



# **INNOVATIVE BIOCONTROL STRATEGIES TO MANAGE CROP AND PEST DISEASES**

EDITED BY: Florence Fontaine, Ana Sofia Duarte and Jochen Fischer  
PUBLISHED IN: *Frontiers in Microbiology*



# frontiers

## Frontiers eBook Copyright Statement

The copyright in the text of individual articles in this eBook is the property of their respective authors or their respective institutions or funders. The copyright in graphics and images within each article may be subject to copyright of other parties. In both cases this is subject to a license granted to Frontiers.

The compilation of articles constituting this eBook is the property of Frontiers.

Each article within this eBook, and the eBook itself, are published under the most recent version of the Creative Commons CC-BY licence.

The version current at the date of publication of this eBook is CC-BY 4.0. If the CC-BY licence is updated, the licence granted by Frontiers is automatically updated to the new version.

When exercising any right under the CC-BY licence, Frontiers must be attributed as the original publisher of the article or eBook, as applicable.

Authors have the responsibility of ensuring that any graphics or other materials which are the property of others may be included in the CC-BY licence, but this should be checked before relying on the CC-BY licence to reproduce those materials. Any copyright notices relating to those materials must be complied with.

Copyright and source acknowledgement notices may not be removed and must be displayed in any copy, derivative work or partial copy which includes the elements in question.

All copyright, and all rights therein, are protected by national and international copyright laws. The above represents a summary only. For further information please read Frontiers' Conditions for Website Use and Copyright Statement, and the applicable CC-BY licence.

ISSN 1664-8714

ISBN 978-2-88976-595-9

DOI 10.3389/978-2-88976-595-9

## About Frontiers

Frontiers is more than just an open-access publisher of scholarly articles: it is a pioneering approach to the world of academia, radically improving the way scholarly research is managed. The grand vision of Frontiers is a world where all people have an equal opportunity to seek, share and generate knowledge. Frontiers provides immediate and permanent online open access to all its publications, but this alone is not enough to realize our grand goals.

## Frontiers Journal Series

The Frontiers Journal Series is a multi-tier and interdisciplinary set of open-access, online journals, promising a paradigm shift from the current review, selection and dissemination processes in academic publishing. All Frontiers journals are driven by researchers for researchers; therefore, they constitute a service to the scholarly community. At the same time, the Frontiers Journal Series operates on a revolutionary invention, the tiered publishing system, initially addressing specific communities of scholars, and gradually climbing up to broader public understanding, thus serving the interests of the lay society, too.

## Dedication to Quality

Each Frontiers article is a landmark of the highest quality, thanks to genuinely collaborative interactions between authors and review editors, who include some of the world's best academicians. Research must be certified by peers before entering a stream of knowledge that may eventually reach the public - and shape society; therefore, Frontiers only applies the most rigorous and unbiased reviews. Frontiers revolutionizes research publishing by freely delivering the most outstanding research, evaluated with no bias from both the academic and social point of view. By applying the most advanced information technologies, Frontiers is catapulting scholarly publishing into a new generation.

## What are Frontiers Research Topics?

Frontiers Research Topics are very popular trademarks of the Frontiers Journals Series: they are collections of at least ten articles, all centered on a particular subject. With their unique mix of varied contributions from Original Research to Review Articles, Frontiers Research Topics unify the most influential researchers, the latest key findings and historical advances in a hot research area! Find out more on how to host your own Frontiers Research Topic or contribute to one as an author by contacting the Frontiers Editorial Office: [frontiersin.org/about/contact](https://frontiersin.org/about/contact)



# INNOVATIVE BIOCONTROL STRATEGIES TO MANAGE CROP AND PEST DISEASES

Topic Editors:

**Florence Fontaine**, Université de Reims Champagne-Ardenne, France

**Ana Sofia Duarte**, Portuguese Catholic University, Portugal

**Jochen Fischer**, Institut für Biotechnologie und Wirkstoff-Forschung (IBWF),  
Germany

**Citation:** Fontaine, F., Duarte, A. S., Fischer, J., eds. (2022). Innovative Biocontrol Strategies to Manage Crop and Pest Diseases. Lausanne: Frontiers Media SA.  
doi: 10.3389/978-2-88976-595-9

# Table of Contents

- 05 Editorial: Innovative Biocontrol Strategies to Manage Crop and Pest Diseases**  
Florence Fontaine, Ana Sofia Duarte and Jochen Fischer
- 07 Isolation, Characterization, and Evaluation of Native Rhizobacterial Consortia Developed From the Rhizosphere of Rice Grown in Organic State Sikkim, India, and Their Effect on Plant Growth**  
Mingma Thundu Sherpa, Laxuman Sharma, Niladri Bag and Sayak Das
- 22 Biocontrol Ability and Mechanism of a Broad-Spectrum Antifungal Strain *Bacillus safensis* sp. QN1NO-4 Against Strawberry Anthracnose Caused by *Colletotrichum fragariae***  
Xiaojuan Li, Miaoyi Zhang, Dengfeng Qi, Dengbo Zhou, Chunlin Qi, Chunyu Li, Siwen Liu, Dandan Xiang, Lu Zhang, Jianghui Xie and Wei Wang
- 36 Monitoring Tritrophic Biocontrol Interactions Between *Bacillus* spp., *Fusarium oxysporum* f. sp. cubense, Tropical Race 4, and Banana Plants in vivo Based on Fluorescent Transformation System**  
Ping He, Shu Li, Shengtao Xu, Huacai Fan, Yongfen Wang, Wei Zhou, Gang Fu, Guangyu Han, Yun-Yue Wang and Si-Jun Zheng
- 49 Cultivar Contributes to the Beneficial Effects of *Bacillus subtilis* PTA-271 and *Trichoderma atroviride* SC1 to Protect Grapevine Against *Neofusicoccum parvum***  
Catarina Leal, Nicolas Richet, Jean-François Guise, David Gramaje, Josep Armengol, Florence Fontaine and Patricia Trotel-Aziz
- 66 Bactericidal Effect of *Pseudomonas oryziphila* sp. nov., a Novel *Pseudomonas* Species Against *Xanthomonas oryzae* Reduces Disease Severity of Bacterial Leaf Streak of Rice**  
Ruihuan Yang, Shengzhang Li, Yilang Li, Yichao Yan, Yuan Fang, Lifang Zou and Gongyou Chen
- 81 Identification of Volatile Organic Compounds in Extremophilic Bacteria and Their Effective Use in Biocontrol of Postharvest Fungal Phytopathogens**  
Laura Toral, Miguel Rodríguez, Fernando Martínez-Checa, Alfredo Montaña, Amparo Cortés-Delgado, Agnieszka Smolinska, Inmaculada Llamas and Inmaculada Sampedro
- 94 Nematicidal Activity of Cyclopiazonic Acid Derived From *Penicillium commune* Against Root-Knot Nematodes and Optimization of the Culture Fermentation Process**  
Van Thi Nguyen, Nan Hee Yu, Yookyung Lee, In Min Hwang, Hung Xuan Bui and Jin-Cheol Kim
- 109 Integrated Metabarcoding and Culturomic-Based Microbiome Profiling of Rice Phyllosphere Reveal Diverse and Functional Bacterial Communities for Blast Disease Suppression**  
Kuleshwar Prasad Sahu, Asharani Patel, Mukesh Kumar, Neelam Sheoran, Sahil Mehta, Bhaskar Reddy, Pierre Eke, Narayanasamy Prabhakaran and Aundy Kumar



- 130 **Biocontrol Potential of *Aspergillus* Species Producing Antimicrobial Metabolites**  
Men Thi Ngo, Minh Van Nguyen, Jae Woo Han, Bomin Kim, Yun Kyung Kim, Myung Soo Park, Hun Kim and Gyung Ja Choi
- 142 **Screening of Cucumber Fusarium Wilt Bio-Inhibitor: High Sporulation *Trichoderma harzianum* Mutant Cultured on Moso Bamboo Medium**  
Ning Zhang, Hao Xu, Jingcong Xie, Jie-yu Cui, Jing Yang, Jian Zhao, Yajuan Tong and Jianchun Jiang
- 152 **Mechanism of a Volatile Organic Compound (6-Methyl-2-Heptanone) Emitted From *Bacillus subtilis* ZD01 Against *Alternaria solani* in Potato**  
Dai Zhang, Ran Qiang, Jing Zhao, Jinglin Zhang, Jianing Cheng, Dongmei Zhao, Yaning Fan, Zhihui Yang and Jiehua Zhu
- 164 **Activity of *Trichoderma asperellum* Strain ICC 012 and *Trichoderma gamsii* Strain ICC 080 Toward Diseases of Esca Complex and Associated Pathogens**  
Stefano Di Marco, Elisa Giorgia Metruccio, Samuele Moretti, Marco Nocentini, Giuseppe Carella, Andrea Pacetti, Enrico Battiston, Fabio Osti and Laura Mugnai
- 181 ***Myxococcus xanthus* R31 Suppresses Tomato Bacterial Wilt by Inhibiting the Pathogen *Ralstonia solanacearum* With Secreted Proteins**  
Honghong Dong, Xin Xu, Ruixiang Gao, Yueqiu Li, Anzhang Li, Qing Yao and Honghui Zhu
- 193 **Interactive Effects of Filamentous Fungi and Cucurbitacin Phytonematicide on Growth of Cowpea and Suppression of *Meloidogyne enterolobii***  
Kgabo Martha Pofu and Phatu William Mashela
- 199 **Modification of Early Response of *Vitis vinifera* to Pathogens Relating to Esca Disease and Biocontrol Agent Vintec® Revealed By Untargeted Metabolomics on Woody Tissues**  
Justine Chervin, Ana Romeo-Oliván, Sylvie Fournier, Virginie Puech-Pages, Bernard Dumas, Alban Jacques and Guillaume Marti
- 213 **Gene *sdaB* Is Involved in the Nematocidal Activity of *Enterobacter ludwigii* AA4 Against the Pine Wood Nematode *Bursaphelenchus xylophilus***  
Yu Zhao, Zhibo Yuan, Shuang Wang, Haoyu Wang, Yanjie Chao, Ronald R. Sederoff, Heike Sederoff, He Yan, Jialiang Pan, Mu Peng, Di Wu, Rainer Borriss and Ben Niu



## OPEN ACCESS

## EDITED AND REVIEWED BY

Jesús Navas-Castillo,  
La Mayora Experimental Station  
(CSIC), Spain

## \*CORRESPONDENCE

Florence Fontaine  
florence.fontaine@univ-reims.fr

## SPECIALTY SECTION

This article was submitted to  
Microbe and Virus Interactions with  
Plants,  
a section of the journal  
Frontiers in Microbiology

RECEIVED 23 September 2022

ACCEPTED 06 October 2022

PUBLISHED 21 October 2022

## CITATION

Fontaine F, Duarte AS and Fischer J  
(2022) Editorial: Innovative biocontrol  
strategies to manage crop and pest  
diseases. *Front. Microbiol.* 13:1052027.  
doi: 10.3389/fmicb.2022.1052027

## COPYRIGHT

© 2022 Fontaine, Duarte and Fischer.  
This is an open-access article  
distributed under the terms of the  
[Creative Commons Attribution License](#)  
(CC BY). The use, distribution or  
reproduction in other forums is  
permitted, provided the original  
author(s) and the copyright owner(s)  
are credited and that the original  
publication in this journal is cited, in  
accordance with accepted academic  
practice. No use, distribution or  
reproduction is permitted which does  
not comply with these terms.

# Editorial: Innovative biocontrol strategies to manage crop and pest diseases

Florence Fontaine<sup>1\*</sup>, Ana Sofia Duarte<sup>2</sup> and Jochen Fischer<sup>3</sup>

<sup>1</sup>Research Unit Résistance Induite et Bioprotection des Plantes RIBP EA 4707, INRAE USC 1488, University of Reims Champagne-Ardenne, Reims, France, <sup>2</sup>Universidade Católica Portuguesa, Faculty of Dental Medicine, Center for Interdisciplinary Research in Health (CIIS), Viseu, Portugal, <sup>3</sup>Institut für Biotechnologie und Wirkstoff-Forschung gGmbH (IBWF), Mainz, Germany

## KEYWORDS

crop protection, biocontrol agent (BCA), fungi, bacteria, sustainability

## Editorial on the Research Topic

[Innovative biocontrol strategies to manage crop and pest diseases](#)

One of the main issues of human life will always be the efficient supply of food. During the last century a shift in agricultural practice made it possible to reduce the amount of labor to feed humanity drastically. But the mechanization of agriculture could not prevent and diminish crop losses due to plant diseases significantly (whether microbial or animal) (Vermeulen et al., 2018; Chidawanyika et al., 2019).

Nevertheless, scientists helped to find solutions for crop protection during all times. In recent years, due to climate change, a more interconnected world and mass production in combination with higher demands on crop protection solutions aiming for a lower impact on the environment new challenges arise every day. Visible to everyone the global climate is changing rapidly and many effects are increasingly manifesting across all biological and environmental systems. Additionally, humans have traded and transported species for centuries, but with an increasing speed and long-range. However, in twentieth century the spreading of species reached a new magnitude and diversity of biological invasions. Biological pests are beneficiaries of both effects. The two main methods for disease control currently available in crop production are application of fungicides (or other pesticides) and the use of plant cultivars resistant or tolerant to their pest organisms. Nevertheless, both methods have differing limitations. Public concerns regarding the health and environmental effects of pesticides, as well as the development of resistant pathogenic strains to fungicides, have reduced their potential. In many important crops, all cultivars and hybrids available to the growers worldwide are susceptible to their pest organisms and genetical modifications of the cultivars are not accepted. One possible solution is the use of biocontrol agents. For that, scientists are attempting to use the current but long-standing war between microorganisms, plants, and animals to develop biological solutions useful for broad agricultural deployment.



The editors aimed for a broad overview shedding light into different corners of modern and innovative plant protection with a focus on strategies using biological approaches.

Therefore, we searched for crop protection solutions using microorganisms and their products to obtain strategies for a modern and advanced agriculture. Some of the articles focus on fungal biocontrol agents (BCAs), such as *Trichoderma* sp. by Di Marco et al., and *Penicillium* sp. by Nguyen et al., while others focus on bacteria, such as *Pseudomonas* sp. by Yang et al. and *Bacillus* sp. as studied by He et al., Leal et al., Li et al., and Zhang N. et al.. Biological control, a phenomenon based on the antagonism between microorganisms, is considered as a sustainable eco-friendly alternative way to prevent or suppress pathogens in agriculture. For example, in this Research Topic, microbial antagonistic strategies against *Neofusicoccum parvum*, an aggressive pathogen associated to Botryosphaeria dieback (BD), are presented for the protection of Chardonnay and Tempranillo (Leal et al.). The most promising biological control trials carried out on a number of fungi that antagonize plant pests and have led to the development of so-called biofungicide products, e.g., Vintec (Chervin et al.). Another promising field of research is based on organic volatile compounds (Toral et al.). In this Research Topic on biocontrol strategies to manage crop and pest diseases, the antagonistic mechanisms of soluble non-volatile bioactive compounds emitted from *Bacillus* have been studied against plant fungal diseases and promising results have been published. The publications cover a wide range of diseases from grapevine trunk diseases to rice pathogens and nematodes on both monocotyledons and dicotyledons to *Alternaria solani* in potato plants (Zhang D. et al.) and bacterial wilt of tomato caused by *Ralstonia solanacearum* (Dong et al.). Innovative approaches also include the application of newly isolated species from marine to soil environments. The included articles allow readers an overview and enable to showcase the variety of crop pests and possible biological control strategies and methods.

The editors of this special Research Topic launched by Frontiers intend to highlight modern research regarding efficient and sustainable plant protection and shed a light on possible and rising new fields in this area.

## References

Chidawanyika, F., Mudavanhu, P., and Nyamukondiwa, C. (2019). Global climate change as a driver of bottom-up and top-down factors in agricultural landscapes and the fate of host-parasitoid interactions. *Front. Ecol. Evol.* 7, 80. doi: 10.3389/fevo.2019.00080

## Author contributions

FF, AD, and JF contributed to writing this Editorial of the Research Topic and approved it for publication.

## Funding

AD was supported by National Funds through FCT—Fundação para a Ciência e a Tecnologia, I.P., under the Project UIDB/04279/2020 and CEECINST/00137/2018/CP1520/CT0013. FF is the supervisor of the academic MALDIVE Chair supported by Grand Reims and URCA.

## Acknowledgments

We thank authors of the papers published in this Research Topic for their valuable contributions. We also thank the editorial board of Frontiers in Microbiology, the submissions team, particularly Talitha Gray and Emmanuel Moro and the Frontiers specialists, especially Camilla Stanton and Victoria Stevenson.

## Conflict of interest

Author JF was employed by Institut für Biotechnologie und Wirkstoff-Forschung gGmbH (IBWF).

The remaining authors declare that the research was conducted in the absence of any commercial or financial relationships that could be construed as a potential conflict of interest.

## Publisher's note

All claims expressed in this article are solely those of the authors and do not necessarily represent those of their affiliated organizations, or those of the publisher, the editors and the reviewers. Any product that may be evaluated in this article, or claim that may be made by its manufacturer, is not guaranteed or endorsed by the publisher.

Vermeulen, S. J., Dinesh, D., Howden, S. M., Cramer, L., and Thornton, P. K. (2018). Transformation in practice: a review of empirical cases of transformational adaptation in agriculture under climate change. *Front. Sustain. Food Syst.* 2, 65. doi: 10.3389/fsufs.2018.00065



# Isolation, Characterization, and Evaluation of Native Rhizobacterial Consortia Developed From the Rhizosphere of Rice Grown in Organic State Sikkim, India, and Their Effect on Plant Growth

## OPEN ACCESS

### Edited by:

Jochen Fischer,  
Institut für Biotechnologie und  
Wirkstoff-Forschung (IBWF), Germany

### Reviewed by:

Tapan Kumar Adhya,  
KIIT University, India  
Hesham Ali El Enshasy,  
University of Technology Malaysia,  
Malaysia  
Upendra Kumar,  
National Rice Research Institute  
(ICAR), India

### \*Correspondence:

Laxuman Sharma  
lsharma@cus.ac.in  
Niladri Bag  
nbag@cus.ac.in

<sup>†</sup>These authors have contributed  
equally to this work

### Specialty section:

This article was submitted to  
Microbe and Virus Interactions with  
Plants,  
a section of the journal  
Frontiers in Microbiology

Received: 23 May 2021

Accepted: 02 August 2021

Published: 06 September 2021

### Citation:

Sherpa MT, Sharma L, Bag N and  
Das S (2021) Isolation,  
Characterization, and Evaluation  
of Native Rhizobacterial Consortia  
Developed From the Rhizosphere  
of Rice Grown in Organic State  
Sikkim, India, and Their Effect on Plant  
Growth. *Front. Microbiol.* 12:713660.  
doi: 10.3389/fmicb.2021.713660

Mingma Thundu Sherpa<sup>1</sup>, Laxuman Sharma<sup>1\*†</sup>, Niladri Bag<sup>1\*†</sup> and Sayak Das<sup>2</sup>

<sup>1</sup> Department of Horticulture, School of Life Sciences, Sikkim University, Gangtok, India, <sup>2</sup> Department of Microbiology,  
School of Life Sciences, Sikkim University, Gangtok, India

Eight rhizospheric bacteria were isolated from the organic paddy fields of Sikkim, India, and identified as *Pseudomonas kribbensis* KSB, *Burkholderia cenocepacia* SRD, *Kosakonia oryzendophytica* YMA7, *Pseudomonas rhodesiae* SRB, *Bacillus* sp. ARA, *Paenibacillus polymyxa* COW3, *Bacillus aryabhattai* PSB2, and *Bacillus megaterium* PSB1. They showed plant growth-promoting attributes in rice and have bio-control potential against phytopathogen *Colletotrichum gloeosporioides* of large cardamom (*Amomum subulatum*). *Burkholderia cenocepacia* SRD showed production of indole acetic acid and ammonia and solubilization of phosphate and potassium and also possessed nitrogen fixation potential. It showed antagonistic activity against two other plant pathogens of large cardamom, viz., *Curvularia eragrostidis* and *Pestalotiopsis* sp., under *in vitro* conditions. The liquid bacterial consortium was prepared using the bacterial strains SRB, PSB1, and COW3 (Consortia-1); PSB2, SRD, and COW3 (Consortia-2); and COW3, KSB, and YMA7 (Consortia-3) to increase the growth and yield of rice plants under organic farming conditions. Greenhouse and field studies showed that the Consortia-3 had the highest plant growth-promoting activity. Consortia-3 demonstrated better agronomic performance in terms of root length (9.5 cm), number of leaflets per plant (5.3), grains per panicle (110.6), test grain weight (27.4 g), dry root weight per plant (0.73 g), and total dry biomass per plant (8.26 g).

**Keywords:** consortia, bio-control, rhizobacteria, bio-fertilizer, organic agriculture, Sikkim, plant growth promoting rhizobacteria

## INTRODUCTION

Northeast India comprises seven sister states, i.e., Assam, Manipur, Meghalaya, Tripura, Mizoram, Arunachal Pradesh, and Nagaland and one brother state, Sikkim. These regions are globally acknowledged for their highest rice diversity (Roy Choudhury et al., 2014). Rice (*Oryza sativa* L.) is one of the main staple food grains of Sikkim that is cultivated in 11,600 ha with a total production



of 20,260 tonnes and a productivity of  $1.84 \text{ t ha}^{-1}$  (Kapoor et al., 2017). It is also described with an epithet “Denzong Valley,” which transcribes to “valley of rice.” Rice is grown during the Kharif season, i.e., monsoon period from July to October. Sikkim alone has greater genetic rice diversity accounting for more than 57 rice accessions documented to date (Kapoor et al., 2017). Among the predominant local rice cultivars, *Attay* is the most common type found all over Sikkim. Depending on the grain size, it can be classified as “*Thulo attay*,” having larger grain size, and “*Sanu attay*,” having small grain size.

Sikkim, the Himalayan state of India, is situated at the  $27^{\circ}\text{N}$ – $28^{\circ}\text{N}$  latitude and  $88^{\circ}\text{E}$ – $89^{\circ}\text{E}$  longitude with an elevation ranging from 300 to 6,000 m above the mean sea level (Sherpa et al., 2015; Najar et al., 2018). The state completely banned the application of synthetic fertilizers and pesticides from 2003 and ultimately attained the certified organic status in 2016. Nutrient management in organic farming has attracted the attention of many researchers for exploring the soil microbes as potent bio-fertilizer that can be used either as a single inoculum or as consortia. Numerous researchers have reported the importance of soil bacteria for the production of plant hormones like indole-3-acetic acid (IAA), gibberellic acid (GA3), solubilization of phosphate, potassium, and nitrogen fixation. The most predominant and economically important soil bacteria isolated from agricultural farmlands are *Burkholderia*, *Delftia*, *Pseudomonas*, *Agrobacterium*, *Azospirillum*, *Azotobacter*, *Rhizobium*, *Clostridium*, and *Serratia* (Bhattacharyya and Jha, 2012; Hao and Chen, 2017; Rajawat et al., 2019; Venieraki et al., 2020). Three species from the genera *Bacillus*, viz., *Bacillus luciferensis* K2, *Bacillus amyloliquefaciens* K12, and *Bacillus subtilis* BioCWB, were isolated from the soils of Sikkim and developed as consortia for use in rice and vegetable cultivation for enhancing their nutrient quality and controlling the pest management of the crops (Panneerselvam et al., 2019, 2020).

*Bacillus* species such as *Bacillus thuringiensis*, *Bacillus megaterium*, *B. subtilis*, and *B. amyloliquefaciens* have also been reported for their effectiveness to suppress diseases and pests in plants. Among their different modes of antagonism, antimicrobial peptides (AMPs) such as *bacillomycin*, *iturin*, *surfactin*, and *fengycin* produced by *Bacillus* spp. have been identified and demonstrated to play an important role in suppressing several plant pathogens. Bacteria are also known to produce volatile compounds and soluble metabolites, which play a key role in plant growth and development, stress tolerance, and disease suppression (Panneerselvam et al., 2019). Sikkim has an entirely organic farming system (Kumar J. et al., 2018), and several management practices including indigenous technologies are available for improving plant growth. However, the application of bacterial consortium particularly of native strain to address the nutrient and pest management has been proved to be holistic and ecologically sustainable strategy for agricultural production (Panneerselvam et al., 2020).

Bacterial consortia were developed from the eight native strains isolated from the rice rhizosphere of the organic farming fields of Sikkim, India. Few previous reports were based on either the monocultures or consortia of bacterial strains from

the same genera such as *Bacillus* sp. showing the plant growth-promoting (PGP) activity (Panneerselvam et al., 2019, 2020). Our consortia were constituted with isolates from different genera having antifungal properties and good nitrogen, potassium, and phosphorous (NPK) performance and had shown promising PGP activity in both tested greenhouse experiments and field study. The consortia developed was tested in local cultivar *Sanu attay*, for various agronomic performance in terms of root length, the number of leaflets per plant, grains per panicle, test grain weight, dry root weight per plant, and total dry biomass per plant, in the test fields at Pakyong organic farming. The present study attempts to identify some of the novel crop-specific multi-potential PGP bacteria from native rice rhizospheric soils.

## MATERIALS AND METHODS

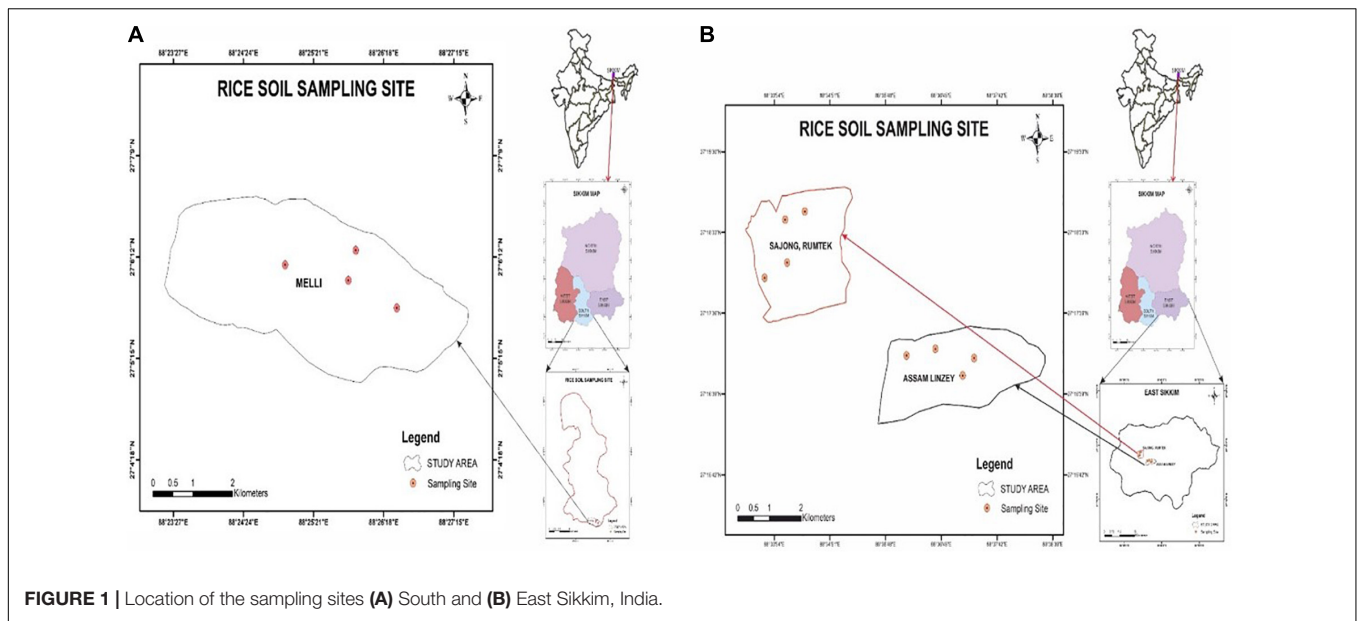
### Sampling Sites

The geographical location of Melli, Sajong, and Assam Lingzey rice fields was determined by GPSMAP 78S (Garmin, Lenexa, KS, United States) as per the manufacturer's guidelines. The study areas were the organic rice fields of the progressive farmers from South Sikkim (Melli, and East Sikkim (Sajong and Assam Lingzey) districts of Sikkim, India. Melli ( $27^{\circ}06'06.32\text{N}$ ;  $88^{\circ}25'38.45\text{E}$ ), Sajong ( $27^{\circ}18'11.13\text{N}$ ;  $88^{\circ}34'26.58\text{E}$ ), and Assam Lingzey ( $27^{\circ}16'55.98\text{N}$ ;  $88^{\circ}37'06.70\text{E}$ ) are located at an elevation of 991, 1,268, and 1289 m above the mean sea level, respectively (Figures 1A,B). Four different sampling sites were chosen for the collection of the rhizosphere soil samples from each of these three villages, i.e., Melli, Sajong, and Assam Lingzey.

The cultivation of the crop was done by the farmers in a well-managed contour terrace on hilly and mountainous topography with ridges almost  $<30\%$  slope. Melli is characterized by a humid subtropical climate with an annual average rainfall of about 3,137 mm and an average temperature of  $23^{\circ}\text{C}$ . Similarly, Sajong and Assam Lingzey are characterized by subtemperate climates with an average rainfall of about 2,578 mm and an average temperature of  $16^{\circ}\text{C}$ . At all the places, the soil was loamy sand; and crops were rain-fed; an assured irrigation source (Bana et al., 2018) was also available.

### Collection of Rhizosphere Soil Samples and Its Physicochemical Analysis

Soil samples were randomly collected from the four different sampling sites at Melli, Sajong, and Assam Lingzey rice fields, during the rainy season of 2019. These samples were collected in triplicates from each of the sampling sites. The field trial was laid out in a split-plot design with local rice cultivar “*Sanu attay*,” a long duration (120 days) variety of paddy. The top 0- to 15-cm soils contained high organic carbon (1%–1.3%) and were slightly acidic in pH (6.5–6.8). One whole paddy plant, after chopping off the shoots, was carefully uprooted (along with the adhering soil; without breaking the secondary and tertiary roots), placed in a polythene bag, labeled and tied (in order to minimize the evaporation loss), and further placed in a box containing ice. The approximate distance of soil adhered to the rice root surface was 12–15 cm. The ice box was transported to a lab where the



roots were shaken to dislodge and separate loosely adhering soil aggregates around primary, secondary, and tertiary roots, and the adhering soils were collected and stored in a refrigerator at 4°C for further studies.

These four soil samples collected from the different sampling sites of a village were pooled together and were used for determination of the physicochemical analysis of the soil for that study area. At all the sampling sites, soils are deep, well-drained, fine-loamy soils with loamy surface, having slight stoniness and moderate erosion. They show a slight degree of profile development and are classified as Cumulic Haplumbre and Pachic Haplumbrepts. They occur in association with moderately deep, coarse soils with loamy surface having slight stoniness and moderate erosion. Associated soils are classified as Typic Udorthents and Typic Haplumbrepts. Most of the area is under paddy cultivation; limited extent is under temperate forest (ENVIS, 2007).

Physicochemical parameters such as soil organic carbon (SOC), nitrogen (N), phosphorus (P), potassium (K), and pH of the rice field soil (before and after application of consortia) were analyzed. SOC and available N/P/K of the soil samples were estimated by the ammonium acetate method (Zhang et al., 2019); and the pH of the soil sample was measured by digital pH meter (Mettler-Toledo, India). The soil:water ratio during the sample collection was 1:2. The soil samples were of loamy sand texture. The pH of the Melli and Sajong soil was between 6.7–6.8 and 6.6–6.8, while soil sample pH of Assam Lingzey was recorded as the lowest among other sites, with a pH of 6.4–6.5. The SOC, available nitrogen, phosphorous, and potassium were measured as 1.1%, 238 kg ha<sup>-1</sup>, 19 kg ha<sup>-1</sup>, and 25 kg ha<sup>-1</sup>, respectively, in Melli soil; those of the soil sample of Sajong were recorded as 1.3%, 235 kg ha<sup>-1</sup>, 18.1 kg ha<sup>-1</sup>, and 22 kg ha<sup>-1</sup>, respectively; and those of Assam Lingzey soil sample were measured as 1%, 239 kg ha<sup>-1</sup>, 16.1 kg ha<sup>-1</sup>, and 21 kg ha<sup>-1</sup>, respectively (Supplementary Table 1).

## Isolation and Screening of Plant Growth-Promoting Rhizobacterial Strains, Their Morphological and Biochemical Characterization, and Molecular Identification

Ten grams of rhizosphere soil from each sampling sites was separately suspended in 90 ml of physiological saline (0.85% of NaCl) in a flask and placed on an orbital shaker (at 100 rpm) at 30°C ± 2°C for 1 h. At the end of shaking, the soil samples were serially diluted up to 10<sup>6</sup> dilutions with physiological saline. Dilutions 10<sup>4</sup>–10<sup>6</sup> were plated on Pikovskayas' agar (PA), Aleksandrov's agar (AA), and Jensen's agar (JA) as described by Panneerselvam et al. (2019, 2020) by spread plate technique and incubated at 30°C ± 2°C for 48 h. The most prominent colonies were isolated and streaked on PA, AA, and JA plates for obtaining pure culture isolates and further were preserved as in glycerol stock stored at –80°C for further studies.

Colony morphology of the pure bacterial isolates was examined. Gram staining was done as per the universal standard method. The physiological characteristics such as the effect of varying temperature, pH, and NaCl concentrations on the isolates were measured by a UV-Vis spectrophotometer. The optimal temperature for growth was examined by incubating the isolates in various temperatures ranging from 5 to 40°C in nutrient broth. The effect of NaCl concentrations was tested in a range of 1%–5% and pH tolerance in the pH ranging from 4 to 10 in nutrient broth at 30 ± 2°C for 48 h (Arya et al., 2015). The biochemical characterization of the isolates was done by qualitative analysis of various enzymes such as indole, methyl red, Voges–Proskauer, and citrate utilization. The carbohydrate assimilation test was performed using glucose, adonitol, arabinose, lactose, sorbitol, mannitol, rhamnose, and sucrose (Najar et al., 2018).

The bacterial genomic DNA was extracted with the help of HiPurA™ kit (HiMedia, Mumbai, India) as per the



manufacturer's instructions. After extraction of genomic DNA, it was stored at  $-80^{\circ}\text{C}$  for further studies. The 16S rRNA genes were polymerase chain reaction (PCR) amplified by using two universal bacterial primers 27F (5'-AGAGTTTGATCCTGGCTCAG-3') and 1492R (5'-CGGTTAC CTTGTTACGACTT-3') (Kumar J. et al., 2018). The amplification was done in 50  $\mu\text{l}$  using 4  $\mu\text{l}$  of each dNTP, 2  $\mu\text{l}$  of  $\text{MgCl}_2$ , 2  $\mu\text{l}$  of template DNA, 1  $\mu\text{l}$  of each primer (forward and reverse), 1  $\mu\text{l}$  of Taq DNA polymerase, and 33  $\mu\text{l}$  of nuclease-free water (HiMedia, India). Reactions were performed in the Mastercycler gradient (Eppendorf, Chennai, India) with the following reaction conditions;  $94^{\circ}\text{C}$  for 5 min for initial denaturation followed by 30 cycles of  $94^{\circ}\text{C}$  for 30 s,  $55^{\circ}\text{C}$  for 1 min,  $72^{\circ}\text{C}$  for 1 min, and the final extension at  $72^{\circ}\text{C}$  for 10 min (thermal cycler PCR system, BIO-RAD C1000; Bio-Rad Laboratories, Singapore) (Najar et al., 2018). The PCR products were purified with the HiPurA<sup>TM</sup> PCR clean up system kit (HiMedia, India) and sequenced by ABI Applied Biosystems<sup>TM</sup> 3500 DNA Analyzer using each universal primer, i.e., 27F and 1492R (Sherpa et al., 2018). The sequences were assembled and aligned with the aid of Codon-Code Aligner software. The sequences were identified using the nucleotide blast tool [National Center for Biotechnology Information (NCBI) search tool], and the phylogenetic tree was created by using the neighbor-joining method with the Jukes-Cantor evolutionary distance measurement using MEGA v.10 (Saitou and Nei, 1987; Erickson, 2010). After the 16S rRNA gene sequences were obtained, they were matched with the GenBank database using the NCBI Basic Local Alignment Search Tool (BLAST). Identified sequences were submitted to NCBI GenBank data, and accession numbers of the selected isolates were obtained.

## In vitro Bioassay for Plant Growth-Promoting Traits

### Solubilization of Insoluble Phosphate and Potassium

The isolates that were screened for their phosphate-solubilizing ability on PA were streaked and incubated for 72 h at  $30^{\circ}\text{C} \pm 2^{\circ}\text{C}$ . The presence of halo zone around the bacterial colony indicated positive isolates. These phosphate solubilization potential isolates were quantitatively estimated in Pikovskayas' medium enriched with tri-calcium phosphate as an insoluble phosphate source (Panneerselvam et al., 2019). Each of the pure isolated bacterial suspension ( $0.5 \text{ ml}$  of  $10^8 \text{ CFU ml}^{-1}$ ) was inoculated in a 250-ml flask containing 100 ml of Pikovskayas' broth. After incubation at 150 rpm at  $30^{\circ}\text{C}$  for 7 days in an incubator, the cultures were centrifuged at 1,000 rpm for 25 min. The supernatant was used to measure the soluble P content colorimetrically as described by Ames (1966). Uninoculated flasks containing the same volume of the medium were established as the controls. The solubilized P content was estimated by subtracting the control P from the final P concentration.

The isolates that were screened for their potassium-solubilizing ability on AA were streaked and incubated for 72 h at  $30^{\circ}\text{C} \pm 2^{\circ}\text{C}$ . The presence of halo zone around the bacterial colony indicated positive isolates. These potassium solubilization

potential isolates were quantitatively estimated in Aleksandrov's medium (Zhang and Kong, 2014; Paul and Sinha, 2017). For the quantitative estimation of potassium solubilization (Sun et al., 2020), cultures were grown in Aleksandrov's broth and incubated for 5 days at  $30^{\circ}\text{C}$  in an incubator. After incubation, 5 ml broth was centrifuged at 10,000 rpm for 15 min; and the supernatant was collected and added to 5 ml of sodium cobalt nitrite solution and was incubated at  $30^{\circ}\text{C}$  for 40 min. It was then centrifuged at 10,000 rpm for 10 min. Optical density was taken at 600 nm in a UV-Vis spectrophotometer. Concentration of potassium produced by cultures was measured with the help of standard graph of KCl obtained in the range of  $100\text{--}1,000 \mu\text{g ml}^{-1}$ .

### Qualitative Estimation of Siderophore Production

The production of bacterial siderophores was qualitatively estimated by the method as per Schwyn and Neilands (1987). Bacteria were streaked on chrome azurol S (CAS) agar media and incubated at  $30^{\circ}\text{C} \pm 2^{\circ}\text{C}$  for 48 h. When the bacteria consumed iron, present in the blue-colored CAS media, orange halos were produced around the colonies, which indicated the presence of siderophores.

### Production of Indole-3-Acetic Acid

Bacterial isolates were grown in nutrient broth supplemented with 0.5% (w/v) tryptophan (i.e., precursor of IAA) and were compared with broths without tryptophan (control) and incubated at  $30^{\circ}\text{C} \pm 2^{\circ}\text{C}$  for 24 h with constant shaking at 150 rpm. The nutrient broth culture was centrifuged at 3,000 rpm for 20 min; and the supernatant was collected in a fresh sterile tube. In a sterile tube, 1 ml of the supernatant was mixed with 2 ml of Salkowski's reagent (2% 0.5  $\text{FeCl}_3$  in 35% perchloric acid solution) and kept in the dark. The absorbance [optical density (OD)] was recorded at 530 nm using a UV-Vis spectrophotometer (Lambda PerkinElmer, Waltham, MA, United States). The amount of produced IAA was measured through a standard curve established by commercially procured IAA ( $0\text{--}100 \mu\text{g ml}^{-1}$ ) as standard.

### Qualitative Analysis of Nitrogen-Fixing Ability

The qualitative nitrogen-fixing ability of the bacterial isolates was evaluated based on their ability to grow on N-free Jensen's media by culturing and incubating them at  $30^{\circ}\text{C} \pm 2^{\circ}\text{C}$  for 48 h (Jimtha et al., 2014; Kumar S. et al., 2018).

### Qualitative and Quantitative Estimation of Ammonia

All the bacterial isolates were qualitatively tested for ammonia production as per Cappuccino and Sherman (1992). The quantitative estimation of ammonia production was assessed by using nutrient broth at  $30^{\circ}\text{C} \pm 2^{\circ}\text{C}$  for 24 h with constant shaking at 150 rpm. Cell-free supernatants of nutrient broth were added with 5% Nessler's reagent, and uninoculated nutrient broth with Nessler's reagent served as a control. Color changes of supernatant from pale to deep yellow were observed for positive isolates. Absorbance was measured at 425 nm, and the amount of ammonia produced was estimated using the ammonium sulfate standard curve of concentrations in ( $0\text{--}100 \text{ mM}$ ) range (Chrouqi et al., 2017).

## Assessment of the *in vitro* Antifungal Activity of Bacterial Isolates

The antifungal activity of the bacterial isolates was evaluated against the fungal pathogens infecting large cardamom (*Amomum subulatum*) of Sikkim by dual culture assay using Potato Carrot Agar (PCA). The following large cardamom fungal pathogens were provided by the Department of Horticulture, Sikkim University, Sikkim, India, viz., *Colletotrichum gloeosporioides* 05 (MN710587), *Curvularia eragrostidis* 04 (MN710527), and *Pestalotiopsis* sp. 02 (MN710582) used for the assay. Agar disc (5 mm) of phytopathogens for 5-day-old culture was placed at one pole of the Petri's plate, and 24-h-old bacterial culture was streaked on the opposite pole (Panneerselvam et al., 2019). Antifungal activity of the bacterial strains was determined by comparing with the control plates inoculated with the fungus only. Inhibition of fungal mycelium (halo zone) around the bacterial colony was a criterion for positive reaction, and its zone of inhibition was measured. The fungal growth was monitored at  $30^{\circ}\text{C} \pm 2^{\circ}\text{C}$  for 120 h; and the three replications per isolate were considered. Fungal colony diameter (growth) was measured, and the percentage of inhibition was calculated as per the methods suggested by Lahlali and Hijri (2010).

$$\text{Percentage of inhibition} = \left( C_d - \frac{T_d}{C_d} \right) \times 100$$

where  $C_d$  is the colony diameter (mm) of the control and  $T_d$  is the colony diameter (mm) of the test plate. Antagonism was also assessed under potato dextrose broth methods wherein first the mycelia dry weight was calculated from which the percentage inhibition by bacteria was calculated as per the formula described by Lahlali and Hijri (2010).

$$\text{Percentage of inhibition} = \left( C^w - \frac{T^w}{C^w} \right) \times 100$$

where  $C^w$  mycelia weight (g) is in the control and  $T^w$  mycelia weight (g) is in the treatment broth.

## *In vitro* Bacterial Compatibility Test

Only the selected bacterial strains were investigated for their compatibility as described by Raja et al. (2006). Each pure bacterial isolate was cultured individually in Luria Bertani broth at  $30^{\circ}\text{C} \pm 2^{\circ}\text{C}$  in a shaker cum incubator at 100 rpm for 48 h. Later on, all the strains were cross-streaked on Luria Bertani agar plate. The cross-streaked plates were incubated at  $30^{\circ}\text{C} \pm 2^{\circ}\text{C}$  for 48 h and then examined for the formation of inhibition zones around the colonies.

## Preparation of Bacterial Consortia

The selected isolates SRB, SRD, PSB1, PSB2, COW3, KSB, and YMA7 were grown until the stationary phase ( $2 \times 10^9$  cells  $\text{ml}^{-1}$ ). Based on the compatibility test, NPK-producing consortia were prepared such as SRB (K), PSB1 (P), and COW3 (N) (Consortia-1); PSB2 (K), SRD (P), and COW3 (N) (Consortia-2); and COW3 (N), KSB (P), and YMA7 (K) (Consortia-3). The selected individual pure bacterial strains having potassium-solubilizing,

phosphorous-solubilizing, and nitrogen-fixing abilities were inoculated into 100-ml conical flask containing each of 50 ml of nutrient broth and was incubated for 48 h at  $30^{\circ}\text{C}$ . The bacterial consortia were prepared by inoculating each of the 200  $\mu\text{l}$  of 48-h-old culture (concentration of  $2 \times 10^9$  CFU  $\text{ml}^{-1}$ ) into 1,000-ml conical flask containing 500 ml of nutrient broth supplemented with 5% sucrose. It was incubated in shaker cum incubator at 150 rpm at  $30^{\circ}\text{C}$  for 48 h. Then the consortia were centrifuged at  $4,000 \times g$  for 5 min and were washed twice with sterile phosphate-buffered saline PBS (1.24 g of  $\text{K}_2\text{HPO}_4$ , 0.39 g of  $\text{KH}_2\text{PO}_4$  and 8.80 g of NaCl per liter). The supernatant was discarded, and the pellet was suspended in PBS buffer. The viable count of the suspension was adjusted by adding sterile distilled water to give a final concentration of  $2 \times 10^9$  cells  $\text{ml}^{-1}$  ( $2 \times 10^9$  CFU  $\text{ml}^{-1}$ ) with the help of a hemocytometer (Marienfeld, Lauda-Königshofen, Germany).

## *In vivo* Root Colonization and Plant Growth Assessment Through Greenhouse Pot Experiment

The effect of the bacterial consortia on plant growth was examined on rice (local cultivar *Sanu Attay*) in a pot at the greenhouse (Department of Horticulture, Sikkim University) in a randomized complete block design method with three replicates. Rice seeds were surface-sterilized with 95% ethanol for 5 min and washed several times with sterilized distilled water.

Three different bacterial consortia [Consortia-1 (*Pseudomonas rhodesiae* SRB + *B. megaterium* PSB1 + *Paenibacillus polymyxa* COW3), Consortia-2 (*Bacillus aryabhattai* PSB2 + *Burkholderia cenocepacia* SRD + *P. polymyxa* COW3), and Consortia-3 (*P. polymyxa* COW3 + *Pseudomonas kribbensis* KSB + *Kosakonia oryzendophytica* YMA7)] were grown in a nutrient broth supplemented with 5% sucrose and was incubated at  $30^{\circ}\text{C}$  for 48 h in an orbital shaker at 150 rpm. Rice seeds were inoculated with each of the bacterial consortia for 5 h at room temperature before planting in pots. Control seeds were also treated in the same manner with sterilized distilled water.

Each pot contained 3 kg of autoclaved sterile soil. Each of the bacterial consortia inoculated seeds was planted 1 cm below the soil surface in each pot. Three replications were conducted for all the treatments. The pots were irrigated with sterile distilled water every day. Rice roots were harvested at the end of the trial, and their dry weight was measured.

## Determination of N, P, and K Uptake by the Rice Plant Grown in Greenhouse Pot Experiment

The availability of N/P/K uptake by the rice plant grown in greenhouse pot was estimated by the analysis of the soil during each treatment, i.e., at initial stage and after 60 days of treatment. In case of the first treatment, i.e., at the initial stage, the soil samples from 0.45 m depth were randomly collected from the pot for each treatment with the three different bacterial consortia. The soil samples were aseptically collected with the help of screw auger. The samples were brought to the laboratory and air-dried under room conditions for 2 days. To remove the

further moisture in the soil, the samples were dried in hot air oven at  $35^{\circ}\text{C} \pm 2^{\circ}\text{C}$  for 6 h. Then the dried soil samples were grinded by wooden roller and thereafter manually sieved through 2 mm stainless steel sieve. The fine-powdered samples were then processed for their chemical analysis through tri-acid mixture.

In case of the second treatment, the effect of the bacterial consortia on nutrient uptake of rice plant was analyzed in the 60-day-old plants. The plant samples from the greenhouse pot experiment were brought to the laboratory, the whole rice plant was air-dried for 2–3 days, and after that, it was dried in a hot air oven at  $60^{\circ}\text{C} \pm 2^{\circ}\text{C}$  overnight to achieve complete dryness of the samples. Once the plant samples were completely dry, they were grinded to powder form and passed through 2 mm stainless steel sieve manually. The filtered powder was then processed for the various chemical assays through tri-acid mixture.

Total nitrogen (N) was assessed by Kjeldahl digestion method; total phosphorous (P) was evaluated by ammonium-molybdate technique in acid digestion procedures; and potassium (K) was estimated by flame photometric methods (Duarah et al., 2011) for both the soil samples (during initial treatment) and plant samples (during second treatment, i.e., after 60 days' growth in a greenhouse pot experiment).

### **In vivo Plant Growth-Promoting Rhizobacteria Activity of the Consortia in Field-Based Trials**

The bacterial consortia were applied at the rice field at Pakyong ( $27^{\circ}13'45.12\text{ N}$  and  $88^{\circ}35'33.26\text{ E}$ , and elevation is 1,272 m above the mean sea level), East Sikkim, in triplicates. Soils are deep, well-drained, fine-loamy soils with loamy surface, have slight stoniness and moderate erosion, and are classified as Cumulic Haplumbre and Pachic Haplumbrepts. The consortia were applied to the field area of  $36.57\text{ m} \times 60.96\text{ m}$  ( $2,229.3\text{ m}^2$ ) where local rice variety *Sanu attay* was organically cultivated. The consortia were administered to 25-day-old rice plant saplings through root dipping method (Fasusi et al., 2021). The uninoculated rice saplings were the controls for the study. The PGP traits were observed in the plants after 60 days by transplanting in organic agricultural farming fields.

### **Statistical Analysis**

Data of bacterial consortia treatments were compared by the least significance difference (LSD) test using R software (Devkota et al., 2019). The differences at the  $p \leq 0.05$  value were considered as significant results.

## **RESULTS**

### **Bacterial Isolation and Biochemical Characterization**

A total of 25 PGP bacteria were screened and isolated from the rice rhizospheric soil. Based on the morphological, biochemical characterization, and PGP attributes, eight bacterial isolates were selected for further analyses. The cell morphology of the isolates was Gram-positive and Gram-negative rods. Most of the isolates

were Voges–Proskauer negative, methyl red positive, and citrate utilization test positive, i.e., seven isolates, six isolates, and seven isolates. The carbohydrate assimilation test showed that most of the isolates fermented carbohydrates like glucose, arabinose, and sucrose (Supplementary Table 2). The physiological analysis showed that isolates could tolerate a wide range of temperature, pH, and NaCl concentrations. Growth was observed up to 5% NaCl concentration (Supplementary Figures 1A,B). The isolates could actively grow in the temperature range from 10 to  $40^{\circ}\text{C}$ . However, most of the isolates showed optimum growth temperature at  $30^{\circ}\text{C}$  (Supplementary Figures 1C,D). The isolates were able to grow in both acidic and alkaline conditions of pH ranging from 4.0 to 10.0 (Supplementary Figures 1E,F). However, the optimum pH for most of the isolates was pH 8.0, although few isolates showed growth up to pH 10 (SRB, KSB, and YMA7).

### **Identification of Bacteria**

Molecular identification revealed the singular dominance of the genus *Bacillus*. The other genera found in this study were *Burkholderia*, *Kosakonia*, and *Pseudomonas*. Identified isolates of *Bacillus* were *B. aryabhatai* PSB2 (MW020338), *B. megaterium* PSB1 (MW020222), and *Bacillus* sp. ARA (MW021509). Similarly, identified isolates of *Pseudomonas* were *P. kribbensis* KSB (MW308683) and *P. rhodesiae* SRB (MW020262), while other identified isolates were *Kosakonia oryzendophytica* YMA7 (MW020337), *P. polymyxa* COW3 (MW020264), and *B. cenocepacia* SRD (MW020263). The alignment and similarity search of 16S rRNA sequence with nr/nt database of NCBI have shown that many of the isolates have a percentage of identity  $>98\%$ . The identified species, the percentage of identity, and their NCBI accession number are given in Table 1. The phylogenetic tree was made with the help of MEGA v.10 software using the maximum likelihood method and the Jukes–Cantor model as shown in Supplementary Figure 2.

### **Plant Growth-Promoting Activity**

In this study, eight efficient isolates were selected based on their PGP traits, in particular, (i) the solubilization of phosphate and potassium; (ii) production of IAA and siderophore; and

**TABLE 1** | Identification of bacteria based on 16S rRNA, the percentage of identity, and NCBI accession numbers.

Isolates	Partial identification based on 16S rRNA gene sequencing	% identity	Accession no.
PSB1	<i>Bacillus megaterium</i>	98	MW020222
COW3	<i>Paenibacillus polymyxa</i>	99	MW020264
SRB	<i>Pseudomonas rhodesiae</i>	99	MW020262
ARA	<i>Bacillus</i> sp.	99	MW021509
KSB	<i>Pseudomonas kribbensis</i>	99	MW308683
YMA7	<i>Kosakonia oryzendophytica</i>	99	MW020337
SRD	<i>Burkholderia cenocepacia</i>	98	MW020263
PSB2	<i>Bacillus aryabhatai</i>	99	MW020338



(iii) ability to fix nitrogen. The selected bacterial isolates were identified as *P. rhodesiae* SRB, *B. megaterium* PSB1, *P. polymyxa* COW3, *B. aryabhattai* PSB2, *B. cenocepacia* SRD, *Bacillus* sp. ARA, *P. kribbensis* KSB, and *K. oryzendophytica* YMA7 (Table 1). The quantitative estimation of phosphate and potassium indicated that isolate *B. cenocepacia* SRD produced significantly higher phosphate ( $530 \mu\text{g ml}^{-1}$ ) and potassium ( $581 \mu\text{g ml}^{-1}$ ) than did the other isolates (Table 2). Similarly, quantitative estimation of IAA and ammonia showed that the isolate *K. oryzendophytica* YMA7 produced a considerably higher extent of IAA ( $84 \mu\text{g ml}^{-1}$ ) and ammonia (61 mM) than did the other isolates (Table 2). However, out of eight isolates, *P. polymyxa* COW3 and *B. aryabhattai* strain PSB2 had only the nitrogen-fixing ability.

## Antagonistic Activity Against Pathogenic Plant Fungi

The dual-plate studies revealed that *B. cenocepacia* SRD had higher antagonistic activity against rice sheath blight and large cardamom leaf spot disease-causing fungi *C. gloeosporioides* (90%–91%), *C. eragrostidis* (43%–49%), and *Pestalotiopsis* sp. (29%–33%) (Supplementary Table 3 and Supplementary Figure 3). Similarly, *K. oryzendophytica* YMA7 showed 56% antagonism against *C. eragrostidis* and *C. gloeosporioides* (53%) and 27% with *Pestalotiopsis* sp., respectively, in both culture plate and broth assay (Supplementary Tables 3, 4). Furthermore, compatibility assays conducted on Nutrient Agar plate deciphered that all the tested isolates have no antagonistic effect on each other such as Consortia-1 (*P. rhodesiae* SRB, *B. megaterium* PSB1, and *P. polymyxa* COW3), Consortia-2 (*B. aryabhattai* PSB2, *B. cenocepacia* SRD, and *P. polymyxa* COW3), and Consortia-3 (*P. polymyxa* COW3, *P. kribbensis* KSB, and *K. oryzendophytica* YMA7).

## Root Growth Stimulation Potential

Greenhouse pot assessments of selected bacterial consortia on rice roots growth have shown the development of the rice root system as a function of IAA production. Consortia-3 (*K. oryzendophytica* YMA7 + *P. kribbensis* KSB + *P. polymyxa* COW3) stimulated the maximum amount of lateral roots on rice plant as compared with other consortia. The root length of rice

exhibited by all the three different bacterial consortia were higher than that of the control.

## Evaluation of Plant Growth-Promoting Traits in Field Study

Three bacterial consortia developed in this study were first tested in greenhouse pot experiments and later on applied to the rice field (Figure 2). Based on the agronomic parameters, significant increases were observed in all the plant growth and yield parameters except leaf number per plant when compared with uninoculated rice plant (Table 3). All the three bacterial consortia significantly improved grains per panicle (C1:45.0, C2:79.0, and C3:110 grain numbers per panicle) (Figures 3, 4 and Supplementary Figures 4, 5), grain weight in grams (C1:24.3 g, C2:24.8 g, and C3:27.8 g) (Figures 3, 4 and Supplementary Figures 4, 5), and root length in cm (C1:6.6 cm, C2:9 cm, and C3:9.5 cm) as compared with uninoculated control rice plants. However, among the three bacterial consortia, Consortia-3-inoculated rice plants showed significantly higher biomass (8.26 g/plant), grains per panicle (110 grain/panicle), test grain weight (27.4 g), root length (9.5 cm), and dry root weight (0.73 g/plant) as compared with the other consortia (Table 3). The combined PGP traits such as phytohormone production and nutrient solubilization abilities were maximally observed in Consortia-3 (*K. oryzendophytica* YMA7 + *P. kribbensis* KSB + *P. polymyxa* COW3). The potential assessment of the bacterial consortia application improved the soil N, P, K value as compared with the control; but in our study, interestingly, the pH value of the experimental field soil decreased from 6.5 to 6.0 (Supplementary Tables 5, 6). This result might be due to the fact that the bacterial colonization in soil decreases pH value due to the secretion of organic acid by bacteria as secondary metabolites.

## Determination of N/P/K Content in Rice Plant

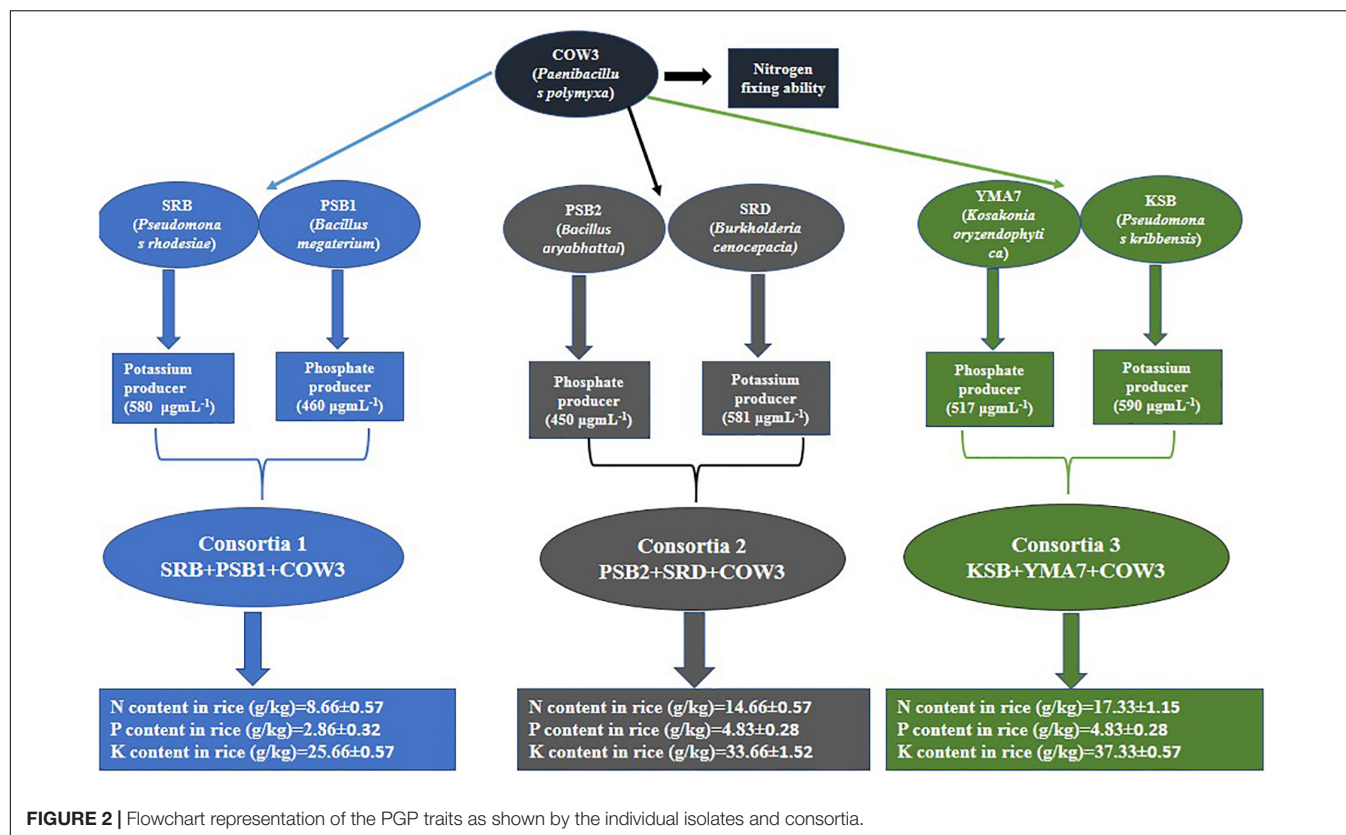
In order to verify whether consortia-based treatment can promote nutrient uptake by rice plants, the content of nitrogen, phosphorus, and potassium in rice plant were determined. Our results showed that significant increase in rice plant N/P/K uptake was observed when the soil was inoculated with different bacterial consortia as compared with the uninoculated control

TABLE 2 | PGP traits of isolated bacterial isolates.

Strain	Phosphate ( $\mu\text{g ml}^{-1}$ )	Potassium ( $\mu\text{g ml}^{-1}$ )	IAA ( $\mu\text{g ml}^{-1}$ )	Ammonia (mM)	Siderophore production	Nitrogen fixation
PSB1	460 $\pm$ 0.25	250 $\pm$ 0.071	21.0 $\pm$ 6.1	7.0 $\pm$ 2.13	++	+
COW3	420 $\pm$ 0.005	250 $\pm$ 0.00	25.0 $\pm$ 0.66	5.0 $\pm$ 0.00	+	+++
SRB	210 $\pm$ 0.003	580 $\pm$ 0.008	5.0 $\pm$ 0.33	10.0 $\pm$ 0.33	+	+
ARA	480 $\pm$ 0.03	570 $\pm$ 0.26	4.0 $\pm$ 0.00	6.0 $\pm$ 0.00	+	++
KSB	410 $\pm$ 0.003	<b>590 <math>\pm</math> 0.01</b>	59.0 $\pm$ 0.33	35.0 $\pm$ 0.33	++	+
YMA7	517 $\pm$ 0.01	570 $\pm$ 0.03	<b>84.0 <math>\pm</math> 1</b>	<b>61.0 <math>\pm</math> 1.2</b>	+++	++
SRD	<b>530 <math>\pm</math> 0.008</b>	581 $\pm$ 0.012	20.0 $\pm$ 0.66	5.0 $\pm$ 0.66	+	++
PSB2	450 $\pm$ 0.006	330 $\pm$ 0.003	10.0 $\pm$ 0.00	2.0 $\pm$ 0.33	+	+

Data are presented as mean of triplicates  $\pm$  standard deviation. “+” denotes weakly positive; “++” denotes moderately positive; and “+++” denotes strongly positive. Bold values indicate the highest value obtained among all the strains for the specific PGP trait. PGP, plant growth promoting; IAA, indole-3-acetic acid.





**TABLE 3 |** Effect of bacterial consortia inoculation on plant growth promotion after 60 days of transplanting of rice at farmer's field.

Microbial consortia	Tiller number per bunch (5 plants)	Root length (cm)	Number of leaflets per plant	Grains per panicle	1,000-grain wt. (g)	Dry root dry wt. per plant (g)	Total dry biomass per plant (g)
C1-Consortia-1 (SRB+PSB+COW3)	14.3 ± 1.45 <sup>ab</sup>	6.6 ± 0.66 <sup>b</sup>	4.0 ± 0.00 <sup>b</sup>	45.0 ± 3.51 <sup>c</sup>	24.3 ± 0.88 <sup>b</sup>	0.49 ± 0.47 <sup>bc</sup>	7.16 ± 0.20 <sup>c</sup>
C2-Consortia-2 (PSB2+SRD+COW3)	15.3 ± 0.33 <sup>a</sup>	9.0 ± 0.00 <sup>a</sup>	5.3 ± 0.33 <sup>a</sup>	79.3 ± 6.56 <sup>b</sup>	24.8 ± 0.57 <sup>b</sup>	0.56 ± 0.41 <sup>b</sup>	7.66 ± 0.28 <sup>b</sup>
C3-Consortia-3 (COW3+KSB+YMA7)	12.6 ± 0.88 <sup>b</sup>	9.5 ± 0.00 <sup>a</sup>	5.3 ± 0.33 <sup>a</sup>	110.6 ± 9.17 <sup>a</sup>	27.4 ± 0.42 <sup>a</sup>	0.73 ± 0.03 <sup>a</sup>	8.26 ± 0.25 <sup>a</sup>
Uninoculated control	12.3 ± 0.88 <sup>b</sup>	3.5 ± 0.28 <sup>c</sup>	4.3 ± 0.33 <sup>b</sup>	66.6 ± 1.73 <sup>b</sup>	18.2 ± 0.34 <sup>b</sup>	0.42 ± 0.09 <sup>c</sup>	6.03 ± 0.05 <sup>d</sup>
LSD ( $p \leq 0.05$ )	2.579	1.412	0.998	19.892	1.968	0.12	0.39
CV	9.44	9.86	10.52	13.20	2.55	11.69	2.71

Values are means ± SE. a, b, c, and d letters on the bars denote differences on the basis of a t-test ( $p < 0.05$ ).

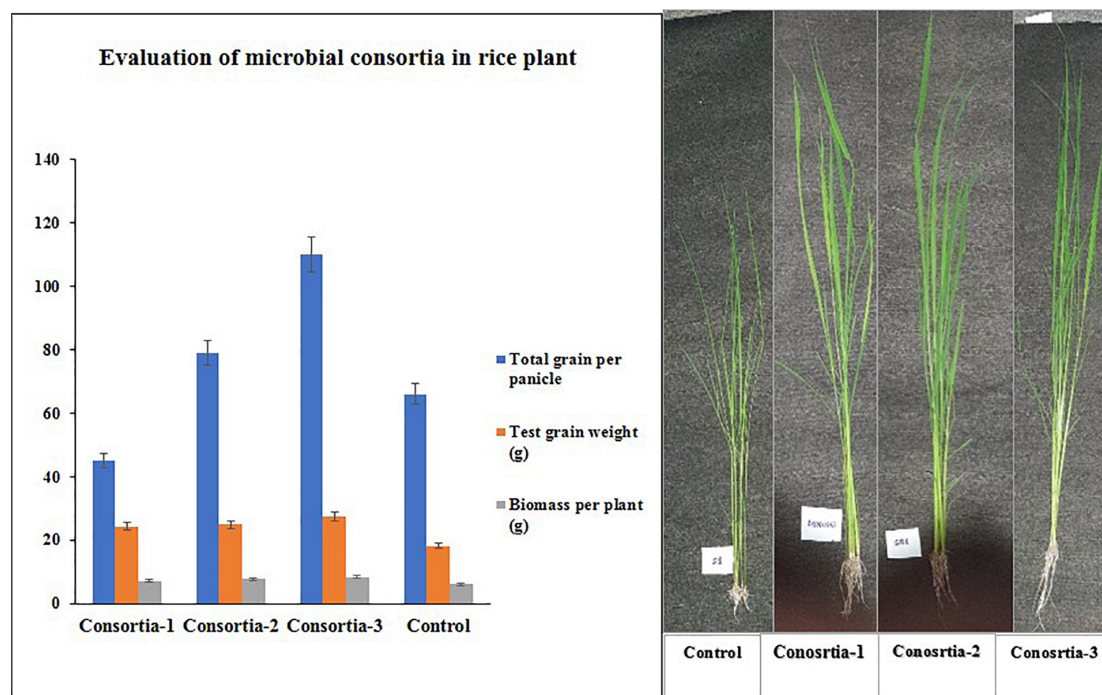
plant. In rice plant, in the soil inoculated with three different bacterial consortia (Consortia-1, Consortia-2, and Consortia-3), the plant N/P/K content was N (8.66, 14.66, and 17.33 g kg<sup>-1</sup>), P (2.86, 4.83, and 4.83 g kg<sup>-1</sup>), and K (25.66, 33.66, 37.33 g kg<sup>-1</sup>) and control plant N/P/K (7.0, 2.16, and 24.66 g kg<sup>-1</sup>) (Figure 5 and Supplementary Table 7).

## DISCUSSION

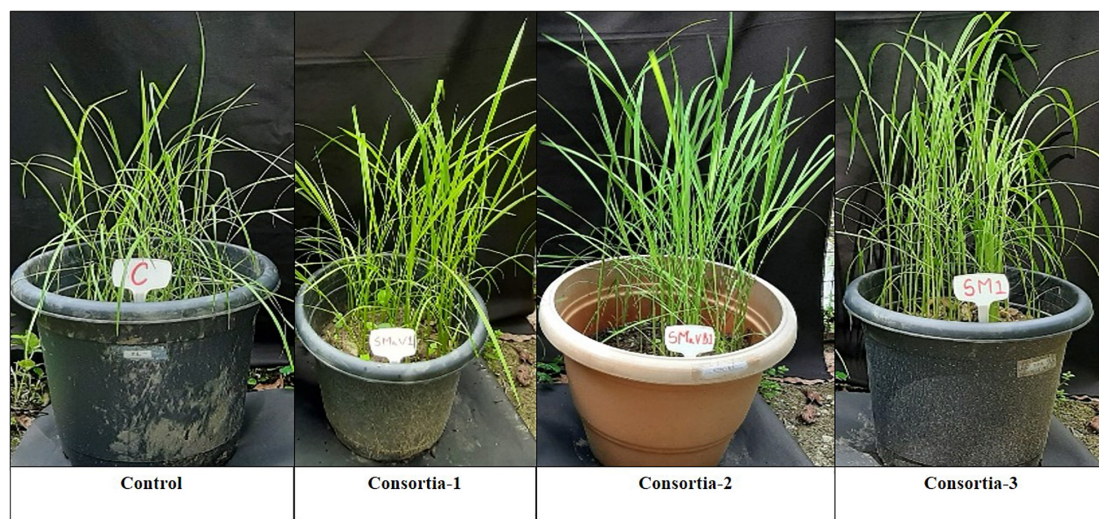
An assortment of abiotic and biotic elements shape soil-and plant-related living spaces and adjust the creations and exercises of their microbial networks, which thus bear upon the nature of

their development of plants and the creation of root exudates (Jain et al., 2020). Bacteria harbor in roots, depending on the incredible variety of natural root exudates, which in the long run influences the growth and development of the plant (Ngalimat et al., 2021). Here, in this study, we examined the impact of rice rhizosphere regulated with local bacterial consortia developed to increase the uptake the N/P/K as nutrients from the soil.

Bacterial isolation was done from soil rhizosphere fractions by 16S rRNA gene sequencing. This technique offers a culture-independent method for tracking dominant bacterial populations in soil (Sultana et al., 2020). To the best of our knowledge, this study represents the first approach using culture-independent method to design a native consortia that can enhance the rice



**FIGURE 3 |** Evaluation of three native consortia (Consortia-1, 2, and 3) on rice plants. Values are means  $\pm$  SE.

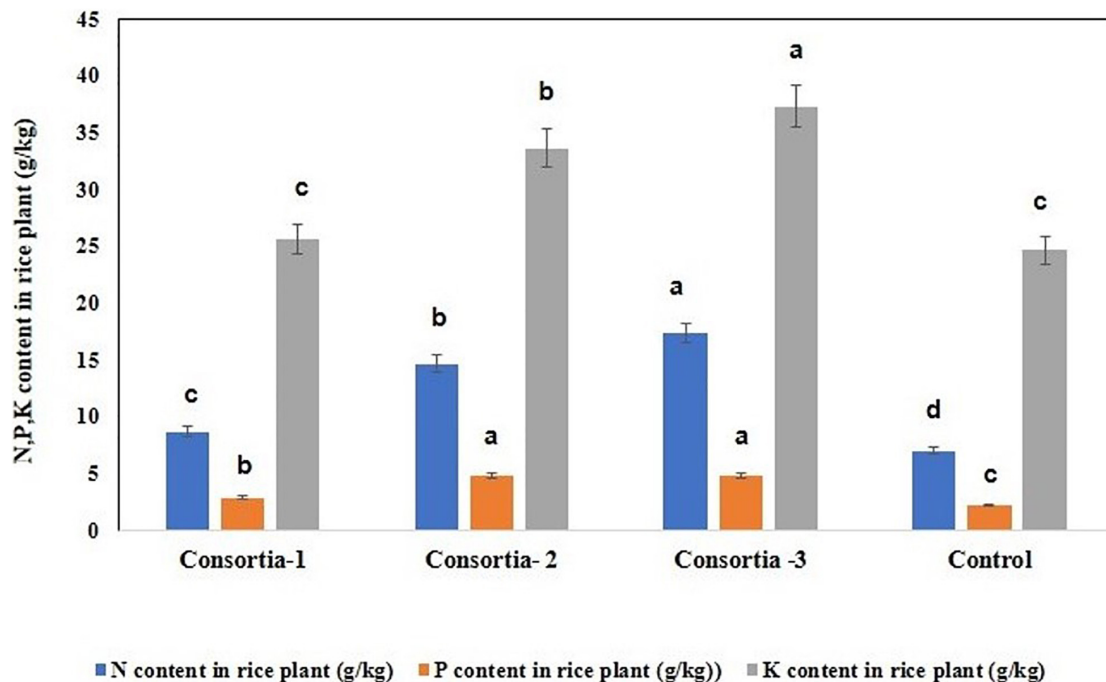


**FIGURE 4 |** Phenotype differences of potted rice plant under different consortia treatments. Consortia-1 (SRB+PSB1+COW3), Consortia-2 (PSB2+SRD+COW3), and Consortia-3 (COW3+KSB+YMA7), and control rice plant.

crop nutrient quality uptake as in N/P/K from the soil of organic farming in Sikkim. In brief, soil samples from three different organic paddy cultivation field sites in Sikkim, India, were chosen [M (loamy sand), S (loamy sand), and AL soil (loamy sand)] to screen and isolate PGP rhizobacteria (PGPR) and design a consortia that can uptake N/P/K nutrients from soil. These bacterial isolates also had antifungal properties that were effective against fungal pathogens. To validate the consortia performance,

chemical analysis of soil (before consortia administration and post-consortia administration) was compared in greenhouse pot experiments. Later on, field-based trials for 60 days on application of consortia were also measured to verify the various agronomic parameters.

Antagonistic and PGPR were screened and isolated from the rhizosphere of rice and was identified through a polyphasic approach, based on morphological, biochemical, and partial



**FIGURE 5 |** Nitrogen, phosphorus, and potassium uptake for rice plant after consortia application (60 days trail). Values are means  $\pm$  SE. abcde letters on the bars denote differences on the basis of a *t*-test ( $p < 0.05$ ).

16S rRNA gene sequencing. The cultures isolated were four *Bacillus* sp. strains (PSB1, PSB2, COW3, and ARA), two *Pseudomonas* sp. strains (SRB and KSB), and one each strain of *Burkholderia* sp. (SRD) and *Kosakonia* sp. (YMA7). 16S rRNA gene sequencing analysis and homology with reference strains from the nucleotide database of NCBI showed that the strains PSB1, PSB3, ARA, COW2, SRB, KSB, SRD, and YMA7 have average nucleotide identity percentage ranges from 98 to 99% with *B. megaterium*, *B. aryabhattai*, *Bacillus* sp., *P. polymyxa*, *P. rhodesiae*, *P. kribbensis*, *B. cenocepacia*, and *K. oryzendophytica*, respectively.

The *B. megaterium* strain PSB1 isolated in this study showed high salt tolerance at 8% NaCl as compared with other isolates.

Many studies revealed that the genus *Pseudomonas* represents the dominance of PGPR for many crops (Qessaoui et al., 2019). In the present investigation, *P. kribbensis* strain KSB showed multiple PGP activities including siderophore production. This result corroborates with previous findings wherein multiple PGP traits have been described from *Pseudomonas* sp. isolated from the rhizospheric soil of wheat, barley, and rice (Ahmad et al., 2008; Sharma et al., 2011).

The member of the genus *Kosakonia* consists of seven different species, *K. oryzendophytica* (Hardoim et al., 2013), *Kosakonia cowanii* (Inoue et al., 2000), *Kosakonia radicincitans* (Kämpfer et al., 2005), *Kosakonia oryzae* (Peng et al., 2009), *Kosakonia arachidis* (Madhaiyan et al., 2010), *Kosakonia sacchari* (Zhu et al., 2013), and *Kosakonia oryzophilus* (Hardoim et al., 2013), which belong to the family Enterobacteriaceae. Except for *K. cowanii*, which is considered to be from clinical origin, other species

of the genus are nitrogen-fixing bacteria, which are commonly associated with plants (Li Y. et al., 2017). They are most frequently found in the nitrogen-fixing bacterial community of some non-leguminous plant, such as rice (Hardoim et al., 2013) and sugarcane (Raju et al., 2020). The *Kosakonia* species contains flagella, which enable them to swim and possibly help in the attachment to the plant surface. It might also produce different secretion systems that help to interact with both host plant and associated microbiota (Becker et al., 2018). The present *in vitro* screening for characteristics generally associated with PGP showed that *K. oryzendophytica* strain YMA7 showed a higher production of IAA ( $84 \mu\text{g ml}^{-1}$ ) and ammonia ( $61 \text{ mM}$ ). It also showed higher solubilization for potassium ( $570 \mu\text{g ml}^{-1}$ ) and phosphate ( $517 \mu\text{g ml}^{-1}$ ). It also produced siderophores. It also produced a high amount of phosphate ( $517 \mu\text{g ml}^{-1}$ ) as compared with *K. oryzendophytica* strain NRCSSDCU262 ( $207 \mu\text{g ml}^{-1}$ ), which is an endophytic-rhizospheric phosphate-solubilizing bacteria (PSB) isolated from cumin grown in agricultural fields of Rajasthan, India (Devi et al., 2020).

Other most important soil bacteria that belong to the genus *Burkholderia* in the class Betaproteobacteria (Castanheira et al., 2015) have also been reported as one of the dominant extracellular PGPR for many crops (Becker et al., 2018). *Burkholderia* species in general have symbiotic relationship with plants, functioning as active rhizospheric components (Castanheira et al., 2015), endophytic plant colonizers, or microsymbionts in legume root nodules, as reported by many researchers (Sutton, 1992). The ability to fix nitrogen was demonstrated by several *Burkholderia* spp. associated with



different plants, for example, maize, coffee (Estrada-de los Santos et al., 2001), sugarcane, and tomato (Lin et al., 2012; Paungfoo-Lonhienne et al., 2014), had already been reported in several studies. In our study, regarding plant growth promotion traits, *B. cenocepacia* SRD showed higher solubilization of phosphate and potassium. It also produced IAA and also showed antagonistic activity against plant fungus *C. gloeosporioides*.

*Colletotrichum* is a broad-spectrum plant pathogen infecting a host range of plants. Its pathogenicity leads to major losses of crops and other agricultural products (Saju et al., 2013). They play a significant role in causing post-harvest loss (Sutton, 1992). The disease symptoms vary on plant species; but generally, it has been observed to affect plant leaves, stems, and fruits of the host plant (Panneerselvam et al., 2019). The antagonistic PGP microbes directly compete with the plant pathogens for nutrition and inhibit or reduce the pathogen growth via hyper-parasitism (Sutton, 1992). Our dual-plate studies on *B. cenocepacia* SRD showed 90%–91% antagonistic activity against *C. gloeosporioides*, which is a rice sheath blight and large cardamom leaf spot disease-causing fungi predominantly found in Sikkim. Mahamuni (2015) found that the *B. cenocepacia* strain VIMP01 solubilized phosphate and potassium and also produced IAA, which was similar to our isolate *B. cenocepacia* SRD.

Phosphorous is considered as the second-most key nutrient after nitrogen for plant growth, although less than 5% of the total soil phosphorous is found in the available form to plants (Otieno et al., 2015). Hence, the capability to solubilize the insoluble form of phosphate is one of the key features of PGP bacteria to boost plant nutrition through an escalation in phosphorous uptake by plants (Taurian et al., 2010). The application of these types of PSB in the soil might contribute to the reduction of excessive usage of the chemical fertilizers, and thereby, it improves the soil health of agricultural lands (Taurian et al., 2010).

In the present investigation, the three bacterial consortia (Consortia-1, Consortia-2, and Consortia-3) were prepared based on solubilization of phosphate and potassium, and nitrogen-fixing ability of the bacterial isolates. Application of bacterial consortia at the rice fields of Pakyong during August 2019 showed that there were significant differences in all the rice plant growth and yield parameters, except leaflets number per plant in the rice plants treated with three different bacterial consortia as compared with uninoculated control. All three consortia significantly improved grains per panicle, grain weight, and root length as compared with uninoculated control plants. But Consortia-3-inoculated rice plants showed higher plant biomass, grains per panicle, grain weight, root length, and dry root weight as compared with control plants and other consortia-inoculated plants. The collective PGP traits and nutrient solubilization properties observed in Consortia-3 were due to the bacterial mixture of *K. oryzaendophytica* YMA7, *P. kribbensis* KSB, and *P. polymyxa* COW3. Our results are in agreement with studies by Di Benedetto et al. (2019) and Devi et al. (2020), who had showed the PGP properties of *Bacillus* spp., *Pseudomonas* spp., and *Kosakonia* spp. Panneerselvam et al. (2019) showed that *B. subtilis* strain BioCWB ( $570 \mu\text{g ml}^{-1}$ ) and *B. luciferensis* strain K2 ( $417.3 \mu\text{g ml}^{-1}$ ) produced higher amounts of phosphates.

Similarly, in our findings, *P. polymyxa* strain COW3 and *Bacillus* sp. strain ARA produced higher phosphates, i.e., 580 and  $579 \mu\text{g ml}^{-1}$ , respectively. In general, the application of Consortia-3 among all the three consortia significantly increased plant growth parameters as compared with those of the uninoculated control plant. Many previous studies have proved that *Bacillus* spp. (*B. aryabhattai*, *B. megaterium*, *Bacillus polymyxa*), *Pseudomonas* spp. (*P. kribbensis*, *P. rhodesiae*), *Burkholderia* spp., and *Kosakonia* spp. possessed PGP attributes, enhanced plant growth, and increased yield in several agricultural and horticultural crops (Park et al., 2017; Devi et al., 2020; Castanheira et al., 2015).

The difficulties encountered by the native bio-inoculants might be distinctive all throughout the planet, as the various abiotic factors such as the edaphic, climatic, and geological conditions of the local environment vary remarkably (Ojuederie et al., 2019; Orozco-Mosqueda et al., 2021). Consequently, for quite a long time, it has been attempted to separate local strains that permit to work on the harvests of similar regions from which they were secluded, which would recommend superior productivity to practice their valuable activities when related with plants in similar sorts of agricultural soils. Consequently, more investigation is needed to relate abiotic angles with the useful properties of each native consortia. Reduction of inorganic farming practices shall also prevent agriculturists from exposure to harmful chemicals that might be toxic not only to the soil but also to human health (Wightwick et al., 2010).

Native PGPR strains might help in plant growth development through various mechanisms. Direct enhancement might be through the improved nutrient accessibility and its proficiency in uptake, by increasing the capacity to solubilize P, to fix  $\text{N}_2$ , and to create siderophores and plant growth hormones, for example, IAA (Glick, 2012). Native PGPR strains are the natural flora of the soil, yet their number is not sufficient to rival different microbes set up in the rhizosphere. Accordingly, the implementation of consortia developed from the native PGPR strains is important to increase the local population of the target microorganism and to boost their helpful properties for plant yield. The utilization of local soil bacterial consortia has many advantages when administered into the plant rhizosphere, as there might be less competition among themselves for nutrient cycling. Furthermore, they are more impervious to the local ecological stress conditions particularly experienced under the anticipated climatic changes (Vimal et al., 2017).

Long-term organic farming/agricultural practices can directionally change the bounty of certain bacterial phyla. Yet there is no adequate comparison of soil bacterial taxa in light of long-term organic farming/agricultural vs. inorganic farming practices. Long-term organic farming might expand the availability of natural C to choose for certain microbial taxa levels that feed fundamentally on natural substrates and multiply significantly, bringing about the progressions in microbial local area structure and soil supplement status (Cederlund et al., 2014). As a result, specific microbial taxa abundances might be considerably expanded by long-term organic farming and also should show some level of associations with soil supplements. Besides, these taxa might show a possible

beneficial impact on crop efficiency and agro-biological system stability (Francioli et al., 2016). Network analysis of the taxa, as estimated by next-generation sequencing, might help with interpreting the complex microbial communities and the role of the environmental standards governing the local area (Barberán et al., 2012; Banerjee et al., 2016). Ongoing analysis through high-throughput sequencing shall un-reveal the microbial variety and local area arrangement under long-term organic farming and inorganic farming (Lentendu et al., 2014; Calleja-Cervantes et al., 2015; Zhou et al., 2015; Chen et al., 2016; Ding et al., 2016; Francioli et al., 2016; Li F. et al., 2017). Notwithstanding, very few studies have been done about which microbial taxa are firmly affected by long-term organic and inorganic farming practices and how these taxa are connected to soil supplement boundaries.

Regarding organic and inorganic farming alone, the former practice ordinarily delivers lower crop yield (Seufert et al., 2012); however, the latter causes more ecological issues (Davidson, 2009). The integrated technique of periodic alteration between organic and inorganic farming is assessed as the best method to upgrade crop productivity and increment of soil organic matter (SOM) level (Wei et al., 2016). In the interim, consolidated organic treatment improves the production of soil invertase, urease, and antacid phosphatase, which are three average microbial exoenzymes engaged with C, N, and P mineralization (Li F. et al., 2017). All the more significantly, in contrast with inorganic farming, the organic treatment improved more measures of explicit bacterial taxa. These taxa are involved in the decay of complex natural matters and soil supplement changes and are accordingly advantageous for plant development by working on supplement accessibility. Subsequently, we need to analyze the bacterial diversity to comprehend the long-term organic farming against inorganic farming in Sikkim. In any case, an essential issue lies in the fact that Sikkim has banned inorganic cultivating practices since 2003, so to mirror inorganic farming in a greenhouse is the solitary choice for better relative investigation.

## CONCLUSION

This is the first-ever study of native consortia developed from the rice rhizosphere of organic farmlands of Sikkim, which are found to be effective as an NPK enhancer so as to help in plant growth promotion. Also, they have antifungal properties that serve as additional crop security against fungal pathogens. We have obtained efficient P-solubilizing, K-solubilizing, N<sub>2</sub>-fixing, IAA-producing, and antagonistic potential bacteria present among the native rice soil rhizosphere. These characteristics are considered as important PGP traits; and the bacterial consortia prepared from N-, P-, and K-producing bacteria have been found effective in improving the growth and N, P, and K contents of tested rice plants. Consortia-3 (*K. oryzaedophytica* YMA7 + *P. kribbensis* KSB + *P. polymyxa* COW3) showed promising PGP traits such as phytohormone production and nutrient solubilization abilities. In the rice plant, in the soil inoculated with bacterial Consortia-3, the N/P/K content was N (17.33 g kg<sup>-1</sup>), P (4.83 g

kg<sup>-1</sup>), and K (37.33 g kg<sup>-1</sup>) as observed against the control plant N/P/K (7.0, 2.16, and 24.66 g kg<sup>-1</sup>, respectively). Three bacterial consortia developed in this study were first tested in greenhouse pot experiments and later applied to the rice field. Based on the agronomic parameters, significant increases were observed in all the plant growth and yield parameters except leaf number per plant when compared with uninoculated rice plants. Consortia-3 significantly improved grains per panicle (110 grain numbers per panicle), grain weight in grams (27.8 g), and root length in cm (9.5 cm) as compared with uninoculated control rice plants. These bacterial consortia can be potential candidates for bio-intensive nutrient management in organic farming systems. Further studies should be focused on the detailed synergistic effect for the production of N, P, K and functional characterization of bacterial consortia for practical applications in the field.

## DATA AVAILABILITY STATEMENT

The datasets presented in this study can be found in online repositories. The names of the repository/repositories and accession number(s) can be found in the article/Supplementary Material.

## AUTHOR CONTRIBUTIONS

MS performed investigation, conceptualization, experiments, visualization, and writing—original draft. NB and LS performed editing of the manuscript, acquired funding and resources, and provided supervision. SD performed statistical and data analysis, visualization, writing, and subediting of the manuscript. All authors contributed to the article and approved the submitted version.

## FUNDING

Himalayan Research Associate (H-RA) Fellowship was provided to MS by the National Mission on Himalayan Studies (NMHS), Ministry of Environment, Forest and Climate Change (MoEF & CC), Government of India.

## ACKNOWLEDGMENTS

The authors want to thank the National Mission on Himalayan Studies (NMHS) for providing the Himalayan Research Fellowship (GBPNI/NMHS-2017-18/HSF-07) and also want to thank Sikkim University for providing laboratory space for research.

## SUPPLEMENTARY MATERIAL

The Supplementary Material for this article can be found online at: <https://www.frontiersin.org/articles/10.3389/fmicb.2021.713660/full#supplementary-material>



## REFERENCES

- Ahmad, F., Ahmad, I., and Khan, M. S. (2008). Screening of free living rhizospheric bacteria for their multiple plant growth promoting activities. *Microbiol. Res.* 163, 173–181. doi: 10.1016/j.micres.2006.04.001
- Ames, B. N. (1966). Assay of inorganic phosphate, total phosphate and phosphatases. *Meth. Enzymol.* 8, 115–118.
- Arya, M., Joshi, G. K., and Gupta, A. K. (2015). Isolation and characterization of thermophilic bacterial strains from Soldhar (Tapovan) hot spring in Central Himalayan. *Ann. Microbiol.* 65, 1457–1464. doi: 10.1007/s13213-014-0984-y
- Bana, R. S., Sepat, S., Rana, K., Pooniya, V., and Choudhary, A. (2018). Moisture-stress management under limited and assured irrigation regimes in wheat (*Triticum aestivum*): effects on crop productivity, water use efficiency, grain quality, nutrient acquisition and soil fertility. *Indian J. Agric. Sci.* 88, 1606–1612.
- Banerjee, S., Kirkby, C. A., Schmutter, D., Bissett, A., Kirkegaard, J. A., and Richardson, A. E. (2016). Network analysis reveals functional redundancy and keystone taxa amongst bacterial and fungal communities during organic matter decomposition in an arable soil. *Soil Biol. Biochem.* 97, 188–198. doi: 10.1016/j.soilbio.2016.03.017
- Barberán, A., Bates, S. T., Casamayor, E. O., and Fierer, N. (2012). Using network analysis to explore co-occurrence patterns in soil microbial communities. *ISME J.* 6, 343–351. doi: 10.1038/ismej.2011.119
- Becker, M., Patz, S., Becker, Y., and Berger, Y. (2018). Comparative genomics reveal a flagellar system, a type VI secretion system and plant growth-promoting gene clusters unique to the endophytic bacterium *Kosakonia radicincitans*. *Front. Microbiol.* 9:1997. doi: 10.3389/fmicb.2018.01997
- Bhattacharyya, P. N., and Jha, D. K. (2012). Plant growth-promoting rhizobacteria (PGPR): emergence in agriculture. *World J. Microbiol. Biotechnol.* 28, 1327–1350. doi: 10.1007/s11274-011-0979-9
- Calleja-Cervantes, M. E., Fernandez-Gonzalez, A. J., Irigoyen, I., Fernandez-Lopez, M., Aparicio-Tejo, P. M., and Menendez, S. (2015). Thirteen years of continued application of composted organic wastes in a vineyard modify soil quality characteristics. *Soil Biol. Biochem.* 90, 241–254. doi: 10.1016/j.soilbio.2015.07.002
- Cappuccino, J. C., and Sherman, N. (1992). *Microbiology, Laboratory Manual*. New York, NY: Benjamin/Cumming Pub. Co.
- Castanheira, N., Dourado, A. C., Kruz, S., and Alves, P. I. L. (2015). Plant growth-promoting *Burkholderia* species isolated from annual ryegrass in Portuguese soils. *J. Appl. Microbiol.* 120, 724–739. doi: 10.1111/jam.13025
- Cederlund, H., Wessen, E., Enwall, K., Jones, C. M., Juhanson, J., Pell, M., et al. (2014). Soil carbon quality and nitrogen fertilization structure bacterial communities with predictable responses of major bacterial phyla. *Appl. Soil Ecol.* 84, 62–68. doi: 10.1016/j.apsoil.2014.06.003
- Chen, C., Zhang, J. N., Lu, M., Qin, C., Chen, Y. H., Yang, L., et al. (2016). Microbial communities of an arable soil treated for 8 years with organic and inorganic fertilizers. *Biol. Fertil. Soils* 52, 455–467. doi: 10.1007/s00374-016-1089-5
- Chrouqi, L., Ouahmane, L., Jadrane, I., Koussa, T., and Al feddy, M. N. (2017). Screening of soil rhizobacteria isolated from wheat plants grown in the Marrakech region (Morocco, North Africa) for plant growth promoting activities. *J. Mat Environ Sci* 8, 3382–3390.
- Davidson, E. A. (2009). The contribution of manure and fertilizer nitrogen to atmospheric nitrous oxide since 1860. *Nat. Geosci.* 2, 659–662. doi: 10.1038/ngeo608
- Devi, D., Gupta, S. D., Mishra, B. K., and Uma. (2020). Isolation and characterization of endophytic rhizospheric phosphate solubilizing bacteria of cumin and their evaluation in vitro. *Int. J. Chem. Sci.* 8, 1583–1593. doi: 10.22271/chemi.2020.v8.i5v.10530
- Devkota, S., Panthi, S., and Shrestha, J. (2019). Response of rice to different organic and inorganic nutrient sources at Parwanipur, Bara district of Nepal. *J. Agric. Nat. Res.* 2, 53–59. doi: 10.3126/janr.v2i1.26041
- Di Benedetto, N. A., Campaniello, D., Bevilacqua, A., and Pia-Cataldi, M. (2019). Isolation, screening, and characterization of plant-growth-promoting bacteria from Durum wheat rhizosphere to improve N and P nutrient use efficiency. *Microorganism* 7:541. doi: 10.3390/microorganisms7110541
- Ding, J. L., Jiang, X., Ma, M. C., Zhou, B. K., Guan, D. W., Zhao, B. S., et al. (2016). Effect of 35 years inorganic fertilizer and manure amendment on structure of bacterial and archaeal communities in black soil of northeast China. *Appl. Soil Ecol.* 105, 187–195. doi: 10.1016/j.apsoil.2016.04.010
- Duarah, I., Deka, M., Saikia, N., and Deka Boruah, H. P. (2011). Phosphate solubilizers enhance NPK fertilizer use efficiency in rice and legume cultivation. *3 Biotech.* 1, 227–238. doi: 10.1007/s13205-011-0028-2
- ENVIS (2007). *Environmental Information System, Forests, Environment and Wildlife Management Department*. Government of Sikkim: ENVIS.
- Erickson, K. (2010). The jukes-cantor model of molecular evolution. *Ecol. Primus.* 20, 438–445. doi: 10.1080/10511970903487705
- Estrada-de los Santos, P., Bustillos-Cristales, R., and Caballero-Mellado, J. (2001). *Burkholderia*, a genus rich in plant associated nitrogen fixers with wide environmental and geographic distribution. *Appl. Environ. Microbiol.* 67, 2790–2798. doi: 10.1128/AEM.67.6.2790-2798.2001
- Fasusi, O. A., Cruz, C., and Babalola, O. O. (2021). Agricultural sustainability: microbial biofertilizers in rhizosphere management. *Agriculture* 11:163. doi: 10.3390/agriculture-e11020163
- Francioli, D., Schulz, E., Lentendu, G., Wubet, T., Buscot, F., and Reitz, T. (2016). Mineral vs. organic amendments: microbial community structure, activity and abundance of agriculturally relevant microbes are driven by long-term fertilization strategies. *Front. Microbiol.* 7:1446. doi: 10.3389/fmicb.2016.01446
- Glick, B. (2012). Plant growth-promoting bacteria: mechanisms and applications. *Scientifica* 2012:963401. doi: 10.6064/2012/96340
- Hao, T., and Chen, S. (2017). Colonization of wheat, maize and cucumber by *Paenibacillus polymyxa* WLY78. *PLoS One* 12:e0169980. doi: 10.1371/journal.pone.0169980
- Hardoim, P. R., Nazir, R., Sessitsch, A., and Elhottová, D. (2013). The new species *Enterobacter oryziphilus* sp. nov. and *Enterobacter oryzendophyticus* sp. nov. are key inhabitants of the endosphere of rice. *BMC Microbiol.* 13:164. doi: 10.1186/1471-2180-13-164
- Inoue, K., Sugiyama, K., Kosako, Y., and Sakazaki, R. (2000). *Enterobacter cowanii* sp. nov., a new species of the family *Enterobacteriaceae*. *Curr. Microbiol.* 41, 417–420. doi: 10.1007/s002840010160
- Jain, A., Chatterjee, A., and Das, S. (2020). Synergistic consortium of beneficial microorganisms in rice rhizosphere promotes host defense to blight-causing *Xanthomonas oryzae* pv. *oryzae*. *Planta* 252:106. doi: 10.1007/s00425-020-03515-x
- Jimtha, J. C., Smitha, P. V., Anisha, C., and Deepthi, T. (2014). Isolation of endophytic bacteria from embryogenic suspension culture of banana and assessment of their plant growth promoting properties. *Plant Cell Tissue Organ Cult.* 118, 57–66. doi: 10.1007/s11240-014-0461-0
- Kämpfer, P., Ruppel, S., and Remus, R. (2005). *Enterobacter radicincitans* sp. nov., a plant growth promoting species of the family *Enterobacteriaceae*. *Syst. Appl. Microbiol.* 28, 213–221. doi: 10.1016/j.syapm.2004.12.007
- Kapoor, C., Avasthe, R., Chettri, P., Gopi, R., and Kalita, H. K. (2017). On-farm status and collection of rice (*Oryza sativa* L.) genetic resources of Sikkim Himalayas. *Indian J. Plant Genet. Resour.* 30, 48–54. doi: 10.5958/0976-1926.2017.00005.5
- Kumar, J., Pradhan, M., and Singhm, N. (2018). *Sustainable Organic Farming in Sikkim: An Inclusive Perspective, Advances in Smart Grid and Renewable Energy*. The Gateway: Springer Nature Singapore, Pvt Ltd, 367–378. doi: 10.1007/978-981-10-4286-7-36
- Kumar, S., Stecher, G., Li, M., and Nnyaz, C. (2018). MEGA X: molecular evolutionary genetics analysis across computing platforms. *Mol. Biol. Evol.* 35, 1547–1549. doi: 10.1093/molbev/msy096
- Lahlali, R., and Hijri, M. (2010). Screening, identification and evaluation of potential biocontrol fungal endophytes against *Rhizoctonia solani* AG3 on potato plants. *FEMS Microbiol. Lett.* 311, 152–159. doi: 10.1111/j.1574-6968.2010.02084.x
- Lentendu, G., Wubet, T., Chatzinotas, A., Wilhelm, C., Buscot, F., and Schlegel, M. (2014). Effects of long-term differential fertilization on eukaryotic microbial communities in an arable soil: a multiple barcoding approach. *Mol. Ecol.* 23, 3341–3355. doi: 10.1111/mec.12819
- Li, F., Chen, L., Zhang, J., Yin, J., and Huang, S. (2017). Bacterial community structure after long-term organic and inorganic fertilization reveals

- important associations between soil nutrients and specific taxa involved in nutrient transformations. *Front. Microbiol.* 8:187. doi: 10.3389/fmicb.2017.0187
- Li, Y., Li, S., Chen, M., and Peng, G. (2017). Complete genome sequence of *Kosakonia oryzae* type strain Ola 51<sup>T</sup>. *Stand Genomic Sci.* 12, 28–35. doi: 10.1186/s40793-017-0240-8
- Lin, L., Li, Z., Hu, C., and Zhang, X. (2012). Plant growth-promoting nitrogen-fixing *enterobacteria* are in association with sugarcane plants growing in Guangxi, China. *Microbes Environ.* 27, 391–399. doi: 10.1264/jsm.2012.011275
- Madhaiyan, M., Poonguzhali, S., Lee, J. S., and Saravanan, V. S. (2010). *Enterobacter arachidis* sp. nov., a plant-growth promoting diazotrophic bacterium isolated from rhizosphere soil of groundnut. *Int. J. Syst. Evol. Microbiol.* 60, 1559–1564. doi: 10.1099/ijs.0.013664-0
- Mahamuni, S. V. (2015). Antifungal properties of *Burkholderia cenocepacia* strain vimp 01 (JQ867371) against *Ceratomyces paradoxa* and *Alternaria alternata*. *Int. J. Bioassays* 4, 4290–4295.
- Najar, I. N., Sherpa, M. T., Das, S., and Das, S. (2018). Microbial ecology of two hot springs of Sikkim: predominate population and geochemistry. *Sci. Total Environ.* 637–638, 730–745. doi: 10.1016/j.scitotenv.2018.05.037
- Ngalimat, M. S., Mohd Hata, E., Zulperi, D., Ismail, S. I., Ismail, M. R., Mohd Zainudin, N., et al. (2021). Plant growth-promoting bacteria as an emerging tool to manage bacterial rice pathogens. *Microorganisms* 9:682. doi: 10.3390/microorganisms90-40682
- Ojuederie, O. B., Olanrewaju, O. S., and Babalola, O. O. (2019). Plant growth promoting rhizobacterial mitigation of drought stress in crop plants: implications for sustainable agriculture. *Agronomy* 9:712.
- Orozco-Mosqueda, M., Flores, A., Rojas-Sánchez, B., Urtis-Flores, C. A., Morales-Cedeño, L. R., Valencia-Marin, M. F., et al. (2021). Plant growth-promoting bacteria as bioinoculants: attributes and challenges for sustainable crop improvement. *Agronomy* 11:1167. doi: 10.3390/agronomy11061167
- Otieno, N., Lally, R. D., Kiwanuka, S., and Lloyd, A. (2015). Plant growth promotion induced by phosphate solubilizing endophytic *Pseudomonas* isolates. *Front. Microbiol.* 6:745. doi: 10.3389/fmicb.2015.00745
- Panneerselvam, P., Senapati, A., Kumar, U., and Sharma, L. (2019). Antagonistic and plant-growth promoting novel *Bacillus* species from long-term organic farming soils from Sikkim, India. *3 Biotech.* 9, 416–428. doi: 10.1007/s13205-019-1938-7
- Panneerselvam, P., Sharma, L., Nayak, A. K., and Senapati, A. (2020). *Development of Microbial Consortium for Plant Growth Promotion, Nutrient and Disease Management in Rice-Horticulture Based Cropping System in Sikkim*. Cuttack: Research Bulletin, NRRI, 8–34.
- Park, Y. G., Mun, B. G., Kang, S. M., and Hussain, A. (2017). *Bacillus aryabhattai* SRB02 tolerates oxidative and nitrosative stress and promotes the growth of soybean by modulating the production of phytohormones. *PLoS One* 12:e0173203. doi: 10.1371/journal.pone.0173203
- Paul, D., and Sinha, S. N. (2017). Isolation and characterization of phosphate solubilizing bacteria *Pseudomonas aeruginosa* KUPSB12 with antibacterial potential from river Ganga, India. *Ann. Agrar. Sci.* 15, 130–136. doi: 10.1016/j.aasci.2016.10.001
- Paungfoo-Lonhienne, C., Lonhienne, T. G. A., Yeoh, Y. K., and Webb, R. I. (2014). A new species of *Burkholderia* isolated from sugarcane roots promotes plant growth. *Microb. Biotechnol.* 7, 142–154. doi: 10.1111/1751-7915.12105
- Peng, G., Zhang, W., Luo, H., and Xie, H. (2009). *Enterobacter oryzae* sp. nov., a nitrogen-fixing bacterium isolated from the wild rice species *Oryza latifolia*. *Int. J. Syst. Evol. Microbiol.* 59, 1650–1655. doi: 10.1099/ijs.0.005967-0
- Qessaoui, R., Bouharroud, R., Furze, J., and Aalaoui, M. E. (2019). Applications of new rhizobacteria *Pseudomonas* isolates in agroecology via fundamental processes complementing plant growth. *Sci. Rep.* 9:12832. doi: 10.1038/s41598-019-49216-8
- Raja, P., Uma, H., Gopal, H., and Govindraj, K. (2006). Impact of bio-inoculants consortium on rice root exudates biological nitrogen fixation and plant growth. *J. Biol. Sci.* 6, 815–823. doi: 10.3923/jbs.2006.815.823
- Rajawat, M. V. S., Ansari, W. A., Singh, D., and Singh, R. (2019). *Potassium Solubilizing Bacteria (KSB). Microbial Interventions in Agriculture and Environment*. The Gateway: Springer Nature Singapore Pvt Ltd, 189–209.
- Raju, C. S., Aslam, A., Thangadurai, D., and Sangeetha, J. (2020). Indole acetic acid (IAA) producing endophytic bacteria on direct somatic embryogenesis and plant regeneration of *Exacum travancoricum* Bedd. *Vegetos* 33, 690–702. doi: 10.1007/s42535-020-00159-w
- Roy Choudhury, D., Singh, N., Singh, A. K., Kumar, S., Srinivasan, K., Tyagi, R. K., et al. (2014). Analysis of genetic diversity and population structure of rice germplasm from north-eastern region of India and development of a core germplasm set. *PLoS One* 9:e113094. doi: 10.1371/journal.pone.0113094
- Saitou, N., and Nei, M. (1987). The neighbor-joining method: a new method for reconstructing phylogenetic trees. *Mol. Biol. Evol.* 4, 406–425. doi: 10.1093/oxfordjournals.molbev.a040454
- Saju, K. A., Deka, T. N., Gupta, U., Biswas, A. K., Sudharshan, M. R., Vijayan, A. K., et al. (2013). Identity of *Colletotrichum* infections in large cardamom (*Amomum subulatum* Roxb.). *J. Spices Aromat. Crops* 22, 101–103.
- Schwyn, B., and Neillands, J. B. (1987). Universal chemical assay for the detection and determination of siderophores. *Anal. Biochem.* 160, 47–56. doi: 10.1016/0003-2697(87)90612-9
- Seufert, V., Ramankutty, N., and Foley, J. A. (2012). Comparing the yields of organic and conventional agriculture. *Nature* 485, 229–232. doi: 10.1038/nature11069
- Sharma, S. K., Bhavdishi, N. J., Ramesh, A., and Joshi, O. P. (2011). Selection of plant growth-promoting *Pseudomonas* spp. that enhanced productivity of soybean-wheat cropping system in Central India. *J. Microbiol. Biotechnol.* 21, 1127–1142. doi: 10.4014/jmb.1012.12018
- Sherpa, M. T., Mathur, A., and Das, S. (2015). Medicinal plants and traditional medicine system of Sikkim: a review. *World J. Pharm. Pharm. Sci.* 2, 161–184.
- Sherpa, M. T., Najar, I. N., Das, S., and Thakur, N. (2018). Bacterial diversity in an alpine debris-free and debris-cover accumulation zone glacier ice, North Sikkim, India. *Indian J. Microbiol.* 58, 470–478. doi: 10.1007/s12088-018-0747-8
- Sultana, S., Paul, S. C., Parveen, S., Alam, S., Rahman, N., Jannat, B., et al. (2020). Isolation and identification of salt-tolerant plant-growth-promoting rhizobacteria and their application for rice cultivation under salt stress. *Can. J. Microbiol.* 66, 144–160. doi: 10.1139/cjm-2019-0323
- Sun, F., Ou, Q., Wang, N., Guo, Z., Ou, Y., Li, N., et al. (2020). Isolation and identification of potassium-solubilizing bacteria from *Mikania micrantha* rhizospheric soil and their effect on *M. micrantha* plants. *Glob. Ecol. Conserv.* 23:e01141. doi: 10.1016/j.gecco.2020.e01141
- Sutton, B. C. (1992). "The genus *Glomerella* and its anamorph *Colletotrichum*," in *Colletotrichum- Biology, Pathology, and Control*, eds J. A. Bailey and M. J. Jeger (Wallingford: CAB International), 1–26.
- Taurian, T., Anzuay, M. S., Angelini, J. G., and Tonelli, M. L. (2010). Phosphate-solubilizing peanut associated bacteria: screening for plant growth-promoting activities. *Plant Soil* 329, 421–431. doi: 10.1007/s11104-009-0168-x
- Venieraki, A., Dimou, M., Vezyri, E., and Kefalogianni, I. (2020). Characterization of nitrogen-fixing bacteria isolated from field-grown barley, oat, and wheat. *J. Microbiol.* 49, 525–534. doi: 10.1007/s12275-011-0457-y
- Vimal, S. R., Singh, J., Arora, N., and Singh, S. (2017). Soil-plant-microbe interactions in stressed agriculture management: a review. *Pedosphere* 27, 177–192. doi: 10.1016/S1002-0160(17)60309-6
- Wei, W. L., Yan, Y., Cao, J., Christie, P., Zhang, F. S., and Fan, M. S. (2016). Effects of combined application of organic amendments and fertilizers on crop yield and soil organic matter: an integrated analysis of long-term experiments. *Agric. Ecosyst. Environ.* 225, 86–92. doi: 10.1016/j.agee.2016.04.004
- Wightwick, A., Walters, R., Allinson, G., Reichman, S., and Menzies, S. R. A. N. (2010). *Environmental Risks of Fungicides Used in Horticultural Production Systems*. Fungicides. Rijeka: InTech, 273–304.

- Zhang, C., and Kong, F. (2014). Isolation and identification of potassium-solubilizing bacteria from tobacco rhizospheric soil and their effect on tobacco plants. *Appl. Soil Ecol.* 82, 18–25. doi: 10.1016/j.apsoil.2014.05.002
- Zhang, S., Lu, X., Zhang, Y., and Nie, G. (2019). Estimation of soil organic matter, total nitrogen and total carbon in sustainable coastal wetlands. *Sustainability* 11, 677–695. doi: 10.3390/su11030667
- Zhou, J., Guan, D. W., Zhou, B. K., Zhao, B. S., Ma, M. C., Qin, J., et al. (2015). Influence of 34-years of fertilization on bacterial communities in an intensively cultivated black soil in northeast China. *Soil Biol. Biochem.* 90, 42–51. doi: 10.1016/j.soilbio.2015.07.005
- Zhu, B., Zhou, Q., Lin, L., and Hu, C. (2013). *Enterobacter sacchari* sp. nov., a nitrogen-fixing bacterium associated with sugar cane (*Saccharum officinarum* L.). *Int. J. Syst. Evol. Microbiol.* 63, 2577–2582. doi: 10.1099/ijs.0.045500-0

**Conflict of Interest:** The authors declare that the research was conducted in the absence of any commercial or financial relationships that could be construed as a potential conflict of interest.

**Publisher's Note:** All claims expressed in this article are solely those of the authors and do not necessarily represent those of their affiliated organizations, or those of the publisher, the editors and the reviewers. Any product that may be evaluated in this article, or claim that may be made by its manufacturer, is not guaranteed or endorsed by the publisher.

Copyright © 2021 Sherpa, Sharma, Bag and Das. This is an open-access article distributed under the terms of the Creative Commons Attribution License (CC BY). The use, distribution or reproduction in other forums is permitted, provided the original author(s) and the copyright owner(s) are credited and that the original publication in this journal is cited, in accordance with accepted academic practice. No use, distribution or reproduction is permitted which does not comply with these terms.



# Biocontrol Ability and Mechanism of a Broad-Spectrum Antifungal Strain *Bacillus safensis* sp. QN1NO-4 Against Strawberry Anthracnose Caused by *Colletotrichum fragariae*

## OPEN ACCESS

### Edited by:

Florence Fontaine,  
Université de Reims  
Champagne-Ardenne, France

### Reviewed by:

Dewa Ngurah Suprpta,  
Udayana University, Indonesia  
Nakkeeran S.,  
Tamil Nadu Agricultural University,  
India

### \*Correspondence:

Wei Wang  
wangweisys@ahau.edu.cn  
Jianghui Xie  
xiejianghui@itbb.org.cn  
Lu Zhang  
luzhangtest@163.com

† These authors have contributed  
equally to this work and share first  
authorship

### Specialty section:

This article was submitted to  
Microbe and Virus Interactions with  
Plants,  
a section of the journal  
Frontiers in Microbiology

Received: 03 July 2021

Accepted: 18 August 2021

Published: 17 September 2021

### Citation:

Li X, Zhang M, Qi D, Zhou D,  
Qi C, Li C, Liu S, Xiang D, Zhang L,  
Xie J and Wang W (2021) Biocontrol  
Ability and Mechanism of a  
Broad-Spectrum Antifungal Strain  
*Bacillus safensis* sp. QN1NO-4  
Against Strawberry Anthracnose  
Caused by *Colletotrichum fragariae*.  
Front. Microbiol. 12:735732.  
doi: 10.3389/fmicb.2021.735732

Xiaojuan Li<sup>1,2,3†</sup>, Miaoyi Zhang<sup>1†</sup>, Dengfeng Qi<sup>1</sup>, Dengbo Zhou<sup>1</sup>, Chunlin Qi<sup>3</sup>, Chunyu Li<sup>4</sup>,  
Siwen Liu<sup>4</sup>, Dandan Xiang<sup>4</sup>, Lu Zhang<sup>2\*</sup>, Jianghui Xie<sup>1\*</sup> and Wei Wang<sup>1\*</sup>

<sup>1</sup> Key Laboratory of Biology and Genetic Resources of Tropical Crops, Ministry of Agriculture, Institute of Tropical Bioscience and Biotechnology, Chinese Academy of Tropical Agricultural Sciences, Haikou, China, <sup>2</sup> Ministry of Education Key Laboratory for Ecology of Tropical Islands, College of Life Science, Hainan Normal University, Haikou, China, <sup>3</sup> College of Ecology and Environment, Hainan University, Haikou, China, <sup>4</sup> Key Laboratory of South Subtropical Fruit Biology and Genetic Resource Utilization, Ministry of Agriculture, Key Laboratory of Tropical and Subtropical Fruit Tree Research of Guangdong Province, Institution of Fruit Tree Research, Guangdong Academy of Agricultural Sciences, Guangzhou, China

Strawberry is a very popular fruit with a special taste, color, and nutritional value. Anthracnose caused by *Colletotrichum fragariae* severely limits fruit shelf life during post-harvest storage. Use of traditional chemical fungicides leads to serious environment pollution and threatens food safety. Biocontrol is considered as a promising strategy to manage the post-harvest fruit diseases. Here, strain QN1NO-4 isolated from noni (*Morinda citrifolia* L.) fruit exhibited a high antifungal activity against *C. fragariae*. Based on its physicochemical profiles and phylogenetic tree of the 16S *rRNA* sequence, strain QN1NO-4 belonged to the genus *Bacillus*. The average nucleotide identity (ANI) calculated by comparing two standard strain genomes was below 95–96%, suggesting that the strain might be a novel species of the genus *Bacillus* and named as *Bacillus safensis* sp. QN1NO-4. Its extract effectively reduced the incidence of strawberry anthracnose of harvested fruit. Fruit weight and TSS contents were also maintained significantly. The antifungal mechanism assays indicated that the extract of the test antagonist inhibited mycelial growth and spore germination of *C. fragariae* *in vitro*. Cells of strain QN1NO-4 demonstrated the cytoplasmic heterogeneity, disappeared organelles, and ruptured ultrastructure. Notably, the strain extract also had a broad-spectrum antifungal activity. Compared with the whole genome of strain QN1NO-4, several functional gene clusters involved in the biosynthesis of active secondary metabolites were observed. Fifteen compounds were identified by gas chromatography–mass spectrometry (GC-MS). Hence, the fruit endophyte *B. safensis* sp. QN1NO-4 is a potential bio-agent identified for the management of post-harvest disease of strawberry fruit.

**Keywords:** *Bacillus safensis*, *Colletotrichum fragariae*, biological control, antifungal properties, strawberry fruit, whole genome sequencing



## INTRODUCTION

Strawberry (*Fragaria × ananassa* Duch.) is one of the most popular fruits with more than 6.1 million tons of annual production in the world (Han et al., 2016; Zhimo et al., 2021). Strawberry fruit is also highly perishable due to mechanical injury and pathogen infection, which limits its shelf life during storage (Rico et al., 2019). Strawberry anthracnose is one of the most serious fungal diseases. It is caused by different *Colletotrichum* fungal species including *Colletotrichum fragariae*, *C. acutatum*, and *C. gloeosporioides* (Denoyes-Rothan et al., 2003; Han et al., 2016). Among the causal agents, *C. fragariae* is an important fungus which causes the disease named anthracnose crown rot (Miller-Butler et al., 2018). The fungi can infect the whole strawberry plant containing fruit, and it has become more destructive in the past decade (Chen et al., 2019; Chung et al., 2020). Currently, the control of strawberry anthracnose is done primarily through chemical fungicides to reduce post-harvest losses (Dukare et al., 2019). However, excessive use of fungicides causes environment pollution and pathogenic resistance (Li et al., 2021; Wang et al., 2021). In some developed countries, use of fungicides has become increasingly limited and even banned (Wisniewski et al., 2016; Wang et al., 2018). Therefore, it is necessary to develop a safer and eco-friendly strategy to manage post-harvest diseases of fruit.

Application of biocontrol agents was considered as an alternative and promising strategy to control plant pathogens (Feliziani et al., 2016; Ye et al., 2021). Biocontrol contributed to minimize the use of chemical pesticides and reduce environmental pollution. In the past few decades, some microorganisms such as yeasts, *Pseudomonas fluorescens*, *Streptomyces* spp., and *Bacillus* species were accepted as important biocontrol agents (Rong et al., 2020; Einloft et al., 2021). They had potential as an alternative to synthetic fungicides. The well-studied *Pichia membranefaciens* and *Pichia guilliermondii* were effective in controlling rhizopus rot of peaches and anthracnose of loquat fruit (Zhao et al., 2019; Zhang et al., 2020). Recent studies demonstrated that *Pseudomonas synxantha* had a biocontrol efficacy against *Monilinia fructicola* and *Monilinia fructigena* in stone fruit (Aiello et al., 2019). *P. fluorescens* can suppress post-harvest gray mold in apples (Zhang et al., 2011; Wallace et al., 2018).

Especially, the *Bacillus* genera were evaluated as outstanding biocontrol agents against fungal pathogens, such as *Bacillus halotolerans* against *Botrytis cinerea* in strawberry fruit (Wang et al., 2021; Ye et al., 2021), *Bacillus* sp. w176 against post-harvest green mold in citrus (Tian et al., 2020), *Bacillus atrophaeus* against anthracnose in soursop and avocado (Guardado-Valdivia et al., 2018), and *Bacillus amyloliquefaciens* against other phytopathogens of fruits (Calvo et al., 2017; Gotor-Vila et al., 2017; Wang et al., 2020; Ye et al., 2021). Several *Bacillus* spp. had been applied as biofertilizers or biopesticides in different crops (Li et al., 2019). They inhibited the pathogenic growth and improved the plant resistance by competition for space or nutrients with pathogens and production of bioactive substances and cell wall-degrading compounds (Ye et al., 2021). Although various *Bacillus* sp. strains are reported in biocontrol of post-harvest fruit,

little work is conducted to identify a broad-spectrum antifungal *Bacillus* strain with an increased efficiency.

In our study, a strain marked with QN1NO-4 with a wide-spectrum antifungal ability is newly isolated from noni fruit. Based on the physicochemical characteristics as well as average nucleotide identity (ANI) assay, the strain is identified as a species of the genus *Bacillus*, called after *Bacillus safensis* sp. QN1NO-4. The isolated extracts successfully inhibit the infection of *C. fragariae* on strawberry fruit during post-harvest and could effectively keep the weight loss and TSS of fruit. The antifungal mechanism is investigated by assaying its effects on spore germination and morphological profile by scanning electron microscopy (SEM) as well as hyphal ultrastructure of *C. fragariae* by transmission electron microscopy (TEM). The complete genome of strain QN1NO-4 reveals a number of key gene clusters of active secondary metabolites. Antimicrobial compounds of strain QN1NO-4 extracts are further identified by gas chromatography-mass spectrometry (GC-MS). These results indicate that the fruit endophyte *B. safensis* sp. QN1NO-4 is a promising biocontrol agent for controlling post-harvest diseases of strawberry fruit.

## MATERIALS AND METHODS

### Fruit Materials

Strawberry (*Fragaria × ananassa* Duch var. Zhang Ji) fruit with similar size (approximately 5-cm diameter), color, and shape was selected from a supermarket. No visible injury and pathogen infection were detected on the fruit surface. After being surface-sterilized with 75% (v/v) of ethanol for 2 min, these fruit samples were rinsed with sterile water for three times and air-dried for 2 h at 25°C.

Noni (*Morinda citrifolia* L.) fruit was collected from a planting farm in Chengmai city (19°58'35"N, 109°55'35"E) of Hainan province, China. Fruit samples were surface-sterilized with 75% (v/v) of ethanol for 5 min, disinfected using 2% of sodium hypochlorite for 20 min, and washed using sterile water for five times.

### Bacterial Isolation

Ten grams of noni fruit was ground in a sterile mortar until paste. One milliliter of homogenate was mixed with 4 ml of Luria-Bertani (LB) medium into a 50-ml conical flask. The mixture was cultured with shaking at 180 rpm for 1 h at room temperature. The suspension was diluted from  $10^{-1}$  to  $10^{-3}$  fold with sterile distilled water. Two hundred microliters of dilution was spread on the LB solid medium and incubated at 28°C for 2 days. A single colony was obtained by repeatedly streaking on LB plates and was kept in 20% (v/v) glycerol at  $-80^{\circ}\text{C}$ .

### Screening of Biocontrol Bacteria Against *C. fragariae*

Fungal pathogen *C. fragariae* (ATCC 58718) was kindly provided by the Institute of Environment and Plant Protection, China Academy of Tropical Agricultural Sciences, Haikou, China. The

antifungal ability of each isolated bacterium was tested against *C. fragariae* using our reported method (Li et al., 2021). Briefly, fungal pathogen was first cultured on a potato dextrose agar (PDA) plate for 7 days. A 5-mm-diameter pathogenic disk was prepared and placed in the middle of the plate. Each isolated bacterium was spotted on the four symmetrical points of the pathogen. The fungal disk alone was used as a control. Five Petri dishes were used for each replicate with a diameter of 90 mm. After culture at 28°C for 7 days, antifungal activity of the isolated bacterium was assessed by determining the radial mycelial growth of fungal pathogen. To further detect the antifungal activity of the isolated bacterium supernatant, the isolate was inoculated in 50 ml of LB liquid medium in a 250-ml conical flask. After being cultured at 150 rpm and 28°C for 3 days, the supernatant was filtered using the Whatman no. 1 qualitative filter paper and sterilized through a 0.22-μm sterile filter (Millipore, Bedford, MA, United States). Twenty microliters of supernatant was spotted at four symmetrical points of the tested pathogens, respectively. An equal amount of LB was used as a control. The antagonistic experiment was kept at 28°C for 7 days. The antifungal activity of the isolated bacterium supernatant was assessed by determining the radial mycelial growth of the fungal pathogen. All experiments were carried out in triplicate.

### Morphological, Physiological, and Biochemical Characteristics of the Selected Isolate

Morphological profiles of the selected isolate were observed after growth at 37°C for 3–4 days. Physiological and biochemical indexes were tested including resistance to pH, temperature and NaCl, enzymatic characteristics, and utilization of carbon and nitrogen sources (Wei et al., 2020). In addition, a disk diffusion method was applied to test the sensitivity of the selected isolate to different antibiotics (Kumar et al., 2014).

### Antifungal Activity Assays of Extract From the Selected Isolate

Extract was prepared according to the previous description with a minor modification (Qi et al., 2019). Briefly, the selected isolate was inoculated in a 5-l Erlenmeyer flask containing 1 l of LB liquid medium. After culture in a rotary shaker (180 rpm) for 3 days at 28°C, an equal volume of ethyl acetate was added to the supernatant. The mixture was subjected to ultrasound for 1 h and then injected into a separating funnel. The organic solvent in the collected extract was evaporated using a rotary vacuum evaporator (N-1300, EYELA, Ailang Instrument Co., Ltd., Shanghai, China). The dried extract was then dissolved in 100% of methanol, and 10 g l<sup>-1</sup> of stock solution was prepared. To detect the antifungal activity assays of the extract, a 5-mm-diameter pathogenic disk was placed in the middle of the PDA plate containing 50 mg l<sup>-1</sup> of extract. After culture at 28°C for 7 days, antifungal activity was assessed by determining the radial mycelial growth of fungal pathogen. All experiments were carried out in triplicate.

### Inhibitory Efficiency of Extract on Mycelial Growth of *C. fragariae*

The stock solution (10 g l<sup>-1</sup>) was diluted into 5, 2.5, 1.25, 0.625, 0.313, 0.156, and 0.078 g l<sup>-1</sup> using a double continuous dilution method (Wei et al., 2020). When 50 ml of the sterilized PDA liquid medium was precooled to 40–50°C, 1 ml of each extract diluent was added to generate different treatment concentrations (1.563, 3.125, 6.25, 12.5, 25, 50, 100, and 200 mg l<sup>-1</sup>, respectively). The inhibition ability of each extract concentration on the mycelial growth of *C. fragariae* was analyzed according to our previous method (Li X.J. et al., 2020). Antifungal activity was measured according to the growth diameter of *C. fragariae* at 28°C for 7 days. The morphological profile of pathogenic mycelia treated with 200 mg l<sup>-1</sup> of extract was observed using an optical microscope (Nikon, E200MV, Japan). The half-maximal effective concentration (*EC*<sub>50</sub>) of the extract against *C. fragariae* was calculated in the light of a toxicity regression equation established by a least square method (Vanewijk and Hoekstra, 1993).

### Inhibitory Efficiency of Extract on Controlling Decay of Strawberry Fruit

Different fold *EC*<sub>50</sub> concentrations (2 × *EC*<sub>50</sub>, 4 × *EC*<sub>50</sub>, and 8 × *EC*<sub>50</sub>) were first prepared. Based on the extract quantity of the 1 × *EC*<sub>50</sub> value, the proper volume of the stock solution (10 mg ml<sup>-1</sup>) was diluted into 8 × *EC*<sub>50</sub> with sterile distilled water. Then, the double continuous dilution method was used to obtain 4 × *EC*<sub>50</sub>, 2 × *EC*<sub>50</sub>, and 1 × *EC*<sub>50</sub>, respectively. The antagonistic ability of the extract was tested for controlling post-harvest anthracnose decay of strawberry fruit according to our previous description (Li et al., 2021). A 2-mm-wide and 1-mm-deep wound was manufactured on the surface of the selected fruit samples using a sterilized needle. Ten microliters of different concentrations of extracts (1 × *EC*<sub>50</sub>, 2 × *EC*<sub>50</sub>, 4 × *EC*<sub>50</sub>, and 8 × *EC*<sub>50</sub>, respectively) was inoculated into fruit wound. An equal volume of sterile water was used as a control. After the treated fruits were air-dried, 10 μl of conidial suspension (1.0 × 10<sup>6</sup> CFU ml<sup>-1</sup>) was added to the wounded site. All fruit samples were kept in an artificial climate cabinet (Ever Scientific Instrument Ltd., Shanghai, China) at 28°C and 85% relative humidity under 12 h light/12 h darkness for 7 days. Twenty-four fruit samples of strawberry were selected for each treatment in three replicates. The disease incidence (DI) was calculated according to the following formula:

$$DI(\%) = (D1/D2) \times 100 \quad (1)$$

where D1 and D2 represent the number of decayed fruits and total fruits, respectively.

### Preservative Effects of Extract on Quality Parameters of Strawberry Fruit

The weight loss and total soluble solids (TSS) of strawberry fruit were determined after treatment with *C. fragariae* and different concentration extracts of the isolated strain for 7 days (Li et al., 2021). Weight loss was expressed as a percentage of fruit weight before and after storage. TSS content was measured using the

refractive index of fruit juice with a MASTER Refractometer (PAL-1, Atago, Japan).

## Antifungal Activity of Secondary Metabolites Against *C. fragariae*

The fungal spores were collected from the PDA medium by rubbing and washing the surface of each petri dish with a sterile L-shaped spreader. The mycelia were removed using a sterile muslin cloth. The spore concentration was adjusted to  $1.0 \times 10^6$  CFU ml<sup>-1</sup> with a hemocytometer (Neubauer, Superior Ltd., Marienfeld, Germany). An equal volume of pathogenic spore suspension ( $1.0 \times 10^6$  CFU ml<sup>-1</sup>) and each concentration extract ( $1 \times EC_{50}$ ,  $2 \times EC_{50}$ ,  $4 \times EC_{50}$ , or  $8 \times EC_{50}$ , respectively) was mixed at 28°C and 85% relative humidity for 12 h. More than 200 spores of *C. fragariae* were used to detect germination using an optical microscope (Nikon, E200MV, Japan) (Pei et al., 2020). Based on the spore germination,  $4 \times EC_{50}$  of extract concentration was selected for the following experiment.

## Morphological Profile of *C. fragariae* Spores Treated With Extract

To detect the effect of extract on the spore morphology of *C. fragariae*, equal volumes of spores ( $1.0 \times 10^6$  CFU ml<sup>-1</sup>) and  $4 \times EC_{50}$  of extracts were completely mixed in a 10-ml sterile centrifugal tube. The mixture was incubated at 28°C for 6 h. After centrifugation at 10,000 rpm for 5 min at 4°C, spores were collected and fixed with 2.5% (v/v) of glutaraldehyde overnight. Then, these fixed spores were washed for three times with a phosphate-buffered saline (PBS, 0.1 mol l<sup>-1</sup>, pH 7.2) for 15 min. The sample was dehydrated using a gradient ethanol solution (30, 50, 70, 80, 90, 95, and 100%, 15 min for each time). The dried samples were coated with gold powder using the ion sputtering instrument (Qi et al., 2019). Platinum was used as the plating material. Samples coated with a film of gold–palladium alloy under vacuum were detected by a scanning electron microscope (SEM, Sigma 500/VP, Zeiss, Germany).

## Ultrastructural Profile of *C. fragariae* Cells Treated With Extract

*C. fragariae* was cultured in the sterilized PDA liquid medium at 28°C and 200 rpm for 5 days. Cells of fungal pathogen were collected and fixed as described in Section “Morphological Profile of *C. fragariae* Spores Treated With Extract.” The pathogenic samples were embedded in Epon 812 resin. An 80-nm-thick section was manufactured by an ultramicrotome (EM UC6, Leica, Germany). The sections were stained with 3% (v/v) of lead citrate for 10 min and 3% (v/v) of saturated uranyl acetate for 30 min. The cell ultrastructure of *C. fragariae* was observed by transmission electron microscopy (TEM, HT7700, Hitachi, Japan).

## Hemolytic Assay of Human Red Blood Cells Treated With Extract

To test the safety of the extract for human, a hemolysis experiment was performed (Li et al., 2021). The human red

blood cells were collected by centrifugation at 1,000 g for 5 min and then were washed with 0.85% (w/v) of normal saline for three times. Two percent of red blood cells was prepared as in our previous description (Li et al., 2021). Four hundred fifty microliters of blood cell solution was mixed with 50 µl of extract ( $1 \times EC_{50}$ ,  $2 \times EC_{50}$ ,  $4 \times EC_{50}$ , or  $8 \times EC_{50}$ ) at 37°C for 1 h. The red blood cells treated with 0.85% (w/v) of normal saline and 0.1% (v/v) of Triton X-100 were used as negative and positive controls, respectively. The release of hemoglobin was monitored by absorbance at 540 nm. Hemolytic activity was expressed as the percentage of total hemoglobin released by extract treatment in comparison with that released by Triton X-100 treatment (Wang et al., 2018).

## Assay of a Broad-Spectrum Antifungal Activity of the Selected Isolate Extract

In order to test whether the selected isolate extract had a broad-spectrum antifungal activity, we selected 10 phytopathogenic fungi, including *C. fragariae* (ATCC 58718), *Fusarium graminearum* (ATCC MYA-4620), *C. acutatum* (ATCC 56815), *F. oxysporum* f. sp. *cucumerinum* (ATCC 204378), *Curvularia lunata* (ATCC 42011), *Pyricularia oryzae* (ATCC 52352), *C. gloeosporioides* Penz. (ATCC 58222), *Alternaria* sp. (ATCC 20492), *C. capsici* (ATCC 48574), and *C. gloeosporioides* (ATCC 16330). These phytopathogenic fungi were kept in our lab. The antifungal activity of the extract was detected against each phytopathogenic fungus according to our previous method (Wei et al., 2020).

## Genome Sequencing and Metabolite Prediction of the Selected Isolate

The genomic DNA of the selected isolate was extracted using the BioTeke Bacterial Genomic DNA Rapid Extraction Kit (DP1301, Beijing Biotech Co., Ltd., China) and quantified using the TBS-380 fluorometer (Turner BioSystems Inc., Sunnyvale, CA, United States). Sequencing was performed on the platform of the Illumina high-throughput sequencing platform (HiSeq). The complete genome was assembled by Majorbio Bio-Pharm Technology Co., Ltd., Shanghai, China. Bioinformatics analysis was carried out using the I-Sanger Cloud Platform 2.0. The ANI was analyzed using the online OrthoANI (Yoon et al., 2017). The G + C content of the strain genome was calculated based on the complete genome sequence. The protein-coding genes were predicted by the Glimmer v3.02 software (Delcher et al., 2007). The unigenes were annotated using the public databases of Gene Ontology (GO<sup>1</sup>), Clusters of Orthologous Groups of proteins (COG<sup>2</sup>), and Kyoto Encyclopedia of Genes and Genomes (KEGG<sup>3</sup>) (Zhang et al., 2020). Gene cluster analysis of secondary metabolite synthesis was carried out by the online antiSMASH v4.2.0 software (Huang et al., 2019).

<sup>1</sup><http://www.geneontology.org/>

<sup>2</sup><http://www.ncbi.nlm.nih.gov/COG>

<sup>3</sup><http://www.genome.jp/kegg/>



## Identification of Chemical Compounds From Extracts

The chemical compounds of the extract were identified by gas chromatography–mass spectrometry (GC-MS) (Ogundajo et al., 2017). The analysis was performed on gas chromatography (5973 Inert XL MSD, Agilent, United States) plus with DB-FFAP (30 m × 0.25 mm × 0.25 μm) and a triple quadrupole mass spectrometer. Helium was used as a carrier gas at 1 ml min<sup>-1</sup>. The temperature program was kept at 70°C for 2 min and increased to 100°C at 5°C min<sup>-1</sup> for 5 min, 250°C at 10°C min<sup>-1</sup> for 35 min, and 280°C at 4°C min<sup>-1</sup> for 5 min. The mass spectrometer was operated in an optimized condition as in our previous description (Li et al., 2021); these data of mass spectra were determined by alignment with the National Institute of the Standards and Technology (NIST) spectral library version 2.0.

## Data Analysis

A one-way analysis of variance (ANOVA) was applied to analyze all data using the SPSS software version 22 (SPSS Inc., Chicago, IL, United States). Data from three independent experiments were expressed as the mean ± standard deviation. A significant difference was evaluated in the light of the LSD multiple-range test at the level of  $p < 0.05$ .

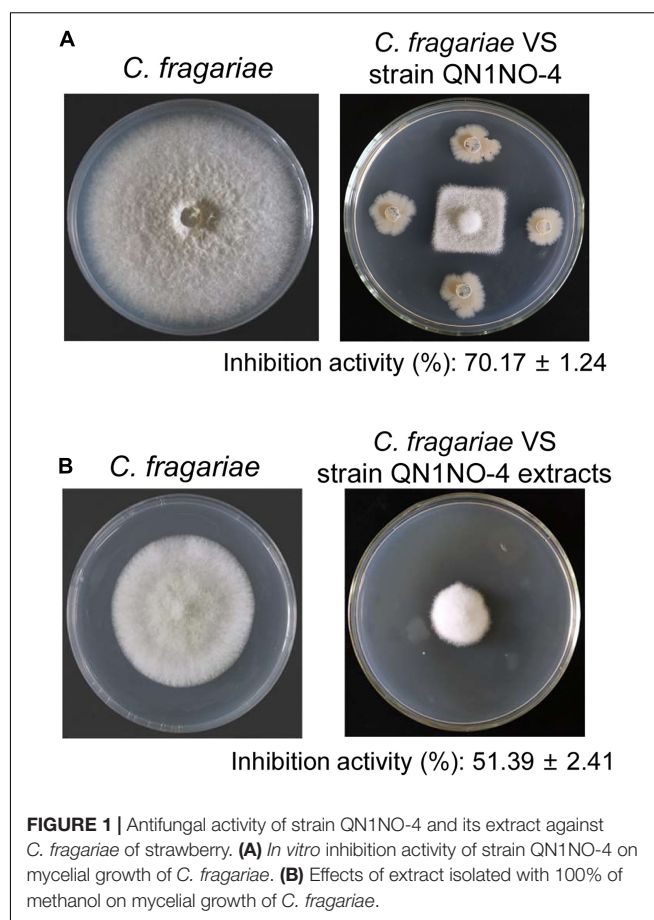
## RESULTS

### Isolation and Screening of Biocontrol Bacteria

A total of 35 endophytic bacteria were isolated from noni fruit. Twenty-nine bacteria had an antifungal activity against *C. fragariae* *in vitro* in **Supplementary Table 1**. The fermentation broth of 10 endophytic bacteria exhibited antagonistic activity against *C. fragariae* (**Supplementary Table 2**). Especially, a strain labeled with QN1NO-4 had the strongest antagonistic activity. Compared with 85.50 mm ± 1.43 of growth diameter of *C. fragariae* in the control plate, the growth diameter was 25.50 mm ± 0.79 in the presence of strain QN1NO-4 (**Figure 1A**). The inhibition activity of mycelial growth was up to 70%. To further analyze antifungal components of strain QN1NO-4, extracts were isolated using 100% of methanol. The inhibition activity was approximately 51% in the PDA solid medium with 50 mg l<sup>-1</sup> of the final extract concentration (**Figure 1B**). Hence, strain QN1NO-4 was selected for the following study.

### Identification and Genome Sequencing of Strain QN1NO-4

Based on the analysis of the morphological properties, strain QN1NO-4 was a round and primrose yellow colony on the LB plate. The colonial margin became much rougher and more irregular along with aging. The physiological and biochemical characteristics showed that strain QN1NO-4 could produce urease, catalase, and nitrate reductase but could not generate hydrogen sulfide. Positive results were detected under analysis of gelatin liquefaction, starch hydrolysis, or V-P test. The



**FIGURE 1** | Antifungal activity of strain QN1NO-4 and its extract against *C. fragariae* of strawberry. **(A)** *In vitro* inhibition activity of strain QN1NO-4 on mycelial growth of *C. fragariae*. **(B)** Effects of extract isolated with 100% of methanol on mycelial growth of *C. fragariae*.

strain could grow on the medium with up to 13% of NaCl, temperature from 30 to 65°C, and pH from 5 to 10. It could utilize all carbon sources and nitrogen sources tested except for L-glutamate and L-tyrosine. In addition, strain QN1NO-4 was sensitive to 18 antibiotics tested except for penicillin and piperacillin (**Table 1**; **Figure 2A** and **Supplementary Tables 3, 4**).

The complete genome of strain QN1NO-4 was sequenced and submitted to the GenBank with accession number of SRR15234655. It contained 3,923,715 bp with 46% of G + C content. The genome consisted of three rRNA genes, 52 tRNA genes, and 3,917 protein-coding genes (**Figure 2B** and **Table 2**). Based on 16S rRNA gene sequences, a phylogenetic tree was constructed using the neighbor-joining method (**Figure 2C**). Strain QN1NO-4 showed a 100% of similarity with the standard strain *B. siamensis* (KCTC 13613). In addition, the ANI value was calculated to further identify the species of strain QN1NO-4. Genomic data of the highest homology standard strains (*B. siamensis* KCTC 13613 and *B. subtilis* NCIB 3610) were downloaded from the EzBioCloud public genome database<sup>4</sup> and then were submitted to the ANI computing platform.<sup>5</sup> The ANI values of strain QN1NO-4 were 94 and 77% in

<sup>4</sup><https://www.ezbiocloud.net/search?Tn=Nocardioides>

<sup>5</sup><https://www.ezbiocloud.net/tools/ani>



**TABLE 1** | Physiological and biochemical characteristics of strain QN1NO-4.

Characteristics	Result
<i>Biochemical test</i>	
Urease production	+
Tween-20	–
Tween-40	–
Tween-60	–
Catalase	+
Oxidase	–
Gelatin liquefaction	+
Starch hydrolysis	+
Decomposition of cellulose	–
Nitrate reduction	+
H <sub>2</sub> S production	–
M/R test	–
V-P test	+
<i>Physiological test</i>	
pH tolerance	5–10 (optimum 7)
NaCl tolerance (%)	1–13 (optimum 5)
Temperature tolerance (°C)	30–65 (optimum 37)

+, positive reaction; –, negative reaction.

comparison with two standard strains *B. siamensis* KCTC 13613 and *B. subtilis* NCIB 3610, respectively (Supplementary Table 5). Both ANI values were below 95–96% of the threshold value for novel species definition (Richter and Rosselló-Móra, 2009). Thus, strain QN1NO-4 might be a novel species

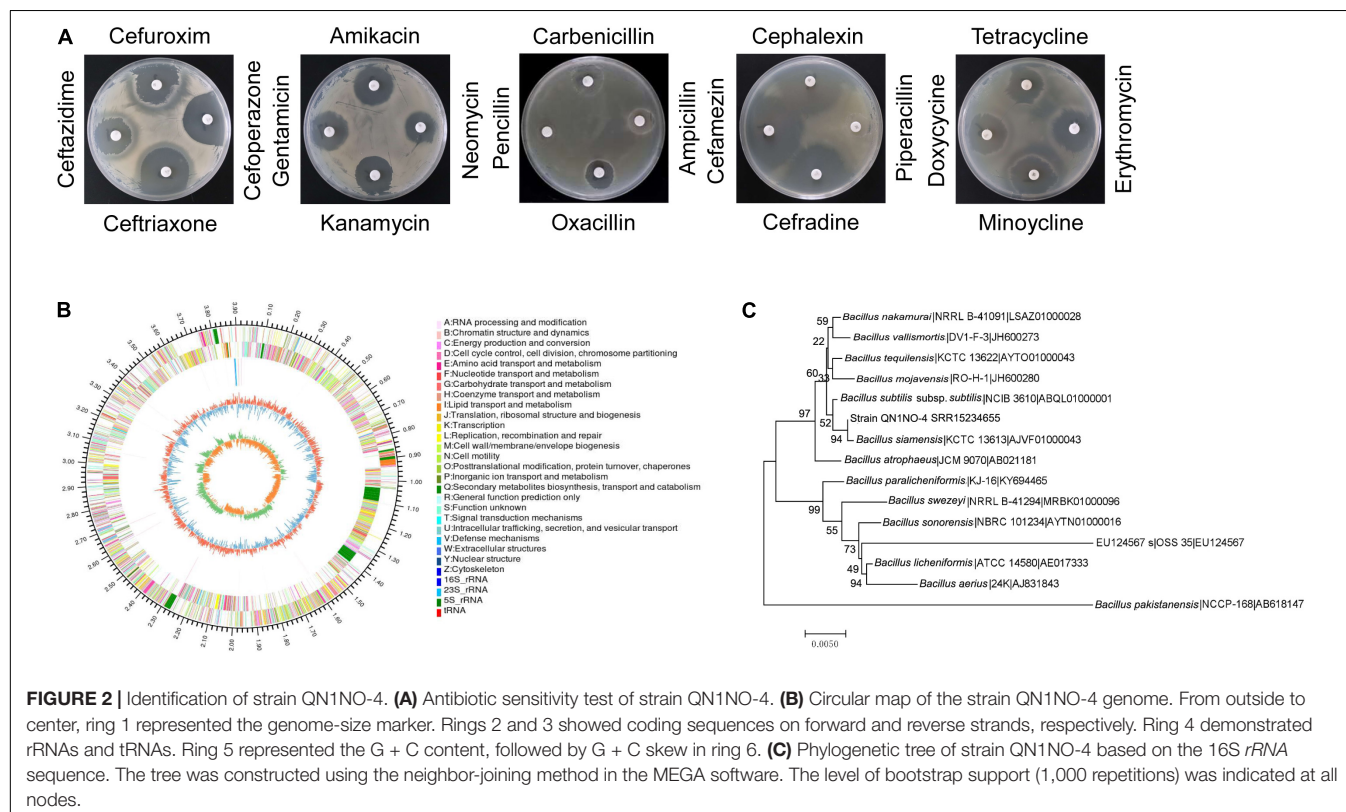
of the genus *Bacillus*, called after *B. safensis* sp. QN1NO-4.

## Determination of the Half-Maximal Effective Concentration Value of the Extract Against *C. fragariae*

The effects of strain QN1NO-4 extracts on mycelial growth of *C. fragariae* were assayed. The inhibitory efficiency showed a dose-dependent manner (Figure 3A). After the strain QN1NO-4 extract was co-incubated with *C. fragariae* at 28°C for 7 days, significant growth inhibition of the pathogen was observed in all the concentration groups (1.563, 3.125, 6.25, 12.5, 25, 50, 100, and 200 mg l<sup>-1</sup>). The inhibitory efficiency was 16, 23, 28, 41, 55, 69, and 83%, respectively (Figure 3B). Compared with the growth diameter of *C. fragariae* (68.00 mm ± 0.1) in the control plate, the half-maximal effective concentration (EC<sub>50</sub>) value of the strain QN1NO-4 extract was 33.81 ± 0.46 mg l<sup>-1</sup> using the toxicity regression equation. The concentration was defined as 1 × EC<sub>50</sub> for the following study.

## Biocontrol Efficiency of Extract on Controlling Strawberry Anthracnose Caused by *C. fragariae*

To investigate the biocontrol efficiency of strain QN1NO-4 against *C. fragariae* in post-harvest strawberry, each concentration extract (1 × EC<sub>50</sub>, 2 × EC<sub>50</sub>, 4 × EC<sub>50</sub>, or 8 × EC<sub>50</sub>, respectively) was used to treat the selected fruit samples (Figure 4A). After artificially co-incubating with



**FIGURE 2** | Identification of strain QN1NO-4. **(A)** Antibiotic sensitivity test of strain QN1NO-4. **(B)** Circular map of the strain QN1NO-4 genome. From outside to center, ring 1 represented the genome-size marker. Rings 2 and 3 showed coding sequences on forward and reverse strands, respectively. Ring 4 demonstrated rRNAs and tRNAs. Ring 5 represented the G + C content, followed by G + C skew in ring 6. **(C)** Phylogenetic tree of strain QN1NO-4 based on the 16S rRNA sequence. The tree was constructed using the neighbor-joining method in the MEGA software. The level of bootstrap support (1,000 repetitions) was indicated at all nodes.

**TABLE 2** | Summary of the strain QN1NO-4 genome.

Attribute	Value	% of total
Genome size (bp)	3,923,715	100
DNA coding region (bp)	3,428,622	87.38
DNA G + C content (bp)	1,824,135	46.49
Total genes	3,972	100
tRNA genes	52	1.31
rRNA genes	3	0.08
Protein-coding genes	3,917	98.62
Genes assigned to COGs	2,967	75.75
Genes assigned to GO	2,554	65.20
Genes assigned to KEGG	2,190	55.91
CRISPR repeat	10	0.26

*C. fragariae* ( $1.0 \times 10^6$  CFU ml<sup>-1</sup>) for 7 days, the DIs and quality parameters of strawberry fruit were measured. Compared with the control group, all treatments alleviated significantly the infection of *C. fragariae* in post-harvest strawberry fruit at 7 days post-inoculation (dpi). The DIs were 67, 46, 29, and 13% in treatment groups of  $1 \times EC_{50}$ ,  $2 \times EC_{50}$ ,  $4 \times EC_{50}$ , and  $8 \times EC_{50}$ , respectively (Figure 4B). Therefore, strain QN1NO-4 extract can inhibit effectively the infection of *C. fragariae* in post-harvest strawberry fruit.

Weight loss and TSS were measured to evaluate the effects of the strain QN1NO-4 extract on the fruit quality of strawberry. Weight loss showed a continuous decrease along with the increasing dose of extract (Figure 4C). Compared with the control group, weight loss was reduced by 4 and 3% after treatment with  $4 \times EC_{50}$  and  $8 \times EC_{50}$ , respectively. No obvious difference was observed between  $1 \times EC_{50}$  and  $2 \times EC_{50}$  treatment groups. Moreover, strain QN1NO-4 extract also delayed the decrease in TSS content during storage. Compared with the control group at 7 dpi, high TSS contents were kept in the treated fruit samples (Figure 4D).

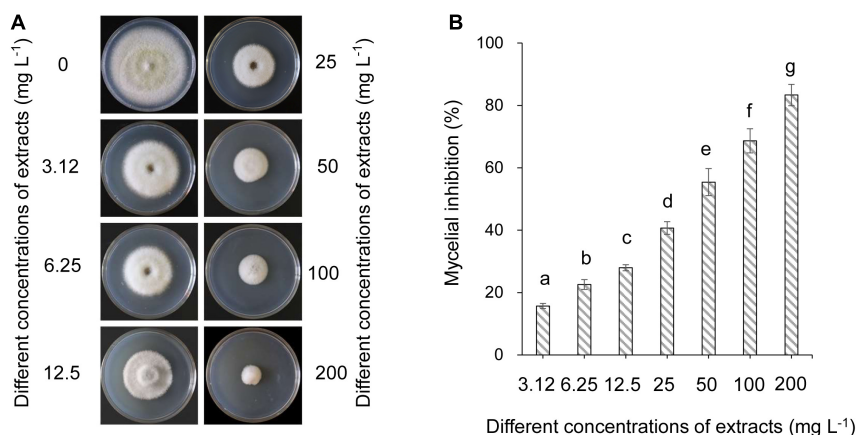
## Effects of Strain QN1NO-4 Extract on Spore Germination, Morphological Profile, and Cell Ultrastructure of *C. fragariae*

To further investigate the possible mechanism of the strain QN1NO-4 extract inhibiting fruit decay of post-harvest strawberry, the spore germination of *C. fragariae* was first analyzed after treatment with extract. The results showed that spore germination was inhibited, and the inhibitory efficiency was gradually increased with the increase of extract concentrations (Figure 5A). In the control group, 95% of spore can germinate, but only 36% and 18% of germination rates were detected in  $1 \times EC_{50}$  and  $2 \times EC_{50}$  treatment groups for 12 h, respectively. Especially, more than  $4 \times EC_{50}$  extract completely inhibited the spore germination of *C. fragariae*. Dense and short hypha at the colony edges were observed in comparison with the sparse and slender mycelia in the control plate (Figure 5B).

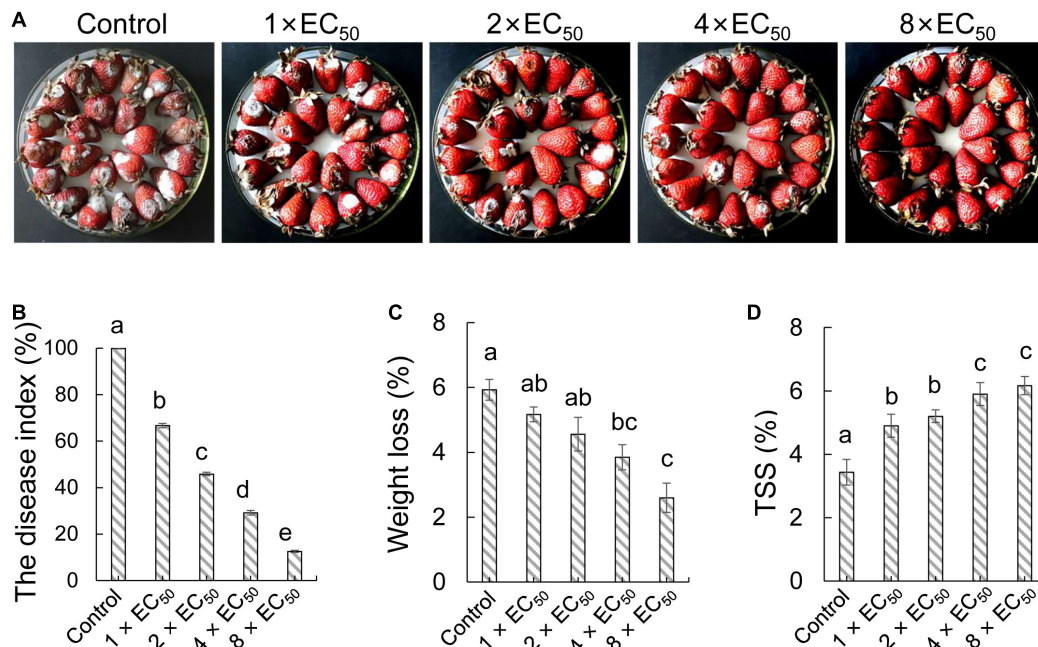
We further analyzed the morphological characteristics of *C. fragariae* spores before and after extract treatment. A wizened and distorted surface of spores was observed in the treatment group of  $4 \times EC_{50}$  extracts for 12 h. The regular and smooth morphology of hypha was displayed in the control group (Figure 5C). By contrast, vacuoles became bigger and disintegrated gradually after treatment with strain H4 extract. The organelle integrity was also broken, and cells showed a cytoplasmic heterogeneity (Figure 5D). In the control group, some complete organelles such as vacuoles and mitochondria could be clearly detected by TEM (Figure 5D).

## Hemolytic Activity Assay of Extract on Eukaryotic Cells

To investigate the toxicity of strain QN1NO-4 extract on eukaryotic cells, the hemolytic activity of extract ( $1 \times EC_{50}$ ,  $2 \times EC_{50}$ ,  $4 \times EC_{50}$ , or  $8 \times EC_{50}$ ) on human red blood cells was assayed using the release of hemoglobin after treatment at



**FIGURE 3** | Determination of the half-maximal effective concentration value of extract against *C. fragariae*. **(A)** Growth inhibition of *C. fragariae* on the PDA medium after treatment with different dose extracts. **(B)** Quantitative analysis of *C. fragariae* growth diameters. Error bars indicated standard errors of the means of three repeated experiments. Different lowercase letters represented a significant difference ( $p < 0.05$ ) of mycelial growth diameter at the same time point using the LSD multiple-range test.



**FIGURE 4 |** *In vivo* effects of strain QN1NO-4 extract on fruit decays and disease incidence caused by *C. fragariae*. **(A)** Disease inhibition of extract on strawberry fruit. Four extract concentrations (1 × EC<sub>50</sub>, 2 × EC<sub>50</sub>, 4 × EC<sub>50</sub>, and 8 × EC<sub>50</sub>) were selected. The treated fruit samples were stored at 28°C for 7 days. **(B)** Quantitative analysis of disease incidence of strawberry fruit treated with different dose extracts. **(C)** Effects of strain QN1NO-4 extract on weight loss of strawberry fruit. **(D)** Effects of strain QN1NO-4 extract on TSS contents of strawberry fruit. Error bars indicated standard errors of the means of three repeated experiments. Different letters indicated a significant difference ( $p < 0.05$ ) among different dose extracts using the LSD multiple-range test.

37°C for 1 h (Supplementary Figure 1). A percentage of 0.1% of Triton X-100 exhibiting 100% of hemolytic activity was selected as a positive control. No obvious hemolytic activity appeared in all treatment groups. Therefore, extract had non-specific cell lytic activity and toxicity to eukaryotic cells.

### Assay of a Broad-Spectrum Antifungal Activity of Strain QN1NO-4 Extract

Based on the prediction of secondary metabolites by genomic sequencing, we further analyzed whether strain QN1NO-4 extract had a broad-spectrum antifungal activity against 10 phytopathogenic fungi selected in our study. After co-incubating for 7 days, the extract exhibited an excellent inhibitory activity for mycelial growth of the selected fungi, ranging from 35 to 56% (Figure 6). The best inhibition activity with 56% was found against *Alternaria* sp., suggesting that the extract had the strongest antifungal activity against the fungi, followed by *C. lunata* (54%) and *F. graminearum* (50%). The minimal inhibition activity of the extract was 35% against *C. gloeosporioides*, indicating that the fungus had the highest tolerable ability for extract treatment.

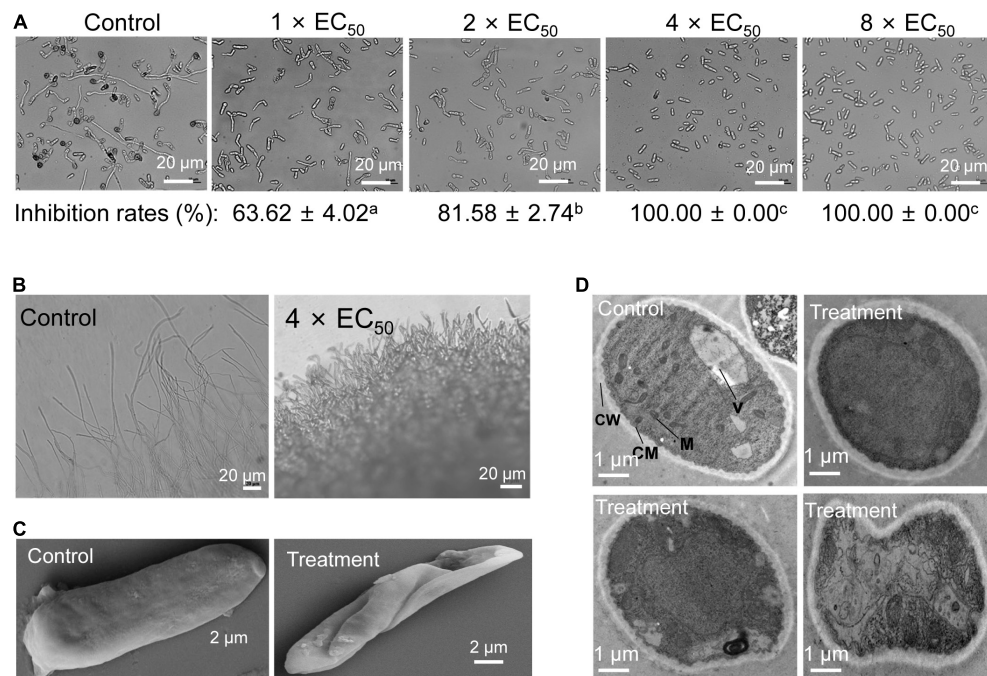
### Genome Annotation and Metabolite Prediction of Strain QN1NO-4

Functional analysis showed that 2,554, 2,967, and 2,190 out of the identified 3,917 protein-coding genes were annotated into GO, COG, and KEGG categories, respectively

(Supplementary Figure 2). For GO categories, the predicted genes were divided into three classes including biological process (27%), cellular components (27%), and molecular function (45%) (Supplementary Figure 2A). For COG categories, these genes were classified into 20 types of four categories. The largest category was metabolism (41%), followed by cellular processes and signaling (18%) as well as information storage and processing (16%). Twenty-five percent of the proportion was classified into the poorly characterized category (Supplementary Figure 2B). KEGG analysis showed that 2,190 of identified protein-coding genes were annotated into 41 pathways (Supplementary Figure 2C). Notably, some pathways including signal transduction, biosynthesis of other secondary metabolites, and metabolism of terpenoids and polyketides were pivotal for disease resistance.

By alignment of antiSMASH software and GenBank, 14 biosynthetic gene clusters containing 457 genes were predicted in the strain QN1NO-4 genome, including three NRPS gene clusters (54 genes), one PKS-like gene cluster (48 genes), one transAT-PKS gene cluster (48 genes), two transAT-PKS-like gene clusters (36 genes), two terpene gene clusters (48 genes), one LAP gene cluster (20 genes), one PKS III gene cluster (48 genes), one beta-lactone gene cluster (50 genes), and one MerR family transcriptional gene cluster (58 genes) (Table 3 and Supplementary Table 6). Among them, eight chemicals produced by gene clusters were involved in the biosynthesis of antimicrobial metabolites, such as bacillibactin, bacilysin, bacillaene, macrolactin, butirosin, diffidin, plantazolicin, and





**FIGURE 5 |** Inhibitory effects of strain QN1NO-4 extract on conidial germination, mycelial morphology, and ultrastructure of *C. fragariae*. **(A)** Conidial germination assay of *C. fragariae* after treatment with 1 ×, 2 ×, 4 ×, or 8 × EC<sub>50</sub> extracts. Bar = 20 μm. CW: cell wall; CM: cell membrane; M: mitochondria; V: vacuole. **(B)** Growth characteristics of *C. fragariae* mycelia treated with 4 × EC<sub>50</sub> of extract. Bar = 20 μm. **(C)** Representative pictures showing the mycelial morphology of *C. fragariae* after treatment with 4 × EC<sub>50</sub> of extracts. Bar = 20 μm. **(D)** Representative pictures showing the ultrastructure of *C. fragariae* after treatment with 4 × EC<sub>50</sub> of extract. Bar = 1 μm.

Pathogenic fungal	<i>F. graminearum</i>	<i>C. lunata</i>	<i>C. gloeosporioides</i>	<i>F. oxysporum</i>	<i>C. fragariae</i>
Mycelial morphology					
Mycelial inhibition (%)	50.31 ± 0.85 <sup>cd</sup>	54.04 ± 1.61 <sup>de</sup>	35.42 ± 1.80 <sup>a</sup>	47.08 ± 2.70 <sup>c</sup>	40.74 ± 2.72 <sup>bf</sup>
Pathogenic fungal	<i>C. gloeosporioides</i> penz.	<i>P. oryae</i>	<i>C. capsici</i>	<i>C. higginsianum</i>	<i>Alternaria</i> sp.
Mycelial morphology					
Mycelial inhibition (%)	41.87 ± 0.75 <sup>b</sup>	48.68 ± 2.63 <sup>c</sup>	40.12 ± 2.98 <sup>bf</sup>	55.93 ± 1.13 <sup>e</sup>	36.57 ± 5.26 <sup>af</sup>

**FIGURE 6 |** A broad-spectrum antifungal activity of strain QN1NO-4 extract against the selected phytopathogenic fungi.

kalimantacin A (**Supplementary Figure 3**). Four gene clusters (cluster1, cluster2, cluster4, and cluster5) presented a 100% similarity with the known compounds. However, 2 out of 14 clusters exhibited a 13% similarity with the predicted compounds, suggesting that these clusters might be involved in the biosynthesis of novel metabolites.

## Bioactive Compound Identification of the Strain QN1NO-4 Extract by GC-MS

GC-MS was employed to analyze the bioactive compounds of the strain QN1NO-4 extract. A total ion current chromatogram

is shown in **Supplementary Figure 4**. Based on retention time, molecular mass, and molecular formula, 15 chemical compounds were identified by the alignment of their mass spectra against the NIST library (**Supplementary Table 7**). These compounds mainly contained hydrocarbons, acids, pyrrolizidine, esters, and phenol. The predicted chemical structures are shown in **Figure 7**, including 2-methyloctanoic acid (1), 2,3-butylene glycol diacetate (2), phenylacetaldehyde (3), 7-hexadecene (4), pantolactone (5), propanoic acid, 3-(methylthio) (6), 2(3H)-benzofuranone (7), 1-octadecene (8), 2,4-bis(1,1-dimethylethyl)-phenol (9), indolizine (10), ethyl palmitate (11), 2-tetradecanol (12), trichloroacetic acid myristyl ester (13), 17b-methyl-5a-androstan-3a,17b-diol (14),



**TABLE 3** | Cluster number and gene number shown in different cluster types.

Cluster type	Cluster number	Gene number
NRPS	3	54
PKS-like	1	48
TransAT-PKS	1	48
TransAT-PKS-like	2	36
Terpene	2	48
LAP	1	20
PKS III	1	48
Beta-lactone	1	50
MerR family transcriptional	1	58
other	1	47
<b>Total</b>	<b>14</b>	<b>457</b>

The bold values represent the total of cluster and gene numbers.

and butyl isobutyl phthalate (15). The peak areas of compounds represented the portions of different compounds in the strain QN1NO-4 extract. Among these compounds, the peak area of 17b-methyl-5a-androstan-3a,17b-diol was 42%, suggesting that it was a dominant compound in strain QN1NO-4 extracts.

## DISCUSSION

Anthraxnose caused by *C. fragariae* is a common and destructive disease of strawberry (Mehmood et al., 2021). Biocontrol has received an increasing attention in controlling post-harvest fruit diseases (Li X.J. et al., 2020). Several endophytes play a vital role in plant protection and plant growth promotion. Many promising endophytic bacteria have been reported as biocontrol candidates against plant pathogens (Morales-Cedeño et al., 2021). Especially, *Bacillus* strains draw more and more attention due to their ability to produce resistant endospores and bioactive metabolites (Zhou et al., 2021). In our present study, a strain labeled QN1NO-4 was isolated from noni fruit and exhibited a strong antifungal ability against *C. fragariae* (Figure 1). According to morphological characteristics as well as genome alignment, strain QN1NO-4 was identified as a novel species of the genus *Bacillus* (Table 1, Figure 2 and Supplementary Tables 3, 4). As potential biocontrol agents, *Bacillus* species had also been successfully used to control other post-harvest diseases of different fruit, such as *Bacillus* species against *B. cinerea* and green mold in strawberry fruit and citrus (Tian et al., 2020; Wang et al., 2021), *B. amyloliquefaciens* against *Penicillium* in oranges and apples (Calvo et al., 2017; Wang et al., 2020; Ye et al., 2021), and *B. atrophaeus* against anthracnose on soursop and avocado (Guardado-Valdivia et al., 2018).

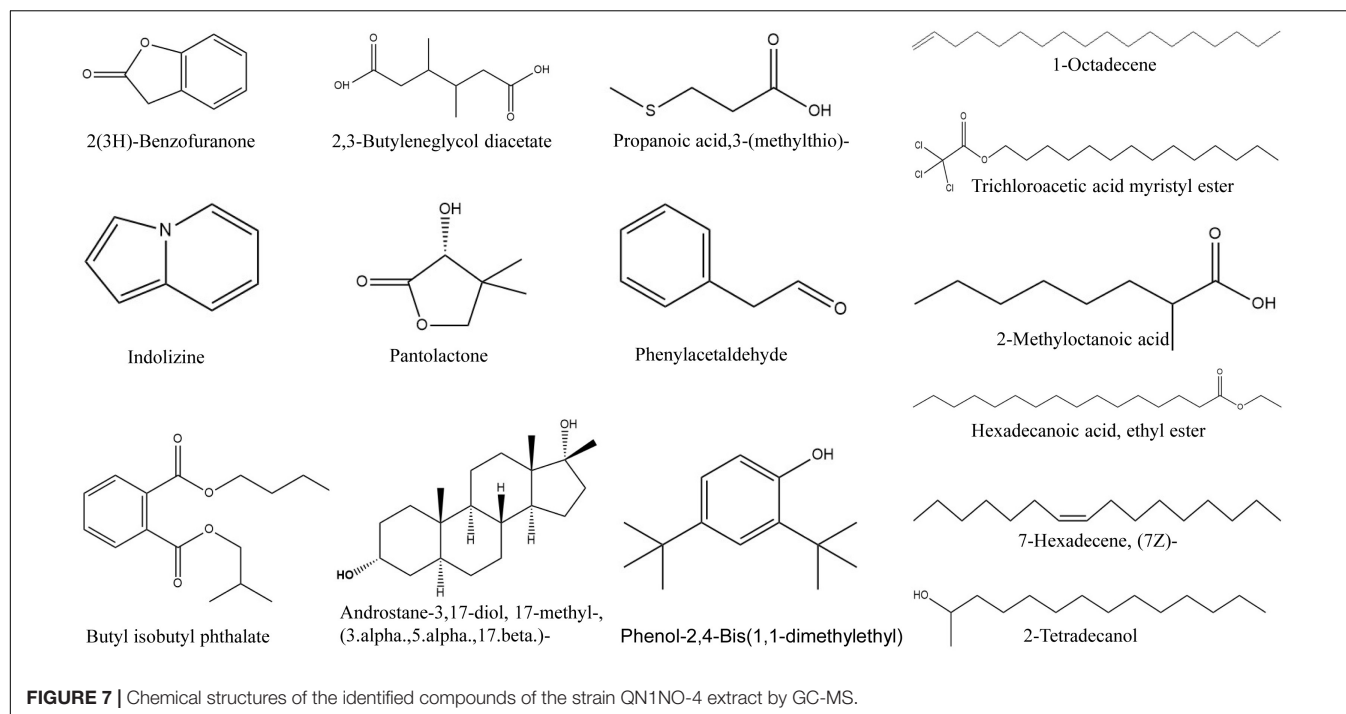
To further elucidate the antifungal mechanism of the strain QN1NO-4 extract against *C. fragariae*, we examined the spore germination, morphology, and ultrastructure of pathogenic cells after extract treatment. Consistent with antifungal activity *in vivo*, more than  $4 \times EC_{50}$  of strain QN1NO-4 extract completely inhibited the spore germination of *C. fragariae*. In addition, the extract also caused the irregular morphology, cell wall thickening, extensive vacuolization, and intracellular organelle degradation of *C. fragariae* (Figure 5D). Inhibition of spore germination

was essential for protecting post-harvest fruit from pathogenic infection (Miyara et al., 2010). A similar germination inhibition of spores was detected in *P. digitatum* treated with *C. lusitanae* and *P. fermentans*, *P. horianna* treated with *Bacillus* species, and *F. incarnatum* treated with *B. amyloliquefaciens* (Dheepa et al., 2016; Perez et al., 2019; Li Y.G. et al., 2020). Moreover, the toxicity and broad antimicrobial activity of the strain QN1NO-4 extract were also determined (Supplementary Figure 1 and Figure 6), suggesting that it is a promising alternative biological fungicide to control post-harvest diseases.

Natural antimicrobials were an attractive source of controlling post-harvest diseases, mitigating the reliance on synthetic fungicides (Kim et al., 2020). We found that the strain QN1NO-4 extract effectively inhibited mycelial growth of *C. fragariae* *in vitro*, and the mycelial inhibition rate depended on a dose-dependent manner (Figure 3A). The previous study showed that a novel peptide produced by *B. amyloliquefaciens* W10 had a strong antifungal activity (Zhang et al., 2017). It suggested that high antagonistic components were different from diverse *Bacillus* species. For example, extracts from different *Bacillus* species significantly inhibited different mycelial growths of *Fusarium solani*, *P. digitatum*, and *Fusarium incarnatum* (Ahmad et al., 2012; Tian et al., 2020). Moreover, the extract effectively kept the fruit quality of post-harvest strawberry by inhibiting fruit weight loss and TSS decrease (Figures 4C,D). Similarly, weight loss in *L. plantarum*-treated litchis was lower than the control fruit (Martínez-Castellanos et al., 2011).

GC-MS was used to further identify antifungal metabolites of strain QN1NO-4. A total of 15 chemical compounds including hydrocarbons, acids, pyrrolizidine, esters, and phenol were identified (Supplementary Table 7 and Figure 7). Among them, 2(3H)-benzofuranone, 2,4-bis(1,1-dimethylethyl)-phenol, and butyl isobutyl phthalate exhibited high antifungal and antibacterial activities. 2(3H)-benzofuranone produced by the indigenous fungus remarkably inhibited the mycelial growth of *M. oryzae* (Fan et al., 2019). 2,4-bis(1,1-Dimethylethyl)-phenol effectively inhibited the spore germination of *P. cinnamomi* and *Aspergillus* and controlled tomato fungal diseases such as early blight and gray mold (Rangel-Sánchez et al., 2014; Gao et al., 2017). Butyl isobutyl phthalate exhibited an antibacterial activity with an MIC value of  $128 \text{ g l}^{-1}$  (Hussain et al., 2017). Interestingly, the compounds in the strain QN1NO-4 extract identified by GC-MS were different from those involved in the synthesis of the above gene clusters (Supplementary Tables 6, 7). It might be because the identification method is not enough to identify all metabolites of strain QN1NO-4 (Wei et al., 2020). Thus, further study was necessary to identify specific active metabolites of strain QN1NO-4, contributing to the broad-spectrum antifungal activity.

Considering the deficiency of the GC-MS method, whole-genome analysis was used to predict rare and novel secondary metabolites, which cannot be detected directly in the fermentation broth using the current technology. In our study, the genome of strain QN1NO-4 was sequenced, revealing numerous unknown and known gene clusters of secondary metabolites (Table 3 and Supplementary Figure 3). These gene clusters might be responsible for the production of microbial



natural products. For example, the biosynthetic gene clusters encoding for polyketides (PKS) and non-ribosomal peptides (NRPS) were identified. They belonged to a structurally varied group of compounds and participated in the biosynthesis of antifungal compounds (Nimaichand et al., 2015; Prasad et al., 2015). In addition, some antimicrobials were also found such as bacillibactin, bacilysin, fengycin, bacillaene, macrolactin, butirosin, diffidicin, plantazolicin, and kalimantacin A (Supplementary Table 6 and Supplementary Figure 3). Bacillibactin was a specific transport system enabling *Bacillus* cells to accumulate and take up limited iron ions from their natural environment (Chen et al., 2009). Bacilysin participated in the antagonistic activity of *B. velezensis* against Gram-negative foodborne pathogens (Nannan et al., 2021). As a potent inhibitor of filamentous fungi, fengycin owned a strong antifungal ability against *V. dahliae* and *B. cinerea* (Li Q.R. et al., 2020; Su et al., 2020). Bacillaene can inhibit prokaryotic protein synthesis (Li Q.R. et al., 2020). Macrolactin effectively inhibited the replication of mammalian Herpes simplex virus and HIV in lymphoblast cells (Gustafson et al., 1989). Butirosin was an aminoglycoside antibiotic produced by *Bacillus circulans* (Llewellyn et al., 2007). Diffidicin exhibited a broad-spectrum antibacterial activity (Anthony et al., 2009). Plantazolicin belonged to a type of polyheterocyclic natural product with highly selective and potent activity against anthrax-causing bacteria (Hao et al., 2015). Thistlethwaite et al. (2017) found that kalimantacin showed a selective and high activity against staphylococci with an MIC value of 0.064 g l<sup>-1</sup>. Considering the novel species of strain QN1NO-4 in our study, some unknown function gene clusters might encode some new secondary metabolites. It will be further proved that strain QN1NO-4 has a broad-spectrum resistance to phytopathogen fungi.

## CONCLUSION

In the present study, a newly isolated strain QN1NO-4 from noni fruit was identified as *B. safensis* sp. and exhibited a strong antifungal ability against *C. fragariae*. Its extract can effectively reduce the fungal disease index and preserve the post-harvest quality of strawberry fruit. Moreover, strain QN1NO-4 extract can significantly inhibit mycelial growth and spore germination of *C. fragariae*, causing morphological and ultrastructure changes of fungal pathogen. Fifteen chemical compounds were identified from strain QN1NO-4 extracts by GC-MS. In addition, the whole-genome analysis revealed that some key function gene clusters in the strain QN1NO-4 genome were involved in the biosynthesis of active secondary metabolites. These diverse gene clusters and metabolites might contribute to its broad-spectrum antifungal activity. Therefore, strain QN1NO-4 is an effective bio-agent for controlling strawberry post-harvest diseases caused by *C. fragariae*.

## DATA AVAILABILITY STATEMENT

The datasets presented in this study can be found in online repositories. The names of the repository/repositories and accession number(s) can be found in the article/Supplementary Material.

## AUTHOR CONTRIBUTIONS

XL, LZ, JX, and WW developed the ideas and designed the experimental plans. LZ, JX, and WW supervised the research and

provided the funding support. XL, MZ, DZ, DQ, CQ, CL, SL, and DX performed the experiments. MZ, DZ, and DQ provided the materials. XL, LZ, and WW analyzed the data and prepared the manuscript. All authors contributed to the article and approved the submitted version.

## FUNDING

This work was supported by the National Key Research and Development Program of China (2020YFD1000104), the National Natural Science Foundation of China (31770476, 32072504), the Natural Science Foundation of Hainan (2019RC293, 320CXTD441), and the China Agriculture Research System (CARS-31).

## SUPPLEMENTARY MATERIAL

The Supplementary Material for this article can be found online at: <https://www.frontiersin.org/articles/10.3389/fmicb.2021.735732/full#supplementary-material>

## REFERENCES

- Ahmad, B., Khan, I., Bashir, S., and Azam, S. (2012). Chemical composition and antifungal, phytotoxic, brine shrimp cytotoxicity, insecticidal and antibacterial activities of the essential oils of *Acacia modesta*. *J. Med. Plants Res.* 6, 4653–4659. doi: 10.5897/JMPR12.016
- Aiello, D., Restuccia, C., Stefani, E., Vitale, A., and Cirvilleri, G. (2019). Postharvest biocontrol ability of *Pseudomonas synxantha* against *Monilinia fruticola* and *Monilinia fructigena* on stone fruit. *Postharvest Biol. Technol.* 149, 83–89. doi: 10.1016/j.postharvbio.2018.11.020
- Anthony, A. A., Marc, O., Badre, H., Yannick, L., Alain, B., Bernard, J., et al. (2009). *Bacillus amyloliquefaciens* GA1 as a source of potent antibiotics and other secondary metabolites for biocontrol of plant pathogens. *Microb. Cell Fact.* 8:63. doi: 10.1186/1475-2859-8-63
- Calvo, H., Marco, P., Blanco, D., Oria, R., and Venturini, M. (2017). Potential of a new strain of *Bacillus amyloliquefaciens* BUZ-14 as a biocontrol agent of postharvest fruit diseases. *Food Microbiol.* 63, 101–110. doi: 10.1016/j.fm.2016.11.004
- Chen, X. H., Koumoutsis, A., Scholz, R., and Borriss, R. (2009). More than anticipated – production of antibiotics and other secondary metabolites by *Bacillus amyloliquefaciens* FZB42. *J. Mol. Microbiol. Biotechnol.* 16, 14–24. doi: 10.1159/000142891
- Chen, X. Y., Dai, D. J., Zhao, S. F., Shen, Y., Wang, H. D., and Zhang, C. Q. (2019). Genetic diversity of *Colletotrichum* spp. causing strawberry anthracnose in Zhejiang, China. *Plant Dis.* 104, 1351–1357. doi: 10.1094/PDIS-09-19-2026-RE
- Chung, P. C., Wu, H. Y., Wang, Y. W., Ariyawansa, H. A., Hu, H. P., Hung, T. H., et al. (2020). Diversity and pathogenicity of *Colletotrichum* species causing strawberry anthracnose in Taiwan and description of a new species, *Colletotrichum miaoliense* sp. nov. *Sci. Rep.* 10:14664. doi: 10.1038/s41598-020-70878-2
- Delcher, A. L., Bratke, K. A., Powers, E. C., and Salzberg, S. L. (2007). Identifying bacterial genes and endosymbiont DNA with Glimmer. *Bioinformatics* 23, 673–679. doi: 10.1093/bioinformatics/btm009
- Denoyes-Rothan, B., Guérin, G., Délye, C., Smith, B., Minz, D., Maymon, M., et al. (2003). Genetic diversity and pathogenic variability among isolates of *Colletotrichum* species from strawberry. *Phytopathology* 93, 219–228. doi: 10.1094/PHYTO.2003.93.2.219
- Dheepa, R., Vinodkumar, S., Renukadevi, P., and Nakkeeran, S. (2016). Phenotypic and molecular characterization of chrysanthemum white rust pathogen *Puccinia horiana* (Henn) and the effect of liquid based formulation of *Bacillus* spp. for the management of chrysanthemum white rust under protected cultivation. *Biol. Control* 103, 172–186. doi: 10.1016/j.biocontrol.2016.09.006
- Dukare, A. S., Paul, S., Nambi, V. E., Gupta, R. K., Singh, R., Sharma, K., et al. (2019). Exploitation of microbial antagonists for the control of postharvest diseases of fruit: a review. *Crit. Rev. Food Sci. Nutr.* 59, 1498–1513. doi: 10.1080/10408398.2017.1417235
- Einloft, T. C., Oliveira, P., Radunz, L. L., and Dionello, R. G. (2021). Biocontrol capabilities of three *Bacillus* isolates towards aflatoxin B1 producer *A. flavus* in vitro and on maize grains. *Food Control* 125:107978. doi: 10.1016/j.foodcont.2021.107978
- Fan, X. Y., Matsumoto, H., Wang, Y., Hu, Y., Liu, Y. F., Fang, H. D., et al. (2019). Microenvironmental interplay predominated by beneficial *Aspergillus* abates fungal pathogen incidence in paddy environment. *Environ. Sci. Technol.* 53, 13042–13052. doi: 10.1021/acs.est.9b04616
- Feliziani, E., Lichter, A., Smilanick, J. L., and Ippolito, A. (2016). Disinfecting agents for controlling fruit and vegetable diseases after harvest. *Postharvest Biol. Technol.* 122, 53–69. doi: 10.1016/j.postharvbio.2016.04.016
- Gao, Z., Zhang, B., Liu, H., Han, J., and Zhang, Y. (2017). Identification of endophytic *Bacillus velezensis* ZSY-1 strain and antifungal activity of its volatile compounds against *Alternaria solani* and *Botrytis cinerea*. *Biol. Control* 105, 27–39. doi: 10.1016/j.biocontrol.2016.11.007
- Gotor-Vila, A., Teixidó, N., Casals, C., Torres, R., De Cal, A., Guijarro, B., et al. (2017). Biological control of brown rot in stone fruit using *Bacillus amyloliquefaciens* CPA-8 under field conditions. *Crop Prot.* 102, 72–80. doi: 10.1016/j.cropro.2017.08.010
- Guardado-Valdivia, L., Tovar-Pérez, E., Chacón-López, A., López-García, U., Gutiérrez-Martínez, P., Stoll, A., et al. (2018). Identification and characterization of a new *Bacillus atrophaeus* strain B5 as biocontrol agent of postharvest anthracnose disease in soursop (*Annona muricata*) and avocado (*Persea americana*). *Microbiol. Res.* 210, 26–32. doi: 10.1016/j.micres.2018.01.007
- Gustafson, K., Roman, M., and Fenical, W. (1989). The macrolactins, a novel class of antiviral and cytotoxic macrolides from a deep-sea marine bacterium. *J. Am. Chem. Soc.* 111, 7519–7524. doi: 10.1021/ja00201a036

**Supplementary Figure 1** | Hemolytic activity of red blood cells treated with strain QN1NO-4 extract.

**Supplementary Figure 2** | Genome annotation of strain QN1NO-4.

**Supplementary Figure 3** | Genome-wide analysis of gene clusters related to the biosynthesis of secondary metabolites in the strain QN1NO-4 genome using the online antiSMASH v4.2.0 software.

**Supplementary Figure 4** | A total ion current chromatogram of strain QN1NO-4 extract.

**Supplementary Table 1** | Antifungal activities of 29 isolated bacteria on mycelial growth of *C. fragariae*.

**Supplementary Table 2** | Antifungal activities of fermentation broth of 10 selected bacteria on mycelial growth of *C. fragariae*.

**Supplementary Table 3** | Carbon source utilization and nitrogen source utilization of strain QN1NO-4.

**Supplementary Table 4** | Sensitivity of strain QN1NO-4 to antibiotics.

**Supplementary Table 5** | Results of average nucleotide identity (ANI).

**Supplementary Table 6** | Prediction and functional annotation of secondary metabolites of strain QN1NO-4 by alignment with the online antiSMASH v4.2.0 software.

**Supplementary Table 7** | Compounds identified of extracts from strain QN1NO-4 by GC-MS.



- Han, Y. C., Zeng, X. G., Xiang, F. Y., Ren, L., Chen, F. Y., and Gu, Y. C. (2016). Distribution and characteristics of *Colletotrichum* spp. associated with anthracnose of strawberry in Hubei, China. *Plant Dis.* 100, 996–1006. doi: 10.1094/PDIS-09-15-1016-RE
- Hao, Y., Blair, P. M., Sharma, A., Mitchell, D. A., and Nair, S. K. (2015). Insights into methyltransferase specificity and bioactivity of derivatives of the antibiotic plantazolicin. *ACS Chem. Biol.* 10, 1209–1216. doi: 10.1021/cb501042a
- Huang, X. L., Kong, F. D., Zhou, S. Q., Huang, D. Y., Zheng, J. P., and Zhu, W. M. (2019). *Streptomyces tirandamycinicus* sp. nov., a novel marine sponge-derived actinobacterium with antibacterial potential against *Streptococcus agalactiae*. *Front. Microbiol.* 10:482. doi: 10.3389/fmicb.2019.00482
- Hussain, A., Rather, M. A., Dar, M. S., Aga, M. A., Ahmad, N., Manzoor, A., et al. (2017). Novel bioactive molecules from *Lentzea violacea* strain AS 08 using one strain-many compounds (OSMAC) approach. *Bioorg. Med. Chem. Lett.* 27, 2579–2582. doi: 10.1016/j.bmcl.2017.03.075
- Kim, J. D., Kang, J. E., and Kim, B. S. (2020). Postharvest disease control efficacy of the polyene macrolide lucensomycin produced by *Streptomyces plumbeus* strain CA5 against gray mold on grapes. *Postharvest Biol. Technol.* 162, 111–115.
- Kumar, V., Naik, B., Gusain, O., and Bisht, G. S. (2014). An actinomycete isolate from solitary wasp mud nest having strong antibacterial activity and kills the candida cells due to the shrinkage and the cytosolic loss. *Front. Microbiol.* 5:446. doi: 10.3389/fmicb.2014.00446
- Li, Q. R., Liao, S. T., Wei, J. H., Xing, D. X., Xiao, Y., and Yang, Q. (2020). Isolation of *Bacillus subtilis* strain SEM-2 from silkworm excrement and characterization of its antagonistic effect against *Fusarium* spp. *Can. J. Microbiol.* 66, 401–412. doi: 10.1139/cjm-2019-0621
- Li, X. J., Jing, T., Zhou, D. B., Zhang, M. Y., Qi, D. F., Zang, X. P., et al. (2021). Biocontrol efficacy and possible mechanism of *Streptomyces* sp. H4 against postharvest anthracnose caused by *Colletotrichum fragariae* on strawberry fruit. *Postharvest Biol. Technol.* 175:111401. doi: 10.1016/j.postharvbio.2020.111401
- Li, X. J., Li, K., Zhou, D. B., Zhang, M. Y., Qi, D. F., Jing, T., et al. (2020). Biological control of banana wilt disease caused by *Fusarium oxysporum* f. sp. *cubense* using *Streptomyces* sp. H4. *Biol. Control* 155:104524. doi: 10.1016/j.biocontrol.2020.104524
- Li, Y., Héloir, M., Zhang, X., Geissler, M., Trouvelot, S., Jacquens, L., et al. (2019). Surfactin and fengycin contribute to the protection of a *Bacillus subtilis* strain against grape downy mildew by both direct effect and defence stimulation. *Mol. Plant Pathol.* 20, 1037–1050. doi: 10.1111/mpp.12809
- Li, Y. G., Cai, Y. A., Liang, Y. B., Ji, P. S., and Xu, L. K. (2020). Assessment of antifungal activities of a biocontrol bacterium BA17 for managing postharvest gray mold of green bean caused by *Botrytis cinerea*. *Postharvest Biol. Technol.* 161:111086. doi: 10.1016/j.postharvbio.2019.111086
- Llewellyn, N. M., Li, Y., and Spencer, J. B. (2007). Biosynthesis of butirosin: transfer and deprotection of the unique amino acid side chain. *Chem. Biol.* 14, 379–386. doi: 10.1016/j.chembiol.2007.02.005
- Martínez-Castellanos, G., Pelayo-Zaldivar, C., Perez-Flores, L. J., Lopez-Luna, A., Gimeno, M., Barzana, E., et al. (2011). Postharvest litchi (*Litchi chinensis* Sonn.) quality preservation by *Lactobacillus plantarum*. *Postharvest Biol. Technol.* 59, 172–178. doi: 10.1016/j.postharvbio.2010.09.005
- Mehmood, N., Yuan, Y., Ali, M., Ali, M., Iftikhar, J., Cheng, C. Z., et al. (2021). Early transcriptional response of terpenoid metabolism to *Colletotrichum gloeosporioides* in a resistant wild strawberry *Fragaria nilgerrensis*. *Phytochemistry* 182:112590. doi: 10.1016/j.phytochem.2020.112590
- Miller-Butler, M. A., Smith, B. J., Babiker, E. M., Kreiser, B. R., and Blythe, E. K. (2018). Comparison of whole plant and detached leaf screening techniques for identifying anthracnose resistance in strawberry plants. *Plant Dis.* 102, 2112–2119. doi: 10.1094/pdis-08-17-1138-re
- Miyara, I., Shafran, H., Davidzon, M., Sherman, A., and Prusky, D. (2010). pH regulation of ammonia secretion by *Colletotrichum gloeosporioides* and its effect on appressorium formation and pathogenicity. *Mol. Plant Microbe Interact.* 23, 304–316. doi: 10.1094/mpmi-23-3-0304
- Morales-Cedeño, L. R., del Carmen Orozco-Mosqueda, M., Loeza-Lara, P. D., Parra-Cota, F. I., Santos-Villalobos, S., and Santoyo, G. (2021). Plant growth-promoting bacterial endophytes as biocontrol agents of pre- and post-harvest diseases: fundamentals, methods of application and future perspectives. *Microbiol. Res.* 242:126612. doi: 10.1016/j.micres.2020.126612
- Nannan, C., Vu, H. Q., Gillis, A., Caulier, S., Nguyen, T. T. T., and Mahillon, J. (2021). Bacilysin within the *Bacillus subtilis* group: gene prevalence versus antagonistic activity against Gram-negative foodborne pathogens. *J. Biotechnol.* 327, 28–35. doi: 10.1016/j.jbiotec.2020.12.017
- Nimaichand, S., Devi, A. M., Tamreihao, K., Ningthoujam, D. S., and Li, W. J. (2015). Actinobacterial diversity in limestonedeposit sites in Hundung, Manipur (India) and their antimicrobial activities. *Front. Microbiol.* 6:413. doi: 10.3389/fmicb.2015.00413
- Ogundajo, A., Okeleye, B., and Ashafa, A. O. (2017). Chemical constituents, in vitro antimicrobial and cytotoxic potentials of the extracts from *Macaranga barteri* Mull-Arg. *Asian Pac. J. Trop. Biomed.* 7, 654–659. doi: 10.1016/j.apjtb.2017.06.014
- Pei, S. P., Liu, R. L., Gao, H. Y., Chen, H. J., Wu, W. J., Fang, X. J., et al. (2020). Inhibitory effect and possible mechanism of carvacrol against *Colletotrichum fruticola*. *Postharvest Biol. Technol.* 163:111126. doi: 10.1016/j.postharvbio.2020.111126
- Perez, M. F., Díaz, M. A., Pereyra, M. M., Córdoba, J. M., Isas, A. S., Sepúlveda, M., et al. (2019). Biocontrol features of *Clavispora lusitaniae* against *Penicillium digitatum* on lemons. *Postharvest Biol. Technol.* 155, 57–64. doi: 10.1016/j.postharvbio.2019.05.012
- Prasad, P., Varshney, D., and Adholeya, A. (2015). Whole genome annotation and comparative genomic analyses of bio-control fungus *Purpureocillium lilacinum*. *BMC Genomics* 16:1004. doi: 10.1186/s12864-015-2229-2
- Qi, D., Zou, L., Zhou, D., Chen, Y., Gao, Z., Feng, R., et al. (2019). Taxonomy and broad-spectrum antifungal activity of *Streptomyces* sp. SCA3-4 isolated from rhizosphere soil of *Opuntia stricta*. *Front. Microbiol.* 10:1390. doi: 10.3389/fmicb.2019.01390
- Rangel-Sánchez, G., Castro-Mercado, E., and García-Pineda, E. (2014). Avocado roots treated with salicylic acid produce phenol-2,4-bis (1,1-dimethylethyl), a compound with antifungal activity. *J. Plant Physiol.* 171, 189–198. doi: 10.1016/j.jplph.2013.07.004
- Richter, M., and Rosselló-Móra, R. (2009). Shifting the genomic gold standard for the prokaryotic species definition. *Proc. Natl. Acad. Sci. U.S.A.* 106, 19126–19131. doi: 10.1073/pnas.0906412106
- Rico, D., Barcenilla, B., Meabe, A., González, C., and Ana, B. (2019). Mechanical properties and quality parameters of Chitosan-edible algae (*Palmaria palmata*) on ready-to-eat strawberries. *J. Sci. Food Agric.* 99, 2651–2921. doi: 10.1002/jsfa.9504
- Rong, S., Hong, X., Li, L., Chen, R., Gao, X., and Xu, Z. (2020). Antifungal activity of endophytic *Bacillus safensis* b21 and its potential application as a biopesticide to control rice blast - sciencedirect. *Pestic. Biochem. Phys.* 162, 69–77. doi: 10.1016/j.pestbp.2019.09.003
- Su, Z. H., Chen, X. Y., Liu, X. M., Guo, Q. G., Li, S. Z., Lu, X. Y., et al. (2020). Genome mining and UHPLC-QTO-MS/MS to identify the potential antimicrobial compounds and determine the specificity of biosynthetic gene clusters in *Bacillus subtilis* NCD-2. *BMC Genomics* 21:767. doi: 10.1186/s12864-020-07160-2
- Thistlethwaite, I. R. G., Bull, F. M., Cui, C. S., Walker, P. D., Gao, S. S., Wang, L. Y., et al. (2017). Elucidation of the relative and absolute stereochemistry of the kalimantacin/batumin antibiotics. *Chem. Sci.* 8, 6196–6201. doi: 10.1039/C7SC01670K
- Tian, Z. H., Chen, C. W., Chen, K., Liu, P., Fan, Q. J., Zhao, J., et al. (2020). Biocontrol and the mechanisms of *Bacillus* sp. w176 against postharvest green mold in citrus. *Postharvest Biol. Technol.* 159:111022. doi: 10.1016/j.postharvbio.2019.111022
- Vanewijk, P., and Hoekstra, J. (1993). Calculation of the EC50 and its confidence interval when subtoxic stimulus is present. *Ecotoxicol. Environ. Saf.* 25, 25–32. doi: 10.1006/eesa.1993.1003
- Wallace, R. L., Hirkala, D. L., and Nelson, L. M. (2018). Mechanisms of action of three isolates of *Pseudomonas fluorescens* active against postharvest grey mold decay of apple during commercial storage. *Biol. Control* 117, 13–20.
- Wang, D. D., Li, J. H., Zhu, G. L., Zhao, K., Jiang, W. W., Li, H. D., et al. (2020). Mechanism of the potential therapeutic candidate *Bacillus subtilis* BSXE-1601 against shrimp pathogenic *Vibrios* and Multifunctional metabolites biosynthetic capability of the strain as predicted by genome analysis. *Front. Microbiol.* 11:581802. doi: 10.3389/fmicb.2020.581802
- Wang, F., Xiao, J., Zhang, Y. Z., Li, R. Y., Liu, L., and Deng, J. (2021). Biocontrol ability and action mechanism of *Bacillus halotolerans* against *Botrytis cinerea* causing grey mould in postharvest strawberry fruit. *Postharvest Biol. Technol.* 174:111456. doi: 10.1016/j.postharvbio.2020.111456



- Wang, W., Deng, L., Yao, S., and Zeng, K. (2018). Control of green and blue mold and sour rot in citrus fruits by the cationic antimicrobial peptide PAF56. *Postharvest Biol. Technol.* 136, 132–138. doi: 10.1016/j.postharvbio.2017.10.015
- Wei, Y., Zhao, Y., Zhou, D., Qi, D., Li, K., and Tang, W. (2020). A newly isolated *Streptomyces* sp. YYS-7 with a broad-spectrum antifungal activity improves the banana plant resistance to *Fusarium oxysporum* f. sp. *cubense* tropical race 4. *Front. Microbiol.* 11:1712. doi: 10.3389/fmicb.2020.01712
- Wisniewski, M., Droby, S., Norelli, J., Liu, J., Schena, L., Agraria, D., et al. (2016). Alternative management technologies for postharvest disease control: the journey from simplicity to complexity. *Postharvest Biol. Technol.* 122, 3–10. doi: 10.1016/j.postharvbio.2016.05.0120925-5214
- Ye, W. Q., Sun, Y. F., Tang, Y. J., and Zhou, W. W. (2021). Biocontrol potential of a broad-spectrum antifungal strain *Bacillus amyloliquefaciens* B4 for postharvest loquat fruit storage. *Postharvest Biol. Technol.* 174:111439. doi: 10.1016/j.postharvbio.2020.111439
- Yoon, S. H., Ha, S. M., Kwon, S., Lim, J., Kim, Y., and Seo, H. (2017). Introducing EzBioCloud: a taxonomically united database of 16S rRNA gene sequences and whole-genome assemblies. *Int. J. Syst. Evol. Microbiol.* 67, 1613–1617. doi: 10.1099/ijsem.0.001755
- Zhang, D., Spadaro, D., Garibaldi, A., and Lodovica, M. (2011). Potential biocontrol activity of a strain of *Pichia guilliermondii* against grey mold of apples and its possible modes of action. *Biol. Control* 57, 193–201.
- Zhang, Q. X., Zhang, Y., Shan, H. H., Tong, Y. H., Chen, X. J., and Liu, F. C. (2017). Isolation and identification of antifungal peptides from *Bacillus amyloliquefaciens* W10. *Sci. Pollut. Res.* 24, 25000–25009. doi: 10.1007/s11356-017-0179-8
- Zhang, X. Y., Wu, F., Gu, N., Yan, X. L., Wang, K. L., Dhanasekaran, S., et al. (2020). Postharvest biological control of Rhizopus rot and the mechanisms involved in induced disease resistance of peaches by *Pichia membranefaciens*. *Postharvest Biol. Technol.* 163, 111–146. doi: 10.1016/j.postharvbio.2020.111146
- Zhao, L., Zhou, Q., Yang, H., Zheng, H., Wen, X., and Sun, W. (2019). Inhibitory effect of *Pichia guilliermondii* Y35-1 against postharvest anthracnose infection in loquat fruit and its effect on quality preservation. *Food Sci.* 40, 170–177.
- Zhimo, V. Y., Ajay, K., Antonio, B., Shoshana, S., Oleg, F., Mohamad, A. T., et al. (2021). Compositional shifts in the strawberry fruit microbiome in response to near-harvest application of *Metschnikowia fructicola*, a yeast biocontrol agent. *Postharvest Biol. Technol.* 175:111469. doi: 10.1016/j.postharvbio.2021.111469
- Zhou, L., Song, C. X., Li, Z. B., and Kuipers, O. P. (2021). Antimicrobial activity screening of rhizosphere soil bacteria from tomato and genome-based analysis of their antimicrobial biosynthetic potential. *BMC Genomics* 22:29. doi: 10.1186/s12864-020-07346-8

**Conflict of Interest:** The authors declare that the research was conducted in the absence of any commercial or financial relationships that could be construed as a potential conflict of interest.

**Publisher's Note:** All claims expressed in this article are solely those of the authors and do not necessarily represent those of their affiliated organizations, or those of the publisher, the editors and the reviewers. Any product that may be evaluated in this article, or claim that may be made by its manufacturer, is not guaranteed or endorsed by the publisher.

Copyright © 2021 Li, Zhang, Qi, Zhou, Qi, Li, Liu, Xiang, Zhang, Xie and Wang. This is an open-access article distributed under the terms of the Creative Commons Attribution License (CC BY). The use, distribution or reproduction in other forums is permitted, provided the original author(s) and the copyright owner(s) are credited and that the original publication in this journal is cited, in accordance with accepted academic practice. No use, distribution or reproduction is permitted which does not comply with these terms.



# Monitoring Tritrophic Biocontrol Interactions Between *Bacillus* spp., *Fusarium oxysporum* f. sp. *cubense*, Tropical Race 4, and Banana Plants *in vivo* Based on Fluorescent Transformation System

## OPEN ACCESS

### Edited by:

Florence Fontaine,  
Université de Reims  
Champagne-Ardenne, France

### Reviewed by:

Mahfuz Rahman,  
West Virginia University,  
United States  
Manoj Kumar Solanki,  
University of Silesia in Katowice,  
Poland

### \*Correspondence:

Si-Jun Zheng  
s.zheng@cgiar.org  
Yun-Yue Wang  
1371209436@qq.com

<sup>†</sup>These authors have contributed  
equally to this work

### Specialty section:

This article was submitted to  
Microbe and Virus Interactions With  
Plants,  
a section of the journal  
Frontiers in Microbiology

Received: 07 August 2021

Accepted: 22 September 2021

Published: 13 October 2021

### Citation:

He P, Li S, Xu S, Fan H, Wang Y,  
Zhou W, Fu G, Han G, Wang Y-Y and  
Zheng S-J (2021) Monitoring  
Tritrophic Biocontrol Interactions  
Between *Bacillus* spp., *Fusarium*  
*oxysporum* f. sp. *cubense*, Tropical  
Race 4, and Banana Plants *in vivo*  
Based on Fluorescent  
Transformation System.  
Front. Microbiol. 12:754918.  
doi: 10.3389/fmicb.2021.754918

Ping He<sup>1,2†</sup>, Shu Li<sup>2†</sup>, Shengtao Xu<sup>2</sup>, Huacai Fan<sup>2</sup>, Yongfen Wang<sup>2,3</sup>, Wei Zhou<sup>4</sup>, Gang Fu<sup>5</sup>,  
Guangyu Han<sup>1</sup>, Yun-Yue Wang<sup>1\*</sup> and Si-Jun Zheng<sup>2,6\*</sup>

<sup>1</sup>State Key Laboratory for Conservation and Utilization of Bio-Resources in Yunnan, Ministry of Education Key Laboratory of Agriculture Biodiversity for Plant Disease Management, College of Plant Protection, Yunnan Agricultural University, Kunming, China, <sup>2</sup>Yunnan Key Laboratory of Green Prevention and Control of Agricultural Transboundary Pests, Agricultural Environment and Resources Institute, Yunnan Academy of Agricultural Sciences, Kunming, China, <sup>3</sup>Institute of Tropical and Subtropical Industry Crops, Yunnan Academy of Agricultural Sciences, Baoshan, China, <sup>4</sup>Biotechnology Research Institute, Guangxi Academy of Agricultural Sciences, Nanning, China, <sup>5</sup>Institute of Plant Protection, Guangxi Academy of Agricultural Sciences, Nanning, China, <sup>6</sup>Bioversity International, Kunming, China

*Bacillus* spp. is effective biocontrol agents for *Fusarium* wilt of banana (FWB), tropical race 4 (TR4). This study explores the colonization by *Bacillus subtilis*, *Bacillus velezensis*, and *Bacillus amyloliquefaciens* of host banana plants and elucidates the mechanism of antagonistic TR4 biocontrol. The authors selected one *B. subtilis* strain, three *B. velezensis* strains, and three *B. amyloliquefaciens* strains that are proven to significantly inhibit TR4 *in vitro*, optimized the genetic transformation conditions and explored their colonization process in banana plants. The results showed that we successfully constructed an optimized fluorescent electro-transformation system (OD<sub>600</sub> of bacteria concentration = 0.7, plasmid concentration = 50 ng/μl, plasmid volume = 2 μl, transformation voltage = 1.8 kV, and transformation capacitance = 400 Ω) of TR4-inhibitory *Bacillus* spp. strains. The red fluorescent protein (RFP)-labeled strains were shown to have high stability with a plasmid-retention frequency above 98%, where bacterial growth rates and TR4 inhibition are unaffected by fluorescent plasmid insertion. *In vivo* colonizing observation by Laser Scanning Confocal Microscopy (LSCM) and Scanning Electron Microscopy (SEM) showed that *Bacillus* spp. can colonize the internal cells of banana plantlets roots. Further, fluorescent observation by LSCM showed these RFP-labeled bacteria exhibit chemotaxis (chemotaxis ratio was 1.85 ± 0.04) toward green fluorescent protein (GFP)-labeled TR4 hyphae in banana plants. We conclude that *B. subtilis*, *B. velezensis*, and *B. amyloliquefaciens* can successfully colonize banana plants and interact with TR4. Monitoring its dynamic interaction with TR4 and its biocontrol mechanism is under further study.

**Keywords:** *Bacillus* spp., biocontrol, electro-transformation, RFP-labeled *Bacillus*, *Bacillus* interaction with TR4

## INTRODUCTION

Fusarium wilt of banana (FWB) caused by *Fusarium oxysporum* f. sp. *cubense*, especially Tropical Race 4 (TR4), is one of the most destructive diseases affecting the crop (Ghag et al., 2015; Presti et al., 2015; Carvalhais et al., 2019). Pathogen spores invade the vascular bundles of banana roots through wounds and then extend to the corms and pseudostems, causing the vascular bundles to become brown and necrotic, the leaves gradually wither and eventually the whole plant dies (Swarupa et al., 2014). Due to its characteristic of surviving in the soil for decades, once the pathogen is introduced into the soil, the infected banana orchard cannot be used for growing susceptible banana cultivars, which seriously affects the sustainable development of the banana industry, as there are few proven TR4-resistant cultivars (Ploetz, 2006, 2015).

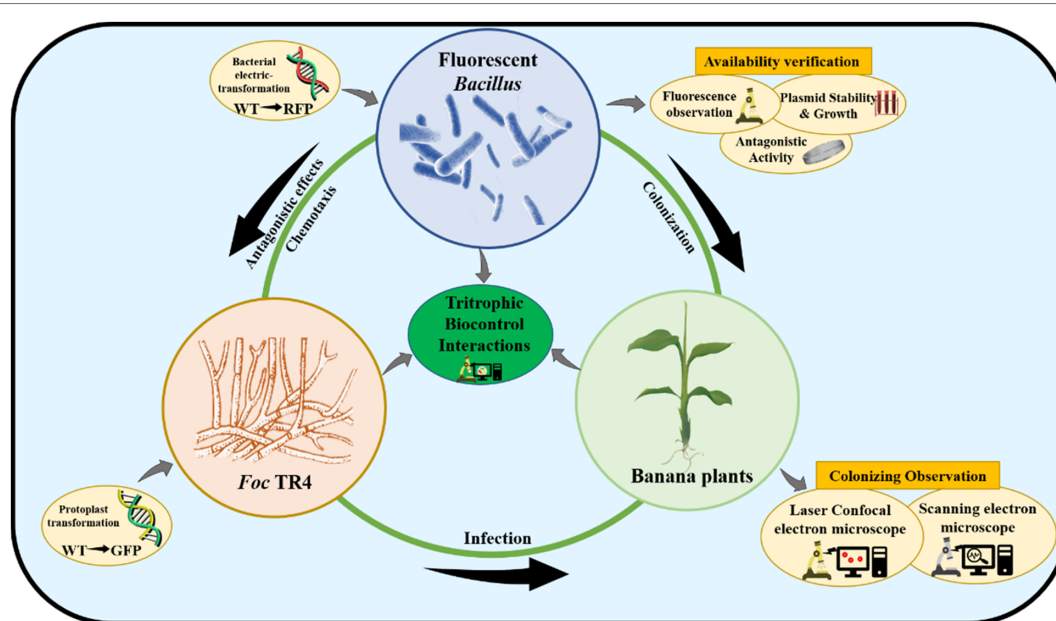
Like all the other *Foc* strains, TR4 cannot be controlled using fungicides and cannot be eradicated from soil using fumigants (ProMusa, 2021). Crop rotation and intercropping have been used to reduce the infections and inoculum levels (Nadarajah et al., 2016). In China, farmers have been growing bananas in the presence of TR4 by rotating or intercropping with Chinese leek (*Allium tuberosum*; Nadarajah et al., 2016; Li et al., 2020a,b). The most effective solution supporting continued production of bananas in infested soils would be replacing susceptible cultivars with resistant ones. However, almost all important banana cultivars are susceptible to TR4 (Ploetz, 2015; Chen et al., 2019; Sun et al., 2019), and most commercial cultivars are triploid and sterile (non-seed bearing) makes banana breeding more difficult (Hwang and Ko, 2004; Heslop-Harrison and Schwarzacher, 2007). At present, few TR4-resistant banana cultivars have been bred and popularized (Daniells, 2011). Furthermore, even those cultivars still have to adapt to local cultivation practices and conditions. As a result, the spread of TR4 has led to an increase in research on biological control and biocontrol agents (BCAs) in suppressing the pathogen (Nadarajah et al., 2016; Bubici et al., 2019; Damodaran et al., 2020).

So far, many microbes such as *Trichoderma* spp., *Pseudomonas* spp., and *Bacillus* spp. have been widely used as BCAs (Bubici et al., 2019). The characteristics of spore-forming and rapid growth of *Bacillus* species confer them with an important advantage over other beneficial biological control microorganisms. In addition, many *Bacillus* species can synthesize a large number of secondary metabolites, which play a key role in antibiosis against detrimental microorganisms (Radhakrishnan et al., 2017; Fira et al., 2018). *Bacillus subtilis* is a representative *Bacillus*, which could produce a variety of antibiotics with different structures and activities; it also exhibits a wide range of antibacterial activities against different plant pathogens under *in vitro* conditions (Stein, 2005). *Bacillus amyloliquefaciens*, a type of Gram-positive bacterium (Priest et al., 1987), highly homologous with *B. subtilis*, has a single nutrient requirement and is harmless to the environment and human health. Due to these positive characteristics, many *B. amyloliquefaciens* strains have been isolated and identified as having significant inhibition

and control effects on *Ceitocybe bescens* and *Fusarium oxysporum* (Guan and Jiang, 2013). Wang et al. (2015) and Xue et al. (2015) found that *B. amyloliquefaciens* combined with organic fertilizers can significantly reduce the incidence of Fusarium wilt. The *B. amyloliquefaciens* isolated by Zhang et al. (2014) showed a good biocontrol effect on banana wilt, and this strain can produce IAA and siderophore, promote the growth of banana plants, and has a high biocontrol potential. *Bacillus velezensis* is also a Gram-positive bacterium that is closely related to *B. amyloliquefaciens*. FZB42 is currently the most researched *B. velezensis* strain, which has been commercialized, and it is effective against various pathogens caused by bacteria and fungi (Borriss et al., 2011). Fan et al. (2011) integrated a plasmid carrying a gene encoding a fluorescent protein into the chromosome of the FZB42 strain and successfully observed the colonization and distribution in the roots of corn, *Arabidopsis*, and duckweed. However, so far there are few reports on the colonization and distribution of *Bacillus* on banana plants. Understanding how these beneficial microorganisms colonize and distribute in host banana plants will provide an important and favorable theoretical basis for using biocontrol strains to control FWB.

Most biocontrol *Bacillus* species are soil microorganisms that colonize the rhizosphere of plants and directly or indirectly promote plant growth through different mechanisms (Compant et al., 2005; Scherwinski et al., 2008; Malfanova et al., 2013). These play an important role in many fields, such as ecological restoration, biocatalysis, and biological control. The successful colonization of biocontrol strains is a prerequisite for the development of biocontrol promotion and disease prevention, and it is vital to explore their interaction processes with plants (Kang, 2019). Fluorescence transformation is currently the most successful approach for studying the colonization of *Bacillus* spp. and the interaction with plants *in vivo* (He, 2014). However, many wild-type *Bacillus* species with good bio-promoting and disease-preventing effects cannot easily form competent cells because of the unknown cellular restriction-repair system, which leads to constraints to a low efficiency of electric shock transformation (Alegre et al., 2004; Yasui et al., 2009). This seriously hinders banana research on horizontal manipulation or modification of *Bacillus*, as well as the further utilization and exploitation of the potential value of these biocontrol agents. Hence, there is a need to develop a reliable and efficient fluorescent-transformation system for monitoring the interactions between *Bacillus*, *Foc* TR4, and banana plants.

In this study, seven *Bacillus* species containing one *B. subtilis*, three *B. velezensis*, and three *B. amyloliquefaciens* strains with strong antagonistic effects on TR4 *in vitro* were selected. In order to obtain stable fluorescent-marked transformants and develop an efficient genetic transformation system, pYP69 carrying red fluorescent protein (RFP) was used as the fluorescent expression vector, which was successfully introduced into wild-type *Bacillus* strains according to the optimized experimental parameters. Furthermore, laser confocal observation confirmed that the fluorescent-transformed strains could be used for monitoring how *Bacillus* colonizes host banana plants (Figure 1).



**FIGURE 1** | The schematic diagram of tritrophic biocontrol interactions.

## MATERIALS AND METHODS

### Source of Strains and Plasmid

*Bacillus subtilis* strain YN1419 (GenBank Accession No. MW647761) was isolated from banana cultivar Brazilian in Xishuangbanna, Yunnan, China. *Bacillus velezensis* strain YN1282-2 (GenBank Accession No. MW663765) was isolated from banana cultivar GCTCV-119. *Bacillus velezensis* N67 (GenBank Accession No. MW672323), WBN06 (GenBank Accession No. MW672324), and *B. amyloliquefaciens* G9R-3 (GenBank Accession No. MW674627; Zhou et al., 2020), HN04 (GenBank Accession No. MW674626) were isolated from Guangxi banana plantations. *Bacillus amyloliquefaciens* YN0904 (GenBank Accession No. MW647760) was isolated from Yunnan banana plantation. All experimental strains had proven strong *Foc* TR4 antagonistic effects *in vitro* (Li et al., 2021). *Foc* TR4 strain 15-1 (Zhang et al., 2018) was isolated from infected banana plants in Xishuangbanna, Yunnan, China. GFP-TR4 was constructed in our laboratory (Zhang et al., 2018) and was used in monitoring the interaction with bacteria. The plasmid pYP69 expressing RFP and the chloramphenicol-resistance gene (Supplementary Figure S1) were obtained as a gift from Dr. Yongmei Li (Plant Protection College of Yunnan Agricultural University, Kunming, China) and Dr. Yiyang Yu (Plant Protection College of Nanjing Agricultural University, Nanjing, China). pYP69 was constructed by the pYC127 as backbone and cloned with mKate2 coding sequence (Chen et al., 2012). The *Escherichia coli* DH5 $\alpha$  was purchased from Beijing Biomed Biotechnology Co., Ltd. (Beijing, China). The strains were stored in 25% glycerol at  $-80^{\circ}\text{C}$ . The isolates were reactivated on nutrition agar (NA) medium at  $37^{\circ}\text{C}$  for 24 h.

### Culture Media

LB broth medium (LB; tryptone 10g, yeast extract 5g, NaCl 10g, pH 7.0 for 1l with deionized water) was used to cultivate the bacteria and prepare the bacterial suspension. Potato Dextrose Agar (PDA) medium (200g potato, 20g glucose, 20g agar, diluted to 1l, natural pH) was used to activate the *Foc* TR4 and conduct the dual-culture experiments. Growth Medium [GM; LB with 3% glycine (Gly), 1% DL-threonine (DL-Thr), 0.03% Tween 80, and 9.1% sorbitol] was used to prepare competent cells. ETM buffer (40 ml glycerol, 360 ml deionized water, 36.4g sorbitol, 36.4g mannitol, 0.25 mM  $\text{KH}_2\text{PO}_4$ , 0.25 mM  $\text{K}_2\text{HPO}_4$ , and 0.5mM  $\text{MgCl}_2$ ) was used to wash away the ion components in competent cells. Recovery Medium (RM; LB with 9.1% sorbitol and 6.92% mannitol) was used for resuspension of competent cells after electroporation.

### Detection of Plasmid pYP69 Expression in *Escherichia coli*

The *Escherichia coli* competent cells were thawed on ice. One microliter pYP69 was mixed gently into competent cells and put it on ice for 30 min stationary. Then, the heat shock was applied at  $42^{\circ}\text{C}$  for 60s, and then, the culture was put on ice for 2 min. Five hundred microliter LB liquid medium was then added to the culture and resuscitated at  $37^{\circ}\text{C}$ , swirling at 180rpm for 60 min, and then, the transformative culture was evenly spread on the 100  $\mu\text{g}/\text{ml}$  ampicillin-resistant medium. The transformative plates were cultured at  $37^{\circ}\text{C}$  for 16h, and then, single colonies were selected to observe fluorescence by the Fluorescence Microscope (Nikon 80I).

### Plasmid Extraction

The *E. coli*-carrying pYP69 plasmid was inoculated into LB liquid medium containing ampicillin (100  $\mu\text{g}/\text{ml}$ ), and cultured



at 37°C, swirling at 220 rpm for 16 h. Plasmid extraction followed the instructions accompanying the OMEGA Plasmid DNA Extraction Kit (E.Z.N. A® Plasmid DNA Mini Kit I).

## Electroporation

### Preparation of Competent Cells

Competent cells preparation (Zhang et al., 2011) was carried out as follows. *Bacillus* strains stored at −80°C were inoculated in the LB solid medium overnight. Each single colony was individually selected and inoculated in 30 ml GM liquid medium by inoculating loop, cultivated at 37°C, 220 rpm for 16 h. Two milliliter cultured bacteria suspension was inoculated into 200 ml GM liquid medium, cultured at 37°C, and swirled at 220 rpm for 3 h. OD<sub>600</sub> value was determined by spectrophotometer (Nanophotometer NP80 Touch). When OD<sub>600</sub> value reached 0.5, 3% Gly, 1% DL-Thr, and 0.03% Tween 80 were added into the culture for cell-wall weakening. The culture was arrested when the OD<sub>600</sub> value reached 0.7. The bacterial suspension was put on ice for 10 min and centrifuged at 4°C, 1,300 g for 10 min; then, 50 ml precooled ETM solution was used to wash away the ion components in the GM medium for three times. About 500 µl ETM was used to suspend the competent cells, competent cells were divided into 100 µl per EP tubes and stored at −80°C.

### Electroporation

The transformation (Kang, 2019) was carried out as follows. Two microliter plasmid pYP69 were added into 100 µl competent cells culture, mixed the plasmid and competent cells, and electroporation was carried out. The electroporation voltage was 1.8 kV, and the capacitance was 400 Ω. After electroporation, 1 ml RM medium was immediately added to the electroporation cup and then transferred to a 1.5 ml centrifuge tube, cultured at 37°C, shook at 220 rpm for 4 h. The culture was spread on the LB solid plate containing 10 µg/ml chloramphenicol, the positive transformants designated according to the format of RFP-*Bacillus*, e.g., RFP-N67, etc., were selected, and the fluorescence labeling was observed under the fluorescence microscope (Excitation wavelength: 555 nm/Emission wavelength: 584 nm).

## Stability Determination of Plasmid pYP69 in *Bacillus*

The activated RFP-*Bacillus* strains were inoculated into liquid LB medium without antibiotics, cultured at 37°C, and shook at 180 rpm, with samples being taken every 5 h and spread on LB solid plates, and bacteria colonies were observed by fluorescence microscope. The percentage of red fluorescent colonies in total cells colonies used to calculate the stability of the plasmid in the RFP-strains. Three replicates were conducted.

## Cell Growth Determination of RFP-Strains

Red fluorescent protein-*Bacillus* and wild-type (WT) strains were inoculated in the LB liquid medium and cultured to the concentration was OD<sub>600</sub> reaching 1.0, and then, the bacteria suspension was transferred to the blank medium at a ratio of 1%.

Bacteria were cultured at 37°C and shook at 180 rpm for 60 h. OD<sub>600</sub> values of samples were measured every hour in the first 6 h. OD<sub>600</sub> was measured every 2 h during 8–20th h, and OD<sub>600</sub> was measured every 4 h during 22nd–60th h. Three replicates were made.

## Antagonistic Activity of RFP-Strains on TR4

The dual-culture method was used to compare the antagonistic activity of the RFP-labeled *Bacillus* and WT strains against *Foc* TR4. TR4 was activated in PDA for 7 days at 28°C, and RFP-labeled bacteria and WT bacteria were activated at 37°C for 24 h. Individual 5 mm diameter disks of TR4 hyphae were placed in the center of each PDA plate. Plates were then inoculated with the RFP strain and the WT strain at 2.5 cm from the center by using inoculating loop. These were cultivated for 7 days, and the growth of TR4 hyphae was measured. The inhibition dual culture assay was carried out in three replicates.

## Colonizing Observation of Biological Control *Bacillus*

A 10 ml red fluorescent bacterial suspension (cultivated 24 h at 37°C and 180 rpm, diluted to  $1 \times 10^6$  cfu/ml) was pour into the tissue-culture bottle which cultured five banana plantlets by MS medium, gently shaking the bottle and placing in a culture incubator (30°C, 80% humidity, 12 h light/12 h dark), with the treatment adding just sterilized water as the control. Five replicates were made. Ten banana plant roots per treatment were randomly selected after inoculation for 7 days, and the roots were washed with flowing sterile water to remove the medium.

For fluorescent microscopy, tissue slices (thickness: 50 nm) were excised by freezing microtome and any bacteria in root tissues were observed by Laser Confocal Electron Microscope (Leica TCS-SP8). Excitation/emission wavelengths were 561 nm/570–640 nm for RFP (mKate2 protein).

For scanning microscopy, the critical point drying sample processing method was conducted. Tissue slices (thickness: 50 nm) were immersed in FAA fixative (5 ml 38% formaldehyde, 5 ml glacial acetic acid, 90 ml 70% ethyl alcohol, and 5 ml glycerol) at 4°C overnight. Then: the fixed samples were immersed in 50, 60, 70, 80, 90, and 95% alcohol successively to dehydrate 30 min was conducted in each alcohol concentration, then the samples were immersed in absolute ethanol for 30 min, and three replicates were conducted. Banana tissue samples were then put into Critical Point Dryer (K850) and Cressington Sputter Coater (108 AUTO) to spray gold coating. The fixed samples were put into Scanning Electron Microscope (ZEISS Sigma 300, Germany) to observe the bacterial colonization.

## Laser Confocal Electron Microscope Observation of Interaction *in vivo*

In order to observe the interactions between strains and TR4 *in vivo*, 3 ml RFP-labeled bacterial culture in 9% physiological saline solution was inoculated into the leaf vascular bundles of the banana cultivar Brazilian by injection (Liu et al., 2020),

and a 5 mm agar disk with GFP-labeled TR4 mycelia (Zhang et al., 2018) was placed on the wound by inoculation loop. The latest fully expanded leaves were selected. Fluorescent observation by laser scanning confocal microscope (Leica TCS-SP8) was carried out after the leaves were cultured in 28 °C, 60% light, and 50% humidity for 7 days. Excitation/emission wavelengths were 561 nm/570–640 nm for RFP (mKate2 protein). Excitation/emission wavelengths were 488 nm/500–540 nm for GFP (AmCyan protein).

## Chemotaxis Assay of Bacteria to Pathogen

Seven day-old *Foc* TR4 were inoculated in 50 ml diluted PDB (1: 50; v: v in H<sub>2</sub>O) at 28 °C with shaking at 150 rpm for 24 h to obtain spores suspension of *Foc* TR4. Suspension was then washed twice with sterile ddH<sub>2</sub>O and incubated for 48 h in 5 ml sterile ddH<sub>2</sub>O at 28 °C and 150 rpm. The supernatant was sterilized by filtration through a 0.22 µm membrane (Millex-GP) for use.

To obtain bacterial suspension,  $1 \times 10^7$  colony ml<sup>-1</sup> RFP-N67 strains were grown in LB overnight at 37 °C, washed either with sterile ddH<sub>2</sub>O, and diluted in ddH<sub>2</sub>O to the OD<sub>600</sub> of 0.1.

Chemotaxis capillary assays (Palmieri et al., 2020) were carried out as follows. 250 µl bacterial suspension was added to the well (1.5 cm × 1.5 cm) in the glass slide together with a 10 µl capillary containing the test compound (*Foc* TR4 hyphal exudate or ddH<sub>2</sub>O). Slides were incubated for 60 min at 28 °C, capillaries were carefully lifted, the content was serially diluted and plated onto LA medium with 10 µg/ml chloramphenicol, and CFUs were counted 24 h after incubation at 37 °C. The chemotaxis ratio was calculated by dividing the number of bacteria in the tube containing the test compound (*Foc* TR4 hyphal exudate) by the number of bacteria in the tube containing the control (ddH<sub>2</sub>O). All experiments included four replicates and were performed three times with similar results.

## Statistical Analysis

Data were analyzed by one-way ANOVA using the SPSS version 18.0 for Windows (Chicago, IL, United States). The figures and charts were drawn using ORIGIN 2018 (Massachusetts, United States).

## RESULTS

### Plasmid pYP69 Expresses Fluorescence in *Escherichia coli*

Before transforming *Bacillus*, we aimed to verify whether this plasmid could be expressed in *E. coli*, preserved, and extracted. Heat-shock transformation was used to transform the plasmid pYP69 into *E. coli* DH5α competent cells. We obtained positive transformants on plates containing ampicillin. Colonies glowed an obvious red color under the fluorescence microscope, and the red *E. coli* cells could still be visualized even after being cultured in the liquid. This verified that RFP-labeled cells can be observed under the fluorescence microscope (Figure 2A), indicating that the plasmid pYP69 can be expressed in *E. coli*.

### Plasmid pYP69 Expresses Fluorescence in *B. subtilis*, *B. velezensis*, and *B. amyloliquefaciens*

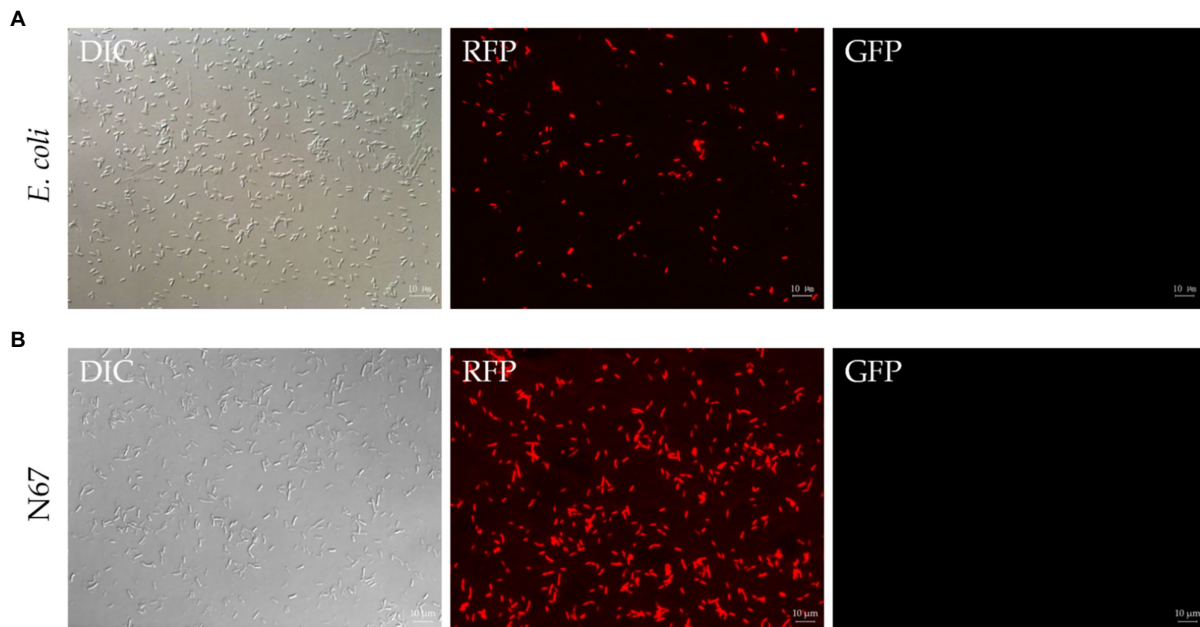
Fluorescence labeling is one of the best methods for tracing bacterial colonization (including *B. subtilis*, *B. velezensis*, and *B. amyloliquefaciens*) in plants. Here, electroporation with optimized conditions was used to transfer the plasmid pYP69 into competent cells of WT *Bacillus* strains. Positive transformants of *Bacillus* were obtained on the solid plate of 10 µg/ml chloramphenicol. These can be seen with the naked eye as the colonies of strains formed on the antibiotic plate gradually become light red. Fluorescence microscope observation results showed that the plasmid pYP69 has been successfully transformed into the WT strains and can express RFP in the *Bacillus* strains (Figure 2B; Supplementary Figures S2A–E). Several repeated experiments showed that although there was still relatively low trans-formants efficiency ( $1 \times 10^2$ – $10^3$  cfu/µg of plasmid DNA); stable transformants from each *Bacillus* strain had already been generated.

### RFP-Labeled Strains Possess High Plasmid Stability

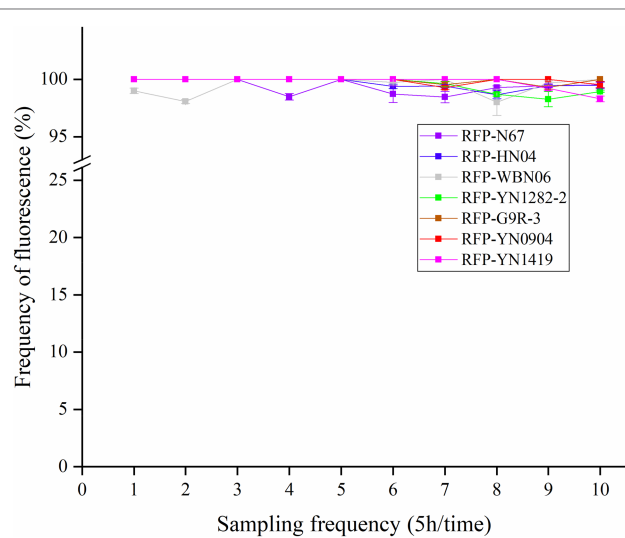
The stability of plasmid expression in the strains is important for the construction of fluorescent strains. Under condition of no antibiotic pressure, the red fluorescent strain was cultured in serial dilutions, and the samples were taken every 5 h. The dilution was evenly spread on a non-resistant plate. The proportion of colonies with fluorescence was counted under a fluorescence microscope to determine the frequency of plasmid retention. We found that the frequency of RFP plasmid cells is all greater than 98% after being cultured for 10 consecutive generations (Figure 3). Results confirmed the plasmid is rarely lost due to the proliferation of bacterial cells, indicating that the plasmid pYP69 can be stably expressed in these *Bacillus* strains, and it can be used for experiment tracing colonization and migration in plants.

### RFP-Labeled Strains Have the Similar Growth Condition of WT-Strains

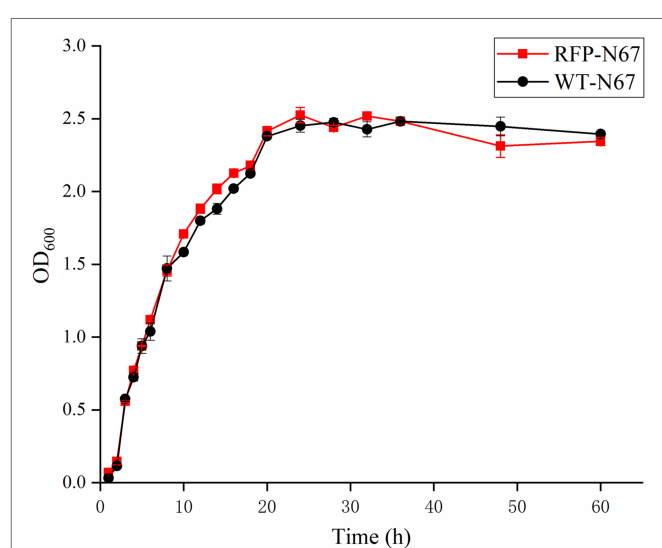
The growth of the RFP-*Bacillus* and WT strains was compared under the same inoculation and culture conditions. The results showed that the growth of RFP-YN0904, RFP-YN1282-2, RFP-WBN06, and RFP-N67 was consistent to WT strains, indicating that the plasmid pYP69 had no significant effect on the growth of these three *B. velezensis*. The wild-type strains of HN04 and G9R-3 grew slight faster in the log phase and reached the stable phase earlier than RFP strains, the wild-type strains YN1419 grew lower before the stable phase than the RFP strain, but they did not significantly affect normal growth of RFP bacteria (Figure 4; Supplementary Figures S3A–E). We speculate that it may be that the introduction of multicopy large plasmids affects the growth rate of *B. amyloliquefaciens* and *B. subtilis*, and good fluorescence performance of the plasmids in the *Bacillus* host may also create an additional metabolic burden on the strains.



**FIGURE 2 |** Fluorescence observation of *Escherichia coli* and N67 under microscopy. DIC, differential interference contrast field; RFP, red fluorescence field; and GFP, green fluorescence field. **(A)** Representative fluorescent micrograph of *E. coli* under fluorescent microscope. Heat-shock transformation was used to transform pYP69 into *E. coli* DH5 $\alpha$  competent cells. The positive transformants on the solid medium containing 100  $\mu$ g/ml ampicillin/ could be observed under the microscope. **(B)** Representative fluorescent micrograph of N67 under fluorescent microscope. Electric-transformation was used to transform pYP69 into N67 competent cells. The positive transformants on the solid medium containing 10  $\mu$ g/ml chloramphenicol could be observed under the microscope. Scale bar: 10  $\mu$ m.



**FIGURE 3 |** Fluorescence plasmid retention frequency of RFP-labeled *Bacillus*. Samples were taken every 5 h. The proportion of colonies on a non-resistant plate with fluorescence was assessed (with three replicates) under fluorescence microscope to determine the frequency of plasmid retention.



**FIGURE 4 |** The growth rate of RFP-N67 compared to wild-type N67. OD<sub>600</sub> measures were used to determine bacterial growth rate. Three replicates were included.

## RFP-Labeled Strains Retain Their Antagonistic Activity Against TR4

The metabolic burden caused by the introduction of exogenous plasmids sometimes affects other functions of the strain. In order to explore the effect on the biological characteristics of

plasmid pYP69 insertion, the antagonistic activities of the RFP-*Bacillus* strain and the WT strain against the pathogenic fungus *Foc* TR4 were compared. The results showed that there was no significant difference in the antagonistic activity of the two types of strains against the tested pathogenic fungi (**Figure 5; Supplementary Table S1**). It shows that the expression of



plasmid pYP69 does not affect the inhibitory activity of the *Bacillus* strains on the growth of the pathogenic fungus.

## ***Bacillus* Can Successfully Colonize Banana Root Cells**

Biocontrol bacteria successfully colonizing plants are a necessary pre-condition for their biocontrol function. To explore the colonization capacity of *Bacillus* in banana plants, we inoculated tissue-cultured banana plantlets with *B. velezensis* RFP-N67. After 7 days of co-culture, we sampled the banana plantlets' roots, and slice observation by Laser Confocal Microscopy (LCM) showed that RFP-N67 colonized the banana roots cells (Figure 6A) and Scanning Electron Microscopy (SEM) confirmed the bacteria could successfully colonized the roots xylem cells (Figures 6B,C). We also found that there were no bacteria in banana plants subject to low inoculation concentrations ( $1 \times 10^3$ – $10^5$  cfu/ml), and that *Bacillus* can enter the root when the inoculation concentration reached a higher density ( $1 \times 10^6$  cfu/ml). However, excessive concentrations could damage banana plantlets.

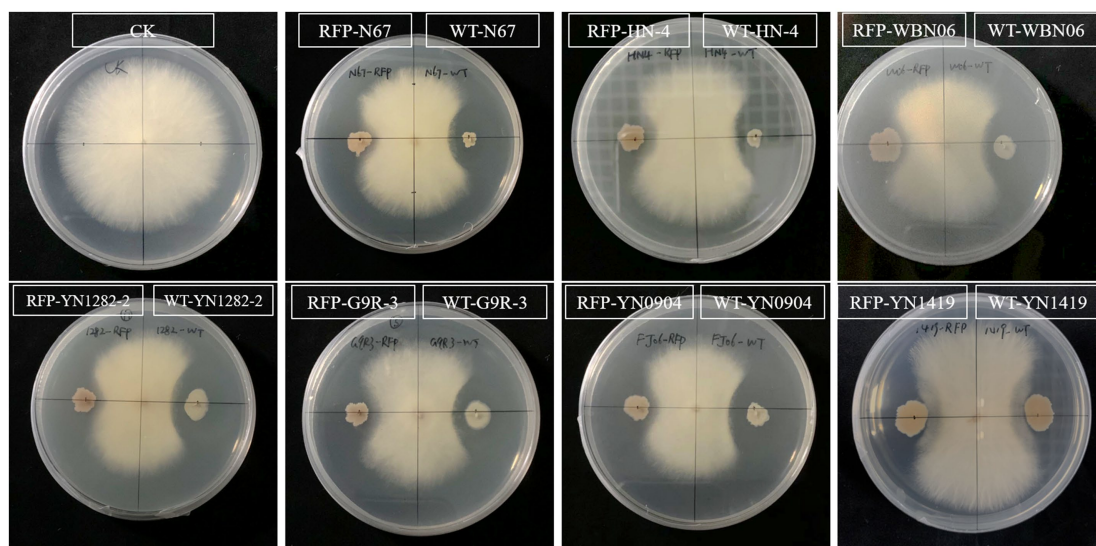
## ***Bacillus* Exhibits Chemotaxis Toward *Foc* TR4 in Banana Plants**

The interactions between beneficial *Bacillus* strains and pathogens are the key to crop disease control. There are few studies on the interactions between biocontrol bacteria and TR4 in banana. Therefore, we selected RFP-labeled *Bacillus* RFP-N67 and used available green fluorescent labeled pathogens GFP-TR4, inoculating banana leaves simultaneously to observe whether they will interact *in vivo*. Leaf phenotypic observation showed that the lesion size in both the front and back sides of the leaves after the treatment inoculated with RFP-N67 and GFP-TR4 was significantly smaller than those found in leaves inoculated

with GFP-TR4 only (Figure 7A). Then, we made ultrathin sections around the leaf lesions and successfully observed RFP-N67 and GFP-TR4 simultaneously under laser confocal microscopy, finding that RFP-N67 often appeared around GFP-TR4 mycelia (Figures 7B,C), and further chemotaxis assay, indicating that RFP-N67 exhibits a strong chemotaxis toward *Foc* TR4 (Figure 7D). Therefore, we can speculate that the biocontrol bacteria RFP-N67 we used can grow and reproduce normally in banana to exert their biocontrol functions, and that in the presence of pathogens, it can be quickly found to inhibit pathogen growth. However, this study only provides histological evidence. Quantitative analysis of specific pathogen growth inhibition needs to be carried out.

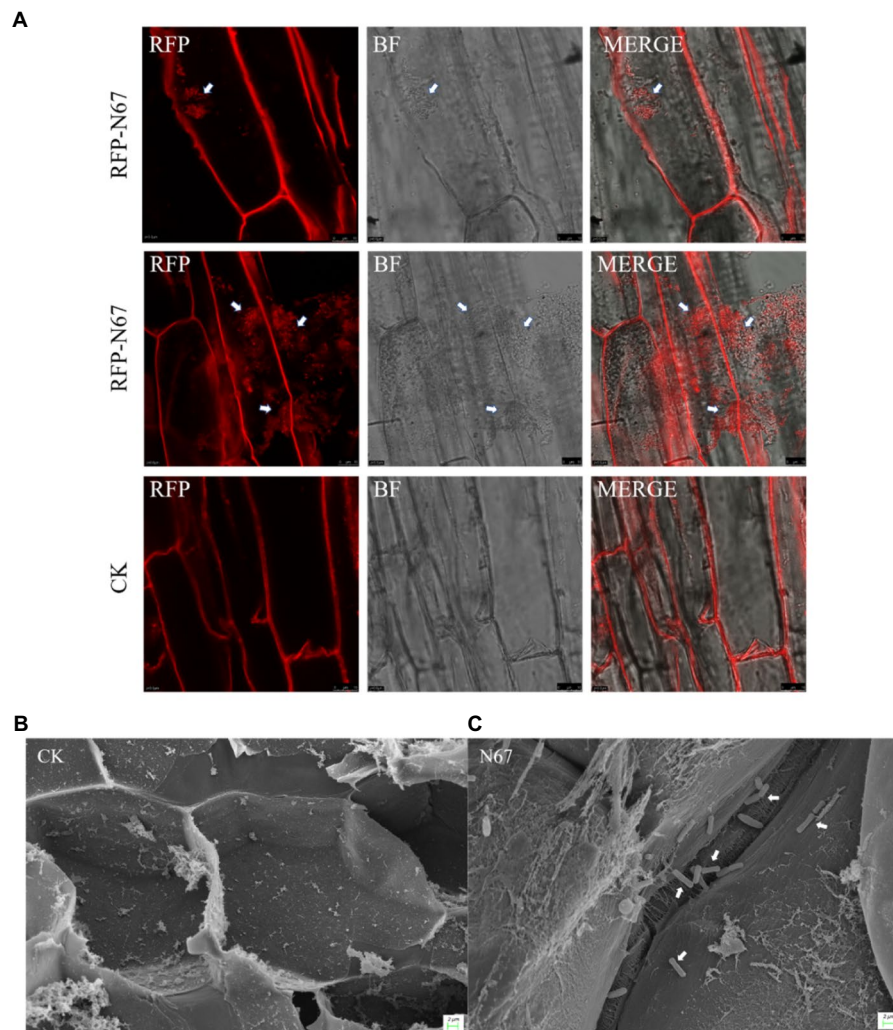
## **DISCUSSION**

Over the last decade, many studies have focused on the interactions of *Foc* with beneficial microorganisms. Generally, researches have centered around “growth promotion,” “systemic resistance induction,” “secondary metabolites syntheses,” etc., which were facilitated by the rapid development of “-omics” tools (Bubici et al., 2019). However, as we know, there are no reliable currently available fluorescent labeled *Bacillus* strains for Banana–Endophyte–Pathogen tritrophic interaction studies. Currently, fluorescence labeling is the best approach for exploring interactions of *Bacillus* spp. with plants *in vivo*. Hence, the fluorescence transformation system we constructed is the first step and of great significance to study the interaction mechanisms associated with TR4 and biological control *Bacillus*. In the process of manipulation, the wild-type *Bacillus* generally has a low transformation efficiency, and some inert *Bacillus* strains cannot even be transformed at all, which seriously affects internal mechanism research of its beneficial properties, such as



**FIGURE 5 |** Antagonistic effect of RFP-labeled *Bacillus* compared to the WT *Bacillus*. The plate inoculated with pathogen only was used as the control (CK). The antagonistic effect of RFP-strains (left) and WT strains (right), respectively, and the pathogen was inoculated in the center. Five replicates were used.



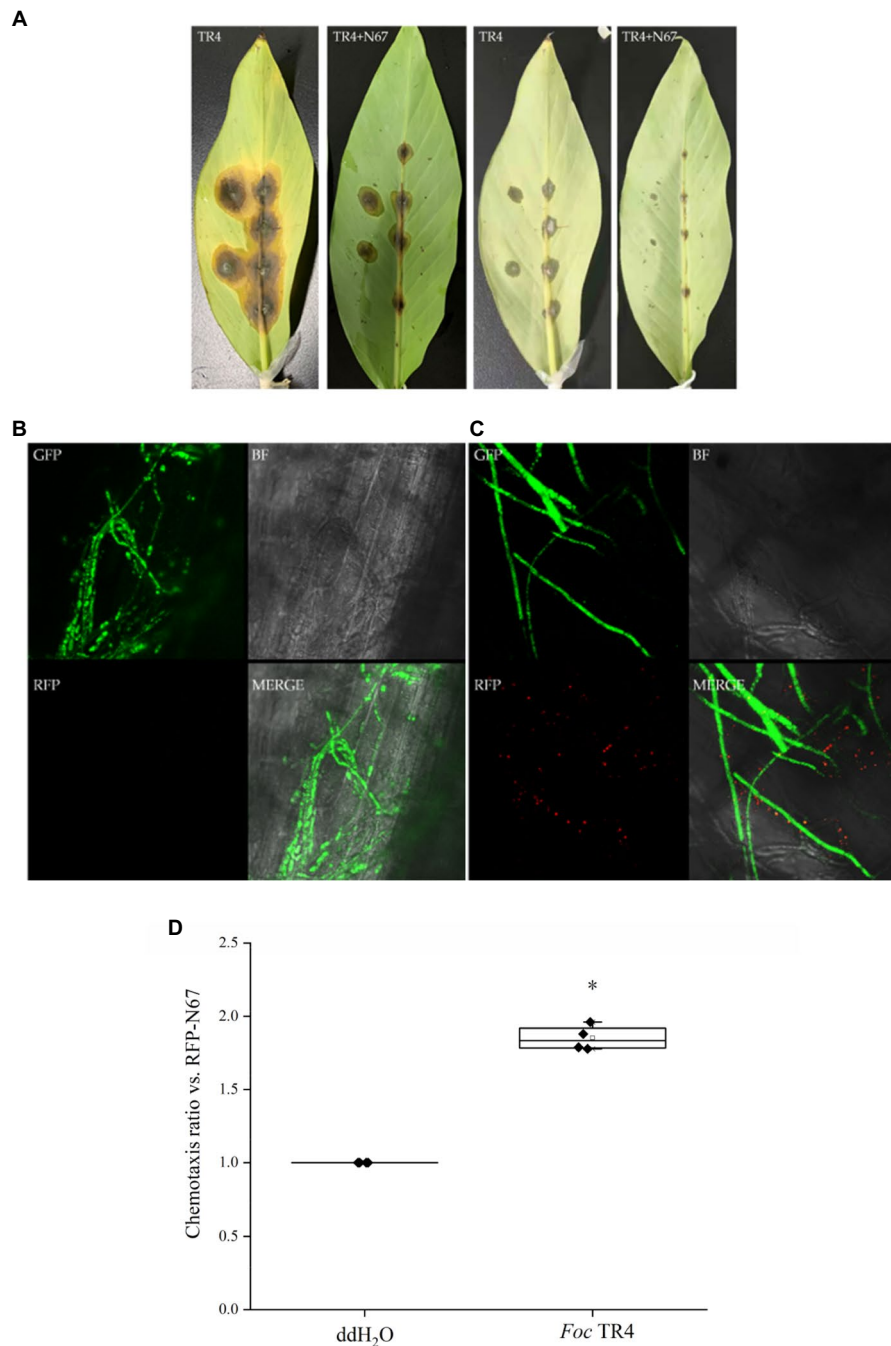


**FIGURE 6 |** *Bacillus velezensis* N67 colonies in banana roots. Banana roots were randomly selected 7 days after inoculant, and the roots were washed with sterile water to remove the medium and bacteria adhering to the surface. Tissue slices were cut out to Laser Confocal Microscopy (LCM) observation and subjected to critical point drying before Scanning Electron Microscopy (SEM) observation. **(A)** Representative fluorescent micrograph of RFP-N67 distributed in banana root cells. Scale bar: 10  $\mu$ m. **(B)** Scanning electron micrograph of control treatment that there were no any bacteria in the banana root cell. **(C)** Representative micrograph of RFP-N67 distributed in banana root xylem cells. The white arrows indicate the bacteria RFP-N67. Three replicates were used. Scale bar: 2  $\mu$ m.

disease prevention, growth promotion, efficient enzyme production, or antibiotics (He, 2014). Currently, the transformation of *Bacillus* mainly includes protoplast transformation, electric shock transformation, natural transformation, and protoplast electric shock transformation (Shen et al., 2013; He, 2014; Kang, 2019; Plucker et al., 2021; Wang, 2021). In this study, we have explored the different methods and conditions of fluorescent transformation of TR4-antagonistic strains. The results showed that we only got the positive transformants by the method of electric shock transformation. Through the natural transformation method, all seven *Bacillus* strains could not form naturally competent cells or positive transformants, even if we tested in the different transformation conditions, such as culture time, plasmid concentration, and recovery time. The low electro-transformation efficiency of wild-type *Bacillus* may be related to the

restriction-repair system in the cell (Zhang et al., 2012). According to the statistics of REBASE (a professional database of restriction endonucleases), approximately 88% bacterial genomes contain restriction-repair systems, and 43% contain four or more restriction-repair systems (Roberts et al., 2007). The restriction-repair system is a barrier for bacteria to exclude external DNA, thus preventing the transformation of bacteriophages and external plasmids, thereby maintaining the integrity and functional stability of its own genetic material. At present, the restriction-repair systems have been found in a variety of bacteria and archaea (Roberts et al., 2003). Finding a way to prevent the wild-type bacteria from degrading the external DNA during the transformation process is the key to improving the efficiency of electric shock transformation.

In the process of cell-wall synthesis, glycine can replace D(L)-alanine in the peptidoglycan component of the bacterial



**FIGURE 7 |** *Bacillus velezensis* RFP-N67 exhibits chemotaxis toward the GFP-TR4 pathogen. N67-RFP in 9% physiological saline solution was injected into the leaf vascular bundles, and the pathogen GFP-TR4 was placed on the injection wound. **(A)** Disease incidence of banana leaves after 7 days' inoculation. The first two pictures show the front side of the leaves, and the last two pictures show the back side of the leaves. Three replicates were used. **(B)** Microscopy of the control treatment, which injected 9% physiological saline solution with no bacteria, inoculated the GFP-TR4 only. **(C)** Representative micrographs of N67-RFP showed significantly chemotropic toward GFP-TR4. BF, bright field; RFP, red fluorescent field; GFP, green fluorescent field; and MERGE, merge image with BF, RFP, and GFP fields. Three replicates were used. **(D)** Chemotaxis ratio of RFP-N67 toward *Foc* TR4. \* indicate the significance between treatments at the 0.05 level.

cell wall, which reduces the degree of cross-linking of peptidoglycan and interferes with the synthesis and assembly of the cell wall, thus loosening the cell wall (Anderson et al., 1966; Zhu et al., 2020). It has been reported that the addition of some compounds that inhibit cell-wall synthesis [such as

glycine, threonine, penicillin, or Tween 80 (affecting cell membranes' fluidity)] during the exponential growth stage of *Bacillus* can improve the transformation efficiency (Holo and Nes, 1989; Zhang et al., 2011). After numerous repeated experiments, we added glycine, sorbitol, threonine, and Tween

80 to the electro-transformation growth medium, finding this helps *Bacillus* more easily absorb external DNA to form positive transformants. Although transformation efficiency is between  $1 \times 10^2$ – $10^3$  cfu/ $\mu$ g of plasmid DNA in the repetitive experiment, indicating our transformation system is still needed to be further optimized, which means that there is still much space for improvement in the transformation of inert *Bacillus* strains. However, this electric shock transformation system is reproducible and stable because we have generated RFP-labeled *Bacillus* in all seven strains from two main banana producing areas, Yunnan and Guangxi provinces, China (Figure 2B; Supplementary Figures S2A–E).

There are other methods that can also improve transformation efficiency: a good way to temporarily inactivate restriction endonuclease in the host bacterium is by incubating at a certain temperature for a couple of times after electric shock. *Corynebacterium glutamicum* was cultured by shaking under low-temperature to prepare electro-transformation competent cells, and then rapidly heat shocked after the electric shock, the results showed that the electro-transformation efficiency was increased fourfold (Rest et al., 1999). Heat-shocking after electric shock transformation of *B. amyloliquefaciens*, increased transformation efficiency by 10-fold (Zhang et al., 2011). In addition, due to the restriction endonuclease and methylase in the wild-type bacteria restriction-repair systems often appearing in pairs, the *in vivo* methylation modification of the exogenous plasmid to be transformed in the same cell can evade restriction-enzyme digestion and degradation of the host wild-type bacteria during the transformation process, thereby improving the transformation efficiency. Through this strategy, the transformation efficiency of *Bifidobacterium adolescentis* ATCC15703 was increased fivefold (Yasui et al., 2009), and the transformation efficiency of *B. amyloliquefaciens* TA208 and *B. cereus* ATCC10987 was increased almost fourfold (Zhang et al., 2012).

A vital factor affecting the expression of fluorescent proteins in *Bacillus* is plasmid instability. In order to explore the stability of plasmid pYP69 in *Bacillus* strains, we detected RFP expression and the loss-ratio of plasmid in the transformed strains with regularly sampling. This showed that within 50h of culture, more than 98% of the cells expressed RFP, indicating that very few cells lost their plasmids (Figure 3), and *Bacillus* growth rate was not affected (Figure 4; Supplementary Figures S3A–E). According to previous reports (Bonfrate et al., 2013), the propagation rate of *Bacillus* in natural environments is 50–100h/generation, and the rate of propagation under laboratory conditions is 20–30 min/generation. Based on this, it could be calculated that the number of fluorescent strain propagations during 50h is about 100–150 generations. In other words, the plasmid pYP69 still exists stably after 100–150 generations, indicating that it has a very strong compatibility with bacteria. Therefore, RFP-labeled *Bacillus* will be suitable for monitoring its colonizing activities in banana host plants in our next research step.

Nowadays, the biological control of banana *Fusarium* wilt is always focused on screening antagonistic strains, while ignoring the research on the colonization of antagonistic bacteria in soil

or plants. Many of the selected antagonistic bacteria have obvious antibacterial effects *in vitro* or pot experiments, but they usually lose biocontrol effects in the field (Jing et al., 2020; Wei et al., 2020). Therefore, the successful colonization of biocontrol bacteria is an important pre-condition for its application and function in field. Some studies have shown that the colonization of plant growth promoting rhizobacteria (PGPR) is affected by abiotic factors, such as soil temperature, texture, water content, and oxygen content. Biotic factors including root exudates, plant growth conditions, bacterial chemotaxis, the nature of self-regulation mechanisms, and bacterial trophic type also affect colonization (Yajing, 2018). At present, a few studies have been carried out on the colonization of strains controlling banana wilt. Dai (Yajing, 2018) detected the quantity of different PGPR in banana soil rhizosphere by fluorescence quantitative PCR. The results indicated that the biomass of three antagonistic bacteria in banana rhizosphere soil was increased significantly, indicating that the three PGPR strains M8, C5, C14 can colonize banana roots (Lin, 2011). Their colonization determination studies used antibiotic-labeled strains and showed that labeled strains could be isolated by wound inoculation, irrigated inoculation, and axil inoculation. The control did not show any bacterial colonies, indicating that with three methods of inoculation, the labeled strains can be colonized in banana. Chao et al. (2010) used the scanning electron microscope to observe biocontrol bacteria FJAT-346-PA-K in tissue-cultured banana plantlets 10 days after inoculation. They successfully found that there were biocontrol bacteria in the roots' internal tissues and banana stems. We inoculated the wild-type strain N67 into tissue-cultured banana plantlets, and it was also confirmed by scanning electron microscope that N67 could successfully colonize the banana root cells (Figures 6B,C). However, this method can only preliminarily judge the existence of biocontrol strains in the plant, and it cannot clearly figure out the internal activity *in vivo*. Therefore, we constructed red fluorescent-labeled strains to observe its dynamic migration in banana plants, and the results showed that the biocontrol strains can successfully colonize the roots but not in the corm or pseudostem due to short incubation period (Figure 6A). We also injected RFP-labeled bacteria into the detached leaf which is proved to be a reliable protocol (Liu et al., 2020). The results showed that the biocontrol strains can successfully colonize and grow in the leaf, as well as displaying a positive chemotaxis response toward TR4 hyphae, indicating that the biocontrol bacteria can effectively interact with and inhibit the pathogen *in vivo* (Figure 7). Other studies have shown that chemoattraction of bacteria could contribute to its root colonization (Palmieri et al., 2020). *Fusarium oxysporum* f. sp. *lycopersici* (Fol) is known to facilitate bacterial movement in search of nutrients which also exhibits chemotaxis toward plant roots (Furuno et al., 2009; Turra et al., 2015). We thus conclude that N67 not only directly inhibits TR4 hyphae growth, but it could also benefit from the capacity of pathogen hyphae trends to plant colonization and thus increases colonization efficiency. Significant progress has been made in other crops by using fluorescent-labeled strains for colonization observation. Kang (2019) observed that the endophytic *B. velezensis* CC09 Bv-GFP can not only effectively colonize wheat roots, but also

migrate to stem and leaf organs to achieve whole plant distribution. He (2014) observed the roots of maize seedlings inoculated with Y2-P43GFPmut3a by fluorescence microscope, showing that Y2 strain successfully colonized root surfaces and interiors. However, as far as we know, there is no research on the *in vivo* interaction of RFP-*Bacillus* for monitoring TR4 in banana, so dynamic migration is our next proposed research.

With the great progress of gene-sequencing technology, more and more *Bacillus* whole genomes have been sequenced. Using such tools, it will be important to explore the potential biocontrol mechanisms among *Bacillus*, pathogens, and plants (Bubici et al., 2019; Carrión et al., 2019; Jiang et al., 2019; Chen et al., 2020; Jing et al., 2020; Wei et al., 2020). The biocontrol mechanisms of *Bacillus* are usually considered to be based on one or more of: (1) Antagonism: *Bacillus* often secretes secretory secondary metabolites that inhibit pathogen growth. (2) Competition: *Bacillus* competes for niches with pathogens and other microorganisms to obtain nutrients and other resources. (3) Inducing systemic resistance: they can activate host defense responses by inducing systemic resistance. (4) Promoting growth: *Bacillus* can provide necessary mineral nutrition and plant hormones (e.g., IAA) for plant hosts to support their life activities. These mechanisms of *Bacillus* are interrelated and synergistic. Of course, the principal *Bacillus* biocontrol mechanism(s) could be different in different crops.

It is an innovative research direction to develop new biopesticides and new agricultural antibiotics by using the antagonistic behavior of microorganisms (Yajing, 2018). It has become an important measure for biological control of TR4 in organic farming by researching “biological fertilizer” (where organic fertilizers are inoculated with biocontrol agents) and banana growth-promoting bacterial agents to increase yield and disease resistance (Ling et al., 2014; Fu et al., 2016). Nowadays, biological control for sustainable banana production has attracted much attention. New biological microorganism agents are urgently needed to replace traditional chemical pesticides, which continue to cause pollution and damage the environment, and degrade soils. Microbial agents as recognized promising “pollution-free pesticides” will play a crucial role in managing agricultural and silvicultural diseases and protecting ecological balance.

## CONCLUSION

We successfully developed an optimized fluorescent electro-transformation system of TR4-inhibitory *Bacillus* spp. strains (OD<sub>600</sub>=0.7, plasmid concentration=50 ng/μl, volume=2 μl, voltage=1.8 kV, and capacitance=400 Ω). The RFP-labeled *Bacillus* strains have high stability, and their growth rates and inhibition effects on TR4 are unaffected by fluorescent plasmid insertion. *In vivo* colonizing observation by Laser Scanning Confocal microscopy (LSCM) and SEM showed that *Bacillus* spp. can colonize the xylem cells of banana plantlets' roots. Further fluorescent observation by LSCM showed these RFP-labeled bacteria exhibit chemotaxis toward the hyphae of

the green fluorescent protein (GFP)-labeled TR4 pathogen in banana leaves.

## DATA AVAILABILITY STATEMENT

The original contributions presented in the study are included in the article/Supplementary Material, further inquiries can be directed to the corresponding authors.

## AUTHOR CONTRIBUTIONS

PH conceived, designed, and performed the experiment, analyzed the data, and wrote the paper. SL conceived, designed, and performed the experiment, and analyzed the data. S-JZ conceived and designed the experiment and prepared the manuscript. SX, HF, YW, and GH analyzed the data. WZ and GF provided the strains sources and analyzed the data. S-JZ and Y-YW supervised the research and provided funding support. All authors contributed to the article and approved the submitted version.

## FUNDING

This research was funded by Science and Technology Department of Yunnan Provincial Government (202001AU070150 and 202102AE090003), Yunling Scholar Programme of Yunnan Provincial Government (YNWR-YLXZ-2018-018), Program for the Innovative Research Team of Green Prevention and Control of Agricultural Transboundary Pests of Yunnan Province (2020–2022), the CGIAR Re-search Program (CRP) on Roots, Tubers, and Bananas (RTB). CRPs are implemented with support from the CGIAR Trust Fund and through bilateral funding agreements. For details, please visit <https://ccafs.cgiar.org/donors>. The views expressed in this document cannot be taken to reflect the official opinions of these organizations.

## ACKNOWLEDGMENTS

We are grateful to Yiyang Yu and Yongmei Li for kindly providing the plasmid. Yongmei Li helped with discussion and ideas during the development of the transformation protocol. Zhijia Gu supported Scanning Electron Microscopy, and Shuiying Zhang supported Laser Confocal Electron Microscope microscopy. We also acknowledge Vincent Johnson of GreenQuills and the Alliance of Bioversity International and CIAT for his editorial review.

## SUPPLEMENTARY MATERIAL

The Supplementary Material for this article can be found online at: <https://www.frontiersin.org/articles/10.3389/fmicb.2021.754918/full#supplementary-material>



## REFERENCES

- Alegre, M. T., Rodriguez, M. C., and Mesas, J. M. (2004). Transformation of *Lactobacillus plantarum* by electroporation with in vitro modified plasmid DNA. *FEMS Microbiol. Lett.* 241, 73–77. doi: 10.1016/j.femsle.2004.10.006
- Anderson, J. S., Meadow, P. M., Haskin, M. A., and Strominger, J. L. (1966). Biosynthesis of the peptidoglycan of bacterial cell walls. *Arch. Biochem. Biophys.* 116, 487–515. doi: 10.1016/0003-9861(66)90056-7
- Bonfrate, L., Tack, J., Grattagliano, I., Cuomo, R., and Portincasa, P. (2013). Microbiota in health and irritable bowel syndrome current knowledge, perspectives and therapeutic options. *Scand. J. Gastroenterol.* 48, 995–1009. doi: 10.3109/00365521.2013.799220z
- Borriss, R., Chen, X. H., Rueckert, C., Blom, J., Becker, A., Baumgarth, B., et al. (2011). Relationship of clades associated with strains DSM 7and FZB42: a proposal for subsp. subsp. nov. and subsp. subsp. nov. based on complete genome sequence comparisons. *Int. J. Syst. Evol. Microbiol.* 61, 1786–1801. doi: 10.1099/ijs.0.023267-0
- Bubici, G., Kaushal, M., Prigigallo, M. I., Gomez-Lama Cabanas, C., and Mercado-Blanco, J. (2019). Biological control agents against Fusarium wilt of Banana. *Front. Microbiol.* 10:616. doi: 10.3389/fmicb.2019.00616
- Carrión, V. J., Perez-Jaramillo, J., Cordovez, V., Tracanna, V., Hollander, M. D., Ruiz-Buck, D., et al. (2019). Pathogen-induced activation of disease-suppressive functions in the endophytic root microbiome. *Science* 366, 606–612. doi: 10.1126/science.aaw9285
- Carvalho, L. C., Henderson, J., Rincon-Florez, V. A., Dwyer, C. O., Czulowski, E., Aitken, E. A. B., et al. (2019). Molecular diagnostics of banana fusarium wilt targeting secreted-in-xylem genes. *Front. Plant Sci.* 10:547. doi: 10.3389/fpls.2019.00547
- Chao, Y., Rongfeng, X., Bo, L., Naisuan, L., and Lu, C. (2010). Endophytic colonization of biocontrol bacterium FJAT\_346\_PA and its efficiency against banana Fusarium wilt. *Acta Phytopathol. Sin.* 37, 493–498. doi: 10.13802/j.cnki.zwbhxb.2010.06.020
- Chen, Y., Cao, S., Chai, Y., Clardy, J., Kolter, R., Guo, J. H., et al. (2012). A *Bacillus subtilis* sensor kinase involved in triggering biofilm formation on the roots of tomato plants. *Mol. Microbiol.* 85, 418–430. doi: 10.1111/j.1365-2958.2012.08109.x
- Chen, Y., Liu, T., Li, Q., Ma, Y., Cheng, J., and Xu, L. (2020). Screening for candidate genes associated with biocontrol mechanisms of *Bacillus pumilus* DX01 using Tn5 transposon mutagenesis and a 2-DE-based comparative proteomic analysis. *Curr. Microbiol.* 77, 3397–3408. doi: 10.1007/s00284-020-02191-0
- Chen, A., Sun, J., Matthews, A., Armas-Egas, L., Chen, N., Hamill, S., et al. (2019). Assessing variations in host resistance to *Fusarium oxysporum* f. sp. cubense race 4 in Musa species, With a focus on the subtropical race 4. *Front. Microbiol.* 10:1062. doi: 10.3389/fmicb.2019.01062
- Compant, S., Duffy, B., Nowak, J., Clement, C., and Barka, E. A. (2005). Use of plant growth-promoting bacteria for biocontrol of plant diseases: principles, mechanisms of action, and future prospects. *Appl. Environ. Microbiol.* 71, 4951–4959. doi: 10.1128/AEM.71.9.4951-4959.2005
- Damodaran, T., Rajan, S., Muthukumar, M., Ram, G., Yadav, K., Kumar, S., et al. (2020). Biological management of Banana Fusarium Wilt caused by *Fusarium oxysporum* f. sp. cubense tropical race 4 using antagonistic fungal isolate CSR-T-3 (*Trichoderma reesei*). *Front. Microbiol.* 11:595845. doi: 10.3389/fmicb.2020.595845
- Daniells, J. W. (2011). Combating Banana wilts—what do resistant cultivars have to offer? *Acta Hort.* 897, 403–411. doi: 10.17660/ActaHortic.2011.897.56
- Fan, B., Chen, X. H., Budiharjo, A., Bleiss, W., Vater, J., and Borriss, R. (2011). Efficient colonization of plant roots by the plant growth promoting bacterium *Bacillus amyloliquefaciens* FZB42, engineered to express green fluorescent protein. *J. Biotechnol.* 151, 303–311. doi: 10.1016/j.jbiotec.2010.12.022
- Fira, D., Dimkic, I., Beric, T., Lozo, J., and Stankovic, S. (2018). Biological control of plant pathogens by bacillus species. *J. Biotechnol.* 285, 44–55. doi: 10.1016/j.jbiotec.2018.07.044
- Fu, L., Ruan, Y., Tao, C., Li, R., and Shen, Q. (2016). Continuous application of bioorganic fertilizer induced resilient culturable bacteria community associated with banana Fusarium wilt suppression. *Sci. Rep.* 6:27731. doi: 10.1038/srep27731
- Furuno, S., Pätzolt, K., Rabe, C., Neu, T. R., Harms, H., and Wick, L. Y. (2009). Fungal mycelia allow chemotactic dispersal of polycyclic aromatic hydrocarbon-degrading bacteria in water-unsaturated systems. *Environ. Microbiol.* 12, 1391–1398. doi: 10.1111/j.1462-2920.2009.02022.x
- Ghag, S. B., Shekhawat, U. K. S., and Ganapathi, T. R. (2015). Fusarium wilt of banana: biology, epidemiology and management. *Int. J. Pest Manag.* 61, 250–263. doi: 10.1080/09670874.2015.1043972
- Guan, X., and Jiang, H. (2013). The research on development of bacillus *Amylolyticus*. *Biotech. World* 4.
- He, P. (2014). Genomic Analysis of B9601-Y2 Strain and Partial Functions Confirmation. Doctor, Huazhong Agricultural University.
- Heslop-Harrison, J. S., and Schwarzacher, T. (2007). Domestication, genomics and the future for banana. *Ann. Bot.* 100, 1073–1084. doi: 10.1093/aob/mcm191
- Holo, H., and Nes, I. F. (1989). High-frequency transformation, by electroporation, of *Lactococcus lactis* subsp. *cremoris* grown with glycine in osmotically stabilized media. *Appl. Environ. Microbiol.* 55, 3119–3123. doi: 10.1128/aem.55.12.3119-3123.1989
- Hwang, S.-C., and Ko, W.-H. (2004). Cavendish Banana cultivars resistant to Fusarium wilt acquired through Somaclonal variation in Taiwan. *Plant Dis.* 88, 580–588. doi: 10.1094/PDIS.2004.88.6.580
- Jiang, C. H., Yao, X. F., Mi, D. D., Li, Z. J., Yang, B. Y., Zheng, Y., et al. (2019). Comparative Transcriptome analysis reveals the biocontrol mechanism of *Bacillus velezensis* F21 Against Fusarium wilt on watermelon. *Front. Microbiol.* 10:652. doi: 10.3389/fmicb.2019.00652
- Jing, T., Zhou, D., Zhang, M., Yun, T., Qi, D., Wei, Y., et al. (2020). Newly isolated *Streptomyces* sp. JBS5-6 as a potential biocontrol agent to control Banana Fusarium wilt: genome sequencing and secondary metabolite cluster profiles. *Front. Microbiol.* 11:602591. doi: 10.3389/fmicb.2020.602591
- Kang, X. (2019). Mechanism of *Bacillus velezensis* CC09 in Controlling Pathogen *Gaeumannomyces graminis* var. *tritici*. Doctor, Nanjing University.
- Li, S., He, P., Fan, H., Liu, L., Yin, K., Yang, B., et al. (2021). A real-time fluorescent reverse transcription quantitative PCR assay for rapid detection of genetic markers' expression associated with *Fusarium* Wilt of banana biocontrol activities in *Bacillus*. *J. Fungi* 7:353. doi: 10.3390/jof7050353
- Li, X., Li, K., Zhou, D., Zhang, M., Qi, D., Jing, T., et al. (2020a). Biological control of Banana wilt disease caused by *Fusarium Oxysporum* f. sp. *Cubense* using *Streptomyces* sp. H4. *Biol. Control* 155:104525. doi: 10.1016/j.biocontrol.2020.104524
- Li, Z., Wang, T., He, C., Cheng, K., Zeng, R., and Song, Y. (2020b). Control of Panama disease of banana by intercropping with Chinese chive (*Allium tuberosum* Rottler): cultivar differences. *BMC Plant Biol.* 20:432. doi: 10.1186/s12870-020-02640-9
- Lin, Z. (2011). Investigation on the Biocontrol Mechanism of *Bacillus subtilis* Strain TR21 against Banana *Fusarium* Wilt. Master, Huazhong Agricultural University.
- Ling, N., Deng, K., Song, Y., Wu, Y., Zhao, J., Raza, W., et al. (2014). Variation of rhizosphere bacterial community in watermelon continuous mono-cropping soil by long-term application of a novel bioorganic fertilizer. *Microbiol. Res.* 169, 570–578. doi: 10.1016/j.micres.2013.10.004
- Liu, S., Li, J., Zhang, Y., Liu, N., Viljoen, A., Mostert, D., et al. (2020). Fusaric acid instigates the invasion of banana by *Fusarium oxysporum* f. sp. *cubense* TR4. *New Phytol.* 225, 913–929. doi: 10.1111/nph.16193
- Malfanova, N., Lugtenberg, B. J. J., and Berg, G. (2013). *Bacterial Endophytes: Who and Where, and What Are They Doing There?* New Jersey: John Wiley & Sons Inc.
- Nadarajah, H., Sreeramanan, S., and Zakaria, L. (2016). Effects of genotype and intercropping with Chinese chives (*Allium tuberosum*) on Fusarium wilt tropical race 4 in banana. *Acta Hort.* 1114, 153–160. doi: 10.17660/ActaHortic.2016.1114.22
- Palmieri, D., Vitale, S., Lima, G., Di Pietro, A., and Turra, D. (2020). A bacterial endophyte exploits chemotaxis of a fungal pathogen for plant colonization. *Nat. Commun.* 11:5264. doi: 10.1038/s41467-020-18994-5
- Ploetz, R. C. (2006). Fusarium wilt of Banana is caused by several pathogens referred to as *Fusarium oxysporum* f. sp. *cubense*. *Phytopathology* 96, 653–656. doi: 10.1094/PHYTO-96-0653
- Ploetz, R. C. (2015). Management of *Fusarium* wilt of banana: a review with special reference to tropical race 4. *Crop Prot.* 73, 7–15. doi: 10.1016/j.cropro.2015.01.007

- Plucker, L., Bosch, K., Geissl, L., Hoffmann, P., and Gohre, V. (2021). Genetic manipulation of the Brassicaceae smut fungus *Thecaphora thlaspeos*. *J. Fungi* 7:38. doi: 10.3390/jof7010038
- Presti, L. L., Lanver, D., Schweizer, G., Tanaka, S., Liang, L., Tollot, M., et al. (2015). Fungal effectors and plant susceptibility. *Annu. Rev. Plant Biol.* 66, 513–545. doi: 10.1146/annurev-arplant-043014-114623
- Priest, F. G., Goodfellow, M., Shute, L. A., and Berkeley, R. C. W. (1987). *Bacillus amyloliquefaciens* sp. nov. norn. rev. *Int. J. Syst. Bacteriol.* 37, 69–71. doi: 10.1099/00207713-37-1-69
- ProMusa (2021). Tropical race 4. Available at: <https://www.promusa.org/Tropical+race+4+--+TR4#footnote61> (Accessed Sep 8, 2021).
- Radhakrishnan, R., Hashem, A., and Abd Allah, E. F. (2017). *Bacillus*: a biological tool for crop improvement through bio-molecular changes in adverse environments. *Front. Physiol.* 8:667. doi: 10.3389/fphys.2017.00667
- Rest, M. E. V. D., Lange, C., and Molenaar, D. (1999). A heat shock following electroporation induces highly efficient transformation of *Corynebacterium glutamicum* with xenogeneic plasmid DNA. *Appl. Microbiol. Biotechnol.* 52, 541–545. doi: 10.1007/s002530051557
- Roberts, R. J., Vincze, T., Posfai, J., and Macelis, D. (2003). REBASE: restriction enzymes and methyltransferases. *Nucleic Acids Res.* 31, 418–420. doi: 10.1093/nar/gkg069
- Roberts, R. J., Vincze, T., Posfai, J., and Macelis, D. (2007). REBASE—enzymes and genes for DNA restriction and modification. *Nucleic Acids Res.* 35, D269–D270. doi: 10.1093/nar/gkl891
- Scherwinski, K., Grosch, R., and Berg, G. (2008). Effect of bacterial antagonists on lettuce: active biocontrol of *Rhizoctonia solani* and negligible, short-term effects on nontarget microorganisms. *FEMS Microbiol. Ecol.* 64, 106–116. doi: 10.1111/j.1574-6941.2007.00421.x
- Shen, X., Chen, Y., Liu, T., Hu, X., and Gu, Z. (2013). Development of a high-efficient transformation system of *Bacillus pumilus* strain DX01 to facilitate gene isolation via gfp-tagged insertional mutagenesis and visualize bacterial colonization of rice roots. *Folia Microbiol.* 58, 409–417. doi: 10.1007/s12223-013-0223-0
- Stein, T. (2005). *Bacillus subtilis* antibiotics: structures, syntheses and specific functions. *Mol. Microbiol.* 56, 845–857. doi: 10.1111/j.1365-2958.2005.04587.x
- Sun, J., Zhang, J., Fang, H., Peng, L., Wei, S., Li, C., et al. (2019). Comparative transcriptome analysis reveals resistance-related genes and pathways in *Musa acuminata* banana ‘Guijiao 9’ in response to *Fusarium* wilt. *Plant Physiol. Biochem.* 141, 83–94. doi: 10.1016/j.plaphy.2019.05.022
- Swarupa, V., Ravishankar, K. V., and Rekha, A. (2014). Plant defense response against *Fusarium oxysporum* and strategies to develop tolerant genotypes in banana. *Planta* 239, 735–751. doi: 10.1007/s00425-013-2024-8
- Turra, D., El Ghalid, M., Rossi, E., and Di Pietro, A. (2015). Fungal pathogen uses sex pheromone receptor for chemotropic sensing of host plant signals. *Nature* 527, 521–524. doi: 10.1038/nature15516
- Wang, P. (2021). Genetic transformation in *Cryptococcus* species. *J. Fungi* 7:56. doi: 10.3390/jof7010056
- Wang, J., Zhao, Y., and Ruan, Y. (2015). Effects of bio-organic fertilizers produced by four *Bacillus amyloliquefaciens* strains on Banana *Fusarium* wilt disease. *Compost Sci. Util.* 23, 185–198. doi: 10.1080/1065657x.2015.1020398
- Wei, Y., Zhao, Y., Zhou, D., Qi, D., Li, K., Tang, W., et al. (2020). A newly isolated *Streptomyces* sp. YYS-7 with a broad-spectrum antifungal activity improves the Banana plant resistance to *Fusarium oxysporum* f. sp. cubense tropical race 4. *Front. Microbiol.* 11:1712. doi: 10.3389/fmicb.2020.01712
- Xue, C., Penton, C. R., Shen, Z., Zhang, R., Huang, Q., Li, R., et al. (2015). Manipulating the banana rhizosphere for biological control of Panama disease. *Sci. Rep.* 5:11124. doi: 10.1038/srep11124
- Yajing, D. (2018). Isolation of Bio-Control Bacteria against *Fusarium* Wilt and their Colonization in Banana Rhizosphere Soil. Master, Fujian Agriculture and Forestry University.
- Yasui, K., Kano, Y., Tanaka, K., Watanabe, K., Shimizu-Kadota, M., Yoshikawa, H., et al. (2009). Improvement of bacterial transformation efficiency using plasmid artificial modification. *Nucleic Acids Res.* 37:e3. doi: 10.1093/nar/gkn884
- Zhang, G.-Q., Bao, P., Zhang, Y., Deng, A.-H., Chen, N., and Wen, T.-Y. (2011). Enhancing electro-transformation competency of recalcitrant *Bacillus amyloliquefaciens* by combining cell-wall weakening and cell-membrane fluidity disturbing. *Anal. Biochem.* 409, 130–137. doi: 10.1016/j.ab.2010.10.013
- Zhang, N., He, X., Zhang, J., Raza, W., Yang, X.-M., Ruan, Y.-Z., et al. (2014). Suppression of *Fusarium* wilt of Banana with application of bio-organic fertilizers. *Pedosphere* 24, 613–624. doi: 10.1016/s1002-0160(14)60047-3
- Zhang, G., Wang, W., Deng, A., Sun, Z., Zhang, Y., Liang, Y., et al. (2012). A mimicking-of-DNA-methylation-patterns pipeline for overcoming the restriction barrier of bacteria. *PLoS Genet.* 8:e1002987. doi: 10.1371/journal.pgen.1002987
- Zhang, L., Yuan, T., Wang, Y., Zhang, D., Bai, T., Xu, S., et al. (2018). Identification and evaluation of resistance to *Fusarium oxysporum* f. sp. cubense tropical race 4 in *Musa acuminata* Pahang. *Euphytica* 214:106. doi: 10.1007/s10681-018-2185-4
- Zhou, W., Tian, D., Li, C., Qin, L., Wei, D., Wei, S., et al. (2020). Isolation and identification of endophytic bacteria G9R-3 in Banana and antagonistic activity evaluation against *Fusarium oxysporum* f.sp.cubense race 4. *South. Chin. J. Agric. Sci.* 33, 1493–1498. doi: 10.16213/j.cnki.scjas.2020.7.024
- Zhu, Y.-C., Sun, D.-X., Deng, Y., An, G.-L., Li, W.-H., Si, W.-J., et al. (2020). Comparative transcriptome analysis of the effect of different heat shock periods on the unfertilized ovule in watermelon (*Citrullus lanatus*). *J. Integr. Agric.* 19, 528–540. doi: 10.1016/s2095-3119(19)62777-2

**Conflict of Interest:** The authors declare that the research was conducted in the absence of any commercial or financial relationships that could be construed as a potential conflict of interest.

**Publisher’s Note:** All claims expressed in this article are solely those of the authors and do not necessarily represent those of their affiliated organizations, or those of the publisher, the editors and the reviewers. Any product that may be evaluated in this article, or claim that may be made by its manufacturer, is not guaranteed or endorsed by the publisher.

Copyright © 2021 He, Li, Xu, Fan, Wang, Zhou, Fu, Han, Wang and Zheng. This is an open-access article distributed under the terms of the Creative Commons Attribution License (CC BY). The use, distribution or reproduction in other forums is permitted, provided the original author(s) and the copyright owner(s) are credited and that the original publication in this journal is cited, in accordance with accepted academic practice. No use, distribution or reproduction is permitted which does not comply with these terms.



# Cultivar Contributes to the Beneficial Effects of *Bacillus subtilis* PTA-271 and *Trichoderma atroviride* SC1 to Protect Grapevine Against *Neofusicoccum parvum*

Catarina Leal<sup>1</sup>, Nicolas Richet<sup>1</sup>, Jean-François Guise<sup>1</sup>, David Gramaje<sup>2</sup>, Josep Armengol<sup>3</sup>, Florence Fontaine<sup>1</sup> and Patricia Trotel-Aziz<sup>1\*</sup>

<sup>1</sup> University of Reims Champagne-Ardenne, Résistance Induite et Bioprotection des Plantes Research Unit, EA 4707, INRAE USC 1488, SFR Condorcet FR CNRS 3417, Reims, France, <sup>2</sup> Instituto de Ciencias de la Vid y del Vino, Consejo Superior de Investigaciones Científicas, Universidad de La Rioja, Gobierno de La Rioja, Logroño, Spain, <sup>3</sup> Instituto Agroforestal Mediterráneo, Universitat Politècnica de València, Valencia, Spain

## OPEN ACCESS

### Edited by:

Fred Asiegbu,  
University of Helsinki, Finland

### Reviewed by:

Pierluigi Revegilia,  
University of Foggia, Italy  
Danai Gkizi,  
Agricultural University of Athens,  
Greece

Regina Billones-Baaijens,  
Charles Sturt University, Australia

### \*Correspondence:

Patricia Trotel-Aziz  
patricia.trotel-aziz@univ-reims.fr

### Specialty section:

This article was submitted to  
Microbe and Virus Interactions with  
Plants,  
a section of the journal  
Frontiers in Microbiology

Received: 16 June 2021

Accepted: 08 September 2021

Published: 14 October 2021

### Citation:

Leal C, Richet N, Guise J-F, Gramaje D, Armengol J, Fontaine F and Trotel-Aziz P (2021) Cultivar Contributes to the Beneficial Effects of *Bacillus subtilis* PTA-271 and *Trichoderma atroviride* SC1 to Protect Grapevine Against *Neofusicoccum parvum*. *Front. Microbiol.* 12:726132. doi: 10.3389/fmicb.2021.726132

Grapevine trunk diseases (GTDs) are a big threat for global viticulture. Without effective chemicals, biocontrol strategies are developed as alternatives to better cope with environmental concerns. A combination of biological control agents (BCAs) could even improve sustainable disease management through complementary ways of protection. In this study, we evaluated the combination of *Bacillus subtilis* (Bs) PTA-271 and *Trichoderma atroviride* (Ta) SC1 for the protection of Chardonnay and Tempranillo rootlings against *Neofusicoccum parvum* Bt67, an aggressive pathogen associated to Botryosphaeria dieback (BD). Indirect benefits offered by each BCA and their combination were then characterized *in planta*, as well as their direct benefits *in vitro*. Results provide evidence that (1) the cultivar contributes to the beneficial effects of Bs PTA-271 and Ta SC1 against *N. parvum*, and that (2) the *in vitro* BCA mutual antagonism switches to the strongest fungistatic effect toward *Np*-Bt67 in a three-way confrontation test. We also report for the first time the beneficial potential of a combination of BCA against *Np*-Bt67 especially in Tempranillo. Our findings highlight a common feature for both cultivars: salicylic acid (SA)-dependent defenses were strongly decreased in plants protected by the BCA, in contrast with symptomatic ones. We thus suggest that (1) the high basal expression of SA-dependent defenses in Tempranillo explains its highest susceptibility to *N. parvum*, and that (2) the cultivar-specific responses to the beneficial Bs PTA-271 and Ta SC1 remain to be further investigated.

**Keywords:** Chardonnay, Tempranillo, biocontrol, *Neofusicoccum parvum*, plant immunity, synergistic effect

## INTRODUCTION

Global environmental changes promote the incidence of plant diseases by increasing the pathogen pressure or make the plants more susceptible to them (O'Brien, 2017; Velásquez et al., 2018). Grapevine trunk diseases (GTDs) are among the most important groups of grapevine diseases all over the world, creating a big concern in all wine-producing countries (Mondello et al., 2018).

Attacking the plant perennial part and leading inevitably to the short- or long-term death of vines, the pathogens responsible of GTDs are described as very injurious for the sustainability of the winemaking industry (Hofstetter et al., 2012). As main restrictors for viticulture, GTDs can lead to high economic losses, less table grape for consumers, and social and environmental disturbances (O'Brien, 2017). Both young and mature vines are affected by GTDs, even as nursery staged plants, reducing both productivity and longevity of the vineyard, thereby causing massive economic losses (Gramaje and Armengol, 2011).

*Botryosphaeria dieback* (BD) is one of the most significant GTDs, triggerable by more than 25 distinct species of Botryosphaeriaceae including the aggressive *Neofusicoccum parvum* (Úrbez-Torres, 2011; Billones-Baaijens and Savocchia, 2019; Reis et al., 2019; Larach et al., 2020). Symptomatic plants develop a low or apoplectic dieback phenotype, including a low budburst rate, a poor vegetative development, external canker, and internal longitudinal necrotic lesions that can lead to a full dead branch (Larignon et al., 2001, 2009; Larignon, 2004; Billones-Baaijens and Savocchia, 2019; Larach et al., 2020). Susceptibility to BD pathogens also differs between cultivars (Travadon et al., 2013; Fontaine et al., 2016a; Chacon et al., 2020; Claverie et al., 2020).

Due to the undetermined period of latency within the vines (asymptomatic state), early detection and management of GTDs remain presently a challenge in both nursery and vineyard, and only few preventives, but no curative methods, are available. Indeed, few chemicals are applied on pruning wounds in vineyards to prevent dissemination of the conidia of fungal pathogens (Sosnowski et al., 2004), preferring cultural practices in vineyard (Mondello et al., 2018) and sanitation methods (Gramaje and Armengol, 2011; Gramaje et al., 2018). However, these kinds of treatments cannot eradicate the pathogens once established in a vineyard (Calzarano et al., 2004; Gramaje and Armengol, 2011). An interesting alternative and complement to the previously cited GTDs control methods in vineyard is the use of biological control agents (BCAs) as reported by Mondello et al. (2018). For instance, several microorganisms have already been evaluated, both *in vitro* and *in planta* against BD pathogens (Hunt et al., 2001; Di Marco et al., 2004; John et al., 2004; Compant et al., 2013; Compant and Mathieu, 2017; Trotel-Aziz et al., 2019). Among them there are bacterial BCAs such as *Pseudomonas*, *Bacillus*, and *Enterobacter* species, and fungal BCAs such as several *Fusarium* and *Trichoderma* species (Mondello et al., 2018). Some of them, such as *Trichoderma atroviride*, *Trichoderma harzianum*, *Bacillus subtilis*, and *Bacillus amyloliquefaciens*, are already commercialized against some GTDs pathogens, or against other hemibiotrophic and necrotrophic pathogens including *Botrytis cinerea*, *Fusarium oxysporum*, or many others (Elad, 2000; Schmidt and Panstruga, 2011; Kuzmanovska et al., 2018; Thambugala et al., 2020; Alfiky and Weisskopf, 2021).

To date, *Trichoderma* species are the most used fungal-based BCA in viticulture (Harman, 2006; Muckherjee et al., 2012; Waghunde et al., 2016) and have been also widely investigated as BCA against GTDs (Di Marco et al., 2002, 2004; John et al., 2008; Halleen et al., 2010; Berbegal et al., 2020;

Martínez-Diz et al., 2021a,b). *Trichoderma* spp. are described to directly antagonize GTD pathogen aggressiveness by competition for nutrients and space, mycoparasitism, cell-wall degrading enzymes, and antibiosis (Harman, 2006; Van Wees et al., 2008; Vinale et al., 2008; Pieterse et al., 2014; Waghunde et al., 2016). *Trichoderma* spp. have also been described as plant growth and defense stimulators (Harman, 2006; Van Wees et al., 2008; Vinale et al., 2008; Pieterse et al., 2014; Waghunde et al., 2016). Among *Trichoderma* spp., *T. atroviride* SC1 was shown to strongly reduce the infections caused by some GTD pathogens in nurseries and established vineyards at the registered dose rate of 2 g/L, equivalent to the density of  $2 \times 10^{10}$  conidia/L recommended by the commercial product (Pertot et al., 2016; Berbegal et al., 2020; Martínez-Diz et al., 2021a). *Bacillus* strains are another group of microorganisms extensively studied as BCA and reported to directly and indirectly protect plants against pathogens with different lifestyles (Magnin-Robert et al., 2007; Trotel-Aziz et al., 2008; Nguyen et al., 2020), including the GTD hemibiotrophic pathogens (Schmidt et al., 2001; Halleen et al., 2010; Rezgui et al., 2016; Kotze et al., 2019; Trotel-Aziz et al., 2019). A broad range of beneficial molecules are produced or encoded by the genome of *Bacillus* spp., both to induce or elicit plant defenses (as with phytohormones precursors, lipopolysaccharides, siderophores, etc.) and to directly compete, antagonize, or alter plant pathogens or their aggressiveness (Kloepper et al., 2004; Ongena and Jacques, 2008; Leal et al., 2021). Among *Bacillus* spp., *B. subtilis* is one of the most frequently tested against GTDs (Mondello et al., 2018), and *B. subtilis* PTA-271 has shown promising results in reducing infections caused by the aggressive strain *N. parvum* Bt67 (Trotel-Aziz et al., 2019). Literature also reports that the combination of two or more BCAs can improve the management of plant diseases (Weller, 1988; Guetsky et al., 2002; El-Tarabily, 2006; Yobo et al., 2011; Magnin-Robert et al., 2013), probably due to additive or synergistic effects of combined mechanisms in a complex changing environment (Meyer and Roberts, 2002).

Beneficial microbial interactions conferred by BCA lead to induced systemic resistance (ISR) in the plant, giving it greater protection to pathogens in spatially separated parts of the plant (Alström, 1991; Van Peer et al., 1991; Wei et al., 1991; De Vleeschauwer and Höfte, 2009). ISR is associated with an early, strong, and rapid activation of plant defenses upon pathogen infection, a phenomenon known as the priming state (Conrath et al., 2001, 2015; Pieterse et al., 2014). Among the BCA-induced defense responses, the most relevant are jasmonate (JA)- and ethylene (ET)-dependent ones, described as useful defenses against necrotrophs (Pieterse et al., 2001, 2014; Verhagen et al., 2004; Van der Ent et al., 2009; Niu et al., 2011; Nie et al., 2017). However, Niu et al. (2011) also reported that some BCAs may mediate ISR in a salicylic acid (SA)-dependent manner. In brief, the diversity of BCA ways of protection may depend on both the BCA and the pathogen, but also on the plant and even the cultivar (Mutawila et al., 2011; Pacifico et al., 2019; Nguyen et al., 2020; Stempien et al., 2020).

In this study, we evaluated the effect of combining a potential BCA, *B. subtilis* PTA-271 (thereafter *Bs* PTA-271), and a BCA-commercial product containing *T. atroviride* SC1 (thereafter *Ta* SC1), on the protection of two distinct grapevine



cultivars, Chardonnay and Tempranillo, potentially showing distinct susceptibilities to GTDs. The pathogen selected was *N. parvum* Bt67 (thereafter *Np*-Bt67), described as a very aggressive pathogen associated to BD. As each BCA has already been recognized as beneficial to at least one cultivar (Trotel-Aziz et al., 2019; Berbegal et al., 2020; Martínez-Diz et al., 2021a), their beneficial effect was additionally investigated on the other cultivar, as single BCA and in dual combination of two BCAs. To compare the two BCAs, densities were aligned to the density optimized for *Bs* PTA-271 with Chardonnay rootlings. After looking for the protective capacity of BCAs *in planta*, their ways of action leading to protection were further explored. Thus, the indirect and direct benefits offered by each BCA and their combination were investigated, focusing on both grapevine immunity and the direct beneficial or detrimental physical interplays among the microorganisms *in vitro* (*Bs* PTA-271, *Ta* SC1, and *Np*-Bt67).

## MATERIALS AND METHODS

### Plant Material and Growth Conditions

Three-node-long cuttings of grapevine *Vitis vinifera* L. cv. Tempranillo (clone RJ-26) and cv Chardonnay (clone 7535) were provided by Viveros Villanueva nursery (Navarra, Spain) and Pommery's vineyards in Reims (France), respectively. Tempranillo cuttings were surface-sterilized for 6 h in a 0.05% cryptonol (8-hydroxyquinoline sulfate) solution, waxed and stored at 4°C in a cold chamber for 3 weeks, and then rehydrated with 0.05% cryptonol solution overnight. Chardonnay cuttings were directly surface-sterilized with 0.05% cryptonol solution overnight. Cuttings of both cv were then rooted as described by Lebon et al. (2005), using an indole-3-butyric acid (1 g/L) solution before being placed by 15 in 350-ml pots containing the soil Sorexto (horticultural soil M4600, Grenoble, France) in a culture chamber (24/20°C day/night, 55–65% relative humidity day/night, and 16-h photoperiod at 400  $\mu\text{mol}/\text{m}^2/\text{s}$ ). They were watered three times a week. Only rootlings that have developed roots (30% rooting rate in 15 weeks) were kept for further experiments and transferred to individual 200-ml pots with the same culture conditions.

### Biocontrol Agent's Growth and Plant Treatments

#### *Bacillus subtilis* PTA-271

*Bacillus subtilis* PTA-271 (GenBank Nucleotide EMBL Accession No. AM293677 for 16S rRNA and DDBJ/ENA/GenBank Accession No. JACERQ000000000 for the whole genome) was isolated in 2001 from the rhizosphere of healthy Chardonnay grapevines (*V. vinifera* L. cv. Chardonnay) from a vineyard located in Champagne (Marne, France) (Trotel-Aziz et al., 2008; Leal et al., 2021). Bacterial growth started by adding 100  $\mu\text{l}$  of glycerol stock suspension to sterile Luria Bertani (LB) medium and incubating at 28°C with agitation (100 rpm). Experiments were performed when the bacterial culture is at the exponential growth phase. After centrifugation (5,000 g, 10 min), the pellet was washed once with a sterile 10 mM  $\text{MgSO}_4$  medium and

resuspended in a same  $\text{MgSO}_4$  medium. Bacterial density was measured by spectrophotometry at 450 and 650 nm, and the mean density was adjusted with a sterile  $\text{MgSO}_4$  medium before treatment according to Trotel-Aziz et al. (2019). The bacterial suspension was applied twice by drenching the soil at the root level of rootlings at a final density of  $10^8$  CFU/g soil. Inoculations were carried out when rootlings were 16 weeks old (considered as day 0) and 2 weeks later (day 15) as indicated in **Figure 1**. Control rootlings were similarly drenched twice with  $\text{MgSO}_4$  solution (**Figure 1**).

#### *Trichoderma atroviride* SC1

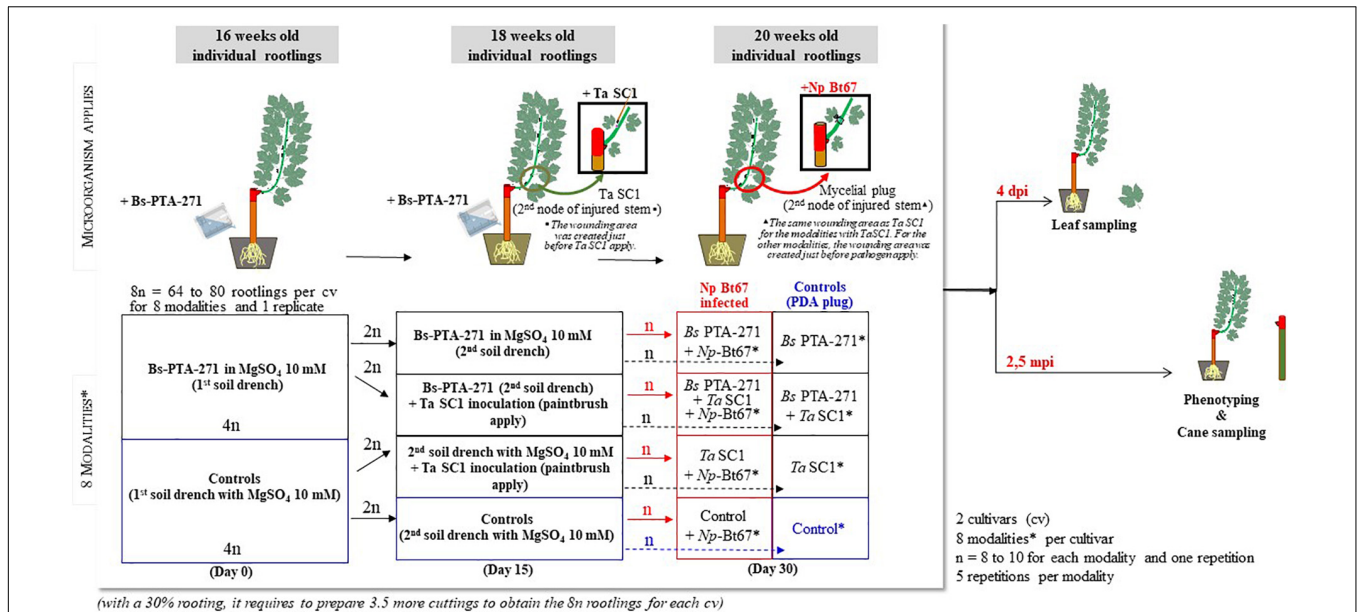
*Trichoderma atroviride* SC1 (Vintec®, Belchim Crop Protection, Bi-PA;  $10^{10}$  conidia per gram of formulated product) was suspended in water at  $10^8$  CFU/ml to compare the effect of each BCA at an equal density. In order to also take advantage of an eliciting effect, the *Ta* SC1 fungal suspension was applied once with a paintbrush to the second node of the previously wounded lignifying stem (5 mm diameter and 1 mm deep; made just before *Ta* SC1 apply) of 18-week-old rootlings (**Figure 1**). The inoculation site was immediately covered with parafilm (day 15).

### Pathogen Strain and Growth

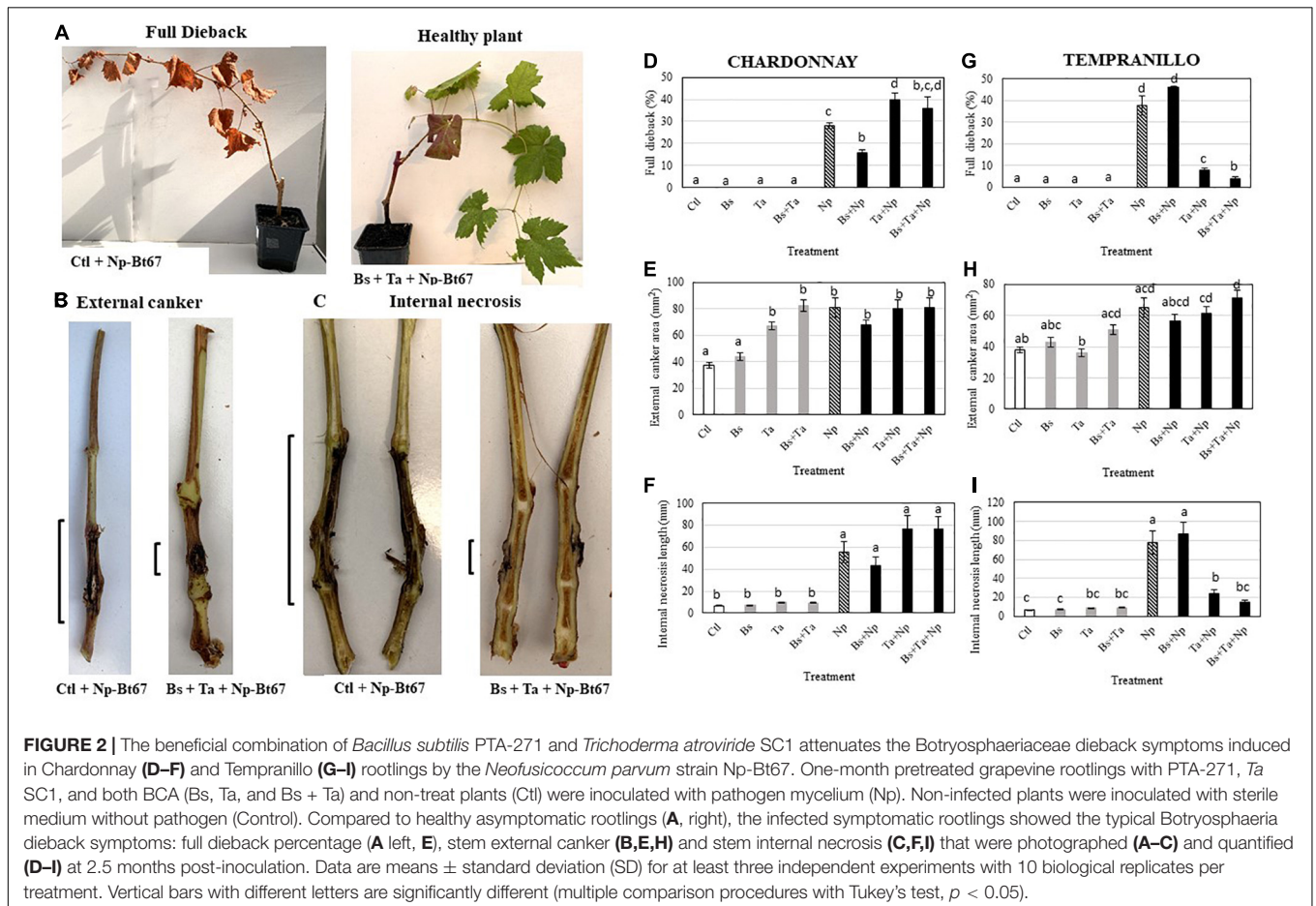
*Neofusicoccum parvum* strain Bt67 isolated from Portuguese vineyards (Estremadura region) is inscribed in the HIA collection (Lisbon University, Portugal). This fungus was maintained on potato dextrose agar (PDA, Sigma, Saint-Quentin-Fallavier, France) plates and stored at 4°C (Trotel-Aziz et al., 2019). The resulting mycelium was plated on PDA medium and incubated in the dark at 22°C for 7 days before inoculation.

### Pathogen Inoculation to Plants, Quantification of Disease Symptoms, and Re-isolation of the Pathogen

Half of the 20-week-old rootlings that were treated with *Bs* PTA-271 (day 0 and day 15) and/or *Ta* SC1 (day 15) were further infected with the pathogen at the wounding area with a 3-mm-diameter mycelial plug from a 7-day-old culture of *Np*-Bt67 strain (day 30), thus at distinct time points (days 0–30) as summarized in **Figure 1**. The inoculation site was then covered with moist hydrophilic cotton before sealing with parafilm. The experiment was composed of five repetitions for each modality (treatment), with 8–10 replicate plants per treatment (**Figure 1**). To confirm that lesions were due to pathogen infection and not to the injury, the control plants were also injured and inoculated with sterile 3-mm PDA plugs (**Figure 1**). Rootlings, namely, “control,” are those that are neither treated with BCA nor infected with the pathogen. After inoculation, vines were kept in the same culture chamber and BD symptoms were assessed at 2.5 months post-inoculation (mpi) (**Figure 1**). Disease symptoms were evaluated as described by Trotel-Aziz et al. (2019) by quantifying the percentage of the full dead shoots from inoculated rootlings (**Figure 2A**, “Full dieback”) and by measuring both the external canker area and the internal necrosis length of the other lignified shoots (**Figures 2B,C**, respectively). To check the success of the infection and the lack of contaminations, re-isolation of pathogen



**FIGURE 1 |** Diagram showing the *Bacillus subtilis* PTA-271 and *Trichoderma atroviride* SC1 inoculations, *Neofusicoccum parvum* strain Np-Bt67 infection, and sample collection process. \*Modalities: Control, Bs PTA-271, Ta SC1, Bs PTA-271 + Ta SC1, Control + Np Bt67, Bs PTA-271 + Np Bt67, Ta SC1 + Np Bt67, Bs PTA-271 + Ta SC1 + Np Bt67.



was performed as described by Pinto et al. (2018), by quickly passing the infected stems onto the flame, then removing the top of the necrotic zone with a scalpel, before plating seven small pieces of tissue per plant onto PDA plates. Plates were then incubated at 28°C for at least 7 days. For every repetition of the experiments, re-isolations were performed with seven of the infected rootlings per infected combination (i.e., Np, Bs + Np, Ta + Np, and Bs + Ta + Np) and each replicate, and one negative control rootling per non-infected combination (i.e., Control, Bs, Ta, and Bs + Ta).

## Direct Confrontation Tests With Biocontrol Agents and Pathogen

Antagonism among microorganisms was checked *in vitro*, using *B. subtilis* PTA-271, *T. atroviride* SC1, and *N. parvum* Np-Bt67, in dual or three-way confrontation tests on PDA plates (9 mm diameter). *Bs* PTA-271 grown in LB medium and *Ta* SC1 resuspended in sterilized water were both used at  $10^8$  CFU/ml (5  $\mu$ l drop), while a 7-day-old mycelium plug (3 mm) was used for the pathogen. Three types of direct confrontation were performed: (A) the pathogen/BCA combinations were plated at the same time, but at distinct areas (i.e., 5 cm away from each other); (B) one or two isolates (*Bs* PTA-271, *Ta* SC1, or *Np*-Bt67) were plated 48 h before the other(s), and at distinct areas; and (C) isolates were plated simultaneously and at the center of the plate. Controls containing one single isolate (*Bs* PTA-271, *Ta* SC1, or *Np*-Bt67) were also made, either on the side of the plate or at the center. All plates were incubated in the dark at 28°C for at least 11 days and photographed daily. Antagonistic effect was characterized by an inhibition zone around the BCA and/or the pathogen. Since the first kind of confrontation (A) added no more information compared to the others (B and C), it was not shown in this study. The experiment was conducted twice with three replicate plates per treatment, and the area occupied by each microorganism was measured daily using ImageJ software (Rueden et al., 2017), based on a reference distance common to all images.

## RNA Extraction and Quantitative Reverse-Transcription Polymerase Chain Reaction Analysis

From the *in planta* assays with rootlings, leaf samples were collected 4 days post-inoculation of pathogen (dpi), ground in liquid nitrogen, and then stored at -80°C. RNA was extracted from powdered 40 leaves of 8 rootlings per replicate of each modality. Total RNA was extracted from 50 mg of leaf powder with Plant RNA Purification Reagent according to manufacturer instructions (Invitrogen, Pontoise, France), and DNase treated as described by the manufacturer's instructions (RQ1 RNase-Free DNase, Promega). RNA quality was checked by agarose gel electrophoresis, and total RNA concentration was measured at 260 nm for each sample using the NanoDrop One spectrophotometer (Ozyme) and adjusted to 100 ng  $\mu$ l<sup>-1</sup>. First-strand cDNA was synthesized from 150 ng of total RNA using the Verso cDNA synthesis kit (Thermo Fisher Scientific, Inc., Waltham, MA, United States). Polymerase chain

reaction (PCR) conditions were the ones described by Gruau et al. (2015). Quantitative reverse-transcription polymerase chain reaction (qRT-PCR) was performed with Absolute Blue qPCR SYBR Green ROX Mix according to manufacturer instructions (Thermo Fisher Scientific, Inc., Waltham, MA, United States), in a BioRad C1000 thermocycler using the BioRad manager software CFX96 Real-Time PCR (BioRad, Hercules, CA, United States). A set of six defense-related genes, selected for their responsiveness to pathogen or priming state induced by beneficial microorganisms (Trotel-Aziz et al., 2019), was tracked by qRT-PCR using specific primers (Table 1). Quantitative RT-PCR reactions were carried out in duplicate in 96-well plates in a 15- $\mu$ l final volume containing Absolute Blue SYBR Green ROX mix including Taq polymerase ThermoPrime, dNTPs, buffer, and MgCl<sub>2</sub> (Thermo Fisher Scientific, Inc., Waltham, MA, United States), 280 nM forward and reverse primers, and 10-fold diluted cDNA according to the manufacturer's protocol. Cycling parameters were 15 min of Taq polymerase activation at 95°C, followed by 40 two-step cycles composed of 10 s of denaturation at 95°C and 45 s of annealing and elongation at 60°C. Melting curve assays were performed from 65 to 95°C at 0.5°C s<sup>-1</sup>, and melting peaks were visualized to check amplification specificity. EF1 and 60SRP genes were used as references and experiments were repeated five times. Relative gene expression was determined with the formula fold induction:  $2(-11Ct)$ , where  $11Ct = [Ct_{TG} (US) - Ct_{RG} (US)] - [Ct_{TG} (RS) - Ct_{RG} (RS)]$ , where Ct is cycle threshold, Ct value is based on the threshold crossing point of individual fluorescence traces of each sample, TG is target gene, RG is reference gene, the US is an unknown sample, and RS is reference sample. Integration of the formula was performed by the CFX Manager 3.1 software (Bio-Rad). Although the genes analyzed were considered significantly up- or downregulated when changes in their expression were >2-fold or <0.5-fold, respectively, we still performed a statistical analysis. Control samples for the rootlings model are cDNA from leaves of rootlings untreated with BCA and inoculated with sterile PDA plugs (1  $\times$  expression level).

## Statistical Analysis

Data of canker area and length of external and internal necrosis of the stems were obtained by the analysis of photos using ImageJ software (Rueden et al., 2017). Statistical analyses were carried out using all the vines of three replicates among five for each modality with RStudio software (Horton and Kleinman, 2015). For modality significance, mean values were compared by Tukey's test ( $p < 0.05$ ). Results of confrontation tests are from one representative repetition out of two showing the same trends. Statistical analyses were carried out using the SigmaStat 3.5 software. For treatment effect, mean values were compared by Tukey's test ( $p < 0.05$ ). Results of gene expression by qRT-PCR analysis correspond to means  $\pm$  SEM deviation from three representative repetitions out of five showing the same trends. Statistical analyses were carried out using the XLSTAT 2021.1.1 5 software (Addinsoft, Paris, France). For treatment effect, mean values were analyzed using one-way analysis of variance (ANOVA). When differences in the means



**TABLE 1** | Primer sequences used for qRT-PCR analysis of defense-related genes (Trotel-Aziz et al., 2019).

Gene	Name	Accession number <sup>1</sup>	Forward primer (5'-3')	Reverse primer (5'-3')	Annealing temperature (°C)	Amplicon size (bp)	Efficiency of primers pairs (%)
60RSP	60S ribosomal protein L18	XM_002270599 <sup>1</sup>	ATCTACCTCAAGCTCCTAGTC	CAATCTTGTCTCCTTTCTCT	60	166	100.0
EF1	Elongation factor 1- $\alpha$	XM_002284888 <sup>1</sup>	AACCAAAATATCCGGAGTAA AAGA	GAACTGGGTGCTTGATAGGC	60	164	100.0
LOX9	Lipoxygenase	NM_001281249 <sup>1</sup>	CCCTTCTTGGCATCTCCCTTA	TGTTGTGTCCAGGGTCCATTC	60	101	90.0
PR1	Pathogenesis-related protein 1	XM_002273752 <sup>1</sup>	GGAGTCCATTAGCACTCCTTTG	CATAATTCTGGGCGTAGGCAG	60	168	90.0
PR2	Class I $\beta$ -1,3-glucanase	NM_001280967 <sup>1</sup>	TCAATGGCTGCAATGGTGC	CGGTCGATGTTGCGAGATTTA	60	155	97.2
GST1	Glutathione-S-transferase	NM_001281248 <sup>1</sup>	TGCATGGAGGAGGAGTTCGT	CAAGGCTATATCCCCATTTCCTTC	60	98	90.0
PAL	Phenylalanine ammonia lyase	XM_003635637 <sup>1</sup>	TCCTCCCGGAAAACAGCTG	TCCTCCAAATGCCTCAAATCA	60	101	92.9
STS	Stilbene synthase	NM_001281117 <sup>1</sup>	AGGAAGCAGCATTGAAGGCTC	TGCACCAGGCATTCTACACC	60	101	94.3

<sup>1</sup> NCBI accession number.

were significant, Fisher's LSD *post hoc* test ( $\alpha = 0.1$ ) was applied to determine which treatments were significantly different from others.

## RESULTS

### Effects of *Bacillus subtilis* PTA-271 and *Trichoderma atroviride* SC1 on Two Cultivars Infected With *Neofusicoccum parvum* Bt67

In control Chardonnay infected with the pathogen, the results of infection showed a rate of  $28 \pm 1.24\%$  for dead shoot (full dieback), of  $80.6 \pm 7.35 \text{ mm}^2$  for external canker size, and of  $55.4 \pm 9.44 \text{ mm}$  for internal necrosis length (see *Np*-Bt67 in **Figures 2D–F**), while in Tempranillo, they reached  $37.5 \pm 4.56\%$ ,  $65.2 \pm 6.23 \text{ mm}^2$ , and of  $77.8 \pm 11.95 \text{ mm}$ , respectively (see *Np*-Bt67 in **Figures 2G–I**).

In BCA-treated Chardonnay rootlings then infected with the pathogen, the results of the biocontrol assays showed that *Bs*-PTA-271-pretreated plants presented a significant lower number of plants with full dieback (by approximately 45%) than the infected control (**Figure 2D**). Infected plants pretreated with *Ta* SC1 did not reduce the full dieback development compared to infected control plants, while infected plants pretreated with both BCAs showed a great variability in the development of full dieback symptoms. Similarly, the external canker area (**Figure 2E**) and the internal necrosis length of infected Chardonnay (**Figure 2F**) were solely slightly reduced in *Bs*-PTA-271-pretreated rootlings (by 16 and 22%, respectively), but insignificantly (**Figure 2E**). In contrast, necrosis length was increased in *Ta* SC1 and both BCAs pretreated plants compared to infected control, although non-significant (**Figure 2F**).

In BCA-treated Tempranillo rootlings then infected with the pathogen, the results of the biocontrol assays showed that *Ta*-SC1- and combined-BCA-pretreated plants showed a

significant lower number of full dieback (by approximately 80 and 91%, respectively) and length of stem internal necrosis (by approximately 70 and 81%, respectively) than the infected control (**Figures 2G,I**, respectively). In contrast, infected plants pretreated with *Bs* PTA-271 showed that neither full dieback development nor internal stem necrosis reduced, compared to infected control plants. Looking at the external canker area (**Figure 2H**), none of the treatments with *Bs*-PTA-271-, *Ta*-SC1-, and combined-BCA-pretreated plants, consecutively infected, induced any significant difference with the infected control. Therefore, external canker may not appear as a relevant indicator for *Np* dieback with this experimental model, for both Tempranillo and Chardonnay.

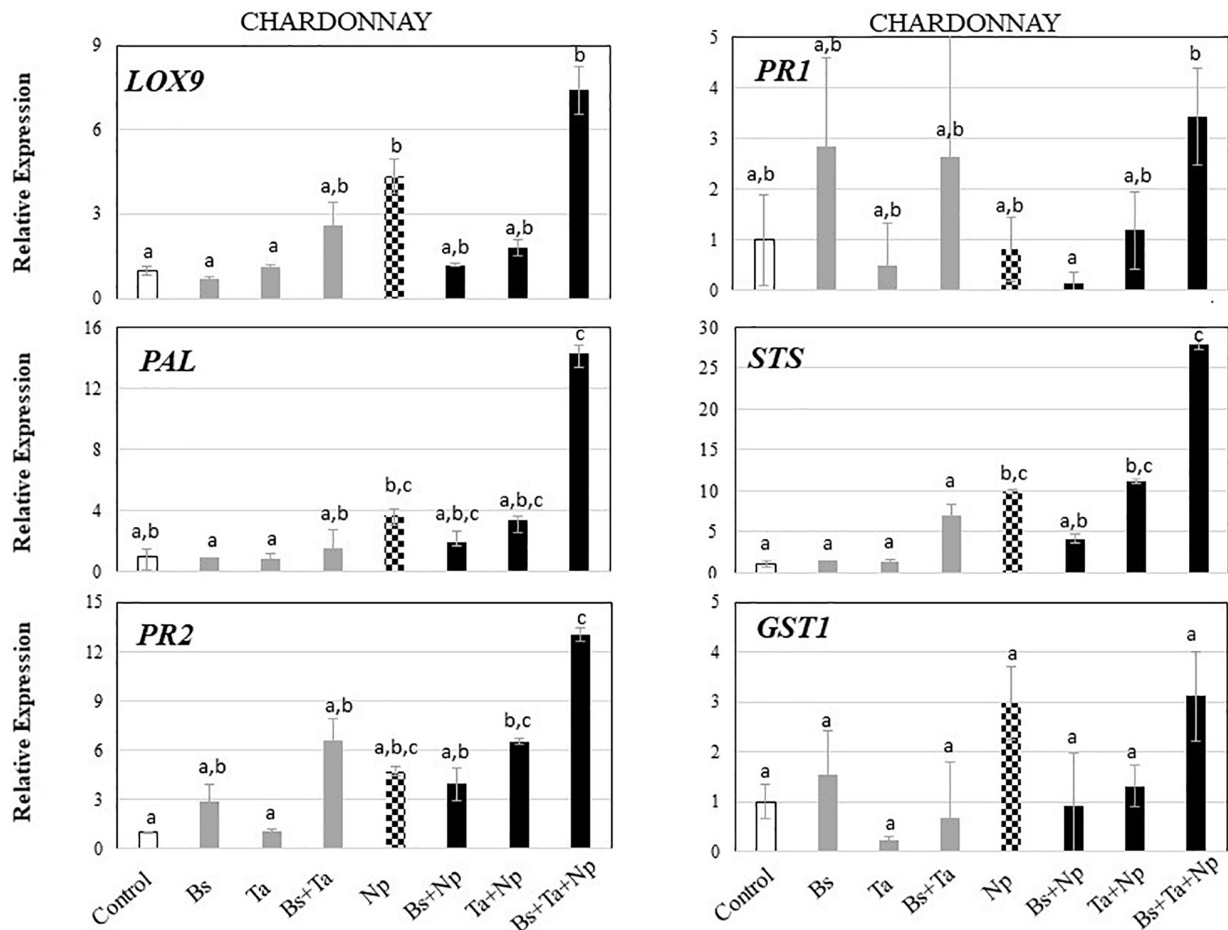
Re-isolations of the pathogen confirmed that (1) there was no background infection elsewhere than in the artificially infected rootlings, satisfying thus the Koch's postulates, and that (2) the pathogen was still alive in both dead and living stems of plants, as well as in infected plants pretreated or not with BCA. From all infected plants, the pathogen was successfully isolated with a percentage of success  $>90\%$  that indicated no fungicidal effect from BCA toward *Np*-Bt67.

### Effects of Biological Control Agents on the Basal Defense of Chardonnay and Tempranillo

The ability of *Bs* PTA-271 or *Ta* SC1 or both BCAs to enhance grapevine immunity was addressed in leaves of control rootlings. Six selected defense genes were targeted by qRT-PCR: the lipoxygenase *LOX9* involved in oxylipin synthesis and described as dependent to JA/ET (Hamiduzzaman et al., 2005; Naznin et al., 2014); *PR1* described to be regulated by SA (Dufour et al., 2013; Naznin et al., 2014; Caarls et al., 2015); the  $\beta$ -1,3-glucanase *PR2* described to be regulated by various phytohormones such as SA, JA, and ET (Liu et al., 2010); the glutathione-S-transferase *GST1* putatively involved in the detoxification process; the



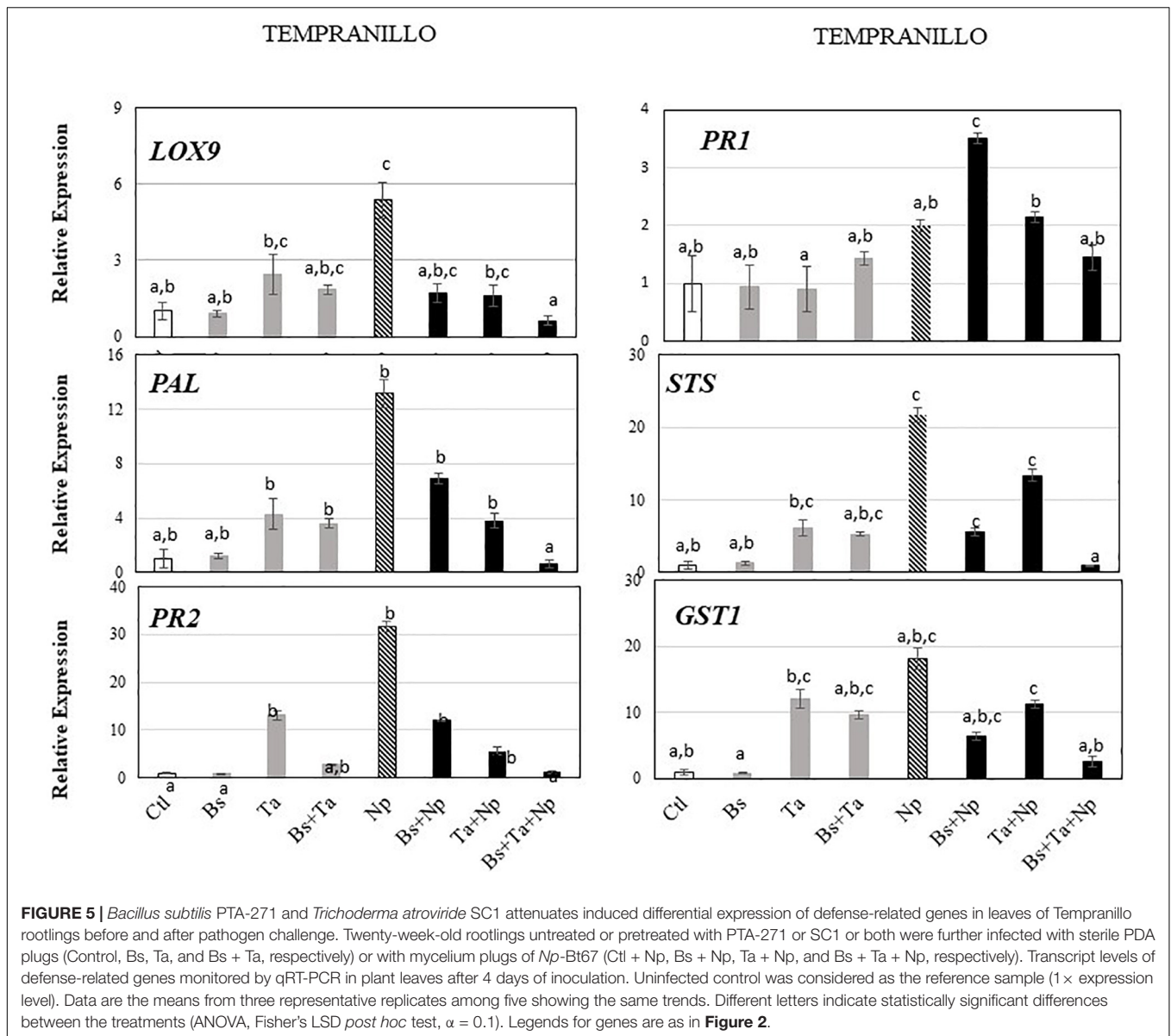




**FIGURE 4** | *Bacillus subtilis* PTA-271 and *Trichoderma atroviride* SC1 attenuates induced differential expression of defense-related genes in leaves of Chardonnay rootlings before and after pathogen challenge. Twenty-week-old rootlings untreated or pretreated with PTA-271 or SC1 or both were further infected with sterile PDA plugs (Control, Bs, Ta, and Bs + Ta, respectively) or with mycelium plugs of Np (CtI + Np, Bs + Np, Ta + Np, and Bs + Ta + Np, respectively). Transcript levels of defense-related genes monitored by qRT-PCR in plant leaves after 4 days of inoculation. Uninfected control was considered as the reference sample (1× expression level). Data are the means from three representative replicates among five showing the same trends. Different letters indicate statistically significant differences between the treatments (ANOVA, Fisher's LSD *post hoc* test,  $\alpha = 0.1$ ). Legends for genes are as in **Figure 2**.

upon pathogen challenge, no post-priming was observed in Bs-PTA-271-pretreated plants since it did not induce any stronger activation of the targeted plant immune defenses compared to Chardonnay-infected control at 4 dpi (**Figure 3**). In contrast, Ta SC1 showed no sign of priming stimulus in control Chardonnay, but it induced similar expression of PR2 (6.5-fold increase) and STS (11.1-fold increase) than infected control (4.7 and 9.8, respectively). Interestingly, the application of both BCAs enabled to reach the highest level of Chardonnay defense gene expression upon pathogen challenge (3.1–27.8) compared to infected control (0.8–9.8), a priming effect shown as consistent according to the discriminating capacity of the qRT-PCR technique, but still not yet significant according to the ANOVA analysis. Anyway, such a synergy at 4 dpi can result from a priming stimulus by Bs PTA-271, followed by a post-primed phase upon pathogen inoculation with a more rapid and strong activation of immune defenses due to interactions among each actor (Bs PTA-271, Ta SC1, Np-Bt67, and Chardonnay).

In leaves of Tempranillo infected with Np-Bt67, the expression of all targeted defense genes was consistently upregulated from 2.0- to 31.5-fold, and significantly for LOX9, PR2, PAL, and STS (**Figure 5** and **Supplementary Figure 1B**). Compared to infected Chardonnay (**Figure 3A**), expression of the basal defense genes was significantly stronger in infected Tempranillo (**Figure 3B**), highlighting a higher basal defense level in Tempranillo toward Np-Bt67 than in Chardonnay at 4 dpi. The ability of each BCA or both to enhance Tempranillo immunity was also addressed (**Figure 5** and **Supplementary Figure 1B**). As reported above, in the absence of pathogen infection, Ta SC1 alone induced a consistent expression of almost all the targeted defenses (2.44–13.03 for LOX9, PR2, GST1, PAL, and STS), suggesting that Ta SC1 may act as a priming stimulus for Tempranillo cultivar, but in a lesser extent when combined with Bs PTA-271 (1.84–9.66). However, upon pathogen challenge, no post-priming was observed in Ta SC1-pretreated rootlings since it did not induce any stronger expression of the targeted immune defenses



than in the Tempranillo-infected control at 4 dpi, but lower (Figure 5 and Supplementary Figure 1B). Regarding *Bs* PTA-271 effect (i.e., Bs + *Np*), while it showed no sign of priming stimulus in control Tempranillo, it induced the expression of almost all targeted defenses, but similarly to *Ta* SC1, thus in a lower extent than the infected control (thus, no more priming in that condition with *Bs* PTA-271). Additionally, the pretreatment with both BCAs induced a lower expression level of Tempranillo defense genes upon pathogen challenge (0.63–2.57) than in infected control (2.0–31.56). However, such apparent non-expression of Tempranillo defenses at 4 dpi did not presume any useful induced defenses at other key times or among other defenses that were not targeted in this study.

Taking the uninfected control of Chardonnay as the reference sample for both cultivars, we can compare the immunity between Tempranillo and Chardonnay upon pathogen challenge

(Figures 3A,B, respectively). As observed in control condition (i.e., high basal expression of *PR1*), infected Tempranillo showed once again a high expression of this targeted gene presumably responsive to SA, compared to Chardonnay. This suggests that Tempranillo would use SA-dependent defense pathways toward *N. parvum*, even when overexpressing *PR2*, *GST1*, *PAL*, and *STS*, unlike Chardonnay. These data thus highlight the possible role of SA signaling in Tempranillo, especially when infected and pretreated with *Bs* PTA-271 (i.e., *PR1*). Curiously, the JA/ET-responsive gene *LOX9* was also highly upregulated in infected Tempranillo, while *LOX9* was severely downregulated in infected Tempranillo pretreated with single or both BCAs, as well as *PR2*, *PAL*, and *STS*. Opposite trends were observed in Chardonnay: (i) no prominent role of SA signaling in infected Chardonnay, especially when pretreated with *Bs* PTA-271; and (ii) *LOX9* was not so highly upregulated in infected Chardonnay (i.e., Ctl + *Np*),



but *LOX9* was upregulated in infected Chardonnay pretreated with both BCAs, and *PR2*, *PAL*, and *STS* with *Ta* SC1 or both BCAs. These data could suggest the prominent role of JA/ET signaling in Chardonnay, especially when infected and pretreated with BCA. Interestingly, *PR2*, *PAL*, and *STS* are common defenses induced by each BCA against *Np*-Bt67 for the two cultivars, possibly through two distinct signaling pathways.

### Direct Beneficial or Detrimental Interplays Between *Bacillus subtilis* PTA-271, *Trichoderma atroviride* SC1, and the Pathogen *Neofusicoccum parvum*-Bt67

Regarding the *in vitro* tests with *Np*-Bt67 (Figure 6), results showed that *Bs* PTA-271 and *Ta* SC1 antagonize *Np*-Bt67 when plated 48 h before the pathogen. As shown in Figures 6A,B, the growth of *Np*-Bt67 was consistently reduced by *Ta* SC1 or *Bs* PTA-271 in dual confrontation compared to the control. However, while the growth of *Np*-Bt67 was completely repressed from day 3 by *Ta* SC1 (Figure 6A), it was half-repressed by *Bs* PTA-271 (Figure 6B), enabling the pathogen to grow consistently less than the control over the same time period. Thus, *Ta* SC1 antagonistic effect was stronger than that of *Bs* PTA-271, although only a fungistatic effect was observed between them (since when transplanted, the pathogen grows back).

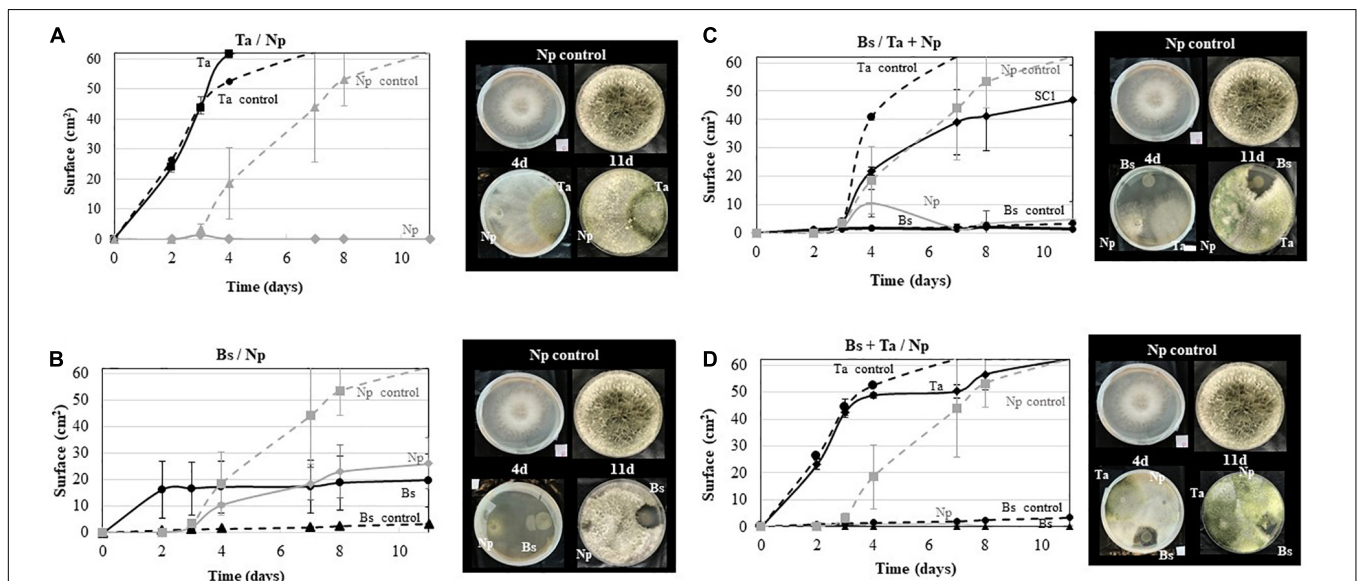
In three-way confrontations (Figures 6C,D), the antagonistic effect of *Bs* PTA-271 against *Np*-Bt67 was still reinforced in the presence of *Ta* SC1, even applied 48 h later (Figure 6C). Such benefit was yet reinforced when the two BCAs were both applied

48 h before the pathogen, in which the growth of *Np*-Bt67 was close to 5 mm<sup>2</sup> (Figure 6D). However, it should be noted that *Ta* SC1 did not grow as fast when applied 48 h after *Bs* PTA-271, since *Ta* SC1 slopes are not parallel but weaker in Figure 6C than in Figure 6D.

To check the *Ta* SC1 capacity to keep its antagonistic effect when applied simultaneously with *Bs* PTA-271, dual confrontations were made between the two BCAs applied in the same area, with or without pathogen (Figure 7). As shown in Figure 7A, the growth of *Ta* SC1 was slowed down with *Bs* PTA-271, leading to a smaller *Ta* SC1 area than for the *Ta* SC1 control over the same time period. Interestingly, this detrimental effect of *Bs* PTA-271 on *Ta* SC1 disappeared in the three-way confrontation with the pathogen *Np*-Bt67 (Figure 7B), being all applied simultaneously at the same area. Thus, *Ta* SC1 and/or *Bs* PTA-271 may keep their strong antagonistic activity when facing a common adversary.

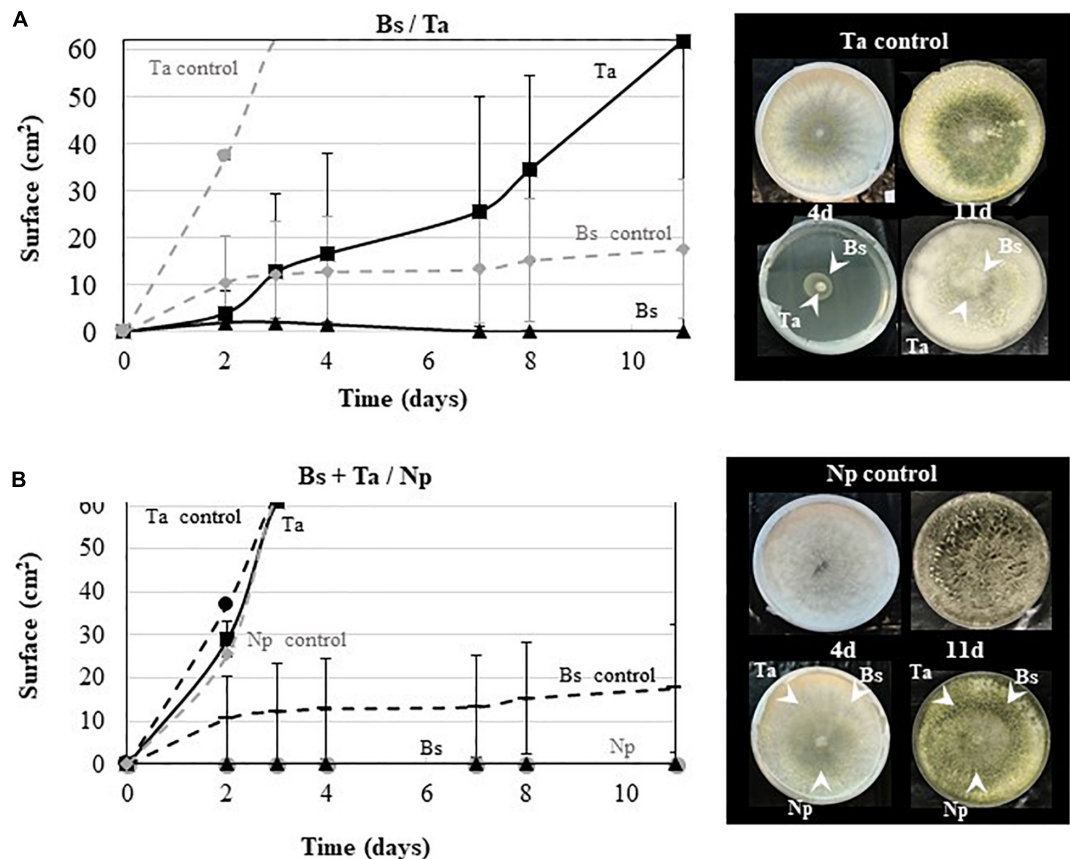
## DISCUSSION

In search of an effective protective BCA combination against *N. parvum*, we investigated a potential BCA and a BCA-commercial product, each already described as protectors against GTDs on distinct cultivars: *B. subtilis* PTA-271 with Chardonnay (Trotel-Aziz et al., 2019) and *T. atroviride* SC1 with different cultivars (Pertot et al., 2016; Berbegal et al., 2020; Martínez-Diz et al., 2021a). This study assessed the combined impact of these two BCAs on two cultivars artificially infected or not with one pathogen. *N. parvum* Bt67 was used, as a very



**FIGURE 6 |** Antagonistic activity of *Bacillus subtilis* PTA-271 and *Trichoderma atroviride* SC1 against the *Neofusicoccum parvum* strain Bt67. **(A)** *T. atroviride* SC1 (*Ta*) was applied 48 h before *N. parvum* (*Np*) in the opposite sides of PDA plates. **(B)** *B. subtilis* PTA-271 (*Bs*) was applied 48 h before *N. parvum* (*Np*-Bt67) in the opposite sides of PDA plates. **(C)** *B. subtilis* PTA-271 (*Bs*) was applied 48 h before *N. parvum* (*Np*) and *T. atroviride* (*Ta*) at distinct areas of the PDA plates. **(D)** *B. subtilis* PTA-271 (*Bs*) and *T. atroviride* SC1 (*Ta*) were applied 48 h before *N. parvum* (*Np*) at distinct areas of the PDA plates. All plates were incubated at 28°C. Pictures of each plate condition were taken from day 1 to day 11 after the first inoculation. Photos on top are the control of *Np*-Bt67 and photos at the bottom indicate the confrontation assay at day 4 (left) and day 11 (right).





**FIGURE 7 |** Antagonistic activity of *Bacillus subtilis* PTA-271 and *Trichoderma atroviride* SC1 against *Neofusicoccum parvum* Bt67. **(A)** *B. subtilis* PTA-271 (Bs) and *T. atroviride* SC1 (Ta) were applied simultaneously in the center of the PDA plates. **(B)** *B. subtilis* PTA-271 (Bs), *T. atroviride* SC1 (Ta), and *N. parvum* (Np) were applied simultaneously in the center of the PDA plates. All plates were incubated at 28°C. Pictures of each plate were taken from day 1 to day 11 after the first inoculation. Photos on top are SC1 control **(A)** and *Np*-Bt67 control **(B)**, and pictures at the bottom indicate the confrontation assay at day 4 (left) and day 11 (right).

aggressive pathogen associated to BD. Our investigation focused on the capacity of single and combined BCAs to counteract BD symptoms on both cultivars. To compare the two BCAs, densities were aligned to the density optimized for *Bs* PTA-271. After looking for the protective capacity of BCA *in planta*, their modes of action leading to protection were further explored. Thus, we investigated whether these BCAs could affect pathogen growth *in vitro* and cultivar immunity upon infection *in planta*.

*Neofusicoccum parvum*-Bt67 caused BD symptoms on the rootlings of the two grapevine cultivars, as shoot full dieback, canker external necrosis, and shoot internal necrosis. Interestingly, the full dieback symptoms were more severe on Tempranillo than on Chardonnay (i.e., 37.5 and 28%, respectively, **Figures 2D,G**), suggesting a greater susceptibility to BD for Tempranillo than Chardonnay, as already reported by Luque et al. (2009) and Cobos et al. (2019). Although there is a lack of comparative data between cultivars, the distinct susceptibility of some cultivars to GTDs has already been reported (Travadon et al., 2013; Fontaine et al., 2016b; Chacon et al., 2020; Reveglia et al., 2021), even within a same cultivar from one region to another or depending on the vintage (Mimiague and Le Gall, 1994). However, in Chardonnay and

Tempranillo rootlings pretreated with one or both BCAs before inoculation of the pathogen, BD symptoms were significantly reduced with *Bs* PTA-271 or *Ta* SC1, respectively. Grapevine effective protection against *Np*-Bt67 has already been reported with *Bs* PTA-271 on Chardonnay rootlings (Trotel-Aziz et al., 2019), and with *Ta* SC1 on Tempranillo in nursery and vineyards conditions (Berbegal et al., 2020; Blundell et al., 2021). Additionally, in our experimental conditions, Chardonnay seems to favor the beneficial effect of *Bs* PTA-271, while Tempranillo favors that of *Ta* SC1 beneficial effect, highlighting the relationship between cultivar response and BCA effect. Manter et al. (2010) suggested that the differences between cultivars may result from minor changes in the composition of their endophyte community, with *Trichoderma* species being among the most common endophytic fungal isolates from Tempranillo (González and Tello, 2011). Therefore, Tempranillo could be subjected to *Trichoderma*'s influence. Similarly, the efficiency of *Bs* PTA-271 toward Chardonnay may be explained by its origin of sampling from an established Chardonnay vineyard, screened from healthy vines (Trotel-Aziz et al., 2008). In combination and according to our experimental conditions, despite cited as compatible strains (Kumar, 2013), *Ta* SC1 + *Bs*

PTA-271 are less protective against *Np*-Bt67 in Chardonnay than *Bs* PTA-271 alone. The authors reported that *Trichoderma* spp. can interfere the plant signaling networks and secrete an arsenal of degrading enzymes (i.e., proteases) and secondary metabolites (Tiwari and Verma, 2019; Alfiky and Weisskopf, 2021), suggesting that *Ta* SC1 may alter both *Bs* PTA-271 integrity and beneficial effects in Chardonnay. However, the application of both BCAs enabled to reach the highest level of Chardonnay defense gene expression upon pathogen challenge (see **Figure 3A**), and the highest protection in Tempranillo cultivar (see **Figure 2G**), highlighting that *Ta* SC1 on its own would not interfere with the beneficial effects of *Bs* PTA-271.

Beneficial effects of combined BCAs have yet been reported in different pathosystems (Yobo et al., 2011; Magnin-Robert et al., 2013), and our study reports for the first time the biocontrol potential of the combination of *Bs* PTA-271 and *Ta* SC1 against *Np*-Bt67 in Tempranillo. Our results showed that *Ta* SC1 efficiently protects Tempranillo, and this protection is still observed in rootlings pretreated with both BCAs (see **Figure 2G**). Thus, a significant benefit is observed when using both BCAs in Tempranillo, despite the fact that they could antagonize each other. In this respect, Leal et al. (2021) reported that the genome of *Bs* PTA-271 encodes for the synthesis of bacillaene, a polyketide already described to antagonize *Trichoderma* spp. (Caulier et al., 2019). Therefore, the positive contribution of *Bs* PTA-271 and *Ta* SC1 to Tempranillo protection against *Np*-Bt67 suggests a fine-tuned orchestrated cooperation of BCAs when facing adversity, as supported by the **Figure 7** results and highlighted by Alfiky and Weisskopf (2021). However, the application of BCAs to rootlings was spatially separated.

Empowered with aggressive molecules, *Bacillus* spp. and *Trichoderma* spp. can possibly exert direct beneficial or detrimental interplays within the host's microbiome, and especially on the other BCA and pathogens such as GTDs fungi (Di Marco et al., 2002; Kloepper et al., 2004; Ongena and Jacques, 2008; Haidar et al., 2016; Trotel-Aziz et al., 2019; Yacoub et al., 2020; Úrbez-Torres et al., 2020; Blundell et al., 2021). *In vitro* dual confrontation tests confirmed the antagonistic activity of *Bs* PTA-271 or *Ta* SC1 toward *Np*-Bt67 since each of them significantly inhibits the mycelium growth of *Np*-Bt67 (see **Figures 6A,B**). This also prompts us the idea that the not-yet-convincing protection assay of *Bs* PTA-271 and *Ta* SC1 in infected Chardonnay would not result from a detrimental effect of *Ta* SC1 on some putative direct effects of *Bs* PTA-271. Indeed, the strong direct antagonistic activity of *Bs* PTA-271 and *Ta* SC1 toward *Np*-Bt67 also operates when the two BCAs were applied both 48 h before the pathogen (see **Figure 6D**). This antagonistic benefit is in accordance with the significant synergy of the protection in Tempranillo by both BCAs (see **Figure 2G**), and it confirms the benefit of using them in combination in Tempranillo to optimize the direct fight against *Np*-Bt67. A similar outcome was reported by Alexander and Phin (2014) using an effective combination of *Bacillus* spp. and *Trichoderma* spp. against *Ganoderma* spp. Such direct effects of BCA against pathogens are important life traits to protect grapevine from BD, still deprived of effective curative treatments nowadays (Mondello et al., 2018). In nursery too, healthy mother plants require a control of their sanitary

status (Pertot et al., 2016), eventually provided by an early inoculation of such beneficial BCA with a strong antagonistic activity toward pathogens.

Direct beneficial or detrimental interplays between BCAs also condition their capacity to live together in symbiosis, even *in planta* as part of the holobiont (Bettenfeld et al., 2020). Dual confrontation was thus also performed between *Bs* PTA-271 and *Ta* SC1. As expected, *Bs* PTA-271 antagonized *Ta* SC1 (see **Figure 7A**; Caulier et al., 2019; Leal et al., 2021). However, this detrimental effect of *Bs* PTA-271 on *Ta* SC1 disappears in a three-way confrontation with *Np*-Bt67, when they were all applied simultaneously at the same area (see **Figure 7B**). These data confirm that *Ta* SC1 and *Bs* PTA-271 can positively interact to better confine *Np*-Bt67 and can lead to a direct positive contribution of this combination to the protection of Tempranillo against *Np*-Bt67. However, such a direct positive contribution of combined BCAs did not operate on the infected Chardonnay rootlings. Our experimental conditions could have altered the ability of *Ta* SC1 to exert its direct fungistatic effect (applied once at  $10^8$  CFU/ml with a paintbrush over a 5-mm<sup>2</sup> area). This also strongly suggests that Chardonnay itself alters the fine-tuned orchestrated cooperation of BCAs, probably targeting the indirect *Ta* SC1 beneficial effect since BCAs are spatially separated. This prompts us to pursue our investigations further in order to decipher the indirect interactions driving to a beneficial outcome in grapevine control of *Np*-Bt67.

According to our previous works, a focus on grapevine systemic immunity was made by targeting six selected defense genes in leaves: the lipoxygenase *LOX9* involved in oxylipin synthesis and described as dependent to JA/ET; *PR1* described to be regulated by SA; the  $\beta$ -1,3-glucanase *PR2* described to be regulated by various phytohormones such as SA, JA, and ET; the glutathione-S-transferase *GST1* putatively involved in the detoxification process; the phenylalanine ammonia-lyase *PAL* catalyzing the first step in the phenylpropanoid pathway; and the stilbene synthase *STS* involved in the synthesis of phytoalexins (Trotel-Aziz et al., 2019). Interestingly, basal immunity results in a weak constitutive expression of the targeted defense genes in Chardonnay compared to Tempranillo (see **Figure 3**), despite the fact that literature described Chardonnay as less susceptible to BD than Tempranillo (Luque et al., 2009). Maybe our six targeted genes are not sufficiently exhaustive to presume at this preliminary stage of the susceptible versus tolerant status of both cultivars. However, looking at the specific red and white cultivar responses, the same studied genes are of interest: those specific to white grape cultivars include transcription factors from the ET pathway and lipid metabolism (e.g., lipoxygenase), while those specific to red grape cultivars are linked to the secondary metabolism in connection with the pathway of phenylpropanoids (e.g., *PAL* and its derivatives) and are expressed more strongly in the red cultivars, to distinguish them from the white ones (Lambert et al., 2012; Massonnet et al., 2017). Upon abiotic or biotic stress, other authors pointed out the highest synthesis of resveratrol in the most tolerant grapevine (Corso et al., 2015; Lakkis et al., 2019), but a gain of protection due to the BCA presence in susceptible cultivar (Lakkis et al., 2019). Considering that susceptible plants rather benefit from the help of BCA to

induce their immunity, unlike resistant plants that already have high basal immunity, we examined the immunity induced by both cultivars studied.

In Tempranillo (see **Figures 3B, 5** and **Supplementary Figure 1B**) under our experimental conditions, application of *Bs*-PTA-271 did not induce significant changes in plant defense responses compared to control, whether infected or not. Since Tempranillo basal immunity strongly upregulates *PR1* as a marker of SA-dependent defenses, we can speculate that high basal SA content might contribute to prevent the beneficial effect of *Bs* PTA-271 on Tempranillo immunity. Our previous study showed that *Bs* PTA-271 primed the expression of the plant JA/ET-dependent defenses in Chardonnay rootlings (Trotel-Aziz et al., 2019), whereas it is reported that early activation of SA signaling could antagonize the expression of these JA/ET-dependent defenses (Pieterse et al., 2012; Van der Does et al., 2013). In this sense, *Bs* PTA-271 did not provide protection in Tempranillo against *Np*-Bt67. These results show therefore that cultivars differing in their basal immunity can condition the success of a BCA protection toward a pathogen. In contrast, *Ta* SC1 alone or together with *Bs* PTA-271 acts as a priming stimulus for Tempranillo, but no post-priming was observed with *Ta* SC1 alone and with *Ta* SC1 + *Bs* PTA-271 upon pathogen challenge. Looking at the defenses induced by these two protective modalities (*Ta* SC1 and *Ta* SC1 + *Bs* PTA-271) against *Np*-Bt67: the SA-dependent defenses (i.e., *PR1*, *PAL*, and *STS*) were rather strongly decreased in protected plants (i.e., asymptomatic despite infected), while they were the highest in symptomatic plants (*Bs* PTA-271). Since Botryosphaeriaceae are known to specifically metabolize grapevine phytoalexins (Stempien et al., 2017), which benefits pathogen fitness, we could suggest that the SA stimulation of the phenylpropanoid pathway and derivatives would wrongly serve the plant. In the case of Tempranillo exposed to Botryosphaeriaceae, the high constitutive expression of SA-dependent defense genes could thus appear as a disadvantage, confirming that Tempranillo would be less tolerant than Chardonnay to BD, as already reported by Luque et al. (2009) and Cobos et al. (2019). Fortunately, in the Tempranillo pretreated with both BCAs, the expressions of genes *PR1*, *PAL*, and *STS* were repressed, and in the Tempranillo pretreated with *Ta* SC1 alone, the expression of the genes *PAL* and *STS* were repressed. Therefore, the beneficial effect of *Ta* SC1 on Tempranillo to control *Np*-Bt67 could result from a repressive effect on detrimental SA-dependent defenses. Complementary approaches are in progress to screen the induced key levers able to trigger ISR in the whole plant. Additionally, the *Ta* SC1 beneficial effect on Tempranillo could also result from a direct antagonism toward *Np*-Bt67 since it is applied in the same area as *Ta* SC1.

In non-infected Chardonnay rootlings (see **Figures 3A, 4** and **Supplementary Figure 1A**), *Ta* SC1 shoot application did not induce any significant changes of the selected targeted responses of plant defenses in leaves, while *Bs* PTA-271 root application upregulated the *PR1* and *PR2* gene expression and the combined application induced the expression of almost all targeted genes at a higher level than *Bs* PTA-271 alone. *Bs* PTA-271, alone or together with *Ta* SC1, may thus act as a priming stimulus in Chardonnay. However, upon pathogen

challenge (4 dpi, designed as a relevant sampling time point for such experiment), *Bs* PTA-271 did not prime any of the targeted defenses, probably due to low to medium pathogen pressure compared to that reported in Trotel-Aziz et al. (2019). However, *Bs* PTA-271 beneficial effect on Chardonnay is supported by the phenotype of the *Bs*-PTA-271 treated rootlings, showing a significant protection for Chardonnay against *Np*-Bt67 at 2.5 mpi. This contrasts with the detected non-benefit provided by the combined application of both BCAs at 2.5 mpi, despite the fact that defenses were primed at 4 dpi, possibly due to a very high level of reactive oxygen species (ROS) that could amplify the plant defenses. It is interesting to note that *GST1* (involved in the ROS detoxification process) is the only useful targeted gene that was weakly expressed in non-protected Chardonnay pre-treated with both BCAs and further infected with *N. parvum* (see **Figure 3A**). This may suggest that when a pathway with high induced defenses is not combined with sufficient ROS detoxification, a plant could potentially trigger many symptoms. In our experimental conditions, Chardonnay therefore favors *Bs* PTA-271's beneficial effect, probably thanks to the different key levers including the induced grapevine immunity. Present at the root level, these results and those reported in Trotel-Aziz et al. (2019) suggest that systemic induced immunity conferred by *Bs* PTA-271 drove the plant ISR against *Np*-Bt67. Amazingly, the application of both BCAs enabled to reach the highest level of Chardonnay defense gene expression upon pathogen challenge (see **Figure 3A**), despite no protection at 2.5 mpi (see **Figure 2D**). Since *Ta* SC1 contributes to actively reducing the SA-dependent defenses in Tempranillo, one can hypothesize that *Ta* SC1 would also promote the *Bs* PTA-271 way of triggering immunity in Chardonnay. The authors also indicated that *Trichoderma* spp. may produce enzymes (i.e., ACC deaminase) able to shunt ET synthesis (Alfiky and Weisskopf, 2021), but in Tempranillo, the application of both BCAs enabled reaching the highest protection (see **Figure 2G**). Thus, it would be surprising that *Ta* SC1 on its own would succeed to interfere with the beneficial effects of *Bs* PTA-271 in Chardonnay. This opens the discussion of how the cultivar interacts with BCAs and the pathogen to condition the beneficial or detrimental outcome against *Np*-Bt67. Complementary approaches are already in progress to screen which are the induced key levers useful to control ISR in the whole plant.

## CONCLUSION

Altogether, our results provide evidence that grapevine susceptibility to BD is cultivar-dependent, as well as the BCA beneficial effects. *Bs* PTA-271 was confirmed as an effective protector for Chardonnay against *Np*-Bt67, and *Ta* SC1 was shown for the first time as a good protector for Tempranillo. This study also reports for the first time the biocontrol potential of the combination of *Bs* PTA-271 and *Ta* SC1 against *Np*-Bt67 in Tempranillo. This is a promising result for an improved efficiency of sustainable biological control in a proven context of lack of effective chemicals to manage GTDs.



Endowed with aggressive molecules, *Bs* PTA-271 and *Ta* SC1 can antagonize each other, but *Bs* PTA-271 inhibits *Np*-Bt67 development with a greater efficiency in a three-way confrontation. This beneficial BCA collaboration against *Np*-Bt67 still operates in Tempranillo and confirms the interest of using both BCAs in combination to optimize the direct fight against *Np*-Bt67. These results are of great interest for effective curative treatments to obtain healthy mother plants in the nursery and to control BD in vineyard. However, the direct beneficial effect of combined BCAs did not operate to protect Chardonnay, suggesting that Chardonnay itself probably alters the fine-tuned orchestrated cooperation of BCAs that drives such direct beneficial effect.

Plant systemic immunity was also affected by each BCA. Our findings suggest a common feature for the two cultivars: the defenses that are greatly diminished in BCA-protected plants appear to be those that are responsive to SA, in contrast to symptomatic plants. For Tempranillo, the high basal expression of SA-dependent defenses may thus explain the highest susceptibility to BD and also the ineffectiveness of *Bs* PTA-271 in our experimental conditions. Complementary approaches are underway to further investigate the responses of each cultivar to both *Bs* PTA-271 and *Ta* SC1 under controlled conditions and upon pathogen challenge.

## DATA AVAILABILITY STATEMENT

The raw data supporting the conclusions of this article will be made available by the authors, without undue reservation.

## AUTHOR CONTRIBUTIONS

CL, PT-A, and FF designed and planned the research. CL performed most of the experiments, analyzed the data, and wrote the manuscript with input and discussion from PT-A, FF, JA, and DG. JA and DG validated the planned research and provided expertise for all stages of this work. J-FG ensured the

quality of the mother cuttings and greenhouse conditions. NR assured the quality of the qRT-PCR analyses and data. All authors contributed to writing and revising the manuscript.

## FUNDING

This work was supported by a French Grant from the Region GRAND-EST France and the City of GRAND-REIMS France through the BIOVIGNE Ph.D. program, whose functioning is supported by BELCHIM Crop Protection France. DG was supported by the Ramón y Cajal program, Spanish Government (RyC-2017-23098).

## ACKNOWLEDGMENTS

We are grateful to Cecilia Rego (Higher Institute of Agronomy, Lisbon University, Portugal) for the pathogen gift. Thanks are also due to Laetitia Parent and Vincent Leclerc for their technical assistance.

## SUPPLEMENTARY MATERIAL

The Supplementary Material for this article can be found online at: <https://www.frontiersin.org/articles/10.3389/fmicb.2021.726132/full#supplementary-material>

**Supplementary Figure 1** | *Bacillus subtilis* PTA-271 and *Trichoderma atroviride* SC1 attenuates induce differential expression of defense-related genes in leaves of Chardonnay (A) and Tempranillo (B) rootlings before and after pathogen challenge. Twenty weeks old rootlings untreated or pretreated with PTA-271 or SC1 or both were further infected with sterile PDA plugs (Control, *Bs*, *Ta*, and *Bs* + *Ta*, respectively) or with mycelium plugs of *Np*-Bt67 (Cti + *Np*, *Bs* + *Np*, *Ta* + *Np*, and *Bs* + *Ta* + *Np*, respectively). Transcript levels of defense-related genes monitored by qRT-PCR in plant leaf after 4 days of inoculation. Uninfected control of each cultivar was considered as a reference sample (1 × expression level) for the same cultivar, and heatmaps represent changes in the transcript expression levels as indicated by the color shading. Data are the means from three representative replicates among five showing the same trends. Legends for genes are as in **Figure 2**.

## REFERENCES

- Alexander, A., and Phin, C. K. (2014). Combination of biological agents in suppressing colonization of *Ganoderma boninense* of basal stem rot. *Am. Eurasian J. Sustain Agric.* 8, 1–7.
- Alfiky, A., and Weisskopf, L. (2021). Deciphering *Trichoderma*–plant–pathogen interactions for better development of biocontrol applications. *J. Fungus.* 7:61. doi: 10.3390/jof7010061
- Alström, S. (1991). Induction of disease resistance in common bean susceptible to halo blight bacterial pathogen after seed bacterization with rhizosphere pseudomonads. *J. Gen. Appl. Microbiol.* 37, 495–501. doi: 10.2323/jgam.37.495
- Berbegal, M., Ramón-Albalat, A., León, M., and Armengol, J. (2020). Evaluation of long-term protection from nursery to vineyard provided by *Trichoderma atroviride* SC1 against fungal grapevine trunk pathogens. *Pest Manag. Sci.* 76, 967–977. doi: 10.1002/ps.5605
- Bettenfeld, P., Fontaine, F., Trouvelot, S., Fernandez, O., and Courty, P. E. (2020). Woody plant declines. What's wrong with the microbiome? *Trends Plant Sci.* 25, 381–394. doi: 10.1016/j.tplants.2019.12.024
- Billones-Baaijens, R., and Savocchia, S. (2019). A review of Botryosphaeriaceae species associated with grapevine trunk diseases in Australia and New Zealand. *Austr. Plant Dis.* 48, 3–18. doi: 10.1007/s13313-018-0585-5
- Blundell, R., Arreguin, M., and Eskalen, A. (2021). *In vitro* evaluation of grapevine endophytes, epiphytes and sap micro-organisms for potential use to control grapevine trunk disease pathogens. *bioRxiv* [Preprint]. doi: 10.1101/2021.02.09.430335
- Caarls, L., Pieterse, C. M., and Van Wees, S. (2015). How salicylic acid takes transcriptional control over jasmonic acid signaling. *Front. Plant Sci.* 6:170. doi: 10.3389/fpls.2015.00170
- Calzarano, F., Di Marco, S., and Cesari, A. (2004). Benefit of fungicide treatment after trunk renewal of vines with different types of esca necrosis. *Phytopathol. Mediterr.* 43, 116–123.
- Caulier, S., Nannan, C., Gillis, A., Licciardi, F., Bragard, C., and Mahillon, J. (2019). Overview of the antimicrobial compounds produced by members of the *Bacillus subtilis* group. *Front. Microbiol.* 10:302. doi: 10.3389/fmicb.2019.00302
- Chacon, J. L., Gramaje, D., Izquierdo, P. M., Martínez, J., and Mena, A. (2020). Evaluation of six red grapevine cultivars inoculated with *Neofusicoccum parvum*. *Eur. J. Plant Pathol.* 158, 811–815. doi: 10.1007/s10658-020-02111-9



- Claverie, M., Notaro, M., Fontaine, F., and Wéry, J. (2020). Current knowledge on Grapevine Trunk Diseases with complex etiology: a systemic approach. *Phytopathol. Mediterr.* 59, 29–53. doi: 10.36253/phyto-11150
- Cobos, R., Calvo-Peña, C., Álvarez-Pérez, J. M., Ibáñez, A., Díez-Galán, A., González-García, S., et al. (2019). Necrotic and cytolytic activity on grapevine leaves produced by Nep1-like proteins of *Diplodia seriata*. *Front. Plant Sci.* 10:1282. doi: 10.3389/fpls.2019.01282
- Compant, S., Brader, G., Muzammil, S., Sessitsch, A., Lebrühi, A., and Mathieu, F. (2013). Use of beneficial bacteria and their secondary metabolites to control grapevine pathogen diseases. *BioControl*. 58, 435–455. doi: 10.1007/s10526-012-9479-6
- Compant, S., and Mathieu, F. (2017). *Biocontrol of Major Grapevine Diseases: Leading Research*. Wallingford: CAB, 160–170.
- Conrath, U., Beckers, G. J., Langenbach, C. J., and Jaskiewicz, M. R. (2015). Priming for enhanced defense. *Annu. Rev. Phytopathol.* 53, 97–119. doi: 10.1146/annurev-phyto-080614-120132
- Conrath, U., Thulke, O., Katz, V., Schwindling, S., and Kohler, A. (2001). Priming as a mechanism in induced systemic resistance of plants. *Eur. J. Plant Pathol.* 107, 113–119.
- Corso, M., Vannozzi, A., Maza, E., Vitulo, N., Meggio, F., Pitacco, A., et al. (2015). Comprehensive transcript profiling of two grapevine rootstock genotypes contrasting in drought susceptibility links the phenylpropanoid pathway to enhanced tolerance. *J. Exp. Bot.* 66, 5739–5752. doi: 10.1093/jxb/erv274
- De Vleeschauwer, D., and Höfte, M. (2009). Rhizobacteria-induced systemic resistance. *Adv. Bot. Res.* 51, 223–281. doi: 10.1016/s0065-2296(09)51006-3
- Di Marco, S., Osti, F., and Cesari, A. (2004). Experiments on the control of esca by *Trichoderma*. *Phytopathol. Mediterr.* 43, 108–115.
- Di Marco, S., Osti, F., Roberti, R., Calzarano, F., and Cesari, A. (2002). Attività di specie di 412 *Trichoderma* nei confronti di *Phaeoemoniella chlamydospora*, patogeno associato al mal dell'esca 413 della vite. *Atti Soc. Ital. Sci. Natl.* 2, 419–424.
- Dufour, M. C., Lambert, C., Bouscalt, J., Mérillon, J. M., and Corio-Costet, M. F. (2013). Benzothiadiazole-primed defence responses and enhanced differential expression of defence genes in *Vitis vinifera* infected with biotrophic pathogens *Erysiphe necator* and *Plasmopara viticola*. *Plant Pathol.* 62, 370–382. doi: 10.1111/j.1365-3059.2012.02628.x
- Elad, Y. (2000). Biological control of foliar pathogens by means of *Trichoderma harzianum* and potential modes of action. *Crop Prot.* 19, 709–714. doi: 10.1016/s0261-2194(00)00094-6
- El-Tarabily, K. A. (2006). Rhizosphere-competent isolates of streptomycete and non-streptomycete actinomycetes capable of producing cell-wall-degrading enzymes to control *Pythium aphanidermatum* damping-off disease of cucumber. *Botany* 84, 211–222. doi: 10.1139/b05-153
- Fontaine, F., Gramaje, D., Armengol, J., Smart, R., Nagy, Z. A., Borgo, M., et al. (2016a). *Grapevine Trunk Diseases. A Review*. Paris: OIV Publications. 24,979-10-91799-60-7.
- Fontaine, F., Pinto, C., Vallet, J., Clément, C., Gomes, A. C., and Spagnolo, A. (2016b). The effects of grapevine trunk diseases (GTDs) on vine physiology. *Eur. J. Plant Pathol.* 144, 707–721. doi: 10.1007/s10658-015-0770-0
- González, V., and Tello, M. L. (2011). The endophytic mycota associated with *Vitis vinifera* in central Spain. *Fungal Divers.* 47, 29–42. doi: 10.1007/s13225-010-0073-x
- Gramaje, D., and Armengol, J. (2011). Fungal trunk pathogens in the grapevine propagation process: potential inoculum sources, detection, identification, and management strategies. *Plant Dis.* 95, 1040–1055. doi: 10.1094/pdis-01-11-0025
- Gramaje, D., Urbez-Torres, J. R., and Sosnowski, M. R. (2018). Managing grapevine trunk diseases with respect to etiology and epidemiology: current strategies and future prospects. *Plant Dis.* 102, 12–39.
- Gruau, C., Tritel-Aziz, P., Guillaume, S., Rabenoelina, F., Clément, C., Baillieul, F., et al. (2015). *Pseudomonas fluorescens* PTA-CT2 triggers local and systemic immune response against *Botrytis cinerea* in grapevine. *Mol. Plant Microbe Interact.* 28, 1117–1129. doi: 10.1094/MPMI-04-15-0092-R
- Guetsky, R., Shtienberg, D., Elad, Y., Fischer, E., and Dinoor, A. (2002). Improving biological control by combining biocontrol agents each with several mechanisms of disease suppression. *Phytopathology* 92, 976–985. doi: 10.1094/phyto.2002.92.9.976
- Haidar, R., Deschamps, A., Roudet, J., Calvo-Garrido, C., Bruez, E., Rey, P., et al. (2016). 451 Multi-organ screening of efficient bacterial control agents against two major pathogens of 452 grapevine. *Biol. Control* 92, 55–65. doi: 10.1016/j.biocontrol.2015.09.003
- Halleen, F., Fourie, P. H., and Lombard, P. J. (2010). Protection of grapevine pruning wounds against *Eutypa lata* by biological and chemical methods. *South Afr. J. Enol. Vitic.* 31, 125–132.
- Hamiduzzaman, M. M., Jakab, G., Barnavon, L., Neuhaus, J. M., and Mauch-Mani, B. (2005).  $\beta$ -Aminobutyric acid-induced resistance against downy mildew in grapevine acts through the potentiation of callose formation and jasmonic acid signaling. *Mol. Plant Microbe Interact.* 18, 819–829. doi: 10.1094/mpmi-18-0819
- Harman, G. E. (2006). Overview of mechanisms and uses of *Trichoderma* spp. *Phytopathology* 96, 190–194. doi: 10.1094/phyto-96-0190
- Hofstetter, V., Buyck, B., Croll, D., Viret, O., Couloux, A., and Gindro, K. (2012). What if esca disease of grapevine were not a fungal disease? *Fungal Divers.* 4, 51–67. doi: 10.1007/s13225-012-0171-z
- Horton, N. J., and Kleinman, K. (2015). *Using R and RStudio for Data Management, Statistical Analysis, and Graphics*. Boca Raton, FL: CRC Press.
- Hunt, J. S., Gale, D. S. J., and Harvey, I. C. (2001). Evaluation of *Trichoderma* as bio-control for protection against wood-invading fungi implicated in grapevine trunk diseases. *Phytopathol. Mediterr.* 40, S485–S486.
- John, S., Scott, E. S., Wicks, T., and Hunt, J. (2004). Interactions between *Eutypa lata* and *Trichoderma harzianum*. *Phytopathol. Mediterr.* 43, 95–104.
- John, S., Wicks, T. J., Hunt, J. S., and Scott, E. S. (2008). Colonisation of grapevine wood by *Trichoderma harzianum* and *Eutypa lata*. *Aust. J. Grape Wine Res.* 14, 18–24.
- Kloepper, J. W., Ryu, M., and Zhang, S. (2004). Induced systemic resistance and promotion of plant growth by *Bacillus* spp. *Phytopathology* 94, 1259–1266. doi: 10.1094/phyto.2004.94.11.1259
- Kotze, R. G., Van der Merwe, C. F., Crampton, B. G., and Kritzing, Q. (2019). A histological assessment of the infection strategy of *Exserohilum turcicum* in maize. *Plant Pathol.* 68, 504–512. doi: 10.1111/ppa.12961
- Kumar (2013). *Trichoderma*: a biological weapon for managing plant diseases and promoting sustainability. *Int. J. Agril. Sci. Vet. Med.* 1, 106–121.
- Kuzmanovska, B., Rusevski, R., Jankulovska, M., and Oreshkovikj, K. B. (2018). Antagonistic activity of *Trichoderma asperellum* and *Trichoderma harzianum* against genetically diverse *Botrytis cinerea* isolates. *Chil. J. Agric. Res.* 78, 391–399. doi: 10.4067/s0718-58392018000300391
- Lakkis, S., Tritel-Aziz, P., Rabenoelina, F., Schwarzenberg, A., Nguema-Ona, E., Clément, C., et al. (2019). Strengthening grapevine resistance by *Pseudomonas fluorescens* PTA-CT2 relies on distinct defense pathways in susceptible and partially resistant genotypes to downy mildew and gray mold diseases. *Front. Plant Sci.* 10:1112. doi: 10.3389/fpls.2019.01112
- Lambert, C., Bisson, J., Waffo-Tégou, P., Papastamoulis, Y., Richard, T., Corio-Costet, M. F., et al. (2012). Phenolics and their antifungal role in grapevine wood decay: focus on the Botryosphaeriaceae family. *J. Agric. Food Chem.* 60, 11859–11868. doi: 10.1021/jf303290g
- Larach, A., Torres, C., Riquelme, N., Valenzuela, M., Salgado, E., Seeger, M., et al. (2020). Yield loss estimation and pathogen identification from *Botryosphaeria* dieback in vineyards of Central Chile over two growing seasons. *Phytopathol. Mediterr.* 59, 537–548.
- Larignon, P., Fontaine, F., Farine, S., Clement, C., and Bertsch, C. (2009). Esca and black dead arm: two major actors of grapevine trunk diseases. *C R Biol.* 332, 765–783. doi: 10.1016/j.crv.2009.05.005
- Larignon, P., Fulchic, R., Cere, L., and Dubos, B. (2001). Observation on black dead arm in French vineyards. *Phytopathol. Mediterr.* 40(Suppl.), S336–S342.
- Larignon, P. (2004). La constitution d'un groupe international de travail sur les maladies du bois et les premiers résultats des expérimentations menées par l'ITV en laboratoire et en pépinières. *Les Maladies du Bois en Midi-Pyrénées* 122, 24–27.
- Leal, C., Fontaine, F., Aziz, A., Egas, C., Clément, C., and Tritel-Aziz, P. (2021). Genome sequence analysis of the beneficial *Bacillus subtilis* PTA-271 isolated from a *Vitis vinifera* (cv. Chardonnay) rhizospheric soil: assets for sustainable biocontrol. *Environ. Microbiol.* 16, 1–14.

- Lebon, G., Duchêne, E., Brun, O., and Clément, C. (2005). Phenology of flowering and starch accumulation in grape (*Vitis vinifera* L.) cuttings and vines. *Ann. Bot.* 95, 943–948. doi: 10.1093/aob/mci108
- Liu, B., Xue, X., Cui, S., Zhang, X., Han, Q., Zhu, L., et al. (2010). Cloning and characterization of a wheat  $\beta$ -1, 3-glucanase gene induced by the stripe rust pathogen *Puccinia striiformis* f. sp. *Mol. Biol. Rep.* 37, 1045–1052. doi: 10.1007/s11033-009-9823-9
- Luque, J., Martos, S., Aroca, A., Raposo, R., and Garcia-Figueres, F. (2009). Symptoms and fungi associated with declining mature grapevine plants in northeast Spain. *Plant Pathol.* 91, 381–390.
- Magnin-Robert, M., Quantinet, D., Couderchet, M., Aziz, A., and Trotel-Aziz, P. (2013). Differential induction of grapevine resistance and defense reactions against *Botrytis cinerea* by bacterial mixtures in vineyards. *BioControl* 58, 117–131. doi: 10.1007/s10526-012-9474-y
- Magnin-Robert, M., Trotel-Aziz, P., Quantinet, D., Biagiatti, S., and Aziz, A. (2007). Biological control of *Botrytis cinerea* by selected grapevine-associated bacteria and stimulation of chitinase and  $\beta$ -1, 3 glucanase activities under field conditions. *Eur. J. Plant Pathol.* 118, 43–57. doi: 10.1007/s10658-007-9111-2
- Manter, D. K., Delgado, A., Holm, G., and Stong, A. (2010). Pyrosequencing reveals a highly diverse and cultivar-specific bacterial endophyte community in potato roots. *Microb. Ecol.* 60, 157–166.
- Martínez-Diz, M. P., Díaz-Losada, E., Andrés-Sodupe, M., Bujanda, R., Maldonado-González, M. M., Ojeda, S., et al. (2021a). Field evaluation of biocontrol agents against black-foot and Petri diseases of grapevine. *Pest Manag. Sci.* 77, 697–708. doi: 10.1002/ps.6064
- Martínez-Diz, M. P., Díaz-Losada, E., Díaz-Fernández, A., Bouzas-Cid, Y., and Gramaje, D. (2021b). Protection of grapevine pruning wounds against *Phaeoemoniella chlamydospora* and *Diplodia seriata* by commercial biological and chemical methods. *Crop Prot.* 143:105465. doi: 10.1016/j.cropro.2020.105465
- Massonnet, M., Fasoli, M., Tornielli, G. B., Altieri, M., Sandri, M., Zuccolotto, P., et al. (2017). Ripening transcriptomic program in red and white grapevine varieties correlates with berry skin anthocyanin accumulation. *Plant Physiol.* 174, 2376–2396. doi: 10.1104/pp.17.00311
- Meyer, S. L. F., and Roberts, D. P. (2002). Combinations of biocontrol agents for management of plant-parasitic nematodes and soilborne plant-pathogenic fungi. *J. Nematol.* 34, 1–8.
- Mimiague, F., and Le Gall, D. (1994). “Bilan sur les enquêtes eutypiose dans le vignoble européen,” in *Quatrième Conférence Internationale sur les Maladies des Plantes*, Bordeaux: Annales ANPP, 1265–1276.
- Mondello, V., Songy, A., Battiston, E., Pinto, C., Coppin, C., Trotel-Aziz, P., et al. (2018). Grapevine trunk diseases: a review of fifteen years of trials for their control with chemicals and biocontrol agents. *Plant Dis.* 102, 1189–1217. doi: 10.1094/pdis-08-17-1181-fe
- Muckherjee, M., Muckherjee, P. K., Horwitz, A., Zachow, C., Berg, G., Zeilinger, S., et al. (2012). Trichoderma-plant-pathogen interactions: advances in genetics of biological control. *Indian J. Microbiol.* 52, 522–529. doi: 10.1007/s12088-012-0308-5
- Mutawila, C., Fourie, P. H., Halleen, F., and Mostert, L. (2011). Grapevine cultivar variation to pruning wound protection by *Trichoderma* species against trunk pathogens. *Phytopathol. Mediterr.* 50, S264–S276.
- Naznin, H. A., Kiyohara, D., Kimura, M., Miyazawa, M., Shimizu, M., and Hyakumachi, M. (2014). Systemic resistance induced by volatile organic compounds emitted by plant growth-promoting fungi in *Arabidopsis thaliana*. *PLoS One* 9:e86882. doi: 10.1371/journal.pone.0086882
- Nguyen, N. H., Trotel-Aziz, P., Villalume, S., Rabenold, F., Schwarzenberg, A., Nguema-Ona, E., et al. (2020). *Bacillus subtilis* and *Pseudomonas fluorescens* trigger common and distinct systemic immune responses in *Arabidopsis thaliana* depending on the pathogen lifestyle. *Vaccines* 8:503. doi: 10.3390/vaccines8030503
- Nie, P., Li, X., Wang, S., Guo, J., Zhao, H., and Niu, D. (2017). Induced systemic resistance against *Botrytis cinerea* by *Bacillus cereus* AR156 through a JA/ET- and NPR1-dependent signaling pathway and activates PAMP-triggered immunity in *Arabidopsis*. *Front. Plant Sci.* 8:238. doi: 10.3389/fpls.2017.00238
- Niu, D. D., Liu, H. X., Jiang, C. H., Wang, Y. P., Wang, Q. Y., Jin, H. L., et al. (2011). The plant growth-promoting rhizobacterium *Bacillus cereus* AR156 induces systemic resistance in *Arabidopsis thaliana* by simultaneously activating salicylate- and jasmonate/ethylene-dependent signaling pathways. *Mol. Plant Microbe Interact.* 24, 533–542. doi: 10.1094/mpmi-09-10-0213
- O'Brien, P. A. (2017). Biological control of plant diseases. *Austr. Plant Pathol.* 46, 293–304.
- Ongena, M., and Jacques, P. (2008). *Bacillus* lipopeptides: versatile weapons for plant disease biocontrol. *Trends Microbiol.* 16, 115–125. doi: 10.1016/j.tim.2007.12.009
- Pacifico, D., Squartini, A., Crucitti, D., Barizza, E., Lo Schiavo, F., Muresu, R., et al. (2019). The role of the endophytic microbiome in the grapevine response to environmental triggers. *Front. Plant Sci.* 10:1256. doi: 10.3389/fpls.2019.01256
- Pertot, I., Prodorutti, D., Colombini, A., and Pasini, L. (2016). *Trichoderma atroviride* SC1 prevents *Phaeoemoniella chlamydospora* and *Phaeoacremonium aleophilum* infection of grapevine plants during the grafting process in nurseries. *BioControl* 61, 257–267. doi: 10.1007/s10526-016-9723-6
- Pieterse, C. M., Van Pelt, J. A., Van Wees, S. C., Ton, J., Léon-Kloosterziel, K. M., Keurentjes, J. J., et al. (2001). Rhizobacteria-mediated induced systemic resistance: triggering, signalling and expression. *Eur. J. Plant Pathol.* 107, 51–61.
- Pieterse, C. M. J., Van der Does, D., Zamioudis, C., Leon-Reyes, A., and Van Wees, S. C. M. (2012). Hormonal modulation of plant immunity. *Annu. Rev. Cell Dev. Biol.* 28, 489–521.
- Pieterse, J., Zamioudis, C., Berendsen, L., Weller, M., Van Wees, M., and Bakker, M. (2014). Induced systemic resistance by beneficial microbes. *Annu. Rev. Phytopathol.* 52, 347–375.
- Pinto, C., Sousa, S., Froufe, H., Egas, C., Clément, C., Fontaine, F., et al. (2018). Draft genome sequence of *Bacillus amyloliquefaciens* subsp. *plantarum* strain Fito\_F321, an endophyte microorganism from *Vitis vinifera* with biocontrol potential. *Stand. Genomic Sci.* 13, 1–12.
- Reis, P., Pierron, R., Larignon, P., Lecomte, P., Abou-Mansour, E., Farine, S., et al. (2019). Vitis methods to understand and develop strategies for diagnosis and sustainable control of grapevine trunk diseases. *Phytopathology* 109, 916–931. doi: 10.1094/phyto-09-18-0349-rvw
- Reveglia, P., Billones-Baaijens, R., Millera Niem, J., Masi, M., Cimmino, A., Evidente, A., et al. (2021). Production of phytotoxic metabolites by *Botryosphaeriaceae* in naturally infected and artificially inoculated grapevines. *Plants* 10:802. doi: 10.3390/plants10040802
- Rezgui, A., Ben Ghnaya-Chakroun, A., Vallance, J., Bruez, E., Hajlaoui, M. R., Sadfi-Zouaoui, N., et al. (2016). Endophytic bacteria with antagonistic traits inhabit the wood tissues of grapevines from Tunisian vineyards. *Biol. Control* 99, 28–37. doi: 10.1016/j.biocontrol.2016.04.005
- Rueden, C. T., Schindelin, J., Hiner, M. C., DeZonia, B. E., Walter, A. E., Arena, E. T., et al. (2017). ImageJ2: ImageJ for the next generation of scientific image data. *BMC Bioinformatics* 18:529. doi: 10.1186/s12859-017-1934-z
- Schmidt, C. S., Lorenz, D., and Wolf, G. A. (2001). Biological control of the grapevine dieback fungus *Eutypa lata* I: screening of bacterial antagonists. *Phytopathology* 149, 427–435.
- Schmidt, S. M., and Panstruga, R. (2011). Pathogenomics of fungal plant parasites: what have we learnt about pathogenesis? *Curr. Opin. Plant Biol.* 14, 392–399. doi: 10.1016/j.pbi.2011.03.006
- Sosnowski, M. R., Creaser, M., and Wicks, T. (2004). Evaluating fungicides as pruning wound treatments to control *Eutypa dieback*. *Aust. N.Z. Grapegrow. Winemak.* 485, 51–53.
- Stempin, E., Goddard, M. L., Wilhelm, K., Tarnus, C., Bertsch, C., and Chong, J. (2017). Grapevine *Botryosphaeria* dieback fungi have specific aggressiveness factor repertory involved in wood decay and stilbene metabolism. *PLoS One* 12:e0188766. doi: 10.1371/journal.pone.0188766
- Stempin, E., Jean, R., Pierron, G., Adendorff, I., Van Jaarsveld, W. J., Halleen, F., et al. (2020). Host defence activation and root colonization of grapevine rootstocks by the biological control fungus *Trichoderma atroviride*. *Phytopathol. Mediterr.* 59, 615–626.
- Thambugala, K. M., Daranagama, D. A., Phillips, A. J., Kannangara, S. D., and Promptutha, I. (2020). Fungi vs. fungi in biocontrol: an overview of fungal antagonists applied against fungal plant pathogens. *Front. Cell Infect. Microbiol.* 10:604923. doi: 10.3389/fcimb.2020.604923
- Tiwari, S., and Verma, T. (2019). “Cellulose as a potential feedstock for cellulose enzyme production,” in *Approaches to Enhance Industrial Production of Fungal Cellulases*, eds M. Srivastava, N. Srivastava, P. W. Ramteke, and P. K. Mishra (Berlin: Springer), 89–116. doi: 10.1007/978-3-030-14726-6\_6
- Travadon, R., Rolshausen, P. E., Gubler, W. D., Cadle-Davidson, L., and Baumgartner, K. (2013). Susceptibility of cultivated and wild *Vitis* spp. to wood

- infection by fungal trunk pathogens. *Plant Dis.* 97, 1529–1536. doi: 10.1094/pdis-05-13-0525-re
- Trotel-Aziz, P., Abou-Mansour, E., Courteaux, B., Rabenoelina, F., Clément, C., Fontaine, F., et al. (2019). *Bacillus subtilis* PTA-271 counteracts *Botryosphaeria* dieback in grapevine, triggering immune responses and detoxification of fungal phytotoxins. *Front. Plant Sci.* 10:25. doi: 10.3389/fpls.2019.00025
- Trotel-Aziz, P., Couderchet, M., Biagianti, S., and Aziz, A. (2008). Characterization of new bacterial biocontrol agents *Acinetobacter*, *Bacillus*, *Pantoea* and *Pseudomonas* spp. mediating grapevine resistance against *Botrytis cinerea*. *Environ. Exp. Bot.* 64, 21–32. doi: 10.1016/j.envexpbot.2007.12.009
- Úrbez-Torres, J. R. (2011). The status of Botryosphaeriaceae species infecting grapevines. *Phytopathol. Mediterr.* 50, 5–45.
- Úrbez-Torres, J. R., Tomaselli, E., Pollard-Flamand, J., Boulé, J., Gerin, D., and Pollastro, S. (2020). Characterization of *Trichoderma* isolates from southern Italy, and their potential biocontrol activity against grapevine trunk disease fungi. *Phytopathol. Mediterr.* 59, 425–439.
- Van der Does, D., Leon-Reyes, A., Koornneef, A., Van Verk, M. C., Rodenburg, N., Pauwels, L., et al. (2013). Salicylic acid suppresses jasmonic acid signaling downstream of SCFCOI1-JAZ by targeting GCC promoter motifs via transcription factor ORA59. *Plant Cell* 25, 744–761. doi: 10.1105/tpc.112.108548
- Van der Ent, S., Van Wees, S. C., and Pieterse, C. M. (2009). Jasmonate signaling in plant interactions with resistance-inducing beneficial microbes. *Phytochemistry* 70, 1581–1588. doi: 10.1016/j.phytochem.2009.06.009
- Van Peer, R., Niemann, G. J., and Schippers, B. (1991). Induced resistance and phytoalexin accumulation in biological control of *Fusarium* wilt of carnation by *Pseudomonas* sp. strain WCS 417 r. *Phytopathology*. 81, 728–734. doi: 10.1094/phyto-81-728
- Van Wees, S. C., Van der Ent, S., and Pieterse, C. M. (2008). Plant immune responses triggered by beneficial microbes. *Curr Opin Plant Biol.* 11, 443–448. doi: 10.1016/j.pbi.2008.05.005
- Velásquez, A. C., Castroverde, C. D. M., and He, S. Y. (2018). Plant–pathogen warfare under changing climate conditions. *Curr. Biol.* 28, R619–R634.
- Verhagen, B. W., Glazebrook, J., Zhu, T., Chang, H. S., Van Loon, L. C., and Pieterse, C. M. (2004). The transcriptome of rhizobacteria-induced systemic resistance in *Arabidopsis*. *Mol Plant Microbe Interact.* 17, 895–908. doi: 10.1094/mpmi.2004.17.8.895
- Vinale, F., Sivasithamparan, K., Ghisalberti, E. L., Marra, R., Barbetti, M. J., Li, H., et al. (2008). A novel role for *Trichoderma* secondary metabolites in the interactions with plants. *Physiol Mol Plant Path.* 72, 80–86. doi: 10.1016/j.pmp.2008.05.005
- Waghunde, R. R., Shelake, R. M., and Sabalpara, A. N. (2016). *Trichoderma*: a significant fungus for agriculture and environment. *Afr J Agric Res.* 11, 1952–1965. doi: 10.5897/ajar2015.10584
- Wei, G., Kloepper, J. W., and Tuzun, S. (1991). Induction of systemic resistance of cucumber to *Colletotrichum orbiculare* by select strains of plant growth-promoting rhizobacteria. *Phytopathology* 81, 1508–1512. doi: 10.1094/phyto-81-1508
- Weller, D. M. (1988). Biological control of soilborne plant pathogens in the rhizosphere with bacteria. *Annu. Rev. Phytopathol.* 26, 379–407. doi: 10.1146/annurev.py.26.090188.002115
- Yacoub, A., Magnin, N., Gerbore, J., Haidar, R., Bruez, E., Compant, S., et al. (2020). The biocontrol root-oomycete, *Pythium Oligandrum*, triggers grapevine resistance and shifts in the transcriptome of the trunk pathogenic fungus, *Phaeoemoniella chlamydospora*. *Int. J. Mol. Sci.* 21:6876. doi: 10.3390/ijms21186876
- Yobo, K. S., Laing, M. D., and Hunter, C. H. (2011). Effects of single and combined inoculations of selected *Trichoderma* and *Bacillus* isolates on growth of dry bean and biological control of *Rhizoctonia solani* damping-off. *Afr. J. Biotechnol.* 10, 8746–8756. doi: 10.5897/ajb10.2213

**Conflict of Interest:** The authors declare that the research was conducted in the absence of any commercial or financial relationships that could be construed as a potential conflict of interest.

**Publisher's Note:** All claims expressed in this article are solely those of the authors and do not necessarily represent those of their affiliated organizations, or those of the publisher, the editors and the reviewers. Any product that may be evaluated in this article, or claim that may be made by its manufacturer, is not guaranteed or endorsed by the publisher.

Copyright © 2021 Leal, Richet, Guise, Gramaje, Armengol, Fontaine and Trotel-Aziz. This is an open-access article distributed under the terms of the Creative Commons Attribution License (CC BY). The use, distribution or reproduction in other forums is permitted, provided the original author(s) and the copyright owner(s) are credited and that the original publication in this journal is cited, in accordance with accepted academic practice. No use, distribution or reproduction is permitted which does not comply with these terms.



# Bactericidal Effect of *Pseudomonas oryziphila* sp. nov., a Novel *Pseudomonas* Species Against *Xanthomonas oryzae* Reduces Disease Severity of Bacterial Leaf Streak of Rice

Ruihuan Yang<sup>1</sup>, Shengzhang Li<sup>1</sup>, Yilang Li<sup>1</sup>, Yichao Yan<sup>1</sup>, Yuan Fang<sup>1</sup>, Lifang Zou<sup>1,2\*</sup> and Gongyou Chen<sup>1,2</sup>

## OPEN ACCESS

### Edited by:

Jochen Fischer,  
Institut für Biotechnologie und  
Wirkstoff-Forschung (IBWF), Germany

### Reviewed by:

Baishi Hu,  
Nanjing Agricultural University, China  
Xiufang Xin,  
CAS Center for Excellence  
in Molecular Plant Sciences, Institute  
of Plant Physiology and Ecology,  
Chinese Academy of Sciences (CAS),  
China

### \*Correspondence:

Lifang Zou  
zoulifang202018@sjtu.edu.cn

### Specialty section:

This article was submitted to  
Microbe and Virus Interactions with  
Plants,  
a section of the journal  
Frontiers in Microbiology

**Received:** 16 August 2021

**Accepted:** 04 October 2021

**Published:** 04 November 2021

### Citation:

Yang R, Li S, Li Y, Yan Y, Fang Y,  
Zou L and Chen G (2021) Bactericidal  
Effect of *Pseudomonas oryziphila* sp.  
nov., a Novel *Pseudomonas* Species  
Against *Xanthomonas oryzae*  
Reduces Disease Severity of Bacterial  
Leaf Streak of Rice.  
Front. Microbiol. 12:759536.  
doi: 10.3389/fmicb.2021.759536

<sup>1</sup> School of Agriculture and Biology, Shanghai Jiao Tong University, Shanghai, China, <sup>2</sup> State Key Laboratory of Microbial Metabolism, Shanghai Jiao Tong University, Shanghai, China

*Pseudomonas* is a diverse genus of Gammaproteobacteria with increasing novel species exhibiting versatile traits including antimicrobial and insecticidal activity, as well as plant growth-promoting, which make them well suited as biocontrol agents of some pathogens. Here we isolated strain 1257 that exhibited strong antagonistic activity against two pathovars of *Xanthomonas oryzae*, especially *X. oryzae* pv. *oryzicola* (Xoc) responsible for the bacterial leaf streak (BLS) in rice. The phylogenetic, genomic, physiological, and biochemical characteristics support that strain 1257 is a representative of a novel *Pseudomonas* species that is most closely related to the entomopathogenic bacterium *Pseudomonas entomophila*. We propose to name it *Pseudomonas oryziphila* sp. nov. Comparative genomics analyses showed that *P. oryziphila* 1257 possesses most of the central metabolic genes of two closely related strains *P. entomophila* L48 and *Pseudomonas mosselii* CFML 90-83, as well as a set of genes encoding the type IV pilus system, suggesting its versatile metabolism and motility properties. Some features, such as insecticidal toxins, phosphate solubilization, indole-3-acetic acid, and phenylacetic acid degradation, were disclosed. Genome-wide random mutagenesis revealed that the non-ribosomal peptide catalyzed by LgrD may be a major active compound of *P. oryziphila* 1257 against Xoc RS105, as well as the critical role of the carbamoyl phosphate and the pentose phosphate pathway that control the biosynthesis of this target compound. Our findings demonstrate that 1257 could effectively inhibit the growth and migration of Xoc in rice tissue to prevent the BLS disease. To our knowledge, this is the first report of a novel *Pseudomonas* species that displays a strong antibacterial activity against Xoc. The results suggest that the *P. oryziphila* strain could be a promising biological control agent for BLS.

**Keywords:** *Pseudomonas oryziphila*, *Xanthomonas oryzae*, bactericidal effect, biocontrol agents, bacterial leaf streak of rice



## INTRODUCTION

*Pseudomonas* species are gram-negative bacteria that are ubiquitous in soil, water, animals, and plant rhizosphere (Weller, 2007). Pseudomonads have the ability to grow rapidly and persist in plant rhizosphere, produce a wide range of secondary metabolites (i.e., antibiotics, siderophores, volatiles, and growth-promoting substances), and adapt to environmental stresses, which make them suitable as biocontrol agents of plant pathogens (Weller, 2007; Couillerot et al., 2009). Certain species of this genus have been demonstrated to be the effective biocontrol or growth-promoting agents. The 2,4-diacetylphloroglucinol (2,4-DAPG)-producing *Pseudomonas fluorescens* can suppress *Gaeumannomyces graminis*, a fungal pathogen, to control the take-all disease of wheat (Thomashow and Weller, 1988; Landa et al., 2003; Kwak et al., 2009). Besides significant suppression of the take-all disease, *P. fluorescens* strain 2-79 increased yields by an average of 17% in field trials (Weller, 2007). Some *Pseudomonas chlororaphis* strains are proficient biocontrol agents of many fungal, bacterial, and oomycete plant pathogens, which attributes to their ability to produce phenazines, pyrrolnitrin, hydrogen cyanide (HCN), siderophores, and volatile organic compounds (VOCs) (Anderson and Kim, 2018; Biessy and Filion, 2018). Phenazines and some VOCs are also involved in the induction of systemic resistance in plants (Raio and Puopolo, 2021). Therefore, there has been high increasing interest in *Pseudomonas* species for commercial and biotechnological applications.

Recent studies have shown that pseudomonads are also a resource reservoir for the control of plant bacterial diseases especially caused by plant pathogenic *Xanthomonas*. *Pseudomonas entomophila* is an entomopathogenic bacterium that is able to kill *Drosophila* larvae and adults. Its entomopathogenic property and hemolytic activity have been associated with insecticidal toxins and cyclic lipopeptides (Vodovar et al., 2005; Vallet-Gely et al., 2010). A recent study showed that *P. entomophila* harbors the bactericidal effect against *Xanthomonas citri* subsp. *citri* (*Xcc*), a causative agent of citrus canker (Villamizar et al., 2020). The saprophytic soil *Pseudomonas putida* has been reported to have the ability to inhibit three *Xanthomonas* bacteria *Xcc*, *Xanthomonas oryzae* pv. *oryzae* (*Xoo*), and *X. oryzae* pv. *oryzicola* (*Xoc*) (Sun et al., 2017). The *P. putida* group members including *Pseudomonas soli* and *Pseudomonas mosselii* produce a mixture of cyclic lipopeptides designated xantholysins that has the specific anti-*Xanthomonas* activity (Li et al., 2013; Pascual et al., 2014). Whether there are some unknown species in *Pseudomonas* genus that have the potential for controlling plant bacterial diseases caused by phytopathogenic *Xanthomonas* remains to be explored.

*Xoc* can infect the host rice causing bacterial leaf streak (BLS) that has gradually become the fourth major disease on rice in some rice-growing regions in southern China, resulting in a yield reduction of 10–30% in some severe cases (Nino-Liu et al., 2006; Ji et al., 2014). To date, no rice variety that is completely immune to *Xoc* was found

(Xu et al., 2021). At present, all rice varieties commonly planted in China are susceptible to *Xoc*, even some hybrid rice varieties are highly susceptible. Currently, bactericides such as bismethiazole or cupric pesticides are frequently used to control BLS in China (Xu et al., 2015; Pan et al., 2017), which has caused *Xoc* to develop resistance. Therefore, an effective and environmentally friendly biocontrol method for BLS is needed.

Our laboratory has been working to develop biological control methods to control BLS. As a part of our work on identifying useful bacterial resources, we screened 223 candidate isolates that exhibited apparent antagonistic activity against the *Xoc* wild-type strain RS105. In our previous studies, three *Bacillus* strains, *Bacillus velezensis* 504, *B. altitudinis* 181-7, and *Bacillus cereus* 512, have been reported to exhibit significantly inhibitory effects on water-soaked lesions caused by *Xoc* in rice leaves (Li et al., 2019; Li S. Z. et al., 2020). In this study, we characterized a *Pseudomonas* strain 1257 from the 223 candidate isolates. The phylogenetic, genomic, physiological, and biochemical characteristics demonstrated that strain 1257 is a representative of a novel *Pseudomonas* species, for which we propose to name *Pseudomonas oryziphila* sp. nov. as its specific antibacterial activity against *Xoo* and *Xoc*. Genomic information showed that *P. oryziphila* 1257 is most closely related to the entomopathogenic bacterium *P. entomophila*. Genome-wide random mutagenesis revealed that a non-ribosomal peptide may be the major active compound involved in biocontrol agent of the *P. oryziphila* strain for BLS. To our knowledge, this is the first report of a novel *Pseudomonas* species that displays a specific antibacterial activity against *Xoc*.

## MATERIALS AND METHODS

### Strains, Plasmids and Primers, Growth Conditions, and Plant Materials

The bacterial strains and plasmids are listed in **Supplementary Table 1**, and primers are listed in **Supplementary Table 2**. All *Xanthomonas* species strains were cultured in nutrient agar (NA) or nutrient broth (NB) medium at 28°C (Cai et al., 2017); *Escherichia coli* DH5 $\alpha$  and EC100D were grown in Luria-Bertani (LB) medium at 37°C. Rice seeds (Yuanfengzhao) were provided by Dr. Youlun Xiao from the Institute of Plant Protection, Hunan Academy of Agricultural Sciences. Antibiotics were used at the following final concentrations ( $\mu\text{g mL}^{-1}$ ) as required: rifampicin (Rif), 75; kanamycin (Km), 25; gentamicin (Gm), 10; and spectinomycin (Sp), 25.

### Isolation of Biocontrol Strains and Antimicrobial Activity Assays

The rhizosphere soil samples from healthy plants were collected from 23 provinces in China. Briefly, a 10-g soil sample with several steel balls was added to a triangular conical flask with 90-mL sterilized water and then was shaken for 20 min at 28°C,

200 revolutions/min (rpm). A 1-mL suspension was diluted to three gradients of  $10^{-3}$ ,  $10^{-4}$ , and  $10^{-5}$  in sterilized water. The *Xoc* RS105 was used as an indicator, through inhibiting its growth to screen biocontrol strains. A 100- $\mu$ L diluted solution was plated onto NA agar plates containing RS105. The plates were incubated at 28°C for 2 days. Colonies with antagonistic activity were transferred and purified and then were further confirmed by the Oxford Cup method. The inhibition zones were measured by Kirby-Bauer (KB) test method. Each inhibitory phenotype was repeated in triplicate. The antagonistic bacterial isolates were collected and stored at -80°C with glycerol (50%, vol/vol). Strain 1257 was isolated from the rhizosphere soil of cabbage collected on September 27, 2017 from Cungu village in Zhuanghang town, Fengxian District, Shanghai, China.

The antimicrobial activity of *P. oryziphila* 1257 was examined using *Xanthomonas* strains, non-*Xanthomonas* strains, and some fungal pathogen strains listed in **Supplementary Table 1**. All bacterial strains were inoculated into NB medium, followed by shaking at 28°C, 200 rpm for 12 h. The harvested cells were suspended and adjusted to a final concentration of OD<sub>600</sub> = 2.0 using NB medium, and then the 200  $\mu$ L solutions were added into the NA medium plates. A 50  $\mu$ L (OD<sub>600</sub> = 2.0) *P. oryziphila* 1257 solution was added into the Oxford Cup. The inhibition zones were measured using KB method and sterile water as the negative control. Three biological replicates were performed. The antifungal activity of *P. oryziphila* 1257 was further studied by confrontation-culture plating method according to the reported protocols.

## Phylogenetic Analysis Based on Multilocus Sequence and Average Nucleotide Identity Calculation

The morphology and physiological and biochemical characteristics of strain 1257 were identified by China Center for Type Culture Collection. Its 16S *rRNA* gene sequence was amplified using universal primers of 27F and 1492R (**Supplementary Table 2**; Dorsch et al., 1992). The 50- $\mu$ L reaction mixtures contained 5  $\mu$ L of 10  $\times$  Ex Taq buffer (Mg<sup>2+</sup> Plus) (20 mM), 4  $\mu$ L of dNTP mixture (10 mM), 1  $\mu$ L of each primer (10  $\mu$ M), 1  $\mu$ L of genomic DNA template (30–50 ng/ $\mu$ L), and 0.25  $\mu$ L of Ex Taq DNA polymerase (TaKaRa, 5 U/ $\mu$ L), with double-distilled water up to 50  $\mu$ L. The polymerase chain reaction (PCR) amplifications were performed according to the following parameters: initial denaturation at 95°C for 8 min and then 32 cycles of 30 s of denaturation at 95°C, 30 s of annealing at 55°C, and 1.5 min of extension at 72°C, and a final extension at 72°C for 10 min. The 1,500-bp fragment was purified and sequenced in BioSune Biotech (Shanghai, China). The complete DNA sequence was used for blast search in the National Center for Biotechnology Information (NCBI) database. The multilocus sequence analysis (MLSA) phylogenetic tree was established and performed. The genome sequences for the other 15 representative *Pseudomonas* species were obtained from the NCBI database. The nucleotide sequences of 10 housekeeping genes *16Sr RNA*, *aroE*, *dnaA*, *guaA*, *gyrB*, *mutL*, *ppsA*, *pyrC*, *recA*, and *rpoB* were aligned using Muscle (version 3.8.425), and the unreliable

comparison points were removed using Gblock (version 0.91b) to ensure that these sequences were suitable for phylogenetic analysis. A maximum likelihood-based phylogenetic method was performed with MEGA 7.0 software, with 1,000 bootstrap replicates; the internodes of branches indicated the percentage (Kumar et al., 2016). The average nucleotide identity (ANI) values among 16 genome sequences including *P. oryziphila* 1257 and other closest strains were calculated using the J Species WS Online Service (Richter et al., 2016). The relatedness of strains *P. oryziphila* 1257, *P. entomophila* L48, and *P. mosselii* CFML 90-83 was further determined by DNA-DNA hybridization as described by Fischer et al. (2011).

## DNA Extraction and Genome Sequencing

The genomic DNA of *P. oryziphila* 1257 was extracted using the Hipure bacterial DNA kit (Magen, Guangzhou, Guangdong, China); DNA quality and integrity were determined by using a Qubit Fluorometer (Invitrogen, United States) and a NanoDrop Spectrophotometer (Thermo scientific, United States). The whole genome was sequenced using the Pacific Biosciences platform and the Illumina Miseq platform at Personalbio (Shanghai, China). The complete genome sequence of *P. oryziphila* 1257 was deposited in GenBank under accession number CP034338.1.

## Gene Family Construction and Collinearity Analysis

For comparative analyses of the orthologous and exclusive genes between 1257 and the other two closest genomes, the protein sequences of *P. oryziphila* 1257, *P. entomophila* L48, and *P. mosselii* CFML 90-83 were filtered to remove low-quality sequences based on length and percent stop codons in FASTA format. Then these proteomes were compared to each other based on an all-versus-all BLASTP alignment with an *E* value of 1e-10, I (Inflation) of 1.5 and at 70% identity. The BLASTP results are retrieved with the MCL program for clustering to construct gene families using OrthoMCL software (version 2.0.8). At last, through the Perl 5.8, DBI libraries to organize and count above clustering results were included.

Collinearity of the conserved and highly orthologous genomic regions were determined and plotted among *P. oryziphila* 1257, *P. entomophila* L48, and *P. mosselii* CFML 90-83 by using Mauve software (version 2.3.1) with default parameters (Darling et al., 2004). The colored, locally collinear blocks (LCBs) show the conserved and highly similar genomic regions. The white areas inside colored regions indicate sequence elements specific to one genome that are not aligned. The height of similarity profile is present inside each block. The colored lines that connect LCBs represent translocations of homologous regions. Blocks above or below the horizontal bar indicated regions that aligned in the forward or reverse orientation, respectively.

## The antiSMASH Analysis

The genomes of *P. oryziphila* 1257, *P. entomophila* L48, and *P. mosselii* CFML 90-83 were analyzed by antiSMASH 5.0 with web server<sup>1</sup> to predict the putative secondary metabolite

<sup>1</sup><https://antismash.secondarymetabolites.org/>

biosynthesis gene clusters (Blin et al., 2019). Detailed gene cluster information was obtained from the GenBank databases.

## Siderophore Production Detection

The chrome azurol S (CAS) assay was used for detecting the siderophore production according to the published methods (Schwyn and Neilands, 1987). Three strains of *P. oryziphila* 1257, *P. entomophila* L48, and *P. mosselii* CFML 90-83 were cultured in LB overnight, and then the suspensions of concentration with OD<sub>600</sub> 2.0 in LB were obtained. A 5-μL solution was spotted on CAS agar plates, incubating at 28°C for 24 h, with three technical replicates.

## EZ-Tn5 Mutagenesis and Screening

Random mutagenesis was performed by electroporation of *P. oryziphila* 1257 competent cell with 1 μL of the EZ-Tn5 < R6Kγori/KAN-2 > Tnp transposome. The electroporated cells were immediately recovered with LB medium to the electroporation cuvette to 1-mL final volume. The medium was mixed gently by a pipette, transferred to a tube, and incubated on a 28°C shaker for 2 h to facilitate the cell outgrowth. Each 200 μL of the cells was plated on four plates containing Km and incubated at 28°C for 2 days. The colonies were moved individually to the NA agar medium containing *Xoc* RS105 and Km to screen the mutants that exhibited absolutely losing, apparently and partially attenuated antagonistic activity against *Xoc* RS105.

The genomic DNA from chosen mutants was digested by *Eco*RI and then were self-ligated by mixing 8 μL of the digested DNA with 1 μL of ligation buffer and 1 μL of T4 DNA ligase (5 units; Thermo). The mixture was incubated at 22°C for 12 h and then inactivated at 70°C for 10 min. An aliquot of 5 μL of the ligation mixture was used to transform *E. coli* EC100D *pir*<sup>+</sup> electrocompetent cells and then were plated on LB plates containing Km. Colonies were screened by amplified with the primers Tn5-F and Tn5-R in **Supplementary Table 2**. Insertion sites were confirmed by sequencing using the forward or reverse EZ-Tn5 < R6Kγori/KAN-2 > transposon-specific primers that were supplied in the kit.

## Construction of the Complemented Strains

Here we selected five mutants of 100-12, 56-11, 62-42, 62-27, and 92-23 to complement. Briefly, the open reading frame sequences with the promoter regions of *lgrD*, *carA*, *carB*, *purF*, and *serC* genes were amplified by PCR with primers listed in **Supplementary Table 2**. The corresponding PCR products were cloned into pML123, resulting in pML-*lgrD* by *Xba*I and *Hind*III digestion resulting in pML-*carA* and pML-*carB* by *Bam*HI and *Xba*I digestion, resulting in pML-*serC* by *Bam*HI and *Sac*I digestion, as well as resulting in pML-*purF* by *Hind*III and *Sac*I digestion. Correct recombinant plasmids were confirmed by PCR using the primers pML123-F and pML123-R listed in **Supplementary Table 2**. Subsequently, the recombinant plasmids were introduced into the corresponding mutants by electroporation.

## Biocontrol Assays

For biocontrol assays in rice fields, 10 leaves from the highly susceptible rice cultivar Yuanfengzao at booting stage were inoculated with *Xoc* RS105 (OD<sub>600</sub> = 0.6) by needle injection. 1257 treatment (1257-Tre) meant that rice leaves were sprayed with 1257 (OD<sub>600</sub> = 1.0) 12 h after inoculation with *Xoc* RS105 suspension. 1257 preventive treatment (1257-Pre) indicated that rice leaves were sprayed with 1257 12 h before inoculation with *Xoc* RS105 suspension. Three independent experiments were performed. The BLS disease severity under all treatments was investigated after 15 days. For biocontrol assays in greenhouse, three leaves from 2-week-old Yuanfengzao were inoculated with *Xoc* RS105-Gus (OD<sub>600</sub> = 0.6) by needleless syringe. The 1257-Tre and 1257-Pre indicated that rice leaves were injected with 1257 at 3 h after and before inoculation with *Xoc* RS105-Gus suspension, respectively. Three pots were injected in one leaf. Two independent experiments were performed. The BLS disease severity under all treatments was observed after 1, 3, 5, and 7 days. The inhibitory percentages (IPs) were calculated by the formula: IP = (1-lesions length of treatment/lesions length of control) × 100. The IP was calculated by using three technical replicates per assay. Student *t* test was used for significance (*p* < 0.05), and the statistical results were treated by GraphPad Prism 8 version.

## β-Glucuronidase Activity Assays

The β-glucuronidase (GUS) activity of *Xoc* RS105-Gus strains including staining and quantitative detection for each treatment in greenhouse was conducted as our previous methods (Li Y. L. et al., 2020; Zou et al., 2021).

## RESULTS

### Isolation of Strain 1257 That Exhibits Strong Antagonistic Activity Against *Xanthomonas oryzae*

To screen beneficial bacterial resources to control BLS, we attained 223 bacterial isolates that displayed evident antibacterial activity against the *Xoc* wild-type strain RS105 from the 248 rhizosphere soil samples collected from 23 provinces in China. Among these isolates, we found that one strain, 1257, strongly inhibited *Xoc* RS105 (with an inhibition zone > 40 mm) and other eight *Xoc* strains isolated from Chinese major rice-growing regions (**Figure 1A** and **Supplementary Figure 1**). We found that 1257 also exhibited antagonistic effect against the *Xoo* wild-type strain PXO99<sup>A</sup>; however, the antibacterial activity against the *Xoc* strains by 1257 was significantly stronger than the *Xoo* strains (**Figure 1A** and **Supplementary Figure 1**). Further antibacterial activity assays showed that 1257 displayed a week antagonistic activity against other five *Xanthomonas* including *Xanthomonas campestris* pv. *phaseoli*, *Xanthomonas axonopodis* pv. *glycines*, *X. campestris* pv. *vesicatoria*, *X. campestris* pv. *malvacearum*, and *X. campestris* pv. *juglandis* (**Figure 1A**), and no evident inhibitory effect against *X. axonopodis* pv. *vasculorum*, *X. axonopodis* pv.



*allii*, and *X. campestris* pv. *musacearum*, as well as other four non-*Xanthomonas* bacterial pathogens such as *Pseudomonas syringae* pv. *tomato* DC3000, *Ralstonia solanacearum*, *Burkholderia glumae*, and *Acidovorax citrulli* (data not shown). The antifungal activity assays showed that 1257 displayed no any inhibitory effect on five fungal pathogens including *Magnaporthe oryzae*, *Fusarium graminearum*, *Fusarium oxysporum*, *Botrytis cinerea*, and *Phytophthora capsici* (data not shown). These results suggest that 1257 exhibits specific inhibitory activity against *Xoc* and *Xoo*, two pathovars of *X. oryzae*.

## 1257 Is a Novel *Pseudomonas* Species Closely Related to *Pseudomonas entomophila*

The partial 16S rRNA gene sequence of 1257 was amplified and aligned with the 16S rRNA gene sequences that have been deposited in the NCBI database. The BLAST analysis indicated that 1257 belongs to the *Pseudomonas* genus; however, the 16S rRNA gene sequence of 1257 exhibited more than 99% similarity with the corresponding sequences of *P. entomophila* L48 (99.54% similarity) and *P. mosselii* CFMT90-83 (99.48% similarity). To define the phylogenetic status of 1257, we sequenced the complete genome of 1257 (Figure 1B), which has been deposited in GenBank under accession number CP034338.1. The dendrogram deduced from 10 housekeeping genes (16S rRNA, *aroE*, *dnaA*, *guaA*, *gyrB*, *mutL*, *ppsA*, *pyrC*, *recA*, and *rpoB*) using MLSA showed that 1257 located in a separate branch with the type strains of *P. entomophila* L48 and *P. mosselii* CFMT90-83 as its nearest neighbors (Figure 1C).

Further, we conducted an ANI analysis between 1257 and other 15 sequenced different species in the phylogenetic tree. All ANI values (ANIb and ANIm) between 1257 and individual species of the genus are in the range of 73.77 to 89.13% (Table 1), which is clearly below the threshold of 95% for species demarcation, indicating that 1257 was distinct to the type strains of all species. 1257 displayed an ANIb value of 86.55% with *P. entomophila* L48, and an ANIb value of 86.72% with *P. mosselii* CFMT90-83, confirming that 1257 should not be grouped into *P. entomophila* or *P. mosselii*. The DNA–DNA hybridization (DDH) value between 1257 and *P. entomophila* L48 was 34.10%, and the DDH value between 1257 and *P. mosselii* CFML 90-83 was 34.70%. These two values were less than the accepted species threshold of 70%. Together, these results suggested that 1257 is a novel species within the *Pseudomonas* genus, which is closely related to *P. entomophila* and *P. mosselii* species.

Additional physiological and biochemical characteristics including enzyme activity, carbon source assimilation and acid production were tested by Biolog system using the Biolog GN2 microplates (Supplementary Table 3). The physiological and biochemical characteristics of *P. entomophila* L48 and *P. mosselii* CFML 90-83 were attained from the previous studies (Dabboussi et al., 2002; Mulet et al., 2012; Supplementary Table 3). These results showed that 1257 exhibited more

than 21 phenotypic features similar to *P. entomophila* L48 and *P. mosselii* CFML 90-83, whereas 1257 differed from *P. entomophila* L48 and *P. mosselii* CFML 90-83 in the utilization of nine carbon sources especially in *N*-acetyl-D-glucosamine, D-arabitol, D-(+)-glucuronic acid, and 2,3-butanediol. 1257 displayed the same as *P. entomophila* L48 in urease activity and in the ability to use L-fucose, psicose,  $\alpha$ -ketobutyric acid, and dimethyl succinate as carbon sources. 1257 differed from *P. entomophila* L48 in the capacity to use glycogen, which is negative for 1257 and *P. mosselii* CFML 90-83. Combined with the antagonistic phenotypes that *P. entomophila* L48 exhibited similar antibacterial activity against *Xoc* RS105 with 1257, but *P. mosselii* CFML 90-83 displayed no inhibitory effect on *Xoc* RS105 (Figure 2A), we concluded that 1257 is most closely related to *P. entomophila*.

Synthetically considering the phylogenetic, genomic, physiological, and biochemical characteristics, we propose strain 1257 as a representative of a novel *Pseudomonas* species, for which we propose to name *P. oryziphila* sp. nov. The type strain is *P. oryziphila* 1257<sup>(T)</sup>.

## Genome Features and Comparative Genomics Analysis

The genome of *P. oryziphila* 1257 is composed of a circular chromosome of 6,049,604 base pairs (Figure 1B) with an overall G + C content of 63.76% and 5,441 protein coding sequences (CDSs), 22 rRNA genes, 76 tRNA genes, and 73 other non-coding RNA genes, without plasmid, which is similar with *P. entomophila* L48, but distinct from *P. mosselii* CFML 90-83 (Table 2). The *P. oryziphila* 1257 genome is larger than that of the *P. entomophila* L48 and smaller than *P. mosselii* CFML 90-83. The collinearity analysis is consistent with the close relatedness among *P. oryziphila*, *P. entomophila*, and *P. mosselii* (Figure 2B). OrthoMCL analysis of the orthologous genes among the three genomes showed that 11,791 genes constitute the core genome, occupying 83.6 to 87.1% of each genome (Figure 2C); 89.6% (12,449 genes) and 88.6% (12,308 genes) of *P. oryziphila* 1257 genes have orthologs in the *P. entomophila* L48 and *P. mosselii* CFML 90-83, respectively (Figure 2C). Based on this analysis, we found that 933 genes (6.7%) are unique to the *P. oryziphila* 1257 genome.

The *P. oryziphila* 1257 genome possesses most of the genes involved in the central metabolic pathways similar with *P. entomophila* L48 and *P. mosselii* CFML 90-83 including pentose phosphate pathway (PPP), the tricarboxylic acid cycle (TCA), and the Entner–Doudoroff (ED) pathway. We found no gene encoding a 6-phosphofructokinase present in the *P. oryziphila* 1257 genome. This is consistent with *P. entomophila* metabolism (Vodovar et al., 2006), indicating that *P. oryziphila* has an incomplete Embden–Meyerhof–Parnas pathway, and relies on a complete ED pathway for hexose utilization.

The *P. oryziphila* 1257 genome contains more than 25 transport-encoding genes, three of which encode TolC, HlyD, and PrtD related to type I secretion system. Notably, 21 genes encoding the type IV pilus system (T4P) were found in the genome of *P. oryziphila* 1257 (Supplementary Figure 2 and





TABLE 1 | ANI analyses between strain 1257 and other representative *Pseudomonas* species.

Reference genomes	Query genome of 1257	
	ANiB and [aligned nucleotides] (%)	ANIm and [aligned nucleotides] (%)
<i>Pseudomonas entomophila</i> L48 (DSM 28517)	86.55 [71.95]	89.10 [69.64]
<i>Pseudomonas mosselii</i> CFML 90-83 (DSM 17497)	86.72 [68.97]	89.13 [67.56]
<i>Pseudomonas taiwanensis</i> CMS (DSM 21245)	83.23 [63.20]	86.86 [53.72]
<i>Pseudomonas plecoglossicida</i> FPC951 (DSM 15088)	84.23 [62.41]	87.64 [56.13]
<i>Pseudomonas monteilii</i> strain 1 (DSM 14164)	83.92 [64.38]	87.21 [57.88]
<i>Pseudomonas putida</i> KT2440 (NBRC 14164)	83.96 [66.37]	87.36 [59.10]
<i>Pseudomonas oryzae</i> L-1 (NBRC 102199)	73.77 [36.02]	83.94 [13.23]
<i>Pseudomonas fuscovaginae</i> LMG 2158 (ICMP 5940)	77.68 [49.92]	85.01 [27.95]
<i>Pseudomonas asplenii</i> 4A7 (DSM17133)	76.48 [54.33]	84.38 [24.32]
<i>Pseudomonas parafulva</i> CB-1 (DSM17004)	81.96 [57.30]	86.37 [44.99]
<i>Pseudomonas cremoricolorata</i> CC-8 (DSM 17059)	80.58 [50.98]	86.14 [38.63]
<i>Pseudomonas koreensis</i> Ps 9-14 (LMG 21318)	77.14 [54.28]	84.65 [28.37]
<i>Pseudomonas fulva</i> YAB-1 (DSM17717)	80.45 [56.12]	85.95 [38.51]
<i>Pseudomonas fluorescens</i> F113 (DSM50090)	76.53 [51.06]	84.47 [23.57]
<i>Pseudomonas aeruginosa</i> PAO1 (DSM50071)	76.10 [46.39]	84.36 [22.89]

ANiB and ANIm values indicate the pairwise comparisons of given genomic sequences with the genome of strain 1257.

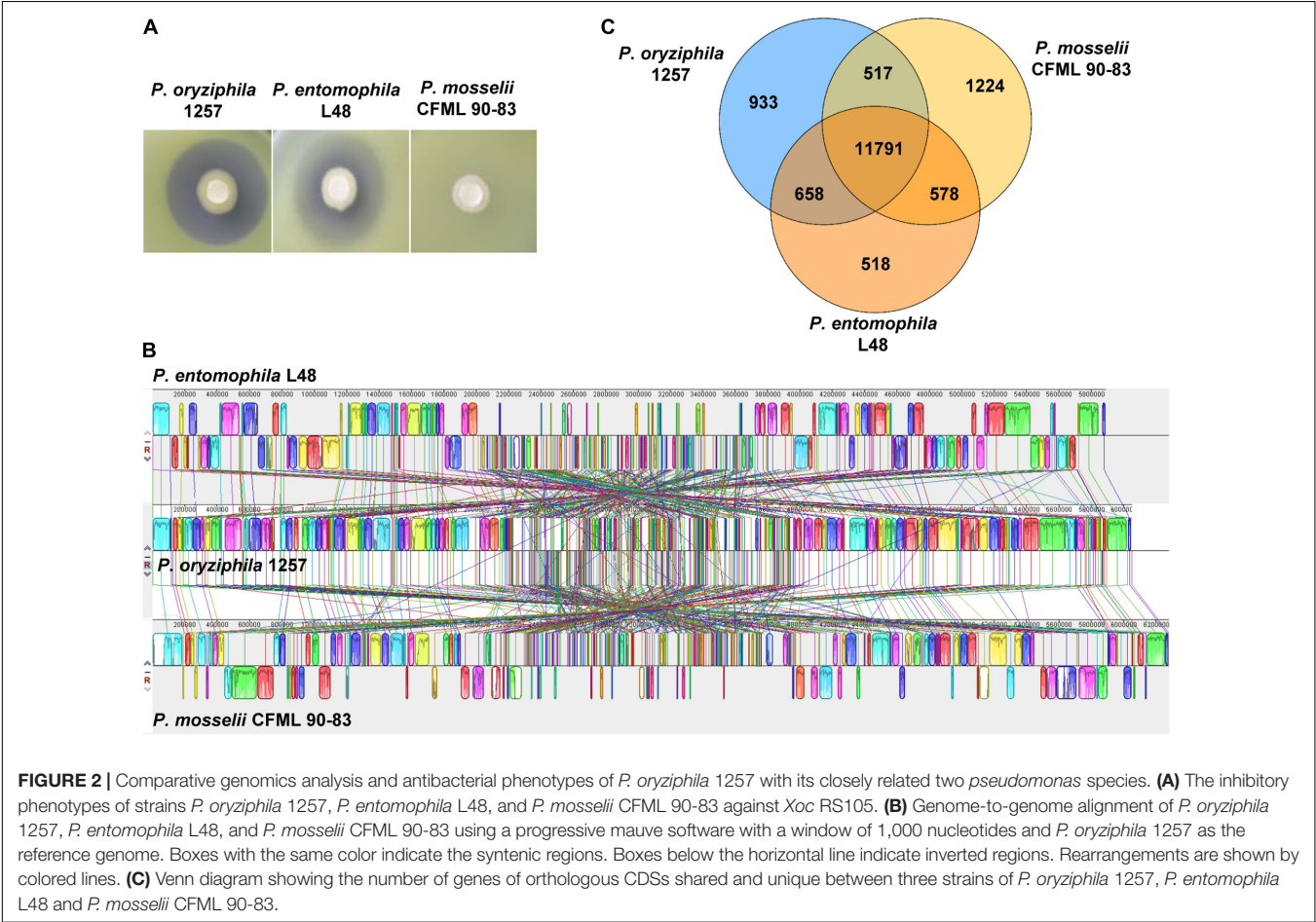


FIGURE 2 | Comparative genomics analysis and antibacterial phenotypes of *P. oryziphila* 1257 with its closely related two *pseudomonas* species. (A) The inhibitory phenotypes of strains *P. oryziphila* 1257, *P. entomophila* L48, and *P. mosselii* CFML 90-83 against *Xoc* RS105. (B) Genome-to-genome alignment of *P. oryziphila* 1257, *P. entomophila* L48, and *P. mosselii* CFML 90-83 using a progressive mauve software with a window of 1,000 nucleotides and *P. oryziphila* 1257 as the reference genome. Boxes with the same color indicate the syntenic regions. Boxes below the horizontal line indicate inverted regions. Rearrangements are shown by colored lines. (C) Venn diagram showing the number of genes of orthologous CDSs shared and unique between three strains of *P. oryziphila* 1257, *P. entomophila* L48 and *P. mosselii* CFML 90-83.

*P. entomophila* and *P. mosselii*. We found that three TcdA-, TcdB-, and TccC-like insecticidal toxin complexes unique to *P. entomophila* are absent from *P. oryziphila* 1257. *P. oryziphila* 1257 possesses the HCN biosynthesis operon (*hcnABC*) but not the genes associated for the biosynthesis of 2,4-DAPG, phenazines, pyoluteorin, pyrrolnitrin, pyochelin, pyocyanine, and xantholysinABCD. We also detected several genes or gene clusters involved in plant–bacteria interactions in the genomes of *P. oryziphila* 1257, including the *iacR* gene involvement in the indole-3-acetic acid (IAA) degradation pathway, the *paa* gene involved in the phenylacetic acid (PAA) degradation pathway, indicating that *P. oryziphila* 1257 might help to balance the delicate IAA and PAA equilibrium in the rhizosphere. A unique *acoABC* operon involved in the biosynthesis of acetoin that has been known as one kind of VOC promoting plant growth was detected in the genome of *P. oryziphila* 1257. Similar to *P. entomophila* and *P. mosselii*, *P. oryziphila* also possesses the pyrroloquinoline quinone (PPQ) biosynthesis genes *pqqE*, *pqqD*, and *pqqB*, which were predicted to participate in phosphate solubilization. These results suggested that *P. oryziphila* 1257 may have the potential to promote plant growth.

The antiSMASH analysis showed that the genome of *P. oryziphila* 1257 contains eight candidate gene clusters encoding a dipeptide *N*-acetylglutaminylglutamine amidc (NAGGN), four non-ribosomal peptide synthetase (NRPS), and two ribosomally synthesized antimicrobial peptides, and a pigment of the aryl polyene (APE) type (Figure 3 and Supplementary Table 6). The NAGGN cluster was predicted to synthesize NAGGN that is unusual dipeptide previously reported only in osmotically stressed *Rhizobium meliloti*, *P. fluorescens*, and *P. aeruginosa* PAO1 (Sagot et al., 2010). The two Bac 1 and Bac 2 clusters were predicted for the bacteriocin biosynthesis. However, these two clusters exhibited no apparent sequence similarity with the known strain. Three of four NRPS were predicted to be the siderophores biosynthetic gene clusters. The NRPS 1 and NRPS 3 are associated with the biosynthesis of pyoverdines. Nearly all fluorescent *Pseudomonas* species produce this yellow-green fluorescent that enable acquisition of Fe (III) ions from the surrounding environment (Gross and Loper, 2009). The genomes of *P. entomophila* L48 and *P. mosselii* CFML 90-83 also contain two independent clusters responsible for the biosynthesis of pyoverdines. In addition to pyoverdine, *P. entomophila* L48 can produce pseudomonine, an isoxazolidone siderophores, and pyochelin, a salicyl-capped siderophores. This is in agreement with our CAS agar diffusion assay, which showed that *P. entomophila* L48 can produce more total siderophores irrespective of chemical nature of the siderophores compared to *P. oryziphila* 1257 and *P. mosselii* CFML 90-83 (Supplementary Figure 4). Blast comparison showed that the NAGGN, NRPS 3, APE, and NRPS 4 cluster is conserved among the genomes of *P. oryziphila*, *P. entomophila*, and *P. mosselii*, whereas *P. entomophila* contains more candidate secondary metabolite biosynthetic gene clusters than that of *P. oryziphila* and *P. mosselii* (Figure 3). Combined with the antagonistic activity of three strains against *Xoc* RS105, we speculate that NRPS cluster but not the siderophores-producing

**TABLE 2 |** General features of genomes of *Pseudomonas oryziphila* (Po) 1257, *Pseudomonas entomophila* (Pe) L48, and *Pseudomonas mosselii* (Pm) CFMT90-83.

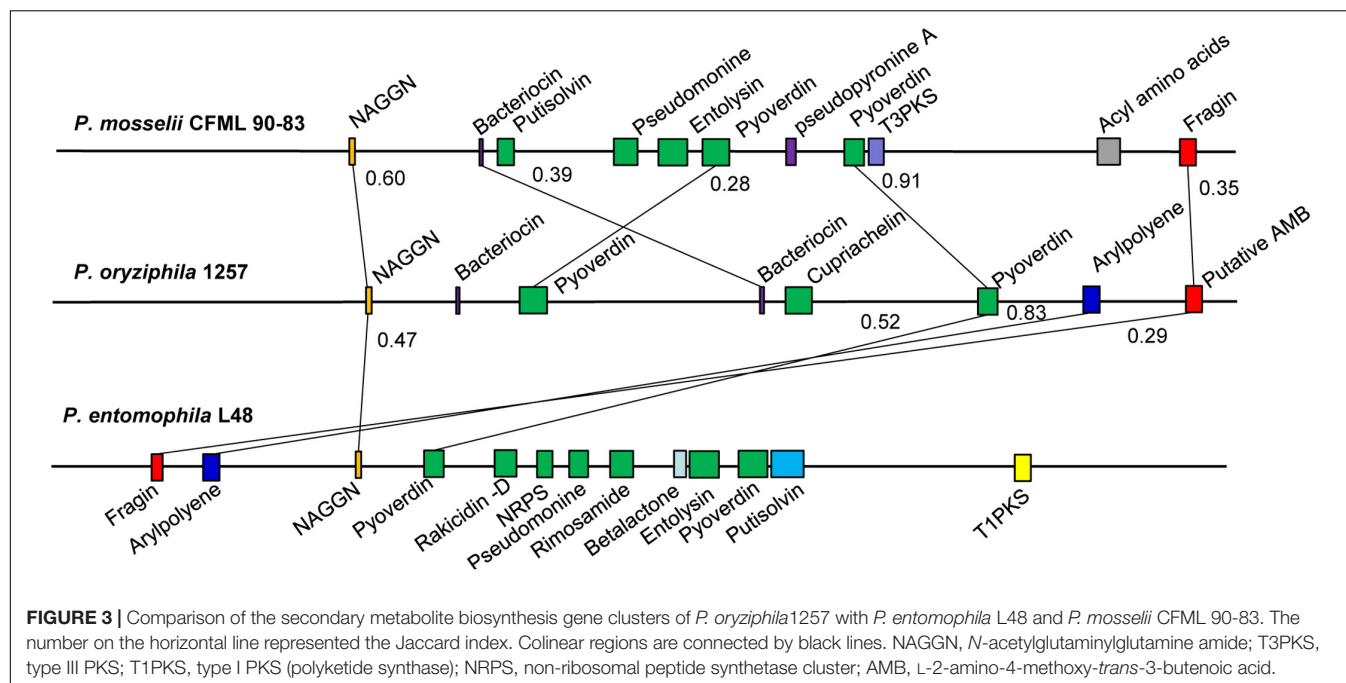
General features	Po 1257	Pe L 48	Pm CFMT90-83
Genome size (Mb)	6.05	5.89	6.28
GC content (%)	63.76	64.20	63.95
rRNA genes	22	22	22
tRNA genes	76	78	80
Other RNA genes	73	4	192
Coding density (%)	86.38	89.1	87.66
Protein coding sequences (CDS)	5,441	5,056	5,731
Plasmid	—	—	+

NRPS cluster may be the target compound of *P. oryziphila* 1257 against *Xoc* RS105.

## Genome-Wide Identification of Antibacterial Mechanisms Against *Xoc*

Our multiple attempts including utilization of ion exchange resin or optimization of the solvent were all failed to obtain the purified compound from 1257 that exhibited antibacterial activity against *Xoc* RS105. However, these attempts indicated that the active substance may be a strong polar compound. To elucidate the antibacterial mechanism of 1257, we used the transposon mutagenesis based on the EZ-Tn5 < R6K<sub>ori</sub>/KAN-2 > Tnp transposome system to screen functional genes associated with antibacterial active compounds. Among the 10,080 mutants, we screened 30 mutants that exhibited absolutely lacking, apparently or partially attenuated antagonistic activity toward *Xoc* RS105 (Supplementary Figure 3). Southern blot analysis indicated that all mutants carried only a single copy of the transposon (data not shown). The Tn5 transposon insertions were mapped to 19 genes including *carAB*, *purMF*, *purCLDK*, *gntR-lgrD*, *sdhA*, *dsbB1*, *tufI*, *serC*, *gph*, *dnaK*, *argG*, *sohB*, and *rRNA2* located in 13 different districts in the genome of 1257 (Figure 4A). In the *carA-carB*, *purM-purF*, *purC-purK*, and *gntR-lgrD* regions, transposons were inserted more frequently. Six independent insertions in the *carB* gene and three independent insertions in the *purL* gene resulted in loss of antagonistic activity of these mutants against *Xoc* RS105. One insertion in the *purF*, *sdhA*, *dsbB1*, *serC*, and *gph* genes also made 1257 lose the antagonistic activity. Two independent insertions in the *purD* and *purK* genes and one insertion in the *carA*, *purM*, *purC*, and *tufI* genes reduced the antagonistic properties of 1257 against *Xoc* RS105. We constructed the full functional segments of the *carA*, *carB*, *purF*, and *serC* genes and introduced the relative plasmids into the corresponding insertion mutants. The complemented strains were found to restore the antagonistic activity against *Xoc* RS105 to the wild-type levels (Figure 4B), indicating the critical role of these genes in biosynthesis of active compounds antagonizing *Xoc* RS105.

To define the biological process involved by the function genes mentioned previously, we exerted a Kyoto Encyclopedia of Genes and Genomes (KEGG) analysis (Figure 5). The *carA*



and *carB* genes encode the carbamoyl phosphate synthetase that catalyzes the synthesis of carbamoyl phosphate (CP), a precursor of arginine and pyrimidines metabolism. ArgG encoded by the *argG* gene is an argininosuccinate synthetase responsible for producing argininosuccinic acid from aspartate. The *sdhA* gene encodes a subunit A of succinate dehydrogenase that is a key enzyme in the TCA cycle. The six *pur* genes encoded PurF, PurD, PurL, PurM, PurC, and PurK, which are metabolic enzymes in the PPP, converting ribose-5P from the glycolytic pathway (PP) into 5-carboxyamino-1-(5-phospho-D-ribose) imidazole (CPR). Together, these analyses indicated that CP and CPR may be the important precursors for synthesis of the activate compounds and also provided some important evidences for further identification of the target compounds.

Three independent insertions have been shown in *dnaK* encoding a chaperone protein foldase DnaK that enable the RNA polymerase to sustain bacterial life in response to the stringent response (Kim et al., 2021). Another two Tn5 insertions in the *sohB* gene encoding a periplasmic serine protease (ClpP class) and *rRNA2* gene encoding the 23s rRNA, respectively, resulted in partially impaired antagonistic activity of the mutants against *Xoc* RS105, indicating that posttranscriptional mechanisms may be involved in the modulation of genes associated with biosynthesis of active compounds.

In particular, two individual insertions have been found in the *gntR* and *lgrD* genes that located in the NRPS 4 cluster exhibiting 40% similarity with the L-2-amino-4-methoxy-*trans*-3-butenic acid (AMB) biosynthetic gene cluster from *P. aeruginosa* PAO1 by the antiSMASH analysis. However, the *gntR* gene encodes a GntR family transcriptional regulator, and the *lgrD* gene encodes a non-ribosomal peptide synthetase of linear gramicidin synthase subunit D. The *gntR* and *lgrD*

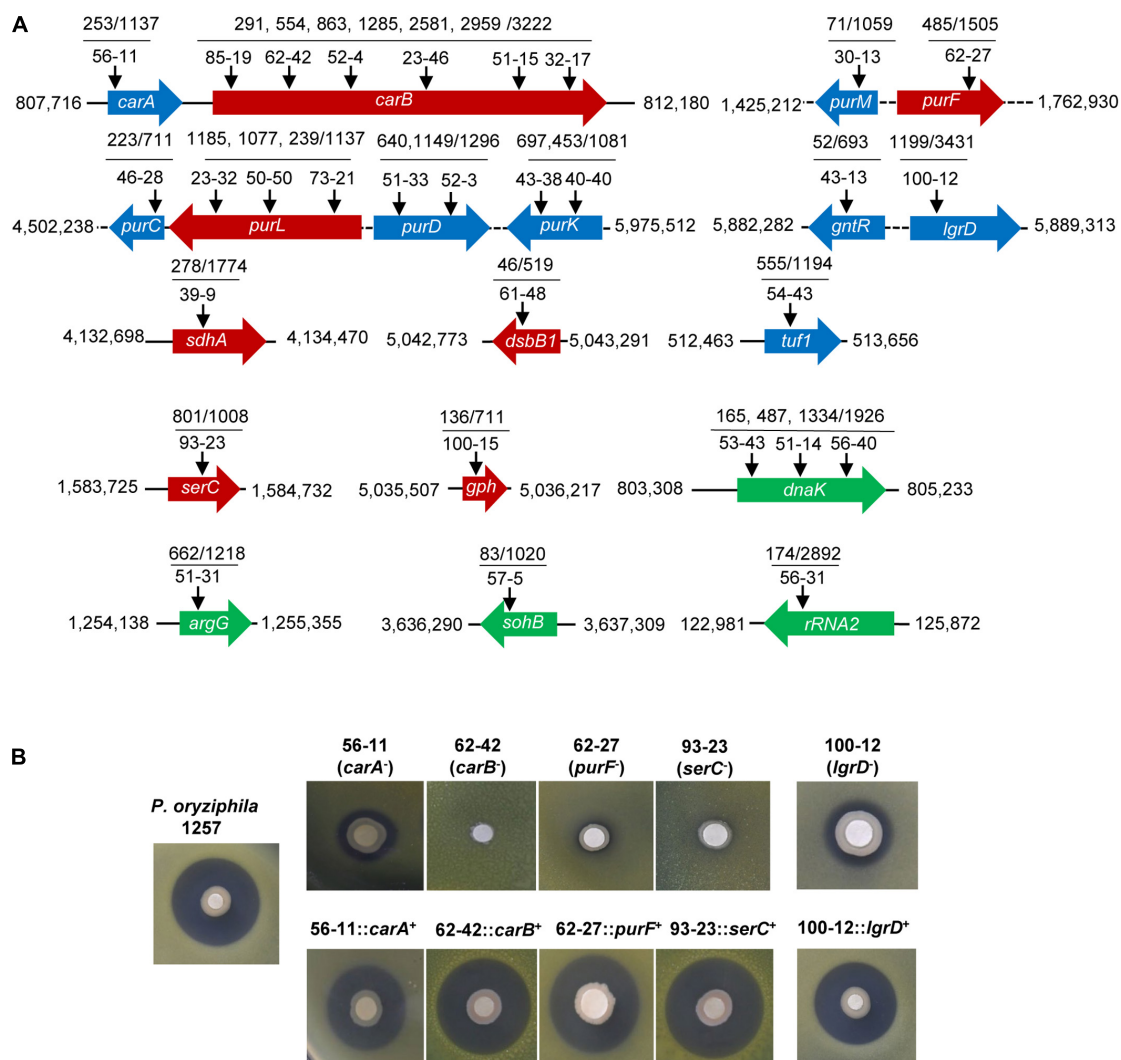
insertion mutants (43-13 and 100-12, respectively) exhibited significantly reduced antibacterial activity against *Xoc* RS105 when compared with the wild-type *P. oryziphila* 1257, whereas the complemented strain of *lgrD* insertion mutant nearly restored the antibacterial activity to the wild-type levels (Figure 4B). These results indicated that the non-ribosomal peptide catalyzed by LgrD may be a major active compound of *P. oryziphila* 1257 against *Xoc* RS105.

Sequence alignments showed that proteins encoded by the 19 genes mentioned previously in *P. oryziphila* 1257 exhibited more similarity with the homologs in *P. entomophila* L48 than *P. mosselii* CFML 90-83 (Supplementary Table 7), further supporting that *P. oryziphila* 1257 is most closely related to *P. entomophila* species.

## Biocontrol Effect of *Pseudomonas oryziphila* 1257 in Bacterial Leaf Streak

To investigate the biocontrol efficiency of *P. oryziphila* 1257 in BLS caused by *Xoc* RS105, we executed a field trial experiment using a highly susceptible cultivar Yuanfengzao as follows: *Xoc* RS105 only (control), rice leaves sprayed with 1257 12 h after inoculation with *Xoc* RS105 suspension (1257-Tre) and rice leaves sprayed with 1257 12 h before inoculation with *Xoc* RS105 suspension (1257-Pre). We first tested the appropriate concentration of 1257 and found that 1257 as OD<sub>600</sub> of 1.0 did not influence the morphology and growth of the rice plants during 15 days in our field trial experiment. Therefore, we used this concentration in all our biocontrol assays. The BLS disease severity under all treatments was investigated after 15 days. Compared with the control treatment, the 1257-Tre and 1257-Pre treatments significantly reduced the severity of BLS in paddy fields with relative control efficiencies of 53.9 and 39.7%,





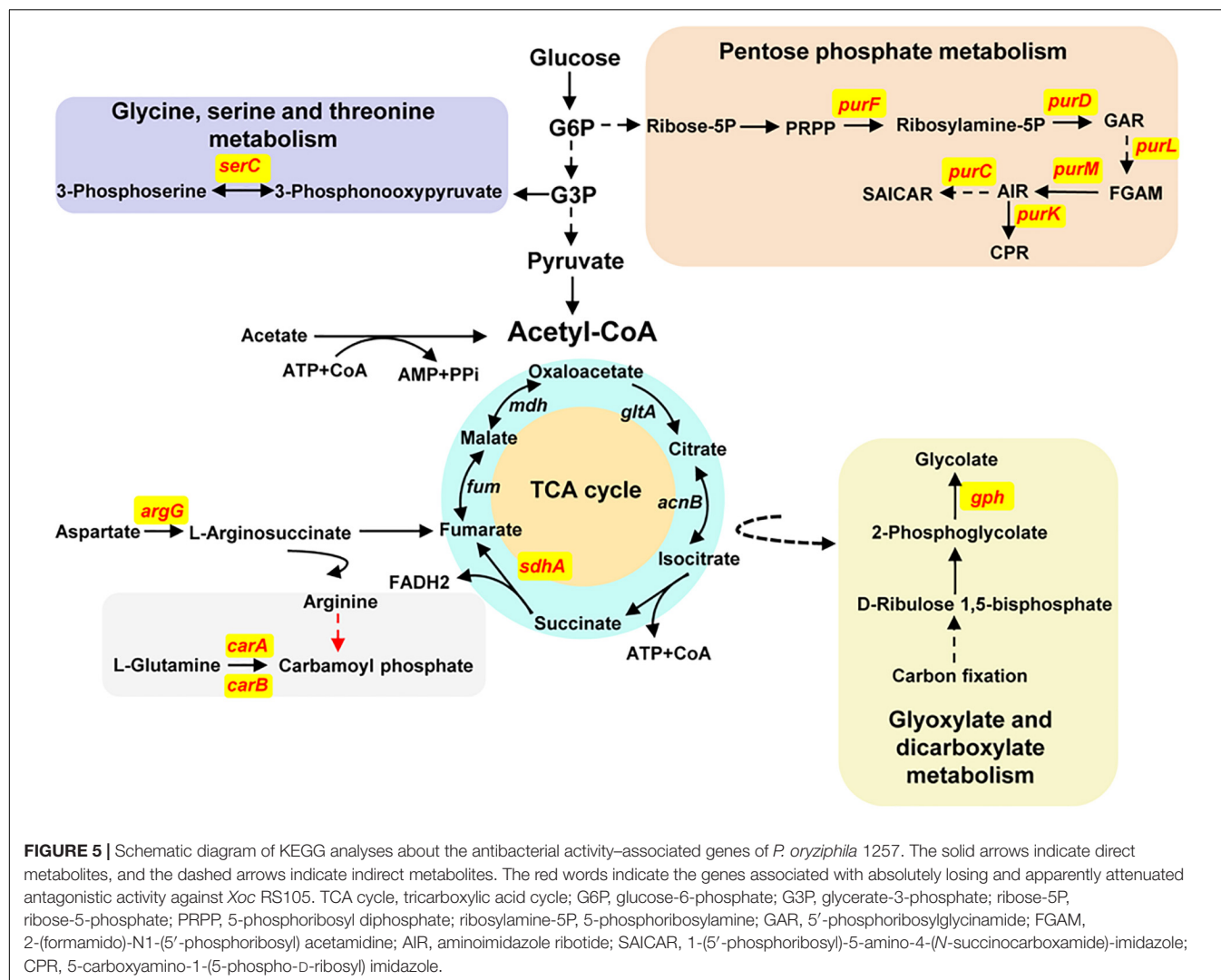
**FIGURE 4 |** Genome-wide identification of the antibacterial functional genes of *P. oryziphila* 1257 against *Xoc* RS105. **(A)** Characterizations of Tn5 insertion mutants of *P. oryziphila* 1257. Arrows represent the Tn5 transposon insertion sites in 19 genes on the 1257 genome. Red, blue, and green arrow boxes indicate genes associated with absolutely losing, apparently, and partially attenuated antagonistic activity against *Xoc* RS105, respectively. **(B)** Antibacterial activity assays of the wild-type *P. oryziphila* 1257, *carA*, *carB*, *purF*, *serC*, and *lgrD* mutants and their corresponding complemented strains.

respectively (**Figure 6A**). This demonstrated that the 1257-Tre treatment exhibited efficient biocontrol of BLS in the field.

Further, we carried out a greenhouse trial experiment using a *Xoc* RS105-Gus strain in which the wild-type *Xoc* RS105 carried a *hrcC-uidA* reporter plasmid as the control treatment. The 1257-Tre and 1257-Pre indicated that rice leaves were injected with 1257 3 h after and before inoculation with *Xoc* RS105-Gus suspension, respectively. The BLS disease severity under all treatments was observed after 1, 3, 5, and 7 days. On the third and fifth day, significantly reduced water-soaked lesions were observed on the leaves of Yuanfengzao by the 1257-Tre and 1257-Pre treatments compared to the control (**Figure 6B**). The relative control efficiencies by the 1257-Tre and 1257-Pre treatments were 66.10% and 54.30% on day 7, respectively.

The GUS histochemical staining with the corresponding leaves showed similar result.

Given that the depth of GUS staining in rice leaves was dependent on bacterial multiplication, we used the quantifiable GUS measurement to determine the growing bacterial population in rice leaves by the control, 1257-Tre, and 1257-Pre treatments using our new method, which is more rapid and accurate than the conventional bacterial number counting (Zou et al., 2021). The quantitative GUS assays showed that the *Xoc* RS105 population-related GUS activity was dramatically lower in the rice leaves treated by 1257 regardless of the 1257-Tre or 1257-Pre treatment than that treated by the control at 1, 3, 5, and 7 days (**Figure 6C**). Taken together, these results indicate that 1257 could effectively inhibit the growth and migration of *Xoc* RS105 in rice tissue

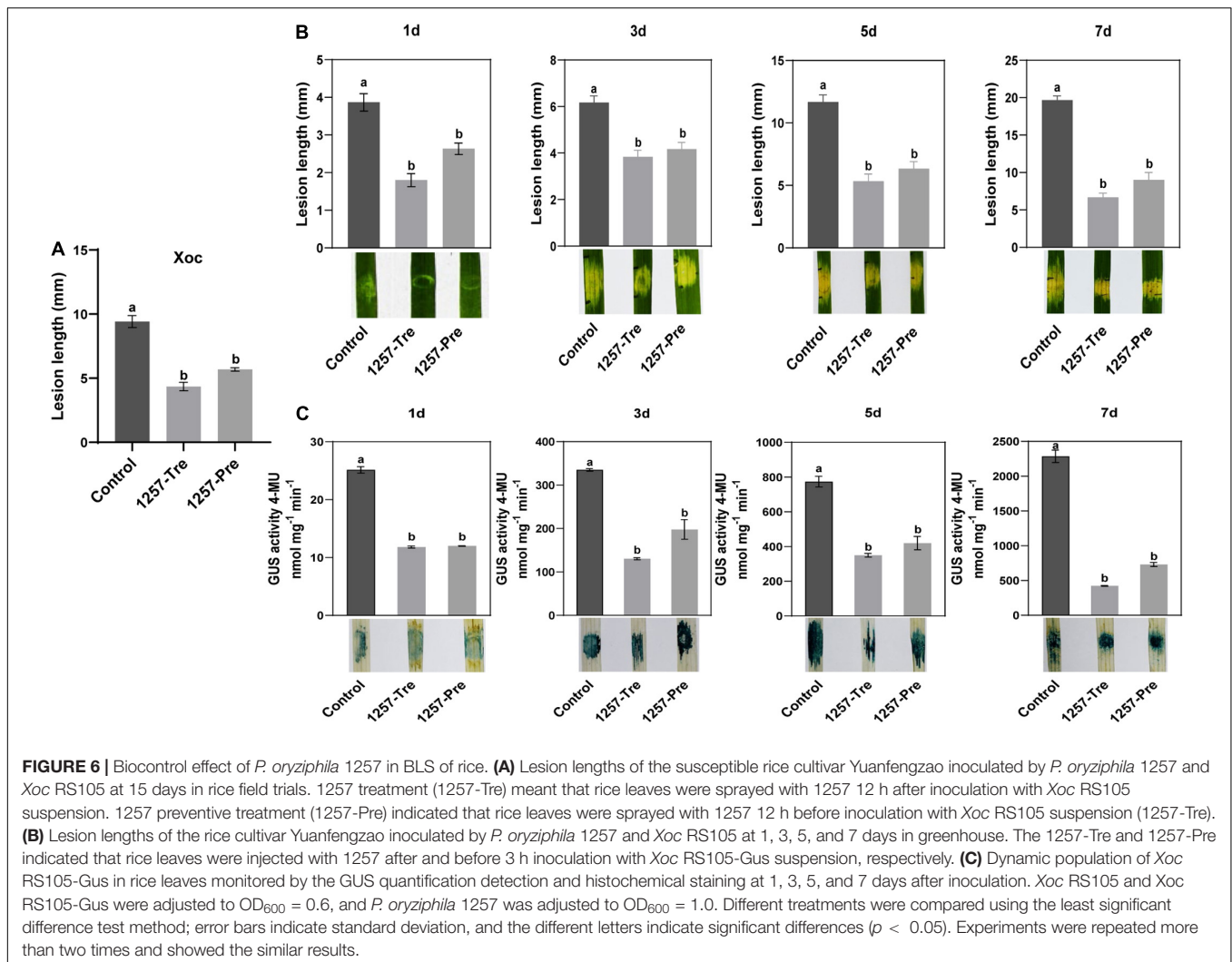


to prevent the BLS disease, making it a promising biological control agent for BLS.

## DISCUSSION

*Xoo* and *Xoc* cause bacterial leaf bright and BLS of rice, respectively, which are two major bacterial diseases of rice in some Asian rice-growing regions (Nino-Liu et al., 2006). In this study, we identified a novel *Pseudomonas* species, *P. oryziphila*, which has the capacity to inhibit *Xoo* and *Xoc* and especially inhibit the growth and migration of *Xoc* in rice tissue to prevent the BLS disease. Genomic information revealed that *P. oryziphila* may have potential to kill insects, solubilize phosphate, move dependently on the T4P system, and degrade IAA and PAA, indicating that it is a versatile bacterium. Our findings collectively indicate that a non-ribosomal peptide may be the major active compound involved in this biocontrol of BLS. The new discovery of *P. oryziphila* also provides more microbial resources for biocontrol of bacterial diseases of rice.

*Pseudomonas* is a diverse genus with more than 200 different species, whereas many new isolates are being classified as a novel species. In 2019, for instance, 16 novel *Pseudomonas* species were described from different sources such as tree bark, sewage, or raw milk (Hofmann et al., 2021). Our results support that strain 1257 is a novel *Pseudomonas* species, which is more closely related to *P. entomophila* than *P. mosselii*. In this study, we used a polyphasic approach including genotypic and phenotypic analyses to characterize this novel species. At first, 1257 could be assigned to the genus *Pseudomonas* by the 16S rRNA-based dendrogram, but not to any validly named species because the 16S rRNA gene sequence of 1257 exhibited more than 99% similarity with the one of the type strains of *P. entomophila* L48 and *P. mosselii* CFMT 90-83. Further MLSA, ANI, and DDH analyses showed that 1257 located in a separate branch with *P. entomophila* and *P. mosselii*; however, the relatedness of this species could not be defined, indicating that sometimes genomic analyses such as MLSA, ANI, and DDH values are not enough to define the close relative relationship of some species. A similar case about the taxonomic characterization of *P.*



*cremoris* sp. nov. was reported in the previous study (Hofmann et al., 2021). For example, ANIm comparisons indicated that the type strain WS 5106 was a novel species within the *P. fluorescens* subgroup, but the pairwise ANIm values of 90.1 and 89.8% showed that WS 5106 was most closely related to *Pseudomonas nabeulensis* CECT 9765<sup>T</sup> and *Pseudomonas kairouanensis* CECT 9766<sup>T</sup> (Hofmann et al., 2021). Therefore, some phenotypic analyses such as physiological and biochemical characteristics, or antagonistic activity, are necessary for further classification status. Our additional phenotypic analyses including enzyme activity, carbon source assimilation, and acid production showed that 1257 exhibited more similar phenotypic features with *P. entomophila* L48 than *P. mosselii* CFML 90-83, supporting that 1257 is most closely related to *P. entomophila*. We designated this novel species as *P. oryziphila* sp. nov., given its specific antibacterial activity against *Xoo* and *Xoc*, which is similar with *P. entomophila* that was named for its unique entomopathogenic property (Vodovar et al., 2005; Mulet et al., 2012).

The collinearity analysis that more than 85% of *P. oryziphila* 1257 genes have orthologs in the *P. entomophila* L48

and *P. mosselii* CFML 90-83 is consistent with the close relatedness among *P. oryziphila*, *P. entomophila*, and *P. mosselii*. Interestingly, comparative genomics analysis revealed that *P. oryziphila* contains a set of T4P biogenesis-associated genes (21 genes) including *pilA* encoding the major pilin protein (Maier and Wong, 2015); the *pilM*, *pilN*, *pilO*, and *pilP* genes encoding the alignment complex (PilM, PilN, PilO, and PilP) (Gold et al., 2015); the *pilT* and *pilC* genes encoding the motor (PilT1, PilT2, and PilC) (McCallum et al., 2019); the *pilQ* genes encoding the outer membrane (OM) pore complex PilQ1 or PilQ2; other genes such as *pilD* encoding a pre-pilin peptidase PilD; *pilS* encoding one of the two-component system PilS (Kilmury and Burrows, 2018); and the minor pilins FimT, PilV, and PilE-encoding genes (Treuner-Lange et al., 2020). These findings indicated that *P. oryziphila* may have a functional T4P. However, only seven T4P homologous genes were found in *P. entomophila* L48, whereas 17 T4P orthologous genes were found in *P. mosselii* CFML 90-83, indicating that T4P biogenesis-associated genes exhibit a high degree of variability among *P. oryziphila*, *P. entomophila*, and *P. mosselii*.

The biocontrol properties of *Pseudomonas* species are largely dependent on its secondary metabolites such as toxins, lipopeptides, polyketides, fatty acids, and phenazines (Gross and Loper, 2009). *P. oryziphila* 1257 contains the insecticidal toxin AprA and hemolytic RTX toxin, which is in agreement with the previous finding in *P. entomophila* L48 (Vodovar et al., 2006). This indicates that *P. oryziphila* strain could be a versatile bacterium capable of inhibiting *X. oryzae* and killing insects or *Drosophila melanogaster*. A similar study has been reported that *P. entomophila* JS2 displayed a clear antibacterial effect against *Xcc* 306, the causal agent of citrus canker (Villamizar et al., 2020). We found that *P. oryziphila* 1257 possesses the HCN biosynthesis operon (*hcnABC*) but not the genes associated for the biosynthesis of 2,4-DAPG, phenazines, pyoluteorin, pyrrolnitrin, pyochelin, pyocyanine, and xantholysinABCD. Xantholysins, a family of lipodepsipeptides produced by some *P. putida* and *P. soli* strains, exhibits *Xanthomonas*-inhibitory activity, including *Xoo*-antagonistic activity (Vallet-Gely et al., 2010; Pascual et al., 2014). Although *P. soli* is closely related to *P. entomophila* and *P. mosselii*, the xantholysin-encoding genes are distinguishable targets between two novel *Pseudomonas* species of *P. oryziphila* and *P. soli*. We also detected several genes or gene clusters including the *iacR* gene (IAA degradation pathway) and the *paa* gene (PAA degradation pathway) in the genomes of *P. oryziphila* 1257, indicating that *P. oryziphila* 1257 might help to balance the delicate IAA and PAA equilibrium in the rhizosphere. The *acoABC* operon putatively participated in the biosynthesis of acetoin, one kind of VOC promoting plant growth (Wu et al., 2019), and PPQ biosynthesis genes *pqqE*, *pqqD*, and *pqqB* predicted to participate in phosphate solubilization were found in the genome of *P. oryziphila* 1257. These findings suggested that *P. oryziphila* 1257 has the potential to promote plant growth, but whether *P. oryziphila* 1257 is a plant growth-promoting rhizobacteria strain needs more experimental evidences.

Our unsuccessful attempts to purify the active substance against *Xoc* RS105 indicated that it could be a strong polar compound; however, the Tn5-based mutagenesis indicated that a non-ribosomal peptide catalyzed by LgrD may be a major active compound of *P. oryziphila* 1257 because the complementary strain of *lgrD* insertion mutant nearly restored the antibacterial activity to the wild-type levels. In our antiSMASH analysis, the *gntR* and *lgrD* genes that located in the NRPS 4 cluster exhibiting 40% similarity with the AMB biosynthetic gene cluster *ambABCDE* of *P. aeruginosa* PAO1. However, the BLAST analysis in NCBI database showed that the *lgrD* gene encodes a non-ribosomal peptide synthetase of linear gramicidin synthase subunit D. Sequence comparison showed that the gramicidin biosynthetic gene cluster of *lgrABCDT* in *Brevibacillus brevis* displayed 55% similarity with the *lgrD*-related cluster in *P. oryziphila* 1257, and LgrD of *P. oryziphila* 1257 exhibited 43% similarity with the AmbB of *P. aeruginosa* PAO1 and 50% similarity with LgrD proteins of *B. brevis*. These results provide some useful clues for further purification of the target active compound; however, the structure of which needs more verifications from biochemical methods such as high-pressure liquid chromatography and nuclear magnetic resonance. From our Tn5 transposon mutant library, we found that one insertion

in the *purF*, *sdhA*, *dsbB1*, *serC*, and *gph* genes made 1257 lose the antagonistic activity. Two independent insertions in the *purD* and *purK* genes and one insertion in the *carA*, *purM*, *purC*, and *tufI* genes reduced the antagonistic properties of 1257 against *Xoc* RS105. Based on the KEGG analyses, we found that these genes were mainly involved in the synthesis of CP and the PPP pathway. Therefore, we speculated that CP and CPR may be the important precursors for synthesis of the activate compounds.

Some studies have shown that most of the bacterial strains applicable for the BLS biocontrol were *Bacillus* strains including *Bacillus amyloliquefaciens*, *B. velezensis* and *B. cereus* (Zhang et al., 2013; Li et al., 2019; Li S. Z. et al., 2020). For instance, compared to the control treatment, *B. amyloliquefaciens* LX-11 significantly reduced the severity of BLS in paddy fields with relative control efficiencies of 60.2% (Zhang et al., 2013). Our results showed that the relative control efficiencies by the *P. oryziphila* 1257 treatments in rice fields and in greenhouses were 53.9 and 66.10%, respectively, which was near to the one by *B. amyloliquefaciens* LX-11. However, there are still some problems in practical use, such as tolerance to stress (high temperature in rice-growing season) and stability of *P. oryziphila* 1257. We are trying to improve the stress tolerance of *P. oryziphila* 1257 through fermentation techniques such as microcapsule bacterial agent to improve its biocontrol effect. Some studies showed that phenazine-1-carboxylic acid (PCA) from *Pseudomonas* species is very effective against *Xoo* and *Xoc* (Xu et al., 2015). PCA as the same name of shenqinmycin has received a pesticide registration certification in China (Jin et al., 2015; Xu et al., 2015). Although *P. oryziphila* 1257 does not produce PCA, there is a long way to go, but it is challenging from purification to commercial use of the antagonistic compounds from *P. oryziphila* 1257 such as PCA. Our results showed that *P. oryziphila* 1257 exhibited specific antagonistic activity against *Xoc* and *Xoo*, whereas whether *P. oryziphila* 1257 is a promising biological control agent for BB needs more evidences from rice field trials.

In summary, we have reported the identification of a novel species, *P. oryziphila*, in the *Pseudomonas* genus. Our results indicated that a non-ribosomal peptide may be one of the major active compounds of *P. oryziphila* 1257 against *Xoc*. Meanwhile, we demonstrated that the type strain *P. oryziphila* 1257<sup>(T)</sup> is an effective biological control agent for BLS, providing a new microbial resource for biological control of bacterial diseases caused by *X. oryzae*.

## DATA AVAILABILITY STATEMENT

The datasets presented in this study can be found in online repositories. The names of the repository/repositories and accession number(s) can be found in the article/Supplementary Material.

## AUTHOR CONTRIBUTIONS

RY and SL designed the research. GC supervised the study. YL, YY, and YF analyzed the data and performed part of the



biocontrol experiments. RY and LZ wrote the manuscript. RY, SL, YL, YY, YF, LZ, and GC critically revised the manuscript and approved the final version. All authors contributed to the article and approved the submitted version.

## FUNDING

This work was financially supported by Shanghai Agriculture Applied Technology Development Program, China (Grant No.G20190202), the National Key R&D Program of China (2017YFD0200400), and the National Natural Science Foundation of China (31772122 to LZ and 31830072 to GC).

## REFERENCES

- Anderson, A. J., and Kim, Y. C. (2018). Biopesticides produced by plant-probiotic *Pseudomonas chlororaphis* isolates. *Crop Protection* 105, 62–69. doi: 10.1016/j.cropro.2017.11.009
- Biessy, A., and Filion, M. (2018). Phenazines in plant-beneficial *Pseudomonas* spp.: biosynthesis, regulation, function and genomics. *Environ. Microbiol.* 20, 3905–3917. doi: 10.1111/1462-2920.14395
- Blin, K., Shaw, S., Steinke, K., Villebro, R., Ziemert, N., Lee, S. Y., et al. (2019). antiSMASH 5.0: updates to the secondary metabolite genome mining pipeline. *Nucleic Acids Res.* 47, W81–W87. doi: 10.1093/nar/gkz310
- Cai, L. L., Cao, Y. Y., Xu, Z. Y., Ma, W. X., Zakria, M., Zou, L. F., et al. (2017). A transcription activator-like effector Tal7 of *Xanthomonas oryzae* pv. *oryzicola* activates rice gene *Os09g29100* to suppress rice immunity. *Sci. Rep.* 7:5089. doi: 10.1038/S41598-017-04800-8
- Couillerot, O., Prigent-Combaret, C., Caballero-Mellado, J., and Moenne-Loccoz, Y. (2009). *Pseudomonas fluorescens* and closely-related fluorescent *pseudomonads* as biocontrol agents of soil-borne phytopathogens. *Lett. Appl. Microbiol.* 48, 505–512. doi: 10.1111/j.1472-765X.2009.02566.x
- Dabboussi, F., Hamze, M., Singer, E., Geoffroy, V., Meyer, J. M., and Izard, D. (2002). *Pseudomonas mosselii* sp. nov., a novel species isolated from clinical specimens. *Int. J. Syst. Evol. Microbiol.* 52, 363–376. doi: 10.1099/00207713-52-2-363
- Darling, A. C., Mau, B., Blattner, F. R., and Perna, N. T. (2004). Mauve: multiple alignment of conserved genomic sequence with rearrangements. *Genome Res.* 14, 1394–1403. doi: 10.1101/gr.2289704
- Dorsch, M., Lane, D., and Stackebrandt, E. (1992). Towards a phylogeny of the genus *Vibrio* based on 16S rRNA sequences. *Int. J. Syst. Evolutionary Microbiol.* 42, 58–63.
- Fischer, S., Brunk, B. P., Chen, F., Gao, X., Harb, O. S., Iodice, J. B., et al. (2011). Using OrthoMCL to assign proteins to OrthoMCL-DB groups or to cluster proteomes into new ortholog groups. *Curr. Protoc. Bioinformatics* 6, 11–19. doi: 10.1002/0471250953.bi0612s35
- Gold, V. A., Salzer, R., Averhoff, B., and Kuhlbrandt, W. (2015). Structure of a type IV pilus machinery in the open and closed state. *Elife* 4:e07380. doi: 10.7554/eLife.07380
- Gross, H., and Loper, J. E. (2009). Genomics of secondary metabolite production by *Pseudomonas* spp. *Nat. Product Rep.* 26, 1408–1446. doi: 10.1039/b817075b
- Hofmann, K., Woller, A., Huptas, C., Wenning, M., Scherer, S., and Doll, E. V. (2021). *Pseudomonas cremoris* sp. nov., a novel proteolytic species isolated from cream. *Int. J. Syst. Evol. Microbiol.* 71, 1–9. doi: 10.1099/ijsem.0.004597
- Ji, Z. Y., Zakria, M., Zou, L. F., Xiong, L., Li, Z., Ji, G. H., et al. (2014). Genetic diversity of transcriptional activator-like effector genes in Chinese isolates of *Xanthomonas oryzae* pv. *oryzicola*. *Phytopathology* 104, 672–682. doi: 10.1094/PHYTO-08-13-0232-R
- Jin, K., Zhou, L., Jiang, H., Sun, S., Fang, Y., Liu, J., et al. (2015). Engineering the central biosynthetic and secondary metabolic pathways of *Pseudomonas aeruginosa* strain PA1201 to improve phenazine-1-carboxylic acid production. *Metab. Eng.* 32, 30–38. doi: 10.1016/j.ymben.2015.09.003

## ACKNOWLEDGMENTS

We thank Youlun Xiao (Institute of Plant Protection, Hunan Academy of Agricultural Sciences, China) for providing rice seeds of Yuanfengzhao. We are thankful to Fazal Haq for critical reading of the manuscript.

## SUPPLEMENTARY MATERIAL

The Supplementary Material for this article can be found online at: <https://www.frontiersin.org/articles/10.3389/fmicb.2021.759536/full#supplementary-material>

- Kilmury, S. L. N., and Burrows, L. L. (2018). The *Pseudomonas aeruginosa* PilSR two-component system regulates both twitching and swimming motilities. *MBio* 9, e1310–e1318. doi: 10.1128/mBio.01310-18
- Kim, J. S., Liu, L., and Vazquez-Torres, A. (2021). The DnaK/DnaJ chaperone system enables RNA polymerase-DksA complex formation in *Salmonella* experiencing oxidative stress. *MBio* 12, 1–17. doi: 10.1128/mBio.03443-20
- Kumar, S., Stecher, G., and Tamura, K. (2016). MEGA7: molecular evolutionary genetics analysis version 7.0 for bigger datasets. *Mol. Biol. Evol.* 33, 1870–1874. doi: 10.1093/molbev/msw054
- Kwak, Y. S., Bakker, P. A., Glandorf, D. C., Rice, J. T., Paulitz, T. C., and Weller, D. M. (2009). Diversity, virulence, and 2,4-diacetylphloroglucinol sensitivity of *Gaeumannomyces graminis* var. *tritici* isolates from Washington state. *Phytopathology* 99, 472–479. doi: 10.1094/PHYTO-99-5-0472
- Landa, B. B., Mavrod, D. M., Thomashow, L. S., and Weller, D. M. (2003). Interactions between strains of 2,4-Diacetylphloroglucinol-producing *Pseudomonas fluorescens* in the rhizosphere of wheat. *Phytopathology* 93, 982–994. doi: 10.1094/PHYTO.2003.93.8.982
- Lee, S. A., Jang, S. H., Kim, B. H., Shibata, T., Yoo, J., Jung, Y., et al. (2018). Insecticidal activity of the metalloprotease AprA occurs through suppression of host cellular and humoral immunity. *Dev. Comp. Immunol.* 81, 116–126. doi: 10.1016/j.dci.2017.11.014
- Li, S., Chen, Y., Yang, R., Zhang, C., Liu, Z., Li, Y., et al. (2019). Isolation and identification of a *Bacillus velezensis* strain against plant pathogenic *Xanthomonas* spp. *Acta Microbiol. Sin.* 59, 1–15.
- Li, S. Z., Liu, Z., Yang, R. H., Chen, Y., Zhong, Y. N., Chen, L. S., et al. (2020). Isolation and identification of a *Bacillus cereus* strain against plant pathogenic *Xanthomonas oryzae*. *Jiangsu Agric. Sci.* 48, 127–136.
- Li, W., Rokni-Zadeh, H., De Vleeschouwer, M., Ghequire, M. G. K., Sinnave, D., Xie, G. L., et al. (2013). The antimicrobial compound xantholysin defines a new group of *Pseudomonas* cyclic lipopeptides. *PLoS One* 8:e62946. doi: 10.1371/journal.pone.0062946
- Li, Y. L., Yan, Y. C., Deng, S. G., Zhang, C. P., Haq, F., Chen, T., et al. (2020). The *Xanthomonas oryzae* pv. *oryzae* type IV pilus alignment subcomplex protein PilN contributes to regulation of bacterial surface-associated behaviours and T3SS system. *Plant Pathol.* 69, 744–755. doi: 10.1111/ppa.13157
- Maier, B., and Wong, G. C. L. (2015). How bacteria use type IV pili machinery on surfaces. *Trends Microbiol.* 23, 775–788. doi: 10.1016/j.tim.2015.09.002
- McCallum, M., Burrows, L. L., and Howell, P. L. (2019). The dynamic structures of the type IV Pilus. *Microbiol. Spectr.* 7, 1–12. doi: 10.1128/microbiolspec.PSIB-0006-2018
- Mulet, M., Gomila, M., Lemaitre, B., Lalucat, J., and Garcia-Valdes, E. (2012). Taxonomic characterisation of *Pseudomonas* strain L48 and formal proposal of *Pseudomonas entomophila* sp. nov. *Syst. Appl. Microbiol.* 35, 145–149. doi: 10.1016/j.syapm.2011.12.003
- Nino-Liu, D. O., Ronald, P. C., and Bogdanove, A. J. (2006). *Xanthomonas oryzae* pathovars: model pathogens of a model crop. *Mol. Plant Pathol.* 7, 303–324. doi: 10.1111/j.1364-3703.2006.00344.x
- Opota, O., Vallet-Gely, I., Vincentelli, R., Kellenberger, C., Iacovache, I., Gonzalez, M. R., et al. (2011). Monalysin, a novel ss-pore-forming toxin from the *Drosophila* pathogen *Pseudomonas entomophila*, contributes to host intestinal

- damage and lethality. *PLoS Pathog.* 7:e1002259. doi: 10.1371/journal.ppat.1002259
- Pan, X., Wu, J., Xu, S., Duan, Y., and Zhou, M. (2017). CatB is critical for total catalase activity and reduces bactericidal effects of phenazine-1-carboxylic acid on *Xanthomonas oryzae* pv. *oryzae* and *X. oryzae* pv. *oryzicola*. *Phytopathology* 107, 163–172. doi: 10.1094/PHYTO-07-16-0251-R
- Pascual, J., Garcia-Lopez, M., Carmona, C., Sousa, T. D., de Pedro, N., Cautain, B., et al. (2014). *Pseudomonas soli* sp. nov., a novel producer of xantholysin congeners. *Syst. Appl. Microbiol.* 37, 412–416. doi: 10.1016/j.syapm.2014.07.003
- Raio, A., and Puopolo, G. (2021). *Pseudomonas chlororaphis* metabolites as biocontrol promoters of plant health and improved crop yield. *World J. Microbiol. Biotechnol.* 37:99. doi: 10.1007/s11274-021-03063-w
- Richter, M., Rossello-Mora, R., Oliver Glockner, F., and Peplies, J. (2016). JSpeciesWS: a web server for prokaryotic species circumscription based on pairwise genome comparison. *Bioinformatics* 32, 929–931. doi: 10.1093/bioinformatics/btv681
- Sagot, B., Gaysinski, M., Mehiri, M., Guignon, J. M., Le Rudulier, D., and Alloing, G. (2010). Osmotically induced synthesis of the dipeptide N-acetylglutaminylglutamine amide is mediated by a new pathway conserved among bacteria. *Proc. Natl. Acad. Sci. U. S. A.* 107, 12652–12657. doi: 10.1073/pnas.1003063107
- Schwyn, B., and Neilands, J. B. (1987). Universal chemical assay for the detection and determination of siderophores. *Anal. Biochem.* 160, 47–56. doi: 10.1016/0003-2697(87)90612-9
- Sun, D. L., Zhuo, T., Hu, X., Fan, X. J., and Zou, H. S. (2017). Identification of a *Pseudomonas putida* as biocontrol agent for tomato bacterial wilt disease. *Biol. Control* 114, 45–50. doi: 10.1016/j.biocontrol.2017.07.015
- Thomashow, L. S., and Weller, D. M. (1988). Role of a phenazine antibiotic from *Pseudomonas fluorescens* in biological control of *Gaeumannomyces graminis* var. *tritici*. *J. Bacteriol.* 170, 3499–3508. doi: 10.1128/jb.170.8.3499-3508.1988
- Treuner-Lange, A., Chang, Y. W., Glatter, T., Herfurth, M., Lindow, S., Chreifi, G., et al. (2020). PilY1 and minor pilins form a complex priming the type IVa pilus in *Myxococcus xanthus*. *Nat. Commun.* 11:5054. doi: 10.1038/s41467-020-18803-z
- Vallet-Gely, I., Novikov, A., Augusto, L., Liehl, P., Bolbach, G., Pechy-Tarr, M., et al. (2010). Association of hemolytic activity of *Pseudomonas entomophila*, a versatile soil bacterium, with cyclic lipopeptide production. *Appl. Environ. Microbiol.* 76, 910–921. doi: 10.1128/AEM.02112-09
- Villamizar, S., Ferro, J. A., Caicedo, J. C., and Alves, L. M. C. (2020). Bactericidal effect of entomopathogenic bacterium *Pseudomonas entomophila* against *Xanthomonas citri* reduces citrus canker disease severity. *Front. Microbiol.* 11:1431. doi: 10.3389/fmicb.2020.01431
- Vodovar, N., Vallenet, D., Cruveiller, S., Rouy, Z., Barbe, V., Acosta, C., et al. (2006). Complete genome sequence of the entomopathogenic and metabolically versatile soil bacterium *Pseudomonas entomophila*. *Nat. Biotechnol.* 24, 673–679. doi: 10.1038/nbt1212
- Vodovar, N., Vinals, M., Liehl, P., Basset, A., Degrouard, J., Spellman, P., et al. (2005). *Drosophila* host defense after oral infection by an entomopathogenic *Pseudomonas* species. *Proc. Natl. Acad. Sci. U. S. A.* 102, 11414–11419. doi: 10.1073/pnas.0502240102
- Weller, D. M. (2007). *Pseudomonas* biocontrol agents of soilborne pathogens: looking back over 30 years. *Phytopathology* 97, 250–256. doi: 10.1094/PHYTO-97-2-0250
- Wu, Y. C., Zhou, J. Y., Li, C. G., and Ma, Y. (2019). Antifungal and plant growth promotion activity of volatile organic compounds produced by *Bacillus amyloliquefaciens*. *Microbiologyopen* 8:e813. doi: 10.1002/mbo3.813
- Xu, S., Pan, X., Luo, J., Wu, J., Zhou, Z., Liang, X., et al. (2015). Effects of phenazine-1-carboxylic acid on the biology of the plant-pathogenic bacterium *Xanthomonas oryzae* pv. *oryzae*. *Pestic Biochem. Physiol.* 117, 39–46. doi: 10.1016/j.pestbp.2014.10.006
- Xu, X., Xu, Z., Li, Z., Zakria, M., Zou, L., and Chen, G. (2021). Increasing resistance to bacterial leaf streak in rice by editing the promoter of susceptibility gene *OsSULRT3;6*. *Plant Biotechnol. J.* 19, 1101–1103. doi: 10.1111/pbi.13602
- Zhang, L., Franks, J., Stolz, D. B., Conway, J. F., and Thibodeau, P. H. (2014). Inducible polymerization and two-dimensional assembly of the repeats-in-toxin (RTX) domain from the *Pseudomonas aeruginosa* alkaline protease. *Biochemistry* 53, 6452–6462. doi: 10.1021/bi5007546
- Zhang, R. S., Chen, S. Y., Wang, X. Y., Luo, C. P., Liu, Y. F., and Chen, Z. Y. (2013). High efficiency application technology with *Bacillus amyloliquefaciens* Lx-11 against rice bacterial leaf streak. *Chin. J. Biol. Control* 29, 595–600.
- Zou, L., Zhang, C., Li, Y., Yang, X., Wang, Y., Yan, Y., et al. (2021). An improved, versatile and efficient modular plasmid assembly system for expression analyses of genes in *Xanthomonas oryzae*. *Mol. Plant Pathol.* 22, 480–492. doi: 10.1111/mpp.13033

**Conflict of Interest:** The authors declare that the research was conducted in the absence of any commercial or financial relationships that could be construed as a potential conflict of interest.

**Publisher's Note:** All claims expressed in this article are solely those of the authors and do not necessarily represent those of their affiliated organizations, or those of the publisher, the editors and the reviewers. Any product that may be evaluated in this article, or claim that may be made by its manufacturer, is not guaranteed or endorsed by the publisher.

Copyright © 2021 Yang, Li, Li, Yan, Fang, Zou and Chen. This is an open-access article distributed under the terms of the Creative Commons Attribution License (CC BY). The use, distribution or reproduction in other forums is permitted, provided the original author(s) and the copyright owner(s) are credited and that the original publication in this journal is cited, in accordance with accepted academic practice. No use, distribution or reproduction is permitted which does not comply with these terms.



# Identification of Volatile Organic Compounds in Extremophilic Bacteria and Their Effective Use in Biocontrol of Postharvest Fungal Phytopathogens

## OPEN ACCESS

### Edited by:

Florence Fontaine,  
Université de Reims Champagne-  
Ardenne, France

### Reviewed by:

Jorge Poveda,  
Public University of Navarre, Spain  
Alessandra Di Francesco,  
University of Bologna, Italy

### \*Correspondence:

Miguel Rodríguez  
miguelrg@correo.ugr.es  
Fernando Martínez-Checa  
fmchecha@ugr.es

<sup>†</sup>These authors have contributed  
equally to this work and share first  
authorship

### Specialty section:

This article was submitted to  
Microbe and Virus Interactions With  
Plants,  
a section of the journal  
Frontiers in Microbiology

**Received:** 09 September 2021

**Accepted:** 11 October 2021

**Published:** 12 November 2021

### Citation:

Toral L, Rodríguez M,  
Martínez-Checa F, Montaña A,  
Cortés-Delgado A, Smolinska A,  
Llamas I and Sampedro I (2021)  
Identification of Volatile Organic  
Compounds in Extremophilic Bacteria  
and Their Effective Use in Biocontrol  
of Postharvest Fungal  
Phytopathogens.  
Front. Microbiol. 12:773092.  
doi: 10.3389/fmicb.2021.773092

Laura Toral<sup>1†</sup>, Miguel Rodríguez<sup>2,3\*†</sup>, Fernando Martínez-Checa<sup>2,3\*</sup>, Alfredo Montaña<sup>4</sup>,  
Amparo Cortés-Delgado<sup>4</sup>, Agnieszka Smolinska<sup>5</sup>, Inmaculada Llamas<sup>2,3</sup> and  
Inmaculada Sampedro<sup>2,3</sup>

<sup>1</sup>Xtrem Biotech S.L., European Business Innovation Center, Avenida de la Innovación, Granada, Spain, <sup>2</sup>Department of Microbiology, Faculty of Pharmacy, Campus de Cartuja s/n, Granada, Spain, <sup>3</sup>Biomedical Research Center (CIBM), Avenida del Conocimiento s/n, Granada, Spain, <sup>4</sup>Department of Food Biotechnology, Instituto de la Grasa, Sevilla, Spain, <sup>5</sup>Department of Pharmacology and Toxicology, Maastricht University, Maastricht, Netherlands

Phytopathogenic fungal growth in postharvest fruits and vegetables is responsible for 20–25% of production losses. Volatile organic compounds (VOCs) have been gaining importance in the food industry as a safe and ecofriendly alternative to pesticides for combating these phytopathogenic fungi. In this study, we analysed the ability of some VOCs produced by strains of the genera *Bacillus*, *Peribacillus*, *Pseudomonas*, *Psychrobacillus* and *Staphylococcus* to inhibit the growth of *Alternaria alternata*, *Botrytis cinerea*, *Fusarium oxysporum*, *Fusarium solani*, *Monilinia fructicola*, *Monilinia laxa* and *Sclerotinia sclerotiorum*, *in vitro* and *in vivo*. We analysed bacterial VOCs by using GC/MS and 87 volatile compounds were identified, in particular acetoin, acetic acid, 2,3-butanediol, isopentanol, dimethyl disulphide and isopentyl isobutanoate. *In vitro* growth inhibition assays and *in vivo* experiments using cherry fruits showed that the best producers of VOCs, *Bacillus atrophaeus* L193, *Bacillus velezensis* XT1 and *Psychrobacillus vulpis* Z8, exhibited the highest antifungal activity against *B. cinerea*, *M. fructicola* and *M. laxa*, which highlights the potential of these strains to control postharvest diseases. Transmission electron microscopy micrographs of bacterial VOC-treated fungi clearly showed antifungal activity which led to an intense degeneration of cellular components of mycelium and cell death.

**Keywords:** volatile compounds, antifungal activity, biocontrol, fungal phytopathogens, postharvest diseases

## INTRODUCTION

The world population has increased by 1 billion over the last 10 years, reaching a total of 7.8 billion currently, which is expected to rise by a further 1 billion by 2030. Regardless of environmental damage and potential risks to human health, the use of chemical fertilisers in agriculture and during postharvest storage has increased and remains at high levels

given the growing demand for food worldwide (Goswami and Deka, 2020). The factors responsible for postharvest losses include fungal pathogen infections which are estimated to account for approximately 20–25% of fruit and vegetable postharvest decay in developed countries and contribute significantly to a deterioration in quality and nutrient composition, mycotoxin contamination and a reduction in the market value of fruit (Frankowski et al., 2001; Mari et al., 2016; Gotor-Vila et al., 2017; Tozlu et al., 2018). Many fungal species of the most diverse genera have been reported to be associated with postharvest diseases in fruits and vegetables worldwide. These include *Penicillium expansum*, *Penicillium italicum* and *Penicillium digitatum* (Cheng et al., 2020; Kanashiro et al., 2020; Yu et al., 2020; Zhang et al., 2020a), *Alternaria alternata* (Tozlu et al., 2018; Garganese et al., 2019), *Phytophthora citrophthora* (Díaz et al., 2020) the necrotrophic pathogens *Sclerotinia sclerotiorum* and *Botrytis cinerea* (Fernando et al., 2005; Giorgio et al., 2015; Massawe et al., 2018; Zhao et al., 2020), *Colletotrichum gloeosporioides* (Jin et al., 2020; Shi et al., 2021), various species belonging to the genus *Fusarium* (Medina-Romero et al., 2017; Go et al., 2019; Lee et al., 2019) and the genus *Monilinia*, known to be the most important fungal pathogen to infect stone fruits (Martini and Mari, 2014; Rungjindamai et al., 2014; Obi et al., 2018).

Although postharvest decay has traditionally been controlled through chemical fungicides, their intensive use can cause problems, such as pathogen resistance, pesticide residues, human health hazards and environmental pollution (Mari et al., 2016; Lim et al., 2017). Moreover, due to the toxicological risks involved, chemicals registered for postharvest use are severely limited while consumer awareness of the need for pesticide-free food has been increasing (Gao et al., 2017; Lastochkina et al., 2020). Thus, given their safe, ecofriendly and sustainability properties, biopesticides, which meet the global strategic requirements of organic agriculture, could be a desirable alternative to traditional pesticides (Wu et al., 2019; Zheng et al., 2019).

A wide range of ecological strategies has emerged with the use of anti-phytopathogenic microorganisms and the use of plant-defence hormones or glucosinolates (Poveda, 2020; Poveda et al., 2020). Given the variety of possible fungal inhibition pathways and the wide range of microbial secondary metabolites, postharvest disease management involving biocontrol agents (BCAs) has, in recent years, focused on the use of volatile organic compounds (VOCs; Ryu et al., 2004; Guevara-Avendano et al., 2019). Species of the genera *Streptomyces*, *Pseudomonas*, *Serratia*, *Xanthomonas*, *Alcaligenes*, *Bacillus* and *Agrobacterium* are reported to be the most frequent producers of these bioactive VOCs (Chaves-Lopez et al., 2015; Schmidt et al., 2015; Asari et al., 2016; Mari et al., 2016; Dias et al., 2017; Gotor-Vila et al., 2017; Lim et al., 2017; Khan et al., 2018).

Microbial volatile organic compounds (MVOCs), which originate from different metabolic pathways during fungal and bacterial growth, contain low molecular weight and high vapour pressure molecules that readily diffuse through water and gas-filled pores in soil environments

(Chaves-Lopez et al., 2015; Parafati et al., 2017; Toffano et al., 2017). From a control perspective, these characteristics expand the area of influence, improve membrane penetration and consequently enhance the lethality of these microorganisms (Logan et al., 2009). Bacterial VOCs inhibit spore germination and mycelial growth of various phytopathogens, promote plant growth and induce plant resistance (Gotor-Vila et al., 2017; Lazazzara et al., 2017; Syed-Ab-Rahman et al., 2019; Di Francesco et al., 2020; Poveda, 2021). However, the composition and antifungal properties of volatiles produced by microorganisms can vary according to the growing medium, oxygen availability, moisture, temperature and pH, as well as the population involved and functional dynamics (Chaves-Lopez et al., 2015; Schmidt et al., 2015). Moreover, MVOCs produced by BCAs can play different regulatory roles in different species, the extent of whose inhibition depends on specific bacterium-fungus interactions (Schmidt et al., 2015; Zheng et al., 2019).

This study thus aims to evaluate the antifungal activity of VOCs produced by bacteria obtained from extreme environments and belonging to the genera *Peribacillus*, *Pseudomonas*, *Staphylococcus*, *Psychrobacillus* and *Bacillus* against seven postharvest fruit pathogens. (i) An *in vitro* approach, together with scanning and transmission microscopy, was used to evaluate the antifungal effect of antipathogenic bacterial VOCs on colony and mycelial growth; (ii) VOCs were identified using headspace solid-phase microextraction coupled with gas chromatography-mass spectrometry (HS-SPME-GC/MS); (iii) the effect of pure compounds on the target pathogens was tested *in vitro*; and (iv) the impact of antifungal activity of bacterial VOCs and synthetic compounds was assayed *in vivo* on fruits. The impact of the culture medium on VOCs composition and its antifungal activity was also evaluated.

## MATERIALS AND METHODS

### Bacterial and Fungal Strains, Growth Media and Culture Conditions

The bacterial strains used in this study had been isolated from different sources: *Peribacillus* sp. N3 from river otter (*Lutra lutra*) faeces and strains *Bacillus atrophaeus* L193 (Rodríguez et al., 2018), *Bacillus velezensis* XT1, a patented strain (Béjar et al., 2014), *Pseudomonas segetis* P6 (Rodríguez et al., 2020b), *Psychrobacillus vulpis* Z8 (Rodríguez et al., 2020a) and *Staphylococcus equorum* subsp. *equorum* EN21 (Vega et al., 2019) from saline and hypersaline environments. We examined the phytopathogenic fungi *A. alternata* CECT 20560, *B. cinerea* (isolated from *Vitis vinifera* L. and kindly provided by the Plant Food Research Group, University of Zaragoza, Spain), *Fusarium oxysporum* CECT 2159, *Fusarium solani* [isolated from *Solanum tuberosum* and kindly provided by the Andalusian Agricultural and Fisheries Research and Training Institute (IFAPA), Cordoba, Spain], *Monilinia fructicola*, *Monilinia laxa* (both isolated from *Prunus persica* L. and kindly provided by the Plant Food Research Group, University of Zaragoza, Spain) and *S. sclerotiorum* CECT 2769.



*Bacillus velezensis* strain XT1 was cultured in nutrient broth (NB) medium (No. 3 NutriSelect® Plus, Merck) while the other bacterial strains were cultured in tryptic soy broth (TSB, Panreac® Applichem) at 28°C and 120 rpm in a rotary shaker unless otherwise stated. Fungal strains were cultured in potato dextrose agar (PDA, Difco®) medium at 21°C. To produce bacterial volatile compounds, strains were cultured in tryptic soy agar (TSA, Panreac® Applichem) medium, Schaeffer's growth (SG) medium (Kovacs, 1928) and the medium optimal for lipopeptide production (MOLP; Ahimou et al., 2000). The pH of each medium was adjusted to 7.2–7.4 using NaOH 1M or HCl 1N.

## Gas Chromatography Analysis of Bacterial Volatile Compounds

The bacterial strains were cultured in flask containing 200 ml of MOLP, SG or TSB for 24 h at 28°C and 120 rpm, and the volatile compounds produced were analysed using HS-SPME-GC/MS according to the procedure described by Montañó et al. (2021). Uninoculated MOLP, SG and TSB samples were analysed as controls in order to remove natural occurring volatile compounds from each medium. An aliquot of each sample (5 ml) was inserted into a 15 ml glass vial and 50 µl of internal standard (5-nonanol; 2 mg L<sup>-1</sup>) was added. The vial was closed and placed in a water bath adjusted to 40°C and stirred at 600 rpm using a stirring bar. After 15 min of equilibration, the headspace volatile compounds were extracted for 30 min using a divinylbenzene/carboxen/polydimethylsiloxane (DVB/CAR/PDMS) fibre (2 cm, 50/30 µm; Supelco, Bellefonte, PA). The volatiles were then desorbed for 15 min at 265°C in a GC injector port interfaced with a mass detector with a scan range of m/z 30–400. Separation was carried out on a VF-WAX MS capillary column (30 m × 0.25 mm × 0.25 µm thickness film) from Agilent Technologies (Santa Clara, CA, United States). The initial oven temperature was 40°C (5 min), followed by 40–195°C at 3°C min<sup>-1</sup> and then held at 195–240°C at 10°C min<sup>-1</sup> for 15 min. Helium was used as the carrier gas at 1 ml min<sup>-1</sup> constant flow. Data processing was carried out using MassHunter software (Agilent Technologies). The volatile compounds were initially identified by comparing MS peaks to those in the NIST 17 MS library. The results were then confirmed by comparing the retention indices to literature data reported for equivalent columns and to authentic standards when available. The volatile compounds were quantified by comparison of peak areas to that of internal standard (5-nonanol). All analyses were done in duplicate (i.e., two vials for each bacterial strain).

## In vitro Antifungal Activity of Bacterial Volatile Compounds

The effects of bacterial volatile compounds on the mycelial growth of the fungal phytopathogens *A. alternata*, *B. cinerea*, *F. oxysporum*, *F. solani*, *M. fructicola*, *M. laxa* and *S. sclerotiorum* were assessed using the bi-plate Petri dish method (Lim et al., 2017), as well as MOLP, SG and TSA media to assess bacterial growth. Briefly, 5 µl from an overnight culture (10<sup>8</sup> CFU ml<sup>-1</sup>)

of each bacterial strain in NB or TSB was spotted in the centre of one of the bi-plate compartments. In the other compartment containing the PDA medium, a mycelium plug (Ø 5 mm) of each fungus from a 15 day culture was removed using a sterile cork borer and deposited on the agar bi-plates. The plates were immediately sealed with a double layer of Parafilm to prevent volatile leakage and then incubated at 28°C for 24 h followed by incubation at 21°C for 15 days. Antifungal activity was measured by the percentage reduction in the mycelial growth with the aid of ImageJ software (Schneider et al., 2012). The experiments were repeated in triplicate using bi-plates with sterile liquid medium instead of bacterial inoculum as control for fungal growth.

## In vivo Biocontrol of Fungal Phytopathogens by Bacterial and Synthetic Volatile Compounds

*In vivo* antifungal activity of bacterial volatile compounds, together with the main synthetic compounds identified by GC/MS, was analysed in cherry fruits (*Prunus avium* cv. Picota) according to the protocol described by Gotor-Vila et al. (2017) and Gao et al. (2018), since cherry fruits are the shared host for all fungal pathogens tested. Briefly, cherries were tap-washed and surface-sterilised by spraying with 1% (w/v) sodium hypochlorite solution followed by 70% (v/v) ethanol and sterile distilled water. Each fruit was wounded using a sterile scalpel, and 10 µl of each fungal suspension (10<sup>6</sup> spore ml<sup>-1</sup>) was deposited. The fruits were placed in 2 L (13 × 13 × 12 cm) plastic boxes with 20 ml of sterile water-soaked medical gauze (13 × 13 cm). Three uncovered Petri dishes containing MOLP medium for each bacterial strain were placed inside the boxes and incubated at 21°C for 7 days. The same protocol was used for testing the synthetic volatile compounds acetic acid, acetoin, 2,3-butenediol, dimethyl disulphide (DMDS), isopentanol and isopentyl isobutanoate using 10 ml glass vials containing 5 ml of a solution of each compound (50 µM) in sterile distilled water. Disease incidence and symptom severity were then determined. Experiments were carried out in triplicate using five fruits per replicate; negative controls consisted of a box containing Petri dishes with uncultured media.

## Microscopic Analysis of Structural Effects of Volatile Compounds

Fungal morphology following bacterial VOC treatments (bi-plate method) was studied using a transmission electron microscopy (TEM) high-resolution FEI Titan G2 50-300 microscope equipped with a high angle annular dark field detector. For this purpose, mycelium blocks were cut into 1 × 1 mm pieces, fixed with 2.5% glutaraldehyde in phosphate buffer (pH 7.2), dehydrated with an ethanol gradient and embedded in Epon 812 resin. Thin sections (70 nm) were cut with a diamond knife (Leica, EM UC7, Germany) and stained with 2% uranyl acetate for 10 min, followed by 3% lead citrate for 3 min.

Untreated fungal samples were used as negative controls for comparative purposes.

## Statistical Analysis

The Shapiro–Wilk test was used to verify data normality, and the data were statistically analysed with the aid of the ANOVA ( $p \leq 0.05$ ) and Tukey tests using SPSS software. In order to detect any groupings of volatile compounds based on the composition of the culture media and the strains, as well as to identify the main components of each group, the data were subjected to principal component analysis (PCA) using SIMCA software version 14.1 (Umetrics, Sweden).

## RESULTS

### Characterisation of Bacterial Volatile Compounds Using GC/MS

The VOCs produced by the six bacterial strains, *B. atrophaeus* L193, *B. velezensis* XT1, *Peribacillus* sp. N3, *P. segetis* P6, *P. vulpis* Z8 and *S. equorum* subsp. *equorum* EN21, grown in 24 h cultures, were identified and quantified using GC/MS following headspace solid-phase microextraction (HS-SPME). The culture media MOLP, SG and TSA were tested in order to determine the impact of their composition on the production of VOCs and their involvement in antifungal activity. A total of 87 compounds were identified after analysing the uninoculated sterile media and each strain culture in all media (**Supplementary Table S1**). Butanal, methyl acetate and 2-methyl-2-butenal compounds, which were found exclusively in MOLP and TSB uninoculated sterile media, were not also detected in the cultured media. The remaining 84 compounds were identified as ketones (21.4%), esters (21.4%), alcohols (15.5%), carboxylic acids (11.9%), sulphur compounds (11.9%), aromatic hydrocarbons (10.7%), aldehydes (4.8%), halogenated compounds (1.2%) and terpenes (1.2%).

Principal component analysis was used to detect VOCs clustering and to determine the relationships between the bacterial strains and culture media. The principal components (PCs), which accounted for the largest variations in data points, were extracted in order to better visualise the data structure in a reduced dimension. The overall PCA dataset consisted of a  $21 \times 87$  matrix, with rows representing 21 bacterial cultures and uncultured media, as well as columns representing volatile compound concentrations. General PCA (**Figure 1**) revealed two main components which, as indicated by the score plot, accounted for 32% of total variance (**Figure 1A**). 19.1% of variance was attributable to principal component 1 (PC1), while 12.9% of variance corresponded to PC2. All culture strains clearly formed a highly correlated group, except for strain *P. vulpis* Z8 cultured in MOLP, SG and TSB media and strain *S. equorum* EN21 cultured in MOLP medium, which were segregated from the main group. The PCA loading plot (**Figure 1B**) shows that this segregation is mainly associated with the volatile compounds butyl isobutanoate (80), isopentyl isobutanoate (82), methanethiol (60), 2-phenylethyl isobutanoate (87), S-methyl thio-3-methylbutanoate (83), butyl propanoate (79) and ethyl 2-methylbutanoate (75) produced by strain *P. vulpis* Z8 for PC1, while PC2 was mainly associated with

the volatile compounds propanoic acid (29), butyl acetate (33), hexanoic acid (38), octanoic acid (39), acetic acid (24), butanoic acid (27), 2,6-diethyl-pyrazine (35) and acetone (1) produced by strain *S. equorum* EN21 in the MOLP medium. These volatile compounds were mostly or exclusively released from strains *P. vulpis* Z8 and *S. equorum* EN21 and at very low levels from other strains.

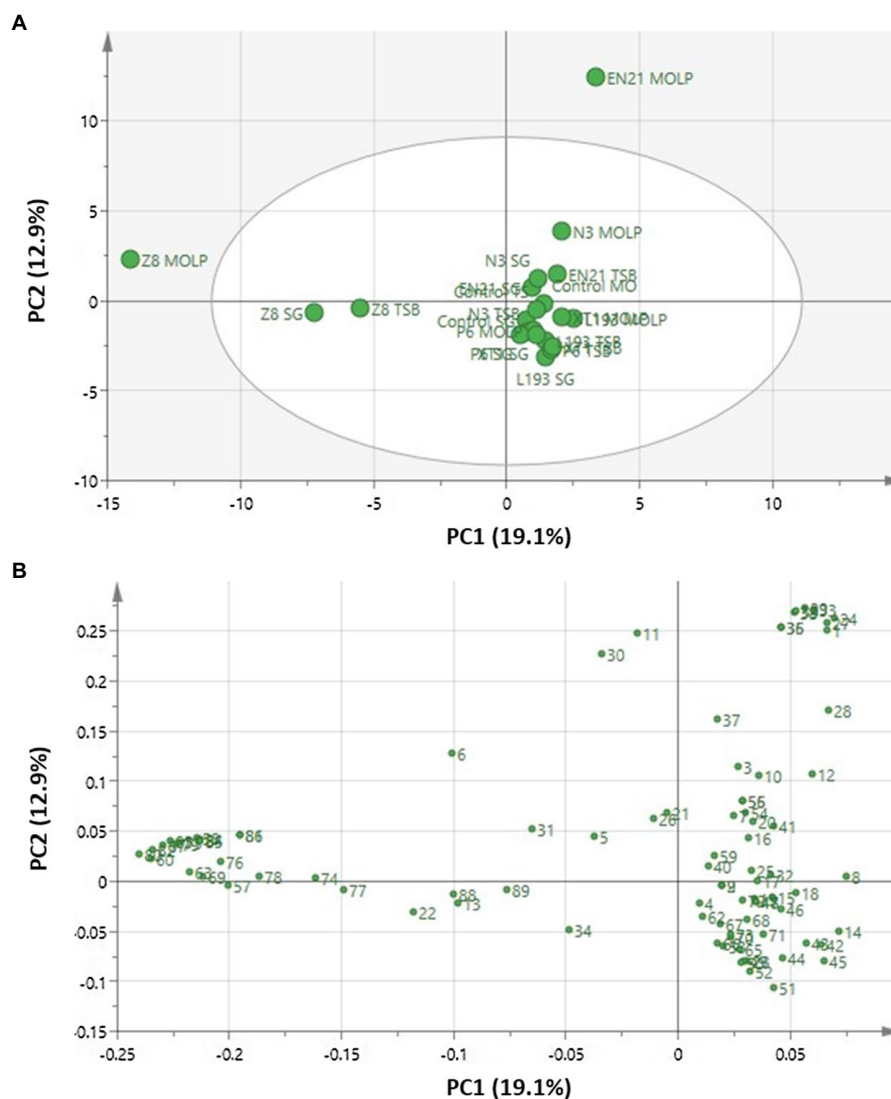
In order to identify the impact of culture media composition on volatile compound production, each bacterial strain was cultured in MOLP, SG and TSB media. Strain *B. atrophaeus* L193 produced 25, 22 and 25 volatile compounds in MOLP, SG and TSB media, respectively, most of which were ketones and aromatic hydrocarbons. In the case of strain *B. velezensis* XT1, the 27, 16 and 27 volatile compounds in MOLP, SG and TSB media, respectively, also mainly corresponded to ketones and aromatic hydrocarbons. With regard to strain *Peribacillus* sp. N3, a total of 37, 20 and 23 compounds were identified in MOLP, SG and TSB media, respectively, most of which were carboxylic acids and ketones. Strain *P. segetis* P6 produced 21, 10 and 21 volatile compounds, mostly ketones, aromatic hydrocarbons and sulphur compounds, in MOLP, SG and TSB media, respectively. In the case of strain *S. equorum* EN21, a total of 28, 18 and 21 volatile compounds, mostly alcohols, carboxylic acids and aromatic hydrocarbons, were detected in MOLP, SG and TSB media, respectively. Finally, with regard to strain *P. vulpis* Z8, a total of 40, 22 and 29 compounds, for the most part esters and sulphur compounds, were identified in MOLP, SG and TSB cultures, respectively.

The main volatile compounds produced by each strain were then selected on the basis of two criteria: their absence from uncultured media and a 2-fold increase in their concentrations in uncultured media. The volatile compounds selected are shown in **Table 1**. High levels of acetoin and 2,3-butanediol were produced by strains *B. atrophaeus* L193 and *B. velezensis* XT1. Acetoin was synthesised in all media, with particularly high levels of production in MOLP, while 2,3-butanediol was only detected in MOLP cultures. Acetic acid was the principal volatile compound detected when strains *Peribacillus* sp. N3 and *S. equorum* EN21 were cultured in MOLP and SG media. High levels of isopentanol were also produced by *S. equorum* EN21 culture in all media, especially TSB. DMDS was the main volatile compound produced by strain *P. segetis* P6 when cultured in SG medium, as well as by strain *P. vulpis* Z8 when cultured in all media. High concentrations of isopentyl isobutanoate were only detected when strain *P. vulpis* Z8 was cultured in all media.

Principal component analysis based on intraspecific differences in medium composition showed a distribution very similar to that previously obtained even though a higher level of correlation was observed for PC1 and PC2 in each medium (**Supplementary Figure S1**).

### In vitro Antifungal Activity of Bacterial Volatile Compounds

The effects of VOCs on the mycelial growth of fungal phytopathogens *A. alternata*, *B. cinerea*, *F. oxysporum*, *F. solani*,



**FIGURE 1 |** Principal component analysis of volatile compounds obtained using HS-SPME and identified with the aid of GC/MS in *B. atrophaeus* L193 (L193), *B. velezensis* XT1 (XT1), *Peribacillus* sp. N3 (N3), *P. segetis* P6 (P6), *S. equorum* EN21 (EN21) and *P. vulpis* Z8 (Z8) grown in MOLP, SG and TSB media, as well as in uncultured control media. **(A)** Score plot. **(B)** Loading plot. Each volatile compound, which is assigned a reference number, can be seen in **Supplementary Table S1**.

*M. fructicola*, *M. laxa* and *S. sclerotiorum* were assessed using the bi-plate Petri dish method, in the three-culture media assayed previously for VOC characterisation.

The highest antifungal activity was observed when strains were cultivated in the MOLP medium. Thus, volatile compounds produced by strains *B. atrophaeus* L193, *B. velezensis* XT1 and *P. vulpis* Z8 synthesised in the MOLP medium greatly inhibited the growth of *S. sclerotiorum* (82, 96 and 56%, respectively), *M. fructicola* (42, 37 and 83%) and *M. laxa* (51, 54 and 15%). With regard to *B. cinerea* plates, *B. atrophaeus* L193 and *B. velezensis* XT1 produced reductions of 27 and 46% in fungal growth, respectively, while *P. vulpis* Z8 shows no effect on the mycelial growth of *B. cinerea* (data not shown). Fungal growth inhibition of some bacterial strains cultured in the MOLP

medium is shown in **Figure 2**. By contrast, no inhibition of mycelial growth was detected against *A. alternata*, *F. oxysporum* and *F. solani* following exposure to VOCs produced by the bacterial strains.

### **In vivo Biocontrol of Fungal Phytopathogens by Bacterial Volatile Compounds**

To examine *in vivo* antifungal activity, VOCs produced by strains *B. atrophaeus* L193, *B. velezensis* XT1 and *P. vulpis* Z8 cultured in the MOLP medium were assayed in cherry fruits, together with some of the principal synthetic volatile compounds characterised by GC/MS. With regard to the

**TABLE 1** | Principal volatile compounds for each strain after culturing in MOLP, SG and TSB media.

Sample	Culture medium	Concentration of principal volatile compounds ( $\mu\text{g L}^{-1}$ )					
		Acetoin	Acetic acid	2,3-butanediol	Isopentanol	Dimethyl disulphide	Isopentyl isobutanoate
Uninoculated media	MOLP	–	3.8 (3.0)	–	–	–	–
	SG	–	–	–	–	–	–
	TSA	–	–	–	–	–	–
<i>B. atrophaeus</i> L193	MOLP	174.0 (10.4)	36.9 (7.1)	268.8 (23.0)	–	–	–
	SG	60.5 (15.6)	10.0 (6.5)	–	–	–	–
	TSA	44.5 (0.3)	3.6 (1.1)	–	–	–	–
<i>B. velezensis</i> XT1	MOLP	111.0 (8.5)	21.9 (0.4)	261.7 (49.3)	–	–	–
	SG	64.0 (9.6)	6.1 (4.1)	–	–	–	–
	TSA	60.0 (0.5)	2.1 (0.0)	–	–	–	–
<i>Peribacillus</i> sp. N3	MOLP	–	32.9 (4.5)	–	7.7 (0.2)	–	–
	SG	–	30.8 (0.4)	–	–	–	–
	TSA	–	–	–	–	5.6 (1.8)	–
<i>P. segetis</i> P6	MOLP	–	–	–	–	3.6 (0.3)	–
	SG	–	–	–	–	46.1 (2.9)	–
	TSA	–	–	–	3.1 (0.1)	–	–
<i>P. vulpis</i> Z8	MOLP	–	–	–	6.1 (1.1)	88.4 (2.7)	82.5 (1.3)
	SG	–	–	–	–	139.7 (1.5)	27.4 (1.9)
	TSA	–	–	–	–	140.1 (4.3)	52.0 (1.1)
<i>S. equorum</i> subsp. <i>equorum</i> EN21	MOLP	–	180.2 (17.1)	–	34.3 (2.1)	–	–
	SG	–	25.6 (1.9)	–	73.4 (3.5)	–	–
	TSA	–	4.1 (2.0)	–	110.6 (27.7)	–	–

Concentrations of each volatile compound are expressed as the mean of two determinations, with standard deviation (SD) indicated in parenthesis – concentration not detected or insignificant.

percentage of disease incidence, the pathogen *M. laxa* was susceptible to VOCs produced by the strains *B. atrophaeus* L193 and *B. velezensis* XT1 (**Figure 3**). In both cases, the VOCs reduced disease incidence by over 50% as compared to the control. For its part, no significant antifungal activity against *M. laxa* was produced by *P. vulpis* Z8 VOCs. Similar results were obtained with regard to the synthetic volatile compounds isopentanol and DMDS. A very different scenario was observed for antifungal activity against the pathogen *M. fructicola*, where VOCs produced by *B. atrophaeus* L193 had no effect, while *P. vulpis* Z8 completely inhibited this pathogen's growth. The VOCs produced by strain *B. velezensis* XT1, and the synthetic compound isopentanol, reduced disease incidence in cherries by 50% as compared to the infection control, while the pathogen *B. cinerea* was completely inhibited by *B. atrophaeus* L193 VOCs. Similarly, strains *P. vulpis* Z8 and *B. velezensis* XT1 reduced the incidence of *B. cinerea* by 48 and 62%, respectively. By contrast, isopentanol and DMDS showed no antifungal activity against *B. cinerea*. The quantity of spores from all pathogenic fungi on the surface of fruits was small and limited to the wound observed when *B. atrophaeus* L193, *B. velezensis* XT1 and *P. vulpis* Z8 VOCs were tested (**Supplementary Figure S2**). On the other hand, while isopentanol and DMDS had no effect on disease sporulation of *M. fructicola* or *B. cinerea*, they did have a slight impact on *M. laxa*. The synthetic compounds acetoin, acetic acid, 2,3-butanediol and isopentyl isobutanoate did not reduce the disease incidence or fungal sporulation of any target pathogens.

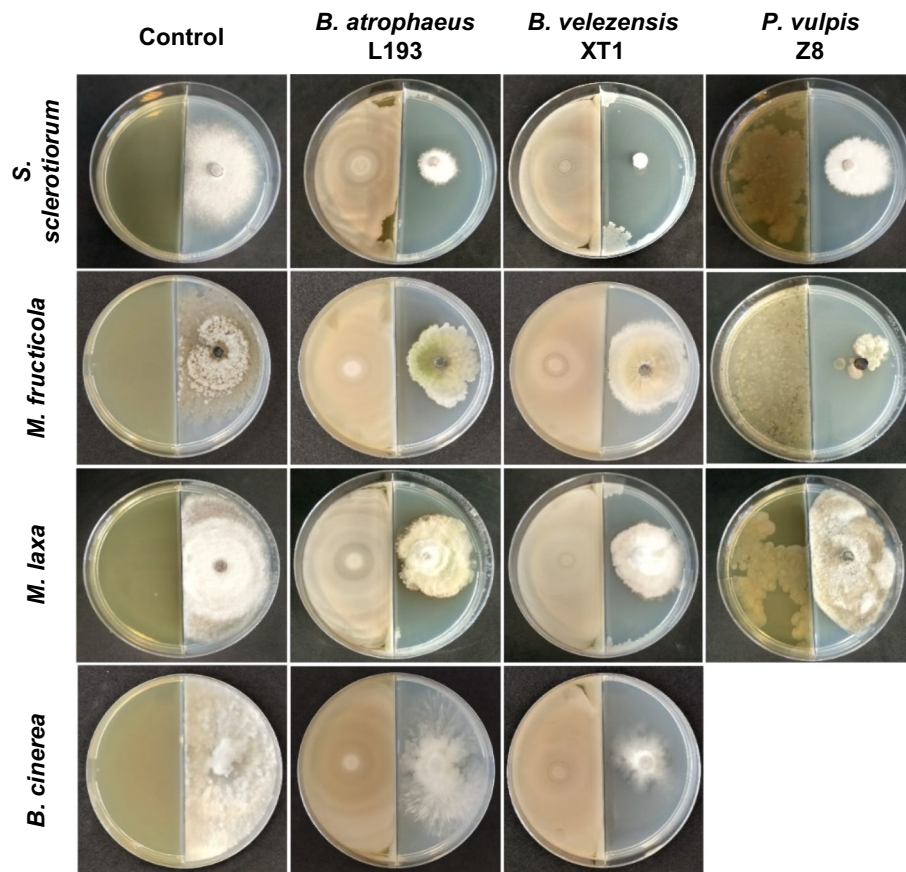
## Microscopic Analysis of Structural Effects of Volatile Compounds

To identify structural disorders caused by bacterial VOC treatment of the phytopathogenic fungi, hyphae were analysed after a 7 day incubation period using TEM. Micrographs of control fungi show well-organised cell walls, as well as cellular membranes, while organelles, such as endoplasmic reticula, abundant mitochondria, nuclei, and vacuoles, can be clearly observed in most of these micrographs (**Figures 4A,D,G**). By contrast, while maintaining the cell wall structure, *B. cinerea* hyphae treated with *B. velezensis* XT1 (**Figure 4B**) and *B. atrophaeus* L193 volatiles (**Figure 4C**) showed severe cytoplasmic cavitation and vacuolation and no organelles were identified. When *M. laxa* was exposed to *B. velezensis* XT1 (**Figure 4E**) and *B. atrophaeus* L193 (**Figure 4F**) VOCs, the hyphal membrane and cell walls appeared to be thinner and degraded, cytoplasmic content was completely coagulated and no organelles could be identified. These effects were also observed in *M. fructicola* hyphae treated with VOCs produced by the *P. vulpis* Z8 strain (**Figure 4H**).

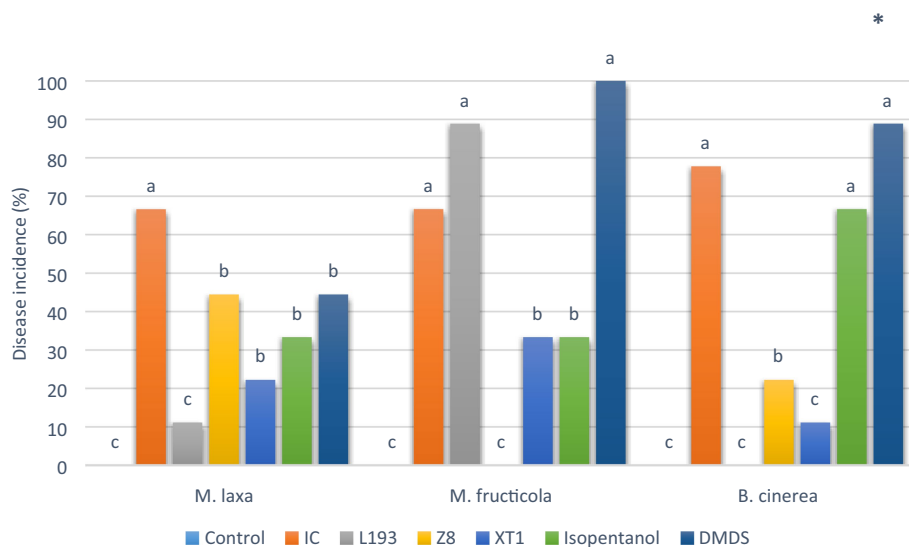
## DISCUSSION

Bacteria emit VOCs that can inhibit the growth of specific microbial populations (Larkin and Stokes, 1967; Chaves-Lopez et al., 2015). These VOCs, which are easily degraded and act over long distances (Gao et al., 2017), exhibit major advantages over conventional fungicides. In this study, we examined the diversity of VOCs produced by extremophilic bacteria and

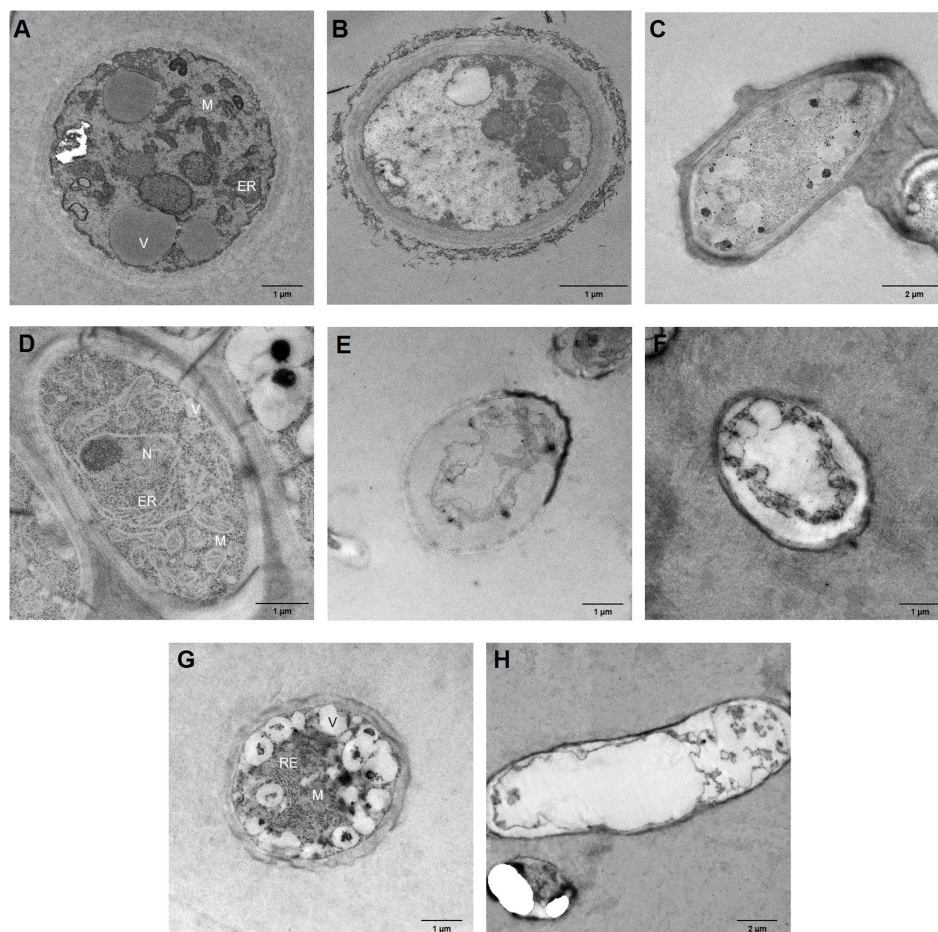




**FIGURE 2** | *In vitro* fungal growth inhibition by bacterial volatile compounds produced by *B. atrophaeus* L193, *B. velezensis* XT1 and *P. vulpis* Z8 when cultured in MOLP medium using the bi-plate method.



**FIGURE 3** | *In vivo* antagonistic activity of volatile organic compounds (VOCs) from *B. atrophaeus* L193, *B. velezensis* XT1 and *P. vulpis* Z8, as well as the synthetic compounds isopentanol and dimethyl disulphide. The figure shows the disease incidence of cherry fruits artificially inoculated with *M. laxa*, *M. fructicola* and *B. cinerea*. Control: control treatment without bacterial VOCs or volatile synthetic compounds. IC: pathogen infection control without VOC treatment. Differences between treatments were tested for statistical significance using Chi-squared test: \* ( $p \leq 0.05$ ), \*\* ( $p \leq 0.01$ ), \*\*\* ( $p \leq 0.001$ ) and ns (not significant).



**FIGURE 4 |** Transmission electron micrographs of fungal hyphae after 7 days of bacterial VOC treatment. **(A)** Untreated *B. cinerea*. **(B)** *B. cinerea* – *B. velezensis* XT1 strain. **(C)** *B. cinerea* – *B. atrophaeus* L193 strain. **(D)** Untreated *M. laxa*. **(E)** *M. laxa* – *B. velezensis* XT1 strain. **(F)** *M. laxa* – *B. atrophaeus* L193 strain. **(G)** Untreated *M. fructicola*. **(H)** *M. fructicola* – *P. vulpis* Z8 strain. ER, endoplasmic reticulum; M, mitochondria; N, nucleus; and V, vacuole.

their antagonistic activity against certain phytopathogenic fungi. Their ability to secrete a wide range of antifungal VOCs could make these bacteria useful in the search for potential biological agents to control postharvest diseases.

Roughly 2,000 compounds produced by almost 1,000 microorganism species are listed in the MVOC database (Lemfack et al., 2018; Caulier et al., 2019). We found acetoin, acetic acid, 2,3-butanediol, isopentanol, dimethylsulfide and isopentyl isobutanoate to be the principal volatile compounds produced by the studied strains.

GC/MS analysis showed that high levels of acetoin and 2,3-butanediol are produced by *Bacillus* strains. Acetoin, which stimulates induced systemic resistance against *Pseudomonas syringae* DC3000 (Sierra, 1957) and plant growth (Kai and Piechulla, 2009) and is produced by other *Bacillus* strains (Asari et al., 2016; Caulier et al., 2019), is synthesised in all media, with particularly high levels detected in MOLP medium, while 2,3-butanediol was exclusively found in MOLP cultures. In addition, the volatile compound 2,3-butanediol is not only known to promote plant growth (Wu et al., 2019) but also

to induce modifications in the expression of genes linked to *Ralstonia solanacearum* and *Pectobacterium carotovorum* pathogenicity (Marquez-Villavicencio Mdel et al., 2011; Tahir et al., 2017).

The antifungal activity of VOCs has been reported to be associated with functional groups (Sasser, 1990; Chaves-Lopez et al., 2015). In addition, solute hydrophobicity affects membrane integrity, which is undermined by the application of lipophilic compounds. This may affect DMDS, the principal volatile compound produced by Z8, and could be responsible for the strong antifungal activity of this bacterium against *Monilia* sp. and *S. sclerotium*. The antifungal activity of this volatile compound has been characterised in *Bacillus* strains (Coosemans, 2005; Caulier et al., 2019) and in *Pseudomonas donghuensis* against *Rhizoctonia solani* (Ossowicki et al., 2017; Guevara-Avendano et al., 2019). DMDS, a sulphur-containing compound produced by *Pseudomonas* sp., also inhibits *Phytophthora infestans* growth and development (De Vrieze et al., 2015; Guevara-Avendano et al., 2019).

Acetic acid is the principal volatile compound produced by strains *Peribacillus* sp. N3 and *S. equorum* EN21 when cultured in MOLP and SG media. Acetic acid has been found to be an effective antifungal compound in several fruits (Baird-Parker, 1963; Fuqua et al., 1994), in low concentrations, reduce *B. cinerea* and *P. expansum* germination to zero (Baird-Parker, 1963) and, at a concentration of 50 mm significantly inhibit the growth of the phytopathogenic fungus *C. gloeosporioides* (Kang et al., 2003). The inhibition by this organic acid is closely related to reduced respiration levels rather than to structural cellular damage. Momma et al. (2006) have described how the treatments of soil with acetic acid suppress the survival of *R. solanacearum*.

In addition, high levels of isopentanol were produced by strain *S. equorum* EN21 in all media, especially in TSB. The antifungal activity of alcohols has been described in previous studies; for example, the phenol 4-chloro-3-methyl has been reported to have a strong antifungal effect on *Alternaria solani* and *B. cinerea* (Gao et al., 2017), allyl alcohol inhibits *S. sclerotiorum* germination in bean plants (Lim et al., 2017), while phenylethyl alcohol inhibits the mycelial growth of *P. italicum* (Li et al., 2010).

High concentrations of isopentyl isobutanoate/isobutyrate were only detected when strain *P. vulpis* Z8 was cultured in all media. To the best of our knowledge, no information concerning the antifungal activity of this compound, which could be responsible for the intense antifungal activity of Z8 against *M. fructicola* or *S. sclerotiorum*, existed prior to our study.

A group of highly correlated VOCs was clearly identified for all the strains investigated except for *P. vulpis* Z8 and *S. equorum* EN21. Several studies have analysed volatile metabolites emitted by clinical *Staphylococcus* sp. strains (Nasir et al., 2018) but only one has identified antifungal volatile agents produced by *Staphylococcus pasteuri* against the commercial truffle species *Tuber borchii* Vittad (Barbieri et al., 2005).

The VOC 2,6-diethyl-pyrazine produced by *S. equorum* strain EN21 is involved in segregating this bacterium from other bacteria. A large proportion of microbial volatiles is pyrazines, which are produced by many strains such *Bacillus subtilis* and are known to exhibit antifungal activity (Chaves-Lopez et al., 2015; Haidar et al., 2016; Caulier et al., 2019). Some of these compounds affect the sporulation and elongation of *B. cinerea* germ tubes (Chaves-Lopez et al., 2015; Haidar et al., 2016; Caulier et al., 2019), while 2,3,5-trimethylpyrazine antifungal activity against bacterium *Fusarium* sp. has also been studied (Guevara-Avendano et al., 2019).

The antifungal activity of bacterial volatile compounds tested *in vitro* demonstrated that strains *B. atrophaeus* L193, *B. velezensis* XT1 and *P. vulpis* Z8 cultured in MOLP medium significantly inhibited the growth of *S. sclerotiorum* and *M. fructicola*. Strains *B. atrophaeus* L193 and *B. velezensis* XT1 reduced the growth of *M. laxa* and *B. cinerea* by between 30 and 55%. Species of the genus *Bacillus* have been reported to be the most common producers of bioactive VOCs (Chaves-Lopez et al., 2015). The *in vitro* activity of VOCs against the major phytopathogenic species *B. subtilis*, *Bacillus amyloliquefaciens* and *B. velezensis* has been studied previously (Chaves-Lopez et al., 2015). However,

few studies have analysed the volatilome produced by *B. atrophaeus*, and, to the best of our knowledge, this is the first study of the antifungal activity of VOCs produced by the genera *Psychrobacillus* and *Peribacillus*.

Our findings show that none of the bacteria tested were effective against all phytopathogenic fungi. Similar results were obtained by Chaves-Lopez et al. (2015) in their study of *Bacillus* strains. The variations in fungal responses could reflect differences in the sites of action or in the ability of fungi to detoxify the metabolites (Chaves-Lopez et al., 2015). Strains *Bacillus* and *Psychrobacillus*, but not *B. frigidotolerans*, showed antifungal activity against major phytopathogens such *Monilinia* and *Sclerotinia*.

Previous *in vitro* studies have demonstrated that VOCs produced by *B. velezensis* inhibit the growth of *B. cinerea* and *M. fructicola* by over 70% (Gao et al., 2017; Guevara-Avendano et al., 2019), which is within the 50–97% range observed in our study of *B. velezensis* XT1 and *B. atrophaeus* L193. We found lower levels of antifungal activity against *Fusarium* for all strains tested, with a 38% reduction observed following exposure to VOCs produced by *B. atrophaeus* strain L193, which is very similar to the reduction observed for other *Bacillus* strains (Yuan et al., 2012; Guevara-Avendano et al., 2019). The bacteria which generally showed the most effective antifungal activity, *B. velezensis* XT1 and *B. atrophaeus* L193, was found to be producers of metabolites with antifungal activity, such as lipopeptides in previous studies (Rodriguez et al., 2018; Toral et al., 2018). Although little is known about VOCs produced by *B. atrophaeus*, the volatilome of *B. atrophaeus* HAB-5 has been identified which has a moderate antifungal effect on the common disease of anthracnose caused by the major fungus *C. gloeosporioides* (Rajaofera et al., 2019). No information on the antifungal activity of volatile compounds produced by *B. atrophaeus* against the major phytopathogens analysed existed prior to our study.

The bacterial genus *Pseudomonas* is also capable of emitting VOCs that inhibit the mycelial growth of *S. sclerotiorum* (Fernando et al., 2005; Guevara-Avendano et al., 2019), although the inhibition rate recorded for *P. segetis* P6 in this study was very low as compared to the other strains tested. Species of the genus *Staphylococcus* are mostly known to cause opportunistic human diseases, some of which are frequently found in rhizospheric soil. Although antifungal activity of the bacterium *S. equorum* against *B. cinerea* has been observed (Sadfi-Zouaoui et al., 2008; Reverchon et al., 2019) to our knowledge, the VOCs produced by this bacterium have not previously been described. In our study, the antifungal activity of *S. equorum* strain EN21 against *F. solani* was found to be very low, with a reduction in fungal growth of only 2%. Reverchon et al. (2019) have shown that VOCs emitted by some *Staphylococcus* species, which are capable of inhibiting the growth of *F. solani* by over 20%, can, however, increase that of *F. oxysporum*.

Overall, our results suggest that the antifungal activity of VOCs produced by the extremophilic bacteria studied is dependent on a combination of a limited number of molecules, while the composition of VOC profiles not only depends on species but also on the growing medium (Larkin and Stokes, 1967;



Chaves-Lopez et al., 2015). The differences in proteins and sugar content in all media reflect differences in the volatiles produced, whose composition and functional properties are known to be influenced by the growth medium (Asari et al., 2016; Lazazzara et al., 2017). The profiles of VOCs obtained in the present study for different *Bacillus* strains confirmed the genetic impact on their composition.

Previous studies have shown that bacterial VOCs can affect the hyphal growth, sporulation and spore germination of fungi (Wenke et al., 2010; Asari et al., 2016). Zhou et al. (2019) have suggested that VOCs produced by *B. subtilis* permeabilize fungal spores and inhibit the germination of *M. fructicola*. Other studies have highlighted how the fungal hyphae of *A. solani* are deformed when treated with VOCs produced by *B. subtilis* strains (Zhang et al., 2020b).

The effects of VOCs produced by the strains tested on the morphology of phytopathogens were evaluated using microscopic analysis. TEM micrographs of fungi treated with bacterial VOCs clearly show the impact of antifungal activity, which causes a marked deterioration in cellular components and cell death and inhibits fungal growth and development. Some studies have previously described a similar destruction of fungal structures and cell death induced by VOCs from *Pseudomonas* spp. strains USB2104 and USB2105, as well as *Bacillus* sp. USB2103, against *S. sclerotiorum* (Giorgio et al., 2015), from *B. subtilis* CF-3 against *M. fructicola* (Zhou et al., 2019) and by synthetic COVs against *B. cinerea* (Liu et al., 2016). By contrast, no antifungal activity mediated by VOCs from species of the genus *Psychrobacillus* was analysed prior to our study.

We investigated the production of several volatile metabolites with different types of biological activity. Previous studies have shown relationships between phytotoxicity and VOCs (Arimura et al., 2010). In some cases, terpenic VOCs inhibited or reduced the germination of seeds of cereals (He et al., 2014). However, exposure of *Arabidopsis thaliana* of alcoholic VOCs showed non-effect on germination (Lee et al., 2014). These studies highlighted the influence of the origin, dose and application form in the antimicrobial activity of VOCs. *In vivo* analyses described the potential of VOCs emitted by *Bacillus* sp. to control postharvest diseases (Zheng et al., 2019). The presence of residual antibiotics produced by these bacteria in fruits constitutes an important health risk because the increased microbial resistance detected in last years (Rashmi et al., 2017). However, VOCs are naturally occurring (emissions by microorganisms) at very low concentrations and do not leave toxic residues on fruit surfaces (Mercier and Smilanick, 2005; Qin et al., 2017). The biological fumigation with VOCs is an

interesting strategy to use against a wide range of storage pathogens and fungal decay.

Our search for extremophilic bacteria capable of withstanding stress conditions identified several good candidate strains for postharvest use as VOCs producers. The antifungal activity of many of the VOCs identified in this work has not been previously studied, and further research is required in order to better understand the mechanistic role of VOCs produced by extreme bacteria in antifungal activity to control postharvest diseases.

## DATA AVAILABILITY STATEMENT

The raw data supporting the conclusions of this article will be made available by the authors, without undue reservation.

## AUTHOR CONTRIBUTIONS

LT, MR, FM-C, IL, and IS conceived and supervised the study and designed the experiments. LT, MR, AS, AM, and AC-D performed the experiments and analysed the data. LT, MR, FM-C, and IS prepared the figures, drafted the manuscript, and wrote the final version of the manuscript. All authors contributed to the article and approved the submitted version.

## FUNDING

This research was funded by grants from the Spanish Ministry of the Economy and Competitiveness (PID2019-106704RB-I00/AEI/10.13039/501100011033) and the European Project for Industrial Doctorates 'H2020' (UGR-Ref. 4726).

## ACKNOWLEDGMENTS

The authors thank Michael O'Shea for correcting the English revision of this manuscript.

## SUPPLEMENTARY MATERIAL

The Supplementary Material for this article can be found online at: <https://www.frontiersin.org/articles/10.3389/fmicb.2021.773092/full#supplementary-material>

## REFERENCES

- Ahimou, F., Jacques, P., and Deleu, M. (2000). Surfactin and iturin A effects on *Bacillus subtilis* surface hydrophobicity. *Enzym. Microb. Technol.* 27, 749–754. doi: 10.1016/S0141-0229(00)00295-7
- Arimura, G.-I., Shiojiri, K., and Karban, R. (2010). Acquired immunity to herbivory and allelopathy caused by airborne plant emissions. *Phytochemistry* 71, 1642–1649. doi: 10.1016/j.phytochem.2010.06.021
- Asari, S., Matzen, S., Petersen, M. A., Bejai, S., and Meijer, J. (2016). Multiple effects of *Bacillus amyloliquefaciens* volatile compounds: plant growth promotion and growth inhibition of phytopathogens. *FEMS Microbiol. Ecol.* 92:fiw070. doi: 10.1093/femsec/fiw070
- Baird-Parker, A. C. (1963). A classification of micrococci and staphylococci based on physiological and biochemical tests. *J. Gen. Microbiol.* 30, 409–427. doi: 10.1099/00221287-30-3-409
- Barbieri, E., Gioacchini, A. M., Zambonelli, A., Bertini, L., and Stocchi, V. (2005). Determination of microbial volatile organic compounds from *Staphylococcus pasteurii* against *Tuber borchii* using solid-phase microextraction and gas chromatography/ion trap mass spectrometry. *Rapid Commun. Mass Spectrom.* 19, 3411–3415. doi: 10.1002/rcm.2209



- Béjar, V., Llamas, I., Ruíz-García, C., and Quesada, E. (2014). *Uso de Bacillus methylotrophicus como estimulante del crecimiento vegetal y medio de control biológico, y cepas aisladas de dicha especie*. Patent No PCT/ES2015/070600. Available at: <https://patents.google.com/patent/ES2561908A1/es>
- Caulier, S., Nannan, C., Gillis, A., Licciardi, F., Bragard, C., and Mahillon, J. (2019). Overview of the antimicrobial compounds produced by members of the *Bacillus subtilis* group. *Front. Microbiol.* 10:302. doi: 10.3389/fmicb.2019.00302
- Chaves-Lopez, C., Serio, A., Gianotti, A., Sacchetti, G., Ndagijimana, M., Ciccarone, C., et al. (2015). Diversity of food-borne *Bacillus* volatile compounds and influence on fungal growth. *J. Appl. Microbiol.* 119, 487–499. doi: 10.1111/jam.12847
- Cheng, Y., Lin, Y., Cao, H., and Li, Z. (2020). Citrus postharvest green mold: recent advances in fungal pathogenicity and fruit resistance. *Microorganisms* 8:449. doi: 10.3390/microorganisms8030449
- Coosemans, J. (2005). *Dimethyl Disulphide (DMS): A Potential Novel Nematicide and Soil Disinfectant*. (Leuven, Belgium: International Society for Horticultural Science), 57–64.
- De Vrieze, M., Pandey, P., Bucheli, T. D., Varadarajan, A. R., Ahrens, C. H., Weisskopf, L., et al. (2015). Volatile organic compounds from native potato-associated *Pseudomonas* as potential anti-oomycete agents. *Front. Microbiol.* 6:1295. doi: 10.3389/fmicb.2015.01295
- Di Francesco, A., Zajc, J., Gunde-Cimerman, N., Aprea, E., Gasperi, F., Placi, N., et al. (2020). Bioactivity of volatile organic compounds by *Aureobasidium* species against gray mold of tomato and table grape. *World J. Microbiol. Biotechnol.* 36:171. doi: 10.1007/s11274-020-02947-7
- Dias, M. P., Bastos, M. S., Xavier, V. B., Cassel, E., Astarita, L. V., and Santarem, E. R. (2017). Plant growth and resistance promoted by *Streptomyces* spp. in tomato. *Plant Physiol. Biochem.* 118, 479–493. doi: 10.1016/j.plaphy.2017.07.017
- Díaz, M. A., Pereyra, M. M., Picón-Montenegro, E., Meinhardt, F., and Dib, J. R. (2020). Killer yeasts for the biological control of postharvest fungal crop diseases. *Microorganisms* 8:1680. doi: 10.3390/microorganisms8111680
- Fernando, W. G. D., Ramarathnam, R., Krishnamoorthy, A. S., and Savchuk, S. C. (2005). Identification and use of potential bacterial organic antifungal volatiles in biocontrol. *Soil Biol. Biochem.* 37, 955–964. doi: 10.1016/j.soilbio.2004.10.021
- Frankowski, J., Lorito, M., Scala, F., Schmid, R., Berg, G., and Bahl, H. (2001). Purification and properties of two chitinolytic enzymes of *Serratia plymuthica* HRO-C48. *Arch. Microbiol.* 176, 421–426. doi: 10.1007/s002030100347
- Fuqua, W. C., Winans, S. C., and Greenberg, E. P. (1994). Quorum sensing in bacteria: the LuxR-LuxI family of cell density-responsive transcriptional regulators. *J. Bacteriol.* 176, 269–275. doi: 10.1128/jb.176.2.269-275.1994
- Gao, H., Li, P., Xu, X., Zeng, Q., and Guan, W. (2018). Research on volatile organic compounds from *Bacillus subtilis* cf-3: biocontrol effects on fruit fungal pathogens and dynamic changes during fermentation. *Front. Microbiol.* 9:456. doi: 10.3389/fmicb.2018.00456
- Gao, Z., Zhang, B., Liu, H., Han, J., and Zhang, Y. (2017). Identification of endophytic *Bacillus velezensis* ZSY-1 strain and antifungal activity of its volatile compounds against *Alternaria solani* and *Botrytis cinerea*. *Biol. Control* 105, 27–39. doi: 10.1016/j.biocontrol.2016.11.007
- Garganese, F., Sanzani, S. M., Di Rella, D., Schena, L., and Ippolito, A. (2019). Pre- and postharvest application of alternative means to control *Alternaria* Brown spot of citrus. *Crop Prot.* 121, 73–79. doi: 10.1016/j.cropro.2019.03.014
- Giorgio, A., De Stradis, A., Lo Cantore, P., and Iacobellis, N. S. (2015). Biocide effects of volatile organic compounds produced by potential biocontrol rhizobacteria on *Sclerotinia sclerotiorum*. *Front. Microbiol.* 6:1056. doi: 10.3389/fmicb.2015.01056
- Go, S.-M., Park, M.-R., Kim, H.-S., Choi, W. S., and Jeong, R.-D. (2019). Antifungal effect of non-thermal atmospheric plasma and its application for control of postharvest *Fusarium oxysporum* decay of paprika. *Food Control* 98, 245–252. doi: 10.1016/j.foodcont.2018.11.028
- Goswami, M., and Deka, S. (2020). Plant growth-promoting rhizobacteria—alleviators of abiotic stresses in soil: a review. *Pedosphere* 30, 40–61. doi: 10.1016/S1002-0160(19)60839-8
- Gotor-Vila, A., Teixido, N., Di Francesco, A., Usall, J., Ugolini, L., Torres, R., et al. (2017). Antifungal effect of volatile organic compounds produced by *Bacillus amyloliquefaciens* CPA-8 against fruit pathogen decays of cherry. *Food Microbiol.* 64, 219–225. doi: 10.1016/j.fm.2017.01.006
- Guevara-Avendano, E., Bejarano-Bolivar, A. A., Kiel-Martinez, A. L., Ramirez-Vazquez, M., Mendez-Bravo, A., Von Wobeser, E. A., et al. (2019). Avocado rhizobacteria emit volatile organic compounds with antifungal activity against *Fusarium solani*, *Fusarium* sp. associated with Kuroshio shot hole borer, and *Colletotrichum gloeosporioides*. *Microbiol. Res.* 219, 74–83. doi: 10.1016/j.micres.2018.11.009
- Haidar, R., Roudet, J., Bonnard, O., Dufour, M. C., Corio-Costet, M. F., Fert, M., et al. (2016). Screening and modes of action of antagonistic bacteria to control the fungal pathogen *Phaeoemoniella chlamydospora* involved in grapevine trunk diseases. *Microbiol. Res.* 192, 172–184. doi: 10.1016/j.micres.2016.07.003
- He, H., Song, Q., Wang, Y., and Yu, S. (2014). Phytotoxic effects of volatile organic compounds in soil water taken from a *Eucalyptus urophylla* plantation. *Plant Soil* 377, 203–215. doi: 10.1007/s11104-013-1989-1
- Jin, P., Wang, H., Tan, Z., Xuan, Z., Dahar, G. Y., Li, Q. X., et al. (2020). Antifungal mechanism of bacillomycin D from *Bacillus velezensis* HN-2 against *Colletotrichum gloeosporioides* Penz. *Pestic. Biochem. Physiol.* 163, 102–107. doi: 10.1016/j.pestbp.2019.11.004
- Kai, M., and Piechulla, B. (2009). Plant growth promotion due to rhizobacterial volatiles an effect of CO<sub>2</sub>? *FEBS Lett.* 583, 3473–3477. doi: 10.1016/j.febslet.2009.09.053
- Kanashiro, A. M., Akiyama, D. Y., Kupper, K. C., and Fill, T. P. (2020). *Penicillium italicum*: an underexplored postharvest pathogen. *Front. Microbiol.* 11:606852. doi: 10.3389/fmicb.2020.606852
- Kang, H. C., Park, Y. H., and Go, S. J. (2003). Growth inhibition of a phytopathogenic fungus, *Colletotrichum* species by acetic acid. *Microbiol. Res.* 158, 321–326. doi: 10.1078/0944-5013-00211
- Khan, N., Martinez-Hidalgo, P., Ice, T. A., Maymon, M., Humm, E. A., Nejat, N., et al. (2018). Antifungal activity of *Bacillus* species against *Fusarium* and analysis of the potential mechanisms used in biocontrol. *Front. Microbiol.* 9:2363. doi: 10.3389/fmicb.2018.02363
- Kovacs, N. (1928). Eine vereinfachte methode zum nachweis der indolbildung durch bakterien. *Z. Immunitätsforsch* 55, 311–315.
- Larkin, J. M., and Stokes, J. L. (1967). Taxonomy of psychrophilic strains of *Bacillus*. *J. Bacteriol.* 94, 889–895. doi: 10.1128/jb.94.4.889-895.1967
- Lastochkina, O., Baymiev, A., Shayahmetova, A., Garshina, D., Koryakov, I., Shpirnaya, I., et al. (2020). Effects of endophytic *Bacillus subtilis* and salicylic acid on postharvest diseases (*Phytophthora infestans*, *Fusarium oxysporum*) development in stored potato tubers. *Plan. Theory* 9:76. doi: 10.3390/plants9010076
- Lazazzara, V., Perazzolli, M., Pertot, I., Biasoli, F., Puopolo, G., and Cappellin, L. (2017). Growth media affect the volatilome and antimicrobial activity against *Phytophthora infestans* in four *Lysobacter* type strains. *Microbiol. Res.* 201, 52–62. doi: 10.1016/j.micres.2017.04.015
- Lee, S., Hung, R., Schink, A. E., Mauro, J., and Bennett, J. W. (2014). *Arabidopsis thaliana* for testing the phytotoxicity of volatile organic compounds. *Plant Growth Regul.* 74, 177–186. doi: 10.1007/s10725-014-9909-9
- Lee, Y. J., Jeong, J. J., Jin, H., Kim, W., Jeun, Y. C., Yu, G. D., et al. (2019). In vitro and in vivo inhibitory effects of gaseous chlorine dioxide against *Fusarium oxysporum* f. sp. batatas isolated from stored sweetpotato: study II. *Plant Pathol. J.* 35, 437–444. doi: 10.5423/PPJ.OA.04.2019.0078
- Lemfack, M. C., Gohlke, B. O., Toguem, S. M. T., Preissner, S., Piechulla, B., and Preissner, R. (2018). mVOC 2.0: a database of microbial volatiles. *Nucleic Acids Res.* 46, D1261–D1265. doi: 10.1093/nar/gkx1016
- Li, Q., Ning, P., Zheng, L., Huang, J., Li, G., and Hsiang, T. (2010). Fumigant activity of volatiles of *Streptomyces globisporus* jk-1 against *Penicillium italicum* on *Citrus microcarpa*. *Postharvest Biol. Technol.* 58, 157–165. doi: 10.1016/j.postharvbio.2010.06.003
- Lim, S. M., Yoon, M. Y., Choi, G. J., Choi, Y. H., Jang, K. S., Shin, T. S., et al. (2017). Diffusible and volatile antifungal compounds produced by an antagonistic *Bacillus velezensis* g341 against various phytopathogenic fungi. *Plant Pathol. J.* 33, 488–498. doi: 10.5423/PPJ.OA.04.2017.0073
- Liu, C., Cui, Z., Yan, X., Qi, Z., Ji, M., and Li, X. (2016). Synthesis, fungicidal activity and mode of action of 4-phenyl-6-trifluoromethyl-2-aminopyrimidines against *Botrytis cinerea*. *Molecules* 21:828. doi: 10.3390/molecules21070828
- Logan, N. A., Berge, O., Bishop, A. H., Busse, H.-J., De Vos, P., Fritze, D., et al. (2009). Proposed minimal standards for describing new taxa of aerobic, endospore-forming bacteria. *Int. J. Syst. Evol. Microbiol.* 59, 2114–2121. doi: 10.1099/ijs.0.013649-0

- Mari, M., Bautista-Baños, S., and Sivakumar, D. (2016). Decay control in the postharvest system: role of microbial and plant volatile organic compounds. *Postharvest Biol. Technol.* 122, 70–81. doi: 10.1016/j.postharvbio.2016.04.014
- Marquez-Villavicencio Mdel, P., Weber, B., Witherell, R. A., Willis, D. K., and Charkowski, A. O. (2011). The 3-hydroxy-2-butanone pathway is required for *Pectobacterium carotovorum* pathogenesis. *PLoS One* 6:e22974. doi: 10.1371/journal.pone.0022974
- Martini, C., and Mari, M. (2014). “*Monilinia fructicola*, *Monilinia laxa* (Monilinia rot, Brown rot)” in *Postharvest Decay*. ed. S. Bautista-Baños (Centro de Desarrollo de Productos Bióticos, Yauatepec Morelos, Mexico: Academic Press), 233–265.
- Massawe, V. C., Hanif, A., Farzand, A., Mburu, D. K., Ochola, S. O., Wu, L., et al. (2018). Volatile compounds of endophytic *Bacillus* spp. have biocontrol activity against *Sclerotinia sclerotiorum*. *Phytopathology* 108, 1373–1385. doi: 10.1094/PHYTO-04-18-0118-R
- Medina-Romero, Y. M., Roque-Flores, G., and Macias-Rubalcava, M. L. (2017). Volatile organic compounds from endophytic fungi as innovative postharvest control of *Fusarium oxysporum* in cherry tomato fruits. *Appl. Microbiol. Biotechnol.* 101, 8209–8222. doi: 10.1007/s00253-017-8542-8
- Mercier, J., and Smilanick, J. L. (2005). Control of green mold and sour rot of stored lemon by biofumigation with *Muscador albus*. *Biol. Control* 32, 401–407. doi: 10.1016/j.biocontrol.2004.12.002
- Momma, N., Yamamoto, K., Simandi, P., and Shishido, M. (2006). Role of organic acids in the mechanisms of biological soil disinfection (BSD). *J. Gen. Plant Pathol.* 72, 247–252. doi: 10.1007/s10327-006-0274-z
- Montaño, A., Cortés-Delgado, A., Sánchez, A. H., and Ruiz-Barba, J. L. (2021). Production of volatile compounds by wild-type yeasts in a natural olive-derived culture medium. *Food Microbiol.* 98:103788. doi: 10.1016/j.fm.2021.103788
- Nasir, M., Bean, H. D., Smolinska, A., Rees, C. A., Zemanick, E. T., and Hill, J. E. (2018). Volatile molecules from bronchoalveolar lavage fluid can ‘rule-in’ *Pseudomonas aeruginosa* and ‘rule-out’ *Staphylococcus aureus* infections in cystic fibrosis patients. *Sci. Rep.* 8:826. doi: 10.1038/s41598-017-18491-8
- Obi, V. I., Barriuso, J. J., and Gogorcena, Y. (2018). Effects of pH and titratable acidity on the growth and development of *Monilinia laxa* (Aderh. & Ruhl.) in vitro and in vivo. *Eur. J. Plant Pathol.* 151, 781–790. doi: 10.1007/s10658-017-1413-4
- Ossowicki, A., Jafra, S., and Garbeva, P. (2017). The antimicrobial volatile power of the rhizospheric isolate *Pseudomonas donghuensis* P482. *PLoS One* 12:e0174362. doi: 10.1371/journal.pone.0174362
- Parafati, L., Vitale, A., Restuccia, C., and Cirvilleri, G. (2017). Performance evaluation of volatile organic compounds by antagonistic yeasts immobilized on hydrogel spheres against gray, green and blue postharvest decays. *Food Microbiol.* 63, 191–198. doi: 10.1016/j.fm.2016.11.021
- Poveda, J. (2020). Use of plant-defense hormones against pathogen-diseases of postharvest fresh produce. *Physiol. Mol. Plant Pathol.* 111:101521. doi: 10.1016/j.pmp.2020.101521
- Poveda, J. (2021). Beneficial effects of microbial volatile organic compounds (MVOs) in plants. *Appl. Soil Ecol.* 168:104118. doi: 10.1016/j.apsoil.2021.104118
- Poveda, J., Eugui, D., and Velasco, P. (2020). Natural control of plant pathogens through glucosinolates: an effective strategy against fungi and oomycetes. *Phytochem. Rev.* 19, 1045–1059. doi: 10.1007/s11101-020-09699-0
- Qin, X., Xiao, H., Cheng, X., Zhou, H., and Si, L. (2017). *Hanseniaspora uvarum* prolongs shelf life of strawberry via volatile production. *Food Microbiol.* 63, 205–212. doi: 10.1016/j.fm.2016.11.005
- Rajaofera, M. J. N., Wang, Y., Dahar, G. Y., Jin, P., Fan, L., Xu, L., et al. (2019). Volatile organic compounds of *Bacillus atrophaeus* HAB-5 inhibit the growth of *Colletotrichum gloeosporioides*. *Pestic. Biochem. Physiol.* 156, 170–176. doi: 10.1016/j.pestbp.2019.02.019
- Rashmi, B., Bharti, S. K., Gogoi, M., Devi, S., and Anita, G. S. (2017). Antibiotic resistance: role of fruits and vegetables in the food basket. *Int. J. Pure Appl. Biosci.* 5, 169–173. doi: 10.18782/2320-7051.5327
- Reverchon, F., García-Quiroz, W., Guevara-Avendano, E., Solis-García, I. A., Ferrera-Rodríguez, O., and Lorea-Hernández, F. (2019). Antifungal potential of *Laureaceae* rhizobacteria from a tropical montane cloud forest against *Fusarium* spp. *Braz. J. Microbiol.* 50, 583–592. doi: 10.1007/s42770-019-00094-2
- Rodríguez, M., Marin, A., Torres, M., Bejar, V., Campos, M., and Sampedro, I. (2018). Aphicidal activity of surfactants produced by *Bacillus atrophaeus* L193. *Front. Microbiol.* 9:3114. doi: 10.3389/fmicb.2018.03114
- Rodríguez, M., Reina, J. C., Bejar, V., and Llamas, I. (2020a). *Psychrobacillus vulpis* sp. nov., a new species isolated from faeces of a red fox in Spain. *Int. J. Syst. Evol. Microbiol.* 70, 882–888. doi: 10.1099/ijsem.0.003840
- Rodríguez, M., Torres, M., Blanco, L., Bejar, V., Sampedro, I., and Llamas, I. (2020b). Plant growth-promoting activity and quorum quenching-mediated biocontrol of bacterial phytopathogens by *Pseudomonas segetis* strain P6. *Sci. Rep.* 10:4121. doi: 10.1038/s41598-020-61084-1
- Rungjindamai, N., Jeffries, P., and Xu, X.-M. (2014). Epidemiology and management of brown rot on stone fruit caused by *Monilinia laxa*. *Eur. J. Plant Pathol.* 140, 1–17. doi: 10.1007/s10658-014-0452-3
- Ryu, C. M., Farag, M. A., Hu, C. H., Reddy, M. S., Kloepper, J. W., and Pare, P. W. (2004). Bacterial volatiles induce systemic resistance in *Arabidopsis*. *Plant Physiol.* 134, 1017–1026. doi: 10.1104/pp.103.026583
- Sadfi-Zouaoui, N., Essghaier, B., Hajlaoui, M. R., Fardeau, M. L., Cayaol, J. L., Ollivier, B., et al. (2008). Ability of moderately halophilic bacteria to control grey mould disease on tomato fruits. *J. Phytopathol.* 156, 42–52.
- Sasser, M. (1990). *Identification of Bacteria by Gas Chromatography of Cellular Fatty Acids*. Newark, DE: MIDI Inc.
- Schmidt, R., Cordovez, V., De Boer, W., Raaijmakers, J., and Garbeva, P. (2015). Volatile affairs in microbial interactions. *ISME J.* 9, 2329–2335. doi: 10.1038/ismej.2015.42
- Schneider, C. A., Rasband, W. S., and Eliceiri, K. W. (2012). NIH Image to ImageJ: 25 years of image analysis. *Nat. Methods* 9, 671–675. doi: 10.1038/nmeth.2089
- Shi, X.-C., Wang, S.-Y., Duan, X.-C., Wang, Y.-Z., Liu, F.-Q., and Laborda, P. (2021). Biocontrol strategies for the management of *Colletotrichum* species in postharvest fruits. *Crop Prot.* 141:105454. doi: 10.1016/j.cropro.2020.105454
- Sierra, G. (1957). A simple method for the detection of lipolytic activity of micro-organisms and some observations on the influence of the contact between cells and fatty substrates. *Antonie Van Leeuwenhoek* 23, 15–22. doi: 10.1007/BF02545855
- Syed-Ab-Rahman, S. F., Carvalhais, L. C., Chua, E. T., Chung, F. Y., Moyle, P. M., Eltanahy, E. G., et al. (2019). Soil bacterial diffusible and volatile organic compounds inhibit *Phytophthora capsici* and promote plant growth. *Sci. Total Environ.* 692, 267–280. doi: 10.1016/j.scitotenv.2019.07.061
- Tahir, H. A., Gu, Q., Wu, H., Niu, Y., Huo, R., and Gao, X. (2017). *Bacillus* volatiles adversely affect the physiology and ultra-structure of *Ralstonia solanacearum* and induce systemic resistance in tobacco against bacterial wilt. *Sci. Rep.* 7:40481. doi: 10.1038/srep40481
- Toffano, L., Fialho, M. B., and Pascholati, S. F. (2017). Potential of fumigation of orange fruits with volatile organic compounds produced by *Saccharomyces cerevisiae* to control citrus black spot disease at postharvest. *Biol. Control* 108, 77–82. doi: 10.1016/j.biocontrol.2017.02.009
- Toral, L., Rodríguez, M., Béjar, V., and Sampedro, I. (2018). Antifungal activity of lipopeptides from *Bacillus methylotrophicus* XT1 CECT 8661 against *Botrytis cinerea*. *Front. Microbiol.* 9:1315. doi: 10.3389/fmicb.2018.01315
- Tozlu, E., Kotan, M. Ş., Tekiner, N., Dikbaş, N., and Kotan, R. (2018). Biological control of postharvest spoilage in fresh mandarins (*Citrus reticulata* Blanco) fruits using bacteria during storage. *Erwerbs-obstbau* 61, 157–164. doi: 10.1007/s10341-018-0412-8
- Vega, C., Rodríguez, M., Llamas, I., Bejar, V., and Sampedro, I. (2019). Silencing of phytopathogen communication by the halotolerant PGPR *Staphylococcus equorum* strain EN21. *Microorganisms* 8:42. doi: 10.3390/microorganisms8010042
- Wenke, K., Kai, M., and Piechulla, B. (2010). Belowground volatiles facilitate interactions between plant roots and soil organisms. *Planta* 231, 499–506. doi: 10.1007/s00425-009-1076-2
- Wu, Y., Zhou, J., Li, C., and Ma, Y. (2019). Antifungal and plant growth promotion activity of volatile organic compounds produced by *Bacillus amyloliquefaciens*. *Microbiology* 8:e00813. doi: 10.1002/mbo3.813
- Yu, L., Qiao, N., Zhao, J., Zhang, H., Tian, F., Zhai, Q., et al. (2020). Postharvest control of *Penicillium expansum* in fruits: a review. *Food Biosci.* 36:100633. doi: 10.1016/j.fbio.2020.100633
- Yuan, J., Raza, W., Shen, Q., and Huang, Q. (2012). Antifungal activity of *Bacillus amyloliquefaciens* NJN-6 volatile compounds against *Fusarium oxysporum* f. sp. cubense. *Appl. Environ. Microbiol.* 78, 5942–5944. doi: 10.1128/AEM.01357-12
- Zhang, H., Godana, E. A., Sui, Y., Yang, Q., Zhang, X., and Zhao, L. (2020a). Biological control as an alternative to synthetic fungicides for the management

- of grey and blue mould diseases of table grapes: a review. *Crit. Rev. Microbiol.* 46, 450–462. doi: 10.1080/1040841X.2020.1794793
- Zhang, D., Yu, S., Yang, Y., Zhang, J., Zhao, D., Pan, Y., et al. (2020b). Antifungal effects of volatiles produced by *Bacillus subtilis* against *Alternaria solani* in potato. *Front. Microbiol.* 11:1196. doi: 10.3389/fmicb.2020.01196
- Zhao, S., Guo, Y., Wang, Q., Luo, H., He, C., and An, B. (2020). Expression of flagellin at yeast surface increases biocontrol efficiency of yeast cells against postharvest disease of tomato caused by *Botrytis cinerea*. *Postharvest Biol. Technol.* 162:111112. doi: 10.1016/j.postharvbio.2019.111112
- Zheng, L., Situ, J.-J., Zhu, Q.-F., Xi, P.-G., Zheng, Y., Liu, H.-X., et al. (2019). Identification of volatile organic compounds for the biocontrol of postharvest litchi fruit pathogen *Peronophythora litchii*. *Postharvest Biol. Technol.* 155, 37–46. doi: 10.1016/j.postharvbio.2019.05.009
- Zhou, M., Li, P., Wu, S., Zhao, P., and Gao, H. (2019). *Bacillus subtilis* CF-3 volatile organic compounds inhibit *Monilinia fructicola* growth in peach fruit. *Front. Microbiol.* 10:1804. doi: 10.3389/fmicb.2019.01804

**Conflict of Interest:** The authors declare that the research was conducted in the absence of any commercial or financial relationships that could be construed as a potential conflict of interest.

**Publisher's Note:** All claims expressed in this article are solely those of the authors and do not necessarily represent those of their affiliated organizations, or those of the publisher, the editors and the reviewers. Any product that may be evaluated in this article, or claim that may be made by its manufacturer, is not guaranteed or endorsed by the publisher.

Copyright © 2021 Toral, Rodríguez, Martínez-Checa, Montaña, Cortés-Delgado, Smolinska, Llamas and Sampedro. This is an open-access article distributed under the terms of the Creative Commons Attribution License (CC BY). The use, distribution or reproduction in other forums is permitted, provided the original author(s) and the copyright owner(s) are credited and that the original publication in this journal is cited, in accordance with accepted academic practice. No use, distribution or reproduction is permitted which does not comply with these terms.



# Nematicidal Activity of Cyclopiazonic Acid Derived From *Penicillium commune* Against Root-Knot Nematodes and Optimization of the Culture Fermentation Process

Van Thi Nguyen<sup>1</sup>, Nan Hee Yu<sup>1</sup>, Yookyung Lee<sup>1</sup>, In Min Hwang<sup>2</sup>, Hung Xuan Bui<sup>3</sup> and Jin-Cheol Kim<sup>1\*</sup>

<sup>1</sup> Department of Agricultural Chemistry, College of Agriculture and Life Sciences, Institute of Environmentally Friendly Agriculture, Chonnam National University, Gwangju, South Korea, <sup>2</sup> Hygienic Safety and Analysis Center, World Institute of Kimchi, Gwangju, South Korea, <sup>3</sup> Department of Entomology and Nematology, Gulf Coast Research and Education Center, University of Florida, Wimauma, FL, United States

## OPEN ACCESS

### Edited by:

Florence Fontaine,  
Université de Reims  
Champagne-Ardenne, France

### Reviewed by:

Tariq Mukhtar,  
Pir Mehr Ali Shah Arid Agriculture  
University, Pakistan  
Nadhem Aissani,  
University of Jendouba, Tunisia  
Sajid Aleem,  
University of Agriculture, Faisalabad,  
Pakistan

### \*Correspondence:

Jin-Cheol Kim  
kjinc@jnu.ac.kr

### Specialty section:

This article was submitted to  
Microbe and Virus Interactions with  
Plants,  
a section of the journal  
Frontiers in Microbiology

Received: 17 June 2021

Accepted: 22 October 2021

Published: 24 November 2021

### Citation:

Nguyen VT, Yu NH, Lee Y,  
Hwang IM, Bui HX and Kim J-C  
(2021) Nematicidal Activity  
of Cyclopiazonic Acid Derived From  
*Penicillium commune* Against  
Root-Knot Nematodes  
and Optimization of the Culture  
Fermentation Process.  
Front. Microbiol. 12:726504.  
doi: 10.3389/fmicb.2021.726504

Among 200 fungal strains isolated from the soil, only one culture filtrate of *Aspergillus flavus* JCK-4087 showed strong nematicidal activity against *Meloidogyne incognita*. The nematicidal metabolite isolated from the culture filtrate of JCK-4087 was identified as cyclopiazonic acid (CPA). Because JCK-4087 also produced aflatoxins, six strains of *Penicillium commune*, which have been reported to be CPA producers, were obtained from the bank and then tested for their CPA productivity. CPA was isolated from the culture filtrate of *P. commune* KACC 45973. CPA killed the second-stage juveniles of *M. incognita*, *M. hapla*, and *M. arenaria* with  $EC_{50-3 \text{ days}}$  4.50, 18.82, and 60.51  $\mu\text{g mL}^{-1}$ , respectively. CPA also significantly inhibited egg hatch of *M. incognita* and *M. hapla* after a total of 28 days of treatment with the concentrations  $> 25 \mu\text{g mL}^{-1}$ . The enhancement of CPA production by *P. commune* KACC 45973 was explored using an optimized medium based on Plackett-Burman design (PBD) and central composite design (CCD). The highest CPA production (381.48  $\mu\text{g mL}^{-1}$ ) was obtained from the optimized medium, exhibiting an increase of 7.88 times when compared with that from potato dextrose broth culture. Application of the wettable power-type formulation of the ethyl acetate extract of the culture filtrate of KACC 45973 reduced gall formation and nematode populations in tomato roots and soils under greenhouse conditions. These results suggest that CPA produced by *P. commune* KACC 45973 can be used as either a biochemical nematicide or a lead molecule for developing chemical nematicides to control root-knot nematodes.

**Keywords:** cyclopiazonic acid, nematicidal activity, Plackett-Burman, central composite design, response surface methodology, root-knot nematode

## INTRODUCTION

Plant-parasitic nematodes (PPNs) are economic burdens in agriculture, owing to their direct and indirect damages that lead to crop yield losses (Bogner et al., 2017); they are estimated to cause an annual yield loss of \$173 billion. Root-knot nematodes (RKNs; *Meloidogyne* spp.) are the most damaging PPNs to various crops (Termorshuizen et al., 2011; Kim et al., 2016; Gamalero and Glick, 2020). RKNs cause nutrient deficiency, stunting, wilting, chlorosis, reduced tillering, immature fruit



drop, and leaf drying (Moens et al., 2009; Palomares-Rius et al., 2017). Among several identified RKN species, *Meloidogyne arenaria*, *M. hapla*, *M. incognita*, and *M. javanica* are commonly reported worldwide (Anwar and McKenry, 2010; Jones et al., 2013; Dong et al., 2014; Kim et al., 2018; Gamalero and Glick, 2020).

Various chemical nematicides have been used to control RKNs on different crops worldwide. However, most chemical nematicides have a broad spectrum of activity, adversely affecting beneficial soil microbes; they often cause a rapid resurgence of soil-borne pathogens (Sánchez-Moreno et al., 2010; Watson et al., 2017). Therefore, developing new, reduced risk nematicides for RKN control is necessary. Recently, various biological control agents have been studied as alternatives to chemical nematicides to control RKNs. Several bacteria and fungi as biological control agents have been reported to have nematicidal activities against RKNs (Martínez-Medina et al., 2017; Ghahremani et al., 2019). Additionally, numerous nematicidal metabolites from fungal biocontrol agents have been reported for the control of RKNs, including thermolides A and B, omphalotins, ophiobolins, bursaphelocides A and B, illinitone A, speudohalonectriins A and B, dichomitin B, and caryopsomycins A-C (Degenkolb and Vilcinskis, 2016).

Several secondary metabolites isolated from the genera *Penicillium* and *Aspergillus* exhibit antimicrobial, anticancer, antiparasitic, insecticidal, and biocontrol activities (El-Hawary et al., 2020; Toghuo and Boyom, 2020). Furthermore, both these genera are commonly found in the soil and have been known to produce various nematicidal metabolites against RKNs (Siddiqui and Akhtar, 2009; Murslain et al., 2014; Jang et al., 2016). Several studies have reported that *Penicillium commune* has potent inhibitory activity against bacteria such as *Staphylococcus aureus*, *Pseudomonas fluorescens*, *P. aeruginosa*, *Bacillus subtilis*, and *Escherichia coli* and fungi such as *Candida glabrata* and *C. albicans* (Gao et al., 2011; Shang et al., 2012; Malhadas et al., 2017). However, the nematicidal metabolites from *P. commune* have not been reported yet.

Optimization of the culture fermentation process is critical to ensure high productivity at a low cost (Calvo et al., 2002; Keller, 2019). The production of secondary microbial metabolites can be enhanced by optimizing physical and chemical conditions (Yang et al., 2016; Zhang et al., 2020). Optimization can be performed using a conventional one-factor-at-a-time approach, a statistical method, or a combination. The conventional approach entails changing one independent factor or variable while keeping the other variables stable. It is labor-intensive, costly, and time-consuming, particularly when many factors are involved. Conversely, the statistical approach is markedly cost-effective, time-efficient, and significantly decreases the number of experimental runs (Rigas et al., 2005; Arul Jose et al., 2013; Nor et al., 2017; Singh et al., 2017; Lim et al., 2019). Three different techniques, such as namely screening, factorial, and response surface methodology, have been used in the statistical method in previous research (Hanrahan and Lu, 2006; Bezerra et al., 2008; No, 2013; Singh et al., 2017; Lim et al., 2020). For screening, the most critical variables affecting

maximum response production were identified by the Plackett–Burman design (PBD). Because PBD focuses on selected main effects and disregards the interaction between variables, another step of optimization using a central composite design (CCD) is required. CCD comprises three parts—a factorial portion, central points, and star points—that mathematically evaluate the interactions among various variables and establish the relationship between response and variables (Raissi and Farsani, 2009; El-Naggar et al., 2016; Kundu et al., 2016; Srivastava et al., 2018). Even though several studies on the fermentation process for producing cyclopiazonic acid (CPA) by *Aspergillus flavus* and *P. commune* were conducted in the 1990s using full factorial design, its production concentrations were low (Gqaleni et al., 1996, 1997).

Initially, we screened 200 fungal isolates against *M. incognita* and found that *A. flavus* JCK-4087 showed very strong nematicidal activity. The nematicidal metabolite was identified as CPA through organic solvent extraction, repeated chromatography, and instrumental analysis. However, *A. flavus* JCK-4087 also produced aflatoxins toxic to mammals (Abnet, 2007; Shephard, 2008; Zain, 2011). Therefore, six strains of *P. commune* were obtained from the Korean Agricultural Culture Collection (KACC), Rural Development Administration, Republic of Korea, which are known as CPA producers (Hermansen et al., 1984; Gqaleni et al., 1996; Ostry et al., 2018), were used in this study. Then, one strain was selected for further study. This research was performed to evaluate the potential of CPA as a biochemical nematicide for the control of root-knot nematode diseases. Therefore, the objectives of this study were (1) to isolate and identify CPA from the fermentation filtrate of *A. flavus* JCK-4087 and *P. commune* KACC 45973, (2) to investigate *in vitro* nematicidal activity of CPA against RKNs, (3) to optimize culture conditions using PBD and CCD for CPA production by *P. commune*, and (4) to evaluate the disease control efficacy of ethyl acetate layer extracted from *P. commune* KACC 45973 against root-knot nematode disease in tomato plants.

## MATERIALS AND METHODS

### Root-Knot Nematode Culture and Preparation

*M. incognita* was obtained from the Korea Research Institute of Chemical Technology (Daejeon, Republic of Korea). Both *M. arenaria* and *M. hapla* were kindly supplied by the National Institute of Agricultural Sciences, Rural Development Administration (Wanju-gun, Jeollabuk-do, Republic of Korea). Second-stage juveniles (J2s) were collected from the populations of *M. arenaria*, *M. hapla*, and *M. incognita* on infected tomato (*Solanum lycopersicum* Mill. cv. Seokwang) plants maintained for at least 2 months at  $28 \pm 2^\circ\text{C}$  and  $75 \pm 5\%$  relative humidity (RH) in a greenhouse at Chonnam National University, Korea. The infected tomato plants were uprooted and washed with tap water; the nematode eggs were extracted with 1% sodium hypochlorite (Jang et al., 2016). Egg suspension was passed through a  $63\ \mu\text{m}$  sieve and then retained in a  $25\ \mu\text{m}$  sieve. The

eggs were washed with distilled water and then hatched using the modified Baermann funnel method at 28°C within 5 days (Viglierchio and Schmitt, 1983). Fresh eggs and J2s were used for further experiments.

## Isolation and Identification of Fungal Strain JCK-4087

The method for isolating 200 fungal strains from soil samples collected from the Gwangju campus of Chonnam National University, Sunchang mountain, and Gok-Seong, Korea, was according to Aziz and Zainol (2018). All the isolated fungal strains were cultured on potato dextrose broth medium (PDB; Becton, Dickinson and Company, Sparks, MD, United States) at 25°C with rotary shaking (150 rpm) for 2 weeks and under static conditions for 3 weeks. Each isolated fungal stock was stored at −80°C in 25% glycerol until further use. The nematicidal activity of 200 culture filtrates were tested against second-stage juveniles (J2s) of *M. incognita* as previously described (Cayrol et al., 1989; Nguyen et al., 2018). A fungal strain JCK-4087 was selected based on its high nematicidal activity against *M. incognita* (data not shown).

Total deoxyribonucleic acid (DNA) of JCK-4087 was extracted and amplified in the internal transcribed spacer (ITS) region, and a PCR was performed as previously reported (Nguyen et al., 2019). Amplified fragments were purified and sequenced at Genotech Crop (Daejeon, South Korea). Additionally,  $\beta$ -tubulin (*Bt2*) and calmodulin (*Cmd*) genes were amplified using the primer pair *Bt2a* and *Bt2b* (Glass and Donaldson, 1995) and *Cmd5* and *Cmd6* (Hong et al., 2005), respectively. The result from ITS, *Bt2*, and *Cmd* sequencing was used to identify JCK-4087 based on the National Center for Biotechnology Information (NCBI) blast database. Multiple sequence alignments were generated with Clustal W and phylogenetic analysis was performed using MEGA version 6 (with the maximum likelihood method), with 1,000 bootstrapping trials (Hasegawa et al., 1985; Tamura et al., 2013; Newman et al., 2016).

## Extraction and Purification of a Nematicidal Metabolite From JCK-4087

The JCK-4087 was cultured on a PDB medium at 25°C on a rotary shaker (150 rpm) for 14 days and then filtered through four cheesecloth layers to segregate culture filtrate and mycelia. Then, the culture filtrate (2.8 L) was partitioned twice with ethyl acetate into a 1:1 ratio (v/v). The crude extract (5.1 g) was loaded onto a chromatography column (3.5 × 60 cm, inner diameter × length) containing silica gel (70–230 mesh, 400 g; Merck, Darmstadt, Germany) and then eluted with chloroform: MeOH (9:1, v/v), yielding eight fractions (F1–F8). These eight fractions were tested for J2s mortality against *M. incognita*. F8 (315 mg), which exhibited nematicidal activity, was further separated using Sep-Pak® Vac 35 cc (10 g) C18 cartridge (Waters Corp., Premier, United Kingdom) with stepwise elution of a mixture of water: methanol (10:0, 9:1, 8:2, 7:3, 6:4, 5:5, 4:6, 3:7, 2:8, 1:9, 0:10, 50 mL per mixture), yielding five fractions (F81–F85). F81 (15.6 mg)

showed nematicidal activity against *Meloidogyne* spp. Thus, one nematicidal metabolite (**1**) was purified, and its purity was evaluated via thin-layer chromatography and high-performance liquid chromatography (HPLC) using a Shimadzu LC-20AT HPLC pump and Shimadzu SPD-M20A PDA detector (Shimadzu Corp., Kyoto, Japan) with a C18 column (Xbridge 5  $\mu$ m, 4.6 × 250 mm, Waters Corp.).

## Structural Determination of a Nematicidal Metabolite

High-resolution electrospray ionization-mass spectrometry (HR-ESI-MS) and nuclear magnetic resonance spectroscopy (NMR) analyses were performed to identify the purified metabolite. HR-ESI-MS analysis of compound **1** was conducted using a Synapt G2 HDMS quadrupole time-of-flight mass spectrometer equipped with an electrospray ion source (Waters Corp.). <sup>1</sup>H- and <sup>13</sup>C-NMR, COSY, HSQC, and HMBC were recorded on Bruker Avance III HD 500 MHz instrument (Bruker Biospin GmbH, Rheinstetten, Germany) and dissolved in methanol-d<sub>4</sub> (Cambridge Isotope Laboratories, Inc., Andover, MA, United States). The internal standard for NMR analysis was tetramethylsilane.

## Quantification of Aflatoxins

Quantitative determination of total aflatoxin was carried out using commercially available Veratox for Aflatoxin ELISA kit (Neogen Food Safety, Lansing, MI, United States) and measured on a Microplate Reader (Benchmark Plus; Bio-Rad, Laboratories Inc., Hercules, CA) at 600 nm (OD<sub>600</sub>).

## Six Fungal Strains From Korean Agricultural Culture Collection

The chemical structure of compound **1** produced by JCK-4087 was determined as CPA and then the fungal strain was identified as *A. flavus*. Because the fungal strain also produced aflatoxins, which are very strong carcinogenic mycotoxins, JCK-4087 cannot be used as a microbial nematicide. Therefore, we obtained six *P. commune* strains, known as CPA producers (Hermansen et al., 1984; Gqaleni et al., 1996; Ostry et al., 2018), from the Korean Agricultural Culture Collection (KACC). The J2s mortality of culture filtrates and ethyl acetate extracts of the six strains was tested against *M. incognita* as described (Cayrol et al., 1989; Nguyen et al., 2018). In addition, the production of CPA in the PDB culture filtrates of the six strains was analyzed by HPLC as described (Pourhosseini et al., 2020). Based on the HPLC results and *in vitro* bioassay, *P. commune* KACC 45973 was selected and then CPA was also isolated from the culture filtrate of the fungal strain using the same method as described above.

## Mortality Assay

Compound **1** extracted from *P. commune* 45973 fungal strain was evaluated J2s of *M. incognita* as previously described (Cayrol et al., 1989; Nguyen et al., 2018). Compound **1** was dissolved in methanol at a concentration of 30 mg mL<sup>−1</sup>, and its toxicity was tested against J2s of *M. arenaria*, *M. hapla*, and *M. incognita*.

1% Methanol was used as a negative control. J2s mortality was evaluated after 3 days of treatment and then calculated according to the following formula (Schneider and Orelli, 1947):

Mortality(%)

$$= \frac{\text{Mortality percent of treatment} - \text{mortality percent of untreated control}}{100 - \text{mortality percent of untreated control}}$$

The experiment was conducted with six replicates per treatment and was performed twice.

## Hatching Assay

Compound **1** dissolved in methanol was employed to immerse approximately 50 egg suspensions of the mixed-development stage in a 96-well tissue plate (Becton, Dickinson and Company, Franklin Lakes, NJ) at concentrations of 0, 5, 25, and 50  $\mu\text{g mL}^{-1}$ . The plates were sealed with parafilm to prevent evaporation and were kept in a humid chamber at  $26 \pm 2^\circ\text{C}$ . The number of eggs and J2s of the three *Meloidogyne* spp. were counted at 0 ( $D_0$ ), 3 ( $D_3$ ), 7 ( $D_7$ ), 15 ( $D_{15}$ ), 21 ( $D_{21}$ ), and 28 ( $D_{28}$ ) days after treatment (Leica DM IL LED; Leica Microsystems CMS GmbH, Wetzlar, Germany). All the experiments were repeated twice with six replicates. The following formula was used to calculate the cumulative percent of egg hatch (Wu et al., 2014):

$$\text{Cumulative percent of egg hatch (\%)} = \frac{J2sDx - J2sDo}{\text{EggDo}} \times 100$$

where Dx = x days after the start of the assay.

## Plackett–Burman Design

PBD was used to determine nutritional and environmental variables affecting the production of compound **1** (Plackett and Burman, 1946). The total number of experiments is  $n+1$ , where  $n$  is the number of variables. With 14 medium components (independent variables) and 20 experimental runs represented in two levels, the design matrix was used to evaluate independent factors that affected compound **1** production, as shown in **Table 1**. On PBD design, five dummy variables (D1–D5) did not affect the data analysis used to estimate experimental error (No, 2013; Phukon et al., 2020). Fourteen different independent variables were evaluated at two levels of high and low [denoted by (+1) and (−1, respectively; **Table 1**). All the trials were carried out in triplicate, and the average concentration of compound **1** determined from the peak areas in HPLC chromatogram was considered the response variable, depending on the first-order Plackett–Burman model:

$$Y = \beta_0 + \sum \beta_i X_i$$

where  $Y$  is the concentration of compound **1** (the response or dependent variable),  $\beta_0$  is the model intercept,  $\beta_i$  is the linear coefficient, and  $X_i$  is the level of the independent variable.

## Response Surface Methodology

The optimal levels of the significant variables and the interactions of these variables during the production of compound **1** were

**TABLE 1** | Coded and actual values of the medium used to produce cyclopiazonic acid by *Penicillium commune* KACC 45973 using Plackett–Burman design.

Symbol code	Variables	Units	Code values	
			− 1	1
A	NaNO <sub>3</sub>	g L <sup>−1</sup>	0	8
B	Tryptone	g L <sup>−1</sup>	0	8
C	Yeast extract	g L <sup>−1</sup>	0	8
D	Glucose	g L <sup>−1</sup>	0	90
E	Starch	g L <sup>−1</sup>	0	90
F	MgSO <sub>4</sub> ·7H <sub>2</sub> O	g L <sup>−1</sup>	0.05	1
G	KCL	g L <sup>−1</sup>	0.05	1
H	FeSO <sub>4</sub> ·7H <sub>2</sub> O	g L <sup>−1</sup>	0.001	0.02
J	K <sub>2</sub> HPO <sub>4</sub>	g L <sup>−1</sup>	1	2
K	PDB	g L <sup>−1</sup>	0	24
L	pH		5	8
M	Agitation speed	rpm	0	150
N	Incubation time	Days	14	21
O	Inoculum size	Plugs	5	10

analyzed by the CCD (Plackett and Burman, 1946; Lim et al., 2019). CCD was used to analyze three factors (NaNO<sub>3</sub>, tryptone, and yeast extract) at five levels [very low, low, intermediate, high, and very high as coded by numbers (−1.68), (−1), (0), (1), and (1.68), respectively]. The experiment was performed in triplicates. The average concentration of compound **1** from the HPLC analysis was considered the value of the response or dependent variable. For predicting the optimal point, the relationship between independent variables and the response or dependent variable was fitted in the quadratic polynomial of the second-order model:

$$Y = \beta_0 + \sum \beta_i X_i + \sum \beta_{ii} X_i^2 + \sum \beta_{ij} X_i X_j$$

where  $Y$  is the predicted response,  $\beta_0$  is the regression coefficient,  $\beta_i$  is the linear coefficient,  $\beta_{ii}$  is the quadratic coefficient,  $\beta_{ij}$  is the interaction coefficient, and  $X_i$  is the levels of independent variables. The interaction and quadratic terms are denoted by the  $X_i^2$  and  $X_i X_j$ .

## Disease Control Efficacy of the Wettable-Powder Type Formulation

The wettable-powder type formulation of the ethyl acetate extract of *P. commune* KACC 45973 (Pc45973–WP20) was prepared as previously described (Kim et al., 2018). The ethyl acetate extract was included in the formulation at a level of 20%. The disease control efficacy of Pc45973–WP20 was evaluated against tomato RKN disease caused by *M. incognita* using pot experiments. Susceptible tomato cv. Seokwang seeds were planted in nursery soil (Bunong horticulture nursery soil, Bunong, Korea) and maintained at  $25 \pm 2^\circ\text{C}$  and  $77 \pm 5\%$  RH for 4 weeks. Pc45973–WP20 was applied at 250, 500, and 1,000-fold dilutions by soil drench (20 mL per pot) twice (1 day before and 6 days after inoculation). A total of 1,500 J2s of *M. incognita* were inoculated into four-leaf stage tomato plants in a 9.5 cm diameter plastic pot containing a pasteurized nursery soil: sand (1:1, v/v) mixture.



Sunchungtan® containing 30% fosthiazate (SL; Farm Hannong Co., Seoul, Republic of Korea) was used as a positive control and applied twice at 4,000-fold dilutions. Distilled water was used as a negative control. The treated plants were arranged in a completely randomized design in the greenhouse at 28–33°C. Their roots were washed with tap water to remove adhered soil particles 6 weeks after the first application (Nguyen et al., 2018). Plant growth parameters, such as plant height and fresh weight of shoot and root, were recorded. Gall index (GI) was used based on a 0–5 galling scale, where 0 = 0–10%, 1 = 11–20%, 2 = 21–50%, 3 = 51–80%, 4 = 81–90%, and 5 = 91–100% root galls (Barker et al., 1985). Eggs and J2s were extracted from the root system and soil and counted under an optical microscope (Leica DM IL LED). Control values of gall index were calculated using the following equation (Yeon et al., 2019; Rajasekharan et al., 2020):

$$\text{Control value (\%)} = \frac{(\text{galling index of untreated control} - \text{galling index of treatment})}{\text{galling index of untreated control}} \times 100$$

Nematodes were collected from a 100 cm<sup>3</sup> soil sample using the modified Baermann technique and were then counted (Hajihassani et al., 2019; Kalaiselvi et al., 2019). The experiment was repeated twice with four replications per treatment.

## Statistical Analysis

The repeated measure ANOVA with SAS University Edition (SAS Institute Inc., Cary, NC) was used to analyze cumulative eggs hatch bioassay. Probability levels of  $P \leq 0.05$  were considered statistically significant. The 50% effective concentration (EC<sub>50</sub>) values were calculated by dose-response curves using the non-linear regression function of GraphPad Prism software version 8.0 (GraphPad Software, Inc.); these values were used for determining paralysis activity. Minitab Statistical Software (version 19, Minitab Inc., United States) was used for optimizing the statistical experimental design and performing regression ANOVA. For *in vitro* experiments, the one-way analysis of variance (ANOVA) with Tukey's test was used with SPSS version 23.0 (SPSS Inc., Chicago, IL, United States).

## RESULTS

### Identification of Fungal Strain JCK-4078

The fungal strain JCK-4078 was identified as *A. flavus* through phylogenetic and BLAST analysis using *ITS*, *Bt2*, and *Cmd* (Supplementary Figure 1). The *ITS*, *Bt2*, and *Cmd* sequences of JCK-4078 were deposited in Genbank under the accession numbers MW786751, MW894649, and MW894650, respectively. The phylogenetic tree constructed using *Cmd* provided better resolution in identifying the strain JCK-4078 than that constructed using *ITS* and *Bt2*.

### Nematicidal Activity of Fungal Strains

Three days after treatment, the culture filtrate of *A. flavus* JCK-4078 showed killing effects against J2s of *M. incognita*

with an EC<sub>50</sub> value of 3.48% (Supplementary Figure 2). Aflatoxin was detected at a concentration of 151 ppb in the culture filtrate of *A. flavus* JCK-4078 (data not shown). Conversely, the culture filtrates of *P. commune* strains obtained from KACC exhibited weak nematicidal activity against J2s of *M. incognita* (Supplementary Figure 3A). However, the ethyl acetate extracts of the six *P. commune* strains caused J2s mortality with EC<sub>50</sub> values ranging from 312.5 to 653.3 µg mL<sup>-1</sup> (Supplementary Figure 3B).

### Isolation and Identification of a Nematicidal Metabolite

One nematicidal metabolite (compound 1) was purified from the crude extract of *A. flavus* JCK-4078. HR-ESI-MS of compound 1 displayed [M + H]<sup>+</sup> molecular ion peak at *m/z* 337.15198 in the positive ion mode and [M + H]<sup>-</sup> molecular ion peak at *m/z* 335.13750 [M - H]<sup>-</sup> in the negative ion mode, indicating its molecular formula to be C<sub>20</sub>H<sub>20</sub>N<sub>2</sub>O<sub>3</sub> (Supplementary Figure 4). The UV-visible absorption spectrum of the compound showed the UV maxima at 223 and 279 nm (data not shown). NMR data of compound 1 are summarized in Supplementary Table 1 based on the <sup>1</sup>H- and <sup>13</sup>C-NMR, COSY, HSQC, and HMBC spectra. All the instrumental data of compound 1 were identical to those of CPA (Holzapfel, 1968; Luk et al., 1977; Lin et al., 2009). Therefore, compound 1 was identified as CPA. Among the six *P. commune* strains obtained from KACC, KACC 45973 produced CPA at the highest level (10.5 µg mL<sup>-1</sup>) in the PDB medium (Supplementary Table 2). Therefore, this fungal strain was used to further study the isolation of CPA, optimization of the culture fermentation process, formulation, and *in vivo* bioassay.

### Mortality and Cumulative Percent of Egg Hatch of Compound 1 Against *Meloidogyne* spp.

The nematicidal activity of CPA was tested against J2s of three *Meloidogyne* species (*M. incognita*, *M. hapla*, and *M. arenaria*). Compound 1 was more effective at causing mortality of *M. incognita* than of *M. arenaria* and *M. hapla* (Table 2). After 3 days, the EC<sub>50</sub> value of compound 1 against J2s of *M. incognita* was 4.5 µg mL<sup>-1</sup>. In comparison, the EC<sub>50</sub> values of compound 1 against *M. arenaria* and *M. hapla* were 60.51 and 18.82 µg mL<sup>-1</sup>, respectively.

Compound 1 also suppressed egg hatch of the three *Meloidogyne* species (Figure 1). The cumulative percentage of egg hatch of *M. incognita* and *M. hapla* at 28 days after exposure to compound 1 at 25 and 50 µg mL<sup>-1</sup> was significantly lower than that of the untreated control of *M. incognita* and *M. hapla*, respectively. The egg hatch of *M. arenaria* was significantly reduced two times when exposed to only 50 µg mL<sup>-1</sup> of compound 1.

### Optimization by Plackett–Burman Design

PBD was used to identify the most significant variables affecting compound 1 production from *P. commune* strain. Compound 1 was produced in a wide range from 1.5 to 204.2 µg mL<sup>-1</sup>.



**TABLE 2** |  $EC_{50}$  values ( $\mu\text{g mL}^{-1}$ ) for cyclopiazonic acid-induced mortality of *Meloidogyne incognita*, *Meloidogyne hapla*, and *Meloidogyne arenaria* after 72 h of nematode immersion in test solution with respective SE and 95% CI values.

Nematode species	$EC_{50}$ ( $\mu\text{g mL}^{-1}$ )	SE	95% CI
<i>M. incognita</i>	4.50	0.012	4.472–4.538
<i>M. hapla</i>	18.82	3.70	11.42–33.10
<i>M. arenaria</i>	60.51	10.96	40.15–110.30

$EC_{50}$ , 50% effective concentration; SE, standard error; CI, confidence interval.

Compound **1** production was the highest in run 11, followed by runs 14 and 17 ( $167.4$  and  $130.8 \mu\text{g mL}^{-1}$ , respectively; **Table 3**).

ANOVA, as well as a sum of squares, mean squares, *F*-value, *t*-value, and *P*-value, were used to test the model's adequacy. The statistical significance was determined using the *P*-value (probability value). Fisher's statistical test (*F*-test) was also used for evaluating the statistical significance of the model. A model *F*-value of 9.49 and a *P*-value of 0.00 imply that the model is significant; there was merely a 0.0001% chance that a "Model *F*-value" this large could occur because of noise. Based on the ANOVA analysis, **Table 4** indicates that the factor that contributed the most to compound **1** production is  $\text{NaNO}_3$ , followed by agitation speed,  $\text{FeSO}_4 \cdot 7\text{H}_2\text{O}$ , tryptone, and yeast extract in that order. The remaining variables did not contribute significantly to CPA production. Out of 14 factors affecting compound **1** production, only 3 factors— $\text{NaNO}_3$  (A), tryptone (B), and yeast extract (C)—both positively and significantly caused an increase in CPA production (**Figure 2** and **Table 4**). However, both agitation speed (M) and  $\text{FeSO}_4 \cdot 7\text{H}_2\text{O}$  (H) exerted significant negative effects.

The value of the coefficient of determination ( $R^2$ ) was 81.85% of the variability in compound **1** production, indicating that only 18.15% of the total variances do not explain the independent factors. The high adjusted  $R^2$  (adj  $R^2$ ) value of 72.23% also points to the accuracy of the model. The predicted  $R^2$  (pred  $R^2$ ) value of 59.16% is in reasonable agreement with the adj  $R^2$  value of 81.73%. It proved that this model is good at predicting compound **1** production, matching between the observed values and the predicted response value.

The first-order polynomial Equation (3) was established based on the results of regression analysis and represents compound

**1** production as a function of the independent variables that deserve the highest response:

$$Y = 605526 + 471500A + 293603B + 280882C - 81339D \\ + 78134E + 82255F + 40002G - 325196H - 26807J \\ - 54016K - 11162L - 403865M + 169532N + 169142O \\ - 219931P + 106629Q + 52084R - 150120S + 101345T(3)$$

where *Y* is compound **1** production, and A, B, C, E, F, H, J, K, L, M, N, and O are  $\text{NaNO}_3$ , tryptone, yeast extract, glucose, starch,  $\text{MgSO}_4 \cdot 7\text{H}_2\text{O}$ , KCL,  $\text{FeSO}_4 \cdot 7\text{H}_2\text{O}$ ,  $\text{K}_2\text{HPO}_4$ , PDB, pH, agitation speed, incubation time, and inoculum size, respectively.

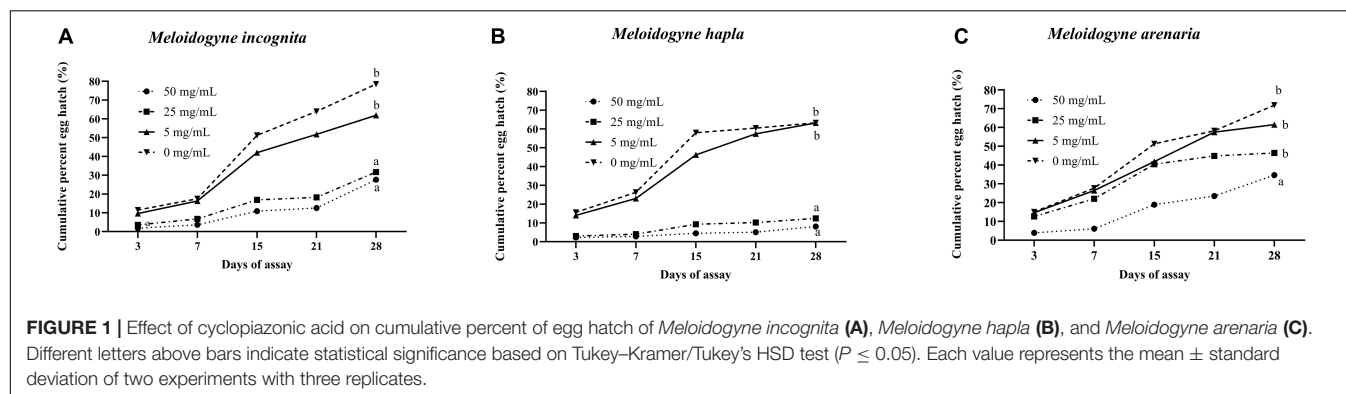
$\text{NaNO}_3$ , tryptone, and yeast extract were chosen as the central points for further optimization using CCD based on the effect, coefficient, contribution, and *P*-value of each variable, as these factors had the most positive significant effects on CPA production.

## Optimization by Response Surface Methodology

In this study, a CCD was employed to optimize different levels of the three main factors ( $\text{NaNO}_3$ , tryptone, and yeast extract) that affect compound **1** production from *P. commune* KACC 45973. Based on the experimental data obtained in **Table 5**, the concentrations of compound **1** ranged from 1.5 to  $343.5 \mu\text{g mL}^{-1}$ . The highest concentration of compound **1** produced from *P. commune* KACC 45973 (which represented the central point of CCD), was detected in run 20 ( $343.5 \mu\text{g mL}^{-1}$ ).

The  $R^2$ -value of 71.07% indicated that the three independent factors predicted 71.07% of the total variance in the dependent variable (compound **1** production) and that the model could not explain 28.93% of the total variance. In the quadratic model, the adj  $R^2$  (62.39%) and pred  $R^2$  (51.89%) values were found with an insignificant lack of fit ( $P > 0.05$ ). All  $R^2$ , adj  $R^2$ , and pred  $R^2$  analyses indicated a good agreement between the experimental and predicted compound **1** and implicated that the analytical model fitted for stimulation of compound **1** production by *P. commune* KACC 45973.

The effects of  $\text{NaNO}_3$ , tryptone, and yeast extract on the CPA production were analyzed based on the predicted response for



**TABLE 3 |** Twenty-trial Plackett–Burman experimental design for evaluation of independent variables with coded values along with the observed cyclopiazonic acid.

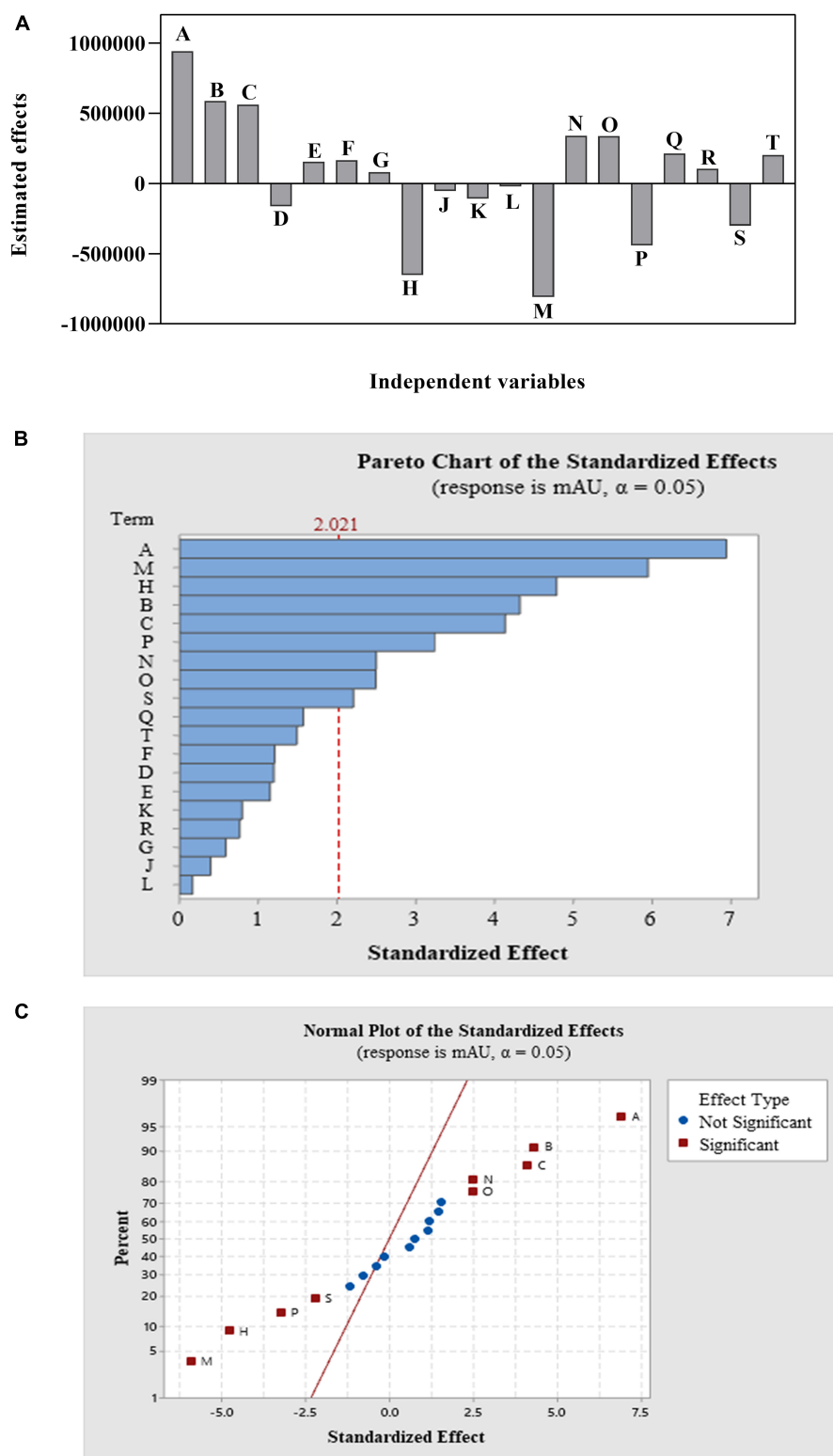
Run	A	B	C	D	E	F	G	H	J	K	L	M	N	O	D1	D2	D3	D4	D5	Actual value	
																				Area (mAU)	Conc.CPA ( $\mu\text{g mL}^{-1}$ )
1	1	–1	–1	1	1	1	–1	1	–1	1	–1	1	–1	–1	–1	1	1	–1	1	87898.0	7.3
2	–1	1	–1	–1	–1	1	1	–1	1	–1	1	1	–1	–1	1	1	1	–1	1	61141.7	5.5
3	–1	–1	–1	1	1	1	1	–1	1	–1	–1	1	1	1	–1	1	–1	1	–1	0.0	1.5
4	1	–1	1	1	–1	1	1	1	1	–1	1	–1	1	–1	–1	–1	–1	–1	1	1434859.7	95.4
5	–1	–1	1	1	1	–1	1	–1	–1	1	1	–1	–1	–1	1	1	–1	1	1	213720.3	15.5
6	1	–1	–1	–1	–1	1	–1	1	1	1	1	–1	–1	1	1	1	–1	1	–1	117458.3	9.2
7	1	–1	1	–1	–1	–1	1	1	–1	–1	–1	1	1	–1	1	1	1	1	–1	75908.0	6.5
8	1	1	–1	1	1	–1	1	1	–1	–1	1	1	–1	1	1	–1	–1	–1	–1	54613.3	5.1
9	–1	–1	–1	–1	–1	–1	–1	–1	–1	–1	–1	–1	–1	–1	–1	–1	–1	–1	–1	32837.0	3.7
10	–1	–1	1	1	–1	1	–1	–1	–1	1	1	1	1	1	1	–1	1	–1	–1	0.0	1.5
11	1	1	1	–1	1	1	–1	–1	–1	–1	–1	–1	1	1	1	1	–1	–1	1	3099019.7	204.2
12	–1	1	1	–1	–1	1	1	1	–1	1	–1	1	–1	1	–1	–1	–1	1	1	100937.7	8.1
13	1	–1	1	–1	1	–1	–1	–1	1	–1	1	1	–1	1	–1	–1	1	1	1	1155138.3	77.1
14	1	1	1	1	–1	–1	1	–1	1	1	–1	–1	–1	1	–1	1	1	–1	–1	2536194.0	167.4
15	–1	1	1	–1	1	–1	–1	1	1	1	1	1	1	–1	–1	1	–1	–1	–1	248304.3	17.8
16	–1	1	1	1	1	1	–1	1	1	–1	–1	–1	–1	–1	1	–1	1	1	–1	0.0	1.5
17	1	1	–1	–1	1	1	1	–1	–1	1	1	–1	1	–1	–1	–1	1	1	–1	1976494.3	130.8
18	1	1	–1	1	–1	–1	–1	–1	1	1	–1	1	1	–1	1	–1	–1	1	1	232676.3	16.7
19	–1	–1	–1	–1	1	–1	1	1	1	1	–1	–1	1	1	1	–1	1	–1	1	1416.7	1.6
20	–1	1	–1	1	–1	–1	–1	1	–1	–1	1	–1	1	1	–1	1	1	1	1	681909.0	46.1

mAU, milli-Absorbance Units; Conc.CPA, concentration of cyclopiazonic acid; D1–D5, dummy1–dummy5.

**TABLE 4 |** Regression statistics and analysis of variance (ANOVA) for the experimental results of Plackett–Burman design used for cyclopiazonic acid production by *Penicillium commune* KACC 45973.

Source	Adj SS	DF	Adj MS	F-value	p-value	Contribution (%)
Model	5.00E+13	19	2.63E+12	9.49	0.00	
Linear	5.00E+13	19	2.63E+12	9.49	0.00	
A- NaNO <sub>3</sub>	1.33E+13	1	1.33E+13	48.09	0.00	21.82
B-Tryptone	5.17E+12	1	5.17E+12	18.65	0.00	8.46
C-Yeast extract	4.73E+12	1	4.73E+12	17.07	0.00	7.75
D-Glucose	3.97E+11	1	3.97E+11	1.43	0.24	0.65
E-Starch	3.66E+11	1	3.66E+11	1.32	0.26	0.60
F-MgSO <sub>4</sub> .7H <sub>2</sub> O	4.06E+11	1	4.06E+11	1.46	0.23	0.66
G-KCL	96010720299	1	96010720299	0.35	0.56	0.16
H-FeSO <sub>4</sub> .7H <sub>2</sub> O	6.35E+12	1	6.35E+12	22.88	0.00	10.38
J- K <sub>2</sub> HPO <sub>4</sub>	43118201686	1	43118201686	0.16	0.69	0.07
K-PDB	1.75E+11	1	1.75E+11	0.63	0.43	0.29
L-pH	7475950426	1	7475950426	0.03	0.87	0.01
M-Agitation speed	9.79E+12	1	9.79E+12	35.29	0.00	16.01
N-Incubation time	1.72E+12	1	1.72E+12	6.22	0.01	2.82
O-Inoculum size	1.72E+12	1	1.72E+12	6.19	0.01	2.81
P-Dummy 1	2.90E+12	1	2.90E+12	10.46	0.00	4.75
Q-Dummy 2	6.82E+11	1	6.82E+11	2.46	0.12	1.12
R-Dummy 3	1.63E+11	1	1.63E+11	0.59	0.44	0.27
S-Dummy 4	1.35E+12	1	1.35E+12	4.87	0.03	2.21
T-Dummy 5	6.16E+11	1	6.16E+11	2.22	0.14	1.01
Error	1.11E+13	40	2.77E+11			
Total	6.11E+13	59				

$R^2$ , 81.85%; Adj  $R^2$ , 73.23%; Pred  $R^2$ , 59.16%; SS, a sum of a square; MS, mean square; DF, degree of freedom; F, Fisher's function; P, level of significance.



**FIGURE 2 |** The main effects of the variables **(A)** and Pareto chart of the standardized effects of 14 variables design at a 95% confidence level **(B)** and the normal plot of the standardized effects of 14 variables design at a 95% confidence level **(C)** of a Plackett–Burman design for cyclopiazonic acid production by *Penicillium commune* KACC 45973.

**TABLE 5 |** Matrix of the central composite design and the corresponding experimental and predicted concentrations of cyclopiazonic acid produced by *Penicillium commune* KACC 45973.

StdOrder	Run	Variables			Area (mAU)	
		A	B	C	Experimental	Predicted
1	1	−1	−1	−1	0.00	469312.00
6	2	1	−1	1	657723.33	1344140.00
10	3	1.68179	0	0	3272122.00	3477750.00
5	4	−1	−1	1	1221872.67	1352719.00
16	5	0	0	0	3315119.33	3307446.00
15	6	0	0	0	3516230.33	3307446.00
20	7	0	0	0	4343611.00	3307446.00
19	8	0	0	0	2572035.67	3307446.00
17	9	0	0	0	4053908.33	3307446.00
3	10	−1	1	−1	862777.33	166334.00
11	11	0	−1.6818	0	296348.67	−26798.40
13	12	0	0	−1.6818	0.00	660673.00
9	13	−1.6818	0	0	0.00	−25874.20
12	14	0	1.68179	0	4334571.00	4671898.00
18	15	0	0	0	2211776.00	3307446.00
2	16	1	−1	−1	2349285.67	1599046.00
4	17	1	1	−1	4482329.00	4341456.00
7	18	−1	1	1	3691986.33	4198043.00
14	19	0	0	1.68179	4483061.00	386568.00
8	20	1	1	1	5229002.33	4984819.00
Variables	Code symbol	Code values				
		−1.68	−1	0	1	1.68
NaNO <sub>3</sub>	A	0	2	5	8	11
Tryptone	B	0	2	5	8	11
Yeast extract	C	0	2	5	8	11

StdOrder, standard order; mAU, milli-Absorbance Units.

producing compound **1** from *P. commune* KACC 45973 that can be expressed using a second-order polynomial model with coded symbols (A–N), as listed in **Supplementary Table 3**.

$$Y = 3307446 + 1041636A + 1396933B + 944201C + 198839AB - 847086AC + 224567BC - 559149A^2 - 348214B^2 - 374352C^2$$

The three-dimensional (3D) response surface and two-dimensional (2D) contour plots were subsequently used to graphically depict the interaction between the three variables. These plots displayed the combined effect of NaNO<sub>3</sub> and tryptone on compound **1** production; the yeast extract was fixed at the central point (5 g L<sup>−1</sup>) (**Figure 3A**). Based on the ANOVA analysis (**Table 6**), both NaNO<sub>3</sub> and tryptone were determined as significant variables affecting CPA production (*p*-value ≤ 0.05). The highest concentration of compound **1** produced was detected when the values of tryptone and NaNO<sub>3</sub> were in the range +1 to +1.68. However, the ANOVA results showed that the interaction coefficient between these two variables was not significant (*p*-value > 0.05) (**Table 6**).

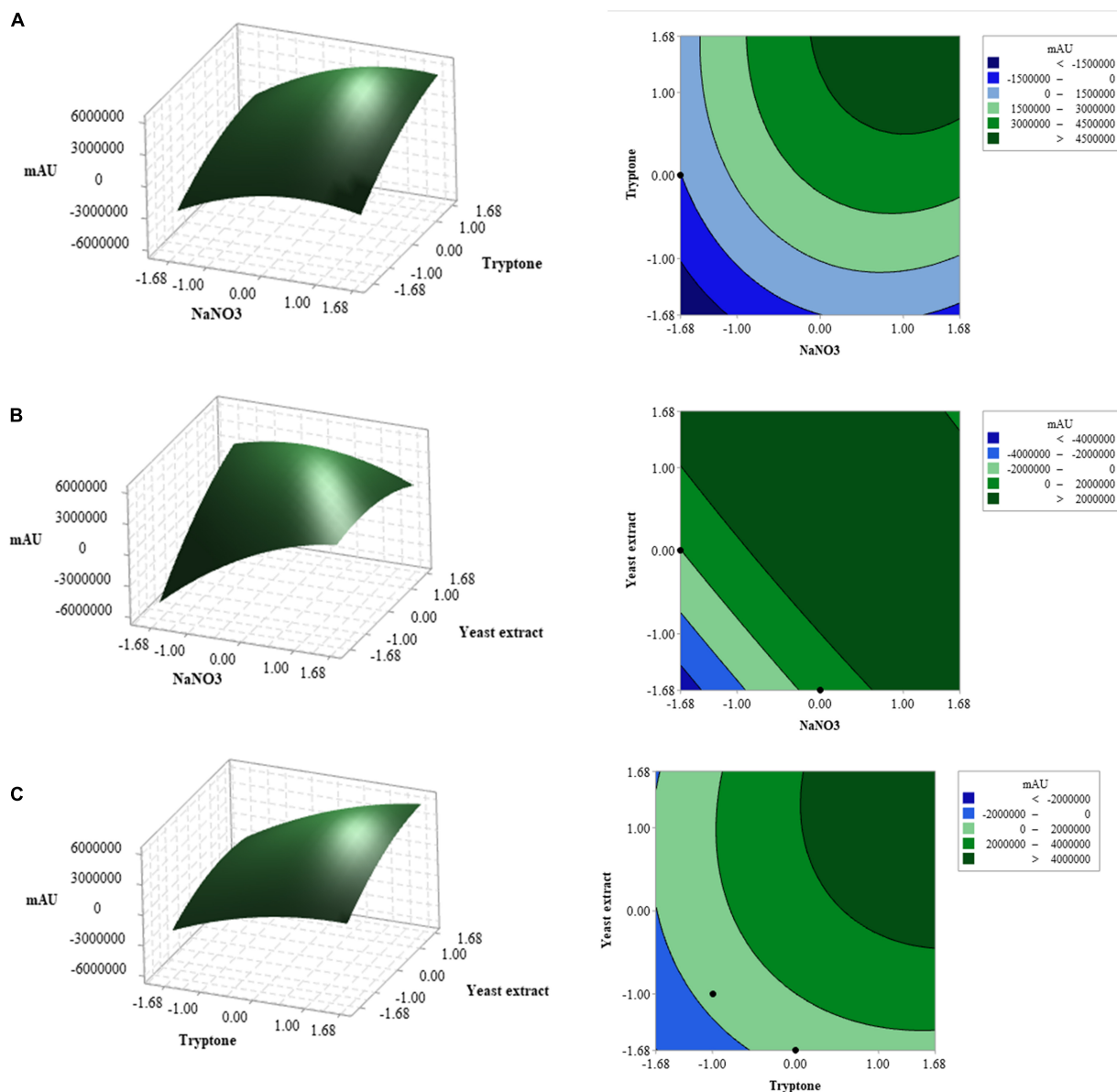
Meanwhile, the combined effects of NaNO<sub>3</sub> and yeast extract on compound **1** production were elucidated in **Figure 3B**; the

concentration of tryptone was kept at the central point (5 g L<sup>−1</sup>). Based on ANOVA results, both NaNO<sub>3</sub> and yeast extract affected compound **1** production, and interaction between these variables was significant at *P*-values ≤ 0.05 (**Table 6**). The maximum response was observed when the NaNO<sub>3</sub> level was near +1 and the yeast extract level was between +1 and +1.68. **Figure 3C** illustrates the 3D response surface and 2D contour plots of compound **1** production by *P. commune* KACC 45973 as a function of tryptone and yeast extract, where the level of NaNO<sub>3</sub> was kept at the center point (5 g L<sup>−1</sup>). The highest production of compound **1** was achieved when the levels of both variables were set in the range from +1 to +1.68. Furthermore, ANOVA analysis revealed that the interaction between the two variables contributed significantly to compound **1** production (*P* ≤ 0.05; **Table 6**).

## Validation of the Models Under the Optimized Setting

Three verification experiments were performed under various optimized medium conditions to confirm the validity and accuracy of the model. The independent factors' design matrix was used along with the experiment results and theoretical values to predict compound **1** production (**Table 7**). The experimentally determined values of maximum compound **1** production and





**FIGURE 3 |** Three-dimensional (3D) response surface plots and two-dimensional (2D) contour plots of three factors affecting cyclopiazonic acid production by *Penicillium commune* KACC 45973. When the interaction of any two factors was plotted, the other factor was set at the central point: (A) tryptone and NaNO<sub>3</sub>, (B) yeast extract and NaNO<sub>3</sub>, and (C) tryptone and yeast extract.

high mortality induced by the culture filtrate from *P. commune* KACC 45973 agreed with the predicted values (Table 7 and Supplementary Table 4). The mortality percent caused by the three optimal media was significantly higher than that by the PDB medium, suggesting that the equations are accurate and reliable for predicting compound 1 production by *P. commune* KACC 45973. Based on the finding, combining the selected factors is the best strategy to optimize the response depicted at the beginning of the study. This model is reasonable to optimize the parameters to increase compound 1 production. The optimum culture conditions for the CPA production by *P. commune* 45973 were determined as follows; liquid medium = the combination

of NaNO<sub>3</sub> (5.04 g L<sup>-1</sup>), tryptone (11 g L<sup>-1</sup>), yeast extract (11 g L<sup>-1</sup>), starch (90 g L<sup>-1</sup>), MgSO<sub>4</sub>·7H<sub>2</sub>O (1 g L<sup>-1</sup>), KCl (1 g L<sup>-1</sup>), FeSO<sub>4</sub>·7H<sub>2</sub>O (0.01 g L<sup>-1</sup>), K<sub>2</sub>HPO<sub>4</sub> (2 g L<sup>-1</sup>), PDB (24 g L<sup>-1</sup>); an incubation time = 21 days; pH = 5.0; inoculum = 10 pieces of 5 mm agar plugs containing mycelia.

## Efficacy of Pc45973–WP20 Against *Meloidogyne incognita* J2s in Planta

From the *in vitro* results, CPA showed the highest nematicidal activity against *M. incognita* when compared with that against the other two *Meloidogyne* species. Thus, we

**TABLE 6 |** Analysis of variance (ANOVA) of the quadratic model for cyclopiazonic acid production by *Penicillium commune* KACC 45973.

Source	Adj SS	DF	Adj MS	F-value	p-value	Contribution (%)
Model	1.59E+14	9	1.77E+13	7.22	0.00	56.52
Linear	1.21E+14	3	4.2E+13	17.17	0.00	43.14
A	2.33E+13	1	3.77E+13	15.4	0.00	8.30
B	6.86E+13	1	7.6E+13	31.09	0.00	24.38
C	2.94E+13	1	3.47E+13	14.2	0.00	10.46
Square	1.9E+13	3	6.57E+12	2.69	0.06	6.75
A <sup>2</sup>	9.81E+12	1	1.32E+13	5.38	0.02	3.49
B <sup>2</sup>	3.72E+12	1	5.18E+12	2.12	0.15	1.32
C <sup>2</sup>	5.45E+12	1	5.98E+12	2.45	0.12	1.94
2-Way interaction	1.86E+13	3	6.21E+12	2.54	0.07	6.63
AB	2.22E+12	1	7.25E+11	0.3	0.59	0.79
AC	1.53E+13	1	1.32E+13	5.38	0.02	5.45
BC	1.11E+12	1	1.11E+12	0.45	0.50	0.40
Error	1.22E+14	50	2.44E+12			43.48
Lack-of-fit	9.63E+12	5	1.93E+12	0.77	0.58	3.43
Pure error	1.13E+14	45	2.5E+12			40.05
Total	2.81E+14	59				100.00

$R^2$ , 71.07%; Adj  $R^2$ , 62.39%; Pred  $R^2$ , 51.89%.

DF, degree of freedom; F, Fisher's function; P, level of significance.

investigated the potential biological control activity of CPA against *M. incognita* in planta. The disease control efficacy of Pc45973–WP20 against *M. incognita* on tomato plants was tested. *M. incognita* population (J2s and eggs) and gall formation on the tomato plants treated with Pc45973–WP 20 were significantly reduced when compared with those on the untreated control in a dose-dependent manner (Table 8). The positive control Sunchungtan completely controlled the gall formation and nematode development in the treated tomato plants. Additionally, there was no significant difference in plant height and fresh root weight among treatments, except with Sunchungtan, which caused phytotoxic effects such as reduced plant growth.

## DISCUSSION

Numerous researchers have focused on developing fungal and bacterial biocontrol agents to control nematodes in agriculture (Abd-Elgawad and Askary, 2018; Forghani and Hajihassani, 2020). Many studies on the two genera *Penicillium* and *Aspergillus* have been conducted to explore various nematicidal metabolites against RKNs (Kusano et al., 2000; Nakahara et al., 2004; Siddiqui and Akhtar, 2009; Murslain et al., 2014; Jang et al., 2016). At 300 mg L<sup>-1</sup>, three compounds isolated from *Penicillium bilaiae* have shown nematicidal activities of 77, 52, and 98% against *Pratylenchus penetrans*, respectively (Nakahara et al., 2004). Furthermore, peniprequinolone, peniprequinolone A and B, 3-methoxy-4-hydroxy-4-(4'-methoxy-4 (4'-methoxyphenyl)) quinolinone, and cyclopenin isolated from *Penicillium* cf. *simplicissimum* have displayed weak nematicidal activity against *P. penetrans* (Kusano et al., 2000). In our previous studies, kojic acid isolated

from *Aspergillus oryzae* exhibited nematicidal activity against *M. incognita* (Kim et al., 2016), and oxalic acid produced by *Aspergillus niger* F22 showed 100% J2s mortality and 95% egg hatch inhibitory activity against *M. incognita* at 2 mmol L<sup>-1</sup> (Jang et al., 2016). In our present study, the culture filtrate of *A. flavus* JCK-4087 showed strong nematicidal activity against *M. incognita*. Recently Naz et al. (2021), also reported that the culture filtrate of one *A. flavus* strain had both eggs hatching inhibitory activity and J2s mortality of *M. incognita*. Compared to J2s mortality between the two *A. flavus* strains, JCK-4087 showed much stronger nematicidal activity than the *A. flavus* strain reported (Naz et al., 2021) with J2s mortality values of 100% at a concentration of 20% for the former and about 40% at a concentration of 25% for the latter.

Both *A. flavus* JCK-4087 and *P. commune* KACC 45973 were found to produce CPA as a nematicidal metabolite. CPA has been reported to be produced by many fungal strains belonging to the genera *Penicillium* and *Aspergillus* (Hermansen et al., 1984; Trucksess et al., 1987; Ostry et al., 2018). The metabolite is toxic at high concentrations (Purchase, 1971; Van Rensburg, 1984; Morrissey et al., 1985) and has antibacterial activity against methicillin-resistant *S. aureus* (MRSA), *B. subtilis*, and *S. aureus* (Shang et al., 2012; Hong et al., 2015). To the best of our knowledge, this is the first report of the effects of CPA on J2s mortality and egg hatch of three *Meloidogyne* species.

In this study, the medium optimized via the statistical optimization approach enhanced CPA production. The first-order model based on PBD has indicated that the most statistically significant variables influencing CPA production were NaNO<sub>3</sub>, tryptone, and yeast extract. The adj  $R^2$  (72.23%) value indicates that the model is reasonable compared to previous studies (Nelofer et al., 2012; El-Naggar et al., 2016). A previous study showed that NaNO<sub>3</sub> caused trap formation and exhibited

**TABLE 7** | Model validation experiments for cyclopiazonic acid (CPA) production from *Penicillium commune* KACC 45973.

No.	NaNO <sub>3</sub> (g L <sup>-1</sup> )	Tryptone (g L <sup>-1</sup> )	Yeast extract (g L <sup>-1</sup> )	CPA yield (μg mL <sup>-1</sup> )			
				Predicted		Experimental	
				MAU	Conc.	MAU	Conc.
Medium 1	5.04	11	11	5,837,215	383.26	5,809,916	381.48
Medium 2	9.1	11	9.45	5,222,246	343.05	5,254,508	345.16
Medium 3	11	11	0.92	4,873,244	320.22	4,677,774	307.44

**TABLE 8** | Effect of the wettable powder formulation of ethyl acetate layer of *Penicillium commune* KACC 45973 (Pc45973-WP20) on gall formation, nematode populations in roots and soils, and shoot and root growth of tomato plants infected with *Meloidogyne incognita*.

Treatments	Conc. (folds)	Nematode population (J2 and eggs)		GI	Control value (%) of gall	Plant		Root weight
		g <sup>-1</sup> root	mL <sup>-1</sup> soil			Height (cm)	Weight (g)	
<b>Pc45973-WP20</b>	250	431.26 ± 37.84 <sup>c</sup>	15.02 ± 1.38 <sup>b</sup>	2.00 ± 0.82 <sup>c</sup>	57.89 ± 16.3 <sup>c</sup>	36.50 ± 4.50 <sup>b</sup>	24.85 ± 3.60 <sup>c</sup>	6.94 ± 1.22 <sup>b</sup>
	500	510.39 ± 53.84 <sup>c</sup>	16.74 ± 2.37 <sup>b</sup>	3.00 ± 0.82 <sup>c</sup>	36.84 ± 16.3 <sup>bc</sup>	41.30 ± 2.50 <sup>b</sup>	24.64 ± 1.45 <sup>c</sup>	7.02 ± 1.10 <sup>b</sup>
	1,000	703.89 ± 63.72 <sup>b</sup>	20.26 ± 4.17 <sup>b</sup>	3.75 ± 0.5 <sup>b</sup>	21.05 ± 10.00 <sup>ab</sup>	40.00 ± 4.10 <sup>b</sup>	24.67 ± 2.66 <sup>c</sup>	6.65 ± 0.29 <sup>b</sup>
<b>Sunchungtan</b>	4,000	0.00 ± 0.00 <sup>d</sup>	5.51 ± 5.60 <sup>c</sup>	0.00 ± 0.00 <sup>d</sup>	100.00 ± 0.00 <sup>d</sup>	13.80 ± 11.10 <sup>a</sup>	3.29 ± 2.83 <sup>a</sup>	1.93 ± 0.52 <sup>a</sup>
<b>Untreated control</b>	—	1233.07 ± 36.47 <sup>a</sup>	32.96 ± 4.23 <sup>a</sup>	4.75 ± 0.50 <sup>a</sup>	0.00 ± 0.00 <sup>a</sup>	31.30 ± 2.50 <sup>b</sup>	17.16 ± 3.68 <sup>b</sup>	6.17 ± 0.19 <sup>b</sup>

Means with same letters are not significantly different ( $p < 0.05$ ) according to Turkey's test. Each value represents the mean ± standard deviation of four repeated values from two trials.

nematicidal activity in *A. oligospora* (Liang et al., 2016). Among the nitrogen sources considered in the present study, NaNO<sub>3</sub> had the highest contribution (21.82%) and exerted significant effects to enhance CPA production (Zarabi et al., 2012). CCD was used to determine the optimal levels of NaNO<sub>3</sub>, tryptone, and yeast extract as selected variables for increasing CPA production. Overall, the maximum CPA production obtained (381.48 mg L<sup>-1</sup>) by *P. commune* KACC 45973 is greater than that by *P. commune* (3.99 mg L<sup>-1</sup>) (Gqaleni et al., 1996) and *A. flavus* (6.256 mg L<sup>-1</sup>) (Gqaleni et al., 1997) in the previous studies. Both *P. commune* IMI87247 and *P. commune* NRRL891 strains have been reported to produce CPA on GMP agar medium but not in submerged medium (Hermansen et al., 1984). In our study, CPA was produced in a submerged medium by *P. commune* KACC 45973.

Additionally, Pc45973-WP20 effectively suppressed the development of tomato RKN disease caused by *M. incognita* in the pot experiment. Similarly previous studies, *Penicillium* and *Aspergillus* species have been reported as potential biocontrol agents against RKNs under greenhouse and field conditions (Siddiqui and Akhtar, 2009; Murslain et al., 2014; Jang et al., 2016). For instance, *Penicillium chrysogenum* reduced galls caused by *Meloidogyne javanica* and *M. incognita* on tomato and cucumber plants under greenhouse conditions (Gotlieb et al., 2003; Sikandar et al., 2019). Furthermore, the compound brefeldin isolated from *Penicillium brefeldianum* HS-1 showed a reduction in gall numbers up to 41.4% after 4 weeks of *M. incognita* inoculation (Miao et al., 2019).

CPA is a mycotoxin that is produced by *Aspergillus* and *Penicillium* (Le Bars, 1979; Trucksess et al., 1987; Lin et al., 2009; Ostry et al., 2018; Rao et al., 2021). Even though CPA

has been detected in a number of food sources such as peanuts, wheat, sunflower, meat, milk, and cheese, few studies have reported CPA as a mycotoxin because of its benign toxicity and low levels (Urano et al., 1992; Dorner et al., 1994; Burdock and Flamm, 2000; Oliveira et al., 2006; Rao et al., 2021). In addition, CPA has not been considered chronically toxic, and it does not affect the immune system (Burdock and Flamm, 2000; King et al., 2011). Hence, CPA can be used as a biochemical biopesticide with the contingency of risk assessments before commercialization.

Chemical nematicides have been used as the most effective means to control RKNs. However, the long-term use of carbamate and organophosphorus nematicides has increased nematode resistance, resulting in reduced field efficacy (Ebene et al., 2019; Desaegeer et al., 2020). This has led to the development of novel chemical nematicides with new action mechanisms. CPA is an ergoline alkaloid and indol-tetramic acid. It is a specific inhibitor of the Ca<sup>2+</sup>-ATPase of sarcoplasmic reticulum (SERCA ATPase) (Seidler et al., 1989; Plenge-Tellechea et al., 2001; Moncoq et al., 2007; Chang et al., 2009). It is selective in inhibiting SERCA ATPase because it does not affect plasma membrane Ca<sup>2+</sup> pumps. CPA has a little different mode of action with other SERCA ATPase inhibitors; CPA depletes 1,4,5-triphosphate-sensitive Ca<sup>2+</sup> stores and does not inhibit L-type calcium-channel activity, but thapsigargin and 2,5-t-butyl hydroquinone do (Nelson et al., 1994). Even though we do not perform any experiment on the mode of action of CPA against *M. incognita*, CPA may show nematicidal activity against J2s and egg hatching of *M. incognita* by inhibiting SERCA ATPase because it has an essential role in the muscle contraction-relaxation cycle. On the other hand, the V-ATPase inhibitor pyocyanin was also reported to show mortality against J2 of *M. incognita*, whereas

ouabain, an inhibitor of the plasma membrane  $\text{Na}^+/\text{K}^+$  ATPase, was ineffective (Caboni et al., 2013). This indicates that the nematicidal activity is quite different among ATPase inhibitors. To our knowledge, there is still no commercial nematicides that used CPA as the active ingredient, thus indicating that CPA can play an important role as a lead molecule to develop new chemical nematicides.

## CONCLUSION

In this study, CPA showed strong J2s mortality and egg hatching inhibitory activity against *Meloidogyne* spp. CPA production of *P. commune* KACC 45973 was enhanced by statistical methods using PBD and CCD. The optimized culture conditions resulted in 7.88-fold higher CPA yields than the basal medium conditions. Our findings indicate that CPA produced by *P. commune* KACC 45973 could be used directly as a biochemical nematicide or indirectly as a lead molecule of synthetic nematicides for controlling RKN diseases.

## REFERENCES

- Abd-Elgawad, M. M., and Askary, T. H. (2018). Fungal and bacterial nematicides in integrated nematode management strategies. *Egypt. J. Biol. Pest Control* 28, 1–24. doi: 10.1186/s41938-018-0080-x
- Abnet, C. C. (2007). Carcinogenic food contaminants. *Cancer Invest.* 25, 189–196. doi: 10.1080/07357900701208733
- Anwar, S., and McKenry, M. (2010). Incidence and reproduction of *Meloidogyne incognita* on vegetable crop genotypes. *Pak. J. Zool.* 42, 135–141.
- Arul Jose, P., Sivakala, K. K., and Jebakumar, S. R. D. (2013). Formulation and statistical optimization of culture medium for improved production of antimicrobial compound by *Streptomyces* sp. JAJ06. *Int. J. Microbiol.* 2013:526260. doi: 10.1155/2013/526260
- Aziz, N. H., and Zainol, N. (2018). Isolation and identification of soil fungi isolates from forest soil for flooded soil recovery. *IOP Conf. Ser. Mater. Sci. Eng.* 342:012028.
- Barker, K. R., Carter, C. C., and Sasser, J. N. (1985). *An Advanced Treatise on Meloidogyne: Methodology*. Raleigh, NC: North Carolina State University Graphics.
- Bezerra, M. A., Santelli, R. E., Oliveira, E. P., Villar, L. S., and Escalera, L. A. (2008). Response surface methodology (RSM) as a tool for optimization in analytical chemistry. *Talanta* 76, 965–977. doi: 10.1016/j.talanta.2008.05.019
- Bogner, C. W., Kamdem, R. S., Sichtermann, G., Matthäus, C., Hölscher, D., Popp, J., et al. (2017). Bioactive secondary metabolites with multiple activities from a fungal endophyte. *Microb. Biotechnol.* 10, 175–188. doi: 10.1111/1751-7915.12467
- Burdock, G., and Flamm, W. (2000). Safety assessment of the mycotoxin cyclopiazonic acid. *Int. J. Toxicol.* 19, 195–218. doi: 10.1080/10915810050074964
- Caboni, P., Aissani, N., Cabras, T., Falqui, A., Marotta, R., Liori, B., et al. (2013). Potent nematicidal activity of phthalaldehyde, salicylaldehyde, and cinnamic aldehyde against *Meloidogyne incognita*. *J. Agric. Food Chem.* 61, 1794–1803. doi: 10.1021/jf305164m
- Calvo, A. M., Wilson, R. A., Bok, J. W., and Keller, N. P. (2002). Relationship between secondary metabolism and fungal development. *Microbiol. Mol. Biol. Rev.* 66, 447–459. doi: 10.1128/mmbr.66.3.447-459.2002
- Cayrol, J.-C., Djian, C., and Pijarowski, L. (1989). Study of the nematicidal properties of the culture filtrate of the nematophagous fungus *Paecilomyces lilacinus*. *Revue. Nématol.* 12, 331–336.
- Chang, P.-K., Ehrlich, K. C., and Fujii, I. (2009). Cyclopiazonic acid biosynthesis of *Aspergillus flavus* and *Aspergillus oryzae*. *Toxins* 1, 74–99. doi: 10.3390/toxins1020074

## DATA AVAILABILITY STATEMENT

The data presented in the study are deposited in the GenBank repository, accession numbers MW786751, MW894649, and MW894650.

## AUTHOR CONTRIBUTIONS

VN and J-CK conceived this study. VN, NY, YL, IH, and J-CK performed the experiments. VN, NY, HB, and J-CK analyzed the data. VN, HB, and J-CK wrote the manuscript. All authors approved the manuscript.

## SUPPLEMENTARY MATERIAL

The Supplementary Material for this article can be found online at: <https://www.frontiersin.org/articles/10.3389/fmicb.2021.726504/full#supplementary-material>

- Degenkolb, T., and Vilcinskas, A. (2016). Metabolites from nematophagous fungi and nematicidal natural products from fungi as alternatives for biological control. Part II: metabolites from nematophagous basidiomycetes and non-nematophagous fungi. *Appl. Microbiol. Biotechnol.* 100, 3813–3824. doi: 10.1007/s00253-015-7234-5
- Desaeger, J., Wram, C., and Zasada, I. (2020). New reduced-risk agricultural nematicides-rationale and review. *J. Nematol.* 52, e2020–e2091. doi: 10.21307/jofnem-2020-091
- Dong, S., Qiao, K., Zhu, Y., Wang, H., Xia, X., and Wang, K. (2014). Managing *Meloidogyne incognita* and *Bemisia tabaci* with thiacloprid in cucumber crops in China. *J. Crop Prot.* 58, 1–5. doi: 10.1016/j.cropro.2013.11.026
- Dorner, J. W., Cole, R. J., Erlington, D. J., Suksupath, S., McDowell, G. H., and Bryden, W. L. (1994). Cyclopiazonic acid residues in milk and eggs. *J. Agric. Food Chem.* 42, 1516–1518. doi: 10.1021/jf00043a023
- Ebone, L. A., Kovaleski, M., and Deuner, C. C. (2019). Nematicides: history, mode, and mechanism action. *Plant Sci. Today* 6, 91–97.
- El-Hawary, S. S., Moawad, A. S., Bahr, H. S., Abdelmohsen, U. R., and Mohammed, R. (2020). Natural product diversity from the endophytic fungi of the genus *Aspergillus*. *RSC Adv.* 10, 22058–22079. doi: 10.1039/D0RA04290K
- El-Naggar, N. E.-A., El-Shweihy, N. M., and El-Ewasy, S. M. (2016). Identification and statistical optimization of fermentation conditions for a newly isolated extracellular cholesterol oxidase-producing *Streptomyces cavourensis* strain NEAE-42. *BMC. Microbiol.* 16:217. doi: 10.1186/s12866-016-0830-4
- Forghani, F., and Hajihassani, A. (2020). Recent advances in the development of environmentally benign treatments to control root-knot nematodes. *Front. Plant Sci.* 11:1125. doi: 10.3389/fpls.2020.01125
- Gamalerio, E., and Glick, B. R. (2020). The use of plant growth-promoting bacteria to prevent nematode damage to plants. *Biology*. 9, 381. doi: 10.3390/biology9110381
- Gao, S.-S., Li, X.-M., Zhang, Y., Li, C.-S., Cui, C.-M., and Wang, B.-G. (2011). Comazaphilones A–F, azaphilone derivatives from the marine sediment-derived fungus *Penicillium commune* QSD-17. *J. Nat. Prod.* 74, 256–261. doi: 10.1021/np100788h
- Ghahremani, Z., Escudero, N., Saus, E., Gabaldón, T., and Sorribas, F. J. (2019). *Pochonia chlamydosporia* Induces plant-dependent systemic resistance to *Meloidogyne incognita*. *Front. Plant Sci.* 10:945. doi: 10.3389/fpls.2019.00945
- Glass, N. L., and Donaldson, G. C. (1995). Development of primer sets designed for use with the PCR to amplify conserved genes from filamentous ascomycetes. *Appl. Environ. Microbiol.* 61, 1323–1330. doi: 10.1128/AEM.61.4.1323-1330.1995
- Gotlieb, D., Oka, Y., Ben-Daniel, B.-H., and Cohen, Y. (2003). Dry mycelium of *Penicillium chrysogenum* protects cucumber and tomato plants against the



- root-knot nematode *Meloidogyne javanica*. *Phytoparasitica* 31, 217–225. doi: 10.1007/BF02980831
- Gqaleni, N., Smith, J. E., Lacey, J., and Gettinby, G. (1996). Production of the mycotoxin cyclopiazonic acid by *Penicillium commune* on solid agar media: effects of water activity, temperature, and incubation time. *J. Food. Prot.* 59, 864–868. doi: 10.4315/0362-028X-59.8.864
- Gqaleni, N., Smith, J. E., Lacey, J., and Gettinby, G. (1997). Effects of temperature, water activity, and incubation time on production of aflatoxins and cyclopiazonic acid by an isolate of *Aspergillus flavus* in surface agar culture. *Appl. Environ. Microbiol.* 63, 1048–1053. doi: 10.1128/AEM.63.3.1048-1053.1997
- Hajihassani, A., Rutter, W. B., and Luo, X. (2019). Resistant pepper carrying N, Me1, and Me3 have different effects on penetration and reproduction of four major *Meloidogyne* species. *J. Nematol.* 51, 1–9. doi: 10.21307/jofnem-2019-020
- Hanrahan, G., and Lu, K. (2006). Application of factorial and response surface methodology in modern experimental design and optimization. *Crit. Rev. Anal. Chem.* 36, 141–151. doi: 10.1080/10408340600969478
- Hasegawa, M., Kishino, H., and Yano, T.-A. (1985). Dating of the human-ape splitting by a molecular clock of mitochondrial DNA. *J. Mol. Evol.* 22, 160–174. doi: 10.1007/BF02101694
- Hermansen, K., Frisvad, J., Emborg, C., and Hansen, J. (1984). Cyclopiazonic acid production by submerged cultures of *Penicillium* and *Aspergillus* strains. *FEMS. Microbiol. Lett.* 21, 253–261. doi: 10.1111/j.1574-6968.1984.tb00220.x
- Holzappel, C. (1968). The isolation and structure of cyclopiazonic acid, a toxic metabolite of *Penicillium cyclopium* westling. *Tetrahedron* 24, 2101–2119. doi: 10.1016/0040-4020(68)88113-x
- Hong, E. J., Kim, N. K., Lee, D., Kim, W. G., and Lee, I. (2015). Overexpression of the laeA gene leads to increased production of cyclopiazonic acid in *Aspergillus fumigatus*. *Fungal. Biol.* 119, 973–983. doi: 10.1016/j.funbio.2015.06.006
- Hong, S. B., Go, S. J., Shin, H. D., Frisvad, J. C., and Samson, R. A. (2005). Polyphasic taxonomy of *Aspergillus fumigatus* and related species. *Mycologia.* 97, 1316–1329. doi: 10.3852/mycologia.97.6.1316
- Jang, J. Y., Choi, Y. H., Shin, T. S., Kim, T. H., Shin, K.-S., Park, H. W., et al. (2016). Biological control of *Meloidogyne incognita* by *Aspergillus niger* F22 producing oxalic acid. *PLoS. One.* 11:e0156230. doi: 10.1371/journal.pone.0156230
- Jones, J. T., Haegeman, A., Danchin, E. G., Gaur, H. S., Helder, J., Jones, M. G., et al. (2013). Top 10 plant-parasitic nematodes in molecular plant pathology. *Mol. Plant Pathol.* 14, 946–961. doi: 10.1111/mpp.12057
- Kalaiselvi, D., Mohankumar, A., Shanmugam, G., Thirupathi, G., Nivitha, S., and Sundararaj, P. (2019). Altitude-related changes in the phytochemical profile of essential oils extracted from *Artemisia nilagirica* and their nematicidal activity against *Meloidogyne incognita*. *Ind. Crop Prod.* 139:111472. doi: 10.1016/j.indcrop.2019.111472
- Keller, N. P. (2019). Fungal secondary metabolism: regulation, function and drug discovery. *Nat. Rev. Microbiol.* 17, 167–180. doi: 10.1038/s41579-018-0121-1
- Kim, T. Y., Jang, J. Y., Jeon, S. J., Lee, H. W., Bae, C.-H., Yeo, J. H., et al. (2016). Nematicidal activity of kojic acid produced by *Aspergillus oryzae* against *Meloidogyne incognita*. *J. Microbiol. Biotechnol.* 26, 1383–1391. doi: 10.4014/jmb.1603.03040
- Kim, T. Y., Jang, J. Y., Yu, N. H., Chi, W. J., Bae, C. H., Yeo, J. H., et al. (2018). Nematicidal activity of grammicin produced by *Xylaria grammica* KCTC 13121BP against *Meloidogyne incognita*. *Pest. Manag. Sci.* 74, 384–391. doi: 10.1002/ps.4717
- King, E. D., Bassi, A. B. Jr., Ross, D. C., and Druebbisch, B. (2011). An industry perspective on the use of “atoxicogenic” strains of *Aspergillus flavus* as biological control agents and the significance of cyclopiazonic acid. *Toxin Rev.* 30, 33–41. doi: 10.3109/15569543.2011.588818
- Kundu, D., Hazra, C., and Chaudhari, A. (2016). Statistical modeling and optimization of culture conditions by response surface methodology for 2, 4- and 2, 6-dinitrotoluene biodegradation using *Rhodococcus pyridinivorans* NT2. *3 Biotech* 6:155. doi: 10.1007/s13205-016-0468-9
- Kusano, M., Koshino, H., Uzawa, J., Fujioka, S., Kawano, T., and Kimura, Y. (2000). Nematicidal alkaloids and related compounds produced by the fungus *Penicillium cf. simplicissimum*. *Biosci. Biotechnol. Biochem.* 64, 2559–2568. doi: 10.1271/bbb.64.2559
- Le Bars, J. (1979). Cyclopiazonic acid production by *Penicillium camemberti* Thom and natural occurrence of this mycotoxin in cheese. *Appl. Environ. Microbiol.* 38, 1052–1055. doi: 10.1128/aem.38.6.1052-1055.1979
- Liang, L., Liu, Z., Liu, L., Li, J., Gao, H., Yang, J., et al. (2016). The nitrate assimilation pathway is involved in the trap formation of *Arthrobotrys oligospora*, a nematode-trapping fungus. *Fungal. Genet. Biol.* 92, 33–39. doi: 10.1016/j.fgb.2016.05.003
- Lim, Y. H., Foo, H. L., Loh, T. C., Mohamad, R., and Abdul Rahim, R. (2020). Rapid evaluation and optimization of medium components governing tryptophan production by *Pediococcus acidilactici* TP-6 isolated from Malaysian food via statistical approaches. *Molecules* 25:779. doi: 10.3390/molecules25040779
- Lim, Y. H., Foo, H. L., Loh, T. C., Mohamad, R., Rahim, R. A., and Idrus, Z. (2019). Optimized medium via statistical approach enhanced threonine production by *Pediococcus pentosaceus* TL-3 isolated from Malaysian food. *Microb. Cell. Fact.* 18:125. doi: 10.1186/s12934-019-1173-2
- Lin, A.-Q., Du, L., Fang, Y.-C., Wang, F.-Z., Zhu, T.-J., Gu, Q.-Q., et al. (2009). iso- $\alpha$ -Cyclopiazonic acid, a new natural product isolated from the marine-derived fungus *Aspergillus flavus* CF-3. *Chem. Nat. Compd.* 45, 677. doi: 10.1007/s10600-009-9433-8
- Luk, K., Kobbe, B., and Townsend, J. (1977). Production of cyclopiazonic acid by *Aspergillus flavus* link. *Appl. Environ. Microbiol.* 33, 211–212. doi: 10.1128/AEM.33.1.211-212.1977
- Malhadas, C., Malheiro, R., Pereira, J. A., de Pinho, P. G., and Baptista, P. (2017). Antimicrobial activity of endophytic fungi from olive tree leaves. *World J. Microbiol. Biotechnol.* 33:46. doi: 10.1007/s11274-017-2216-7
- Martinez-Medina, A., Fernandez, I., Lok, G. B., Pozo, M. J., Pieterse, C. M., and Van Wees, S. C. (2017). Shifting from priming of salicylic acid to jasmonic acid-regulated defences by *Trichoderma* protects tomato against the root knot nematode *Meloidogyne incognita*. *New Phytol.* 213, 1363–1377. doi: 10.1111/nph.14251
- Miao, G.-P., Han, J., Zhang, K.-G., Wang, S.-C., and Wang, C.-R. (2019). Protection of melon against *Fusarium* wilt-root knot nematode complex by endophytic fungi *Penicillium brefeldianum* HS-1. *Symbiosis* 77, 83–89. doi: 10.1007/s13199-018-0565-0
- Moen, M., Perry, R. N., and Starr, J. L. (2009). “Meloidogyne species—a diverse group of novel and important plant parasites,” in *Root-Knot Nematodes*, eds R. N. Perry, M. Moens, and J. L. Starr (Wallingford: CAB), 483.
- Moncoq, K., Trieber, C. A., and Young, H. S. (2007). The molecular basis for cyclopiazonic acid inhibition of the sarcoplasmic reticulum calcium pump. *J. Biol. Chem.* 282, 9748–9757. doi: 10.1074/jbc.M611653200
- Morrissey, R. E., Norred, W. P., Cole, R. J., and Dörner, J. (1985). Toxicity of the mycotoxin, cyclopiazonic acid, to Sprague-Dawley rats. *Toxicol. Appl. Pharmacol.* 77, 94–107. doi: 10.1016/0041-008X(85)90271-6
- Murslain, M., Javed, N., Khan, S. A., Khan, H. U., Abbas, H., and Kamran, M. (2014). Combined efficacy of *Moringa oleifera* leaves and a fungus, *Trichoderma harzianum* against *Meloidogyne javanica* on eggplant. *Pak. J. Zool.* 46, 827–832.
- Nakahara, S., Kusano, M., Fujioka, S., Shimada, A., and Kimura, Y. (2004). Penipratynolene, a novel nematicide from *Penicillium bilaiae* Chalabuda. *Biosci. Biotechnol. Biochem.* 68, 257–259. doi: 10.1271/bbb.68.257
- Naz, I., Khan, R. A. A., Masood, T., Baig, A., Siddique, I., and Haq, S. (2021). Biological control of root knot nematode, *Meloidogyne incognita*, in vitro, greenhouse and field in cucumber. *Biol. Control* 152:104429. doi: 10.1016/j.biocontrol.2020.104429
- Nelofer, R., Ramanan, R. N., Abd Rahman, R. N. Z. R., Basri, M., and Ariff, A. B. (2012). Comparison of the estimation capabilities of response surface methodology and artificial neural network for the optimization of recombinant lipase production by *E. coli* BL21. *J. Ind. Microbiol. Biotechnol.* 39, 243–254. doi: 10.1007/s10295-011-1019-3
- Nelson, E., Li, C., Bangalore, R., Benson, T., Kass, R., and Hinkle, P. (1994). Inhibition of L-type calcium-channel activity by thapsigargin and 2, 5-t-butylhydroquinone, but not by cyclopiazonic acid. *Biochem. J.* 302, 147–154. doi: 10.1042/bj3020147
- Newman, L., Duffus, A. L., and Lee, C. (2016). Using the free program MEGA to build phylogenetic trees from molecular data. *Am. Biol. Teach.* 78, 608–612. doi: 10.1525/abt.2016.78.7.608
- Nguyen, H. T., Kim, S., Yu, N. H., Park, A. R., Yoon, H., Bae, C. H., et al. (2019). Antimicrobial activities of an oxygenated cyclohexanone derivative isolated from *Amphirosellinia nigrospora* JS-1675 against various plant pathogenic bacteria and fungi. *J. Appl. Microbiol.* 126, 894–904. doi: 10.1111/jam.14138
- Nguyen, L. T. T., Jang, J. Y., Kim, T. Y., Yu, N. H., Park, A. R., Lee, S., et al. (2018). Nematicidal activity of verrucarins A and roridin A isolated from

- Myrothecium verrucaria* against *Meloidogyne incognita*. *Pestic. Biochem. Physiol.* 148, 133–143.
- No, A. (2013). Experimental design and optimisation (4): plackett–burman designs. *Anal. Methods* 5, 1901–1903.
- Nor, N. M., Mohamed, M. S., Loh, T. C., Foo, H. L., Rahim, R. A., Tan, J. S., et al. (2017). Comparative analyses on medium optimization using one-factor-at-a-time, response surface methodology, and artificial neural network for lysine–methionine biosynthesis by *Pediococcus pentosaceus* RF-1. *Biotechnol. Biotechnol. Equip.* 31, 935–947. doi: 10.1080/13102818.2017.1335177.
- Oliveira, C., Rosmaninho, J., and Rosim, R. (2006). Aflatoxin M1 and cyclopiazonic acid in fluid milk traded in São Paulo. *Brazil. Food Addit. Contam.* 23, 196–201.
- Ostry, V., Toman, J., Grosse, Y., and Malir, F. (2018). Cyclopiazonic acid: 50th anniversary of its discovery. *World Mycotoxin J.* 11, 135–148.
- Palomares-Rius, J. E., Escobar, C., Cabrera, J., Vovlas, A., and Castillo, P. (2017). Anatomical alterations in plant tissues induced by plant-parasitic nematodes. *Front. Plant. Sci.* 8:1987. doi: 10.3389/fpls.2017.01987
- Phukon, L. C., Chourasia, R., Kumari, M., Godan, T. K., Sahoo, D., Parameswaran, B., et al. (2020). Production and characterisation of lipase for application in detergent industry from a novel *Pseudomonas helmanticensis* HS6. *Bioresour. Technol.* 309:123352. doi: 10.1016/j.biortech.2020.123352
- Plackett, R. L., and Burman, J. P. (1946). The design of optimum multifactorial experiments. *Biometrika* 33, 305–325. doi: 10.1093/biomet/33.4.305
- Plenge-Tellechea, F., Soler, F., and Fernandez-Belda, F. (2001). On the inhibition mechanism of sarcoplasmic or endoplasmic reticulum  $Ca^{2+}$ -ATPases by cyclopiazonic acid. *J. Biol. Chem.* 272, 2794–2800. doi: 10.1074/jbc.272.5.2794
- Pourhosseini, R., Sedaghati, E., Fani, S. R., Nadi, M., Moradi, M., and Ahmadi, Z. (2020). Potential of cyclopiazonic acid production in non-aflatoxinogenic strains of *Aspergillus flavus* of Iranian Pistachio. *PHJ* 3, 6–17. doi: 10.22123/PHJ.2021.262373.1067
- Purchase, I. (1971). The acute toxicity of the mycotoxin cyclopiazonic acid to rats. *Toxicol. Appl. Pharmacol.* 18, 114–123. doi: 10.1016/0041-008x(71)90320-6
- Raissi, S., and Farsani, R.-E. (2009). Statistical process optimization through multi-response surface methodology. *World Acad. Sci. Eng. Technol.* 51, 267–271.
- Rajasekharan, S. K., Kim, S., Kim, J.-C., and Lee, J. (2020). Nematicidal activity of 5-iodoindole against root-knot nematodes. *Pestic. Biochem. Physiol.* 163, 76–83.
- Rao, V. K., Navale, V., Ajmera, S., and Dhuri, V. (2021). *Aspergillus* derived mycotoxins in food and the environment: prevalence, Detection, and Toxicity. *Toxicol. Rep.* 8, 1008–1030. doi: 10.1016/j.toxrep.2021.04.013
- Rigas, F., Dritsa, V., Marchant, R., Papadopoulou, K., Avramides, E., and Hatzianestis, I. (2005). Biodegradation of lindane by *Pleurotus ostreatus* via central composite design. *Environ. Int.* 31, 191–196. doi: 10.1016/j.envint.2004.09.024
- Sánchez-Moreno, S., Jiménez, L., Alonso-Prados, J., and García-Baudin, J. (2010). Nematodes as indicators of fumigant effects on soil food webs in strawberry crops in Southern Spain. *Ecol. Indic.* 10, 148–156. doi: 10.1016/j.ecolind.2009.04.010
- Schneider, P., and Orelli, O. (1947). *Entomologisches Praktikum*. Aarau: Verlag, HR Sauerländer Co.
- Seidler, N. W., Jona, I., Vegh, M., and Martonosi, A. (1989). Cyclopiazonic acid is a specific inhibitor of the  $Ca^{2+}$ -ATPase of sarcoplasmic reticulum. *J. Biol. Chem.* 264, 17816–17823.
- Shang, Z., Li, X., Meng, L., Li, C., Gao, S., Huang, C., et al. (2012). Chemical profile of the secondary metabolites produced by a deep-sea sediment-derived fungus *Penicillium commune* SD-118. *Chin. J. Ocean. Limnol.* 30, 305–314. doi: 10.1007/s00343-012-1075-1
- Shephard, G. S. (2008). Risk assessment of aflatoxins in food in Africa. *Food Addit. Contam.* 25, 1246–1256. doi: 10.1080/02652030802036222
- Siddiqui, Z. A., and Akhtar, M. S. (2009). Effects of antagonistic fungi, plant growth-promoting rhizobacteria, and arbuscular mycorrhizal fungi alone and in combination on the reproduction of *Meloidogyne incognita* and growth of tomato. *J. Gen. Plant. Pathol.* 75, 144. doi: 10.1007/s10327-009-0154-4
- Sikandar, A., Zhang, M., Zhu, X., Wang, Y., Ahmed, M., Iqbal, M., et al. (2019). Efficacy of *Penicillium chrysogenum* strain SNEF1216 against root-knot nematodes (*Meloidogyne incognita*) in cucumber (*Cucumis sativus* L.) under greenhouse conditions. *Sci. Rep.* 17, 12451–12464.
- Singh, V., Haque, S., Niwas, R., Srivastava, A., Pasupuleti, M., and Tripathi, C. K. M. (2017). Strategies for fermentation medium optimization: an in-depth review. *Front. Microbiol.* 7:2087. doi: 10.3389/fmicb.2016.02087
- Srivastava, A., Singh, V., Haque, S., Pandey, S., Mishra, M., Jawed, A., et al. (2018). Response surface methodology-genetic algorithm based medium optimization, purification, and characterization of cholesterol oxidase from *Streptomyces rimosus*. *Sci. Rep.* 8:10913. doi: 10.1038/s41598-018-29241-9
- Tamura, K., Stecher, G., Peterson, D., Filipski, A., and Kumar, S. (2013). MEGA6: molecular evolutionary genetics analysis version 6.0. *Mol. Biol. Evol.* 30, 2725–2729. doi: 10.1093/molbev/mst197
- Termorshuizen, A., Korthals, G., and Thoden, T. (2011). Organic amendments and their influences on plant-parasitic and free-living nematodes: a promising method for nematode management? *J. Nematol.* 13, 133–153. doi: 10.1163/138855410X541834
- Toghueo, R. M. K., and Boyom, F. F. (2020). Endophytic *Penicillium* species and their agricultural, biotechnological, and pharmaceutical applications. *3 Biotech* 10, 1–35. doi: 10.1007/s13205-020-2081-1
- Trucksess, M. W., Mislivec, P. B., Young, K., Bruce, V. R., and Page, S. W. (1987). Cyclopiazonic acid production by cultures of *Aspergillus* and *Penicillium* species isolated from dried beans, corn meal, macaroni, and pecans. *J. Assoc. Off. Anal. Chem.* 70, 123–126. doi: 10.1093/jaoac/70.1.123
- Urano, T., Trucksess, M. W., Beaver, R. W., Wilson, D. M., Dorner, J. W., and Dowell, F. E. (1992). Co-occurrence of cyclopiazonic acid and aflatoxins in corn and peanuts. *J. AOAC Int.* 75, 838–841. doi: 10.1093/jaoac/75.5.838
- Van Rensburg, S. (1984). Subacute toxicity of the mycotoxin cyclopiazonic acid. *Food Chem. Toxicol.* 22, 993–998. doi: 10.1016/0278-6915(84)90149-2
- Viglierchio, D., and Schmitt, R. V. (1983). On the methodology of nematode extraction from field samples: baermann funnel modifications. *J. Nematol.* 15, 438.
- Watson, T. T., Nelson, L. M., Neilsen, D., Neilsen, G. H., and Forge, T. A. (2017). Soil amendments influence *Pratylenchus penetrans* populations, beneficial rhizosphere microorganisms, and growth of newly planted sweet cherry. *Appl. Soil Ecol.* 117, 212–220. doi: 10.1016/j.apsoil.2017.04.014
- Wu, H., Masler, E. P., Rogers, S. T., Chen, C., and Chitwood, D. J. (2014). Benzyl isothiocyanate affects development, hatching and reproduction of the soybean cyst nematode *Heterodera glycines*. *J. Nematol.* 16, 495–504. doi: 10.1163/15685411-00002781
- Yang, C., Zhao, D., Tan, Z., Zhu, X., Liu, X., Duan, Y., et al. (2016). Ferment optimization of biocontrol fungus SNEf against *Meloidogyne incognita* by response surface methodology. *Chin. J. Biol. Control* 32, 503–510.
- Yeon, J., Park, A. R., Kim, Y. J., Seo, H. J., Yu, N. H., Ha, S., et al. (2019). Control of root-knot nematodes by a mixture of maleic acid and copper sulfate. *Plant Pathol. J.* 141, 61–68. doi: 10.5423/PPJ.OA.08.2019.0225
- Zain, M. E. (2011). Impact of mycotoxins on humans and animals. *J. Saudi Chem. Soc.* 15, 129–144. doi: 10.1016/j.jscs.2010.06.006
- Zarabi, M., Hasanzadeh, M., Mohammadifar, M., Sahebany, N., and Etebarian, H. R. (2012). Effect of cultural condition on biomass production of some nematophagous fungi as biological control agent. *Egypt. Acad. J. Biol. Sci.* 5, 115–126. doi: 10.21608/EAJBSA.2012.14947
- Zhang, S., Gan, Y., Liu, J., Zhou, J., and Xu, B. (2020). Optimization of the fermentation media and parameters for the bio-control potential of *Trichoderma longibrachiatum* T6 against Nematodes. *Front. Microbiol.* 11:574601. doi: 10.3389/fmicb.2020.574601

**Conflict of Interest:** The authors declare that the research was conducted in the absence of any commercial or financial relationships that could be construed as a potential conflict of interest.

**Publisher's Note:** All claims expressed in this article are solely those of the authors and do not necessarily represent those of their affiliated organizations, or those of the publisher, the editors and the reviewers. Any product that may be evaluated in this article, or claim that may be made by its manufacturer, is not guaranteed or endorsed by the publisher.

Copyright © 2021 Nguyen, Yu, Lee, Hwang, Bui and Kim. This is an open-access article distributed under the terms of the Creative Commons Attribution License (CC BY). The use, distribution or reproduction in other forums is permitted, provided the original author(s) and the copyright owner(s) are credited and that the original publication in this journal is cited, in accordance with accepted academic practice. No use, distribution or reproduction is permitted which does not comply with these terms.



## OPEN ACCESS

## Edited by:

Florence Fontaine,  
Université de Reims  
Champagne-Ardenne, France

## Reviewed by:

Kulandaivelu Velmourougane,  
Central Institute for Cotton Research  
(ICAR), India  
Chunxu Song,  
China Agricultural University, China

## \*Correspondence:

Aundy Kumar  
kumar@iari.res.in  
orcid.org/0000-0002-7401-9885

## † Present address:

Pierre Eke,  
College of Technology, Department  
of Crop Production Technology,  
University of Bamenda, Bamili, North  
West Region, Cameroon  
Narayanasamy Prabhakaran,  
Research and Development Centre,  
T. Stanes & Company Ltd.,  
Coimbatore, India

## Specialty section:

This article was submitted to  
Microbe and Virus Interactions with  
Plants,  
a section of the journal  
Frontiers in Microbiology

Received: 21 September 2021

Accepted: 20 October 2021

Published: 30 November 2021

## Citation:

Sahu KP, Patel A, Kumar M,  
Sheoran N, Mehta S, Reddy B, Eke P,  
Prabhakaran N and Kumar A (2021)  
Integrated Metabarcoding  
and Culturomic-Based Microbiome  
Profiling of Rice Phyllosphere Reveal  
Diverse and Functional Bacterial  
Communities for Blast Disease  
Suppression.  
Front. Microbiol. 12:780458.  
doi: 10.3389/fmicb.2021.780458

# Integrated Metabarcoding and Culturomic-Based Microbiome Profiling of Rice Phyllosphere Reveal Diverse and Functional Bacterial Communities for Blast Disease Suppression

Kuleshwar Prasad Sahu<sup>1</sup>, Asharani Patel<sup>1</sup>, Mukesh Kumar<sup>1</sup>, Neelam Sheoran<sup>1</sup>, Sahil Mehta<sup>2</sup>, Bhaskar Reddy<sup>1</sup>, Pierre Eke<sup>††</sup>, Narayanasamy Prabhakaran<sup>††</sup> and Aundy Kumar<sup>1\*</sup>

<sup>1</sup> Division of Plant Pathology, ICAR-Indian Agricultural Research Institute, New Delhi, India, <sup>2</sup> Crop Improvement Group, International Centre for Genetic Engineering and Biotechnology, New Delhi, India

Phyllosphere—the harsh foliar plant part exposed to vagaries of environmental and climatic variables is a unique habitat for microbial communities. In the present work, we profiled the phyllosphere microbiome of the rice plants using 16S rRNA gene amplicon sequencing (hereafter termed metabarcoding) and the conventional microbiological methods (culturomics) to decipher the microbiome assemblage, composition, and their functions such as antibiosis and defense induction against rice blast disease. The blast susceptible rice genotype (PRR78) harbored far more diverse bacterial species (294 species) than the resistant genotype (Pusa1602) that showed 193 species. Our metabarcoding of bacterial communities in phyllosphere revealed the predominance of the phylum, Proteobacteria, and its members *Pantoea*, *Enterobacter*, *Pseudomonas*, and *Erwinia* on the phyllosphere of both rice genotypes. The microbiological culturomic validation of metabarcoding-taxonomic annotation further confirmed the prevalence of 31 bacterial isolates representing 11 genera and 16 species with the maximum abundance of *Pantoea*. The phyllosphere-associated bacterial members displayed antifungal activity on rice blast fungus, *Magnaporthe oryzae*, by volatile and non-volatile metabolites. Upon phyllobacterization of rice cultivar PB1, the bacterial species such as *Enterobacter sacchari*, *Microbacterium testaceum*, *Pantoea ananatis*, *Pantoea dispersa*, *Pantoea vagans*, *Pseudomonas oryzae*, *Rhizobium* sp., and *Sphingomonas* sp. elicited a defense response and contributed to the suppression of blast disease. qRT-PCR-based gene expression analysis indicated over expression of defense-associated genes such as *OsCEBiP*, *OsCERK1*, and phytohormone-associated genes such as *OsPAD4*, *OsEDS1*, *OsPR1.1*, *OsNPR1*, *OsPDF2.2*, and *OsFMO* in phyllobacterized rice seedlings. The phyllosphere bacterial species showing blast suppressive activity on rice were found non-plant



pathogenic in tobacco infiltration assay. Our comparative microbiome interrogation of the rice phyllosphere culminated in the isolation and identification of agriculturally significant bacterial communities for blast disease management in rice farming through phylломicrobiome engineering in the future.

**Keywords:** antibiosis, blast, defense genes, *Magnaporthe oryzae*, microbiome, phyllosphere, rice, immunocompetence

## INTRODUCTION

Microbial communities have an evolutionary association with plant populations where they function as metaorganisms in the natural environment. Here, the microbial activities in total termed microbiomes play a pivotal role in plant development and survival (Hartmann et al., 2008; Bulgarelli et al., 2013; Berg et al., 2016). The microbial communities associated with the plants are called plant microbiome and microbial metagenome that often confer functional flexibility to the plant genome (Sessitsch et al., 2012). The plant microbiomes are presumed to modulate a variety of plant functions. However, the ecological role of the phyllosphere microbial communities on plant functional ecology is among the most understudied and underrated aspects in plant biology.

The microbial life on the foliar niche, the phyllosphere microbiome, is constantly exposed to vagaries of weather events, and other agronomic practices in crop husbandry (Lindow and Leveau, 2002). Currently, the epiphytic phyllosphere microbiomes and their natural functions are increasingly investigated in crops like rice, wheat, maize, and soybean (Andrews and Harris, 2000; Bertani et al., 2016; Compant et al., 2019; Sahu et al., 2020). It is further reported that plant-associated bacteria are prolific for the secretion of primary and secondary metabolites and volatiles for plant growth, developmental regulation, and defense against stresses (Munjal et al., 2016; Rascovan et al., 2016; Sheoran et al., 2016; Gómez Expósito et al., 2017; Eke et al., 2019; Ashajyothi et al., 2020; Vandana et al., 2021).

Rice is the primary staple for the nearly three billion world population and contributes to global food security. Rice production is affected by several biotic and abiotic stresses; among them, blast disease caused by ascomycetous fungus *Magnaporthe oryzae* (anamorph *Pyricularia oryzae* Sacc.) is responsible for nearly 30.0% of losses, which can feed 60 million population if prevented preemptively (Dean et al., 2005; Scheuermann et al., 2012; Yasuda et al., 2015; Hashim et al., 2018; Mehta et al., 2019; Prakash et al., 2021). Deployment of fungicides and blast-resistant cultivars are among the blast-combating strategies widely practiced. However, both strategies are under scanner as the chemicals are no longer encouraged due to safety considerations, and the host resistance is not durable (Nalley et al., 2016; Asibi et al., 2019; Sella et al., 2021). Recently, the fungicide residues intercepted on the Indian rice imports have prompted many countries to reject consignments from international trade (Al-Antary et al., 2020). Under this scenario, there is a growing demand among the various stakeholders of the rice production system for an alternative

blast mitigation strategy. One promising yet unexplored strategy is the biological control of blast disease by deploying leaf microbiota that shares the same microecological niche with the blast pathogen, *M. oryzae*. So far, the potential of phyllosphere microbial communities sharing the leaf microhabitat with *Magnaporthe*—the incitant of blast disease has not yet been harnessed to mitigate the disease in any crop. Hence, the present investigation was carried out to explore the phyllo-microbiome of rice and exploit them for blast disease suppression by microbiome reengineering.

## MATERIALS AND METHODS

### Study Location and Sampling for Microbiome Analysis

The 16S rRNA gene amplicon sequencing by NGS (hereafter cited as metabarcoding; Berg et al., 2020), combined with conventional culturomic investigation of phylломicrobiome, was conducted. For this, we planted rice genotypes in a blast-endemic mountain ecosystem in Palampur, Himachal Pradesh, India (32°6'4.7"N and 76°32'39.79"E) located at an altitude of 1,275 m above mean sea level [weather conditions: mean temperature 22–23°C; precipitation 700–1,000 mm; RH 60.0%; sunshine hours 300–350; source: <https://en.climate-data.org>; [www.worldweatheronline.com](http://www.worldweatheronline.com)]. The rice genotypes were grown during the rice-growing season in August to September 2014. Briefly, rice genotypes PRR78—a blast susceptible variety, and Pusa1602—a near-isogenic line of PRR78 introgressed with *Pi2* gene conferring complete resistance to blast disease (Singh et al., 2012), were planted in parallel rows with a spacing of 20 cm by adopting all crop husbandry practices. Leaf samples were excised at 15 and 30 days post-sowing in sterilized falcon tubes and brought to the laboratory in an insulated cool container maintained at a temperature of 4.0 ± 1.0°C and processed for microbiome analysis by metabarcoding and culturomic analysis.

### Profiling of Phylломicrobiome by Metabarcoding

#### Extraction and Isolation of Epiphytic Microbial Community Genomic DNA

Leaf (5.0 g) samples were shaken with 50 ml of sterile phosphate buffer saline [PBS, g L<sup>-1</sup> NaCl 8; KCl 0.2; Na<sub>2</sub>HPO<sub>4</sub> 1.44; KH<sub>2</sub>PO<sub>4</sub> 0.24; pH-7.4] amended with 0.1% Tween-20 (PBS-T) to dislodge the epiphytic microbiome. The leaf epiphytic microbiome was extracted six times serially in 50 ml of



PBS-T by agitating for 30 min at 250 rpm and vortexing for 10 s. Thus, the collected epiphytic-microbial suspension (300 ml) was collected aseptically in a presterilized container and centrifuged at  $12,000 \times g$  for 60 min at  $4.0^{\circ}\text{C}$  to collect the epiphytic microbial cells. Thus, the obtained pellet was processed to isolate genomic DNA by the cetyltrimethyl ammonium bromide (CTAB) method reported by Moore et al. (2004) with slight modifications like avoidance of phenol in the extraction steps. The quality and quantity of microbial community genomic DNA was determined electrophoretically, spectrophotometrically (Nanodrop 2000, Thermo Scientific, United States), and fluorometrically using Qubit dsDNA BR Assay (Thermo Fisher Scientific Inc., United States).

### Preparation of Sequencing Libraries for $2 \times 300$ -bp Run Chemistry

The amplicon libraries were prepared using *Nextera XT Index Kit* (Illumina Inc.) as per the 16S rRNA Gene Amplicon Sequencing Library Preparation Protocol (Part no. 15044223 Rev. B). PCR primers for the amplification of the 490-bp hypervariable region of V3–V4 of 16S rRNA gene of Eubacteria were designed, synthesized, and used. The sequences of the primers are V3F: 5'CCTACGGGNGGCWGCAG3' and V4R: 5'GACTACHVGGGTATCTAATCC3'. The target amplicons were generated using the fusion primer that consists of Illumina adaptors and multiplex index sequence as per the instructions of the manufacturer. The amplicon libraries were purified by  $1 \times$  AMPure XP beads and checked on Agilent High Sensitivity (HS) chip on Bioanalyzer 2100 and quantified on fluorometer by Qubit dsDNA HS-Assay kit (Life Technologies, United States). Quality-passed libraries were equimolar pooled and then sequenced using the Illumina MiSeq platform with  $2 \times 300$ -bp paired-end sequencing chemistry following the protocols of the manufacturer (Illumina, San Diego, CA, United States).

### Bioinformatic Analyses

Initially, the sequenced raw forward reads (R1) and reverse reads (R2) were scanned and analyzed using the FastQC version (Andrews, 2018) to assess the quality of 16S rRNA amplicon reads. Thus, the obtained raw reads were end trimmed and curated using Trimmomatic v0.35 (Bolger et al., 2014) with the following command and settings: (i) remove adapter sequences, (ii) ambiguous reads (reads with unknown nucleotides "N" larger than 5.0%), and (iii) low-quality sequences [reads with more than 10.0% quality threshold (quality value)  $< 20$  Phred score]. The resultant quality-passed read pairs were joined using PEAR (Paired-End reAdmergeR) version 0.9.8 (Zhang et al., 2014) with default parameters. The joined paired reads were further processed for downstream taxonomic classification where unpaired reads were discarded. The taxonomic classification of resultant high-quality reads was performed using MG-RAST v4.0, wherein (i) 16S rRNA gene sequence reads were sorted using Sortme RNA, (ii) sorted reads were clustered at  $\geq 97\%$  similarity using CD-HIT method, and (iii) clustered reads were taxonomically classified using SILVA SSU database. The clustered reads and taxon abundance downloaded  $> 100$  bases and 90.0% similarity

through the best hit classification. Furthermore, PAST v2.17c (Hammer et al., 2001) was used for the determination of  $\alpha$ -diversity.

## Phyllosphere Microbiome Interrogation by Culturomic Methods

### Isolation and Characterization of the Culturable Epiphytic Microbiome

Another set of leaves (500 mg) excised from the rice genotypes were analyzed using the culturomic method on nutrient agar medium [NA, g  $\text{L}^{-1}$ ; peptone 5.0; beef extract 3.0; NaCl 5.0; agar 15.0; pH  $7.0 \pm 0.2$ ]. Briefly, the leaf was agitated with 50 ml of sterile phosphate buffer saline amended with 0.1% Tween-20 (PBST) for 30 min at 250 rpm followed by vortexing for 10 s; the aliquot, thus, obtained was decimally diluted up to  $10^{-5}$ . An aliquot of 1.0 ml at  $10^{-3}$ ,  $10^{-4}$ , and  $10^{-5}$  from each sample was pour plated in nutrient agar media supplemented with 2,3,5-tetrazolium chloride (50 mg  $\text{L}^{-1}$ ) and incubated at  $28 \pm 2^{\circ}\text{C}$  for 72 h for morphotyping the bacterial colonies. The culturable bacterial population and their diversity were assessed and quantified based on morphological traits, such as size, shape, color, texture, and margin. The pure culture of the representative isolates was preserved in  $-80$  and  $-20^{\circ}\text{C}$  as glycerol stock (30% V/V) for downstream work.

### Identification of Epiphytic Bacterial Species by 16S rRNA Gene Sequencing

Genomic DNA was isolated by the CTAB method described by Moore et al. (2004) with minor modifications as mentioned previously. Isolated and purified genomic DNA was quantitated and quality analyzed as described above. Finally, the genomic DNA reconstituted at  $100 \text{ ng } \mu\text{L}^{-1}$  was used as a template in PCR amplification. Box PCR-based DNA fingerprinting was performed for diversity analysis as well as to eliminate the duplicate isolates from the collection (Versalovic et al., 1994); this PCR-based DNA profiling technique specifically amplifies the non-coding conserved sequences in the bacterial genome and is considered a highly discriminatory DNA-fingerprinting technique (Kumar et al., 2004; Eke et al., 2019). Amplicon profiles were resolved in 1.0% agarose gel at 30 V for 10–12 h and imaged (QuantityOne, BioRad, United States). Isolates showing identical amplicon profiles were presumed to be duplicates. PCR amplification of the 16S rRNA gene was performed using primer sets, 27F (27F: 5'-AGAGTTTGATCCTGGCTCAG-3') and 1492R (1492R: 5'-GGTACCTTGTTACGACTT-3'), to amplify the 1,465-bp region (Sheoran et al., 2015; Munjal et al., 2016). Then the PCR amplicons resolved in the agarose gel (1.0 %) were purified and eluted using an elution kit according to the instructions of the manufacturer (Promega Corporation, United States). The amplicons were sequenced bidirectionally to achieve maximum coverage of the sequences and analyzed using the nucleotide-Basic Local Alignment Search Tool (BLAST) algorithm at the National Center for Biological Information (NCBI); the bacterial species identity was confirmed by closest match. The diversity analysis of culturable

phyllosphere bacterial species was calculated using Shannon diversity indices.

## Activity Screening of Epiphytic Phyllospheric Bacteria on *Magnaporthe oryzae*

### Antifungal Activity *in vitro*

Airborne volatile organic compounds emitted, and diffusible metabolites secreted, during bacterial growth were tested for antifungal activities on *M. oryzae*. Here, we conducted dual-culture confrontation assays, and mycelial inhibition over mock was calculated as described (Sheoran et al., 2015; Munjal et al., 2016). Additionally, the fungicidal or fungistatic nature of the antifungal activity of volatiles on *M. oryzae* was also determined. Here, the volatile exposed mycelia of *M. oryzae* showing complete inhibition were further incubated after replacing bacterial volatile with lid. Depending on the mycelial growth, the bacterial volatile was either categorized as fungicidal or fungistatic on *M. oryzae* (Sahu et al., 2020). The radial mycelial growth of *M. oryzae* was measured, and mycelial inhibition (%) over mock was calculated using the following formula

$$I = \frac{C-T}{C} \times 100$$

where I = percent inhibition

C = colony diameter in control

T = colony diameter in treatment

### Blast-Suppressive Activity *in planta*

The bacterial isolates showing inhibition of mycelial growth of *M. oryzae* were selected for *in planta* blast control assay. Here, blast-susceptible rice genotype, Pusa Basmati 1, was allowed to germinate in the bacterial cell suspension set at three different bacterial densities ( $\sim 10^6$ ,  $10^7$ , and  $10^8$  CFU ml<sup>-1</sup>) for 5 days. Upon germination, the transplants were further grown in a climate-controlled greenhouse set at a temperature of  $28.0 \pm 2.0^\circ\text{C}$ , relative humidity of  $90.0 \pm 10.0\%$ , and light/dark cycles of 14/10 h. Thus, the obtained 3-week-old seedlings were foliar sprayed (booster spray) with phyllosphere bacterial suspension ( $\sim 10^6$ ,  $10^7$ , and  $10^8$  CFU ml<sup>-1</sup>) and challenged with the conidia of *M. oryzae*-1637 prepared in water ( $2.0 \times 10^5$  conidia ml<sup>-1</sup>) (Rajashankara et al., 2017). Blast disease severity was determined 7 days post-inoculation on a 0.0–5.0 disease rating scale where 0.0 = no evidence of infection; 1.0 = brown specks <0.5 mm in diameter; 2.0 = brown specks of 0.5–1.0 mm in diameter; 3.0 = round to elliptical lesions of about 1–3 mm in diameter; 4.0 = typical spindle-shaped blast lesion of 3.0 mm or more with little or no coalescence of the lesion; 5.0 = the same as 4.0 but half or more leaves killed by coalescence of lesions. Plants scored 0.0–2.0 were rated resistant, 3.0 as moderately susceptible, and 4.0–5.0 as susceptible (Mackill and Bonman, 1992). The disease severity was calculated using the following formula.

$$\text{Disease severity} = \frac{\sum (\text{Scale} \times \text{Number of plants infected}) \times 100}{\text{Total number of plants} \times \text{Maximum disease scale}}$$

Furthermore, the percent reduction in disease severity compared with control was estimated using the following formula:

$$\text{Reduction in Blast Severity} = \frac{C-T}{C} \times 100$$

C = disease severity in control

T = disease severity in treatment

## Phenotyping for Phyllosphere Microbiome Conferred Immunocompetence

The bacterial isolates showing antifungal activity on *M. oryzae* were selected for the immunocompetence assay. Here, the germination and phenotypic alterations induced on rice seedlings by bacterial isolates were monitored and scored. In this assay, the blast susceptible Pusa Basmati 1 was subjected to germination for 5 days in the presence of bacterial cells at varying densities such as  $10^6$ ,  $10^7$ ,  $10^8$ , and  $10^9$  (CFU mL<sup>-1</sup>). Similarly, seeds germinated in sterile double distilled water served as control. The experiment was performed in three replications with 50 seeds in each replication and repeated twice. The seed germination (%) was calculated using the following formula to evaluate the effect of bacterial interaction on germination.

$$\text{Seed germination (\%)} = \frac{\text{Number of germinated seeds}}{\text{Total number of seeds}} \times 100$$

To test the effect of bacterial colonization on the shoot and root growth, five randomly selected seedlings were scored. The percent deviation in shoot and root growth was calculated against the untreated mock seedlings using the following formula. Here, while the negative value indicated growth inhibition, the positive score indicated growth promotion.

$$G = \frac{T-C}{C} \times 100$$

where G = percent growth of shoot/root

C = length of shoot/root in control

T = length of shoot/root in the treatment

## Assessment of Immunocompetence by qPCR

Having confirmed the blast-suppressive potential of the phyllosphere bacterial species, we performed qPCR experiments to decipher the effect of bacterial supplementation on the expression of genes involved in defense pathways in rice. A total of nine phyllosphere bacterial isolates such as *Pantoea vagans* OsEp-Plm-30B3, *Pantoea ananatis* OsEp-Plm-15B6, *Enterobacter sacchari* OsEp-Plm-15B10, *P. ananatis* OsEp-Plm-30B17, *Pantoea dispersa* OsEp-Plm-15B14, *Rhizobium* sp. OsEp-Plm-30B4, *Microbacterium testaceum* OsEp-Plm-30B1, *Pseudomonas oryzae* sp. OsEp-Plm-15B16, and *Sphingomonas* sp. OsEp-Plm-15B2 that showed blast-suppressive activity on rice was chosen for the study.

Briefly, whole seedlings of Pusa Basmati 1, bacterized with  $2 \times 10^7$  CFU ml<sup>-1</sup> and sampled at 24-h interval for three consecutive days were immediately snap frozen in liquid nitrogen to stop all the cellular metabolic activity and then stored instantly at  $-80^\circ\text{C}$  until further use. The total RNA was isolated using the SV Tool RNA isolation system according to the instructions of the manufacturer (Promega, Madison, WI, United States). The quality and quantity of RNA were assessed spectrophotometrically (NanoDrop 2000, Thermo Scientific, United States) and electrophoretically.

## Transcriptional Analysis of Genes Associated With Immunocompetence

Eight rice genes, such as *OsCEBiP* (Akamatsu et al., 2013), *OsCERK1* (Kouzai et al., 2014), *OsPAD4* (Ke et al., 2014), *OsEDS1* (Ke et al., 2019), *OsNPR1* (Sugano et al., 2010), *OsPDF2.2* (Thomma et al., 2002), *OsFMO1* (Koch et al., 2006; Mishina and Zeier, 2006), and *OsPR1.1* (Breen et al., 2017), which were reported to play a role in rice defense, were selected; PCR primers targeting the above defense genes are furnished in **Supplementary Tables 1, 2**. qPCR was performed in Real-Time Thermal Cycler (LightCycler 96, Roche Life Science, Switzerland) using GoTaq® 1-Step RT-qPCR System (Promega Corporation, United States); qPCR reaction conditions were as follows: one cycle of reverse transcription at 37°C for 15 min followed by reverse transcriptase inactivation step at 95°C for 10 min followed by 30 cycles at 95°C for 10 s, annealing at 58°C for 30 s and extension at 72°C for 30 s followed by three-step melting at 95°C for 10 s, 63°C for 60 s, and 97°C for 1.0 s, and then a final cooling at 37°C for 30 s. Later, cyclic threshold data points were analyzed for the determination of gene expression relative to the reference housekeeping *OsActin* gene using the software LightCycler®96 Roche. The mean *Ct* values were considered for the calculation of  $2^{-\Delta\Delta C_T}$  to estimate the fold changes in gene expression.

## Hypersensitive Reaction on Tobacco

Upon bacterial infiltration on tobacco leaves, potential plant pathogenic bacteria are known to induce hypersensitive reactions (HR) (Klement, 1963); this is considered as a test to ascertain the plant pathogenic nature of bacterial isolates. The best performing nine bacterial isolates for suppression of blast disease were selected for this assay. Tobacco (*Nicotiana tabacum*) plants were grown under greenhouse conditions at 20°C, 50–60% relative humidity, and 12/12-h light/dark per day. Fully expanded leaves of 2 to 3-month-old plantlets were used in all experiments. Bacterial inoculum ( $1.0 \times 10^8$  CFU ml<sup>-1</sup>, absorbance at 600 nm = 1.0 OD) was infiltrated onto the leaves using a sterile hypodermal syringe. Thus, treated plants were incubated at 25–30°C under greenhouse conditions (12/12 h of dark/light photoperiods). Similarly, leaves infiltrated with sterile distilled water alone served as a negative control, and a well-known bacterial pathogen, *Ralstonia solanacearum*, served as a positive control. Plant responses to the bacterial infiltration on tobacco leaves were recorded after 24-h post-inoculation.

## Statistical Analysis

All datasets were analyzed using the data analytical tool available in MS Office Excel 2013. The analyzed data obtained were subjected to significance testing by analysis of variance (ANOVA) at a  $p \leq 0.05$  level of significance. Furthermore, various parameters like the standard error of the mean (SEm), standard error of the difference between two means (SEd), critical difference (CD), and coefficient of variation (CV) were estimated. For figures and tables, the values are represented as the mean of all biological and technical replicates. For the qPCR data analysis, the fold change values calculated for the defense genes

were imported into the GraphPad Prism program (<https://www.graphpad.com/scientific-software/prism>), and two-way ANOVA was conducted using Bonferroni *post-hoc* test for determining the statistical significance at \* $p \leq 0.05$ , \*\* $p = 0.001$ , and \*\*\* $p = 0.0001$ .

## RESULTS

### 16S rRNA Barcode Sequence Read Statistics and Diversity Indices

Phyllosphere microbiome profiling of blast-susceptible (PRR78) and blast-resistant rice (Pusa1602) genotypes planted in blast-endemic locations was conducted using integrated 16S rRNA gene amplicon sequencing and microbiological methods. The total curated sequence generated is in the range of 4, 31,222 for Pusa1602 and 1, 81,250 for PRR78 reads (**Table 1**). The  $\alpha$ -diversity indices (Shannon diversity) were 1.25 for Pusa1602 and 1.85 for PRR78. Other diversity indices were also marginally higher for PRR78 than Pusa1602 revealing that the blast-susceptible genotype harbored more diverse microbial species than the resistant type (**Table 1**).

### Structure and Composition of Phyllosphere Microbiome on Blast-Susceptible and Resistant Rice Genotypes

The metabarcoding-assisted taxonomic profiling of the phyllosphere microbiome of two rice genotypes revealed the abundance of bacterial phyla, Proteobacteria (70.7–91.0%), and class Gamma Proteobacteria on both the genotypes (70.4–91.0%). Bacterial communities belong to the order *Enterobacteriales* (89.2%) followed by *Pseudomonadales* (1.7%) was found dominant on Pusa1602, while *Enterobacteriales* (68.0%) followed by *Bacteroidales* (3.7%) and *Pseudomonadales* (2.2%) were in high frequency on susceptible genotype, PRR78. Further at the family level, *Enterobacteriaceae* (89.2%) followed

**TABLE 1** | Metabarcoding statistics and diversity indices of phyllosphere microbiome.

Parameters	Sample origin: Mid Himalayan mountain—Palampur, India	
	Pusa1602	PRR78
MG-RAST accession number*	mgm4619774.3	mgm4621255.3
Number of base pairs	201,387,096	221,346,634
Total number of sequences	4,39,681	4,68,994
Total number of reads	431,222	181,250
Simpson	0.6304	0.6936
Shannon	1.253	1.851
Evenness	0.01813	0.02166
Fisher- $\alpha$	19.03	33.71
Berger-Parker	0.4339	0.5018
Chao-1	310.4	421.7
Observed species	193	294

\*<https://www.mg-rast.org/>.



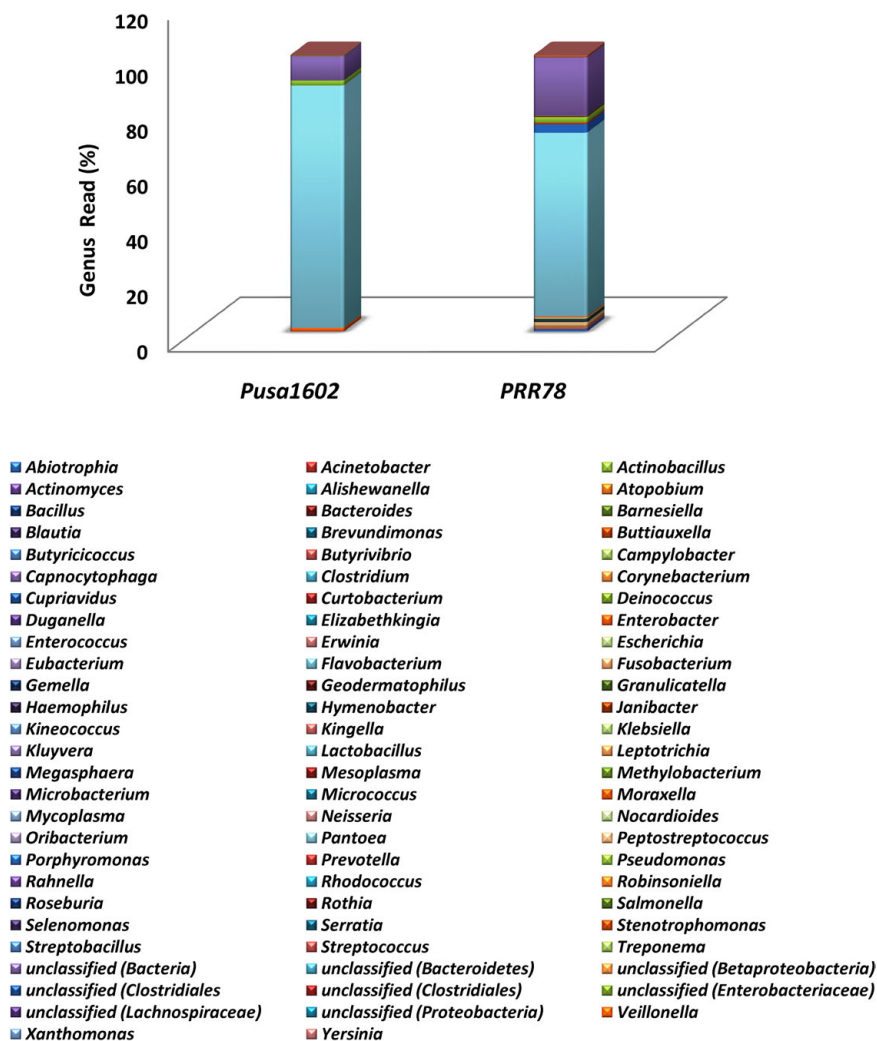
by *Pseudomonadaceae* (1.7%) in the resistant genotype and *Enterobacteriaceae* (68.0%) followed by *Porphyromonadaceae* (3.0%) and *Pseudomonadaceae* (2.0%) in the susceptible genotype were found overrepresented. Bacterial genus *Pantoea* (67.3–87.7%) was the most dominant bacteria on both the genotypes. Other dominant genera are *Pseudomonas*, *Enterobacter*, *Buttiauxella*, and *Erwinia* in the resistant genotype and *Porphyromonas*, *Pseudomonas*, *Abiotrophia*, *Enterobacter*, and *Gemella* in the susceptible genotype (Figure 1, Supplementary Figure 1, and Supplementary Table 3).

## Validation of Metabarcoding Sequence Data by Culturomic Methods

### Enumeration of Cultivable Microbiome and Identification of Bacterial Communities

Both the genotypes recorded the nearly identical epiphytic bacterial population ( $1.55\text{--}5.6 \log \text{CFU g}^{-1}$ )

(Supplementary Table 4). A total of 37 distinct morphotypes of bacterial isolates were enumerated with a diversity index ranging from 1.48 to 1.82 for all the cultured phyllosphere microbiome. The 30-day-old phyllosphere showed more bacterial population (21 morphotypes) and diversity compared with the 15-day seedlings (16 morphotypes). The results of diversity indices further revealed more bacterial diversity in the susceptible genotypes than in the resistant genotypes. The diversity indices of epiphytic bacteria on the rice phyllosphere are presented in Supplementary Table 5. BOX-PCR DNA fingerprinting of all 37 morphotypes culminated in 31 distinct BOX Amplicon Groups (Supplementary Figure 2). Isolates with identical amplicon profiles were considered duplicates, and a representative isolate for each of the BOX groups was retained and subjected to downstream work. The bacterial species identity was established through a 16S rRNA gene sequence analysis. The 31 distinct BOX amplicon groups represented 11 genera and 16 species. We also observed high-frequency occurrence of bacterial species



**FIGURE 1 |** Genus-level relative abundance of phyllosphere bacterial communities on rice genotypes; refer to **Supplementary Figure 1** for other taxonomic hierarchy.



like *Acinetobacter* (2), *Curtobacterium* (3), *Enterobacter* (4), *Microbacterium* (4), *Pantoea* (9), *Pseudomonas* (2), *Rhizobium* (2), and *Sphingomonas* (2) on the rice phyllosphere (Table 2 and Supplementary Figures 3, 4a–k). All cultured bacterial genera were also found among the mapped reads in the metabarcoding analysis (Figure 2 and Table 3).

## Activity Screening Against Rice Blast Fungus *Magnaporthe oryzae*

### Screening for Antifungal Activity

Dual-plate confrontation assay showed inhibition of the mycelial growth of *M. oryzae* by both volatiles and secreted metabolites produced by bacterial species. Among the 31 bacteria evaluated, 11 phyllosphere-associated bacterial isolates displayed over 40.0% inhibition of mycelial growth by their secreted metabolites (Table 4 and Supplementary Figure 5). The antagonistic bacterial isolates represented species, such as *Acinetobacter calcoaceticus*, *Enterobacter cloacae*, *E. sacchari*, *P. ananatis*, *P. vagans*, *P. oryzihabitans*, and *Sphingomonas* sp. Similarly, a total of 12 of them completely inhibited the growth of

*M. oryzae* (100% inhibition) by bacterial volatile organic compounds (Table 4 and Supplementary Figure 6). The antifungal volatile emitting bacterial isolates represented the species, such as *E. sacchari*, *M. testaceum*, *P. ananatis*, *P. dispersa*, *P. vagans*, *P. oryzihabitans*, and *Rhizobium* sp. Furthermore, while the volatile of seven bacterial isolates displayed fungicidal activity, the other five bacteria released fungistatic volatiles against *M. oryzae* as mycelial growth re-emerged upon removal of the volatile exposure (Supplementary Figure 7 and Supplementary Table 6).


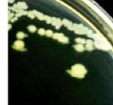

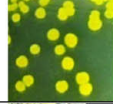





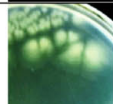
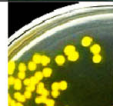
## Suppressive Effect of Phylломicrobiome on Blast Disease

Blast-susceptible rice cultivar, Pusa Basmati 1, was used for evaluating the blast-suppressive effects of rice phylломicrobiome. A total of 13 bacterial isolates representing *Pantoea* (eight strains), *Enterobacter* (one), *Microbacterium* (one), *Pseudomonas* (one), *Rhizobium* (one), and *Sphingomonas* (one) were evaluated at three different cell densities. Blast incidence and severity were scored as per the blast score chart recommended by

**TABLE 2 |** Identification of cultivated phyllosphere bacterial isolates by 16S rRNA gene sequencing.

Sequence ID	Organism	Sequence length (bp)	*Host	GenBank accession
OsEp_Plm_15B9	<i>Acinetobacter calcoaceticus</i>	1,409	PRR78	MT367784
OsEp_Plm_15B13	<i>Curtobacterium</i> sp.	1,400	PRR78	MT367788
OsEp_Plm_30B20	<i>Enterobacter ludwigii</i>	1,422	PRR78	MT367806
OsEp_Plm_30B8	<i>Pantoea ananatis</i>	1,401	PRR78	MT367799
OsEp_Plm_15B16	<i>Pseudomonas oryzihabitans</i>	1,403	PRR78	MT367791
OsEp_Plm_15B8	<i>Rhizobium taibaishanense</i>	1,349	PRR78	MT367783
OsEp_Plm_30B9	<i>Sphingomonas pseudosanguinis</i>	1,400	PRR78	MT367800
OsEp_Plm_15B4	<i>Acidovorax avenae</i>	1,400	PRR78 and Pusa1602	MT367779
OsEp_Plm_15B15	<i>Acinetobacter radioresistens</i>	1,402	PRR78 and Pusa1602	MT367790
OsEp_Plm_30B7	<i>Agrobacterium vitis</i>	1,400	PRR78 and Pusa1602	MT367798
OsEp_Plm_15B3	<i>Curtobacterium luteum</i>	1,391	PRR78 and Pusa1602	MT367778
OsEp_Plm_15B12	<i>Curtobacterium luteum</i>	1,393	PRR78 and Pusa1602	MT367787
OsEp_Plm_30B10	<i>Enterobacter cloacae</i>	1,403	PRR78 and Pusa1602	MT367801
OsEp_Plm_15B10	<i>Enterobacter sacchari</i>	1,419	PRR78 and Pusa1602	MT367785
OsEp_Plm_15B11	<i>Enterobacter</i> sp.	1,402	PRR78 and Pusa1602	MT367786
OsEp_Plm_15B7	<i>Enterococcus faecium</i>	1,409	PRR78 and Pusa1602	MT367782
OsEp_Plm_15B5	<i>Microbacterium</i> sp.	1,379	PRR78 and Pusa1602	MT367780
OsEp_Plm_15B1	<i>Microbacterium testaceum</i>	1,400	PRR78 and Pusa1602	MT367776
OsEp_Plm_30B1	<i>Microbacterium testaceum</i>	1,398	PRR78 and Pusa1602	MT367792
OsEp_Plm_30B5	<i>Microbacterium testaceum</i>	1,401	PRR78 and Pusa1602	MT367796
OsEp_Plm_15B6	<i>Pantoea ananatis</i>	1,405	PRR78 and Pusa1602	MT367781
OsEp_Plm_30B2	<i>Pantoea ananatis</i>	1,404	PRR78 and Pusa1602	MT367793
OsEp_Plm_30B6	<i>Pantoea ananatis</i>	1,408	PRR78 and Pusa1602	MT367797
OsEp_Plm_30B15	<i>Pantoea ananatis</i>	1,412	PRR78 and Pusa1602	MT367803
OsEp_Plm_30B17	<i>Pantoea ananatis</i>	1,384	PRR78 and Pusa1602	MT367804
OsEp_Plm_30B19	<i>Pantoea ananatis</i>	1,417	PRR78 and Pusa1602	MT367805
OsEp_Plm_15B14	<i>Pantoea dispersa</i>	1,410	PRR78 and Pusa1602	MT367789
OsEp_Plm_30B3	<i>Pantoea vagans</i>	1,409	PRR78 and Pusa1602	MT367794
OsEp_Plm_30B14	<i>Pseudomonas</i> sp.	1,408	PRR78 and Pusa1602	MT367802
OsEp_Plm_30B4	<i>Rhizobium</i> sp.	1,360	PRR78 and Pusa1602	MT367795
OsEp_Plm_15B2	<i>Sphingomonas</i> sp.	1,373	PRR78 and Pusa1602	MT367777

\*Isolated from rice leaf excised from PRR78 and Pusa1602 planted in Palampur, Himachal Pradesh, India.

Bacterial Genera	Metabarcoding method		Culturomic method		High abundance of yellow pigmented bacterial isolates
	Blast Resistant Pusa1602	Blast Susceptible PRR78	Blast Resistant Pusa1602	Blast Susceptible PRR78	
	*Mapped Reads (%)	*Mapped Reads (%)	#Species	#Species	
<i>Acidovorax</i>	-	-	<i>Acidovorax avenae</i>	<i>Acidovorax avenae</i>	
<i>Acinetobacter</i>	0.005	-	<i>Acinetobacter radioresistens</i>	<i>Acinetobacter calcoaceticus</i> <i>Acinetobacter radioresistens</i>	
<i>Agrobacterium</i>	-	-	<i>Agrobacterium vitis</i>	<i>Agrobacterium vitis</i>	
<i>Curtobacterium</i>	0.008	0.005	<i>Curtobacterium luteum</i> (2)	<i>Curtobacterium luteum</i> (2) <i>Curtobacterium</i> sp.	
<i>Enterobacter</i>	0.843	0.614	<i>Enterobacter cloacae</i>  <i>Enterobacter sacchari</i>  <i>Enterobacter</i> sp.	<i>Enterobacter cloacae</i> <i>Enterobacter ludwigii</i> <i>Enterobacter sacchari</i> <i>Enterobacter</i> sp.	
<i>Enterococcus</i>	0.008	0.069	<i>Enterococcus faecium</i>	<i>Enterococcus faecium</i>	
<i>Microbacterium</i>	0.006	0.008	<i>Microbacterium</i> sp. <i>Microbacterium testaceum</i> (3)	<i>Microbacterium</i> sp. <i>Microbacterium testaceum</i> (3)	
<i>Pantoea</i>	87.751	66.357	<i>Pantoea ananatis</i> (6) <i>Pantoea dispersa</i> <i>Pantoea vagans</i>	<i>Pantoea ananatis</i> (7) <i>Pantoea dispersa</i> <i>Pantoea vagans</i>	
<i>Pseudomonas</i>	1.746	2.042	<i>Pseudomonas</i> sp.	<i>Pseudomonas oryzae</i> <i>Pseudomonas</i> sp.	
<i>Rhizobium</i>	-	-	<i>Rhizobium</i> sp.	<i>Rhizobium</i> sp. <i>Rhizobium taibaishanense</i>	
<i>Sphingomonas</i>	-	-	<i>Sphingomonas</i> sp.	<i>Sphingomonas pseudosanguinis</i> <i>Sphingomonas</i> sp.	

**FIGURE 2 |** Microbiological culturomic validation of bacterial species composition in phyllosphere; bacterial species belonging to yellow-pigmented *Curtobacterium*, *Enterobacter*, *Microbacterium*, *Pseudomonas*, *Pantoea*, and *Sphingomonas* were found dominant on the phyllosphere. Data in parentheses represent the number of isolates cultured. \*Species identity in Silva Database. #Species identity in GenBank database.

**TABLE 3 |** Quantification and identification of bacterial population on rice phyllosymbiont by integrated metabarcoding and culturomic methods.

Genus	Metabarcoding method				Culturomic method	
	Blast-resistant Pusa1602		Blast-susceptible PRR78		Blast-resistant Pusa1602	Blast-susceptible PRR78
	*Read count	Reads (%)	*Read count	Reads (%)	Log CFU g <sup>-1</sup>	Log CFU g <sup>-1</sup>
<i>Pantoea</i>	423,893	87.751	137,297	66.357	4.73	5.17
<i>Pseudomonas</i>	8,433	1.746	4,226	2.042	3.23	4.47
<i>Enterobacter</i>	4,071	0.843	1,270	0.614	4.13	5.00
<i>Buttiauxella</i>	1,210	0.250	—	—	—	—
<i>Erwinia</i>	501	0.104	264	0.128	—	—
<i>Klebsiella</i>	402	0.083	769	0.372	—	—
<i>Clostridium</i>	144	0.030	172	0.083	—	—
<i>Salmonella</i>	141	0.029	97	0.047	—	—
<i>Bacteroides</i>	116	0.024	346	0.167	—	—
<i>Enterococcus</i>	40	0.008	142	0.069	3.65	2.16
<i>Curtobacterium</i>	38	0.008	10	0.005	2.24	4.64
<i>Kineococcus</i>	35	0.007	139	0.067	—	—
<i>Microbacterium</i>	27	0.006	16	0.008	5.66	5.90
<i>Acinetobacter</i>	22	0.005	—	—	3.49	3.74
<i>Abiotrophia</i>	—	—	1,522	0.736	—	—
<i>Acidovorax</i>	—	—	—	—	4.54	5.37
<i>Agrobacterium</i>	—	—	—	—	3.87	2.47
<i>Butyrivibrio</i>	—	—	134	0.065	—	—
<i>Campylobacter</i>	—	—	101	0.049	—	—
<i>Capnocytophaga</i>	—	—	518	0.250	—	—
<i>Elizabethkingia</i>	—	—	206	0.100	—	—
<i>Escherichia</i>	—	—	755	0.365	—	—
<i>Flavobacterium</i>	—	—	152	0.073	—	—
<i>Fusobacterium</i>	—	—	1,093	0.528	—	—
<i>Gemella</i>	—	—	1,213	0.586	—	—
<i>Granulicatella</i>	—	—	807	0.390	—	—
<i>Haemophilus</i>	—	—	475	0.230	—	—
<i>Kluyvera</i>	—	—	135	0.065	—	—
<i>Leptotrichia</i>	—	—	220	0.106	—	—
<i>Moraxella</i>	—	—	382	0.185	—	—
<i>Neisseria</i>	—	—	450	0.217	—	—
<i>Porphyromonas</i>	—	—	6,355	3.071	—	—
<i>Prevotella</i>	—	—	1,064	0.514	—	—
<i>Rhizobium</i>	—	—	—	—	5.13	5.43
<i>Rothia</i>	—	—	696	0.336	—	—
<i>Sphingomonas</i>	—	—	—	—	4.17	4.82
<i>Streptobacillus</i>	—	—	107	0.052	—	—
<i>Veillonella</i>	—	—	608	0.294	—	—

\*Genus with less than 10 reads were not considered.

Mackill and Bonman (1992). Most of the bacterial isolates were found to reduce the blast disease development in the plants of the susceptible rice cultivar at all tested doses. Maximum reduction in disease severity was shown by *P. vagans* OsEp-Plm-30B3 (81.9%), *P. ananatis* OsEp-Plm-15B6 (81.5%), *E. sacchari* OsEp-Plm-15B10 (78.1%), *P. ananatis* OsEp-Plm-30B17 (77.7%), *P. dispersa* OsEp-Plm-15B14 (76.2%), *Rhizobium* sp. OsEp-Plm-30B4 (69.8%), *M. testaceum* OsEp-Plm-30B1 (67.5%), *P. oryzae* OsEp-Plm-15B16 (52.4%), and *Sphingomonas* sp. OsEp-Plm-15B2 (51.8%) (Figure 3 and Table 5). Nine of the 13

bacterial isolates showed over 50% reduction of blast severity in all bacterial titers. Interestingly, the reduction in blast severity could not be correlated with the bacterial cell densities used for phyllobacterization.

## Phenotyping for Phyllosymbiont Conferred Immunocompetence

An experiment was conducted to study the potential of phyllosphere bacteria to confer immunocompetence in rice.

**TABLE 4 |** Antifungal activity of phyllosphere bacteria by secreted metabolites and volatile compounds against *Magnaporthe oryzae*.

Bacterial isolates	Mycelial inhibition (%)	
	Volatile compounds	Secretory compounds
1. <i>Enterobacter sacchari</i> OsEp-Plm-15B10	100.0	57.4
2. <i>Microbacterium testaceum</i> OsEp-Plm-30B1	100.0	38.9
3. <i>Pantoea dispersa</i> OsEp-Plm-15B14	100.0	35.2
4. <i>Pantoea ananatis</i> OsEp-Plm-15B6	100.0	19.4
5. <i>Pantoea ananatis</i> OsEp-Plm-30B2	100.0	53.7
6. <i>Pantoea vagans</i> OsEp-Plm-30B3	100.0	47.2
7. <i>Pantoea ananatis</i> OsEp-Plm-30B6	100.0	45.4
8. <i>Pantoea ananatis</i> OsEp-Plm-30B8	100.0	7.4
9. <i>Pantoea ananatis</i> OsEp-Plm-30B17	100.0	52.8
10. <i>Pantoea ananatis</i> OsEp-Plm-30B19	100.0	8.3
11. <i>Pseudomonas oryzae</i> OsEp-Plm-15B16	100.0	41.7
12. <i>Rhizobium</i> sp. OsEp-Plm-30B4	100.0	5.6
13. <i>Sphingomonas</i> sp. OsEp-Plm-15B2	62.9	53.7
14. <i>Agrobacterium vitis</i> OsEp-Plm-30B7	77.9	15.7
15. <i>Enterobacter cloacae</i> OsEp-Plm-30B10	76.4	46.3
16. <i>Pantoea ananatis</i> OsEp-Plm-30B15	57.9	13.9
17. <i>Microbacterium testaceum</i> OsEp-Plm-30B5	57.1	4.6
18. <i>Enterobacter ludwigii</i> OsEp-Plm-30B20	56.4	4.6
19. <i>Curtobacterium luteum</i> OsEp-Plm-15B12	48.6	8.3
20. <i>Acidovorax avenae</i> OsEp-Plm-15B4	45.7	6.5
21. <i>Acinetobacter radioresistens</i> OsEp-Plm-15B15	45.7	8.3
22. <i>Microbacterium testaceum</i> OsEp-Plm-15B1	42.9	7.4
23. <i>Curtobacterium</i> sp. OsEp-Plm-15B13	38.6	7.4
24. <i>Acinetobacter calcoaceticus</i> OsEp-Plm-15B9	37.9	44.4
25. <i>Enterococcus faecium</i> OsEp-Plm-15B7	35.0	23.2
26. <i>Sphingomonas pseudosanguinis</i> OsEp-Plm-30B9	35.0	6.5
27. <i>Microbacterium</i> sp. OsEp-Plm-15B5	34.3	8.3
28. <i>Rhizobium taiwanense</i> OsEp-Plm-15B8	32.9	8.3
29. <i>Enterobacter</i> sp. OsEp-Plm-15B11	32.1	39.8
30. <i>Pseudomonas</i> sp. OsEp-Plm-30B14	31.4	3.7
31. <i>Curtobacterium luteum</i> OsEp-Plm-15B3	29.3	11.1
Mock	0.0	0.0
C.D.	12.0	4.8
SE (m)	4.3	1.7
SE (d)	6.1	2.4
C.V. (%)	13.2	12.8
F (calc.)	52.1	130.5
F (tab.)	1.6	1.6

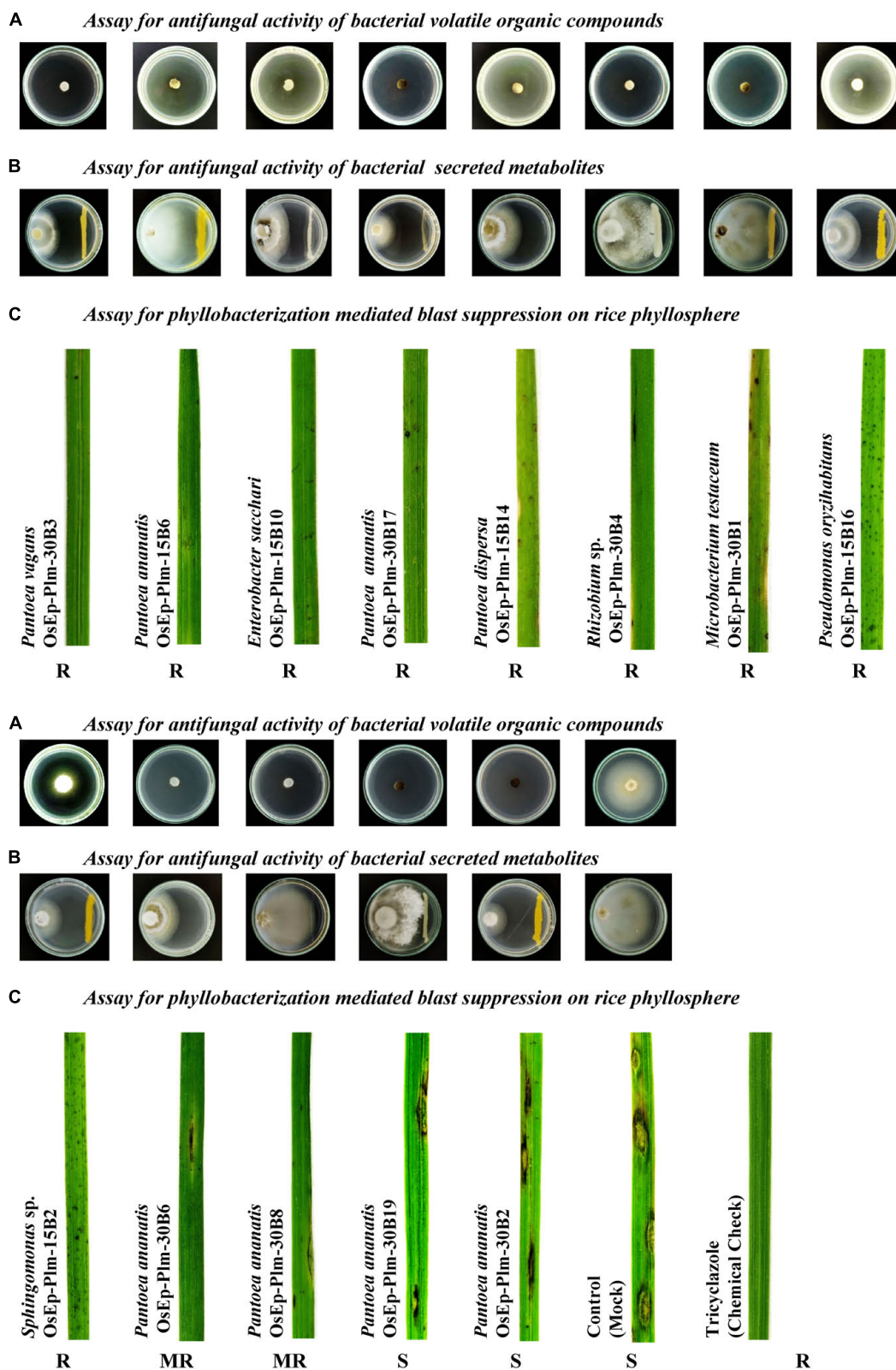
Seedling growth inhibition due to microbial interactions is touted as a phenotypic marker for the induced immune response in plants. Here, the seed germination and the seedling emergence were monitored during bacterial interaction that showed germination in the range of 40.0–86.7% across various bacterial inoculations. Maximum germination was observed in *E. sacchari* OsEp-Plm-15B10, while the minimum germination was observed in *P. ananatis* OsEp-Plm-30B2 (Supplementary Figure 8 and Supplementary Table 7). However, the germinability of rice seeds reduced upon increasing bacterial density with poor germination observed at a titer of  $10^9$  CFU ml<sup>-1</sup>. The bacterial inoculation on seeds and seedlings appeared to trigger the plant phenotypic alteration

especially on the shoot and root growth. All nine bacterial isolates representing six genera induced a density-dependent alteration on the shoot and root emergence and growth (Supplementary Tables 8, 9). In particular, the shoot and root growth of rice was found inhibited at high bacterial titer ( $10^9$  CFU ml<sup>-1</sup>) (Figure 4).

### qPCR Assay on Phyllobacterization-Mediated Immunocompetence

The rice seedlings displaying the altered growth pattern were subjected to transcriptional analysis by qPCR. Defense genes





**FIGURE 3 |** Suppressive effects of phyllosphere bacterial inoculation on *Magnaporthe oryzae* and the rice blast disease. **(A)** Phyllosphere bacteria displayed volatile mediated antifungal activity on *Magnaporthe oryzae*. **(B)** A few isolates showed secreted metabolite mediated antifungal activity on *Magnaporthe oryzae*. **(C)** Nine of the tested 13 bacteria isolates showed blast-suppressive activity on rice leaf.

**TABLE 5** | Suppressive effects of phyllobacterization on rice blast disease.

Bacterial species/isolate	Bacterial dose (0.01 OD at A600 nm = ~10 <sup>6</sup> cfu per ml)		Bacterial dose (0.1 OD at A600 nm = ~10 <sup>7</sup> cfu per ml)		Bacterial dose (1.0 OD at A600 nm = ~10 <sup>8</sup> cfu per ml)		Mean	
	*Blast severity	**Reduction in severity (%)	*Blast severity	**Reduction in severity (%)	*Blast severity	**Reduction in severity (%)	*Blast severity	**Reduction in severity (%)
<i>Pantoea vagans</i> OsEp-Plm-30B3	11.3	77.9	7.0	86.2	9.4	81.5	9.2	81.9
<i>Pantoea ananatis</i> OsEp-Plm-15B6	8.1	84.0	13.3	73.8	6.8	86.7	9.4	81.5
<i>Enterobacter sacchari</i> OsEp-Plm-15B10	11.7	76.9	13.0	74.5	8.7	83.0	11.1	78.1
<i>Pantoea ananatis</i> OsEp-Plm-30B17	15.8	68.9	12.1	76.3	6.2	87.9	11.3	77.7
<i>Pantoea dispersa</i> OsEp-Plm-15B14	8.0	84.3	15.5	69.5	12.8	74.9	12.1	76.2
<i>Rhizobium</i> sp. OsEp-Plm-30B4	13.4	73.7	18.3	63.9	14.3	71.9	15.3	69.8
<i>Microbacterium testaceum</i> OsEp-Plm-30B1	19.0	62.6	11.4	77.5	19.1	62.5	16.5	67.5
<i>Pseudomonas oryzae</i> OsEp-Plm-15B16	22.4	55.9	21.9	56.9	28.3	44.4	24.2	52.4
<i>Sphingomonas</i> sp. OsEp-Plm-15B2	20.9	58.9	24.2	52.5	28.5	43.9	24.5	51.8
<i>Pantoea ananatis</i> OsEp-Plm-30B6	21.5	57.7	28.9	43.2	34.8	31.6	28.4	44.2
<i>Pantoea ananatis</i> OsEp-Plm-30B8	29.5	41.9	26.9	47.1	32.2	36.6	29.6	41.9
<i>Pantoea ananatis</i> OsEp-Plm-30B19	41.7	18.0	42.2	17.0	35.0	31.1	39.6	22.0
<i>Pantoea ananatis</i> OsEp-Plm-30B2	54.6	-7.5	42.9	15.7	39.0	23.2	45.5	10.5
Control	50.8	0.0	50.8	0.0	50.8	0.0	50.8	0.0
Tricyclazole	6.8	86.7	10.1	80.1	8.1	84.0	8.33	83.6

\*Disease severity was calculated using the following formula:

$$\text{Disease severity} = \frac{\sum (\text{Scale} \times \text{Number of plants infected}) \times 100}{\text{Total number of plants} \times \text{Maximum disease scale}}$$

\*\*Blast severity reduction was estimated using the following formula:

$$\text{Blast severity reduction} = \frac{C-T}{C} \times 100$$

C = disease severity in control.







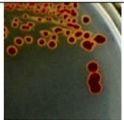
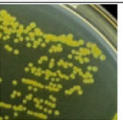

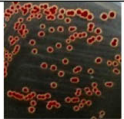
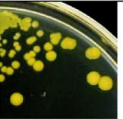
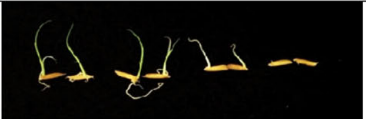
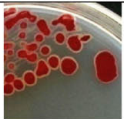


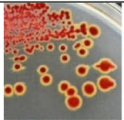
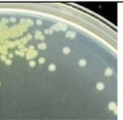
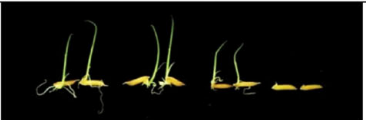
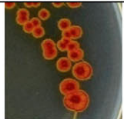

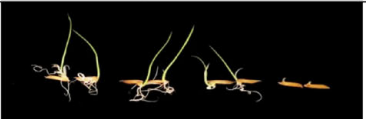
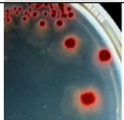
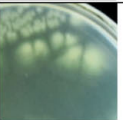
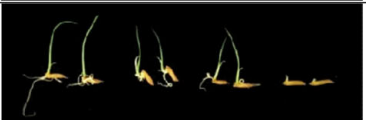
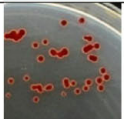
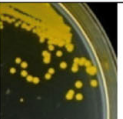

T = disease severity in treatment.

such as *OsCEBiP*, *OsCERK1*, *OsPAD4*, *OsNPR1*, *OsEDS1*, *OsPDF2.2*, *OsFMO1*, and *OsPR1.1* showed marginal to a high level of expression in phyllobacterized rice seedlings compared with the untreated control compared with *OsActin* used as a reference gene. Interestingly, *Sphingomonas* sp. OsEp-Plm-15B2, *P. ananatis* OsEp-Plm-15B6, *E. sacchari* OsEp-Plm-15B10, *P. dispersa* OsEp-Plm-15B14, *P. oryzae* OsEp-Plm-15B16, *M. testaceum* OsEp-Plm-30B1, *P. vagans* OsEp-Plm-30B3 *Rhizobium* sp. OsEp-Plm-30B4, and *P. ananatis* OsEp-Plm-30B17 sustained the overexpression of *OsCEBiP* in rice seedlings in all three-time points. *P. ananatis* OsEp-Plm-15B6 and *P. dispersa* OsEp-Plm-15B14 showed significant

upregulation in almost all the defense-related genes at least for one-time point. *E. sacchari* OsEp-Plm-15B10 showed sustained upregulation of all the genes for 48 h after bacterial treatment. The epiphytic bacteria-mediated activation of defense genes was more pronounced during the early time points peaking at 48 hpi with a sharp drop at 72 h of bacterial interaction (**Figure 5** and **Supplementary Table 10**).

## Hypersensitive Reaction on Tobacco

Rice phyllospheric bacteria upon infiltration in tobacco leaf did not trigger any necrotic reactions even after 48 h. The expression of quick necrosis due to the hypersensitive reaction

Phyllosphere bacterial speceis	Colonies on nutrient media		Bacterial Titer (CFU mL <sup>-1</sup> )			
	NA+ Tetrazolium	NA	10 <sup>6-7</sup>	10 <sup>7-8</sup>	10 <sup>8-9</sup>	10 <sup>9-10</sup>
<i>Enterobacter sacchari</i> sEp-Plm-15B10						
<i>Microbacterium testaceum</i> OsEp-Plm-30B1						
<i>Pantoea ananatis</i> OsEp-Plm-15B6						
<i>Pantoea ananatis</i> OsEp-Plm-30B17						
<i>Pantoea dispersa</i> OsEp-Plm-15B14						
<i>Pantoea vagans</i> OsEp-Plm-30B3						
<i>Pseudomonas oryzae</i> OsEp-Plm-15B16						
<i>Rhizobium</i> sp. OsEp-Plm-30B4						
<i>Sphingomonas</i> sp. OsEp-Plm-15B2						

**FIGURE 4 |** Assay for phyllosphere-conferred immunocompetence. Seedling growth inhibition as a phenotypic marker of microbiome-conferred immunocompetence, observed with nine blast-suppressive bacterial isolates, represented six genera such as *Enterobacter*, *Microbacterium*, *Pantoea*, *Pseudomonas*, *Rhizobium*, and *Sphingomonas*. The rice phyllosphere bacteria showed various shades of yellow pigmentation; the pink color appearance of the bacterial colony is due to the reduction of tetrazolium dye into insoluble formazan; the inhibition of shoot and root growth—an indicator of innate immunity, can be seen in plantlets interacting with high bacterial titer.

was observed in the pathogen, *R. solanacearum*, which infiltrated a leaf indicating that the rice phyllosphere-associated bacterial isolates are non-pathogenic on plants (**Supplementary Figure 9**).

## DISCUSSION

The foliar plant niches termed phyllosphere is one of the habitats for a diverse microbiota where the dynamic plant–microbe interactions are believed to impact plant performance in the

ecosystem. With assistance from the microbial genome and their metabolic capabilities, the plants are exposed to a plethora of unpredictable, yet competitive or cooperative, microbial interactions (Vorholt, 2012; Hardoim et al., 2015; Reinhold-Hurek et al., 2015; Brader et al., 2017; Lemanceau et al., 2017). In recent years, the impact of microbe–microbe interactions on the host–microbial pathogen interaction outcomes is gaining the attention of researchers. Studies have shown that the microbiome structure, assemblage, and compositions are directly influenced by both micro and macro abiotic



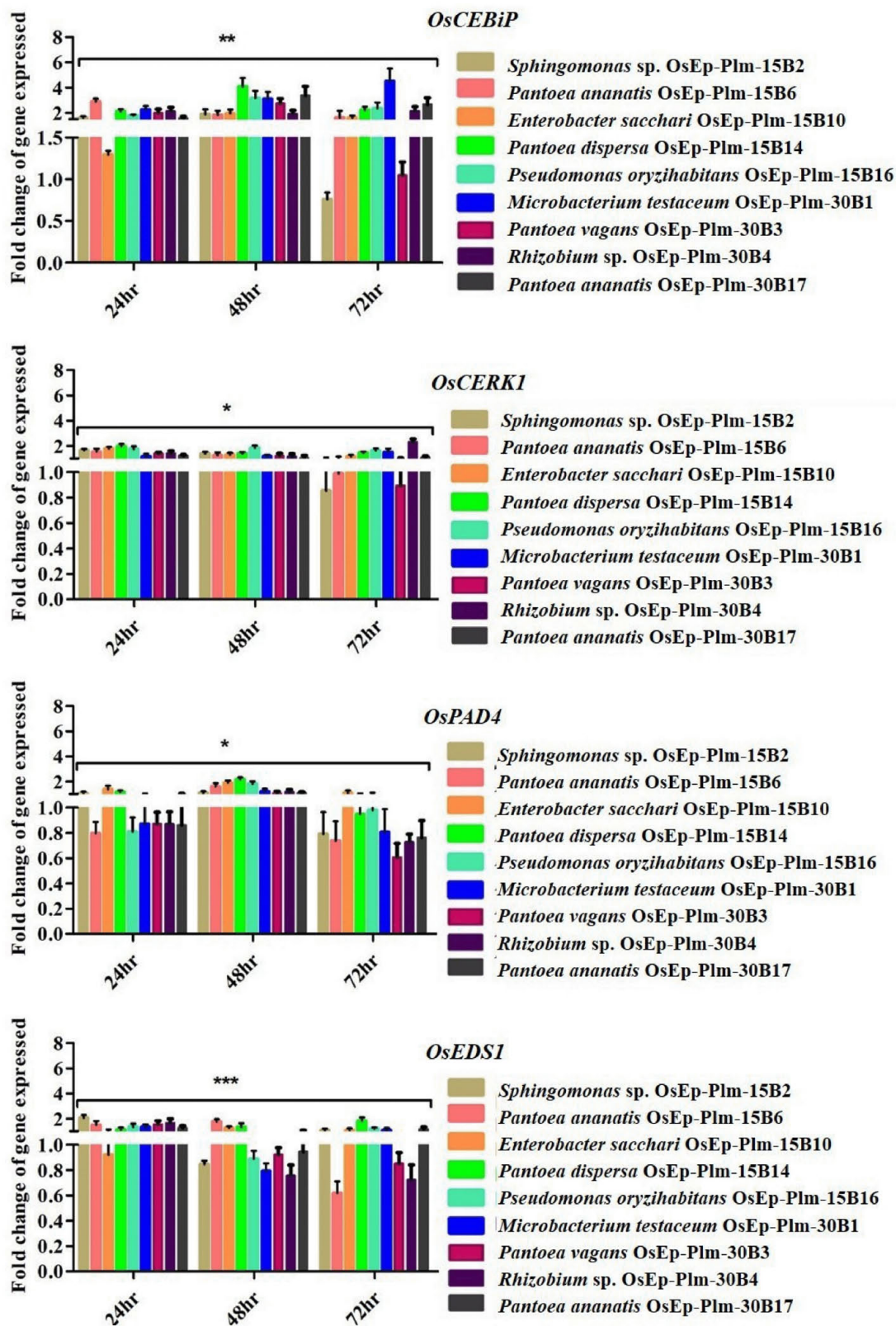
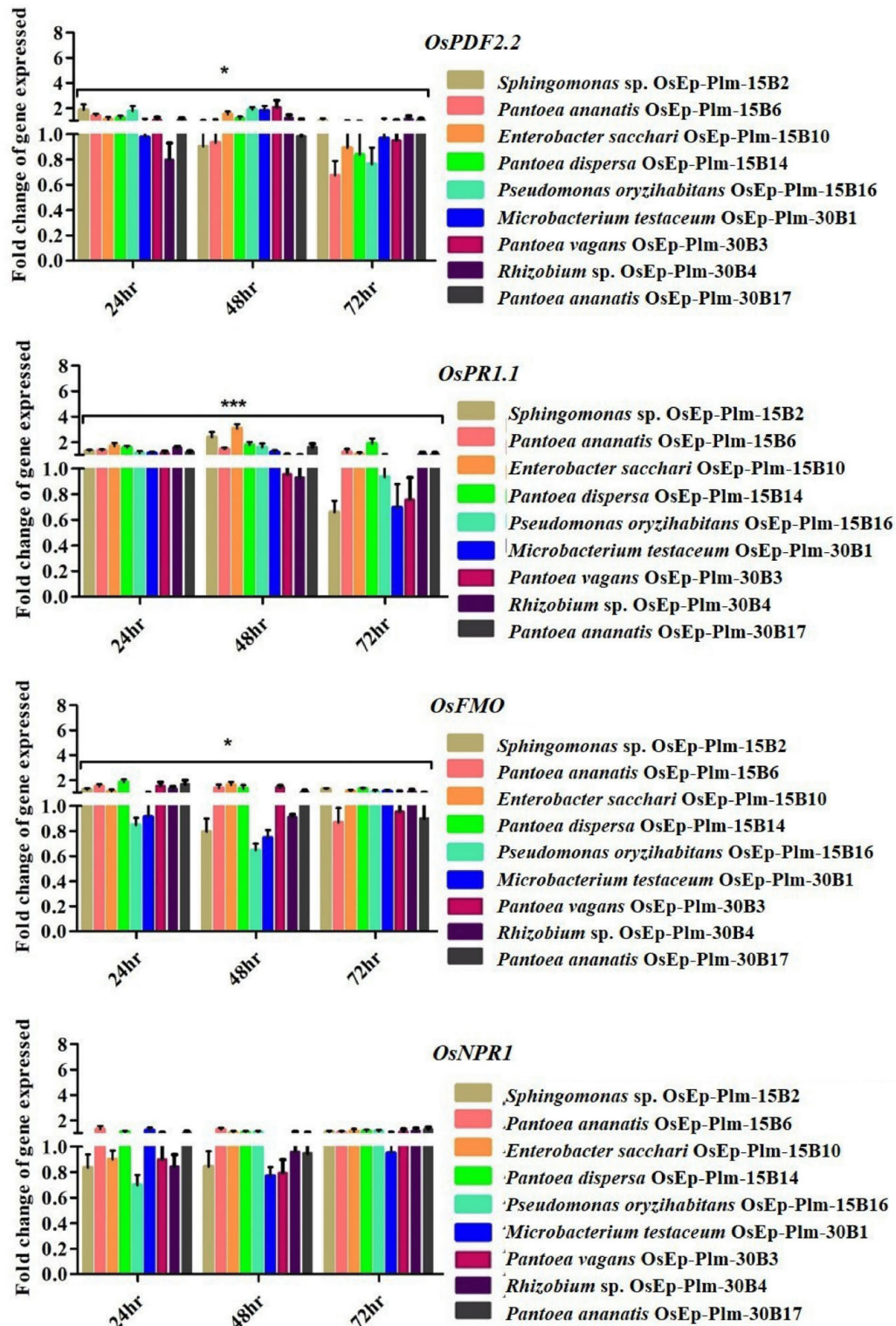
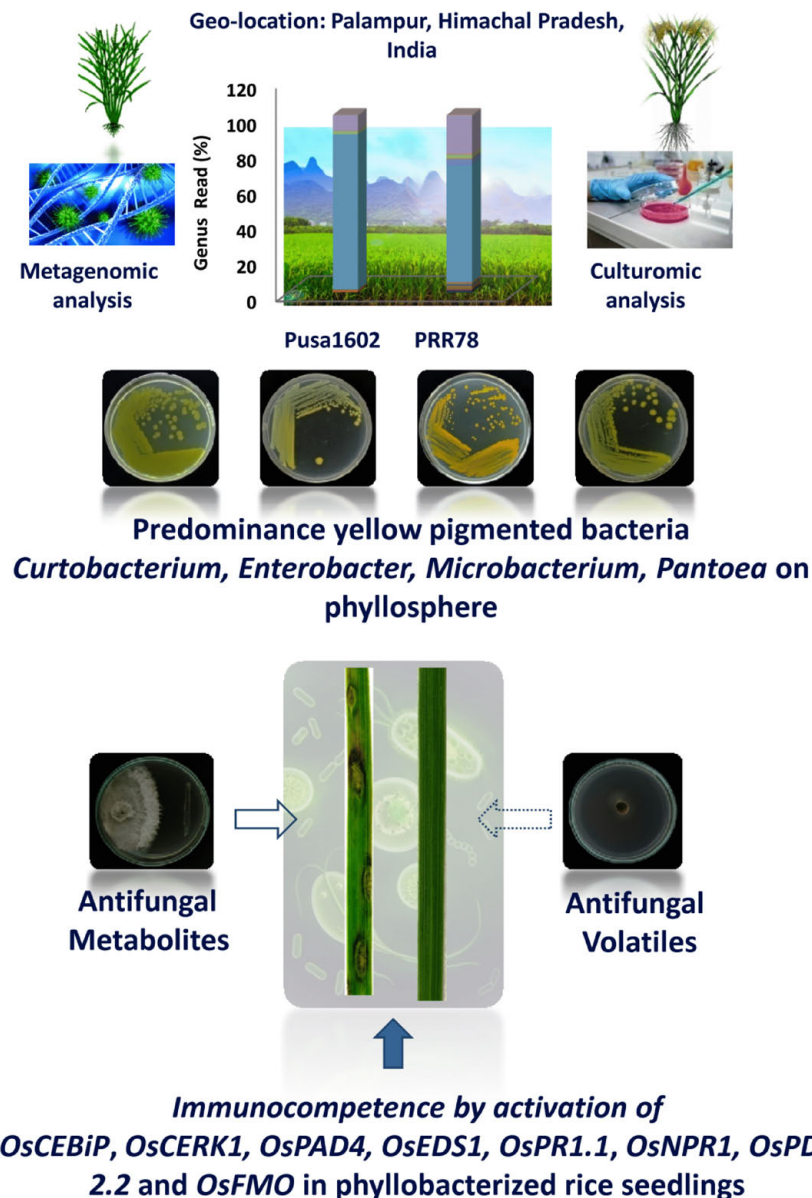


FIGURE 5 | (Continued)





**FIGURE 5 |** qPCR-based transcriptional analysis of defense gene expression in rice seedlings upon phylobacterization. The fold change values obtained for the defense genes were imported into the GraphPad Prism program (<https://www.graphpad.com/scientific-software/prism/>), and two-way ANOVA was conducted using Bonferroni *post-hoc* test for determining the statistical significance at  $p \leq 0.05$ ,  $**p = 0.001$ , and  $***p = 0.0001$ . Refer to **Supplementary Table 10** for data pertaining to fold changes of gene expression.



**FIGURE 6 |** Phyllosphere microbiome-assisted suppression of rice blast disease. Blast suppressiveness by the predominant and pigmented bacterial isolates of phyllosphere can be attributed to both antifungal activity on *Magnaporthe oryzae* as well as induced defense in rice as evident from enhanced expression of many defense genes.

and biotic factors (Jacobs et al., 2005). Most of the previous microbiome studies have focused primarily on metagenomic or amplicon sequence surveys, and a few attempts have been made to validate the microbial mNGS datasets using classical microbiological culturomic tools. Strikingly, we have compared the phyllosphere microbiome of blast disease-resistant and -susceptible rice genotypes planted in a blast endemic location in India. We recorded marginally high bacterial diversity and species richness on PRR78 that could be attributed to the innate susceptibility of the genotypes owing to the absence of functional NBS-LRR type of receptors termed as R-genes. Besides, the susceptible leaf

showing early necrotic symptoms might have paved way for the inevitable microbial succession on the phyllosphere.

In the present work, we not only microbiologically validated the bacterial community structure in the phyllosphere but also functionally characterized them for harnessing their antifungal and defense-inducing potential against rice blast disease. The NGS metabarcoding-based microbiome profiling revealed the predominance of phylum Proteobacteria on the rice phyllosphere. The predominance of Proteobacteria consisting of bacterial communities belonging to *Enterobacteriaceae* and *Pseudomonadaceae* is reported on the phyllosphere by many

workers (Knief et al., 2012; Ren et al., 2014; Roman-Reyna et al., 2019; Yasmin et al., 2020). At the lower taxonomic genus hierarchy, *Pantoea* followed by *Pseudomonas* and *Enterobacter* were overrepresented on both the rice genotypes. Our findings are in agreement with many other reports that highlighted the ubiquitous occurrence of *Pantoea* as the most abundant bacterial genera on the phyllosphere (Cottyn et al., 2009; Cothier et al., 2010; Kim et al., 2020; Stone and Jackson, 2020; Dhankhar et al., 2021). The microbiological investigation culminated in the isolation of 37 distinct morphotypes on the rice phyllosphere; here, the 4-week-old seedling harbored more bacterial morphotypes compared with the 15-day-old seedlings implying that microbial biomass on plant niches expands with the age of the plants. The morphotypes could be identified as belonging to 31 distinct amplicon groups in BOX-AIR-PCR fingerprinting based on shared amplicon profiles of the isolates. The BOX PCR DNA fingerprinting is one of the widely used molecular tools in bacterial typing and biogeography studies of microbial isolates (Versalovic et al., 1994; Brusetti et al., 2008).

The 16S rRNA gene sequence database search confirmed the identity of cultured bacterial isolates as belonging to *Acinetobacter*, *Enterobacter*, *Pantoea*, *Pseudomonas*, and *Sphingomonas* on blast-resistant and -susceptible genotypes. *Pantoea*, *Enterobacter*, *Microbacterium*, and *Curtobacterium* are recently reported as a member of the core microbiome of the rice leaf endosphere (Kumar et al., 2021). The genus *Microbacterium* too is frequently observed on the rice phyllosphere and spermosphere by several researchers in the past (Kaku et al., 2000; Leveau and Lindow, 2001; Midha et al., 2016). Characteristically, most of the phyllosphere bacterial genera produced shades of pigmentation as observed in *Acinetobacter* (pale brown), *Curtobacterium* (dark yellow), *Enterobacter* (pale brown to yellow), *Microbacterium* (yellow), *Pantoea* (yellow), *Pseudomonas* (pale brown to yellow), and *Sphingomonas* (dark yellow) (**Supplementary Figures 4a–k**). Production of dark pigmentation is one of the adaptive traits of bacteria and other microbes that encounter harsh environmental abiotic stresses like solar radiation and light on the phyllosphere (Green, 1992; Jacobs et al., 2005). Pigmentation on phyllospheric bacteria is believed to protect them from harmful ultraviolet radiation (Sundin and Jacobs, 1999). The rice phyllosphere is considered as the preferred habitat for yellow-pigmented *Pantoea* and pink-pigmented methylotrophs, which can survive under nutritional and moisture stress as well as can withstand harmful  $\gamma$ -ray radiation (Green, 1992). The effect of solar radiation on the composition and activities of the phyllosphere microbial community is reported by Carvalho and Castillo (2018).

The bacterial isolates showed antifungal activity on *M. oryzae* by their secreted compounds and volatile organic compounds, while *Enterobacter*, *Microbacterium*, *Pantoea*, *Pseudomonas*, and *Rhizobium* showed volatile mediated antifungal activity, and the *Acinetobacter* and *Sphingomonas* displayed secretory metabolite-mediated antagonism. The antagonistic potential of these bacterial species has been exploited for combating crop diseases caused by several fungal pathogens. For instance, the antagonistic potential of *Acinetobacter baumannii* (Liu et al., 2007),

*Enterobacter* sp. (Gong et al., 2019), *M. testaceum* (Mannaa et al., 2017), *P. ananatis* (Gasser et al., 2012), *P. dispersa* (Jiang et al., 2019), *P. vagans* (Stockwell et al., 2010), *P. oryzihabitans* (Vagelas and Gowen, 2012; Rariz et al., 2017; Horuz and Aysan, 2018), and *Sphingomonas* sp. (Innerebner et al., 2011; Wachowska et al., 2013) is reported. Among them, *P. vagans* strain C9-1, isolated from apple has been registered by Nufarms America Inc., Burr Ridge, IL as “BlightBan C9-1” for the biological control of fire blight of apple caused by *Erwinia amylovora*. Isolates belonging to *Sphingomonas* have also been reported to promote plant growth, confer tolerance against abiotic stresses, and offer protection against plant pathogens (Luo et al., 2020; Turner, 2020).

Currently, growing evidence for microbe-induced seedling growth alteration as a phenotypic marker of activated innate immunity is published (Wang et al., 2021). We observed that the phyllosphere bacterial species in a density-dependent manner impacted the seed germination with consequent seedling growth alterations upon seed inoculation. The results are in agreement with the studies of Damodaran et al. (2013) and Zhu et al. (2017) who observed varying effects of endophytic and rhizosphere bacteria on seed germination. The seedling growth assay enabled us to identify the bacterial species that conferred immune competence in rice seedlings. Whereas the seedling growth was found inhibited at a higher dose ( $10^9$  cells per ml), the lower doses ( $10^6$ – $10^8$  cells per ml) showed characteristic non-lethal seedling inhibition presumably owing to a tradeoff between growth and immunity. To confirm this, we performed the qPCR-based temporal transcriptional analysis of defense genes involved in innate immunity on phyllobacterized rice seedlings.

Phyllobacterized rice seedlings showed an elevated expression of defense genes, such as *OsCEBiP*, *OsCERK*, *OsPRI.1*, *OsNPR1*, *OsPDF2.2*, *OsFMO*, and *OsPAD4*. Significant up-regulation of almost all tested defense-related genes at least for a one-time point was shown by *P. ananatis* (OsEp-Plm-15B6) and *P. dispersa* (OsEp-Plm-15B14). Notably, *E. sacchari* (OsEp-Plm-15B10) showed sustained expression of all the genes 48 hpi. Among the genes, significant expression of *OsCEBiP* and *OsCERK* was observed in phyllobacterized rice seedlings. Both *OsCEBiP* and *OsCERK* are reported to be activating MAMP-triggered immune (MTI) responses in plants upon chitin and peptidoglycan perception (Akamatsu et al., 2013; Kouzai et al., 2014). Defense genes, such as *OsPAD4* and *OsEDS1* participating in the jasmonic acid-mediated ISR, were also found induced in rice seedlings upon bacterization. Induction of *OsPAD4* contributes to the accumulation of rice phytoalexin, mamilactone-A, and contributes to basal resistance (Hasegawa et al., 2010; Ke et al., 2014, 2019). Marginal induction of *OsNPR1*, *OsFMO*, *OsPDF2.2*, and *OsPRI.1* was observed in phyllobacterized rice seedlings. Among them, *OsNPR1*—the key regulator of salicylic acid (SA)-mediated defense signaling is believed to control resource and energy redistribution during the defense reaction (Sugano et al., 2010). Likewise, *OsFMO1* is known to modulate systemic acquired resistance in plants against pathogens (Koch et al., 2006; Mishina and Zeier, 2006). While *OsPDF2.2* codes for antifungal plant defensin (Thomma et al., 2002), the *OsPRI.1* codes for an acidic pathogenesis-related



protein to modulate SA-mediated systemic acquired resistance (Brader et al., 2017).

Phyllosphere bacterial species evaluated against rice blast under artificial epiphytotic trial in greenhouse showed a reduction in blast disease (50 % over mock) at all tested bacterial titers. Upon prophylactic foliar application (or phyllobacterization), the species belonging to *Pantoea*, *Enterobacter*, *Microbacterium*, *Pseudomonas*, *Sphingomonas*, and *Rhizobium* showed significant blast suppression at all tested doses. However, we could not observe any dosage response for enhanced blast suppression revealing the sufficiency of bacterial augmentation at  $10^{6-7}$  cells per ml for reducing blast disease. Suppression of blast disease by *Bacillus*, *Streptomyces*, *Pseudomonas*, *Pantoea*, *Paenibacillus*, *Burkholderia*, *Enterobacter*, *Paraburkholderia*, and *Actinomycetes* was earlier reported in the literature (Gómez Expósito et al., 2017; Harsonowati et al., 2017; Schlatter et al., 2017). Rice blast suppression by *Microbacterium*, *Pseudomonas*, and *Stenotrophomonas* are attributed to the direct antifungal antibiosis and the indirect defense activation as evident from the expression of rice defense genes (Ashajyothi et al., 2020; Sahu et al., 2020). Recently, bacterial volatile belonging to pyrazines is reported to modulate defense against blast disease (Patel et al., 2020). Taken together, it is concluded that the enrichment of phyllosphere bacterial communities on the leaf can inflict antifungal antibiosis on *M. oryzae* and defense elicitation in rice to reduce the incidence and severity of blast disease.

Having confirmed the blast-suppressive potential of phyllosphere bacterial communities, we conducted a tobacco infiltration HR assay to ascertain the biosafety of the phyllosphere bacterial isolate (Klement, 1963). The tobacco HR assay has been recognized to test the pathogenic nature of plant-associated bacterial species (Kucheryava et al., 1999; Medina-Salazar et al., 2020; Sadeghi and Khodakaramian, 2020). None of the phyllosphere bacterial isolates showed any necrotic lesions, while comparing with *R. solanacearum* served as a positive check. Shades of faded yellowing observed with few phyllosphere bacterial isolates are indicative of activated defense.

In conclusion, the phyllosphere bacterial communities suppressed the blast disease by the dual action of antifungal secreted and volatile metabolites as well as by microbe conferred immunocompetence (Figure 6). The present investigation on phyllosphere microbiome analysis of rice culminated in several potential hitherto unexplored bacterial communities for microbiome-assisted crop protection, especially against rice blast disease.

## REFERENCES

- Akamatsu, A., Wong, H. L., Fujiwara, M., Okuda, J., Nishide, K., Uno, K., et al. (2013). An OsCEBiP/OsCERK1-OsRacGEF1-OsRac1 module is an essential early component of chitin-induced rice immunity. *Cell Host Microbe* 13, 465–476. doi: 10.1016/j.chom.2013.03.007
- Al-Antary, T. M., Alawi, M. A., Masaedeh, M., and Haddad, N. A. (2020). Multi-Residue Analysis of 405 Pesticides in Agricultural Crops in Middle Governorates of Jordan in 2018 and 2019 Using QuEChERS Method Followed by LC-MS/MS and GC-ECD. *Fresenius Environ. Bull.* 29, 2534–2539.
- Andrews, J. H., and Harris, R. F. (2000). The ecology and biogeography of microorganisms on plant surfaces. *Annu. Rev. Phytopathol.* 38, 145–180. doi: 10.1146/annurev.phyto.38.1.145
- Andrews, S. (2018). *FastQC: A Quality Control Tool for High Throughput Sequence Data*. Cambridge: Babraham Institute.
- Ashajyothi, M., Kumar, A., Sheoran, N., Ganesan, P., Gogoi, R., Subbaiyan, G. K., et al. (2020). Black pepper (*Piper nigrum* L.) associated endophytic *Pseudomonas putida* BP25 alters root phenotype and induces defense in rice (*Oryza sativa* L.) against blast disease incited by *Magnaporthe oryzae*. *Biol. Control* 143:104181. doi: 10.1016/j.biocontrol.2019.104181

## DATA AVAILABILITY STATEMENT

The datasets presented in this study can be found in online repositories. The names of the repository/repositories and accession number(s) can be found in the article/Supplementary Material.

## AUTHOR CONTRIBUTIONS

KS conceptualized the study, developed the methodology, investigated and validated the study, performed the formal analysis, and wrote the original draft. AK conceptualized and investigated the study, provided the resources, wrote, reviewed, and edited the manuscript, and was in charge of the visualization, supervision, and project administration. AP, MK, and NS developed the methodology and validated the study. SM and BR performed the formal analysis. PE and NP validated the study. All authors read and approved the final manuscript.

## FUNDING

KS offers his sincere thanks to the Council of Scientific and Industrial Research (CSIR) for financial support in the form of Junior and Senior Research Fellowships [File No: 09/083(0367)/2016-EMR-I] for the Ph.D. program. KS and AK were grateful to NAHEP-CAAST on “Genomics assisted crop improvement and management” for financial assistance.

## ACKNOWLEDGMENTS

We thank the Director, IARI, and Dean, PG School, Indian Council of Agricultural Research–Indian Agricultural Research Institute, New Delhi, for the logistic support and encouragement. We gratefully acknowledge the research grant provided by Genomics-Assisted Crop Improvement and Management (NAHEP/CAAST/2018-19/07), ICAR-IARI, New Delhi.

## SUPPLEMENTARY MATERIAL

The Supplementary Material for this article can be found online at: <https://www.frontiersin.org/articles/10.3389/fmicb.2021.780458/full#supplementary-material>



- Asibi, A. E., Chai, Q., and Coulter, J. A. (2019). Rice blast: a disease with implications for global food security. *Agronomy* 9:451. doi: 10.3390/agronomy9080451
- Berg, G., Rybakova, D., Fischer, D., Cernava, T., Vergès, M.-C. C., Charles, T., et al. (2020). Microbiome definition re-visited: old concepts and new challenges. *Microbiome* 8:103. doi: 10.1186/s40168-020-00875-0
- Berg, G., Rybakova, D., Grube, M., and Köberl, M. (2016). The plant microbiome explored: implications for experimental botany. *J. Exp. Bot.* 67, 995–1002. doi: 10.1093/jxb/erv466
- Bertani, I., Abbruscato, P., Piffanelli, P., Subramoni, S., and Venturi, V. (2016). Rice bacterial endophytes: isolation of a collection, identification of beneficial strains, and microbiome analysis. *Environ. Microbiol. Rep.* 8, 388–398. doi: 10.1111/1758-2229.12403
- Bolger, A. M., Lohse, M., and Usadel, B. (2014). Trimmomatic: a flexible trimmer for Illumina sequence data. *Bioinformatics* 30, 2114–2120. doi: 10.1093/bioinformatics/btu170
- Brader, G., Compant, S., Vescio, K., Mitter, B., Trognitz, F., Ma, L.-J., et al. (2017). Ecology and genomic insights into plant-pathogenic and plant-nonpathogenic endophytes. *Annu. Rev. Phytopathol.* 55, 61–83. doi: 10.1146/annurev-phyto-080516-035641
- Breen, S., Williams, S. J., Outram, M., Kobe, B., and Solomon, P. S. (2017). Emerging insights into the functions of pathogenesis-related protein 1. *Trends Plant Sci.* 22, 871–879. doi: 10.1016/j.tplants.2017.06.013
- Bruseti, L., Malkhazova, I., Gtari, M., Tamagnini, L., Borin, S., Merabishvili, M., et al. (2008). Fluorescent-BOX-PCR for resolving bacterial genetic diversity, endemism, and biogeography. *BMC Microbiol.* 8:220. doi: 10.1186/1471-2180-8-220
- Bulgarelli, D., Schlaeppi, K., Spaepen, S., Van Themaat, E. V. L., and Schulze-Lefert, P. (2013). Structure and functions of the bacterial microbiota of plants. *Annu. Rev. Plant Biol.* 64, 807–838. doi: 10.1146/annurev-arplant-050312-120106
- Carvalho, S. D., and Castillo, J. A. (2018). Influence of light on plant–phyllosphere interaction. *Front. Plant Sci.* 9:1482. doi: 10.3389/fpls.2018.01482
- Compant, S., Samad, A., Faist, H., and Sessitsch, A. (2019). A review on the plant microbiome: ecology, functions, and emerging trends in microbial application. *J. Adv. Res.* 19, 29–37. doi: 10.1016/j.jare.2019.03.004
- Cother, E., Noble, D., Van De Ven, R., Lanoiselet, V., Ash, G., Vuthy, N., et al. (2010). Bacterial pathogens of rice in the Kingdom of Cambodia and description of a new pathogen causing a serious sheath rot disease. *Plant Pathol.* 59, 944–953. doi: 10.1111/j.1365-3059.2010.02310.x
- Cottyn, B., Debode, J., Regalado, E., Mew, T., and Swings, J. (2009). Phenotypic and genetic diversity of rice seed-associated bacteria and their role in pathogenicity and biological control. *J. Appl. Microbiol.* 107, 885–897. doi: 10.1111/j.1365-2672.2009.04268.x
- Damodaran, T., Sharma, D., Mishra, V., Jha, S., Kannan, R., Sah, V., et al. (2013). Isolation of Salt Tolerant Endophytic and Rhizospheric Bacteria by Natural Selection and screening for promising plant growth-promoting Rhizobacteria (PGPR) and growth vigour in Tomato under sodic environment. *Afr. J. Microbiol. Res.* 7, 5082–5089. doi: 10.5897/AJMR2013.6003
- Dean, R. A., Talbot, N. J., Ebbole, D. J., Farman, M. L., Mitchell, T. K., Orbach, M. J., et al. (2005). The genome sequence of the rice blast fungus *Magnaporthe oryzae*. *Nature* 434, 980–986. doi: 10.1038/nature03449
- Dhankhar, R., Mohanty, A., and Gulati, P. (2021). “Microbial diversity of Phyllosphere: exploring the unexplored,” in *Phytomicrobiome Interactions and Sustainable Agriculture*, eds A. Verma, J. K. Saini, A. E. L. Hesham and H. B. Singh (Hoboken, NJ: John Wiley & Sons Ltd), 66–90. doi: 10.1002/9781119644798.ch5
- Eke, P., Kumar, A., Sahu, K. P., Wakam, L. N., Sheoran, N., Ashajoyti, M., et al. (2019). Endophytic bacteria of desert triangular spurge (*Euphorbia antiquorum* L.) confer drought tolerance and induce growth promotion in tomato (*Solanum lycopersicum* L.). *Microbiol. Res.* 228:126302. doi: 10.1016/j.micres.2019.126302
- Gasser, F., Cardinale, M., Schildberger, B., and Berg, G. (2012). Biocontrol of *Botrytis cinerea* by successful introduction of *Pantoea ananatis* in the grapevine phyllosphere. *Int. J. Wine Res.* 4, 53–63. doi: 10.2147/ijwr.s31339
- Gómez Expósito, R., De Bruijn, I., Postma, J., and Raaijmakers, J. M. (2017). Current insights into the role of rhizosphere bacteria in disease suppressive soils. *Front. Microbiol.* 8:2529. doi: 10.3389/fmicb.2017.02529
- Gong, A.-D., Dong, F.-Y., Hu, M.-J., Kong, X.-W., Wei, F.-F., Gong, S.-J., et al. (2019). Antifungal activity of volatile emitted from *Enterobacter asburiae* Vt-7 against *Aspergillus flavus* and aflatoxins in peanuts during storage. *Food Control* 106:106718. doi: 10.1016/j.foodcont.2019.106718
- Green, P. (1992). “The genus methylobacterium,” in *The Prokaryotes*, 2nd Edn, eds A. Balows, H. G. Trüper, M. Dworkin, W. Harder, and K. H. Schleifer (Berlin: Springer-Verlag), 2342–2349. doi: 10.1007/0-387-30745-1\_14
- Hammer, Ø., Harper, D. A., and Ryan, P. D. (2001). PAST: paleontological statistics software package for education and data analysis. *Palaeontol. Electronica* 4, 1–9.
- Hardoim, P. R., Van Overbeek, L. S., Berg, G., Pirttilä, A. M., Compant, S., Campisano, A., et al. (2015). The hidden world within plants: ecological and evolutionary considerations for defining functioning of microbial endophytes. *Microbiol. Mol. Biol. Rev.* 79, 293–320. doi: 10.1128/mmbr.00050-14
- Harsonowati, W., Astuti, R. I., and Wahyudi, A. T. (2017). Leaf blast disease reduction by rice-phyllosphere actinomycetes producing bioactive compounds. *J. Gen. Plant Pathol.* 83, 98–108. doi: 10.1007/s10327-017-0700-4
- Hartmann, A., Rothballer, M., and Schmid, M. (2008). Lorenz Hiltner, a pioneer in rhizosphere microbial ecology and soil bacteriology research. *Plant Soil* 312, 7–14. doi: 10.1007/s11104-007-9514-z
- Hasegawa, M., Mitsuhara, I., Seo, S., Imai, T., Koga, J., Okada, K., et al. (2010). Phytoalexin accumulation in the interaction between rice and the blast fungus. *Mol. Plant Microbe Interact.* 23, 1000–1011. doi: 10.1094/mpmi-23-8-1000
- Hashim, I., Mamiro, D. P., Mabagala, R. B., and Tefera, T. (2018). Smallholder farmers’ knowledge, perception and management of rice blast disease in upland rice production in Tanzania. *J. Agric. Sci.* 10, 137–145.
- Horuz, S., and Aysan, Y. (2018). Biological control of watermelon seedling blight caused by *Acidovorax citrulli* using antagonistic bacteria from the genera *Curtobacterium*, *Microbacterium*, and *Pseudomonas*. *Plant Prot. Sci.* 54, 138–146. doi: 10.17221/168/2016-pps
- Innerebner, G., Knief, C., and Vorholt, J. A. (2011). Protection of *Arabidopsis thaliana* against leaf-pathogenic *Pseudomonas syringae* by *Sphingomonas* strains in a controlled model system. *Appl. Environ. Microbiol.* 77, 3202–3210. doi: 10.1128/aem.00133-11
- Jacobs, J., Carroll, T., and Sundin, G. (2005). The role of pigmentation, ultraviolet radiation tolerance, and leaf colonization strategies in the epiphytic survival of phyllosphere bacteria. *Microb. Ecol.* 49, 104–113. doi: 10.1007/s00248-003-1061-4
- Jiang, L., Jeong, J. C., Lee, J.-S., Park, J. M., Yang, J.-W., Lee, M. H., et al. (2019). Potential of *Pantoea dispersa* as an effective biocontrol agent for black rot in sweet potato. *Sci. Rep.* 9:16354. doi: 10.1038/s41598-019-52804-3
- Kaku, H., Subandiyah, S., and Ochiai, H. (2000). Red stripe of rice [*Oryza sativa*] is caused by a bacterium *Microbacterium* sp. *J. Gen. Plant Pathol.* 66, 149–152. doi: 10.1007/pl00012937
- Ke, Y., Kang, Y., Wu, M., Liu, H., Hui, S., Zhang, Q., et al. (2019). Jasmonic acid-involved *OsEDS1* signaling in Rice-bacteria interactions. *Rice* 12:25. doi: 10.1186/s12284-019-0283-0
- Ke, Y., Liu, H., Li, X., Xiao, J., and Wang, S. (2014). Rice *OsPAD4* functions differently from *ArabidopsisAtPAD4* in host-pathogen interactions. *Plant J.* 78, 619–631. doi: 10.1111/tj.12500
- Kim, H., Lee, K. K., Jeon, J., Harris, W. A., and Lee, Y.-H. (2020). Domestication of *Oryza* species eco-evolutionarily shapes bacterial and fungal communities in rice seed. *Microbiome* 8:20. doi: 10.1186/s40168-020-00805-0
- Klement, Z. (1963). Rapid detection of the pathogenicity of phytopathogenic pseudomonads. *Nature* 199, 299–300. doi: 10.1038/199299b0
- Knief, C., Delmotte, N., Chaffron, S., Stark, M., Innerebner, G., Wassmann, R., et al. (2012). Metaproteomic analysis of microbial communities in the phyllosphere and rhizosphere of rice. *ISME J.* 6, 1378–1390. doi: 10.1038/ismej.2011.192
- Koch, M., Vorwerk, S., Masur, C., Sharifi-Sirchi, G., Olivieri, N., and Schlaich, N. L. (2006). A role for a flavin-containing mono-oxygenase in resistance against microbial pathogens in *Arabidopsis*. *Plant J.* 47, 629–639. doi: 10.1111/j.1365-3113.2006.02813.x
- Kouzai, Y., Mochizuki, S., Nakajima, K., Desaki, Y., Hayafune, M., Miyazaki, H., et al. (2014). Targeted gene disruption of *OsCERK1* reveals its indispensable role in chitin perception and involvement in the peptidoglycan response and immunity in rice. *Mol. Plant Microbe Interact.* 27, 975–982.
- Kucheryava, N., Fiss, M., Auling, G., and Kroppenstedt, R. M. (1999). Isolation and characterization of epiphytic bacteria from the phyllosphere of apple, antagonistic in vitro to *Venturia inaequalis*, the causal agent of apple scab. *Syst. Appl. Microbiol.* 22, 472–478. doi: 10.1016/s0723-2020(99)80057-5

- Kumar, A., Sarma, Y., and Anandaraj, M. (2004). Evaluation of genetic diversity of *Ralstonia solanacearum* causing bacterial wilt of ginger using REP-PCR and PCR-RFLP. *Curr. Sci.* 87, 1555–1561.
- Kumar, M., Kumar, A., Sahu, K. P., Patel, A., Reddy, B., Sheoran, N., et al. (2021). Deciphering core-microbiome of rice leaf endosphere: revelation by metagenomic and microbiological analysis of aromatic and non-aromatic genotypes grown in three geographical zones. *Microbiol. Res.* 246:126704. doi: 10.1016/j.micres.2021.126704
- Lemanceau, P., Blouin, M., Muller, D., and Moënné-Loccoz, Y. (2017). Let the core microbiota be functional. *Trends Plant Sci.* 22, 583–595. doi: 10.1016/j.tplants.2017.04.008
- Leveau, J. H., and Lindow, S. E. (2001). Appetite of an epiphyte: quantitative monitoring of bacterial sugar consumption in the phyllosphere. *Proc. Natl. Acad. Sci. U.S.A.* 98, 3446–3453. doi: 10.1073/pnas.061629598
- Lindow, S. E., and Leveau, J. H. (2002). Phyllosphere microbiology. *Curr. Opin. Biotechnol.* 13, 238–243. doi: 10.1016/s0958-1669(02)00313-0
- Liu, C., Chen, X., Liu, T., Lian, B., Gu, Y., Caer, V., et al. (2007). Study of the antifungal activity of *Acinetobacter baumannii* LCH001 in vitro and identification of its antifungal components. *Appl. Microbiol. Biotechnol.* 76, 459–466. doi: 10.1007/s00253-007-1010-0
- Luo, Y., Zhou, M., Zhao, Q., Wang, F., Gao, J., Sheng, H., et al. (2020). Complete genome sequence of *Sphingomonas* sp. Cra20, a drought-resistant and plant growth-promoting rhizobacteria. *Genomics* 112, 3648–3657. doi: 10.1016/j.ygeno.2020.04.013
- Mackill, D., and Bonman, J. (1992). Inheritance of blast resistance in near-isogenic lines of rice. *Phytopathology* 82, 746–749. doi: 10.1094/phyto-82-746
- Mannaa, M., Oh, J., and Kim, K. D. (2017). Microbe-mediated control of *Aspergillus flavus* in stored rice grains with a focus on aflatoxin inhibition and biodegradation. *Ann. Appl. Biol.* 171, 376–392. doi: 10.1111/aab.12381
- Medina-Salazar, S. A., Rodriguez-Aguilar, M., Vallejo-Pérez, M. R., Flores-Ramirez, R., Marin-Sanchez, J., Aguilar-Benitez, G., et al. (2020). Biodiversity of epiphytic *Pseudomonas* strains isolated from leaves of pepper and lettuce. *Biologia* 75, 773–784. doi: 10.2478/s11756-019-00392-y
- Mehta, S., Singh, B., Dhakate, P., Rahman, M., and Islam, M. A. (2019). “Rice, marker-assisted breeding, and disease resistance,” in *Disease Resistance in Crop Plants*, ed. S. H. Wani (Cham: Springer), 83–111. doi: 10.1007/978-3-030-20728-1\_5
- Midha, S., Bansal, K., Sharma, S., Kumar, N., Patil, P. P., Chaudhry, V., et al. (2016). Genomic resource of rice seed associated bacteria. *Front. Microbiol.* 6:1551. doi: 10.3389/fmicb.2015.01551
- Mishina, T. E., and Zeier, J. (2006). The *Arabidopsis* flavin-dependent monooxygenase *FMO1* is an essential component of biologically induced systemic acquired resistance. *Plant Physiol.* 141, 1666–1675. doi: 10.1104/pp.106.081257
- Moore, E., Arnscheidt, A., Krüger, A., Strömpl, C., and Mau, M. (2004). “Simplified protocols for the preparation of genomic DNA from bacterial cultures,” in *Molecular Microbial Ecology Manual*, eds G. Kowalchuk, F. J. De Bruijn, I. Head, A. D. L. Akkermans, and J. D. van Elsas (London: Kluwer Academic Publishers), 1–15. doi: 10.1007/978-1-4020-2177-0\_101
- Munjal, V., Nadakkakath, A. V., Sheoran, N., Kundu, A., Venugopal, V., Subaharan, K., et al. (2016). Genotyping and identification of broad-spectrum antimicrobial volatiles in black pepper root endophytic biocontrol agent, *Bacillus megaterium* BP17. *Biol. Control* 92, 66–76. doi: 10.1016/j.biocontrol.2015.09.005
- Nalley, L., Tsiboe, F., Durand-Morat, A., Shew, A., and Thoma, G. (2016). Economic and environmental impact of rice blast pathogen (*Magnaporthe oryzae*) alleviation in the United States. *PLoS One* 11:e0167295. doi: 10.1371/journal.pone.0167295
- Patel, A., Kumar, A., Sheoran, N., Kumar, M., Sahu, K. P., Ganesan, P., et al. (2020). Antifungal and defense elicitor activities of pyrazines identified in endophytic *Pseudomonas putida* BP25 against fungal blast incited by *Magnaporthe oryzae* in rice. *J. Plant Dis. Prot.* 128, 261–272. doi: 10.1007/s41348-020-00373-3
- Prakash, G., Patel, A., Prakash, I., Sahu, K. P., Hosahatti, R., and Kumar, A. (2021). “Microconidia: understanding its role in the fungus *Magnaporthe oryzae* Inciting Rice Blast Disease,” in *Blast Disease of Cereal Crops*, eds S. C. Nayaka, R. Hosahatti, G. Prakash, C. T. Satyavathi, and T. R. Sharma (Cham: Springer), 143–150. doi: 10.1007/978-3-030-60585-8\_10
- Rajashekara, H., Prakash, G., Pandian, R., Sarkel, S., Dubey, A., Sharma, P., et al. (2017). An efficient technique for isolation and mass multiplication of *Magnaporthe oryzae* from blast infected samples. *Indian Phytopathol.* 69, 260–265.
- Rariz, G., Ferrando, L., Echegoyen, N., and Scavino, A. F. (2017). Antagonism between *Azospirillum brasilense* Az39 and *Pseudomonas oryzae* habitan, a seed-borne endophyte, in growing rice plants. *Rev. Agron. Noroeste Argent.* 37, 45–56.
- Rascovan, N., Carbonetto, B., Perrig, D., Díaz, M., Canciani, W., Abalo, M., et al. (2016). Integrated analysis of root microbiomes of soybean and wheat from agricultural fields. *Sci. Rep.* 6:28084. doi: 10.1038/srep28084
- Reinhold-Hurek, B., Büniger, W., Burbano, C. S., Sabale, M., and Hurek, T. (2015). Roots shaping their microbiome: global hotspots for microbial activity. *Annu. Rev. Phytopathol.* 53, 403–424. doi: 10.1146/annurev-phyto-082712-102342
- Ren, G., Zhang, H., Lin, X., Zhu, J., and Jia, Z. (2014). Response of phyllosphere bacterial communities to elevated CO<sub>2</sub> during rice growing season. *Appl. Microbiol. Biotechnol.* 98, 9459–9471. doi: 10.1007/s00253-014-5915-0
- Roman-Reyna, V., Pinili, D., Borjaa, F. N., Quibod, I., Groen, S. C., Mulyaningsih, E. S., et al. (2019). *The Rice Leaf Microbiome has a Conserved Community Structure Controlled by Complex Host-Microbe Interactions*. Available online at: [https://papers.ssrn.com/sol3/papers.cfm?abstract\\_id=3382544](https://papers.ssrn.com/sol3/papers.cfm?abstract_id=3382544) (accessed May 2019).
- Sadeghi, K., and Khodakaramian, G. (2020). Characteristics and Ice Nucleation Activity of Sugarcane Epiphytic and Endophytic Bacteria and Their Role in Host Frostbite. *Sugar Tech* 22, 291–302. doi: 10.1007/s12355-019-00759-0
- Sahu, K. P., Kumar, A., Patel, A., Kumar, M., Gopalakrishnan, S., Prakash, G., et al. (2020). Rice Blast Lesions: an Unexplored Phyllosphere Microhabitat for Novel Antagonistic Bacterial Species Against *Magnaporthe oryzae*. *Microb. Ecol.* 81, 731–745. doi: 10.1007/s00248-020-01617-3
- Scheuermann, K. K., Raimondi, J. V., Marschalek, R., De Andrade, A., and Wickert, E. (2012). “*Magnaporthe oryzae* genetic diversity and its outcomes on the search for durable resistance,” in *The Molecular Basis of Plant Genetic Diversity*, ed. M. Caliskan (Rijeka: IntechOpen), 331–356. doi: 10.5772/33479
- Schlatter, D., Kinkel, L., Thomashow, L., Weller, D., and Paulitz, T. (2017). Disease suppressive soils: new insights from the soil microbiome. *Phytopathology* 107, 1284–1297. doi: 10.1094/phyto-03-17-0111-rwv
- Sella, L., Vu, V. V., Quarantin, A., Caracciolo, R., Govind, R., Bolzonello, A., et al. (2021). “Sustainable methods to control *Pyricularia oryzae*, the causal agent of rice blast disease,” in *Innovations in Land, Water and Energy for Vietnam’s Sustainable Development*, ed. M. Anderle (Berlin: Springer), 67–82. doi: 10.1007/978-3-030-51260-6\_7
- Sessitsch, A., Hardoim, P., Döring, J., Weilharter, A., Krause, A., Woyke, T., et al. (2012). Functional characteristics of an endophyte community colonizing rice roots as revealed by metagenomic analysis. *Mol. Plant Microbe Interact.* 25, 28–36. doi: 10.1094/mpmi-08-11-0204
- Sheoran, N., Kumar, A., Munjal, V., Nadakkakath, A. V., and Eapen, S. J. (2016). *Pseudomonas putida* BP25 alters root phenotype and triggers salicylic acid signaling as a feedback loop in regulating endophytic colonization in *Arabidopsis thaliana*. *Physiol. Mol. Plant Pathol.* 93, 99–111. doi: 10.1016/j.pmp.2016.01.008
- Sheoran, N., Nadakkakath, A. V., Munjal, V., Kundu, A., Subaharan, K., Venugopal, V., et al. (2015). Genetic analysis of plant endophytic *Pseudomonas putida* BP25 and chemo-profiling of its antimicrobial volatile organic compounds. *Microbiol. Res.* 173, 66–78. doi: 10.1016/j.micres.2015.02.001
- Singh, V. K., Singh, A., Singh, S., Ellur, R. K., Choudhary, V., Sarkel, S., et al. (2012). Incorporation of blast resistance into “PRR78”, an elite Basmati rice restorer line, through marker-assisted backcross breeding. *Field Crops Res.* 128, 8–16. doi: 10.1016/j.fcr.2011.12.003
- Stockwell, V., Johnson, K., Sugar, D., and Loper, J. (2010). Control of fire blight by *Pseudomonas fluorescens* A506 and *Pantoea vagans* C9-1 applied as single strains and mixed inocula. *Phytopathology* 100, 1330–1339. doi: 10.1094/phyto-03-10-0097
- Stone, B. W., and Jackson, C. R. (2020). Seasonal patterns contribute more towards phyllosphere bacterial community structure than short-term perturbations. *Microb. Ecol.* 81, 146–156. doi: 10.1007/s00248-020-01564-z

- Sugano, S., Jiang, C.-J., Miyazawa, S.-I., Masumoto, C., Yazawa, K., Hayashi, N., et al. (2010). Role of *OsNPR1* in rice defense program as revealed by genome-wide expression analysis. *Plant Mol. Biol.* 74, 549–562. doi: 10.1007/s11103-010-9695-3
- Sundin, G., and Jacobs, J. (1999). Ultraviolet radiation (UVR) sensitivity analysis and UVR survival strategies of a bacterial community from the phyllosphere of field-grown peanut (*Arachis hypogaea* L.). *Microb. Ecol.* 38, 27–38. doi: 10.1007/s002489900152
- Thomma, B. P., Cammue, B. P., and Thevissen, K. (2002). Plant defensins. *Planta* 216, 193–202. doi: 10.1007/s00425-002-0902-6
- Turner, A. D. (2020). Exploring Interactions of Phyllosphere Epiphytes with Plant Pathogenic Bacteria *Pseudomonas* and *Xanthomonas* on Tomato. Available online at: [https://csuepress.columbusstate.edu/theses\\_dissertations/395](https://csuepress.columbusstate.edu/theses_dissertations/395) (accessed September 2, 2021).
- Vagelas, I., and Gowen, S. (2012). Control of *Fusarium oxysporum* and root-knot nematodes (*Meloidogyne* spp.) with *Pseudomonas oryzae* habitans. *Pak. J. Phytopathol.* 24, 32–38.
- Vandana, U. K., Rajkumari, J., Singha, L. P., Satish, L., Alavilli, H., Sudheer, P. D., et al. (2021). The endophytic microbiome as a hotspot of synergistic interactions, with prospects of plant growth promotion. *Biology* 10:101. doi: 10.3390/biology10020101
- Versalovic, J., Schneider, M., De Bruijn, F., and Lupski, J. R. (1994). Genomic fingerprinting of bacteria using repetitive sequence-based polymerase chain reaction. *Methods Mol. Cell. Biol.* 5, 25–40. doi: 10.1007/978-1-4615-6369-3\_34
- Vorholt, J. A. (2012). Microbial life in the phyllosphere. *Nat. Rev. Microbiol.* 10, 828–840. doi: 10.1038/nrmicro2910
- Wachowska, U., Irzykowski, W., Jędryczka, M., Stasiulewicz-Paluch, A. D., and Głowacka, K. (2013). Biological control of winter wheat pathogens with the use of antagonistic *Spingomonas* bacteria under greenhouse conditions. *Biocontrol Sci. Technol.* 23, 1110–1122.
- Wang, Y., Holland, J., and Balint-Kurti, P. (2021). Development and use of a seedling growth retardation assay to quantify and map loci underlying variation in the maize basal defense response. *PhytoFrontiers*. 1, 149–159. doi: 10.1094/phytofr-12-20-0038-r
- Yasmin, S., Hakim, S., Zaheer, A., Mirza, B., and Mirza, M. S. (2020). Metagenomic Analysis of Bacterial Community Associated with Rhizosphere and Phyllosphere of Basmati Rice. *bioRxiv* [Preprint]. doi: 10.1101/2020.04.09.034009
- Yasuda, N., Mitsunaga, T., Hayashi, K., Koizumi, S., and Fujita, Y. (2015). Effects of pyramiding quantitative resistance genes *pi21*, *Pi34*, and *Pi35* on rice leaf blast disease. *Plant Dis.* 99, 904–909. doi: 10.1094/pdis-02-14-0214-re
- Zhang, J., Kobert, K., Flouri, T., and Stamatakis, A. (2014). PEAR: a fast and accurate Illumina Paired-End reAd mergeR. *Bioinformatics* 30, 614–620. doi: 10.1093/bioinformatics/btt593
- Zhu, Y. L., She, X.-P., Wang, J. S., and Lv, H. Y. (2017). Endophytic bacterial effects on seed germination and mobilization of reserves in *Ammodendron biofolium*. *Pak. J. Bot.* 49, 2029–2035.

**Conflict of Interest:** The authors declare that the research was conducted in the absence of any commercial or financial relationships that could be construed as a potential conflict of interest.

The reviewer KV declared a shared affiliation with the authors, to the handling editor at the time of the review.

**Publisher's Note:** All claims expressed in this article are solely those of the authors and do not necessarily represent those of their affiliated organizations, or those of the publisher, the editors and the reviewers. Any product that may be evaluated in this article, or claim that may be made by its manufacturer, is not guaranteed or endorsed by the publisher.

Copyright © 2021 Sahu, Patel, Kumar, Sheoran, Mehta, Reddy, Eke, Prabhakaran and Kumar. This is an open-access article distributed under the terms of the Creative Commons Attribution License (CC BY). The use, distribution or reproduction in other forums is permitted, provided the original author(s) and the copyright owner(s) are credited and that the original publication in this journal is cited, in accordance with accepted academic practice. No use, distribution or reproduction is permitted which does not comply with these terms.



# Biocontrol Potential of *Aspergillus* Species Producing Antimicrobial Metabolites

Men Thi Ngo<sup>1,2</sup>, Minh Van Nguyen<sup>1,2</sup>, Jae Woo Han<sup>1</sup>, Bomin Kim<sup>1,2</sup>, Yun Kyung Kim<sup>1,2</sup>, Myung Soo Park<sup>3</sup>, Hun Kim<sup>1,2\*</sup> and Gyung Ja Choi<sup>1,2\*</sup>

<sup>1</sup>Center for Eco-friendly New Materials, Korea Research Institute of Chemical Technology, Daejeon, South Korea,

<sup>2</sup>Department of Medicinal Chemistry and Pharmacology, University of Science and Technology, Daejeon, South Korea,

<sup>3</sup>School of Biological Sciences, Seoul National University, Seoul, South Korea

## OPEN ACCESS

### Edited by:

Jochen Fischer,  
Institut für Biotechnologie und  
Wirkstoff-Forschung (IBWF),  
Germany

### Reviewed by:

Laith Khalil Tawfeeq Al-Ani,  
Universiti Sains Malaysia, Malaysia  
Karthik Loganathan,  
Salem Microbes Pvt Ltd, India

### \*Correspondence:

Hun Kim  
hunkim@kriict.re.kr  
Gyung Ja Choi  
kjchoi@kriict.re.kr

### Specialty section:

This article was submitted to  
Microbe and Virus Interactions With  
Plants,  
a section of the journal  
Frontiers in Microbiology

Received: 29 October 2021

Accepted: 30 November 2021

Published: 23 December 2021

### Citation:

Ngo MT, Nguyen MV, Han JW,  
Kim B, Kim YK, Park MS, Kim H and  
Choi GJ (2021) Biocontrol Potential  
of *Aspergillus* Species Producing  
Antimicrobial Metabolites.  
Front. Microbiol. 12:804333.  
doi: 10.3389/fmicb.2021.804333

Microbial metabolites have been recognized as an important source for the discovery of new antifungal agents because of their diverse chemical structures with novel modes of action. In the course of our screening for new antifungal agents from microbes, we found that culture filtrates of two fungal species *Aspergillus candidus* SFC20200425-M11 and *Aspergillus montenegroi* SFC20200425-M27 have the potentials to reduce the development of fungal plant diseases such as tomato late blight and wheat leaf rust. From these two *Aspergillus* spp., we isolated a total of seven active compounds, including two new compounds (**4** and **6**), and identified their chemical structures based on the NMR spectral analyses: sphaeropsidin A (**1**), (*R*)-formosusin A (**2**), (*R*)-variotin (**3**), candidusin (**4**), asperlin (**5**), montenegrol (**6**), and protulactone A (**7**). Based on the results of the *in vitro* bioassays of 11 plant pathogenic fungi and bacteria, sphaeropsidin A (**1**), (*R*)-formosusin A (**2**), (*R*)-variotin (**3**), and asperlin (**5**) exhibited a wide range of antimicrobial activity. Furthermore, when plants were treated with sphaeropsidin A (**1**) and (*R*)-formosusin A (**2**) at a concentration of 500 µg/ml, sphaeropsidin A (**1**) exhibited an efficacy disease control value of 96 and 90% compared to non-treated control against tomato late blight and wheat leaf rust, and (*R*)-formosusin A (**2**) strongly reduced the development of tomato gray mold by 82%. Asperlin (**5**) at a concentration of 500 µg/ml effectively controlled the development of tomato late blight and wheat leaf rust with a disease control value of 95%. Given that culture filtrates and active compounds derived from two *Aspergillus* spp. exhibited disease control efficacies, our results suggest that the *Aspergillus*-produced antifungal compounds could be useful for the development of new natural fungicides.

**Keywords:** *Aspergillus candidus*, *Aspergillus montenegroi*, plant disease, biocontrol, antimicrobial compound

## INTRODUCTION

The world population is expected to reach up to 9.7 billion people by 2050, postulating that the required agricultural food production increases up to at least 50–110% (Godfray et al., 2010; Raymaekers et al., 2020). Considering that the additional agricultural area is limited, the reduction of crop yield losses caused by plant pathogens has gained the most



attention contributing to food security (Mauser et al., 2015; Raymaekers et al., 2020). Although the use of synthetic pesticides has been recognized as one of the most effective methods to control plant diseases, the overuse of chemical pesticides has led to severe problems, such as resistance, toxicity in humans and animals, and environmental pollution (Hüter, 2011). To compensate for the shortcomings of chemical pesticides, the development and use of biological pesticides based on natural resources exhibiting a promising antimicrobial activity have been crucial in agriculture (Dayan et al., 2009; Choi et al., 2010).

To date, there are over 23,000 known microbial secondary metabolites that are significant sources for life-saving drugs, and 42% of which are produced by fungi (Demain, 2014; Chandra et al., 2020). The genus *Aspergillus* has been recognized as an enormous source of lead compounds with promising diverse structures and biological activities (Sadorn et al., 2016). Notably, from 2015 to 2019, 362 secondary metabolites were isolated from different *Aspergillus* species, including alkaloids, butenolides, and cytochalasins, which showed diverse biological activities such as antimicrobial, anti-inflammatory, and anticancer activities (El-hawary et al., 2020). Regarding the antimicrobial activity, it has been reported that aspetritones and candidusin derivatives isolated from the culture of *Aspergillus tritici* SP2-8-1 exhibited antibacterial activity against the methicillin-resistant strain *Staphylococcus aureus* (Wang et al., 2017). Two new compounds, aspergillethers A and B, from the endophytic fungus *Aspergillus versicolor* exhibited significant *in vitro* antibacterial and antifungal activities toward *S. aureus*, *Bacillus cereus*, and *Candida albicans* (Mohamed et al., 2020). Despite efforts to find secondary metabolites showing antimicrobial activity, to date, relatively few *Aspergillus* species have been considered as biological agents for plant protection (Zhao et al., 2018; El-Sayed and Ali, 2020).

With the production of antimicrobial metabolites, some fungal species have been reported as a potent material for controlling plant diseases. For example, the basidiomycete fungus *Crinipellis rhizomaticola* culture filtrate and its active compounds crinipellins suppressed the development of rice blast and pepper anthracnose caused by *Magnaporthe oryzae* and *Collectotrichum coccodes*, respectively (Han et al., 2018). Jang et al. (2016) also showed that a culture filtrate of *Aspergillus niger* F22 was highly active against a root-knot nematode *Meloidogyne incognita* by which a nematocidal component oxalic acid affected the mortality of second-stage juveniles and the inhibition of egg hatching. Later, the strain *A. niger* F22 was registered as a natural nematocidal agent in the Korean market (Lee et al., 2017).

The marine environment has been investigated for new natural resources containing bioactive compounds with benefits for the health of humans, animals, and plants (Sohn and Oh, 2010). For this endeavor, marine-derived resources have gained much attention in the past decades (Buttachon et al., 2018). In particular, marine-derived fungi have been considered as a rich source of secondary metabolites with promising antimicrobial effects (Neuhaus et al., 2019; Wang et al., 2021), representing unprecedented scaffolds for further drug design

for specific modes of action (Xu et al., 2015; Willems et al., 2020). In the current study, our main goals were (1) to find *Aspergillus* species derived from a marine environment that have *in vitro* and *in vivo* antimicrobial properties against plant pathogens and (2) to identify the active metabolites from the selected *Aspergillus* species. Based on the *in vitro* antimicrobial activity and plant disease control efficacies of the fungal cultures containing the identified active compounds, our results could provide valuable information to develop new biological control agents for crops.

## MATERIALS AND METHODS

### Fungal and Bacterial Strains Used in This Study

The eight strains of *Aspergillus* species used in this study were kindly provided by Dr. Myung Soo Park (Marine Fungal Resource Bank, Seoul National University; **Supplementary Table S1**). Of these strains, SFC20200425-M11 and SFC20200425-M27 showing a promising plant disease control efficacy were deposited as a patent microorganism to the Korean Agricultural Culture Collection (KACC, Wanju, South Korea).

For the *in vitro* antifungal activity assay, six plant pathogenic fungi provided by the KACC were used: *Alternaria brassicicola* (KACC 40036), *Botrytis cinerea* (KACC 48736), *C. coccodes* (KACC 48737), *Fusarium oxysporum* (KACC 40043), *M. oryzae* (KACC 46552), and *Phytophthora infestans* (KACC 48738). Additionally, we used two obligate parasitic fungi *Puccinia triticina* and *Blumeria graminis* f. sp. *hordei*, which were maintained on their host plants, for the disease control efficacy assay (Choi et al., 2010; Shin et al., 2017; Han et al., 2018). For the antibacterial activity assay, the five following bacterial species were used: *Agrobacterium tumefaciens* SL2434, *Clavibacter michiganensis* SL4135, *Pseudomonas syringae* SL308, *Ralstonia solanacearum* SL1944, and *Erwinia amylovora* TS3128. All bacteria were provided by the National Academy of Agricultural Sciences (Wanju, Korea), except for *R. solanacearum* provided by Dr. SW Lee of Dong-A University (Vu et al., 2017). The fungi and bacteria were maintained on potato dextrose agar (PDA; BD Difco, Sparks, MD, United States) medium and tryptic soy agar (TSA; BD Difco) medium, respectively, and kept at 4°C before use.

### Phylogenetic Analysis

For the isolation of genomic DNA (gDNA), each fungal species was grown in 50 ml of potato dextrose broth (PDB; BD Difco) medium at 25°C for 4 days on a rotary shaker (150 rpm). The gDNA was extracted using the cetyltrimethylammonium bromide (CTAB) procedure as previously described (Han et al., 2018). For phylogenetic analysis, the calmodulin (*CaM*) gene was amplified by the primer set CF1D (5'-CAGGTCTCCGA GTACAAG-3') and CF4 (5'-CAGGTCTCCGAGTACAAGTTTY TGCATCATRAGYTGGAC-3'; Lee et al., 2016). The resulting amplicon was purified using the GeneAll Expin™ PCR purification kit (GeneAll, Seoul, South Korea) and then analyzed

using corresponding PCR primers by Macrogen (Seoul, Korea). The resulting sequences were analyzed with the BLASTn program of the NCBI.<sup>1</sup> The sequences were aligned using ClustalW implemented in MEGA version X, and distances were estimated based on the Tamura-Nei model (Tamura and Nei, 1993). A phylogenetic tree was generated using the neighbor-joining method with 1,000 bootstrap analyses (Saitou and Nei, 1987).

## Isolation Procedures of Antimicrobial Metabolites

Twenty mycelial disks (8 mm in diameter) of each fungal strain, SFC20200425-M11 and SFC20200425-M27, were inoculated into 400 ml PDB medium in a 2 L-baffled Erlenmeyer flask and incubated on a rotary shaker at 150 rpm and 25°C for 10 days. The culture broths of SFC20200425-M11 (3.6 L) and SFC20200425-M27 (1.6 L) were centrifuged at 10,000 × *g* for 30 min and then filtered through two layers of Whatman No. 1 filter paper (Maidstone, United Kingdom). The culture filtrates were partitioned with an equal volume of ethyl acetate (EtOAc) and *n*-butanol (BuOH), sequentially. Each layer was concentrated to dryness by a rotary evaporator (Rotavapor R-300; Büchi, Flawil, Switzerland).

From the culture filtrate of SFC20200425-M11, the EtOAc (370 mg), BuOH (640 mg), and water (6.8 g) extracts were obtained. The EtOAc extract was applied onto a silica gel column (40–63 µm; Merck, Darmstadt, Germany), using an isocratic elution of *n*-hexane/EtOAc (3:1, v/v) to give five fractions (E1–E5). The E3 and E4 fractions were pure compounds **1** (51 mg) and **2** (35 mg), respectively. Fraction E5 (152 mg) was further separated by preparative thin-layer chromatography (TLC) using Kieselgel 60 F254 glass plates (Merck). The TLC plates were developed with *n*-hexane/EtOAc (60:40, v/v) to give five fractions (E51–E55). Fraction E55 was a pure compound **4** (13 mg), and fraction E52 was further purified by high-pressure liquid chromatography (HPLC) using the Shimadzu LC-6 AD system (Kyoto, Japan). The Capcell Pak C18 column (20 × 250 mm, 5 µm; Shiseido, Tokyo, Japan) was used for preparative HPLC and eluted with 68% aqueous methanol at a flow rate of 5 ml/min to give compound **3** (2 mg).

Among the obtained EtOAc (338 mg), BuOH (340 mg), and water (3.1 g) extracts from the culture broth of SFC20200425-M27, the EtOAc extract was purified by preparative HPLC. The column was eluted with 30% aqueous methanol to give compound **5** (91.2 mg). Next, the BuOH extract was separated by an Isolera One mid-pressure liquid chromatography (MPLC) system (Biotage, Uppsala, Sweden) equipped with the Biotage SNAP Ultra C18 cartridge (60 g). The column was eluted with a linear gradient of aqueous methanol (2–100%, v/v) to give two fractions (B1 and B2). Fraction B2 was pure compound **7** (21 mg). The fraction B1 (70 mg) was further purified by preparative HPLC. The column was eluted with 8% aqueous methanol to give compound **6** (22 mg). The isolation schemes for all compounds **1–7** are presented in **Supplementary Figures S1 and S2**.

## General Experimental Procedures for Chemical Structural Elucidation

Chemical structures of the purified compounds were determined by spectroscopic analyses and comparison with previous literature data. High-resolution electrospray ionization mass spectrometry (HRESIMS) data were obtained by the Synapt G2 system (Waters, Milford, MA, United States). The 1D and 2D nuclear magnetic resonance (NMR) spectra were recorded by a Bruker Advance 500 MHz spectrometer (Rheinstetten, Germany) in chloroform-*d*<sub>3</sub>, methanol-*d*<sub>4</sub>, or pyridine-*d*<sub>5</sub> (Cambridge Isotope Laboratories, Andover, MA, United States). Chemical shifts were referenced to the solvent peaks ( $\delta_{\text{H}}$  7.26 and  $\delta_{\text{C}}$  77.2 for chloroform-*d*<sub>3</sub>;  $\delta_{\text{H}}$  4.87 and  $\delta_{\text{C}}$  49.0 for methanol-*d*<sub>4</sub>;  $\delta_{\text{H}}$  8.71 and  $\delta_{\text{C}}$  149.9 for pyridine-*d*<sub>5</sub>).

## Esterification of Compound 4

To determine the absolute configuration of the secondary alcohol compound **4**, Mosher's method using  $\alpha$ -methoxy- $\alpha$ -trifluoromethylphenylacetic acid (MTPA) esters was performed as previously described by Nguyen et al. (2018). Briefly, the (*R/S*)-MTPA esters of **4** (**4a** and **4b**) were prepared using Mosher's esterification method. Compounds **4** (0.5 mg) and 4-(dimethylamino)-pyridine (0.2 mg) were mixed into a 5 ml vial, and then, the mixture was dried *in vacuo*. Pyridine-*d*<sub>5</sub> (0.5 ml) and (*R*)-MPTA or (*S*)-MPTA (Sigma-Aldrich, St Louis, MO, United States; 6.0 µl) were immediately put into the vial, and then the vial was sealed and shaken to mix evenly. The reaction was carried out at room temperature for 12 h. The reactant was transferred into an NMR tube to measure the <sup>1</sup>H-NMR and <sup>1</sup>H–<sup>1</sup>H COSY spectra.

## In vitro Antimicrobial Assay

The values for the minimum inhibitory concentration (MIC) of the purified compounds **1–7** were determined against plant pathogenic fungi and bacteria by the broth microdilution method using 96-well microtiter plates modified according to previous methods for the testing of potential antimicrobial natural products (Espinell-Ingroff et al., 2005; Vu et al., 2017; Ngo et al., 2019). Briefly, fungal spore suspensions (5 × 10<sup>4</sup> spores/ml) or bacterial cell suspensions (2 × 10<sup>5</sup> CFU/ml) were added to each well of a 96-well microtiter plate containing PDB or tryptic soy broth (TSB; BD Difco) medium, respectively. The purified compounds dissolved in methanol were added and then serially two-fold diluted to reach the final concentrations ranging from 0.06 to 250 µg/ml. The microtiter plates were incubated for 1–2 days, and the MIC values were determined by visual inspection of complete growth inhibition (Espinell-Ingroff et al., 2005). Blasticidin-S and oxytetracycline were used as positive controls for the antifungal and antibacterial assays, respectively. The medium containing 1% methanol was used as a negative control.

## Disease Control Efficacy Assay

Six plant diseases caused by fungi were used for the plant disease control efficacy assay: rice blast (RCB, caused by *M. oryzae*), tomato gray mold (TGM, caused by *B. cinerea*), tomato

<sup>1</sup><http://www.ncbi.nlm.nih.gov>

late blight (TLB, caused by *P. infestans*), wheat leaf rust (WLR, caused by *P. tritricina*), barley powdery mildew (BPM, caused by *B. graminis* f. sp. *hordei*), and pepper anthracnose (PAN, caused by *C. coccodes*). We performed the plant disease control efficacy assay as previously described (Lee et al., 2007; Ngo et al., 2021). Briefly, rice (*Oryza sativa* L, cv. Chucheong), tomato (*Solanum lycopersicum* cv. Seokwang), wheat (*Triticum aestivum* cv. Geumgang), barley (*Hordeum sativum* cv. Hanyoung), and pepper (*Capsicum annuum* cv. Hyangchon) were used as host plants, which were grown in a greenhouse at  $25 \pm 5^\circ\text{C}$  for 3–4 weeks. One day before pathogen inoculation, the culture filtrates were directly applied onto the plant by spraying. The plants were also treated with the solvent extracts (1,000  $\mu\text{g}/\text{ml}$ ) and pure compounds (125, 250, and 500  $\mu\text{g}/\text{ml}$ ), which were dissolved in 5% aqueous methanol (v/v), using the same method for the culture filtrates. When the culture filtrates, solvent extracts, and pure compounds were applied to the plants, the samples contained 0.025% Tween 20 (w/v) as a wetting agent. Chemical fungicides (blasticidin S, validamycin, fludioxonil, dimethomorph, flusilazole, and dithianon) and 5% aqueous methanol were used as positive and negative controls, respectively. The treated plants were inoculated with spore suspensions ( $5 \times 10^4$  spores/ml) of each fungal pathogen and incubated as previously described (Ngo et al., 2021). The experiment was conducted twice with three replicates for each treatment. The disease control efficacy was calculated with the following equation: control efficacy (%) =  $100 \times [1 - B/A]$ , where A is the mean lesion area (%) on the leaves of the control plants, and B is the mean lesion area (%) on the leaves of the treated plants (Lee et al., 2007).

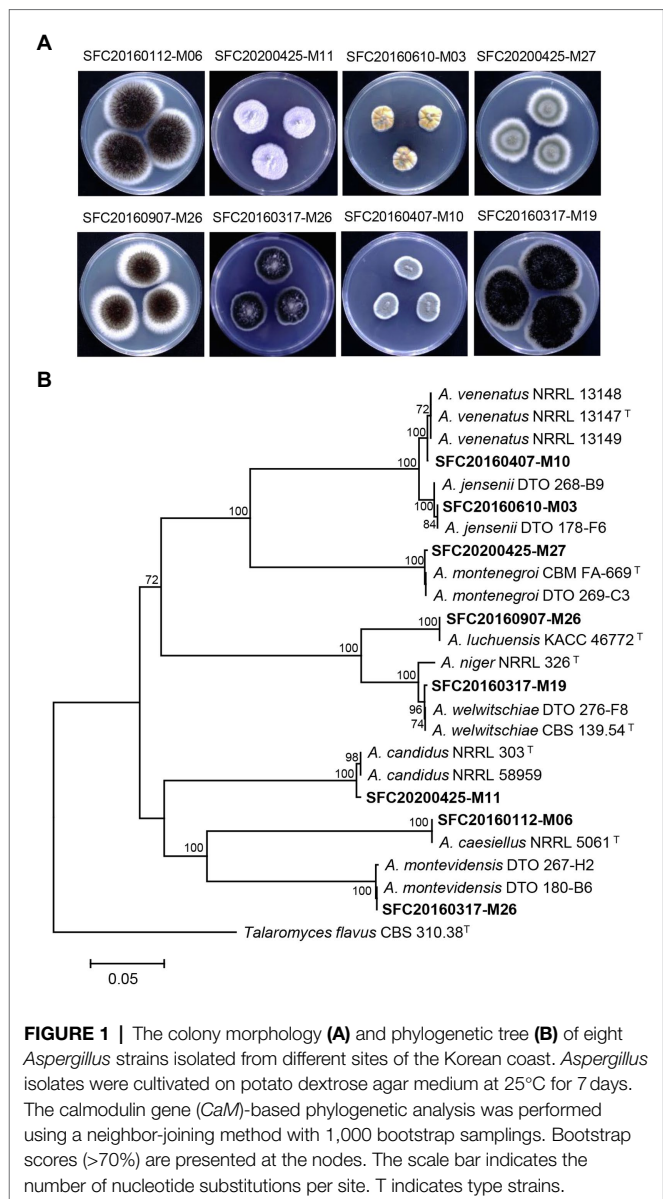
## Statistical Analysis

Data were subjected to one-way ANOVA, and the means of the treatments were separated by Duncan's multiple range test ( $p < 0.05$ ) using the R-software (Version 4.0.5). All values are expressed as the mean  $\pm$  standard deviation. Significant differences ( $p < 0.05$ ) were indicated with different small letters in each bar.

## RESULTS AND DISCUSSION

### Identification of the Marine-Derived *Aspergillus* Species

Marine-derived fungi have been considered as a rich source of bioactive compounds with promising antimicrobial effects and plant disease control efficacy (Xu et al., 2015; Wang et al., 2021). In this study, a total of eight marine-derived *Aspergillus* spp. was isolated from different sites of the Korean coast (Supplementary Table S1). After cultivation on PDA medium for 7 days, eight strains of marine-derived *Aspergillus* showed different colony morphologies (Figure 1A). The *CaM* gene-based phylogenetic tree was constructed for the identification of the *Aspergillus* species (Figure 1B). In a previous study, two *Aspergillus* strains SFC20160112-M06 and SFC20160407-M10 were identified as *Aspergillus caesiellus* and *A. venenatus*, respectively (Lee et al., 2016). Here, six *Aspergillus* strains SFC20160610-M03, SFC20200425-M27, SFC20160907-M26, SFC20160317-M19, SFC20200425-M11, and SFC20160317-M26 were identified as *A. jensenii*, *A. montenegroi*, *A. luchuensis*, *A. welwitschiae*, *A. candidus*, and *A. montevidensis*, respectively (Figure 1B).



**FIGURE 1 |** The colony morphology (A) and phylogenetic tree (B) of eight *Aspergillus* strains isolated from different sites of the Korean coast. *Aspergillus* isolates were cultivated on potato dextrose agar medium at  $25^\circ\text{C}$  for 7 days. The calmodulin gene (*CaM*)-based phylogenetic analysis was performed using a neighbor-joining method with 1,000 bootstrap samplings. Bootstrap scores ( $>70\%$ ) are presented at the nodes. The scale bar indicates the number of nucleotide substitutions per site. T indicates type strains.

SFC20160317-M19, SFC20200425-M11, and SFC20160317-M26 were identified as *A. jensenii*, *A. montenegroi*, *A. luchuensis*, *A. welwitschiae*, *A. candidus*, and *A. montevidensis*, respectively (Figure 1B).

### Plant Disease Control Efficacy of the Culture Filtrates and Their Partitioned Fractions

To explore the potential of these *Aspergillus* strains in plant disease control, the disease control efficacy of the culture filtrates was investigated against six plant diseases RCB, TGM, TLB, WLR, BPM, and PAN (Table 1). When the plants were treated with each culture filtrate, the culture filtrate of *A. candidus* SFC20200425-M11 significantly reduced the disease development of TGM and PAN with control values of 82 and 91%, respectively, compared to the non-treatment control (Table 1). In contrast,



**TABLE 1** | *In vivo* antifungal activity of *Aspergillus* species against plant pathogenic fungi.

Treatment	Conc. (μg/ml)	Disease control (%)					
		RCB	TGM	TLB	WLR	BPM	PAN
<i>Aspergillus caesiellus</i> (SFC20160112-M06)	cf	0 <sup>e</sup>	0 <sup>d</sup>	0 <sup>c</sup>	0 <sup>d</sup>	0 <sup>e</sup>	10 ± 7 <sup>c</sup>
<i>A. candidus</i> (SFC20200425-M11)	cf	0 <sup>e</sup>	82 ± 5 <sup>b</sup>	36 ± 10 <sup>b</sup>	20 ± 0 <sup>c</sup>	25 ± 12 <sup>cd</sup>	91 ± 5 <sup>a</sup>
<i>A. jensenii</i> (SFC20160610-M03)	cf	17 ± 13 <sup>de</sup>	0 <sup>d</sup>	0 <sup>c</sup>	60 ± 9 <sup>b</sup>	33 ± 0 <sup>c</sup>	0 <sup>c</sup>
<i>A. luchuensis</i> (SFC20160907-M26)	cf	pt	0 <sup>d</sup>	0 <sup>c</sup>	pt	pt	75 ± 9 <sup>a</sup>
<i>A. montenegroi</i> (SFC20200425-M27)	cf	33 ± 0 <sup>d</sup>	0 <sup>d</sup>	98 ± 1 <sup>a</sup>	100 <sup>a</sup>	0 <sup>e</sup>	35 ± 7 <sup>b</sup>
<i>A. montevideensis</i> (SFC20160317-M26)	cf	0 <sup>e</sup>	0 <sup>d</sup>	0 <sup>c</sup>	0 <sup>d</sup>	0 <sup>e</sup>	10 ± 7 <sup>c</sup>
<i>A. venenatus</i> (SFC20160407-M10)	cf	pt	pt	pt	pt	pt	pt
<i>A. welwitschiae</i> (SFC20160317-M19)	cf	pt	pt	pt	pt	pt	pt
<i>A. candidus</i> EtOAc extract	1,000	56 ± 9 <sup>c</sup>	100 <sup>a</sup>	94 ± 2 <sup>a</sup>	73 ± 9 <sup>b</sup>	8 ± 6 <sup>de</sup>	91 ± 5 <sup>a</sup>
<i>A. candidus</i> BuOH extract	1,000	0 <sup>e</sup>	21 ± 10 <sup>c</sup>	0 <sup>c</sup>	20 ± 0 <sup>c</sup>	0 <sup>e</sup>	0 <sup>c</sup>
<i>A. candidus</i> water extract	1,000	0 <sup>e</sup>	0 <sup>d</sup>	0 <sup>c</sup>	0 <sup>d</sup>	0 <sup>e</sup>	0 <sup>c</sup>
<i>A. montenegroi</i> EtOAc extract	1,000	79 ± 5 <sup>abc</sup>	7 ± 5 <sup>cd</sup>	84 ± 10 <sup>a</sup>	100 <sup>a</sup>	58 ± 12 <sup>b</sup>	85 ± 4 <sup>a</sup>
<i>A. montenegroi</i> BuOH extract	1,000	85 ± 4 <sup>ab</sup>	0 <sup>d</sup>	82 ± 5 <sup>a</sup>	100 <sup>a</sup>	8 ± 6 <sup>de</sup>	85 ± 4 <sup>a</sup>
<i>A. montenegroi</i> water extract	1,000	0 <sup>e</sup>	0 <sup>d</sup>	0 <sup>c</sup>	0 <sup>d</sup>	0 <sup>e</sup>	0 <sup>c</sup>
Blasticidin-S	1	69 ± 9 <sup>bc</sup>	–	–	–	–	–
	50	100 <sup>a</sup>	–	–	–	–	–
	20	–	94 ± 2 <sup>ab</sup>	–	–	–	–
Fenhexamide	100	–	100 <sup>a</sup>	–	–	–	–
Dimethomorph	2	–	–	50 ± 10 <sup>b</sup>	–	–	–
	10	–	–	100 <sup>a</sup>	–	–	–
Flusilazole	2	–	–	–	60 ± 9 <sup>b</sup>	–	–
	10	–	–	–	100 <sup>a</sup>	–	–
Benomyl	20	–	–	–	–	77 ± 0 <sup>b</sup>	–
	100	–	–	–	–	100 <sup>a</sup>	–
Dithianon	10	–	–	–	–	–	11 ± 7 <sup>c</sup>
	50	–	–	–	–	–	93 ± 1 <sup>a</sup>

Disease control values (%) represent the mean of three replicates. Values with different letters are significantly different at  $p < 0.05$  according to Duncan's multiple range test. RCB, rice blast; TGM, tomato gray mold; TLB, tomato late blight; WLR, wheat leaf rust; BPM, barley powdery mildew; PAN, pepper anthracnose; cf, culture filtrate; pt, phytotoxicity; and –, not tested. The values represent the mean ± standard deviation of two runs with three replicates. Different small letters in each column indicate a significant difference at  $p < 0.05$ .

there were weak or no effects on RCB, TLB, WLR, and BPM. The culture filtrate of *A. montenegroi* SFC20200425-M27 exhibited disease control values of 98 and 100% for TLB and WLR, respectively, whereas the development of RCB, TGM, BPM, and PAN were weak or not inhibited by this culture filtrate (Table 1). The culture filtrates of *A. caesiellus* SFC20160112-M06, *A. jensenii* SFC20160610-M03, and *A. montevideensis* SFC20160317-M26 showed weak or no disease control efficacies (Table 1). Moreover, the culture filtrates of *A. luchuensis* SFC20160907-M26, *A. venenatus* SFC20160407-M10, and *A. welwitschiae* SFC20160317-M19 exhibited phytotoxic symptoms on the foliage parts of the plants (Table 1). Thus, among the eight *Aspergillus* strains, *A. candidus* SFC20200425-M11 and *A. montenegroi* SFC20200425-M27 were selected as potential biocontrol agents in which they may produce antifungal compounds for plant diseases control.

To identify active compounds in the culture filtrates, we explored the disease control efficacy of the solvent extracts derived from the culture filtrates. When each extract was sprayed at a concentration of 1,000 μg/ml onto the plants 24 h before the inoculation of the fungal pathogens, the EtOAc extract of *A. candidus* SFC20200425-M11 exhibited a broad spectrum of disease control efficacy against TGM, TLB, WLR, and PAN with control values of 100, 94, 73, and 91%, respectively, compared to the non-treatment controls (Table 1). However, the BuOH and water extracts had no significant effects on all

tested plant diseases (Table 1). These results suggest that the EtOAc extract of *A. candidus* SFC20200425-M11 might contain antifungal substances.

In contrast to the solvent extracts of the *A. candidus* culture, both the EtOAc and BuOH extracts of *A. montenegroi* SFC20200425-M27 effectively controlled plant diseases. The EtOAc showed control values of 79, 84, 100, and 85% against RCB, TLB, WLR, and PAN, respectively (Table 1). The BuOH extract also exhibited disease control efficacies against RCB, TLB, WLR, and PAN with control values of 85, 82, 100, and 85%, respectively (Table 1). The water extract had no effect on all tested plant diseases (Table 1). These results suggest that *A. candidus* SFC20200425-M11 and *A. montenegroi* SFC20200425-M27 produce antifungal substances that have lipophilic properties.

## Chemical Identification of the Active Metabolites

Based on the results of the disease control efficacy assays, the EtOAc extract of *A. candidus* SFC20200425-M11 and the EtOAc and BuOH extracts of *A. montenegroi* SFC20200425-M27 were further separated by various chromatographic procedures with the guidance of *in vitro* antifungal assays against *B. cinerea* or *P. infestans*. Compounds 1–4 were isolated from the EtOAc extract of *A. candidus* SFC20200425-M11, and compounds 5–7



were isolated from the EtOAc and BuOH extracts of *A. montenegroi* SFC20200425-M27. By comparing our spectroscopic data (Supplementary Table S2) of the isolated compounds with those reported in the literature (Yonehara et al., 1959; Ellestad et al., 1972; Mizuba et al., 1975; Sohn and Oh, 2010; Mizushina et al., 2014), five of them were identified as known compounds: sphaeropsidin A (1), (*R*)-formosusin A (2), (*R*)-variotin (3), asperlin (5), and protulactone A (7). For the structural determination of the new compounds 4 and 6, MS and NMR spectroscopic analyses were performed (Table 2; Supplementary Figures S3–S17). All the chemical structures of compounds 1–7 are shown in Figure 2.

The HRESIMS spectrum of compound 4 showed a quasi-molecular ion at  $m/z$  332.1833  $[M+Na]^+$ , which was consistent with the molecular formula  $C_{17}H_{27}NO_4$  (calculated  $m/z$  332.1838 for  $C_{17}H_{27}NO_4Na$ ; Supplementary Figure S3). The  $^{13}C$ -NMR and HSQC spectra revealed two methyls ( $\delta_C$  13.0 and 14.1), seven  $sp^3$  methylenes ( $\delta_C$  17.2, 22.7, 27.5, 33.6, 37.3, 44.1, and 45.4), three olefinic methines ( $\delta_C$  129.5, 135.0, and 135.4), two oxygenated methines ( $\delta_C$  68.5, 68.6), one olefinic quaternary carbon ( $\delta_C$  134.3), and two ketone carbons ( $\delta_C$  173.1 and 175.8; Table 2; Supplementary Figures S4–S6). The *N*-substituted  $\gamma$ -lactam moiety of compound 4 was confirmed by  $^1H$ - $^1H$  COSY correlations among H-2', H-3', and H-4' along with the HMBC correlations from H-2', H-3', and H-4' to C-1' (Supplementary Figures S7 and S8). It was also confirmed by the HMBC correlations from H-13 to C-5, C-6, and C-7, together with  $^1H$ - $^1H$  COSY correlations among H-2, H-3, H-4, and H-5 and among H-7, H-8, H-9, H-10, H-11, and H-12. Two parts of the structure were connected through ketone carbon C-1, which was confirmed by the correlations in the HMBC experiment from H-2, H-3, and H-4' to C-1. The coupling constants between H-4 and H-5 ( $J=15.7$  Hz) indicated the *trans* (*E*) geometry of the double bond (Table 2). Another double bond was determined to be *E* based on NOESY correlations from H-4 to H-13 and from H-5 to H-7 (Figure 3A). The planar structure of compound 4 was similar to that of *R*-variotin (3), except for the presence of one aliphatic methylene at C-2 and a hydroxyl group at C-3 instead of the double bond at C-2. The absolute configuration at C-3 and C-8 was established by the NOESY experiment and Mosher's method (Supplementary Figures S9–S13). In the NOESY experiment, correlations were observed from H-5 to H-3, from H-5 to H-7, from H-13 to H-4, and from H-13 to H-8 (Figure 3A). The secondary alcohol groups were reacted with *R*-(–)- and *S*-(+)- $\alpha$ -methoxy- $\alpha$ -(trifluoromethyl)phenylacetyl chloride (MTPA) to give *S*- and *R*-MTPA esters, 4a and 4b, respectively (Figure 3B). The  $^1H$  NMR chemical shift differences ( $\Delta\delta_{S-R}$ ) between 4a and 4b are shown in Figure 3B. Positive  $\Delta\delta_{S-R}$  values for H-4 and H-5 together with negative  $\Delta\delta_{S-R}$  values for H-2', H-3', H-4', and H-2 indicated the *S* configuration of C-3 (Figure 3B). The absolute configuration of C-8 was determined as *R* based on positive  $\Delta\delta_{S-R}$  values for H-9, H-10, H-11, and H-12 and a negative  $\Delta\delta_{S-R}$  value for H-7 (Figure 3B). Thus, the structure of 4 was elucidated as 1-((3*S*,4*E*,6*E*,8*R*)-3,8-dihydroxy-6-methyldodeca-4,6-dienoyl) pyrrolidin-2-one and designated as candidusin.

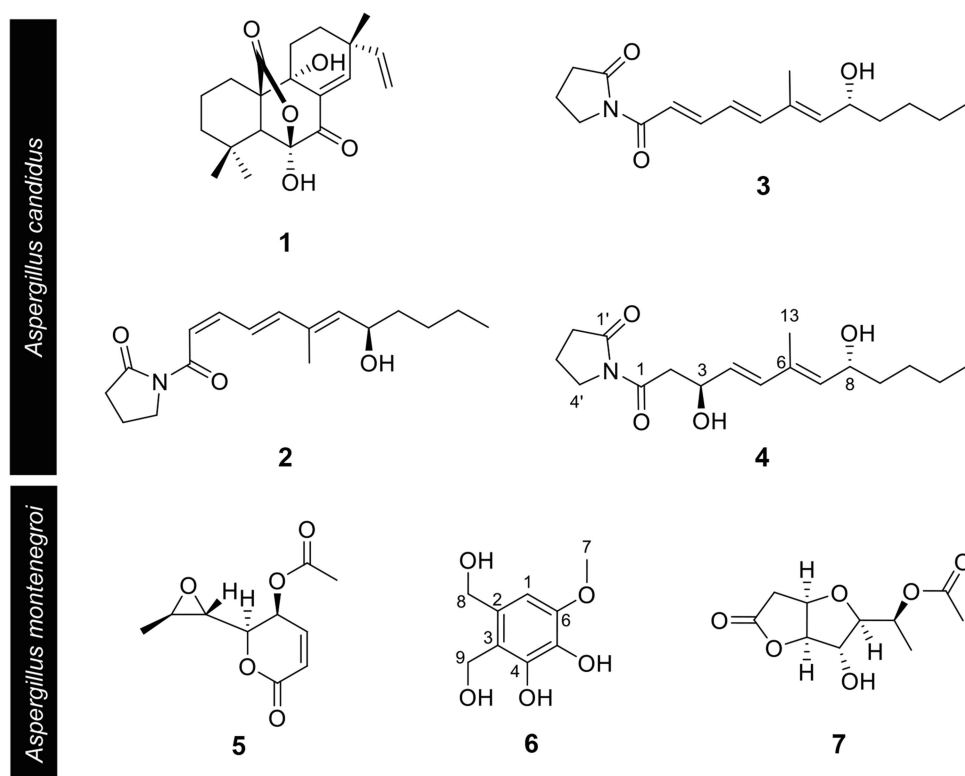
**TABLE 2 |** The  $^1H$  and  $^{13}C$  NMR data (500 and 125 MHz) for new compounds 4 and 6.

Position	Candidusin (4) in chloroform- <i>d</i>		Motenegrol (6) in methanol- <i>d</i> <sub>4</sub>	
	$\delta_H$ (J in Hz)	$\delta_C$ , Type	$\delta_H$ (J in Hz)	$\delta_C$ , Type
1	–	173.1, CO	6.53, s	104.9, CH
2	3.13, d (4.0); 3.12, d (8.3)	44.1, CH <sub>2</sub>	–	132.2, C
3	4.66, m	68.6, CH	–	119.9, C
4	5.69, dd (15.7, 6.3)	129.5, CH	–	145.8, C
5	6.27, d (15.7)	135.0, CH	–	134.5, C
6	–	134.3, C	–	148.6, C
7	5.42, d (8.7)	135.4, CH	3.81, s	56.4, CH <sub>3</sub>
8	4.43, q (6.7)	68.5, CH	4.58, s	63.6, CH <sub>2</sub>
9	1.58, m; 1.42, m	37.3, CH <sub>2</sub>	4.71, s	56.6, CH <sub>2</sub>
10	1.28*	27.5, CH <sub>2</sub>	–	–
11	1.28*	22.7, CH <sub>2</sub>	–	–
12	0.86, t (7.0)	14.1, CH <sub>3</sub>	–	–
13	1.76, d (1.2)	13.0, CH <sub>3</sub>	–	–
1'	–	175.8, CO	–	–
2'	2.58, t (8.1)	33.6, CH <sub>2</sub>	–	–
3'	2.02, m	17.2, CH <sub>2</sub>	–	–
4'	3.79, t (7.2)	45.4, CH <sub>2</sub>	–	–

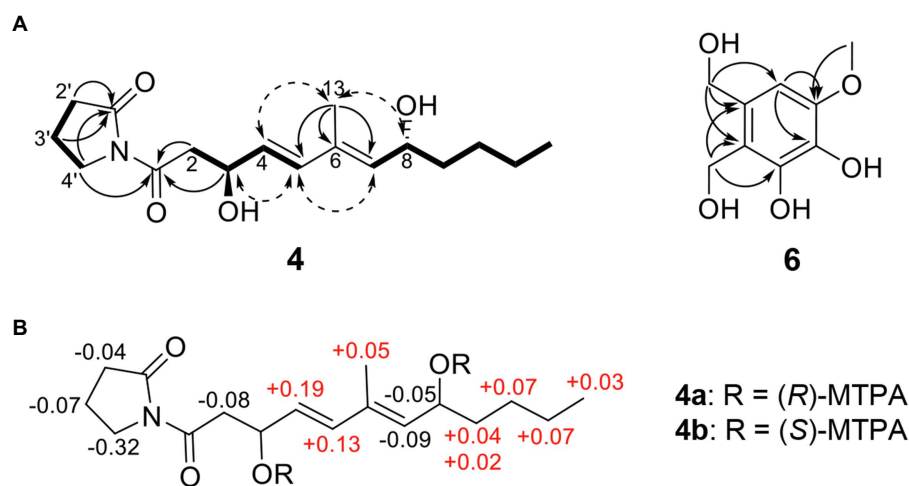
All proton and carbon positions are assigned by  $^1H$ - $^1H$  COSY, HSQC, and HMBC experiments. Em dashes indicate "not detected." \*(Asterisks) indicate overlapped signals.

The molecular formula of compound 6 was determined to be  $C_9H_{12}O_5$  based on the HRESIMS peaks of  $m/z$  223.0581  $[M+Na]^+$  and 205.0476  $[M+Na-H_2O]^+$  (calculated 223.0582 and 205.0477 for  $C_9H_{12}O_5Na$  and  $C_9H_{10}O_4Na$ ; Supplementary Figure S14). The  $^1H$  NMR spectrum of compound 6 exhibited signals for one aromatic proton at  $\delta_H$  6.53, two oxygenated methylene groups at  $\delta_H$  4.71 and 4.58, and one methoxy group at  $\delta_H$  3.81 (Table 2; Supplementary Figure S15). The  $^{13}C$  NMR spectrum of compound 6 contained nine signals, including one methoxy ( $\delta_C$  56.4), two oxygenated methylenes ( $\delta_C$  56.6 and 63.6), one aromatic methine ( $\delta_C$  104.9), and five quaternary aromatic carbons ( $\delta_C$  119.9, 132.2, 134.5, 145.8, and 148.6; Table 2; Supplementary Figure S16). These data suggest that compound 6 has a penta-substituted benzene ring. The positions of five substituents were determined by the HMBC correlations as follows: from an oxygenated methylene proton H-8 ( $\delta_H$  4.58) to C-1, C-2, and C-3; from an oxygenated methylene proton H-9 ( $\delta_H$  4.73) to C-2, C-3, and C-4; from an aromatic methine proton H-1 ( $\delta_H$  6.53) to C-5 and C-6; and a methoxy proton H-7 ( $\delta_H$  3.81) to C-6 (Supplementary Figure S17). Those data suggested that the substituted two oxygenated methylenes, two hydroxyls, and one methoxy group were placed on C-2, C-3, C-4, C-5, and C-6, respectively. Therefore, the structure of compound 6 was elucidated as 2,3-dihydroxymethyl-4,5-dihydroxy-6-methoxybenzene and named motenegrol.

Candidusin (4): colorless oil;  $[\alpha]_D^{25} = -10$  ( $c=0.1$ , methanol); IR (ATR)  $\nu_{max}/cm$ : 3,371, 2,972, 2,926, 1,730, 1,645, 1,549, 1,439, 1,369, 1,242, and 1,173;  $^1H$ - and  $^{13}C$ -NMR (500 and 125 MHz, chloroform-*d*) data: see Table 2; Supplementary Figures S4 and S5; HRESIMS:  $m/z$  332.1833  $[M+Na]^+$  (calculated  $m/z$  332.1838 for  $C_{17}H_{27}NO_4Na$ ; Supplementary Figure S3).



**FIGURE 2** | Chemical structures of compounds **1–7** isolated from *Aspergillus candidus* SFC20200425-M11 and *Aspergillus montenegroi* SFC20200425-M27. Sphaeropsidin A (**1**), (*R*)-formosusin A (**2**), (*R*)-variotin (**3**), and candidusin (**4**) were isolated from *Aspergillus candidus*. Asperlin (**5**), montenegrol (**6**), and protulatone A (**7**) were isolated from *A. montenegroi*.



**FIGURE 3** | Structural identification of new compounds. **(A)** Key HMBC (arrow), COSY (bold line), and NOESY (dotted arrow) correlations of compounds **4** and **6**. **(B)** The  $\Delta\delta^S - \delta^R$  values for (*R*)- and (*S*)-MTPA esters of compound **4**.

(*S*)-MTPA ester of **4** (**4a**):  $^1\text{H}$  NMR (Pyridine- $d_5$ , 500 MHz):  $\delta_{\text{H}}$  6.6244 (H-5), 6.0912 (H-4), 5.9078 (H-8), 5.4669 (H-7), 3.3667 (H-2), 3.1911 (H-4'), 2.4020 (H-2'), 1.9070 (H-13), 1.9069 (H-3'), 1.7134 (H-9a), 1.5270 (H-9b), 1.1980 (H-10, H-11), and 0.7707 (H-12).

(*R*)-MTPA ester of **4** (**4b**):  $^1\text{H}$  NMR (Pyridine- $d_5$ , 500 MHz):  $\delta_{\text{H}}$  6.4908 (H-5), 5.9625 (H-8), 5.9035 (H-4), 5.5533 (H-7), 3.5116 (H-4'), 3.4503 (H-2), 2.4464 (H-2'), 1.9755 (H-3'), 1.8536 (H-13), 1.6724 (H-9a), 1.5073 (H-9b), 1.1267 (H-10, H-11), and 0.7374 (H-12).

Montenegrol (6): yellow oil;  $^1\text{H}$ - and  $^{13}\text{C}$ -NMR (500 and 125 MHz, methanol- $d_4$ ) data: see **Table 2**; **Supplementary Figures S15 and S16**; HRESIMS:  $m/z$  223.0687  $[\text{M} + \text{Na}]^+$  (calculated  $m/z$  223.0582 for  $\text{C}_9\text{H}_{12}\text{O}_5\text{Na}$ ; **Supplementary Figure S14**).

## In vitro Antimicrobial Activity of the Pure Compounds 1–7

The isolated compounds 1–7 were evaluated for their *in vitro* antifungal and antibacterial property against six plant pathogenic fungi (*A. brassicicola*, *B. cinerea*, *C. coccodes*, *F. oxysporum*, *M. oryzae*, and *P. infestans*) and five plant pathogenic bacteria (*A. tumefaciens*, *C. michiganensis*, *P. syringae*, *R. solanacearum*, and *E. amylovora*). All MIC values of the isolated compounds 1–7 are presented in **Table 3**. Of compounds 1–4 identified from the culture filtrate of *A. candidus* SFC20200425-M11, sphaeropsidin A (1), (*R*)-formosusin A (2), and (*R*)-variotin (3) exhibited an antifungal activity against all tested fungal pathogens, but not for the bacterial pathogens. In particular, sphaeropsidin A (1) exhibited promising antifungal activities against *P. infestans*, *C. coccodes*, *A. brassicicola*, and *B. cinerea* with MIC values of 0.3, 8, 16, and 63  $\mu\text{g/ml}$ , respectively. (*R*)-formosusin A (2) showed the most potential antifungal activity against *C. coccodes* with a MIC value of 1  $\mu\text{g/ml}$ , followed by *B. cinerea*, *M. oryzae*, *F. oxysporum*, and *A. brassicicola* with MIC values of 4, 4, 16, and 16  $\mu\text{g/ml}$ , respectively. (*R*)-variotin (3) exhibited promising antifungal activities against *C. coccodes*, *A. brassicicola*, and *B. cinerea* with MIC values of 8, 16, and 16  $\mu\text{g/ml}$ , respectively. Among the fungal pathogens tested, *C. coccodes* was the most sensitive to sphaeropsidin A (1), (*R*)-formosusin A (2), and (*R*)-variotin (3) with MIC values ranging from 1 to 8  $\mu\text{g/ml}$ . Despite the structural similarity with formosusin A (2) and (*R*)-variotin (3), the new compound candidusin (4) exclusively showed a moderate antifungal activity against *A. brassicicola* with a MIC value of 250  $\mu\text{g/ml}$ .

Of three isolated compounds 5–7 from the culture filtrate of *A. montenegroi* SFC20200425-M27, asperlin (5) was the most effective in suppressing the growth of *P. infestans*, *M. oryzae*, and *C. coccodes* (MICs=1, 31, and 250  $\mu\text{g/ml}$ , respectively).

Montenegrol (6) and protulactone A (7) showed a moderate activity to inhibit the growth of *P. infestans* with MIC values of 250 and 125  $\mu\text{g/ml}$ , respectively. Intriguingly, among all the tested compounds in this study, only asperlin (5) showed an antibacterial activity against *C. michiganensis* and *E. amylovora* with MIC values of 125 and 250  $\mu\text{g/ml}$ , respectively.

## Plant Disease Control Efficacy of Active Compounds

Considering the *in vitro* antimicrobial activity and yield of the isolated compounds, we examined the disease control efficacy of sphaeropsidin A (1), (*R*)-formosusin A (2), and asperlin (5). When plants were treated with each compound, sphaeropsidin A (1) strongly reduced the disease development of TLB by at least 94% at all the treated concentrations compared to the non-treatment control. Sphaeropsidin A (1) also exhibited disease control values of 53 and 90% against WLR at a concentration of 250 and 500  $\mu\text{g/ml}$ , respectively (**Figure 4**). Despite these vigorous disease control activities against TLB and WLR, sphaeropsidin A (1) showed weak or no disease control effects against RCB, TGM, BPM, and PAN at a high concentration of 500  $\mu\text{g/ml}$  (**Supplementary Table S3**). In the case of (*R*)-formosusin A (2), it reduced in a concentration dependent manner the development of TGM with control values of 21, 57, and 82% at concentrations of 125, 250, and 500  $\mu\text{g/ml}$ , respectively (**Figure 5**). Similar to sphaeropsidin A (1), asperlin (5) also reduced the development of TLB with control values of more than 90% at concentrations of 125–500  $\mu\text{g/ml}$  and exhibited disease control values of 83 and 95% against WLR at the concentration of 250 and 500  $\mu\text{g/ml}$ , respectively (**Figure 6**). In addition to the plant disease control efficacies, there were no phytotoxic symptoms observed on the treated plants (data not shown).

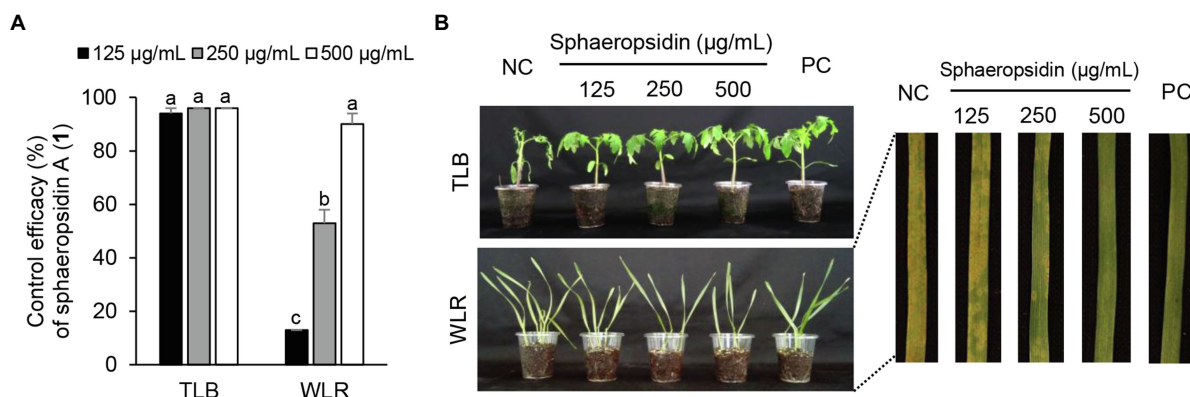
## Major Active Compounds of *Aspergillus candidus* SFC20200425-M11 and *Aspergillus montenegroi* SFC20200425-M27

In the current study, sphaeropsidin A (1) was isolated as one of the major antifungal compounds produced by *A. candidus*

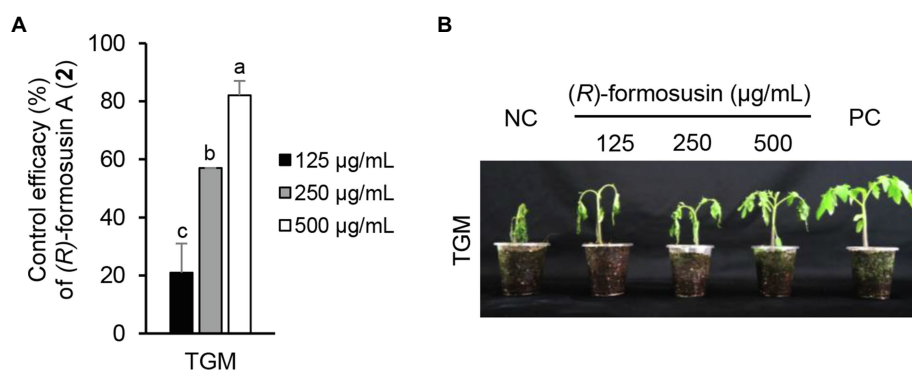
**TABLE 3** | *In vitro* antimicrobial activity of compounds 1–7 against plant pathogen.

Plant Pathogen		MIC ( $\mu\text{g/ml}$ )						
		1	2	3	4	5	6	7
Fungus	<i>Alternaria brassicicola</i>	16	16	16	250	–	–	–
	<i>Botrytis cinerea</i>	63	4	16	–	–	–	–
	<i>Colletotrichum coccodes</i>	8	1	8	–	250	–	–
	<i>Fusarium oxysporum</i>	250	16	63	–	–	–	–
	<i>Magnaporthe oryzae</i>	125	4	125	–	31	–	–
	<i>Phytophthora infestans</i>	0.3	250	250	–	1	250	125
Bacterium	<i>Agrobacterium tumefaciens</i>	–	–	–	–	–	–	–
	<i>Clavibacter michiganensis</i>	–	–	–	–	125	–	–
	<i>Pseudomonas syringae</i>	–	–	–	–	–	–	–
	<i>Ralstonia solanacearum</i>	–	–	–	–	–	–	–
	<i>Erwinia amylovora</i>	–	–	–	–	250	–	–

1, sphaeropsidin A; 2, (*R*)-formosusin A; 3, (*R*)-variotin; 4, candidusin; 5, asperlin; 6, montenegrol; 7, protulactone A. Em dashes indicate MIC > 250  $\mu\text{g/ml}$ .



**FIGURE 4 |** Effects of sphaeropsidin A (**1**) isolated from *Aspergillus candidus* SFC20200425-M11 on the development of tomato late blight (TLB) and wheat leaf rust (WLR) caused by *Phytophthora infestans* and *Puccinia triticina*. **(A)** Control efficacy of sphaeropsidin A (**1**) against TLB and WLR. The bars represent the mean  $\pm$  standard deviation of two runs with three replicates. Different small letters in each bar indicate a significant difference at  $p < 0.05$  (Duncan's multiple range test). **(B)** Representatives of plants treated with sphaeropsidin A (**1**) at a concentration of 125, 250, and 500  $\mu\text{g/mL}$ . Plants were inoculated with sporangia or spores of *P. infestans* or *P. triticina* 1 day after treatment with sphaeropsidin A (**1**). Treatment with Tween 20 solution containing 5% methanol and chemical fungicides (dimethomorph for TLB and flusilazole for WLR) were prepared as negative and positive controls (NC and PC), respectively.



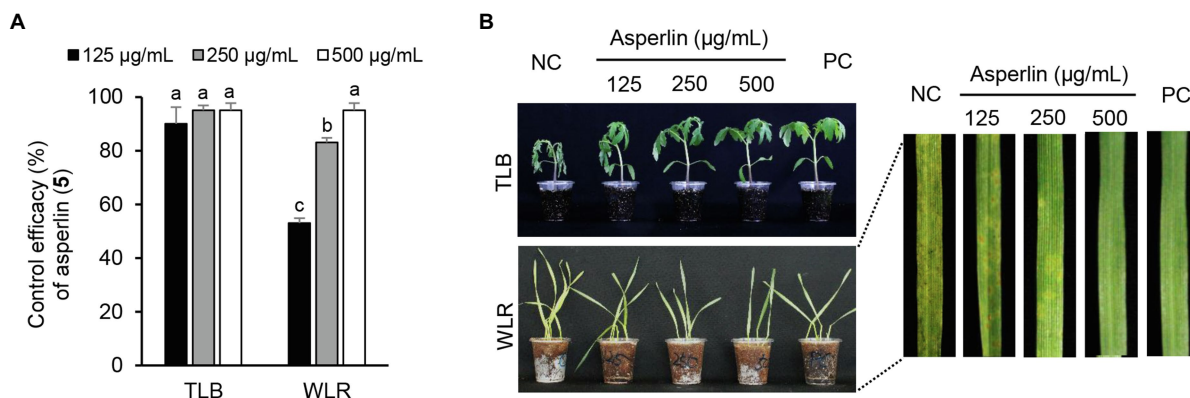
**FIGURE 5 |** Effect of (*R*)-formosusin (**2**) isolated from *Aspergillus candidus* SFC20200425-M11 on the development of tomato gray mold (TGM) caused by *Botrytis cinerea*. **(A)** Control efficacy of (*R*)-formosusin (**2**) against TGM. The bars represent the mean  $\pm$  standard deviation of two runs with three replicates. Different small letters in each bar indicate a significant difference at  $p < 0.05$  (Duncan's multiple range test). **(B)** Representatives of plants treated with (*R*)-formosusin (**2**) at a concentration of 125, 250, and 500  $\mu\text{g/mL}$ . Plants were inoculated with spores of *B. cinerea* 1 day after treatment with (*R*)-formosusin (**2**). Treatment with the Tween 20 solution containing 5% methanol and a chemical fungicide (fenhexamide) were prepared as negative and positive controls (NC and PC), respectively.

SFC20200425-M11. Sphaeropsidin A (**1**), an unarranged pimarane diterpene, was first isolated from the fermentation of the fungus *Aspergillus chevalieri* (Ellestad et al., 1972). Since then, sphaeropsidin A (**1**) and its derivatives have been identified from various fungal species such as *Aspergillus porosus*, *Sphaeropsis sapinea* f. sp. *cupressi*, and *Diplodia* spp. (Evidente et al., 1997; Neuhaus et al., 2019). In terms of antimicrobial activity, there were several studies presenting the potent antifungal activity of sphaeropsidin A (**1**) against plant and human pathogenic fungi (Evidente et al., 1996, 1997; Sparapano et al., 2004; Weber et al., 2007). Based on the structure–activity relationship studies, Sparapano et al. (2004) showed that the tricyclic pimarane system (particularly C-ring) and the vinyl group at C-13 are essential for the activity of sphaeropsidin A. In this study, we also showed that sphaeropsidin A (**1**) exhibits *in vitro* and *in vivo* antifungal activity against plant

pathogenic fungi (Table 3; Figure 4). To the best of our knowledge, this is the first study to present the *in vivo* disease control efficacy of sphaeropsidin A (**1**) against TLB by *P. infestans* and WLR by *P. triticina* (Figure 4). Beyond the antifungal activity of sphaeropsidin A (**1**), it has also been reported to be effective against plant and human pathogenic bacteria such as *Staphylococcus haemolyticus*, *Pseudomonas aeruginosa*, and *Xanthomonas oryzae* pv. *oryzae* (Evidente et al., 2011; Roschetto et al., 2020). However, in this study, no antibacterial activity of sphaeropsidin A (**1**) was observed against plant pathogenic bacteria at a concentration of 250  $\mu\text{g/mL}$ .

The other active compounds of *A. candidus* SFC20200425-M11 were (*R*)-formosusin A (**2**) and (*R*)-variotin (**3**). (*R*)-formosusin A (**2**) is a *cis*-olefin analog of (*R*)-variotin (**3**; Yonehara et al., 1959; Omolo et al., 2000; Mizushima et al., 2014; Yajima et al., 2016). (*R*)-formosusin A (**2**) was first isolated from *Paecilomyces*





**FIGURE 6 |** Effects of asperlin (5) isolated from *Aspergillus montenegroi* SFC20200425-M27 on the development of tomato late blight (TLB) and wheat leaf rust (WLR) caused by *Phytophthora infestans* and *Puccinia tritricina*. **(A)** Control efficacy of asperlin (5) against TLB and WLR. The bars represent the mean  $\pm$  standard deviation of two runs with three replicates. Different small letters in each bar indicate a significant difference at  $p < 0.05$  (Duncan's multiple range test). **(B)** Representatives of plants treated with asperlin (5) at a concentration of 125, 250, and 500 µg/mL. Plants were inoculated with sporangia or spores of *P. infestans* or *P. tritricina* 1 day after treatment with asperlin (5). Treatment with Tween 20 solution containing 5% methanol and chemical fungicides (dimethomorph for TLB and flusilazole for WLR) were prepared as negative and positive controls (NC and PC), respectively.

*formosus* (Mizushima et al., 2014), and its absolute configuration of (*R*)-formosusin A (2) was established by Yajima et al. (2016). (*R*)-formosusin A (2) has been known to inhibit a mammalian DNA polymerase involved in the DNA repair pathway (Beard and Wilson, 2006; Mizushima et al., 2014), but its antifungal activity has not been investigated. In contrast, (*R*)-variotin (3) has been reported as a broad-spectrum antifungal compound (Yonehara et al., 1959). Considering the structural similarity of (*R*)-formosusin A (2) and (*R*)-variotin (3), it may be evident that (*R*)-formosusin A (2) exhibits an antifungal activity against plant pathogenic fungi. As expected, we found that (*R*)-formosusin A (2) has an antifungal activity against plant pathogenic fungi, and it was more active than (*R*)-variotin (3) against *B. cinerea*, *C. coccodes*, and *M. oryzae* (Table 3). However, although the new derivative candidusin (4) in this study was structurally similar to (*R*)-formosusin A (2) and (*R*)-variotin (3) containing an enone moiety, we did not observe an antifungal activity at a concentration of 250 µg/mL, except for *A. brassicicola* (Table 3). This observation could be supported by the antimicrobial results of the diarylheptanoids from the black and green alder, which showed more significant activity of compounds containing the enone moiety in the aliphatic chain (Novaković et al., 2015).

Of the isolated compounds 5–7 from the culture broth of *A. montenegroi* SFC20200425-M27, asperlin (5) showed the most potent activity against the plant pathogenic fungi *P. infestans* and *M. oryzae*, and against the plant pathogenic bacteria *C. michiganensis* and *E. amylovora* (Table 3). Asperlin (5) is a polyketide antibiotic that was first isolated from *Aspergillus nidulans*, and its various biological activities such as antifungal, anti-inflammatory, and anti-atherosclerotic have been extensively studied (Argoudelis and Zieserl, 1966; Komai, 2003; Lee et al., 2011; Zhou et al., 2017; Wu et al., 2019). Here, we report for the first time that asperlin (5) exhibits an *in vivo* antifungal activity against TLB and WLR.

## CONCLUSION

Evaluation of antagonistic microbes is vital for a better understanding of the ecological significance of the biocontrol of plant diseases. In this study, our results showed that *A. candidus* SFC20200425-M11 and *A. montenegroi* SFC20200425-M27 isolated from a marine environment exhibit a biocontrol potential for the first time. Although a variety of secondary metabolites and their biological activities have been reported from *A. candidus*, there is limited information on *A. candidus* and its secondary metabolites in plant disease control efficacy. Given that *A. candidus* and *A. montenegroi* culture filtrates effectively control various plant diseases, we isolated and identified two new compounds (4 and 6), along with five known compounds (1–3, 5, and 7). The *in vitro* results revealed the broad antifungal spectrum of sphaeropsidin A (1), (*R*)-formosusin A (2), (*R*)-variotin (3), and asperlin (5), and these natural compounds exhibited plant disease control efficacies. In addition to the antifungal activity, asperlin (5) exclusively showed an antibacterial activity against *C. michiganensis* and *E. amylovora*. Taken together, our results suggest that *Aspergillus* spp. and their antimicrobial compounds have great potential to be developed as new biocontrol agents or used as active ingredients for natural pesticides in agricultural fields.

## DATA AVAILABILITY STATEMENT

The original contributions presented in the study are included in the article/Supplementary Material; further inquiries can be directed to the corresponding authors.

## AUTHOR CONTRIBUTIONS

HK and GC provided the study idea and supervision. MN, BK, YK, and MP contributed to the experimental performance.

MN, JH, and HK contributed to the manuscript preparation. MN, JH, HK, and GC contributed to the structure elucidation, revising, and proofreading of the manuscript. All authors contributed to the article and approved the submitted version.

## FUNDING

This study was supported by the Cooperative Research Program for Agricultural Science and Technology Development (project PJ016028), Rural Development Administration, Republic of Korea.

## REFERENCES

- Argoudelis, A. D., and Zieserl, J. F. (1966). The structure of U-13,933, a new antibiotic. *Tetrahedron Lett.* 7, 1969–1973. doi: 10.1016/S0040-4039(00)76280-0
- Beard, W. A., and Wilson, S. H. (2006). Structure and mechanism of DNA polymerase  $\beta$ . *Chem. Rev.* 106, 361–382. doi: 10.1021/cr0404904
- Buttachon, S., Ramos, S. A., Inácio, A., Dethoup, T., Gales, L., Lee, M., et al. (2018). Bis-indolyl benzenoids, hydroxypyrrolidine derivatives and other constituents from cultures of the marine sponge-associated fungus *Aspergillus candidus* KUFA0062. *Mar. Drugs* 16:119. doi: 10.3390/md16040119
- Chandra, P., Sharma, R. K., and Arora, D. S. (2020). Antioxidant compounds from microbial sources: A review. *Food Res. Int.* 129:108849. doi: 10.1016/j.foodres.2019.108849
- Choi, G. J., Jang, K. S., Choi, Y. H., Yu, J. H., and Kim, J.-C. (2010). Antifungal activity of lower alkyl fatty acid esters against powdery mildews. *Plant Pathol. J.* 26, 360–366. doi: 10.5423/PPJ.2010.26.4.360
- Dayan, F. E., Cantrell, C. L., and Duke, S. O. (2009). Natural products in crop protection. *Biorg. Med. Chem.* 17, 4022–4034. doi: 10.1016/j.bmc.2009.01.046
- Demain, A. L. (2014). Importance of microbial natural products and the need to revitalize their discovery. *J. Ind. Microbiol. Biotechnol.* 41, 185–201. doi: 10.1007/s10295-013-1325-z
- El-hawary, S. S., Moawad, A. S., Bahr, H. S., Abdelmohsen, U. R., and Mohammed, R. (2020). Natural product diversity from the endophytic fungi of the genus *Aspergillus*. *RSC Adv.* 10, 22058–22079. doi: 10.1039/D0RA04290K
- Ellestad, G., Kunstmann, M., Miranda, P., and Morton, G. (1972). Structures of fungal diterpene antibiotics LL-S491 $\beta$  and  $\gamma$ . *J. Am. Chem. Soc.* 94, 6206–6208. doi: 10.1021/ja00772a054
- El-Sayed, A. S., and Ali, G. S. (2020). *Aspergillus flavipes* is a novel efficient biocontrol agent of *Phytophthora parasitica*. *Biol. Control* 140:104072. doi: 10.1016/j.biocontrol.2019.104072
- Espinel-Ingraff, A., Fothergill, A., Ghannoum, M., Manavathu, E., Ostrosky-Zeichner, L., Pfaller, M., et al. (2005). Quality control and reference guidelines for CLSI broth microdilution susceptibility method (M 38-A document) for amphotericin B, itraconazole, posaconazole, and voriconazole. *J. Clin. Microbiol.* 43, 5243–5246. doi: 10.1128/JCM.43.10.5243-5246.2005
- Evidente, A., Sparapano, L., Fierro, O., Bruno, G., Giordano, F., and Motta, A. (1997). Sphaeropsidins B and C, phytotoxic pimarane diterpenes from *Sphaeropsis sapinea* f. sp. *cupressi* and *Diplodia mutila*. *Phytochemistry* 45, 705–713. doi: 10.1016/S0031-9422(97)00006-X
- Evidente, A., Sparapano, L., Motta, A., Giordano, F., Fierro, O., and Frisullo, S. (1996). A phytotoxic pimarane diterpene of *Sphaeropsis sapinea* f. sp. *cupressi*, the pathogen of a canker disease of cypress. *Phytochemistry* 42, 1541–1546. doi: 10.1016/0031-9422(96)00206-3
- Evidente, A., Venturi, V., Masi, M., Degrassi, G., Cimmino, A., Maddau, L., et al. (2011). *In vitro* antibacterial activity of sphaeropsidins and chemical derivatives toward *Xanthomonas oryzae* pv. *oryzae*, the causal agent of rice bacterial blight. *J. Nat. Prod.* 74, 2520–2525. doi: 10.1021/np200625m
- Godfray, H. C. J., Beddington, J. R., Crute, I. R., Haddad, L., Lawrence, D., Muir, J. F., et al. (2010). Food security: The challenge of feeding 9 billion people. *Science* 327, 812–818. doi: 10.1126/science.1185383
- Han, J. W., Oh, M., Lee, Y. J., Choi, J., Choi, G. J., and Kim, H. (2018). Crinipellins A and I, two diterpenoids from the basidiomycete fungus *Crinipellis rhizomaticola*, as potential natural fungicides. *Molecules* 23:2377. doi: 10.3390/molecules23092377
- Hüter, O. F. (2011). Use of natural products in the crop protection industry. *Phytochem. Rev.* 10, 185–194. doi: 10.1007/s11101-010-9168-y
- Jang, J. Y., Choi, Y. H., Shin, T. S., Kim, T. H., Shin, K. S., Park, H. W., et al. (2016). Biological control of *Meloidogyne incognita* by *Aspergillus Niger* F22 producing oxalic acid. *PLoS One* 11:e0156230. doi: 10.1371/journal.pone.0156230
- Komai, S. (2003). Antifungal activity of pyranone and furanone derivatives, isolated from *Aspergillus* sp. IFM51759, against *Aspergillus fumigatus*. *Mycotoxins* 53, 11–18. doi: 10.2520/myco.53.11
- Lee, D. S., Jeong, G. S., Li, B., Lee, S. U., Oh, H. C., and Kim, Y. C. (2011). Asperlin from the marine-derived fungus *Aspergillus* sp. SF-5044 exerts anti-inflammatory effects through heme oxygenase-1 expression in murine macrophages. *J. Pharmacol. Sci.* 116, 283–295. doi: 10.1254/jphs.10219FP
- Lee, H. R., Jung, J., Riu, M., and Ryu, C. M. (2017). A new frontier for biological control against plant pathogenic nematodes and insect pests I: by microbes. *Res. Plant Dis.* 23, 114–149. doi: 10.5423/RPD.2017.23.2.114
- Lee, S., Park, M. S., and Lim, Y. W. (2016). Diversity of marine-derived *Aspergillus* from tidal mudflats and sea sand in Korea. *Mycobiology* 44, 237–247. doi: 10.5941/MYCO.2016.44.4.237
- Lee, T. H., Yeh, M. H., Chang, C. I., Lee, C. K., Shao, Y. Y., and Kuo, Y. H. (2007). New lignans from the heartwood of *Cunninghamia lanceolata*. *Biosci. Biotechnol. Biochem.* 71, 2075–2078. doi: 10.1271/bbb.70162
- Mausser, W., Klepper, G., Zabel, F., Delzeit, R., Hank, T., Putzenlechner, B., et al. (2015). Global biomass production potentials exceed expected future demand without the need for cropland expansion. *Nat. Commun.* 6:8946. doi: 10.1038/ncomms9946
- Mizuba, S., Lee, K., and Jiu, J. (1975). Three antimicrobial metabolites from *Aspergillus caespitosus*. *Can. J. Microbiol.* 21, 1781–1787. doi: 10.1139/m75-259
- Mizushima, Y., Suzuki-Fukudome, H., Takeuchi, T., Takemoto, K., Kuriyama, I., Yoshida, H., et al. (2014). Formosusin A, a novel specific inhibitor of mammalian DNA polymerase  $\beta$  from the fungus *Paecilomyces formosus*. *Biorg. Med. Chem.* 22, 1070–1076. doi: 10.1016/j.bmc.2013.12.038
- Mohamed, G. A., Ibrahim, S. R., and Asfour, H. Z. (2020). Antimicrobial metabolites from the endophytic fungus *Aspergillus versicolor*. *Phytochem. Lett.* 35, 152–155. doi: 10.1016/j.phytol.2019.12.003
- Neuhaus, G. F., Adpressa, D. A., Bruhn, T., and Loesgen, S. (2019). Polyketides from marine-derived *Aspergillus porosus*: challenges and opportunities for determining absolute configuration. *J. Nat. Prod.* 82, 2780–2789. doi: 10.1021/acs.jnatprod.9b00416
- Ngo, M. T., Han, J. W., Nguyen, M. V., Dang, Q. L., Kim, H., and Choi, G. J. (2021). Antifungal properties of natural products from *Pterocarya tonkinensis* against phytopathogenic fungi. *Pest Manag. Sci.* 77, 1864–1872. doi: 10.1002/ps.6211
- Ngo, M. T., Han, J. W., Yoon, S., Bae, S., Kim, S. Y., Kim, H., et al. (2019). Discovery of new triterpenoid saponins isolated from *Maesa japonica* with antifungal activity against rice blast fungus *Magnaporthe oryzae*. *J. Agric. Food Chem.* 67, 7706–7715. doi: 10.1021/acs.jafc.9b02236
- Nguyen, V. M., Han, B. S., Choi, H. Y., Byun, J., Park, J. S., and Kim, W. G. (2018). Genkwalathins A and B, new lathyrane-type diterpenes from *Daphne genkwa*. *Nat. Prod. Res.* 32, 1782–1790. doi: 10.1080/14786419.2017.1402322

## ACKNOWLEDGMENTS

We thank to Dr. Jung Hoon Choi (Department of Biochemical Analysis, Korea Basic Science Institute) for recording HRESIMS data.

## SUPPLEMENTARY MATERIAL

The Supplementary Material for this article can be found online at: <https://www.frontiersin.org/articles/10.3389/fmicb.2021.804333/full#supplementary-material>

- Novaković, M., Novaković, I., Cvetković, M., Sladić, D., and Tešević, V. (2015). Antimicrobial activity of the diarylheptanoids from the black and green alder. *Braz. J. Bot.* 38, 441–446. doi: 10.1007/s40415-015-0151-0
- Omolo, J. O., Anke, H., Chhabra, S., and Sterner, O. (2000). New variotin analogues from *Aspergillus viridi-nutans*. *J. Nat. Prod.* 63, 975–977. doi: 10.1021/np990509b
- Raymaekers, K., Ponet, L., Holtappels, D., Berckmans, B., and Cammue, B. P. A. (2020). Screening for novel biocontrol agents applicable in plant disease management – A review. *Biol. Control* 144:104240. doi: 10.1016/j.biocontrol.2020.104240
- Roschetto, E., Masi, M., Esposito, M., Di Lecce, R., Delicato, A., Maddau, L., et al. (2020). Anti-biofilm activity of the fungal phytotoxin sphaeropsidin A against clinical isolates of antibiotic-resistant bacteria. *Toxins* 12:444. doi: 10.3390/toxins12070444
- Sadorn, K., Saepua, S., Boonyuen, N., Laksanacharoen, P., Rachatawee, P., Prabpai, S., et al. (2016). Allahabadolactones A and B from the endophytic fungus, *Aspergillus allahabadii* BCC45335. *Tetrahedron* 72, 489–495. doi: 10.1016/j.tet.2015.11.056
- Saitou, N., and Nei, M. (1987). The neighbor-joining method: A new method for reconstructing phylogenetic trees. *Mol. Biol. Evol.* 4, 406–425. doi: 10.1093/oxfordjournals.molbev.a040454
- Shin, T. S., Yu, N. H., Lee, J., Choi, G. J., Kim, J. C., and Shin, C. S. (2017). Development of a biofungicide using a mycoparasitic fungus *Simplicillium lamellicola* BCP and its control efficacy against gray mold diseases of tomato and ginseng. *Plant Pathol. J.* 33, 337–344. doi: 10.5423/PPJ.FT.04.2017.0087
- Sohn, J. H., and Oh, H. C. (2010). Protulactones A and B: two new polyketides from the marine-derived fungus *Aspergillus* sp. SF-5044. *Bull. Kor. Chem. Soc.* 31, 1695–1698. doi: 10.5012/bkcs.2010.31.6.1695
- Sparapano, L., Bruno, G., Fierro, O., and Evidente, A. (2004). Studies on structure–activity relationship of sphaeropsidins A–F, phytotoxins produced by *Sphaeropsis sapinea* f. sp. *cupressi*. *Phytochemistry* 65, 189–198. doi: 10.1016/j.phytochem.2003.11.006
- Tamura, K., and Nei, M. (1993). Estimation of the number of nucleotide substitutions in the control region of mitochondrial DNA in humans and chimpanzees. *Mol. Biol. Evol.* 10, 512–526. doi: 10.1093/oxfordjournals.molbev.a040023
- Vu, T. T., Kim, H., Tran, V. K., Vu, H. D., Hoang, T. X., Han, J. W., et al. (2017). Antibacterial activity of tannins isolated from *Sapium baccatum* extract and use for control of tomato bacterial wilt. *PLoS One* 12:e0181499. doi: 10.1371/journal.pone.0181499
- Wang, W., Liao, Y., Tang, C., Huang, X., Luo, Z., Chen, J., et al. (2017). Cytotoxic and antibacterial compounds from the coral-derived fungus *Aspergillus tritici* SP2-8-1. *Mar. Drugs* 15, 348. doi: 10.3390/md15110348
- Wang, C., Tang, S., and Cao, S. (2021). Antimicrobial compounds from marine fungi. *Phytochem. Rev.* 20, 85–117. doi: 10.1007/s11101-020-09705-5
- Weber, R. W. S., Kappe, R., Paululat, T., Mösker, E., and Anke, H. (2007). Anti-*Candida* metabolites from endophytic fungi. *Phytochemistry* 68, 886–892. doi: 10.1016/j.phytochem.2006.12.017
- Willems, T., De Mol, M. L., De Bruycker, A., De Maeseneire, S. L., and Soetaert, W. K. (2020). Alkaloids from marine fungi: promising antimicrobials. *Antibiotics* 9:340. doi: 10.3390/antibiotics9060340
- Wu, C., Zhou, Y., Qi, G., Liu, D., Cao, X., Yu, J., et al. (2019). Asperlin stimulates energy expenditure and modulates gut microbiota in HFD-fed mice. *Mar. Drugs* 17:38. doi: 10.3390/md17010038
- Xu, L., Meng, W., Cao, C., Wang, J., Shan, W., and Wang, Q. (2015). Antibacterial and antifungal compounds from marine fungi. *Mar. Drugs* 13, 3479–3513. doi: 10.3390/md13063479
- Yajima, A., Iizuka, Y., Katsuta, R., and Nukada, T. (2016). Synthesis and absolute configuration of formosusin A, a specific inhibitor of mammalian DNA polymerase  $\beta$ . *Tetrahedron Lett.* 57, 2012–2015. doi: 10.1016/j.tetlet.2016.03.094
- Yonehara, H., Takeuchi, S., Umezawa, H., and Sumiki, Y. (1959). Variotin, a new antifungal antibiotic, produced by *Paecilomyces varioti* Bainier var. *antibioticus*. *J. Antibiot.* 12, 109–110
- Zhao, J., Liu, W., Liu, D., Lu, C., Zhang, D., Wu, H., et al. (2018). Identification and evaluation of *Aspergillus tubingensis* as a potential biocontrol agent against grey mould on tomato. *J. Gen. Plant Pathol.* 84, 148–159. doi: 10.1007/s10327-018-0764-9
- Zhou, Y., Chen, R., Liu, D., Wu, C., Guo, P., and Lin, W. (2017). Asperlin inhibits LPS-evoked foam cell formation and prevents atherosclerosis in ApoE<sup>−/−</sup> mice. *Mar. Drugs* 15, 358. doi: 10.3390/md15110358

**Conflict of Interest:** The authors declare that the research was conducted in the absence of any commercial or financial relationships that could be construed as a potential conflict of interest.

**Publisher's Note:** All claims expressed in this article are solely those of the authors and do not necessarily represent those of their affiliated organizations, or those of the publisher, the editors and the reviewers. Any product that may be evaluated in this article, or claim that may be made by its manufacturer, is not guaranteed or endorsed by the publisher.

Copyright © 2021 Ngo, Nguyen, Han, Kim, Kim, Park, Kim and Choi. This is an open-access article distributed under the terms of the Creative Commons Attribution License (CC BY). The use, distribution or reproduction in other forums is permitted, provided the original author(s) and the copyright owner(s) are credited and that the original publication in this journal is cited, in accordance with accepted academic practice. No use, distribution or reproduction is permitted which does not comply with these terms.



OPEN ACCESS

**Edited by:**

Florence Fontaine,  
Université de Reims  
Champagne-Ardenne, France

**Reviewed by:**

Quan Bu,  
Jiangsu University, China  
Xin Zhou,  
Nanjing Forestry University, China  
Zhe Ling,  
Nanjing Forestry University, China  
Jochen Fischer,  
Institut für Biotechnologie und  
Wirkstoff-Forschung (IBWF), Germany  
Ana Sofia Duarte,  
Portuguese Catholic University,  
Portugal

**\*Correspondence:**

Jingcong Xie  
Xiejingcong@icifp.cn  
Jianchun Jiang  
Jiangjianchun@icifp.cn

**Specialty section:**

This article was submitted to  
Microbe and Virus Interactions with  
Plants,  
a section of the journal  
Frontiers in Microbiology

**Received:** 23 August 2021

**Accepted:** 13 December 2021

**Published:** 31 December 2021

**Citation:**

Zhang N, Xu H, Xie J, Cui J-y,  
Yang J, Zhao J, Tong Y and Jiang J  
(2021) Screening of Cucumber  
Fusarium Wilt Bio-Inhibitor: High  
Sporulation *Trichoderma harzianum*  
Mutant Cultured on Moso Bamboo  
Medium. *Front. Microbiol.* 12:763006.  
doi: 10.3389/fmicb.2021.763006

# Screening of Cucumber Fusarium Wilt Bio-Inhibitor: High Sporulation *Trichoderma harzianum* Mutant Cultured on Moso Bamboo Medium

Ning Zhang<sup>1,2</sup>, Hao Xu<sup>1,2</sup>, Jingcong Xie<sup>1,2\*</sup>, Jie-yu Cui<sup>3</sup>, Jing Yang<sup>1,2</sup>, Jian Zhao<sup>1,2</sup>, Yajuan Tong<sup>1,2</sup> and Jianchun Jiang<sup>1,2\*</sup>

<sup>1</sup> Institute of Chemical Industry of Forest Products, Chinese Academy of Forestry, National Engineering Laboratory for Biomass Chemical Utilization, Key Laboratory of Chemical Engineering of Forest Products, National Forestry and Grassland Administration, Key Laboratory of Biomass Energy and Material, Nanjing, China, <sup>2</sup> Co-Innovation Center of Efficient Processing and Utilization of Forest Resources, Nanjing Forestry University, Nanjing, China, <sup>3</sup> College of Chemical Engineering, Nanjing Forestry University, Nanjing, China

Cucumber fusarium wilt is a soil-borne disease which causes serious production decrease in cucumber cultivation world widely. Extensive using of chemical pesticides has caused serious environmental pollution and economic losses, therefore, it is particularly urgent to develop efficient, safe and pollution-free biopesticide. In this study, a mutant strain of *Trichoderma harzianum* cultivated in moso bamboo medium was proved to be an efficient bio-inhibitor of the disease. The mutant strain *T. harzianum* T334, was obtained by three microwave mutagenesis cycles with an irradiation power of 600 W and irradiation time of 40 s. In contrast to the original strain, the inhibition rate on cucumber fusarium wilt of the strain T334 increased from 63 to 78%. In this work, disk milling pretreatment of moso bamboo has shown significant beneficial effects on both biotransformation and sporulation of T334. Its sporulation reached  $3.7 \times 10^9$  cfu/g in mushroom bags with 90% bamboo stem powder (pretreated by disk milli), 9.5% bamboo leaf powder and 0.5% wheat bran when the ratio of solid to liquid was 4:6, the inoculum amount was 10%, and the culture temperature was 28°C. These results provide an alternative bioinhibitor for the control of cucumber fusarium wilt, and a potential usage of moso bamboo in the production of microbial pesticide.

**Keywords:** moso bamboo, *Trichoderma harzianum*, cucumber fusarium wilt, microwave mutagenesis, mutagenesis

## HIGHLIGHTS

- Cucumber fusarium wilt inhibition rate of T334 was increased by microwave mutagenesis.
- Sporulation of T334 was increased after microwave mutagenesis.
- Biotransformation rate of moso bamboo was improved after disk milling pretreatment.
- Bamboo stem and leaves are suitable for fermenting production of the mutant T334.



## INTRODUCTION

Cucumber fusarium wilt (Jia et al., 2015) is one of the most difficult diseases to control in cucumber cultivation. It is world widely known as “plant cancer,” which is a systemic disease transmitted by soil and invades the root or root neck (Gao et al., 2020). Cucumber fusarium wilt spreads quickly and it only takes 2–3 years from sporadic onset to large-scale onset. The incidence rate can be as high as 70%, and the yield loss is 10–50% or even no harvest in the 3 years of continuous cropping in the same plot. The disease not only harms cucumber, but also harms watermelon, melon, winter melon and so on. The pathogen of Cucumber fusarium wilt is *Fusarium oxysporum* f. sp. *cucumebrium*, which overwinters in soil, and diseased plant residues and seeds with mycelium, sclerotium and thick cucumebrium spores become the source of infection at the beginning of the next year and can be transmitted over a long distance with the help of rain and irrigation water (Li et al., 2016). At present, the prevention and control techniques for Cucumber fusarium wilt mainly include selection of disease-resistant varieties, avoidance of continuous cropping, grafting and application of chemical pesticides. Although the extensive use of chemical pesticides has controlled the disease, it has, at the same time, killed the beneficial microorganisms in the environment, seriously damaged the agricultural ecosystem and caused environmental pollution. In addition, the resistance of pathogens increases year by year, which has resulted in a high incidence rate of the disease and difficulty in its prevention (Jia et al., 2015). Therefore, it is particularly urgent to develop high-efficiency, safe and pollution-free green biological pesticides (Cao et al., 2011).

Research on the biological control of Cucumber fusarium wilt has mainly focused on fungi, actinomycetes and bacteria (José et al., 2015). Among them, *T. harzianum* has been attracting the interest of many researchers because it can inhibit plant pathogenic fungi, promote plant growth and induce plant defense through its hyperparasitism and production of antibiotics, including polyketones, amino acids and their derivatives, terpenes, imidazoles, etc. (Khaledi and Taheri, 2016). Although the fermentation technology of *T. harzianum* has been significantly improved, and some products have been put into the market, the backward production technology and the low control effect compared with chemical pesticides limit its wide application. Increment in control effect can be achieved by using microbial genetic breeding techniques including mutation breeding, crossbreeding, metabolic control breeding and genetic engineering breeding etc. By comparison, advanced physical mutagenesis techniques, such as microwave (Sarkar et al., 2015) and low energy ion implantation (Wu et al., 2012; Liu et al., 2015), provide more and more possibilities in parameter selection and control. Combined with sensitive screening factors, they have been well applied in industrial microbial genetics and breeding (Xu et al., 2010; Yan et al., 2014).

On the other hand, the key to the application of *T. harzianum* in agricultural production lies in the number of spores. Fungicides with a high number of spores can germinate and propagate rapidly in the field, form dominant colonies, and

then produce metabolites that act on the plant and its growth microenvironment, exerting biological control and promoting plant growth (Yücel et al., 2017). In addition, if the number of spores is high, the shelf life of the fungicide will be longer. At present, wheat bran is the main component in the medium for *T. harzianum* cultivation. The problem with wheat bran is that mycelial growth is too vigorous, and spores are insufficient during the process of cell growth. Therefore, it is key to improve sporulation and develop a culture medium that is suitable for the growth of *T. harzianum*.

Previous studies have found that bamboo powder can be used for the culture of *T. harzianum*, and a selective medium composed of oxygen carrier powder and bamboo powder for *T. harzianum* culture was invented (Qin et al., 2016). However, further analysis of the effect of the pretreatment method on the fibers and lignocellulosic composition after fermentation are still required to determine the bamboo potential for *T. harzianum* production. The analysis results showed that bamboo contains 25–45% cellulose, 20–25% hemicellulose and 20–30% lignin. Compared with straw and wheat straw, bamboo shows little difference in cellulose content but higher lignin content. Compared with hardwood and cork, bamboo has basically the same lignin content but lower cellulose and hemicellulose content (Singh et al., 2016). Therefore, research on biotransformation with bamboo as the substrate has a certain uniqueness. Like other lignocelluloses, the resistance of bamboo fiber to enzymatic hydrolysis is also the bottleneck of bamboo fiber biotransformation (Yang et al., 2011). It is difficult to reduce the crystallinity of cellulose and increase the specific surface area and porosity of substrate as much as possible. Papermaking beating treatment is a process in which fiber is cut off and disported by the mechanical action of beating equipment. Beating treatment can produce a series of effects, such as deformation, wetness swelling, fibrillation and cutting (Salgueiro et al., 2016). As a technology for papermaking beating treatment, the disk mill involves a continuous beating process. This strategy reduces the particle size and increases the specific surface area, thereby improving the biological accessibility of raw materials (Liu et al., 2016).

In this paper we applied the technique of microwave to irradiate *T. harzianum* and selected a mutant with higher inhibition rate on cucumber fusarium wilt. Fatality and mutation rate of different operation parameters of microwave mutagenesis (microwave powers and times) were tested, and then genetic stability of the mutant was investigated. Moso bamboo stem powder, which was pretreated by disk milling, and moso bamboo leaves were used as the medium to ferment *T. harzianum* mutant. The microstructure (IR, XRD, and SEM) of moso bamboo after pretreatment and fermentation were also tested.

## MATERIALS AND METHODS

### Materials

Moso bamboo powder was supplied by the China National Bamboo Research Center. Moso bamboo leaves were collected from Nanjing Forestry University. *Trichoderma harzianum*

(CMCC 3.5488) was purchased from the China General Microbiological Culture Collection Center. The pathogenic strain, *Fusarium oxysporum* f. sp. *cucumerinum* (CICC 2532) was purchased from the China Center of Industrial Culture Collection.

## Pretreatment Method for Moso Bamboo Materials

The moso bamboo powder was dried to a constant weight and then milled five times by a FSP-300 high-concentration experimental disk mill. The screw rotation speed was 280 rpm, the water supply pressure was 0.5 MPa, the cooling water flow was 2 L/min, and the dilution water flow was 3 L/min (Romuli et al., 2015). The freeness of the obtained material reached 170 ~ 180 mL. The fresh moso bamboo leaves were dried to constant weight, ground and passed through a 0.178 mm sieve.

## Medium

Solid medium (mass per 1,000 mL of medium): glucose 20 g,  $\text{KH}_2\text{PO}_4$  3 g,  $\text{MgSO}_4 \cdot 7\text{H}_2\text{O}$  1.5 g,  $(\text{NH}_4)_2\text{SO}_4$  0.75 g, wheat bran decoction (Cavalcante et al., 2008) (100 g of bran, 900 g of water, boiling for 20 min, filtered through four layers of gauze) 80 g, agar 15 g. Separate medium formula (mass per 1,000 mL of medium): 1.5 g of sodium deoxycholate was added to the solid medium; liquid medium (mass per 1,000 mL of medium): glucose 20 g,  $\text{KH}_2\text{PO}_4$  3 g,  $\text{MgSO}_4 \cdot 7\text{H}_2\text{O}$  1.5 g,  $(\text{NH}_4)_2\text{SO}_4$  0.75 g, bran water 80 g. Solid fermentation medium: Moso bamboo pretreated with 90 g of disk mill material, 9.5 g of moso bamboo leaf powder, 0.5 g of bran, and 150 mL of liquid medium.

## Fermentation Method

Seed liquid fermentation method (Gu et al., 2008): Appropriate amounts of spores of *T. harzianum* were inserted into liquid medium. The liquid filling quantity was 50 mL in a 250 mL triangular bottle, the rotation speed was 180 r/min, and the culture time was 48 h at 28°C. Solid-state fermentation method: The fermentation medium was placed in a 1,000 mL beaker or mushroom culture bags of 20 cm × 28 cm, sterilized by moist heat, cooled to room temperature, inserted into 5% *T. harzianum* seed liquid, and placed in a 28°C incubator for 7–10 days. After 48 h of inoculation, the culture medium and mycelium were mixed evenly every 48 h, and an appropriate amount of sterile water was added until the end of the fermentation.

## Breeding of *T. harzianum* by Microwave Mutation

### Microwave Mutagenesis Method

Microwave mutagenesis was carried out with MWD-520 microwave digestion system which was produced by Shanghai Metash Instruments Co., Ltd. Physiological saline was added to the separation medium of *T. harzianum*, and the spores were washed and poured into a sterilized triangular flask equipped with a magnetic stirrer to disperse the spores for use (Osula et al., 2015). The concentration of spore suspension was controlled at  $10^7 \sim 10^8$  cfu/mL. The spore suspension was transferred into a 1.5 mL centrifuge tube, and the centrifuge tube was placed

into a microwave digestion tube containing ice cubes (Jia et al., 2003). The spore suspension was irradiated with power levels of 200, 400, 600, 800, and 1,000 W, and the treatment time was 0 ~ 180 s (Li, 2001). Then, the spore suspension was coated on the separation medium plate, and the number of colonies was counted after incubation at 28°C for 2 days to calculate the lethal rate of microwaves under different irradiation powers and times, according to the equation (1).

$$\text{Lethal rate(\%)} = \frac{(N_0 - N_c)}{N_0} \times 100 \quad (1)$$

$N_0$  — Colony number of coated plate without microwave irradiation;

$N_c$  — Colony number of the coated plate after microwave irradiation for different times.

### Screening Method of the *T. harzianum* Mutant

Primary screening of mutant strains (point confrontation experiment): *Fusarium oxysporum* f. sp. *cucumebrium* and irradiated *T. harzianum* and were inoculated symmetrically on solid medium at the same time (Karkachi et al., 2012). The distance between them was approximately 3 cm. The plates that were only inoculated with *Fusarium oxysporum* f. sp. *cucumebrium* were used as a control. Then, the diameters of *Fusarium oxysporum* f. sp. *cucumebrium* on the experimental and the control plates were measured regularly. The inhibition rate of *T. harzianum* on *Fusarium oxysporum* f. sp. *cucumebrium* was calculated according to the equation (2).

$$\text{Inhibition rate(\%)} = \frac{(D_0 - D_c)}{D_0} \times 100 \quad (2)$$

$D_0$  — Diameter of the colony without microwave irradiation;

$D_c$  — Diameter of the colony after microwave irradiation.

Compared with the original strain, the mutant was defined as positive if the inhibition rate was confirmed to be a 5% increase after incubation; inversely, the mutant was defined as negative if a 5% decrease was confirmed.

Secondary screening of mutant strains: the mutant strain with a significantly increased inhibition rate was selected, inserted into the solid fermentation medium at a 5% inoculation volume, and placed in a 28°C incubator for 7 days. In this way, mutant strains with high antibacterial efficiency and high spore yield were selected.

### Genetic Stability

To ensure the genetic stability of the mutant strains, the genetic stability was tested. The inhibition rate and sporulation after solid fermentation were detected. *T. harzianum* was mutagenized three times and passaged five times, and three parallel samples were made in each generation.

## Analytical Methods

### Determination of the Number of Spores

Solid culture (0.5 g) was diluted 100 times with sterile water containing 1% Tween, stirred on a magnetic stirrer for 20 min, and the number of spores was counted under a microscope with a hemocytometer.

## Infrared Spectrum Analysis

A Nicolet iS10 Fourier infrared spectrometer produced by Thermo Nicolet Corporation was used to detect the structural changes of the samples. The scanning wavenumber range was 4,000–500  $\text{cm}^{-1}$ . The calculation method of the relative intensity of the absorption peak was the ratio of the absorbance of the corresponding characteristic wavenumber to the absorbance of 1,372  $\text{cm}^{-1}$  (Chandel et al., 2014). The experimental results were the average of three experimental repeats.

## X-Ray Diffraction Analysis

A D8 Focus X-ray diffractometer (XRD) produced by Bruker Corporation was used to determine the relative crystallinity of the samples. The detection wavelength was 0.15406 nm, and the sampling interval was 0.02°. Then, the crystallinity was calculated according to the equation (Segal et al., 1959). The experimental results were the average of three experimental repeats.

$$Crl(\%) = \frac{(I_{002} - I_{am})}{I_{002}} \times 100 \quad (3)$$

$Crl(\%)$  — The percentage of relative crystallinity;

$I_{002}$  — The maximum intensity (arbitrary unit) of the lattice diffraction angle;

$I_{am}$  — The scattering intensity of the non-crystalline background diffraction when the  $2\theta$  angle is close to 18°.

## Scanning Electron Microscope Analysis

Observation was carried out with a 3400-I scanning electron microscope (SEM) produced by Hitachi Limited. The Moso bamboo raw material, the raw material after pretreatment with a disk mill, and the culture medium after fermentation were observed at 1,000 times and 2,000 times magnification, respectively.

# RESULTS AND DISCUSSION

## Breeding of *T. harzianum* Mutants by Microwave Irradiation

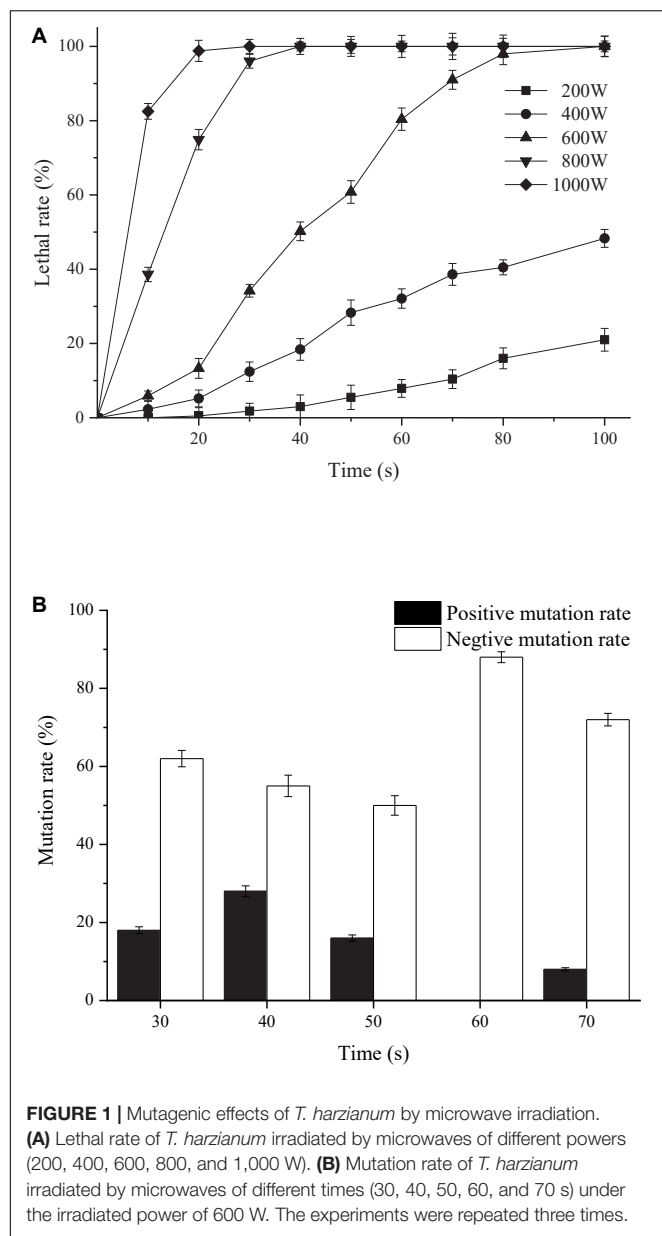
### Mutagenic Effects of *T. harzianum* by Microwave Irradiation

Existing studies have shown that microwave irradiation can cause damage or weakening of hydrogen bonding and base stacking chemical forces of microbial DNA molecules and change the three-dimensional structure of DNA, which leads to the occurrence of mutations (Mazinani et al., 2017). It can be seen from **Figure 1A** that the lethal rate of *T. harzianum* increased with the increase of irradiation power and the length of irradiation time; when the irradiation power was 200 W, the lethal rate was less than 20% within 100 s; when the irradiation was 400 W, the lethal rate within 100 s was less than 50%. When the irradiation power was 600 W and the irradiation time was 20 ~ 60 s, the lethal rate was concentrated at 40 ~ 80%, while continuing to increase the irradiation power, the lethal rate increased to 100%. According to the repair theory (Stuckey and Storici, 2013), the repair capacity of the cell depends on

the irradiation intensity or tends to be saturated with increasing irradiation intensity. The irradiation intensity continued to increase, and the lethal rate was no longer significant, indicating that the repair system of the cell was activated. Of course, if the irradiation intensity exceeded the repair ability of the cell, the strains would die. Therefore, the optimal irradiation time can be determined at the turning point of the lethal rate curve from a sharp increase to a stable level. Based on the lethal situation of *T. harzianum* (**Figure 1A**), the optimal irradiation power was 600 W, and the irradiation time was 30 ~ 70 s. At optimal irradiation condition, different mutation rate of *T. harzianum* was exhibited under different irradiation times (**Figure 1B**). When the irradiation time was 40 s, the positive mutation rate of the strain reached 28%, and the negative mutation was the lowest at 50 s. When the irradiation time was 60 s, no positive mutation was obtained. To select the colony most likely to have a higher sporulation, the subsequent mutagenesis operations were performed with an irradiation time of 40 s.

## Screening of the *T. harzianum* Mutant and Genetic Stability

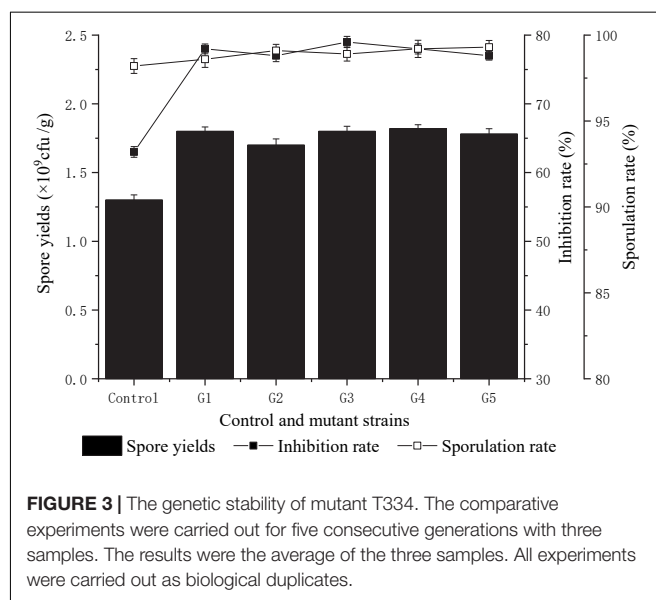
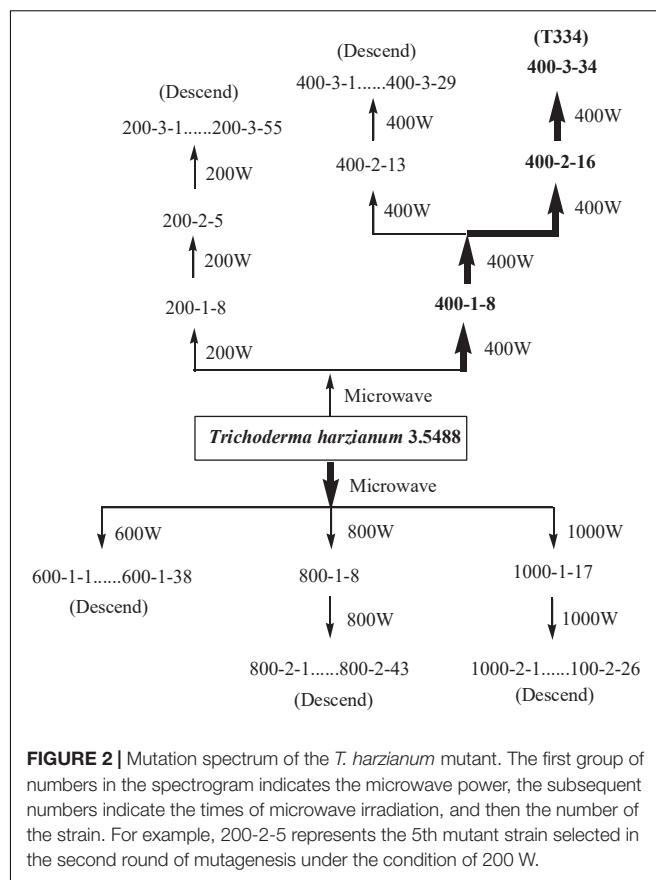
Compared with *Fusarium oxysporum* f. sp. *cucumerinum*, *T. harzianum* grew rapidly and had competitive advantages in nutrients and space. In this study, the rapid growth of *T. harzianum* was used for mutation screening. Twenty-four hours after inoculation, the colonies of *T. harzianum* were much larger than those of *Fusarium oxysporum* f. sp. *cucumerinum*, and at 48 h, parts of both colonies began to contact each other gradually. After 72 h, an obvious antimicrobial line was formed between the two colonies where they were in contact, and *T. harzianum* began to surround *Fusarium oxysporum* f. sp. *cucumerinum*. Ninety-six hours later, *T. harzianum* completely surrounded *Fusarium oxysporum* f. sp. *cucumerinum*. With the increase in the number of spores on both sides, the colonies of *T. harzianum* began to be produced on the white colony of *Fusarium oxysporum* f. sp. *cucumerinum* and increased. Finally, the colony of *Fusarium oxysporum* f. sp. *cucumerinum* was disintegrated. By measuring the colony diameter of *Fusarium oxysporum* f. sp. *cucumerinum* after incubation of 96 h, the inhibitory effect of *T. harzianum* on *Fusarium oxysporum* f. sp. *cucumerinum* was investigated. The mutation screening process is shown in **Figure 2**. After three microwave mutations, a mutant 400-3-34 (abbreviated as T334) was obtained, and its inhibition rate of *Fusarium oxysporum* f. sp. *cucumerinum* reached 78% and increased 23.81% compared with the original strain. It can be seen from the growth trend that the mutant T334 grew faster, and spores grew vigorously. Its sporulation increased from  $1.3 \times 10^9$  cfu/g to  $1.8 \times 10^9$  cfu/g, and the sporulation and inhibition rate of T334 remained stable after five generations of flask culture. The experimental results are shown in **Figure 3**. The mutagenesis effect of microwave irradiation on *T. harzianum* was preliminarily studied, the results of existing studies showed that microwave irradiation could cause changes in the activity of antioxidant enzymes in *T. harzianum*, including superoxide dismutase (SOD), peroxidase (POD), catalase (CAT), polyphenol oxidase (PPO) and so on (Kushwah et al., 2013). We speculated



that this not only affected the survival rate of *T. harzianum* after mutagenesis, but also may be related to its antimicrobial activity and sporulation (Li et al., 2011).

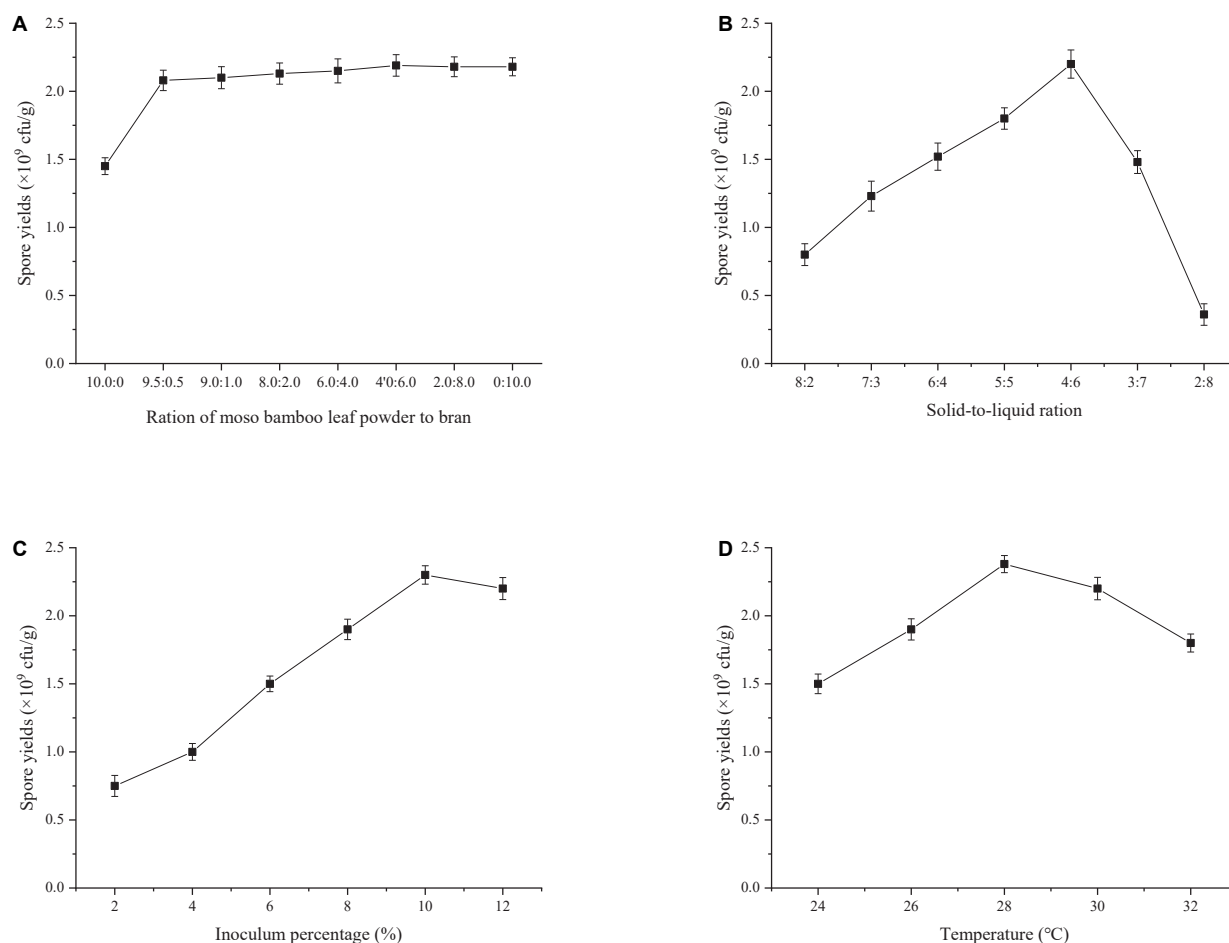
## Effect of Fermentation Conditions on Spore Production

Previous experiments found that 90% bamboo powder was the most suitable medium for the growth of *T. harzianum*. In this study, the ratio of bamboo leaf powder to wheat bran in the remaining 10% was optimized. The results (Figure 4A) showed that the sporulation of T334 increased rapidly when the wheat bran content in bamboo leaf powder increased to 0.5%, but the increase was not significant (the increase was less than 5%) when its content continued to increase, which indicated



that 9.5% wheat bran in the medium could be replaced by bamboo leaf powder. Under this condition, the sporulation of T334 was  $2.08 \times 10^9$  cfu/g; the solid-liquid ratio of the medium directly affected the sporulation of T334. The water storage capacity of bamboo powder was weak, and the excess liquid medium accumulated at the bottom of the beaker could not be





**FIGURE 4 |** Effects of fermentation conditions on spore production. After each factor was optimized, the optimal condition was substituted into the optimization experiment of the next factor. The experiments were repeated three times. **(A)** Effect of the ratio of moso bamboo leaf to bran on sporulation (10:0, 9.5:0.5, 9.0:1.0, 8.0:2.0, 6.0:4.0, 20:8.0, and 0:10.0). Solid-to-liquid ratio (5:5), inoculum percentage (8%), fermentation temperature (28°C). **(B)** Effect of solid-to-liquid ratio on sporulation (8:2, 7:3, 6:4, 5:5, 4:6, 3:7, 2:8). The ratio of moso bamboo leaf to bran (9.5:0.5), inoculum percentage (8%), fermentation temperature (28°C). **(C)** Effect of inoculum percentage on sporulation (2, 4, 6, 8, 10, and 12%). The ratio of moso bamboo leaf to bran (9.5:0.5), solid-to-liquid ratio (4:6), fermentation temperature (28°C). **(D)** Effect on fermentation temperature on spore production (24, 26, 28, 30, and 32°C). The ratio of moso bamboo leaf to bran (9.5:0.5), solid-to-liquid ratio (4:6), inoculum percentage (10%).

used. However, if the liquid medium was insufficient, it could not provide enough soluble nutrition for the growth of T334. Repeated observations showed that the sporulation of T334 was highest when the ratio of solid to liquid was 4:6 (see **Figure 4B**). During the experiment, it was found that there was a strong relationship between the growth of T334 and the inoculation amount. Low inoculation amounts slowed the growth of T334 and prolonged the fermentation cycle. The results showed that sporulation was better when the inoculation amount was 10% (**Figure 4C**), and sporulation did not increase with increasing inoculation amount. The fermentation temperature experimental results (**Figure 4D**) showed that the optimal spore producing temperature of T334 was 28°C, and the mycelia could grow well within the experimental temperature range. According to the above fermentation conditions, fermentation experiments were carried out in mushroom culture bags of 20 cm  $\times$  28 cm, and the sporulation of T334 could reach  $3.72 \times 10^9$  cfu/g.

## Effect of Pretreatment and T334 Fermentation on the Chemical Composition and Microstructure of Moso Bamboo

### Chemical Composition Analysis

After pretreatment by disk milling, the material was dried together with the solution for use, so the total mass loss and the contents of cellulose and lignin did not change much. After the spores were separated after fermentation, the fermentation medium was washed with water to remove the bamboo leaf residues, and the composition changes of the remaining bamboo powder were determined. The results (**Table 1**) showed that the content of hemicellulose in bamboo powder decreased by 67.59%, and the content of cellulose decreased by approximately 13.77%. Therefore, bamboo stem powder helped to increase the amount of air in the fermentation medium for its loose texture, and

**TABLE 1** | Chemical composition change before and after fermentation.

Samples	Solid remain	Cellulose (%)		Hemicellulose (%)		Lignin (%)	
	(%)	Content	removal	Content	removal	Content	removal
Moso bamboo material	100.00	38.96	—	27.52	—	22.24	—
Before fermentation	96.26	38.67	4.46	26.04/	8.92	22.50/	2.61
After fermentation	78.51	42.79	13.77	11.36/	67.59	26.37/	6.91

provided sufficient carbon source and nutrients for the growth of *T. harzianum*.

### FIR Analysis

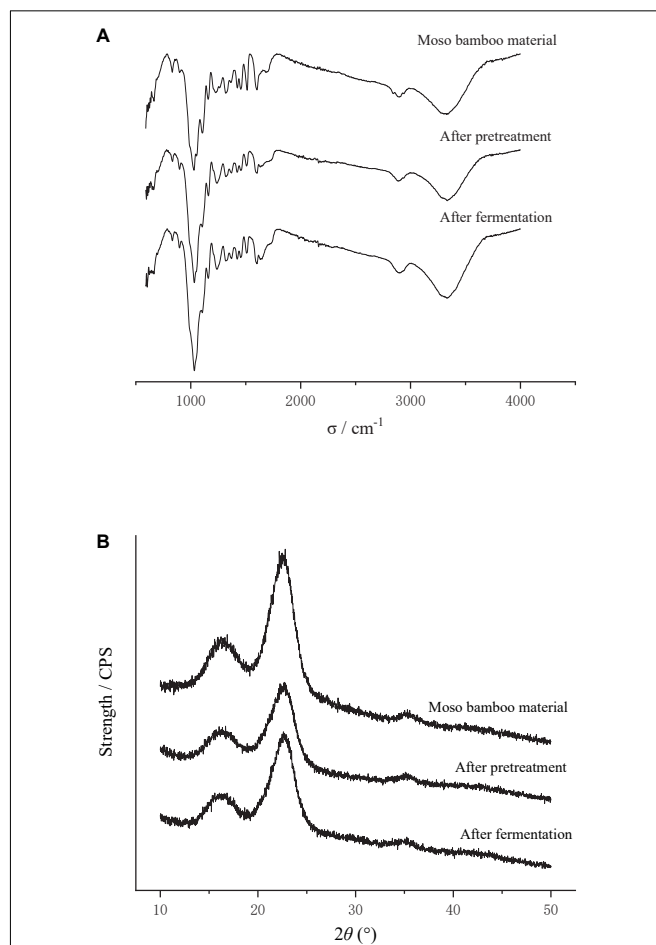
The moso bamboo raw material, the pretreated material and the after-fermentation material were scanned by infrared spectroscopy, and the relative absorption intensity in the infrared spectrum is shown in **Table 1**. After pretreatment by disk milling, the absorption peak intensity of the moso bamboo material at 3,400, 2,900 and 1,432  $\text{cm}^{-1}$  decreased (**Table 2**), which indicated that the intramolecular hydrogen bond, intermolecular hydrogen bond and methylene bond were broken. The absorption peak intensity at 1,163 and 898  $\text{cm}^{-1}$  increased (**Table 2**), which showed that the disk milling treatment was helpful for the depolymerization and separation of cellulose, hemicellulose and lignin but did not destroy the  $\beta$ -glycoside bond and C-O-C bond between glucose and cellulose, which was beneficial to the growth and utilization of microorganisms. After fermentation, the absorption peak intensities at 3,400, 1,432, 1,372, and 898  $\text{cm}^{-1}$  were all reduced (**Table 2**), indicating that the fermentation of T334 caused the hydrogen bond and methylene bond in the molecular structure of moso bamboo to break. The  $\beta$ -glucoside bond of the glucose molecule inside the cellulose molecule and the C-O-C bond of the glucose molecule were destroyed (Liu et al., 2012). The reduction in the absorption strength of the above structure also showed that the growth of T334 consumed a lot of carbon sources, while the absorption peak intensity at 2,900  $\text{cm}^{-1}$  increased (**Table 2**), which indicated that more intermolecular hydrogen bonds were formed in culture during the growth and reproduction of T334, and the formation of intermolecular hydrogen bonds allowed the solute to be better surrounded by water molecules and dispersed into water, which helped the growth and reproduction of T334 (Wang et al., 2020). In addition, T334 could secrete cellulase, which in turn contributed to the degradation of culture medium.

**TABLE 2** | Structure attribution and relative intensity change of infrared absorption peak (Kim and Lee, 2005).

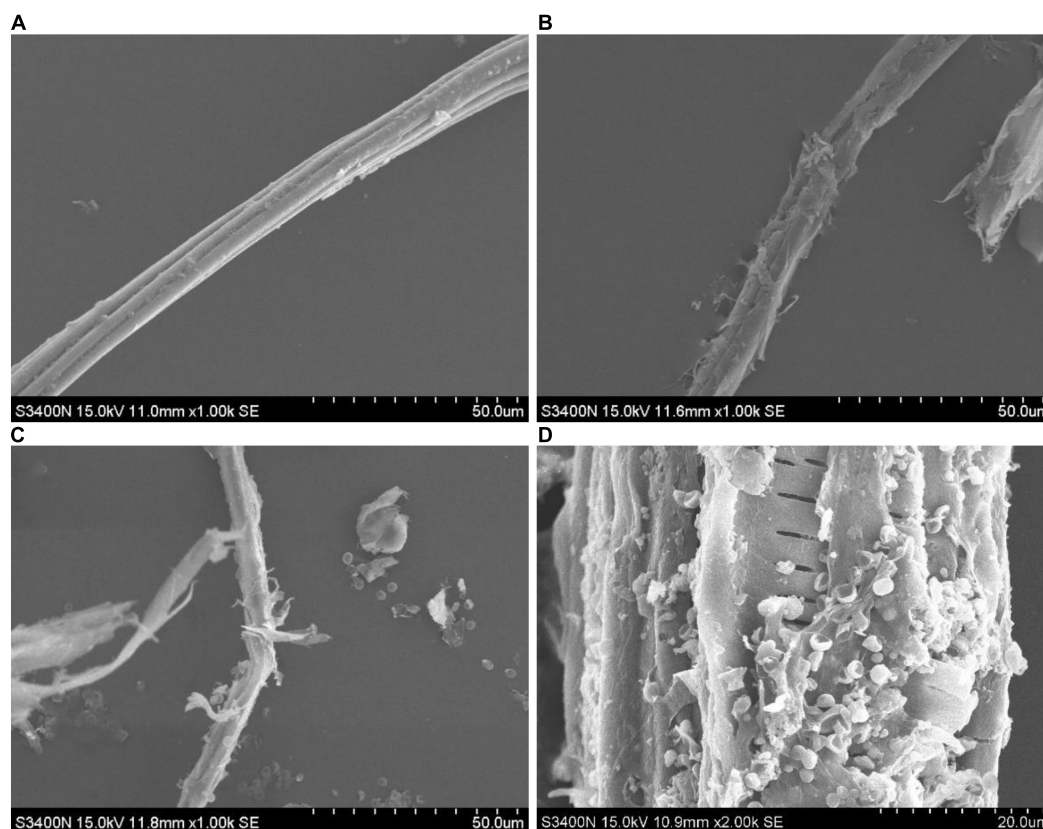
Wave length $\sigma/\text{cm}^{-1}$	Response peak	Moso bamboo	After pretreatment	After fermentation
3,400	Intramolecular -OH	2.020	1.999	2.162
2,900	Intermolecular -OH	1.614	1.346	1.509
1,432	Cellulose -CH <sub>2</sub>	1.2625	0.810	0.850
1,372	Cellulose and hemicellulose -CH	1.000	1.000	1.000
1,163	Cellulose and hemicellulose C-O-C	1.701	2.027	1.648
898	$\beta$ -Glucoside bond	0.687	0.834	0.635

### X-Ray Diffraction Analysis of Medium

**Figure 5** shows the X-ray diffraction curves before and after the fermentation of bamboo culture medium, and the changes of crystallinity was calculated according to equation (3). The results showed that the crystallinity of moso bamboo fiber



**FIGURE 5** | Effect of pretreatment and T334 fermentation on the microstructure of moso bamboo. **(A)** Infrared spectrum of moso bamboo pretreated by disk mill and after fermentation. Samples of the moso bamboo raw material, after pretreatment and after fermentation were scanned with a Nicolet iS10 Fourier Infrared Spectrometer, and the wavelength was 500–4,000  $\text{cm}^{-1}$ . Each sample was scanned three times, and the result was the average of three times. **(B)** X-ray diffraction pattern of moso bamboo pretreated by disk mill and after fermentation. Samples of the moso bamboo raw material, after pretreatment and after fermentation were scanned with a D8 Focus X-ray Diffraction instrument. The detection wavelength was 0.15406 nm, and the sampling interval was 0.02°. Each sample was scanned three times, and the result was the average of three times.



**FIGURE 6 |** SEM image of moso bamboo culture medium. Samples of the moso bamboo raw material, after pretreatment and after fermentation were scanned using a 3400-I scanning electron microscope. **(A)** Moso bamboo material. **(B)** Material pretreated by disk milling. **(C)** Moso bamboo culture medium after fermentation at 1,000 $\times$  magnification. **(D)** Moso bamboo culture medium after fermentation at 2,000 $\times$  magnification.

decreased by 30% after disk milling, which indicates that the crystallization area of moso bamboo fiber was destroyed, resulting from the destruction of the intramolecular hydrogen bonds, intermolecular hydrogen bonds and methylene bonds in the bamboo fibers. After fermentation, the crystallinity reached 0.459 and increased 36.0% compared to the material that was pretreated by the disk mill. The reason may be that the growth of T334 mainly resulted in a disordered structure on the surface of the moso bamboo fiber, resulting in a decrease in the amorphous structure and an increase in the crystalline structure (Ju et al., 2015). In the same way, the increase in crystallization of the fermentation substrate also led to the slowing down of the fermentation process to the end. The results of chemical component analysis showed that cellulose and lignin were the main residues in the fermentation substrate after fermentation, and the premise of continuous fermentation was the continuous depolymerization of cellulose and the removal of lignin.

### Scanning Electron Microscopy of Culture Medium

It can be seen from the scanning electron microscopy that the surface of the moso bamboo raw material was smooth, and the fibers were arranged in order, as shown in **Figure 6A**. After pretreatment by disk milling, the moso bamboo fibers were obviously broomed and divided into filaments, and such

structural changes were undoubtedly conducive to the growth and reproduction of the mycelium, as shown in **Figure 6B**. After fermentation (**Figure 6C**), the mycelium of T334 and the bamboo fiber were intertwined, and many spores could be seen inside and outside the sporangium. From 2,000 $\times$  magnification (**Figure 6D**), we can see the orderly arrangement of fiber structure inside. On the other hand, the growth of T334 also contributed to further degradation of the bamboo fiber. The degradation process resulted in degradation of the surface amorphous area, which was more easily degraded first, and then the degradation of the crystallized area with high crystallinity.

## CONCLUSION

An improved biocontrol agent *T. harzianum* T334 was obtained by microwave mutagenesis. Compared with the original strain, the inhibition rate of the mutated strain against cucumber fusarium wilt increased by 23.81% from 63 to 78%. Moso bamboo was investigated as a new material for fermenting production of the microbial pesticide T334, and whole bamboo utilization was realized with 90% moso bamboo stem powder (pretreated by disk mill), 9.5% moso bamboo leaf powder and 0.5% wheat

bran. Under optimal fermentation conditions (solid to liquid 4:6, inoculum 10%, and fermentation at 28°C), the sporulation reached  $3.72 \times 10^9$  cfu/g when cultured in mushroom bags. After fermentation, the content of hemicellulose in bamboo powder decreased by 67.59%, and the content of cellulose decreased by 13.77%. The crystallinity of bamboo medium increased from 0.337 to 0.459, which indicated that the growth and reproduction of T334 consumed nutrients in the medium of moso bamboo and also changed its microstructure.

## DATA AVAILABILITY STATEMENT

The original contributions presented in the study are included in the article/**Supplementary Material**, further inquiries can be directed to the corresponding author/s.

## AUTHOR CONTRIBUTIONS

JJ and JX conceived and designed the experiments. NZ, HX, JX, and J-YC performed the experiments. NZ, JY, and JZ analyzed

the data. HX, JY, YT, and JZ contributed to the reagents, materials, and analysis tools. NZ wrote the manuscript. JJ, NZ, and JX revised and approved the final version of the manuscript. All authors contributed to the article and approved the submitted version.

## FUNDING

This study was financially supported by National Natural Science Foundation of China (Grant No. 31770636), Basic Scientific Research Project of Jiangsu Province Biomass Energy and Material Laboratory (Grant No. JSBEM-S-2017011), and Natural Science Foundation of Jiangsu Province (Grant Nos. BK20180153 and BK20200162).

## SUPPLEMENTARY MATERIAL

The Supplementary Material for this article can be found online at: <https://www.frontiersin.org/articles/10.3389/fmicb.2021.763006/full#supplementary-material>

## REFERENCES

- Cao, Y., Zhang, Z., Ling, N., Yuan, Y., Zheng, X., Shen, B., et al. (2011). *Bacillus subtilis* SQR 9 can control fusarium wilt in cucumber by colonizing plant roots. *Biol. Fertil. Soils*. 47, 495–506. doi: 10.1007/s00374-011-0556-2
- Cavalcante, R. S., Lima, H., Pinto, G. A., Gava, C. A., and Rodrigues, S. (2008). Effect of moisture on *Trichoderma* conidia production on corn and wheat bran by solid state fermentation. *Food Bioproc. Tech.* 1, 100–104. doi: 10.1007/s11947-007-0034-x
- Chandel, A. K., Antunes, F. A., Anjos, V., Bell, M. J., Rodrigues, L. N., Polikarpov, I., et al. (2014). Multi-scale structural and chemical analysis of sugarcane bagasse in the process of sequential acid–base pretreatment and ethanol production by *Scheffersomyces shehatae* and *Saccharomyces cerevisiae*. *Biotechnol. Biofuels*. 7, 63–79. doi: 10.1186/1754-6834-7-63
- Gao, X., Li, K., Ma, Z., Zou, H., and Wang, J. (2020). Cucumber fusarium wilt resistance induced by intercropping with celery differs from that induced by the cucumber genotype and is related to sulfur-containing allelochemicals. *Sci. Hortic.* 271, 109475–109485. doi: 10.1016/j.scienta.2020.109475
- Gu, J. G., Lv, X. Y., Hu, D. D., Li, S. G., and Jiang, R. B. (2008). Production of chlamydospores of *Trichoderma longibrachiatum* ACCC30150 and *Trichoderma harzianum* ACCC30371 by liquid fermentation. *Chin. J. Bio. Control* 24, 253–256.
- Jia, H. H., Zhou, H., and Wei, P. (2003). Advances in research and application of microwave mutagenesis. *Ind. Microbiol.* 33, 46–50.
- Jia, K., Gao, Y. H., Huang, X. Q., Guo, R. J., and Li, S. D. (2015). Rhizosphere inhibition of cucumber fusarium wilt by different surfactin-excreting strains of *Bacillus subtilis*. *Plant Pathol.* 31, 140–151. doi: 10.5423/PPJ.OA.10.2014.0113
- José, L. H. M., María, I. S. P., Juan, M. G. P., Jesús, D. Q. V., and Langarica, H. R. G. (2015). Antibiosis of *Trichoderma* spp strains native to northeastern Mexico against the pathogenic fungus *Macrophomina phaseolina*. *Braz. J. Microbiol.* 46, 1093–1101. doi: 10.1590/S1517-838246420120177
- Ju, X., Bowden, M., Brown, E. E., and Zhang, X. (2015). An improved x-ray diffraction method for cellulose crystallinity measurement. *Carbohydr. Polym.* 123, 476–481. doi: 10.1016/j.carbpol.2014.12.071
- Karkachi, N. E., Gharbi, S., Kihal, M., and Henni, J. E. (2012). Biological control of *Fusarium oxysporum* f.sp. *lycopersici* isolated from Algerian tomato by *Pseudomonas fluorescens*, *Bacillus cereus*, *Serratia marcescens* and *Trichoderma harzianum*. *Res. J. Agro.* 4, 31–34. doi: 10.3923/rjagr.2010.31.34
- Khaledi, N., and Taheri, P. (2016). Biocontrol mechanisms of *Trichoderma harzianum* against soybean charcoal rot caused by *Macrophomina phaseolina*. *J. Plant Prot. Res.* 56, 21–31. doi: 10.1515/jppr-2016-0004
- Kim, T. H., and Lee, Y. Y. (2005). Pretreatment and fractionation of corn stover by ammonia recycle percolation process. *Bioresour. Technol.* 96, 2007–2013. doi: 10.1016/j.biortech.2005.01.015
- Kushwah, P., Mishra, T., and Kothari, V. (2013). Effect of microwave radiation on growth, enzyme activity (amylase and pectinase), and/or exopolysaccharide production in *Bacillus subtilis*, *Streptococcus mutans*, *Xanthomonas campestris* and *Pectobacterium carotovora*. *Br. Microb. Res. J.* 3, 645–653. doi: 10.9734/bmrj/2013/5036
- Li, J. F., Zhang, S. Q., Shi, S. L., and Huo, P. H. (2011). Mutational approach for N<sub>2</sub>-fixing and P-solubilizing mutant strains of *Klebsiella pneumoniae* RSN19 by microwave mutagenesis. *World J. Microb. Biot.* 27, 1481–1489. doi: 10.1007/s11274-010-0600-7
- Li, R., Shen, Z. Z., Li, S., Zhang, R. F., Fu, L., and Deng, X. H. (2016). Novel soil fumigation method for suppressing cucumber fusarium wilt disease associated with soil microflora alterations. *App. Soil. Ecol.* 101, 28–36. doi: 10.1016/j.apsoil.2016.01.004
- Li, Y. Q. (2001). Study on the screening high yield xylanase producing strain *Aspergillus Niger* by microwave mutagenesis. *J. Microbiol.* 17, 50–53.
- Liu, B., Zheng, S., Ma, X., Bo, Y., Yue, J., Dong, W., et al. (2015). Mutation breeding of extracellular polysaccharide-producing microalgae *Cryptocodinium cohnii* by a novel mutagenesis with atmospheric and room temperature plasma. *Int. J. Mol. Sci.* 16, 8201–8212. doi: 10.3390/ijms16048201
- Liu, Q., Li, W., Ma, Q., An, S., Li, M., Jameel, H., et al. (2016). Pretreatment of corn stover for sugar production using a two-stage dilute acid followed by wet-milling pretreatment process. *Bioresour. Technol.* 211, 435–442. doi: 10.1016/j.biortech.2016.03.131
- Liu, X. H., Xu, C. H., Sun, S. Q., Huang, J., Zhang, K., Li, G. Y., et al. (2012). Discrimination of different genuine danshen and their extracts by fourier transform infrared spectroscopy combined with two-dimensional correlation infrared spectroscopy. *Spectrochim. Acta Part A* 97, 290–296. doi: 10.1016/j.saa.2012.06.013
- Mazinani, S. A., Moradi, F., Stuart, J. A., and Yan, H. (2017). Microwave irradiation of PC3 cells at constant culture temperature alters the incorporation of BODIPY into cells and reduction of MTT. *ChemistrySelect* 2, 7983–7986. doi: 10.1002/slct.201701445
- Osula, O., Swatkoski, S., and Cotter, R. J. (2015). Identification of protein sumoylation sites by mass spectrometry using combined microwave-assisted



- aspartic acid cleavage and tryptic digestion. *J. Mass Spectrom.* 47, 644–654. doi: 10.1002/jms.2959
- Qin, Z. R., Wang, Y. F., Guo, J., Zhang, D. D., and Wang, X. L. (2016). *A Selective Medium for Trichoderma Harzianum Culture*. China: 201610586285.0. Hefei: Hefei Dingtu Intellectual Property Agency Office.
- Romuli, S., Karaj, S., and Müller, J. (2015). Influence of physical properties of *Jatropha curcas* L. seeds on shelling performance using a modified disc mill. *Ind. Crops Prod.* 77, 1053–1062. doi: 10.1016/j.indcrop.2015.10.014
- Salgueiro, A. M., Evtuguin, D. V., Saraiva, J. A., and Almeida, F. (2016). High pressure-promoted xylanase treatment to enhance papermaking properties of recycled pulp. *Appl. Microbiol. Biotechnol.* 100, 1–9. doi: 10.1007/s00253-016-7703-5
- Sarkar, S., Selvamurthy, W., and Gupta, M. M. (2015). Biological consequences of microwave stress: implications for mutagenesis and carcinogenesis. *IETE Technical. Rev.* 14, 153–163. doi: 10.1080/02564602.1997.11416665
- Segal, L., Creely, J. J., Martin, A. E., and Conrad, C. M. (1959). An empirical method for estimating the degree of crystallinity of native cellulose using the x-ray diffractometer. *Text. Res. J.* 29, 786–794. doi: 10.1177/004051755902901003
- Singh, R., Krishna, B. B., Kumar, J., and Bhaskar, T. (2016). Opportunities for utilization of non-conventional energy sources for biomass pretreatment. *Bioresour. Technol.* 199, 398–407. doi: 10.1016/j.biortech.2015.08.117
- Stuckey, S., and Storici, F. (2013). Gene knockouts, in vivo site-directed mutagenesis and other modifications using the delitto perfetto system in *Saccharomyces cerevisiae*. *Method Enzymol.* 533, 103–131. doi: 10.1016/B978-0-12-420067-8.00008-8
- Wang, W., Wang, X. M., Zhang, Y., Yu, Q., Tan, X. S., Zhuang, X. S., et al. (2020). Effect of sodium hydroxide pretreatment on physicochemical changes and enzymatic hydrolysis of herbaceous and woody lignocelluloses. *Ind. Crops Prod.* 145, 112145–112152. doi: 10.1016/j.indcrop.2020.112145
- Wu, L. Q., Miao, F. X., Gu, H. K., and Shang, H. Z. (2012). Breeding of High-yield salinomycin-producing streptomyces albus strains by low energy N<sup>+</sup> ion beam irradiation. *Agri. Biotechnol.* 1, 55–56.
- Xu, T. T., Bai, Z. Z., Wang, L. J., and He, B. F. (2010). Breeding of D(-)-lactic acid high producing strain by low-energy ion implantation and preliminary analysis of related metabolism. *Appl. Biochem. Biotechnol.* 60, 314–321. doi: 10.1007/s12010-008-8274-4
- Yan, S., Wang, S., Zhai, Z., Chen, X., and Wu, J. (2014). Mutation breeding of salt-tolerant and ethanol-producing strain *S.cerevisiae* H058 by low-energy ion implantation. *Adv. J. Food Sci. Technol.* 6, 941–946. doi: 10.19026/ajfst.6.136
- Yang, B., Dai, Z., Ding, S. Y., and Charles, E. W. (2011). Enzymatic hydrolysis of cellulosic Biomass. *Biofuels* 2, 421–449. doi: 10.4155/bfs.11.116
- Yücel, S., Karaçancı, Ş., and Ay, T. (2017). Activity and bioformulation of trichoderma harzianum for management of tomato diseases caused by soilborne pathogens. *Acta Hort.* 1164, 339–344. doi: 10.17660/actahortic.2017.1164.43

**Conflict of Interest:** The authors declare that the research was conducted in the absence of any commercial or financial relationships that could be construed as a potential conflict of interest.

The reviewers ZL and XZ declared a shared affiliation with the author, J-YC, to the handling editor at the time of review.

**Publisher's Note:** All claims expressed in this article are solely those of the authors and do not necessarily represent those of their affiliated organizations, or those of the publisher, the editors and the reviewers. Any product that may be evaluated in this article, or claim that may be made by its manufacturer, is not guaranteed or endorsed by the publisher.

Copyright © 2021 Zhang, Xu, Xie, Cui, Yang, Zhao, Tong and Jiang. This is an open-access article distributed under the terms of the Creative Commons Attribution License (CC BY). The use, distribution or reproduction in other forums is permitted, provided the original author(s) and the copyright owner(s) are credited and that the original publication in this journal is cited, in accordance with accepted academic practice. No use, distribution or reproduction is permitted which does not comply with these terms.



# Mechanism of a Volatile Organic Compound (6-Methyl-2-Heptanone) Emitted From *Bacillus subtilis* ZD01 Against *Alternaria solani* in Potato

Dai Zhang<sup>1</sup>, Ran Qiang<sup>1</sup>, Jing Zhao<sup>1</sup>, Jinglin Zhang<sup>2</sup>, Jianing Cheng<sup>3</sup>, Dongmei Zhao<sup>1</sup>, Yaning Fan<sup>1</sup>, Zhihui Yang<sup>1\*</sup> and Jiehua Zhu<sup>1\*</sup>

<sup>1</sup> College of Plant Protection, Hebei Agricultural University, Baoding, China, <sup>2</sup> Beijing Laboratory for Food Quality and Safety, Beijing Technology and Business University, Beijing, China, <sup>3</sup> Agricultural Business Training and Entrepreneurship Center, Hebei Agricultural University, Baoding, China

## OPEN ACCESS

### Edited by:

Florence Fontaine,  
Université de Reims  
Champagne-Ardenne, France

### Reviewed by:

Ana Vazquez,  
Universidad Católica de Córdoba,  
Argentina  
Valeria Scala,  
Centro di Ricerca Difesa e  
Sperimentazione (CREA-DC), Italy

### \*Correspondence:

Zhihui Yang  
13933291416@163.com  
Jiehua Zhu  
zhujiehua356@126.com

### Specialty section:

This article was submitted to  
Microbe and Virus Interactions with  
Plants,  
a section of the journal  
Frontiers in Microbiology

**Received:** 03 November 2021

**Accepted:** 08 December 2021

**Published:** 13 January 2022

### Citation:

Zhang D, Qiang R, Zhao J,  
Zhang J, Cheng J, Zhao D, Fan Y,  
Yang Z and Zhu J (2022) Mechanism  
of a Volatile Organic Compound  
(6-Methyl-2-Heptanone) Emitted  
From *Bacillus subtilis* ZD01 Against  
*Alternaria solani* in Potato.  
Front. Microbiol. 12:808337.  
doi: 10.3389/fmicb.2021.808337

The antagonistic mechanisms of soluble non-volatile bioactive compounds, such as proteins and lipopeptides emitted from *Bacillus* have been widely studied. However, there are limited studies on the antifungal mechanisms of volatile organic compounds (VOCs) produced by *Bacillus* against plant fungal diseases. In this study, the antagonistic mechanisms of one specific VOC, 6-methyl-2-heptanone, against *Alternaria solani* were investigated. To optimize the extraction conditions of headspace solid-phase microextraction, a 50/30- $\mu$ m divinylbenzene/carboxen/polydimethylsiloxane fiber at 50°C for 40 min was used. For gas chromatography-mass spectrometry using a free fatty acid phase capillary column, 6-methyl-2-heptanone accounted for the highest content, at 22.27%, of the total VOCs from *Bacillus subtilis* ZD01, which inhibited *A. solani* mycelial growth strongly *in vitro*. Therefore, 6-methyl-2-heptanone was selected as the main active chemical to elucidate the action mechanisms against *A. solani*. Scanning and transmission electron microscopy analyses revealed that after exposure to an EC<sub>50</sub> dose of 6-methyl-2-heptanone, *A. solani* hyphal cells had a wide range of abnormalities. 6-Methyl-2-heptanone also caused the capture of cellular fluorescent green label and the release of adenosine triphosphate (ATP) from outer membranes *A. solani* cells, which may enhance 6-methyl-2-heptanone ability to reach the cytoplasmic membrane. In addition, 6-methyl-2-heptanone showed strong inhibitory effect on *A. solani* conidial germination. It also damaged conidial internal structures, with the treated group having collapsed shrunken small vesicles as observed by transmission electron microscopy. Because 6-methyl-2-heptanone showed strong effects on mycelial integrity and conidial structure, the expression levels of related pathogenic genes in *A. solani* treated with 6-methyl-2-heptanone were investigated. The qRT-PCR results showed that transcriptional expression levels of *slt2* and *wetA* genes were strongly down-regulated after exposure to 6-methyl-2-heptanone. Finally, because identifying the functions of pathogenic genes will be important for the biological control of *A. solani*, the *wetA* gene was identified as a conidia-associated gene that plays roles in regulating sporulation yield and conidial maturation. These findings provide further insights into the mechanisms of VOCs secreted by *Bacillus* against *A. solani*.

**Keywords:** *Alternaria solani*, *Bacillus subtilis*, 6-methyl-2-heptanone, antifungal activity, conidial genes

## INTRODUCTION

Potato early blight caused by *Alternaria solani* is a main factor in the death of potato leaves, and it results in substantial yield losses (Morgan et al., 2002; Pasche et al., 2007; Peters et al., 2008). Fungicides are the main effective methods of controlling potato early blight disease. However, because of increased fungal pathogen drug resistance, environmental pollution and human health risks induced by the abuse of chemical fungicides (Wang and Liu, 2007; Maachia et al., 2015), there is a greater need for alternative environmentally friendly effective methods to control fungal diseases of potato.

Biological control has been widely regarded as a potential substitute for chemical fungicides owing to its environmental safety and high efficiency. The use of *Bacillus* strains as the biocontrol microorganisms is presently a promising strategy for controlling plant pathogens (Chaurasia et al., 2005; Zheng et al., 2013). *Bacillus* strains exhibit significant antifungal activities against various pathogenic fungi, such as *Penicillium digitatum*, *Monilinia fructicola*, and *Botrytis cinerea* (Wichitra et al., 2008; Senthil et al., 2011; Banani et al., 2015; Maachia et al., 2015; Liu et al., 2018). Recently, the use of volatile organic compounds (VOCs) produced by *Bacillus* strains was proposed as an alternative control method for plant fungal diseases (Chen et al., 2008; Gao et al., 2017; Haiyan et al., 2018; Massawe et al., 2018; Zhang X. Y. et al., 2020) because of their strong inhibitory effects on plant fungi (Chaves-López et al., 2015; Raza et al., 2016a,b; Gotor-Vila et al., 2017; Calvo et al., 2020). In addition, various VOCs produced by *Bacillus* strains have been identified as effective compounds (e.g., 2-nonanone, 2-methylpyrazine, and benzothiazole) (Arrebola et al., 2010; Raza et al., 2015; Khan et al., 2018; Liu et al., 2018; Xie et al., 2018; Wu et al., 2019; Calvo et al., 2020).

Recent research on the VOCs produced by *Bacillus* strains has primarily focused on evaluating volatile mixture biocontrol effects, including disease incidences in inoculated plants, spore germination, mycelial growth inhibition, and reduced sporulation, as well as the identification of exact VOC components (Kai et al., 2009; Schreinemachers and Tipraqsa, 2012; Khan et al., 2018; Tran et al., 2020). However, little is known about the biocontrol effects of specific identified VOC compounds. Moreover, the VOC types secreted by *Bacillus* strains are varied, including aldehydes, ketones, alcohols, and esters (Morath et al., 2012; Chantal et al., 2014). Additionally, different volatile chemicals do not have the same effects on, or the same degree of inhibition against, all fungi. This may be because different fungi respond to different component(s) of the volatile mixture and have different sites of action (Kai et al., 2009). For example, 3-methyl-1-butanol inhibits the mycelial growth of *Fusarium oxysporum* f. sp. *lactucae* but has no antifungal activity against *A. alternata* and *B. cinerea* (Chaves-López et al., 2015). Therefore, it is essential to study the biocontrol functions of *Bacillus*-specific volatiles to further determine the action modes of VOCs secreted by *Bacillus* on fungal pathogens.

In our previous study, VOCs secreted by *B. subtilis* ZD01 exhibited significant antifungal activity against *A. solani* (Zhang D. et al., 2020). In this study, we discovered that

6-methyl-2-heptanone was the dominant component in the VOCs, and it also shows strong antagonistic effects against *A. solani* (Zhang D. et al., 2020). Therefore, we speculated that 6-methyl-2-heptanone plays the most important role in pathogen inhibition. Consequently, we investigated the inhibitory effects of 6-methyl-2-heptanone produced by *B. subtilis* strain ZD01 on *A. solani*. Moreover, we identified the function of the *wetA* gene in *A. solani*. The results increase our knowledge of bacterial and fungal interactions mediated by VOCs and provide a potential strategy for potato early blight disease control.

## RESULTS

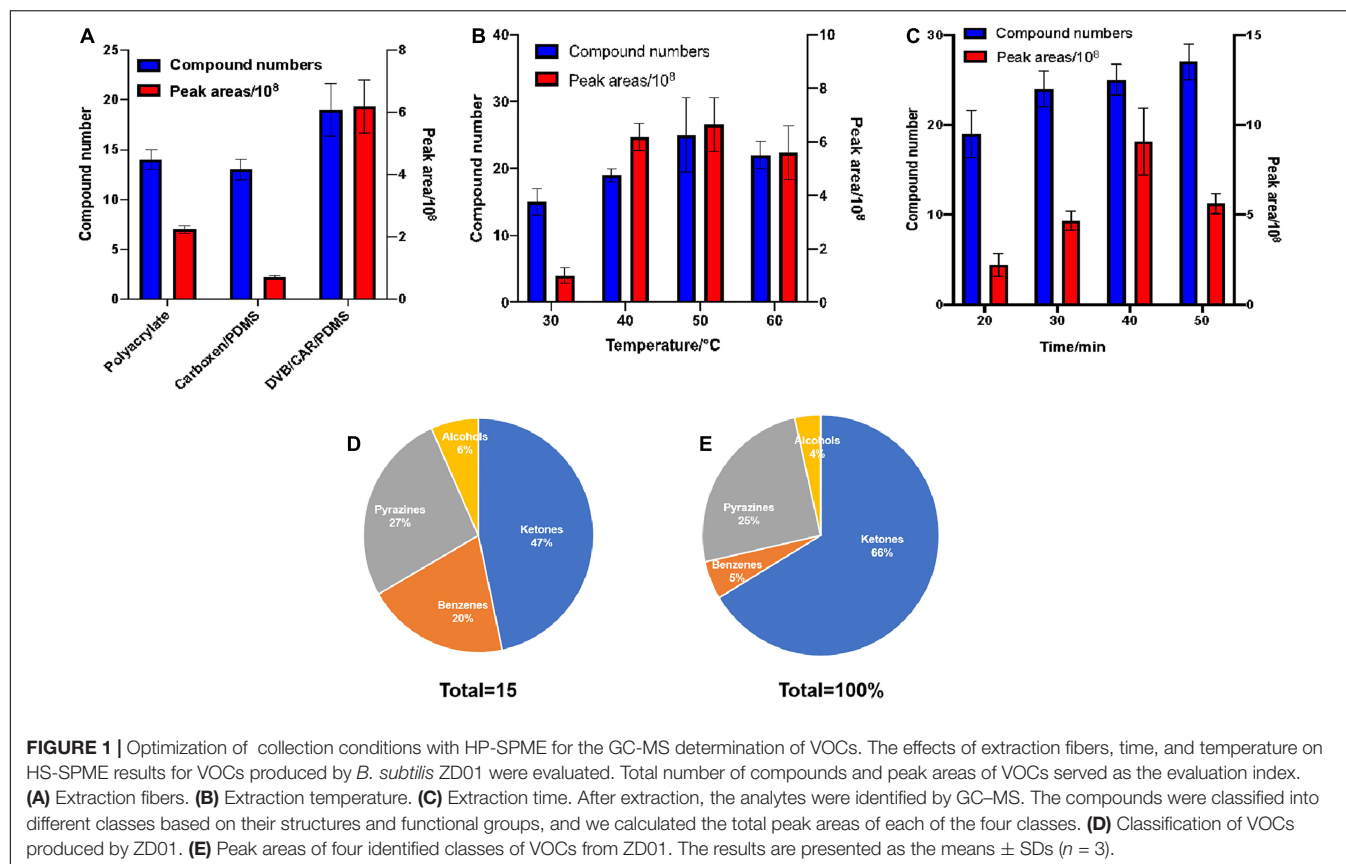
### Optimization of Extraction Conditions and Identification of Volatile Organic Compounds Produced by *B. subtilis* ZD01

Different extraction conditions for headspace solid-phase microextraction (HS-SPME) affect the extracting efficiency. Moreover, columns with different polarities also affect gas chromatography-mass spectrometry (GC-MS) analyses. In this study, the effects of extraction fibers, time, and temperature conditions on the HS-SPME of VOCs produced by *B. subtilis* ZD01 were evaluated, and a free fatty acid phase (FFAP) capillary column (60 m × 0.25 mm × 0.25 μm) was used for GC-MS analyses of the produced volatiles. The total number of compounds and peak areas of the VOCs were used as the evaluation index.

Three kinds of extraction fibers [85-μm polyacrylate, 50/30-μm divinylbenzene/carboxen/polydimethylsiloxane (DVB/CAR/PDMS) and 75-μm CAR/PDMS] were tested. The 85-μm polyacrylate, 75-μm CAR/PDMS, and 50/30-μm DVB/CAR/PDMS fibers allowed GC-MS resolutions of 14, 13, and 19 distinct VOCs, respectively. In addition, a larger total peak area for the VOCs was obtained using 50/30-μm DVB/CAR/PDMS compared with the other extraction fibers (Figure 1A). Thus, the use of 50/30-μm DVB/CAR/PDMS increased the number and contents of VOCs. Consequently, we chose 50/30-μm DVB/CAR/PDMS as the extraction fiber for the following experiments.

The effect of extraction temperature on the GC-MS characterization of VOCs was analyzed. As shown in Figure 1B, 15, 19, 25, and 22, total compounds were detected by GC-MS at extraction temperatures of 30, 40, 50, and 60°C, respectively. In addition, the peak area of the total compounds was greatest at 50°C. Compared with other extraction temperatures, at 50°C the numbers and peak area of the total compounds detected by GC-MS were increased obviously. Thus, 50°C was selected as the extraction temperature.

We also evaluated the potential influence of extraction time on the GC-MS analysis of VOCs using 50/30-μm DVB/CAR/PDMS at 50°C. The extraction times of 20, 30, 40, and 50 min allowed GC-MS identification of 19, 24, 25, and 27 VOCs, respectively. In addition, the peak area of the total compounds was maximum at 40 min, which was much greater than at the other time



**FIGURE 1 |** Optimization of collection conditions with HP-SPME for the GC-MS determination of VOCs. The effects of extraction fibers, time, and temperature on HS-SPME results for VOCs produced by *B. subtilis* ZD01 were evaluated. Total number of compounds and peak areas of VOCs served as the evaluation index. (A) Extraction fibers. (B) Extraction temperature. (C) Extraction time. After extraction, the analytes were identified by GC-MS. The compounds were classified into different classes based on their structures and functional groups, and we calculated the total peak areas of each of the four classes. (D) Classification of VOCs produced by ZD01. (E) Peak areas of four identified classes of VOCs from ZD01. The results are presented as the means  $\pm$  SDs ( $n = 3$ ).

points (Figure 1C). Therefore, we selected to use the 50/30- $\mu\text{m}$  DVB/CAR/PDMS fiber at  $50^{\circ}\text{C}$  for 40 min as the extraction conditions for GC-MS.

Gas chromatography-mass spectrometry with a FFAP capillary column ( $60\text{ m} \times 0.25\text{ mm} \times 0.25\text{ }\mu\text{m}$ ) was used to detect the volatiles of ZD01 samples and control samples (Luria-Bertani medium alone) under optimized extraction conditions (50/30  $\mu\text{m}$  DVB/CAR/PDMS fiber at  $50^{\circ}\text{C}$  with 40 min). LB medium without *Bacillus* inoculation was used as a control. Identical volatile compounds produced by ZD01 and LB medium were eliminated. In total, 15 volatiles specifically released by ZD01 were obtained, including 7 ketones, 4 pyrazines, 3 benzenes, and 1 alcohol (Figures 1D,E and Table 1). Among them, 6-methyl-2-heptanone showed the largest peak area, at 22.27% of the total VOCs. Moreover, 6-methyl-2-heptanone was identified as having an 8.88% peak area of the total VOCs by GC-MS using an HP-5 capillary column and has shown strong antagonistic effects on *A. solani* (Zhang D. et al., 2020). Therefore, 6-methyl-2-heptanone may be the main active chemical; therefore, it was selected as a potential agent for controlling potato early blight.

## 6-Methyl-2-Heptanone Inhibited Mycelial Growth and Induced Structural Changes in *A. solani* in vitro

Because 6-methyl-2-heptanone may be a potential agent for controlling potato early blight, pure 6-methyl-2-heptanone

purchased from a company was tested for antifungal activity. In detail, divided dishes were used to evaluate the inhibition of 6-methyl-2-heptanone against *A. solani* mycelial growth and its pathogenicity. 6-Methyl-2-heptanone suppressed mycelial growth by more than 78% at its highest dose (15  $\mu\text{L}$ ) (Figure 2A). For this compound, an  $\text{EC}_{50}$  value of 10.88  $\mu\text{L}$  was obtained.

Mycelial structures play vital roles in the infection process, and they form a special structure, the penetration peg, before invading plant leaves. Thus, we evaluated the potential effects of 6-methyl-2-heptanone on *A. solani* mycelial ultrastructures. Scanning electron microscopy (SEM) was used to study the surface morphological changes of *A. solani*. As shown in Figure 2B, the control hyphae had smooth surfaces and intact morphology. In contrast, some 6-methyl-2-heptanone-treated hyphae had wrinkled surface cells (red arrows, Figure 2B). Hyphae exhibited swelling tissues on the surface (yellow arrows, Figure 2B) after exposure to 6-methyl-2-heptanone. Moreover, compared with normal hyphae, some of the *A. solani* 6-methyl-2-heptanone-treated mycelia were deformed and significantly enlarged (green arrows, Figure 2B).

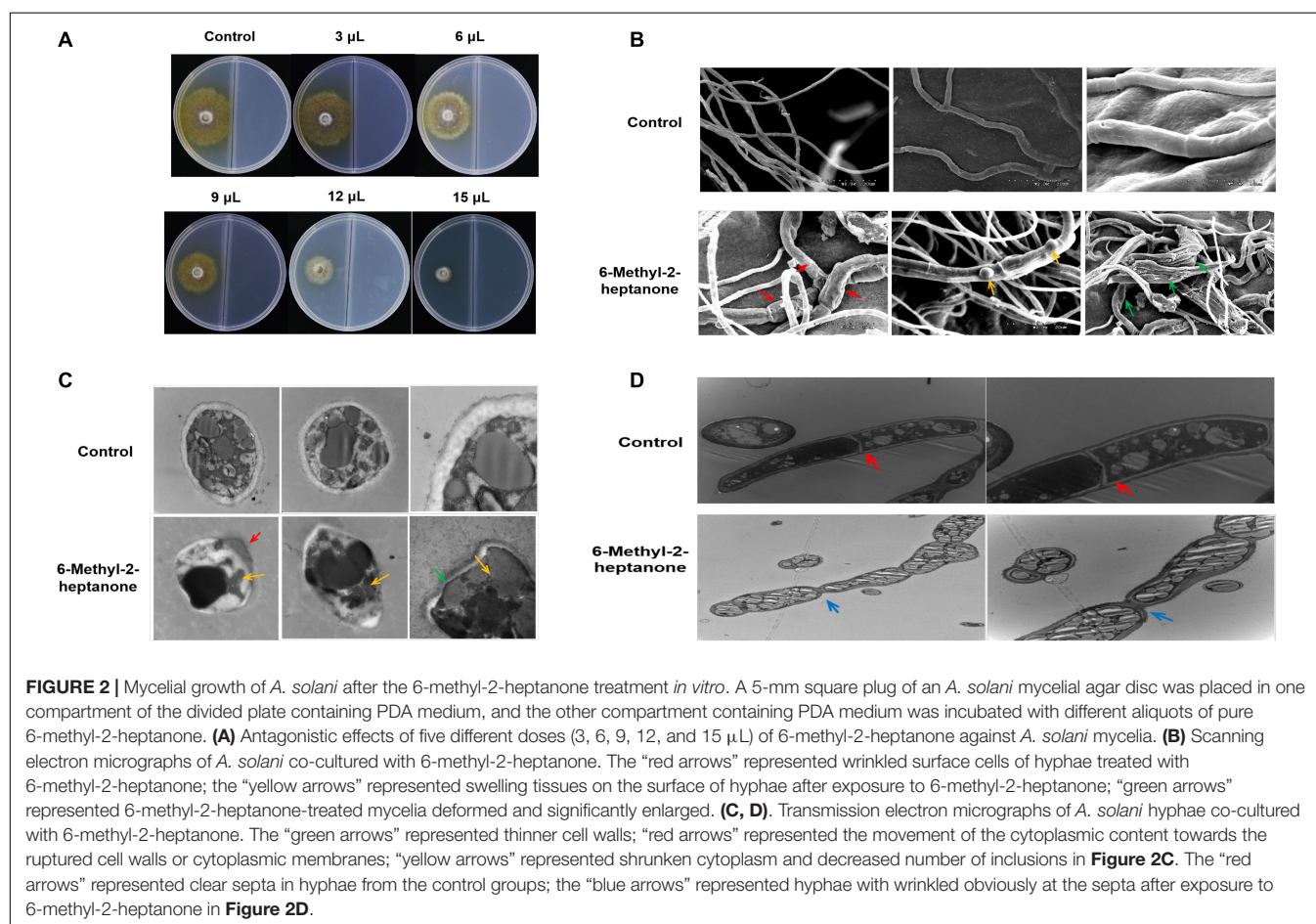
Because the 6-methyl-2-heptanone-treated *A. solani* hyphae showed serious surface structure abnormalities, their internal structure used transmission electron microscopy (TEM). As shown in Figure 2C, in cross-sections, hyphae from control groups were elliptical-shaped with a clear outer cell-wall edge, cytoplasmic membrane and uniform periplasmic space. The cytoplasm was evenly distributed, with a consistent electron



**TABLE 1** | Volatile compounds produced by *Bacillus subtilis* ZD01 identified under optimal conditions using an free fatty acid phase (FFAP) chromatographic column.

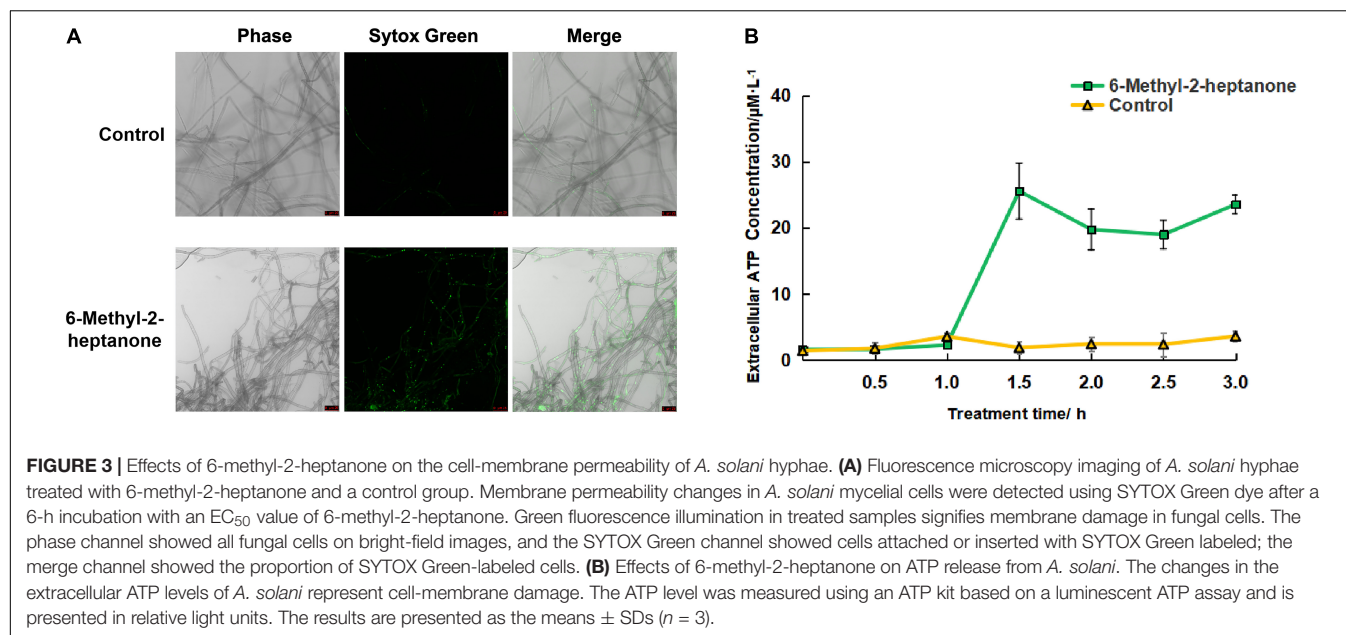
No.	Chemicals	CAS	Retaining time (min)	SI	RSI	Peak area ratio (%)
1	3-Methyl-2-pentanone	565-61-7	7.27	863	913	3.32
2	2-Heptanone	110-43-0	10.22	867	877	4.42
3	6-Methyl-2-heptanone	928-68-7	11.46	888	892	22.27
4	5-Methyl-2-heptanone	18217-12-4	11.90	855	858	19.08
5	Methyl-pyrazine	109-08-0	12.41	939	941	6.65
6	2,5-Dimethylpyrazine	123-32-0	13.73	944	946	12.47
7	6-Methyl-2-heptanol	4730-22-7	14.58	874	885	3.53
8	2-Ethyl-5-methyl-pyrazine	13360-64-0	15.20	687	826	3.87
9	2-Methyl-5-(1-methylethyl)pyrazine	13925-05-8	15.81	845	975	2.00
10	2-Decanone	693-54-9	16.59	821	871	10.77
11	Acetophenone	98-86-2	21.90	639	863	4.70
12	2-Ethyl-6-methyl-phenol	1687-64-5	26.59	693	871	3.24
13	Phenylethyl alcohol	60-12-8	27.44	688	882	1.34
14	1,2-Benzisothiazole	272-16-2	28.63	772	922	0.53
15	2-Nonadecanone	629-66-3	30.45	731	869	1.81

SI, strength indexes; RSI, relative strength indexes.



density. Nuclei, vacuoles, and mitochondria were also distributed randomly in the cells (Figure 2C). Compared with the undamaged control cells, a wide range of misshapen and severely deformed cells were observed in treated *A. solani*. Cell walls

were thinner (green arrows, Figure 2C) and even damaged (red arrows, Figure 2C), which resulted in the movement of the cytoplasmic content toward the ruptured cell walls or cytoplasmic membranes (red arrow, Figure 2C). The cytoplasm



was shrunken, and the number of inclusions decreased (yellow arrows, **Figure 2C**). Longitudinal sections of hyphae from the control groups were normal size with similar width and had clear septa (red arrows, **Figure 2D**). However, in the treated group, the mycelia were inflated. Many hyphae also appeared wrinkled obviously at the septa after exposure to 6-methyl-2-heptanone (blue arrows, **Figure 2D**). Moreover, more and larger lipid droplets were observed in the cytoplasm of treated samples compared with the control groups, which had only a few dark internal lipid droplets (**Figures 2C,D**).

### The Cell-Membrane Permeability of *A. solani* Hyphae Changed After the 6-Methyl-2-Heptanone Treatment

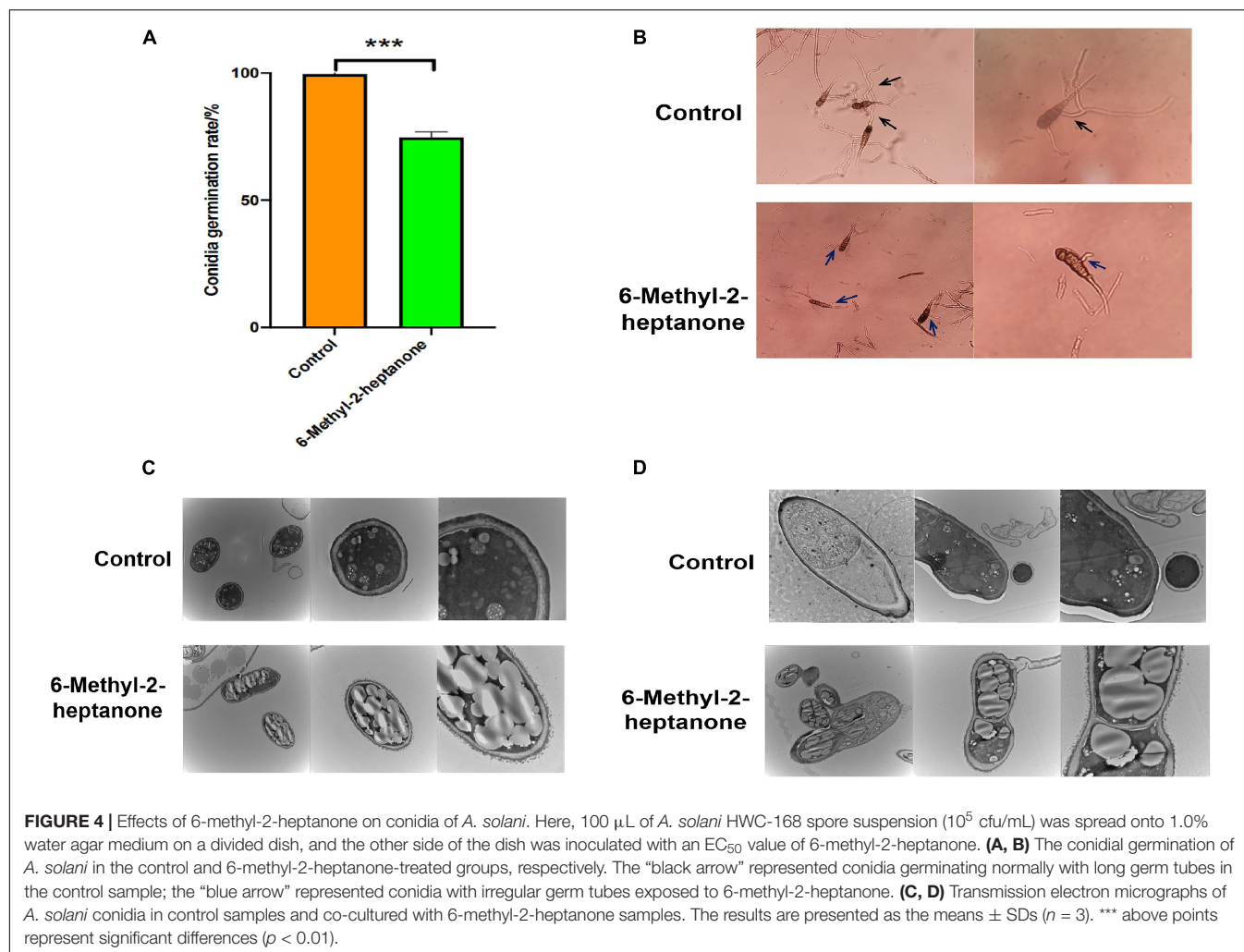
To further identify the mechanisms by which 6-methyl-2-heptanone produces the antifungal activity against *A. solani* hyphal cells, we used SYTOX Green labeling to detect the membrane permeability. As shown in **Figure 3A**, none of the cells fluorescent green in the control group. In contrast, some cells fluorescent green in samples that had been exposed in the EC<sub>50</sub> value of 6-methyl-2-heptanone for 4 days.

To further identify the damaging effects of 6-methyl-2-heptanone on cell membranes, the adenosine triphosphate (ATP) contents released into the extra-cellular medium were used as an indicator of the effects of 6-methyl-2-heptanone on the membranes of fungal hyphae. As shown in **Figure 3B**, the extracellular ATP level of *A. solani* rapidly increased after 1 h exposure to the EC<sub>50</sub> value of 6-methyl-2-heptanone. In contrast, the extracellular ATP levels of the control cells were constantly low, from 0.5 to 3 h, which suggested that 6-methyl-2-heptanone caused serious ATP leakage from *A. solani* hyphal cells. Thus, the results further indicated that 6-methyl-2-heptanone increased *A. solani* cell-membrane permeability.

### 6-Methyl-2-Heptanone Inhibited Conidial Vitality and Damaged Internal Structures of *A. solani* Conidia

In addition to mycelia, conidial vitality also plays a crucial role during the infection of fungal pathogens. Conidia resist severe environmental conditions and are spread by wind and rain. After adhering to potato leaves, conidia form penetration pegs, special mycelial structures, which infect potato leaves. Therefore, the capacity of 6-methyl-2-heptanone to suppress conidial vitality was evaluated *in vitro*. As shown in **Figure 4A**, the germination rate of conidia treated with the EC<sub>50</sub> value of 6-methyl-2-heptanone was 74.73% ± 2.11%, whereas it was 99.62% ± 1.67% in the control group, which suggested that 6-methyl-2-heptanone inhibited *A. solani* conidial germination significantly (*p* < 0.05). Conidia in the control sample germinated normally and formed long germ tubes (black arrow, **Figure 4B**) to infect plants. However, conidia exposed to 6-methyl-2-heptanone formed irregular germ tubes (blue arrow, **Figure 4B**). This shorter tube did not have the ability to penetrate and invade host epidermal cell junctions.

Transmission electron microscopy was then used to detect the degree of damage to conidial structures. The majority of *A. solani* conidia treated with 6-methyl-2-heptanone showed severe morphological disruptions. Collapsed shrunken were detected. Additionally, more extracellular secretions occurred around the conidial cell-wall surface, and larger lipid droplets appeared within the conidia (**Figures 4C,D**). In the control group not exposed to 6-methyl-2-heptanone, conidia exhibited regular shapes, uniformly distributed cytoplasm and apparently intact envelopes. We also observed electron dense cytoplasm and robust ultra-structures in the control group (**Figures 4C,D**). The findings confirmed that 6-methyl-2-heptanone damaged conidial structures.



## 6-Methyl-2-Heptanone Downregulated the Expression of Pathogenic Genes in *A. solani*

Because 6-methyl-2-heptanone showed strong effects on mycelial integrity and conidial structures, we further investigated the action mode of 6-methyl-2-heptanone against *A. solani* by examining the expression levels of pathogenic mycelia- and conidia-related genes. In our previous study, we determined that the *slt2* gene is involved in mycelial growth, penetration, and pathogenicity (Zhang D. et al., 2020). Moreover, fungi spread through spores, and conidia also play a key role in the *A. solani* infection process. The complete genome of *A. solani* HWC-168 has been sequenced and analyzed (Zhang et al., 2018), and one typical gene, *wetA*, related to conidia was found in the genome. Therefore, we investigated the effects of 6-methyl-2-heptanone transcription on the expression profiles of *slt2* and *wetA* in *A. solani* using qRT-PCR.

After *A. solani* strain HWC-168 was exposed to 6-methyl-2-heptanone for 2 h and 6 h, the expression of *wetA* was strongly repressed (approximately 1.31- and 0.96-fold, respectively) (Figure 5A). The transcriptional expression of *slt2* was induced

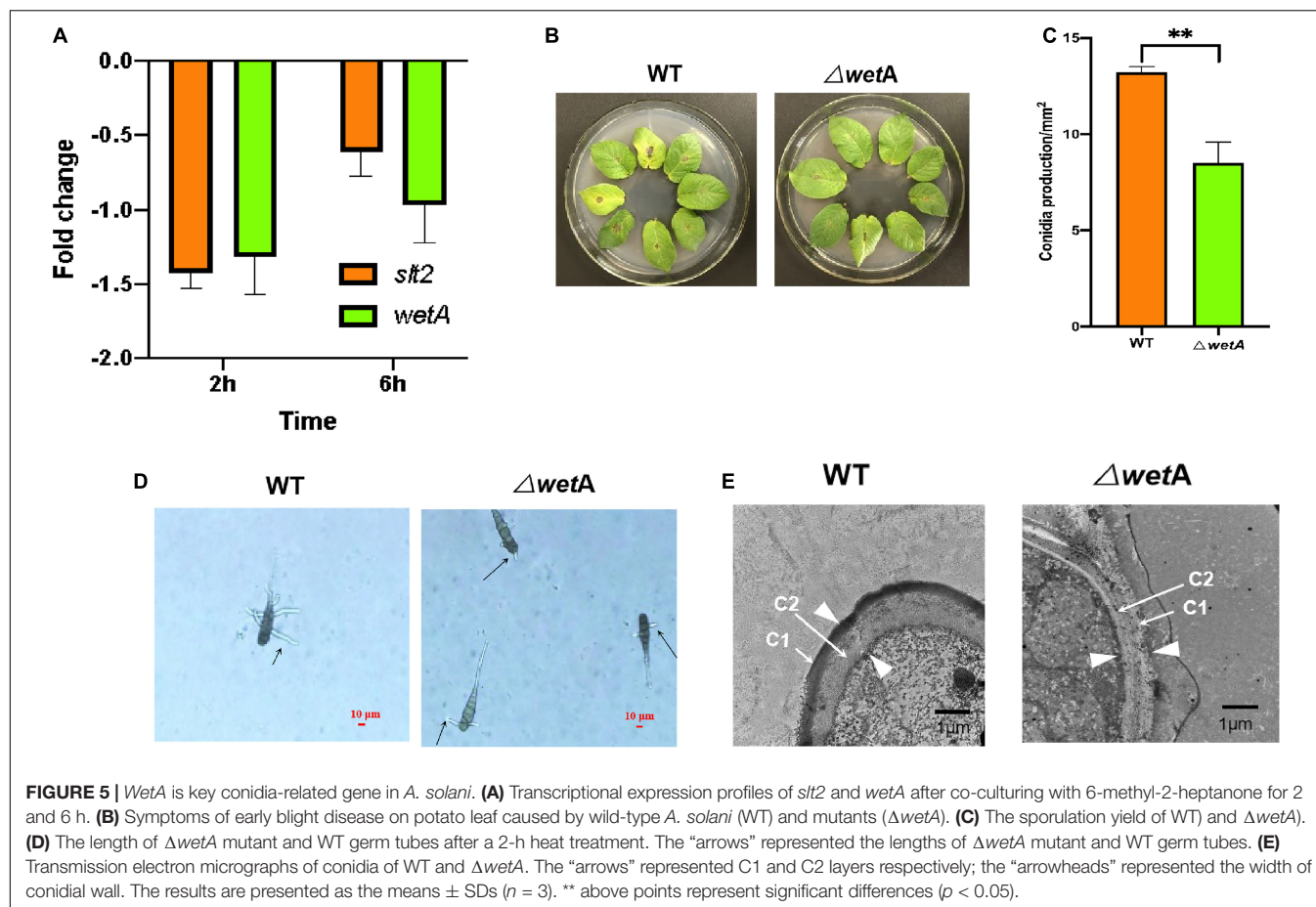
(approximately 1.42-fold) compared with the control group and then repressed (approximately 0.61-fold) in the presence of VOCs after 2- and 6-h co-culturing (Figure 5A). The down-regulated expression levels of *slt2* and *wetA* were consistent with the virulence reduction in *A. solani*.

## *WetA* Is a Conidia-Associated Gene in *A. solani*

Identifying the functions of pathogenic genes is important for determining pathogenic mechanisms and biological control approaches for *A. solani*. Moreover, little is known about the functions of *A. solani* pathogenesis-related genes. Because 6-methyl-2-heptanone showed a strong effect on the transcriptional expression of *wetA* in conidia, we compared the *wetA* gene sequence in *A. solani* with those of 22 fungi. The *wetA* gene in *A. solani* is closely related to the *wetA* gene in *Alternaria alternata* (Supplementary Figure 1). Then, the functions of *wetA* were determined using gene knockouts and phenotype verification.

To determine whether *wetA* affects the pathogenicity of *A. solani*, the virulence of the deletion mutants and the wild-type





(WT) strain were compared *in vivo* using potato leaf tests. As shown in **Figure 5B**, potato leaves inoculated with WT HWC-168 showed obvious lesions and yellow halos. The lesion diameters extended to  $0.50 \pm 0.07$  cm after a 7-day incubation at  $25^{\circ}\text{C}$ , whereas for the leaves inoculated with  $\Delta wetA$  mutants, the lesion diameters were limited to  $0.20 \pm 0.06$  cm. Thus, the deletion of *wetA* significantly reduced the pathogenicity of *A. solani* ( $p < 0.05$ ).

Then, we evaluated the sporulation and conidia germination of deletion mutants and the WT strain under *in vitro* conditions. As shown in **Figure 5C**, the sporulation yield of the *wetA* deletion mutant per area was  $8.51 \pm 1.09 \times 10^2/\text{mm}^2$ , whereas that of the WT strain was  $13.21 \pm 0.28 \times 10^2/\text{mm}^2$ . Compared with the WT strain, the sporulation yield of the *wetA* deletion mutant per area decreased significantly ( $p < 0.05$ ). These results suggested that *wetA* has a significant role in sporulation. Moreover, we examined the conidial germination of WT *A. solani* and mutants ( $\Delta wetA$ ) after a 2-h heat treatment. The conidial germination of WT was  $40.67\% \pm 2.52\%$ , whereas that of the  $\Delta wetA$  mutants was limited to  $27.33\% \pm 1.17\%$ . The lengths of  $\Delta wetA$  mutant and WT germ tubes were  $18.56 \pm 2.89$   $\mu\text{m}$  and  $57.96 \pm 4.90$   $\mu\text{m}$ , respectively (**Figure 5D**). The results indicated that expression of the *wetA* gene had strong inhibitory effects on conidial germination and germ tube elongation under heat-treatment conditions.

To examine the role of *wetA* in conidial vitality, WT and *wetA* mutant conidia in *A. solani* were compared using TEM. As shown in **Figure 5E**, WT conidia formed a crenulated electron-dense C1 layer and a condensed electron-light C2 layer. In the *wetA* mutants, although the C1 and C2 layers were formed, the C1 layer was not crenulated and the C2 layer failed to condense, resulting in a thicker conidial wall than in the WT strain. Moreover, the C1 layer was subtended by projections from the C2 layer in the WT strain, and this was not observed in the *wetA* mutant strain. These data indicated that the *wetA* mutant exhibits conidial wall defects similar to those found in *Aspergillus nidulans* (Sewall et al., 1990; Marshall and Timberlake, 1991) and that *wetA* plays an essential role in conidial wall completion and spore maturation.

## DISCUSSION

Mycelial growth, hyphal morphology, and conidial germination are significant factors in the plant infection processes of fungal pathogens. Consequently, most previous studies focused on plant fungal mycelial morphology and spore germination after being treated with VOC mixtures emitted by bacterial strains (Chaurasia et al., 2005; Effmert et al., 2012; Morath et al., 2012; Zheng et al., 2013; Chantal et al., 2014; Xie et al., 2018; Li et al.,



2019; Martins et al., 2019; Wu et al., 2019; Tran et al., 2020). For example, the VOCs of *Bacillus velezensis* 5YN8 suppress the mycelial growth and conidial formation of *B. cinerea* BC1301 (Jiang et al., 2018). Excessive vesication or thickened cell walls in conidia and increased plasma membrane retractions have been observed by TEM in mycelia of *B. cinerea* fumigated with *Bacillus* VOCs (Li et al., 2012). In our previous study, we also found that volatiles secreted by the ZD01 strain inhibit mycelial growth and conidial germination (Zhang D. et al., 2020). Thus, most of studies have focused on the effects of volatile mixtures produced by *Bacillus* strains against plant fungi. However, the action sites of different component(s) of the volatile mixtures may vary in different fungi, and little is known about the action mechanisms of specific effective substances in VOCs on plant pathogens.

In our study, 6-methyl-2-heptanone accounted for relatively large contents, at 22.27 and 8.88% of the total VOCs from *B. subtilis* ZD01, using FFAP and HP-5 capillary columns, respectively, in GC-MS analyses, and it inhibited *A. solani* mycelial growth strongly *in vitro* (Zhang D. et al., 2020). Furthermore, 6-methyl-2-heptanone is produced by *Bacillus* strains and shows significant antifungal activities against plant pathogens. For example, 6-methyl-2-heptanone produced by *Bacillus vallismortis* 12a and *Bacillus altitudinis* 14b completely inhibits the mycelial growth of *Monilinia fructicola* (Liu et al., 2018). Therefore, 6-methyl-2-heptanone may be a key active chemical component of VOCs emitted from *Bacillus* strains that can be used for controlling plant disease. Consequently, we selected it as a specific effective substance to elucidate the action mechanisms against *A. solani*. We found that 6-methyl-2-heptanone damaged cell-wall integrity and changed cell-membrane permeability. Cell walls and membranes are crucial for maintaining cell viability (Bowman and Free, 2006; Ruiz-Herrera et al., 2006; Shao et al., 2013; Tao et al., 2014). It is, therefore, necessary to reveal the interactions of bioactive VOCs with model membranes.

Currently, little is known about the functions of *A. solani* pathogenesis-related genes, which may be important for the biological control of plant pathogens. In this study, the function of the *wetA* gene, which is involved in conidial vitality in *A. solani*, was identified using a constructed knockout mutant and phenotypical characterization. The *wetA* mutant strain failed to form condensed C1 and C2 layers, which was consistent with previous studies (Sewall et al., 1990; Marshall and Timberlake, 1991). In *A. nidulans*, the *wetA* gene is required late in development for the synthesis of crucial cell-wall layers (Marshall and Timberlake, 1991). The inner wall layer of *wetA* mutant conidia did not condense during Stage II, and they form large cytoplasmic vacuoles that undergo lysis (Sewall et al., 1990). Here, the WT C1 layer was slightly more crenulated than that of the  $\Delta wetA$  strain. The C2 layer appears condensed in the WT but not in the *wetA* mutant strain (Sewall et al., 1990). Therefore, *wetA* plays crucial roles in the sporulation and conidial wall formation of *A. solani*, which had further effects on its pathogenicity in *in vivo* tests.

In summary, this study first elucidated the action mechanism of *B. subtilis* ZD01 metabolite 6-methyl-2-heptanone to control *A. solani* and shed light on the potential biocontrol

mechanism of 6-methyl-2-heptanone against *A. solani* in potato (Figure 6). 6-Methyl-2-heptanone caused hyphal deformity and damaged the cell integrity and membrane permeability of *A. solani* hyphae, which could not form the penetration pegs. Additionally, it inhibited conidial germination and altered conidial structures. Moreover, 6-methyl-2-heptanone down-regulated the transcriptional expression levels of *slt2* and *wetA* genes, which are involved in mycelial vitality, sporulation, and conidial maturity. Future research will focus on increasing the safety of 6-methyl-2-heptanone treatments and determining the action sites of 6-methyl-2-heptanone produced by *B. subtilis* ZD01 against *A. solani*.

## EXPERIMENTAL PROCEDURES

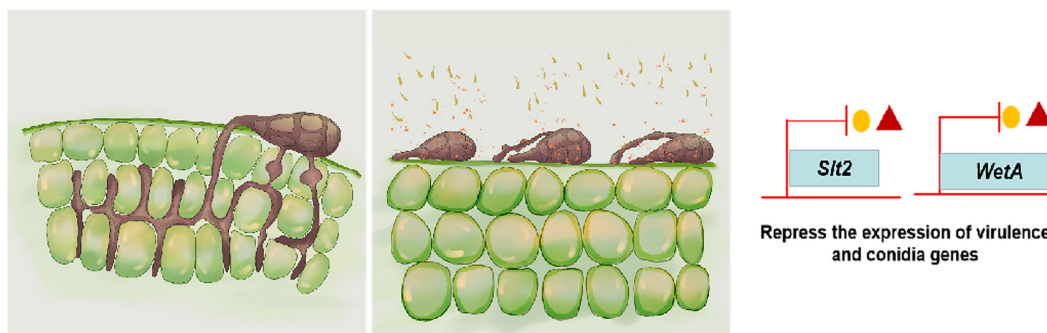
### Optimization of Volatile Organic Compound Collection Conditions

Here, 20  $\mu$ L of *Bacillus* strain suspension ( $1 \times 10^8$  cfu/mL) was inoculated into 6 mL LB medium in a 20-mL headspace-vial. The vials were firmly sealed using parafilm and rubber lids, and then, they were incubated at 25°C for 4 days before VOC collection. HS-SPME and GC-MS were used to analyze the samples.

A SPME holder from Supelco, Inc. (Bellefonte, PA, United States) was used to perform HS-SPME manually. The SPME fibers were also purchased from Supelco, Inc. The extraction conditions were optimized in accordance with a previous method (Zhang et al., 2021). Briefly, the vials were water-bathed in a heated metal block with the SPME fiber inserted in the headspaces under different extraction conditions for optimization. We used the extraction fiber, temperature, and time as factors. We chose 85- $\mu$ m Polyacrylate, 75- $\mu$ m Carboxen/PDMS, and 50/30- $\mu$ m DVB/CAR/PDMS as the extraction fibers for optimization at 40°C condition for 40 min. Next, the extraction temperature was optimized using the optimal fiber for 40 min at 30, 40, 50, and 60°C. To optimize the extraction time, the VOCs were extracted for 20, 30, 40, and 50 min with the optimized fiber and temperature. Finally, the VOCs were extracted using the optimized conditions. The experiment was repeated three times. All the strains used in this study are listed in Supplementary Table 1.

### Analysis of Volatile Organic Compounds From *B. subtilis* ZD01 by Gas Chromatography-Mass Spectrometry

After extraction, the analytes were desorbed for 5 min at 250°C in the injector of the GC with the purge valve off (split-less mode). Capillary GC-MS was carried out using a Thermo Trace 1310 gas chromatographer (Thermo Fisher Scientific, Waltham, MA, United States). The samples were analyzed on a FFAP capillary column (60 m  $\times$  0.25 mm  $\times$  0.25  $\mu$ m, Thermo Fisher Scientific). The temperature of the injection port was 230°C. The flow rate was 1 mL/min. We used the following temperature program: start at 50°C; increase to 220°C at 5°C/min; and hold at 220°C for 15 min.



**FIGURE 6 |** A model for the mode of action of 6-methyl-2-heptanone produced by ZD01 against *A. solani*. 6-Methyl-2-heptanone changes the structures of mycelia and conidia of *A. solani*, which subsequently leads to the suppression of fungal growth, mycelium penetration, conidia vitality, and germination, as well as relative virulence and conidia-related gene expression levels. As a result, *A. solani* failed to infect potato leaves.

A Thermo TSQ-8000 MS was used for peak separation and detection. The MS was operated in electron ionization mode at 70 eV with a source temperature of 280°C using a continuous scan from 45 *m/z* to 450 *m/z*. The ionization source and transfer line temperatures were both 230°C, and electron ionization mode was used. The analysis was performed in full-scan mode. Mass spectral data for the volatile compounds were compared with data in the National Institute of Standards and Technology (NIST) Mass Spectrum Library. The VOCs in treated samples that were not found in the control were considered the final *Bacillus*-produced VOCs. The experiment was repeated three times.

For each detected peak, a standard mixture of hydrocarbons from C<sub>7</sub> to C<sub>27</sub> (Bailingwei Inc., Beijing, China) was prepared. The sample and the hydrocarbon standard mixture were co-injected into the GC, and the retention times were used to calculate retention indices. A linear retention index was calculated using GC retention index standards in accordance with the method of Van den Dool and Kratz (1963). The relative strength indexes of chemicals that matched chemicals in the NIST library with scores greater than 800 were used.

### Inhibition Assay of 6-Methyl-2-Heptanone Against *A. solani* *in vitro*

To test the inhibition on mycelial growth, pure 6-methyl-2-heptanone was purchased from Shanghai Macklin Biochemical Technology Co., Ltd. In this test, the divided plate method was used (Xie et al., 2018), and the plate allocation of the different treatments was randomized. Briefly, a 5-mm square plug from an *A. solani* mycelial agar disk was placed in one compartment of the divided plate containing PDA medium, and the other compartment containing PDA medium was incubated with different aliquots of pure compound. The doses of 6-methyl-2-heptanone were 3, 6, 9, 12, and 15  $\mu$ L, respectively. The dishes were immediately sealed with parafilm and incubated at 25°C for 4 days. Pathogens and plates not containing the pure compound were used as controls. The sample unit was represented by six replicates per dose. The inhibitory rate on mycelial growth

was calculated in accordance with the following formula, and EC<sub>50</sub> values were calculated as the effective concentrations that inhibited fungal mycelial growth by 50% in comparison with the control.

Inhibitory rate on mycelium growth (%) = (the diameter of control – the diameter of treatment group)/the diameter of control  $\times$  100%.

The efficiency of 6-methyl-2-heptanone against *A. solani* conidial germination was also tested using the divided plate assay. For this purpose, 100  $\mu$ L of *A. solani* HWC-168 spore suspension (10<sup>5</sup> cfu/mL) was spread onto half of the 1.0% water agar medium in a divided dish, and the other side of dish was inoculated with the EC<sub>50</sub> value of 6-methyl-2-heptanone. The spore suspension and LB plates with sterile water were used as controls. Dishes were immediately sealed with parafilm. The plates were incubated at 25°C for 6–8 h, and sporulation was assessed. The experiment was repeated in triplicate.

Inhibitory rate on conidial germination (%) = (the conidial germination of control – the conidial germination of treatment group)/the conidial germination of control  $\times$  100%.

### Scanning Electron Microscopy

Scanning electron microscopy was conducted to determine the effects of 6-methyl-2-heptanone on the hyphae of *A. solani* at the ultra-structural level. The *A. solani* mycelia were inoculated as described in the above divided plate assay and cultured with EC<sub>50</sub> doses of 6-methyl-2-heptanone at 25°C for 4 days. The plates without 6-methyl-2-heptanone were used as controls. Then, mycelia of each group were harvested and fixed in 2% glutaraldehyde (Solarbio, Beijing, China) at 4°C and dehydrated with gradient ethanol solutions (50, 70, 80, 90, and 100%) for 20 min. Afterward, ethanol was replaced by 100% tertiary butyl ethanol. Cells were then freeze-dried, coated with gold, and imaged using a Hitachi S-3500N field emission SEM (Hitachi, Tokyo, Japan).

### Transmission Electron Microscopy

Transmission electron microscopy was used to observe internal morphological changes in *A. solani* colonies. For groups exposed

to pure 6-methyl-2-heptanone, the *A. solani* mycelia and conidia were treated with  $EC_{50}$  doses of 6-methyl-2-heptanone as described in the above divided plate assay. The plates without 6-methyl-2-heptanone were used as controls. Then, hyphae and conidia were collected. For fungal deletion and WT strains, conidia were collected. The conidia were collected by centrifugation ( $5,000 \times g$  for 15 min at  $20^{\circ}C$ ). Hyphae and conidia were washed and fixed with 2% glutaraldehyde for 30 min at  $4^{\circ}C$ . The specimens were prepared in accordance with Yamanaka et al. (2005) for TEM analysis. Ultra-structural changes in the cells were observed using a Hitachi H-7650 transmission electron microscope (Hitachi).

## Extracellular Adenosine Triphosphate Measurement Assay

The same design as described above was used to investigate the effects of 6-methyl-2-heptanone on outer mycelial ATP contents. For *A. solani*, a 5-mm square plug of mycelial agar disks was placed in one compartment of the divided plate containing PDA medium, and the plate was incubated at  $25^{\circ}C$  for 4 days. Then, an  $EC_{50}$  dose of 6-methyl-2-heptanone was added to the other compartment and incubated for 0.5, 1.0, 1.5, 2.0, 2.5, and 3.0 h at  $25^{\circ}C$ . The plates without 6-methyl-2-heptanone were used as controls. The *A. solani* cells and the supernatants were collected by centrifugation ( $12,000 \times g$  for 5 min at  $4^{\circ}C$ ). The extracellular ATP level was determined using an Enhanced ATP Assay Kit (Beyotime Biotechnology Inc., Shanghai, China) and a multi-function microplate reader (Tecan Spark, Salzburg, Austria). The ATP kit was based on a luminescent ATP assay protocol that involved the lysis of each cell sample and the addition of luciferase and luciferin, followed by the measurement of the emitted light. The experiment was repeated in triplicate.

## Fluorescence Microscopy Imaging

For *A. solani*, a 5-mm square plug of a mycelial agar disk was placed in one compartment of a divided plate containing PDA medium, and the plate was incubated at  $25^{\circ}C$  for 4 days. One section of the cells was treated with an  $EC_{50}$  dose of 6-methyl-2-heptanone for 6 h at  $25^{\circ}C$ , and the other section was treated with sterile saline for 6 h at  $25^{\circ}C$ . The mycelia were collected and re-suspended in sterile saline. Then,  $0.8 \mu M$  SYTOX Green solution (Invitrogen Corporation, Carlsbad, CA, United States) was added to all the cells. The samples were incubated for 15 min in the dark. Afterward, mycelia were rinsed two times with 8.5% sterile saline, re-suspended in sterile saline, and immediately measured for fluorescence. Green fluorescent signaling in *A. solani* was visualized using a Nikon Ti2-U fluorescence microscope (Nikon Corporation, Tokyo, Japan). The excitation wavelength was 488 nm, and the emission wavelength was 538 nm (Mu Oz et al., 2013).

## Quantitative Real-Time PCR

Total RNAs of *A. solani* cells co-cultured with 6-methyl-2-heptanone for 2 and 6 h were extracted using a Bacterial RNA Kit (Omega Bio-Tek, Norcross, GA, United States) in accordance with the manufacturer's instructions. First-strand cDNA was

obtained using reverse transcriptase (TransGen Biotech, Beijing, China) with random hexamer primers. Real-time PCR was performed with SYBR Premix Ex Taq<sup>TM</sup> (TransGen Biotech). The actin gene was used as an internal reference gene. The specific primers used are listed in **Supplementary Table 2**. The relative expression levels of specific genes were calculated using the  $2^{-\Delta\Delta CT}$  method (Livak and Schmittgen, 2001).

## Construction of Fungal Deletion Strains

Gene deletion vector construction and the transformation of *A. solani* were performed using the double-joint PCR method with minor modifications (Yu et al., 2004). The primers used for flanking sequence amplification for each gene are listed in **Supplementary Table 2**. A hygromycin resistance cassette replaced the open reading frame of *wetA*, and the constructed fragment was inserted into the pEASY-T1 cloning vector (**Supplementary Table 1**). After transforming the constructed plasmid into HWC-168, the subsequent deletion mutants were verified by PCR using the *wetA*-F/R primer set (**Supplementary Table 2**).

## In vivo Antagonistic Activity of *WetA* Mutants

To determine the pathogenicity of different *A. solani* strains, 20  $\mu L$  of conidial suspensions ( $10^5$  cfu/mL) of WT and *wetA* mutants were inoculated onto the center of one piece of fresh potato leaf. After 5 days of growth under a 12-h/12-h light/dark cycle at  $25^{\circ}C$ , the lesion diameters were measured.

## Statistical Analysis

Three independent experiments were performed for each assay. Data were analyzed using SPSS 20.0 Windows Software (SPSS Inc., Chicago, IL, United States). Least significant differences were calculated to compare results at the 0.05 level.

## DATA AVAILABILITY STATEMENT

The datasets presented in this study can be found in online repositories. The names of the repository/repositories and accession number(s) can be found below: <https://www.ncbi.nlm.nih.gov/genbank/>, CP046448.1.

## AUTHOR CONTRIBUTIONS

DZ, RQ, and YF performed the experiments. DZ wrote the manuscript. JZ and JC provided data curation and methodology. DMZ provided technical assistance. DZ, ZY, and JHZ designed the experiments. ZY and JHZ provided supervision and project administration. All authors contributed to the article and approved the submitted version.

## FUNDING

This work was funded by the National Natural Science Foundation of China (32001956), Research on the Cultivation



of Innovation Ability of Postgraduate Students in Education Department of Hebei Province, China (CXZZBS2021036), China Agriculture Research System of MOF and MARA (CARS-09-P18), and Modern Agro-Industry Technology Research System in Hebei Province, China (HBCT2018080205).

## REFERENCES

- Arrebola, E., Dharini, S., and Lise, K. (2010). Effect of volatile compounds produced by *Bacillus* strains on postharvest decay in citrus. *Biol. Control* 53, 122–128. doi: 10.1016/j.biocontrol.2009.11.010
- Banani, H., Davide, S., Dianpeng, Z., Slavica, M., Garibaldi, A., and Maria, L. G. (2015). Postharvest application of a novel chitinase cloned from *Metschnikowia fructicola* and overexpressed in *Pichia pastoris* to control brown rot of peaches. *Int. J. Food Microbiol.* 199, 54–61. doi: 10.1016/j.ijfoodmicro.2015.01.002
- Bowman, S. M., and Free, S. J. (2006). The structure and synthesis of the fungal cell wall. *Bioessays* 28, 799–808. doi: 10.1002/bies.20441
- Calvo, H., Isabel, M., Esther, A., Ana, P., Domingo, B., and María, E. V. (2020). Antifungal activity of the volatile organic compounds produced by *Bacillus velezensis* strains against postharvest fungal pathogens. *Postharvest Biol. Technol.* 166:111208. doi: 10.1016/j.postharvbio.2020.111208
- Chantal, L. M., Janette, N., Mathias, D., Robert, P., and Birgit, P. (2014). mVOC: a database of microbial volatiles. *Nucleic Acids Res.* 44:1016. doi: 10.1093/nar/gkx1016
- Chaves-López, C., Serio, A., Gianotti, A., Sacchetti, G., Ndagijimana, M., Ciccarone, C., et al. (2015). Diversity of food-borne *Bacillus* volatile compounds and influence on fungal growth. *J. Appl. Microbiol.* 119, 487–499. doi: 10.1111/jam.12847
- Chaurasia, B., Pandey, A., Palni, L. M. S., Trivedi, P., Kumar, B., and Colvin, N. (2005). Diffusible and volatile compounds produced by an antagonistic *Bacillus subtilis* strain cause structural deformations in pathogenic fungi *in vitro*. *Microbiol. Res.* 160, 75–81. doi: 10.1016/j.micres.2004.09.013
- Chen, H., Xiao, X., Wang, J., Wu, L., Zheng, Z., and Yu, Z. (2008). Antagonistic effects of volatiles generated by *Bacillus subtilis* on spore germination and hyphal growth of the plant pathogen, *botrytis cinerea*. *Biotechnol. Lett.* 30, 919–923. doi: 10.1007/s10529-007-9626-9
- Effmert, U., Kalderás, J., Warnke, R., and Piechulla, B. (2012). Volatile mediated interactions between bacteria and fungi in the soil. *J. Chem. Ecol.* 38, 665–703. doi: 10.1007/s10886-012-0135-5
- Gao, Z., Zhang, B., Liu, H., Han, J., and Zhang, Y. (2017). Identification of endophytic *Bacillus velezensis* ZSY-1 strain and antifungal activity of its volatile compounds against *Alternaria solani* and *Botrytis cinerea*. *Biol. Control* 150, 27–39. doi: 10.1016/j.biocontrol.2016.11.007
- Gotor-Vila, A., Teixido, N., Francesco, A. D., Usall, J., Ugolini, L., Torres, R., et al. (2017). Antifungal effect of volatile organic compounds produced by *Bacillus amyloliquefaciens* CPA-8 against fruit pathogen decays of cherry. *Food Microbiol.* 64, 219–225. doi: 10.1016/j.fm.2017.01.006
- Haiyan, G., Li, P. Z., Xu, X. X., Zeng, Q., and Guan, W. Q. (2018). Research on volatile organic compounds from *Bacillus subtilis* CF-3: biocontrol effects on fruit fungal pathogens and dynamic changes during fermentation. *Front. Microbiol.* 9:456. doi: 10.3389/fmicb.2018.00456
- Jiang, C. H., Liao, M., Jie, Wang, H. K., Zheng, M. Z., Xu, J. J., and Guo, J. H. (2018). *Bacillus velezensis*, a potential and efficient biocontrol agent in control of pepper gray mold caused by *botrytis cinerea*. *Biol. Control* 126, 147–157.
- Kai, M., Haustein, M., Molina, F., Petri, A., Scholz, B., and Piechulla, B. (2009). Bacterial volatiles and their action potential. *Appl. Microbiol. Biotechnol.* 81, 1001–1012. doi: 10.1007/s00253-008-1760-3
- Khan, N., Martínez-Hidalgo, P., Ice, T. A., Maymon, M., Humm, E. A., Nejat, N., et al. (2018). Antifungal activity of bacillus species against fusarium and analysis of the potential mechanisms used in biocontrol. *Front. Microbiol.* 9:2363. doi: 10.3389/FMICB.2018.02363
- Li, Q., Ning, P., Zheng, L., Huang, J. B., Li, G. Q., and Tom, H. (2012). Effects of volatile substances of *Streptomyces globisporus* JK-1 on control of *Botrytis cinerea* on tomato fruit. *Biol. Control* 61, 113–120. doi: 10.1016/j.biocontrol.2011.10.014
- Li, Z., Situ, J. J., Zhu, Q. F., Xi, P. G., Zheng, Y., Liu, H. X., et al. (2019). Identification of volatile organic compounds for the biocontrol of postharvest litchi fruit pathogen *Peronophythora litchii*. *Postharvest Biol. Technol.* 155, 37–46. doi: 10.1016/j.postharvbio.2019.05.009
- Liu, C., Yin, X. H., Wang, Q. G., Peng, Y., Ma, Y. R., Liu, P., et al. (2018). Antagonistic activities of volatiles produced by two *Bacillus* strains against monilinia fructicola in peach fruit. *J. Sci. Food Agric.* 98, 5756–5763. doi: 10.1002/jsfa.9125
- Livak, K. J., and Schmittgen, T. D. (2001). Analysis of relative gene expression data using real-time quantitative PCR and the 2- $\Delta\Delta$ CT method. *Methods* 25, 402–408. doi: 10.1006/meth.2001.1262
- Maachia, B., Rafik, E., Chérif, M., Nandal, P., and Bernard, P. (2015). Biological control of the grapevine diseases 'grey mold' and 'powdery mildew' by *Bacillus* B27 and B29 strains. *Indian J. Exp. Biol.* 53, 109–115.
- Marshall, M. A., and Timberlake, W. E. (1991). *Aspergillus nidulans* wetA activates spore-specific gene expression. *Mol. Cell. Biol.* 11, 55–62. doi: 10.1128/mcb.11.1.55-62.1991
- Martins, S. J., de Faria, A. F., Pedrosa, M. P., Cunha, M. G., da Rocha, M. R., and de Medeiros, F. H. V. (2019). Microbial volatiles organic compounds control anthracnose (*Colletotrichum lindemuthianum*) in common bean (*Phaseolus vulgaris* L.). *Biol. Control* 131, 36–42. doi: 10.1016/j.biocontrol.2019.01.003
- Massawe, V. C., Rao, A. H., Farzand, A., Mburu, D. K., and Gao, X. (2018). Volatile organic compounds of endophytic bacillus spp. have biocontrol activity against sclerotinia sclerotiorum. *Phytopathology* 108, 1373–1385. doi: 10.1094/PHYTO-04-18-0118-R
- Morath, S. U., Hung, R., and Bennett, J. W. (2012). Fungal volatile organic compounds: a review with emphasis on their biotechnological potential. *Fungal Biol. Rev.* 26, 73–83. doi: 10.1016/j.fbr.2012.07.001
- Morgan, G. D., Stevenson, W. R., Macguidwin, A. E., Kelling, K. A., and Zhu, J. (2002). Plant pathogen population dynamics in potato fields. *J. Nematol.* 34, 189–193.
- Mu Oz, A., Gandía, M., Harries, E., Carmona, L., Read, N. D., and Marcos, J. F. (2013). Understanding the mechanism of action of cell-penetrating antifungal peptides using the rationally designed hexapeptide PAF26 as a model. *Fungal Biol. Rev.* 26, 146–155. doi: 10.1016/j.fbr.2012.10.003
- Pasche, J. S., Wharam, C. M., and Gudmestad, N. C. (2007). Shift in sensitivity of *alternaria solani* in response to Q o I fungicides. *Plant Dis.* 88, 181–187. doi: 10.1094/PDIS.2004.88.2.181
- Peters, R. D., Drake, K. A., Gudmestad, N. C., Pasche, J. S., and Shinnars-Carnelley, T. (2008). First report of reduced sensitivity to a QoI fungicide in isolates of *alternaria solani* causing early blight of potato in Canada. *Plant Dis.* 92, 1707–1707. doi: 10.1094/PDIS-92-12-1707B
- Raza, W., Ling, N., Yang, L., Huang, Q., and Shen, Q. (2016a). Response of tomato wilt pathogen *Ralstonia solanacearum* to the volatile organic compounds produced by a biocontrol strain *Bacillus amyloliquefaciens* SQR-9. *Sci. Rep.* 6:24856. doi: 10.1038/srep24856
- Raza, W., Wang, J., Wu, Y., Ling, N., Wei, Z., Huang, Q., et al. (2016b). Effects of volatile organic compounds produced by *Bacillus amyloliquefaciens* on the growth and virulence traits of tomato bacterial wilt pathogen *Ralstonia solanacearum*. *Appl. Microbiol. Biotechnol.* 100, 7639–7650. doi: 10.1007/s00253-016-7584-7
- Raza, W., Yuan, J., Ling, N., Huang, Q., and Shen, Q. (2015). Production of volatile organic compounds by an antagonistic strain *Paenibacillus polymyxa* WR-2 in the presence of root exudates and organic fertilizer and their antifungal activity against *Fusarium oxysporum* f. sp. niveum. *Biol. Control* 80, 89–95. doi: 10.1016/j.biocontrol.2014.09.004
- Ruiz-Herrera, J., Elorza, M. V., Valentín, E., and Sentandreu, R. (2006). Molecular organization of the cell wall of *Candida albicans* and its relation to pathogenicity. *FEMS Yeast Res.* 6, 14–29. doi: 10.1111/j.1567-1364.2005.00017.x

## SUPPLEMENTARY MATERIAL

The Supplementary Material for this article can be found online at: <https://www.frontiersin.org/articles/10.3389/fmicb.2021.808337/full#supplementary-material>



- Schreinemachers, P., and Tipraqsa. (2012). Agricultural pesticides and land use intensification in high, middle and low income countries. *Food Policy* 6, 616–626. doi: 10.1016/j.foodpol.2012.06.003
- Senthil, R., Prabakar, K., Rajendran, L., and Karthikeyan, G. (2011). Efficacy of different biological control agents against major postharvest pathogens of grapes under room temperature storage conditions. *Phytopathol. Mediterranea* 50, 55–65.
- Sewall, T. C., Mims, C. W., and Timberlake, W. E. (1990). Conidium differentiation in *Aspergillus nidulans* wild-type and wet-white (wetA) mutant strains. *Developmental Biology* 138, 499–508. doi: 10.1016/0012-1606(90)90215-5
- Shao, X., Cheng, S., Wang, H., Yu, D., and Mungai, C. (2013). The possible mechanism of antifungal action of tea tree oil on *Botrytis cinerea*. *J. Appl. Microbiol.* 114, 1642–1649. doi: 10.1111/jam.12193
- Tao, N., OuYang, Q., and Jia, L. (2014). Citral inhibits mycelial growth of *Penicillium italicum* by a membrane damage mechanism. *Food Control* 41, 116–121. doi: 10.1016/j.foodcont.2014.01.010
- Tran, T. D., Del, C. C., Hnasko, R., Gorski, L., and McGarvey, J. A. (2020). *Bacillus amyloliquefaciens* ALB65 inhibits the growth of listeria monocytogenes on cantaloupe melons. *Appl. Environ. Microbiol.* 87:e01926-20. doi: 10.1128/AEM.01926-20
- Van den Dool, H., and Kratz, P. (1963). A generalization of the retention index system including linear temperature programmed gasliquid partition chromatography. *J. Chromatogr.* 11, 463–471. doi: 10.1016/s0021-9673(01)80947-x
- Wang, C. J., and Liu, Z. Q. (2007). Foliar uptake of pesticides—present status and future challenge. *Pesticide Biochem. Physiol.* 87, 1–8. doi: 10.1016/j.pestbp.2006.04.004
- Wichitra, L., Punpen, H., and Samerchai, C. (2008). Growth inhibitory properties of *Bacillus subtilis* strains and their metabolites against the green mold pathogen (*Penicillium digitatum* Sacc.) of citrus fruit. *Postharvest Biol. Technol.* 48, 113–121. doi: 10.1016/j.postharvbio.2007.09.024
- Wu, Y. C., Zhou, J. Y., Li, C. G., and Yan, M. (2019). Antifungal and plant growth promotion activity of volatile organic compounds produced by *Bacillus amyloliquefaciens*. *Microbiol. Open* 8:813. doi: 10.1002/mbo3.813
- Xie, S., Zang, H., Wu, H., Uddin, R. F., and Gao, X. (2018). Antibacterial effects of volatiles produced by *Bacillus* strain D13 against *Xanthomonas oryzae* pv. *oryzae*. *Mol Plant Pathol.* 19, 49–58. doi: 10.1111/mpp.12494
- Yamanaka, M., Hara, K., and Kudo, J. (2005). Bactericidal actions of a silver ion solution on *Escherichia coli*, studied by energy-filtering transmission electron microscopy and proteomic analysis. *Appl. Environ. Microbiol.* 71, 7589–7593. doi: 10.1128/AEM.71.11.7589-7593.2005
- Yu, J. H., Hamari, Z., Han, K. H., Seo, J. A., Reyes-Domínguez, Y., and Scazzocchio, C. (2004). Double-joint PCR: a PCR-based molecular tool for gene manipulations in filamentous fungi. *Fungal Genet. Biol.* 41, 973–981. doi: 10.1016/j.fgb.2004.08.001
- Zhang, D., He, J. Y., Haddadi, P., Zhu, J. H., Yang, Z. H., and Ma, L. S. (2018). Genome sequence of the potato pathogenic fungus *Alternaria solani* HWC-168 reveals clues for its conidiation and virulence. *BioMed Central* 18:176. doi: 10.1186/s12866-018-1324-3
- Zhang, D., Yu, S. Q., Yang, Y. Q., Zhang, J. L., and Zhu, J. H. (2020). Antifungal effects of volatiles produced by *Bacillus subtilis* against *Alternaria solani* in potato. *Frontiers in Microbiology* 11:1196. doi: 10.3389/fmicb.2020.01196
- Zhang, D., Yu, S. Q., Zhao, D. M., Zhang, J. L., Pan, Y., Yang, Y. Q., et al. (2021). Inhibitory effects of non-volatiles lipopeptides and volatiles ketones metabolites secreted by *Bacillus velezensis* C16 against *Alternaria solani*. *Biol. Control* 152:104421. doi: 10.1016/j.biocontrol.2020.104421
- Zhang, X. Y., Gao, Z. F., Zhang, X. X., Bai, W. B., Zhang, L. X., and Pei, H. B. (2020). Control effects of *Bacillus siamensis* G-3 volatile compounds on raspberry postharvest diseases caused by *Botrytis cinerea* and *Rhizopus stolonifer*. *Biol. Control* 141:104135. doi: 10.1016/j.biocontrol.2019.104135
- Zheng, M., Shi, J. Y., Shi, J., Wang, Q., and Li, Y. (2013). Antimicrobial effects of volatiles produced by two antagonistic *Bacillus* strains on the anthracnose pathogen in postharvest mangos. *Biol. Control* 65, 200–206. doi: 10.1016/j.biocontrol.2013.02.004

**Conflict of Interest:** The authors declare that the research was conducted in the absence of any commercial or financial relationships that could be construed as a potential conflict of interest.

**Publisher's Note:** All claims expressed in this article are solely those of the authors and do not necessarily represent those of their affiliated organizations, or those of the publisher, the editors and the reviewers. Any product that may be evaluated in this article, or claim that may be made by its manufacturer, is not guaranteed or endorsed by the publisher.

Copyright © 2022 Zhang, Qiang, Zhao, Zhang, Cheng, Zhao, Fan, Yang and Zhu. This is an open-access article distributed under the terms of the Creative Commons Attribution License (CC BY). The use, distribution or reproduction in other forums is permitted, provided the original author(s) and the copyright owner(s) are credited and that the original publication in this journal is cited, in accordance with accepted academic practice. No use, distribution or reproduction is permitted which does not comply with these terms.



## OPEN ACCESS

### Edited by:

Ana Sofia Duarte,  
Catholic University of Portugal,  
Portugal

### Reviewed by:

Vladimiro Guarnaccia,  
University of Turin, Italy  
Emmanouil A. Markakis,  
Institute of Olive Tree, Subtropical  
Plants and Viticulture, Hellenic  
Agricultural Organization – DEMETER,  
Greece

### \*Correspondence:

Samuele Moretti  
samuele.moretti@uha.fr  
Fabio Osti  
fabio.osti@ibe.cnr.it

### † Present address:

Samuele Moretti,  
Laboratoire Vigne, Biotechnologies et  
Environnement UPR 3991, Université  
de Haute-Alsace, Colmar, France

### Specialty section:

This article was submitted to  
Microbe and Virus Interactions with  
Plants,  
a section of the journal  
Frontiers in Microbiology

**Received:** 11 November 2021

**Accepted:** 16 December 2021

**Published:** 28 January 2022

### Citation:

Di Marco S, Metruccio EG,  
Moretti S, Nocentini M, Carella G,  
Pacetti A, Battiston E, Osti F and  
Mugnai L (2022) Activity  
of *Trichoderma asperellum* Strain ICC  
012 and *Trichoderma gamsii* Strain  
ICC 080 Toward Diseases of Esca  
Complex and Associated Pathogens.  
Front. Microbiol. 12:813410.  
doi: 10.3389/fmicb.2021.813410

# Activity of *Trichoderma asperellum* Strain ICC 012 and *Trichoderma gamsii* Strain ICC 080 Toward Diseases of Esca Complex and Associated Pathogens

Stefano Di Marco<sup>1</sup>, Elisa Giorgia Metruccio<sup>1</sup>, Samuele Moretti<sup>2\*†</sup>, Marco Nocentini<sup>2</sup>,  
Giuseppe Carella<sup>2</sup>, Andrea Pacetti<sup>2</sup>, Enrico Battiston<sup>2</sup>, Fabio Osti<sup>1\*</sup> and Laura Mugnai<sup>2</sup>

<sup>1</sup> Institute of BioEconomy, National Research Council, Bologna, Italy, <sup>2</sup> Plant Pathology and Entomology Section, Department of Agricultural, Food, Environmental and Forestry Science and Technology (DAGRI), University of Florence, Florence, Italy

Grapevine trunk diseases are widespread in all grape-growing countries. The diseases included in the Esca complex of diseases are particularly common in European vineyards. Their distinctive foliar symptoms are well known to be associated not only with losses in quantity, as with all grapevine wood diseases, but also with losses in the quality of the crop. Protection of pruning wounds is known to reduce infections in artificial inoculations and, to some extent, reduce the external leaf symptoms. The application of biological control agents in the field is typically started at the first appearance of symptoms. In this article, the two strains belonging to two different species, *Trichoderma asperellum* ICC 012 and *T. gamsii* ICC 080, which are present in a commercial formulation, were tested *in vitro*, *in vivo* in artificial inoculation, and in the field in long-term experiments where the wounds on four young asymptomatic vineyards were protected since 1 or 2 years after planting. The *in vitro* trials highlighted the different temperature requirements of the two strains, the direct mycoparasitizing activity of *T. asperellum*, and the indirect activity shown by both *Trichoderma* strains. The *in vivo* trials confirmed the ability of the two strains to reduce the colonization following artificial inoculations with the high, unnatural concentration of spores used in artificial infections, even if with variable efficacy, and with long persistence as they could be reisolated 7 months post-application. The preventive applications carried out over 9 years showed a very high reduction in symptom development in the treated vines, on annual and cumulated incidence and on the death of vines, with disease reduction varying from 66 to almost 90%. Early and annual application of protection to the pruning wounds appears to be the best method for reducing damages caused by grapevine leaf stripe disease (a disease of the Esca complex of diseases). *Trichoderma* appears to offer an efficient, environmentally friendly, and long-lasting protection in the presence of a natural inoculum concentration.

**Keywords:** biocontrol agent, biological control, Esca complex, grapevine trunk diseases, *Trichoderma*

## INTRODUCTION

Grapevine trunk diseases (GTD), in recent decades, have shown an increasing impact on grapevine cultivation, causing severe losses in viticulture (Mondello et al., 2018a). The spread of the diseases is due to multiple interacting factors, such as the dissemination of potentially infected propagation material and, above all, the adoption of methods of production in vineyards that favored fungal infections or weakened the vine defense mechanisms (Surico et al., 2004; Gramaje and Di Marco, 2015; Lecomte et al., 2018). Therefore, the increasing spread of GTDs in almost all grape-growing areas and the onset of symptoms, even on young vines, have attracted the attention of winegrowers and researchers on such diseases.

The most relevant and damaging GTD in Europe was commonly known as “Esca disease” of grapevine (Larignon and Dubos, 1997; Bertsch et al., 2013; Guerin-Dubrana et al., 2019) but has been re-defined by some authors, based on research carried out in the recent decades, as a complex of different diseases (Mugnai et al., 1999; Surico, 2009), where grapevine leaf stripe disease (GLSD), without or with wood decay (Esca proper), is characterized by the typical leaf stripe symptoms.

Tracheomycotic pathogens, like *Phaeomoniella chlamydospora* (*Pch*) and *Phaeoacremonium* species [mainly *Phaeoacremonium minimum* (*Pmin*)], and the basidiomycete *Fomitiporia mediterranea* (*Fmed*) are commonly considered as the main pathogens associated with Esca complex of diseases (ECDs), inducing wood discoloration and decay, respectively. Moreover, fungal canker agents, like botryosphaeriaceous species, are very often isolated from affected vines (Bertsch et al., 2013; Gramaje et al., 2018).

The infected plants can show various types of symptoms in the canopy (among which the leaf stripe symptom is one of the most characteristic feature; **Figure 1**) and in the wood (wood rot and central and sectorial discolorations and necrosis) (Mugnai et al., 1999). The role of various pathogens associated to leaf symptoms has not been clarified completely yet, and the relationship with white rot presence and extent has recently been reviewed (Moretti et al., 2021). The leaf symptoms have been reproduced only on very few occasions by the inoculation of different pathogens (Sparapano et al., 2001; Reis et al., 2016; Markakis et al., 2017). GLSD appears not to be linked to specific fungal agents but as a reaction of the plant to the activity of fungal wood colonization affecting the plant physiology and the quality of production (Calzarano et al., 2004b, 2017a; Lorrain et al., 2012; Pouzoulet et al., 2014; Fontaine et al., 2016; Mary et al., 2017; Bortolami et al., 2021; Del Frari et al., 2021).

Foliar symptom expression shows almost unique peculiarities, as their intermittent occurrence in the vineyard (Marchi et al., 2006; Guerin-Dubrana et al., 2019) is a very rare phenomenon that has been observed in another wood disease, the “decay of kiwi fruit” that has many common factors with ECDs (Di Marco and Osti, 2008). The erratic nature of foliar symptom expression could be associated with phytotoxins produced by tracheomycotic pathogens, alterations of phytoalexins and photosynthetic functions, and disorders of sap flow or hydraulic failures (Claverie et al., 2020;

Calzarano et al., 2021; Ouadi et al., 2021) modulated by environmental and meteorological factors, such as rainfall and temperature (Marchi et al., 2006; Calzarano et al., 2018). Nevertheless, the deterioration of the wood by pathogens and the correlation between incidence and severity of foliar symptom expression and yield losses are unquestionable. In that respect, ECDs control aims to reduce the risk and effects of wood infection (Mondello et al., 2018a).

Management of infected vines includes different approaches like trunk renewal (Egger et al., 1998; Calzarano et al., 2004a; Gramaje et al., 2018), wood surgery or curettage (Bruez et al., 2020; Pacetti et al., 2021), vine training for an optimal sap flux (Lecomte et al., 2018), or re-grafting of infected plants in the vineyard as alternative to replanting (Mondello et al., 2018a). Foliar treatments can also reduce disease incidence as (i) with fosetyl Al application in a downy mildew strategy (Di Marco et al., 2011a), (ii) a nutrient mixture based on calcium, magnesium, and seaweed (Calzarano et al., 2007, 2017b; Calzarano and Di Marco, 2018), or (iii) even winter treatments with a copper formulation (Di Marco et al., 2011b; Calzarano et al., 2014). Nevertheless, the best way to control wood pathogens remains to be reduction of the risk of infection, and many efforts have been focused on the protection of pruning wounds, as pathogens, mostly spread by airborne spores, can cause new infections mainly through the pruning wounds (Mugnai et al., 1999; Bertsch et al., 2013).

Pruning wounds are susceptible to infections for a long time, at least up to 4 months (Eskalen et al., 2007; Serra et al., 2008). The susceptibility of wounds is linked to many factors, such as (i) age of the wound at the time of infection (Eskalen et al., 2007), (ii) cultivar (Feliciano et al., 2004; Mutawila et al., 2011a), (iii) type and/or time of pruning (Rolshausen et al., 2010; Elena and Luque, 2016), and (iv) climatic conditions, such as frequency of rain events (Eskalen and Gubler, 2001; Rolshausen et al., 2010) or weekly temperatures (Serra et al., 2008). The protection of pruning wounds from GTDs has been achieved by application of different fungicides (Mondello et al., 2018b) as well as by applying new specific formulations as a paste (Diaz et al., 2013). A new product based on a polymer and fungicides and known as pyraclostrobin + boscalid (Tessior®), applied in the vineyard with special equipment on each pruning wound, was proposed against ECDs and registered in some European countries (Lengyel et al., 2019).

The long susceptibility of pruning wounds to infections and the need for long-lasting colonization and activity, combined with the need for sustainable tools, promoted the setting up of wound protection with biological control agents, such as *Trichoderma* species (Di Marco et al., 2004; Van Niekerk et al., 2011; Bigot et al., 2020; Brown et al., 2021) and *Bacillus* spp. (Alfonzo et al., 2012; Mondello et al., 2018a).

The *Trichoderma* species are filamentous ascomycetes usually living in the root and soil ecosystem and widely applied as bio-control agents. The bio-control is due to various antimicrobial activities, including mycoparasitism, antibiosis, competition for nutrients and/or space, and induction of plant resistance (Harman et al., 2004). Research on the use



of *Trichoderma* toward GTDs was primarily performed in the nursery during the process of production of propagation material with applications in hydration, grafting, callusing, and nursery field (Halleen et al., 2001; Hunt et al., 2001; Di Marco et al., 2002, 2004; Fourie and Halleen, 2004, 2006; Di Marco and Osti, 2007; Mounier et al., 2016; Pertot et al., 2016).

Pruning wound protection was initially performed with strains of *Trichoderma longibrachiatum* (strain 6) or *Trichoderma harzianum* (strain T39) that were able to colonize the pruning wound surface for up to 2 months in the vineyard, while applications to pruning wounds on potted vines before artificial inoculation with *Pch* prevented necrosis in xylem tissue below the wound (Di Marco et al., 2004). Other studies showed the activity of *Trichoderma* species in protecting pruning wounds from infections by different GTD pathogens, including *Pch* (Kotze et al., 2011). Further research pointed out that the activity of *Trichoderma* species is also dependent on the interaction with the host-plant cultivar (Mutawila et al., 2011a). The growth and interaction between *T. harzianum*, *Eutypa lata*, and *Pch* showed that the bio-control agent was able to grow deeper in the presence of the pathogens than when applied alone on the wound (Mutawila et al., 2011b). *Trichoderma atroviride* strain SC1 colonized the wounds for several months after its application, protecting the plants throughout the growth season (Prodorutti et al., 2012). Several *Trichoderma*-based products were registered against ECDs. *Trichoderma atroviride* I-1237 (Esquive®) was demonstrated to be effective in wound protection against “Esca”, black dead arm, and *Eutypa dieback*, reducing leaf symptom expression after at least a 2-year application (Mounier et al., 2016) and reducing the infections on pruned canes artificially inoculated with *Pch* and *Neofusicoccum parvum* (Reis et al., 2017). *Trichoderma atroviride* SC1 (Vintec®) reduced the infections when applied in the nursery and in the vineyard (Berbegal et al., 2020). Some activity of *T. atroviride* SC1 and *T. atroviride* I-1237, even if significantly lower than that of new synthetic fungicide formulations, was observed on wounds artificially infected with *Pch* and *Diplodia seriata* (Martinez-Diz et al., 2021). Decreased incidence and severity of foliar symptoms of Esca were obtained in vineyard pruning wounds treated with Remedier®, a bio-fungicide composed of *Trichoderma asperellum* ICC 012 and *Trichoderma gamsii* ICC 080 in a formulation developed by Isagro Company (Aloi et al., 2017; Bigot et al., 2020).

This study aimed to characterize the protective activity of a *Trichoderma*-based commercial product, Remedier®, when applied in a really preventive approach in yet asymptomatic vineyards, demonstrating that its constant use over a long length of time gives an increasing efficacy as a strong reduction agent of ECDs symptom development. The *in vitro* activity of the two individual strains at different temperatures was assessed against three GTD pathogens (*Pch*, as the main tracheomycotic pathogen of ECDs; *N. parvum*, as an important canker agent; and the white-rot agent *F. mediterranea*). In the vineyard, the activity of the registered formulation Remedier® and the viability of both *Trichoderma* species



**FIGURE 1 |** Leaf stripe symptoms, often described as tiger stripe leaves, are the most distinctive symptom of grapevine leaf stripe disease, within the Esca complex of diseases.

after different times of application were assessed for their efficacy to protect pruning wounds inoculated with *Pch*. Finally, the effect of a field spray application of Remedier® was evaluated on the annual and cumulative leaf stripe symptoms incidence and the percentage of apoplexy and mortality over a multiple-year survey carried out in four vineyards located in two different regions of Italy that were treated to protect them from infections since after 1 or 2 years from planting.

## MATERIALS AND METHODS

### *In vitro* Growth of *Trichoderma* Strains at Different Temperatures

Isagro S.p.A (Novara, Italy) provided fungal colonies of *T. asperellum* strain ICC 012 (*Tasp*) and *T. gamsii* strain ICC 080 (*Tgam*), which are the active ingredients of the commercial bio-fungicide Remedier®. *Trichoderma* colonies were grown on marine agar (MA; Difco, Detroit, MI, United States) in Petri dishes and maintained at  $25 \pm 1^\circ\text{C}$  with a 12-h photoperiod. Plates of MA were inoculated by placing a plug of *Tasp* or *Tgam* face down at the center of the dish. The plates were then incubated at 10, 13, 18, and  $23 \pm 1^\circ\text{C}$  with a 12-h photoperiod, and colony radii were recorded daily. There were five replicates for each *Trichoderma* strain-temperature combination. Measurements of



daily growth of the two strains at the different temperatures were continued until the colonies reached the edge of the dish or stopped growing.

### **In vitro Activity of the Two *Trichoderma* Strains Against Selected Wood Pathogens at Different Temperatures**

Each *Trichoderma* strain was tested against *Pch* CBS229.95, *Fmed* strain PVFi-201.03, and *N. parvum* (Np) PVFi-np22 (maintained in the collection of DAGRI, University of Florence, Florence, Italy). All fungal colonies were grown under the conditions described above.

A mycelial plug (5 mm in diameter) of a colony of *Tasp* or *Tgam* was put face down at the periphery of a Petri dish, and a colonized agar plug of each pathogen isolate was placed at the opposite side along the diameter of the same plate. Plates containing only a plug of each *Trichoderma* strain or pathogen strain served as control. The plates were incubated at 10, 13, 18, and  $23 \pm 1^\circ\text{C}$  with a 12-h photoperiod, and colony radii along the diameter were measured daily until the *Trichoderma* strain and pathogen colonies in the same plate stopped growing. There were five replicates for each *Trichoderma*–pathogen–temperature combination.

The direct (competitive growth) or indirect (production of volatile and non-volatile compounds) activity of the *Trichoderma* strains was assessed as follows:

Direct activity of *Trichoderma* was recorded as (i) the day when the *Trichoderma* strain and pathogen colonies came into contact, (ii) the day when maximum overgrowth, the ability of the *Trichoderma* strain to overlap and grow over the pathogen colony, occurred and at what percentage, and (iii) the day when the *Trichoderma* strain sporulated on the pathogen colony. At the maximum *Trichoderma* overgrowth, the colony area of the pathogen and the area overlapped by *Trichoderma* were measured by video image analysis. The images were taken with a CCD camera (model TK-880, JVC, Yokohama, Japan) interfaced with a computer by an ELVIS board and Chameleon software (Sky Instruments Ltd., Llandrindod Wells, Powys, Wales, United Kingdom). The percentage of maximum overgrowth was calculated by dividing the overlapped colony area by the colony area multiplied by 100.

Indirect activity of *Trichoderma* was recorded as (i) the day when the pathogen colony stopped growing and (ii) the day and the percentage of maximum colony growth inhibition assessed on the day immediately before the contact between the *Trichoderma* strain tested and the pathogen. In case there was no contact, the day when both the *Trichoderma* strain and pathogen stopped growing was recorded. Inhibition of the pathogen colony at each temperature was calculated as follows: radius of the pathogen colony without *Trichoderma* minus radius of the pathogen colony in the presence of *Trichoderma* divided by the radius of the pathogen colony without *Trichoderma* multiplied by 100. Both radii of pathogen

colonies grown with or without *Trichoderma* were assessed on the same day.

### **Artificial Inoculations on Grapevine Canes Treated With the *Trichoderma* Formulation in an In-Field Trial**

All field trials were carried out with the commercial product Remedier containing® 2% *T. asperellum* strain ICC 012 (*Tasp*) and 2% of *T. gamsii* strain ICC 080 (*Tgam*). As a parallel test, inoculation of canes previously protected by spraying the commercial product Remedier® was carried out. The same number of control canes were included in all tests. In the untreated control canes, no protection nor artificial inoculation was applied. The trial was carried out in a vineyard of 20-year-old “Sangiovese” grapevines located in San Casciano in Val di Pesa, Florence, Italy, where vine rows where no ECDs foliar symptoms had been recorded in the previous 3 years were selected. In 2009 and 2010, at BBCH growth stage 00 (winter buds), canes on the cordon that were as much as possible perpendicular to the soil were selected. The canes were pre-pruned at the end of February, and a few centimeters were cut from the tip of the pruned cane to provide a fresh wound on the day when the treatment was applied. Following the recommendation of the producer, the commercial *Trichoderma* formulation was prepared by pouring the product into water at room temperature at about 24 h before the application so as to start the germination of the spores. On the following day, the treatment was applied by a hand sprayer at the label concentration ( $250 \text{ g hL}^{-1}$ ) up to dripping. At 4 days after treatment,  $100 \mu\text{L}$  of a  $1 \times 10^5 \text{ Pch mL}^{-1}$  conidial suspension was applied to the wound of each cane.

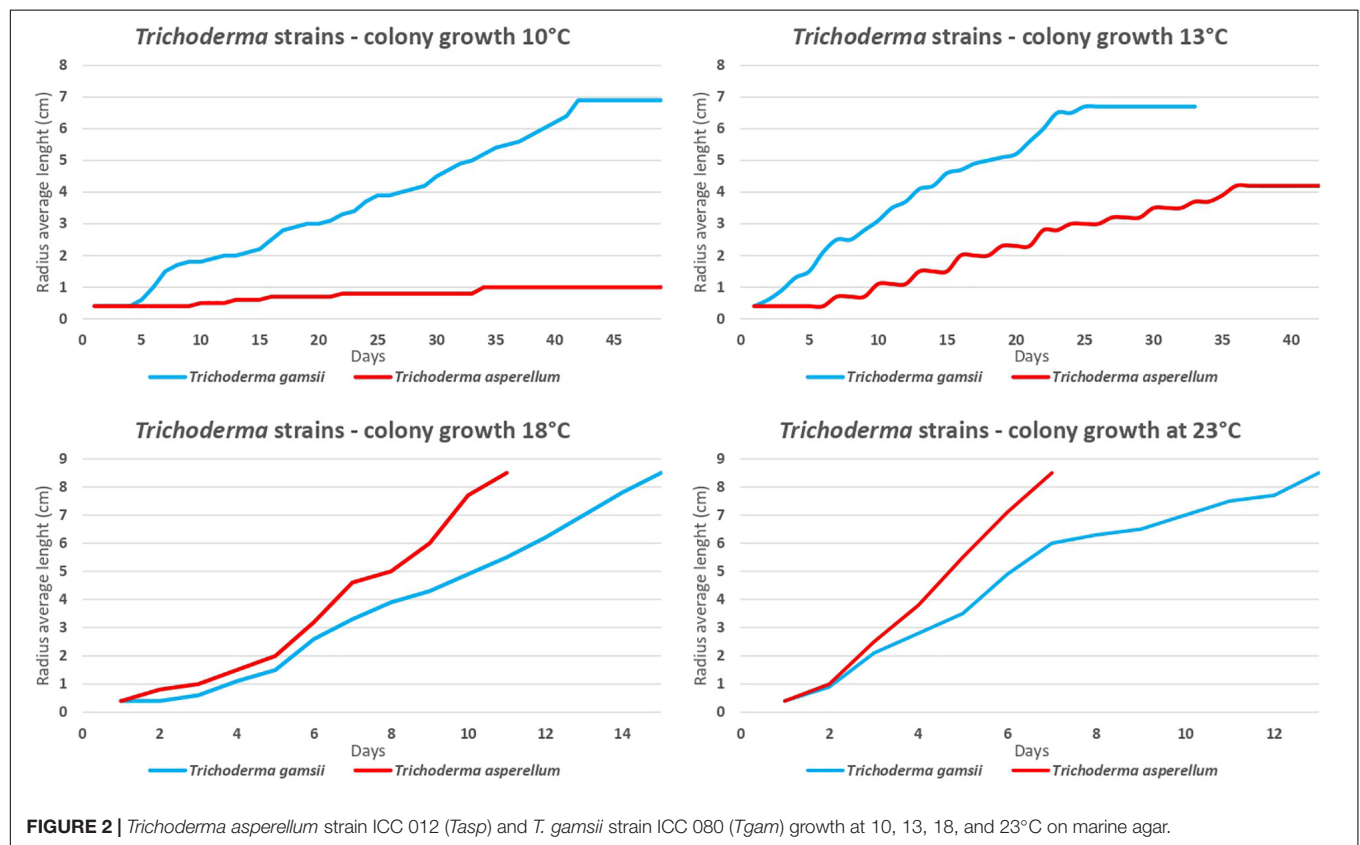
Forty-five canes were used per treatment (three replicates of 15 canes each). After 7 months, re-isolations were made from the canes. The canes were quickly soaked in ethanol and flamed, the bark was removed, and the canes were flamed again after spraying with ethanol. Three 2-mm-thick wood disks or transversal sections were sampled from each cane at 0.5, 2, and 6 cm away from the cut and inoculated end. Moreover, the first external slice was also analyzed to assess the survival of the *Trichoderma* species. Each slice, 2 mm in thickness, was cut in six fragments that were plated on MA agar. The colonies that developed in the following 60 days were identified from their morphology (characteristics of the colony and micromorphology).

### **Colonization and Persistence of the *Trichoderma* Formulation on Artificially Inoculated Canes**

The colonization ability and persistence of the two strains of *Tasp* and *Tgam* present in the commercial product were assessed in a further trial setup in 2010 in the same vineyard in San Casciano in Val di Pesa (Florence). A further lot of 90 canes was treated with Remedier® immediately after the trimming cut as detailed above. The same number of canes was left unprotected as untreated control to check for possible natural *Trichoderma* infections. Re-isolation was carried out by sampling 15 canes at 3, 7, and 15 days (to assess establishment speed) and 1, 2, and 7 months after the spray application (to assess persistence

**TABLE 1** | List of the vineyards where the on-field applications of the *Trichoderma* formulations on pruning wounds were carried out.

Vineyard code and cultivar	Region	Locality, province	Year of planting	Time of pruning	Soil	Trichoderma application			Number of plants per plot at the beginning of the trial	
						First	Last	Time	Control	Trichoderma-treated
V1 Trebbiano	Emilia-Romagna	S. Andrea, Ravenna	2009	Mid-February	Medium texture	2011	2019	Early April	488	486
V2 Lambrusco	Emilia-Romagna	Cavezzo, Modena	2009	Mid-March	Medium texture	2011	2019	Early April	799	800
V3 Trebbiano	Emilia-Romagna	Bagnara, Ravenna	2009	Mid-February	Medium texture	2011	2018	Early April	362	384
V4 Cabernet Franc	Friuli Venezia Giulia	Tauriano, Pordenone	2009	Mid-March	Medium texture	2010	2019	Late March	600	600



over time). In both trials, 6 wood chips per cane, taken from the first 5 mm of the cut end in each trimming cut, were plated on MA. Colonization and persistence were evaluated as the number of canes with at least one colony (incidence) and as the total number of wood chips colonized by each of the two *Trichoderma* species (severity).

## Efficacy of Application of the *Trichoderma*-Based Product in the Vineyard

The field trials details are shown in **Table 1**. The vineyards, Guyot trained, were located in two regions of Central and Northern Italy: Emilia-Romagna and Friuli Venezia Giulia. In

each vineyard, at the year before the start of the experiments (September), a time 0 survey was carried out to assess the absence of ECDs symptoms. In the following spring (March), two plots were selected in each vineyard: one was treated with the *Trichoderma* commercial formulation, and the other one was used as untreated control. In each vineyard, around 500 vines per plot (2 plots per vineyard) were monitored each year and mapped (**Table 1**).

*Trichoderma* applications were carried out every year with the same modality for the following 9 years. The trials were conducted in commercial vineyards planted in the previous year. Except for the wound protection treatment, both plots in each vineyard received the same treatments against pests and foliar diseases.

**TABLE 2** | *In vitro* direct activity of the *Trichoderma asperellum* strain (Tasp) on *Phaeomoniella chlamydospora*, *Neofusicoccum parvum*, and *Fomitiporia mediterranea*.

Temperature (°C)	<i>Phaeomoniella chlamydospora</i>				<i>Fomitiporia mediterranea</i>				<i>Neofusicoccum parvum</i>			
	Contact	Maximum overgrowth		Sporulation	Contact	Maximum overgrowth		Sporulation	Contact	Maximum overgrowth		Sporulation
	Day <sup>a</sup>	Day <sup>a</sup>	% <sup>a</sup>	Day <sup>a</sup>	Day	Day	%	Day	Day	%	Day	Day
10	– <sup>b</sup>	– <sup>b</sup>	– <sup>b</sup>	–	–	–	–	–	–	–	–	–
13	–	–	–	–	37a <sup>c</sup>	–	–	–	20a	–	–	–
18	10a	12a	100°	12°	7b	11a	100a	11a	6b	10a	28.2a	14a
23	4b	9a	100°	6b	7b	9a	100a	9a	4b	6b	42b	9b

<sup>a</sup>Days after plug deposition in the plate.

<sup>b</sup>For each pathogen, the dash within a column indicated that no contact, overgrowth, or sporulation occurred, and statistical analysis was not performed.

<sup>c</sup>For each pathogen, data followed by the same letter within columns did not differ significantly according to ANOVA ( $P < 0.05$ ).

As mentioned above, the commercial formulation of *Trichoderma* was prepared 24 h before its application to start the germination of the spores. The product was applied at 250 g hL<sup>-1</sup> formulation, with a volume of 400 L ha<sup>-1</sup>, thus distributing 1 kg of product per hectare. A single application per year was carried out in late March until early April.

Every year, the vineyards were monitored at the end of August to early September, time of greatest disease expression. The position of each plant in the plot and its condition and symptoms were recorded each year, following an arbitrary scale of symptom severity on a two-dimensional map to follow the evolution of the disease on a single plant over the years of investigation, as healthy (“H”) or with low severity (“A”) of foliar symptoms and high severity (“B”) of foliar symptoms when expressing 5–30% or >30% symptoms of the whole vine canopy.

The frequency of occurrence of the two levels of symptoms (A or B) was calculated by dividing the total number of vines with A or B symptom level in a given year by the total number of standing plants of the same age in that year multiplied by 100. Furthermore, the frequency of plants showing apoplexy (APO), as wilting of foliage and clusters of the whole plant, was calculated by dividing the number of plants showing symptoms of apoplexy in a given year by the total standing coetaneous plants in that year multiplied by 100.

The annual incidence was calculated by dividing the number of plants with leaf symptoms in a given year by the total number of standing coetaneous plants (H + A + B + APO) in that year multiplied by 100. The cumulated incidence was calculated in each year of survey by dividing the standing plants with leaf symptoms in that year or in at least one of the previous years of survey by the total number of standing coetaneous plants observed in the first year of survey multiplied by 100. The cumulated number of dead plants was calculated each year of the survey by dividing the total number of plants that died after showing foliar symptoms or apoplectic symptoms in that or in a previous year of investigation by the total number of standing coetaneous plants in the first year of survey and multiplying by 100.

In each year, the efficacy of the protective action was calculated as the percentage of vines that had been symptomatic at least once during the survey in the treated or untreated plots (cumulated incidence) over the total number of vines that had been

symptomatic at least once over the years (cumulated incidence) in each vineyard.

## Statistical Analyses

### *In vitro* Trials

For each pathogen, analysis of variance (ANOVA) was used to determine the significance of the differences between the treatments in the daily mycelium growth rate of the two *Trichoderma* strains and their inhibition activity against pathogens *in vitro*. In the case of indirect activity, results were submitted to ANOVA, and Tukey's test was used to assess the difference among treatments ( $P = 0.05$ ). Statistical analyses were performed using SAS system software, version 9.1 (SAS Institute, Cary, NC, United States).

## Artificial Inoculations on Grapevine Canes Treated With the *Trichoderma* Formulation in an In-Field Trial

Data normality was checked with the Shapiro–Wilk test. The data were analyzed statistically using Kruskal–Wallis non-parametric and Dunn's *post hoc* tests; the significance values were adjusted by Bonferroni correction via SPSS 27 software (SPSS Inc., Chicago, IL, United States). The statistical significance level was set at  $P = 0.05$ .

### Application of the *Trichoderma*-Based Product in the Vineyard

The activity of *Trichoderma* on annual disease incidence, cumulated disease incidence, symptom A and symptom B incidence, apoplexy incidence, and cumulated numbers of dead plants were analyzed by  $\chi^2$  test. All the plants of each plot were considered to compare *Trichoderma* and control treatments. Where differences in distribution between the two treatments were significant, asterisks were placed (\* $P < 0.05$ ,  $P < 0.01$ , and \*\*\* $P < 0.001$  significance levels, respectively). Statistical analyses were performed using Prism 5 (GraphPad Software, San Diego, CA, United States). The reduction in the cumulative percentages of symptomatic vines was calculated using Abbott's formula (Abbott, 1925) for comparison among treatments and untreated control.

## RESULTS

### *In vitro* Growth of *Trichoderma* Strains at Different Temperatures

*Trichoderma asperellum* strain ICC 012 (*Tasp*) and *T. gamsii* strain ICC 080 (*Tgam*) showed different growth rates at different temperatures. *Tasp* had a higher radius length ( $P < 0.05$ ) at 18°C from the 4th day after the beginning of the trial and at 23°C from the 3rd day compared to *Tgam*. The radius length of *Tgam* increased faster ( $P < 0.05$ ) than *Tasp* at 10 and 13°C from the 5th and 2nd day from the beginning of the trial (Figure 2). On the whole, *Tasp* grew faster at higher temperatures, while *Tgam* grew faster at lower temperatures.

### *In vitro* Activity of *Trichoderma* Species Against Selected Wood Pathogens at Different Temperatures

The pathogens grew at 13, 18, and 23°C. *Np* grew also at 10°C, while the other pathogens did not grow beyond 1 mm.

#### Direct Activity

*Tasp* overgrew the pathogen colonies at 18 and 23°C. At 23°C, *Tasp* was significantly ( $P < 0.05$ ) faster than at 18°C in reaching the pathogen colony of *Pch* and displayed maximum overgrowth after 2–5 days from contact with the colonies of the pathogen. At both temperatures, overgrowth was complete (100%) for *Pch* and *Fmed* and partial for *Np*, where the percentage of overgrowth at 23°C was significantly ( $P < 0.05$ ) faster than at 18°C (Table 2).

*Tasp* sporulated earlier at 23°C than at 18°C (significantly different at  $P < 0.05$  for *Pch* and *Np*). In the interaction with *Np*, *Tasp* sporulation was less efficient compared to *Pch* and *Fmed*, occurring 4 days after the maximum overgrowth. The maximum overgrowth percentage ranged from 28% at 18°C to 42% at 23°C, and the values were significantly different ( $P < 0.05$ , Table 2). *Tgam* was not able to overgrow the pathogens.

#### Indirect Activity

In general, *Tasp* did not reduce the growth of the pathogens except for *Np* at 13°C, where growth was reduced by 48%, and on *Fmed*, where growth was reduced by 52% (Table 3). In contrast, *Tgam* stopped and reduced the growth of all pathogens at all temperatures at which pathogens grew. Pathogen colonies were stopped more rapidly at higher temperatures. The percentage of *Np* colony growth inhibition was significantly ( $P < 0.05$ ) higher (63.5%) at 10°C, whereas the greatest inhibition occurred at 18 and 23°C on *Fmed* (65%) and *Pch* (55.5%), respectively (Table 3).

### Artificial Inoculations on Grapevine Canes Treated With the *Trichoderma* Formulation in an In-Field Trial

The commercial *Trichoderma* formulation significantly reduced ( $P = 0.05$ ) the colonization by *Pch* in the first-year trial in 2009 when it almost completely stopped pathogen invasion in canes at 0.5, 2, and 6 cm from the wound, as can be seen compared with the positive control, i.e., inoculated but non-protected canes (Table 4—2009). In the same trial, *Trichoderma* was still present

**TABLE 3 |** Indirect activity of *T. asperellum* (*Tasp*) and *T. gamsii* (*Tgam*) strains in stopping or reducing the growth of the pathogen colony in dual culture with *Phaeomoniella chlamydospora* (*Pch*), *Neofusicoccum parvum* (*Np*), and *Fomitiporia mediterranea* (*Fmed*).

Pathogen	Temperature	Growth stop	Highest growth inhibition <sup>b</sup>	
	(°C)	Day <sup>a</sup>	Day <sup>a</sup>	(%)
<b><i>Tasp</i> activity on pathogen growth</b>				
<i>Pch</i>	10	— <sup>c</sup>	—	—
	13	—	—	—
	18	—	—	—
	23	—	—	—
<i>Np</i>	10	—	—	—
	13	6	18	48
	18	—	—	—
	23	—	—	—
<i>Fmed</i>	10	—	—	—
	13	23	34	52
	18	—	—	—
	23	—	—	—
<b><i>Tgam</i> activity on pathogen growth</b>				
<i>Pch</i>	10	— <sup>c</sup>	—	—
	13	9	15	8.7c <sup>d</sup>
	18	9	9	24b
	23	9	15	55.5a
<i>Np</i>	10	14	24	63.5a
	13	8	10	46b
	18	6	8	15c
	23	4	6	38b
<i>Fmed</i>	10	—	—	—
	13	19	42	17a
	18	10	16	65b
	23	6	10	61b

<sup>a</sup>Days of growth in Petri plates.

<sup>b</sup>The reduction was assessed immediately before the contact between *Trichoderma* and pathogen colonies.

<sup>c</sup>The colony of the pathogen did not grow.

<sup>d</sup>For each pathogen, data followed by the same letter within columns did not differ significantly according to Turkey's test ( $P \leq 0.05$ ).

and re-isolated from 24% of the sampled wood fragments. In the following year, the results were quite different, as the colonization by the pathogen was quite high in the first analyzed section, at 0.5%, reaching a high severity (Table 4—2010). Nevertheless, the pathogen, even if present in the first section, was reduced at 2- and 6-cm distance from the wound. The number of canes with at least one infection was reduced to 31% of the canes. *Trichoderma* was re-isolated from 87% of the control-treated canes.

### Colonization and Persistence of the *Trichoderma* Formulation on Artificially Inoculated Canes

The ability of the two *Trichoderma* strains to colonize fresh pruning wounds was evaluated as the total number of wood chips colonized divided by the total number of sampled chips. Colonization was confirmed to be stable over time, and after



**TABLE 4 |** Colonization of canes by *Phaeomoniella chlamydospora* (*Pch*) and *Trichoderma* species following preventive treatment by the *Trichoderma* formulation and/or artificial inoculation with *Pch*.

Cane wood analyzed	Untreated, non-inoculated	Untreated, inoculated ( <i>Pch</i> )	Treated ( <i>Trichoderma</i> ), non-inoculated	Treated ( <i>Trichoderma</i> ), inoculated ( <i>Pch</i> )
<b>2009</b>				
Whole cane <sup>a</sup> ( <i>Pch</i> )	0.6 ± 2.4b <sup>b</sup>	15.9 ± 14.9a	0.0 ± 0.0b	0.1 ± 0.8b
Section A <sup>c</sup> ( <i>Pch</i> )	0.0 ± 0.0b	12.6 ± 20.1a	0.0 ± 0.0b	0.0 ± 0.0b
Section B ( <i>Pch</i> )	0.0 ± 0.0b	16.7 ± 21.9a	0.0 ± 0.0b	0.4 ± 2.5b
Section C ( <i>Pch</i> )	1.8 ± 7.3b	18.5 ± 26.4a	0.0 ± 0.0b	0.0 ± 0.0b
Whole cane <sup>a</sup> ( <i>Trichoderma</i> )	0.1 ± 0.8b	0.4 ± 2.5b	24.6 ± 22.4a	20.1 ± 18.4a
Section A ( <i>Trichoderma</i> )	0.4 ± 2.5b	0.7 ± 5.0b	43.0 ± 38.2a	31.1 ± 35.8a
Section B ( <i>Trichoderma</i> )	0.0 ± 0.0b	0.0 ± 0.0b	21.8 ± 32.9a	17.0 ± 30.5a
Section C ( <i>Trichoderma</i> )	0.0 ± 0.0b	0.4 ± 2.5b	8.9 ± 25.8ab	12.2 ± 24.7a
<b>2010</b>				
Whole cane <sup>a</sup> ( <i>Pch</i> )	0.4 ± 2.0b2	20.0 ± 19.3a	0.0 ± 0.0b	17.0 ± 13.6a
Section A ( <i>Pch</i> )	1.1 ± 6.1b	36.1 ± 32.5a	0.0 ± 0.0b	46.7 ± 36.7a
Section B ( <i>Pch</i> )	0.0 ± 0.0b	17.8 ± 28.3a	0.0 ± 0.0b	4.4 ± 9.7ab
Section C ( <i>Pch</i> )	0.0 ± 0.0b	6.1 ± 18.8a	0.0 ± 0.0b	0.0 ± 0.0b
Whole cane <sup>a</sup> ( <i>Trichoderma</i> )	0.0 ± 0.0b	0.0 ± 0.0b	2.8 ± 6.6a	0.6 ± 1.7ab
Section A ( <i>Trichoderma</i> )	0.0 ± 0.0b	0.0 ± 0.0b	6.1 ± 14.2a	1.1 ± 4.2ab
Section B ( <i>Trichoderma</i> )	0.0 ± 0.0a	0.0 ± 0.0a	2.2 ± 12.2a	0.6 ± 3.0a
Section C ( <i>Trichoderma</i> )	0.0 ± 0.0a	0.0 ± 0.0a	0.0 ± 0.0a	0.0 ± 0.0a

The canes were pruned and treated in March 2009 and March 2010 in a cv Sangiovese vineyard. Re-isolation of the inoculated/applied fungi was carried out after 7 months in both years.

<sup>a</sup>In the whole cane, for each treatment, all the data from the three sections were averaged and statistically analyzed.

<sup>b</sup>Values are means ± standard deviation of three replicates, with 15 canes each. Values in the same row followed by different letters indicate significant differences based on Dunn's test at  $p = 0.05$ .

<sup>c</sup>Sections A, B, and C are obtained at 0.5, 2, and 6 cm from the surface of the pruning wound, respectively.

2 months from application, it was still present in up to 83.3% of the wood fragments plated. Even after 7 months, 60% of the wood fragments were still colonized by the *Trichoderma* strains. The *Tasp* strain, which is the one that is more efficient in direct activity against the wood pathogens tested, was more abundantly isolated in the first part of the season, while both strains were equally present on the wounds in the last part of the season (Table 5).

## Application of *Trichoderma* Formulation in Young Asymptomatic Vineyards

ECDs foliar symptoms appeared at 4–5 years after planting in the untreated plots. The *Trichoderma* treatments delayed the appearance of symptoms by 2 years (V3-Trebbiano and V4-Cabernet Franc) or 3 years (V1-Trebbiano and V2-Lambrusco). Furthermore, in all vineyards, since the first appearance of symptoms, a reduction in the percentage of symptomatic plants in the treated plots was clearly recorded (Figure 3).

The reduction in the annual incidence was confirmed over the years from the onset of foliar symptoms and was significantly different in 80.8% of the year/vineyard combinations, 38.1% of which were at  $P < 0.001$ , 28.6% at  $P < 0.01$ , and 33.3% at  $P < 0.05$  (Figure 3). The percentage of plants that showed symptoms in at least 1 year of the survey ranged from 8.4 to 26% in the untreated plot, whereas in the treated plots the percentage ranged from 1 to 8.7% (Figure 4). A statistically significant reduction of the cumulated incidence in the treated plot was observed the year after (2 years in V2-Lambrusco) the appearance

of the foliar symptoms. This reduction was always significantly different (81.8% at  $P < 0.001$  and 18.2% at  $P < 0.01$ ) throughout the survey (Figure 4).

The low level (A) of foliar symptom severity was the most frequent level of symptom in the first years of disease appearance in these young vineyards (Figure 5). The *Trichoderma* application reduced the incidence of the A symptom; this reduction was noticed in 92.6% of the year/vineyard combination and was statistically significant in 63% of the year/vineyard combinations. The V3-Trebbiano and V4-Cabernet Franc vineyards showed a slight increase of A symptoms in the treated plots only in the last year of application/investigation (Figure 5A), but this was not statistically significant. The incidence of severe symptom (B) was low, except in V4-Cabernet Franc where the severe symptoms were about 5% in 2017 and 2018. In such cases, however, symptom B was significantly lower ( $P < 0.001$ ) in the treated plot (Figure 5B).

The apoplectic symptom (Figure 6) was mainly observed in V2-Cabernet Franc with an incidence of <2.5%. In this vineyard, *Trichoderma* reduced the incidence of apoplexy in 5 out of 6 years (4 years with statistically significant differences).

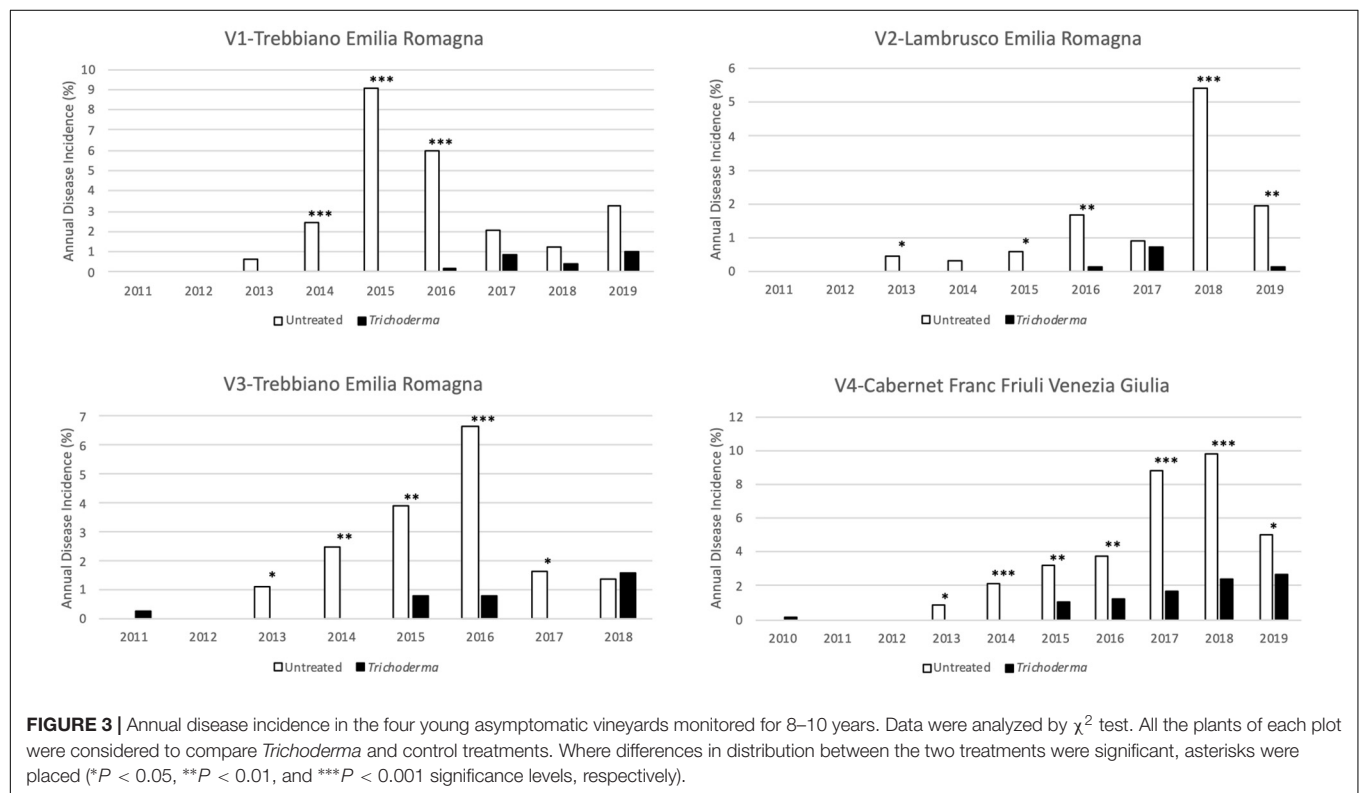
Although death of the vines, as to be expected in such young vineyards, was absent (V1-Trebbiano) or lower than 1.5% in the other vineyards, the application of *Trichoderma* always reduced vine death, with significantly different values in 2 out of 3 vineyards (Figure 7).

As reported in Table 1, the number of vines surveyed in the two plots (treated and untreated) in each vineyard was

**TABLE 5 |** Persistence of the colonization of fresh pruning wounds over time of the *Trichoderma* species applied as a commercial formulation (Remedier®).

Time after treatment	Wood chips analyzed	Wood chips with <i>Trichoderma</i> spp.		<i>Trichoderma</i> species re-isolation (%)		Average temperature (°C)	Average rain (mm)
	No.	No.	%	% <i>T. asperellum</i>	% <i>T. gamsii</i>		
Colonization (100% of the inoculated canes at each sampling time and at least one colony of <i>Trichoderma</i> )							
3 days	90	54	60.0	75	25	9	106.6
7 days	90	60	67.0	78	22	9	106.6
15 days	90	71	78.9	92	8	9	106.6
Persistence (100% of the inoculated canes at each sampling time and at least one colony of <i>Trichoderma</i> )							
1 month	90	81	90.0	50	40	9	106.6
2 months	90	75	83.3	53	30	14.2	11.8
7 months	90	54	60.0	53	47	17.8	17.6

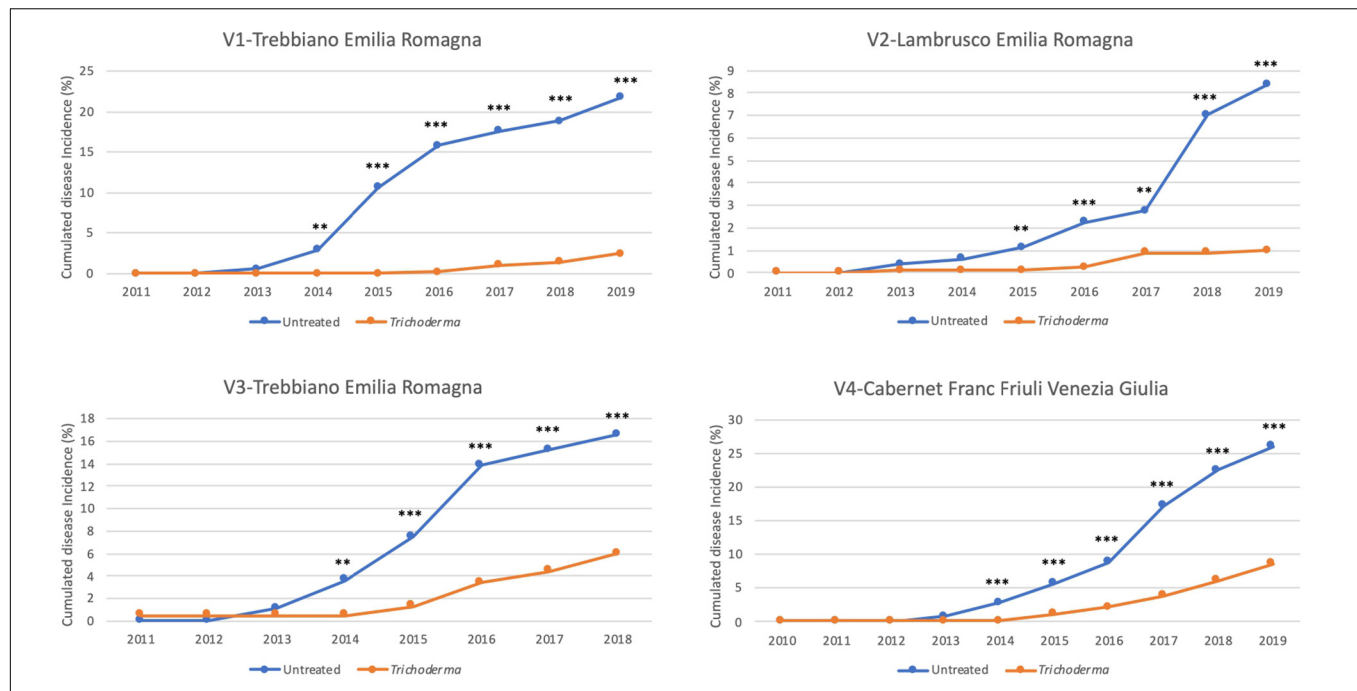
Re-isolation from the first 5 mm of the cut end in the pruning wound of 15 treated canes for each timing was analyzed after variable timing from application. Values are based on the total number of wood chips analyzed (six wood chips per cane, at 15 canes per treatment).



identical in V2 and V4 vineyards and very close in V1 and V4. Therefore, as an overview of the efficacy of the protection of the pruning wounds by the *Trichoderma*-based product, a significant reduction in the symptoms given by the early protection of the wounds (Figure 8) was observed. The reduction in the number of vines that had been symptomatic at least once by the end of the 9-year surveys (cumulated incidence) divided by the total number of symptomatic vines in the two plots of that vineyard was ranging as follows: 88.7 (V1), 88.1 (V2), 71.7 (V3), and 61.7% (V4, which was the vineyard with the most susceptible cultivar).

## DISCUSSION

This study is the first one carried out to test wound protection over a period of several years on several young vineyards that never showed GLSD foliar symptoms before. The study was carried out in commercial vineyards located in different Italian regions planted with different cultivars and showed that the protection activity of *Trichoderma* treatments applied on pruning wounds gives a remarkable reduction on the subsequent development of foliar symptoms and mortality associated with GLSD within the ECDs.



**FIGURE 4 |** Yearly cumulated disease incidence in the four young asymptomatic vineyards monitored for 8–10 years. Data were analyzed by  $\chi^2$  test. All the plants of each plot were considered to compare *Trichoderma* and control treatments. Where differences in distribution between the two treatments were significant, asterisks were placed (\*\* $P < 0.01$  and \*\*\* $P < 0.001$  significance levels, respectively).

The study demonstrated the protective potential of *Trichoderma* applications against some of the associated GTD fungal pathogens *in vitro* and in artificial inoculation experiments. The *in vitro* trials with two single strains of *T. asperellum* and *T. gamsii* present in the commercial formulation applied in the field demonstrated that both strains inhibited or reduced, with different modes of action, the growth of selected GTD pathogens such as *Pch*, *Np*, and *Fmed*. Only *T. asperellum* ICC 012 showed direct activity as competitive growth.

Several studies have already shown that *T. asperellum* strains were effective against different pathogens through a combination of modes of action, such as antibiosis, mycoparasitism, competition for nutrients, volatile compounds, and induced resistance (Verma et al., 2007; Kott et al., 2015; Wu et al., 2017). The inhibitory efficacy of *T. asperellum* ICC 012 increased at higher temperatures, regardless of the pathogen species. This agrees with Qui et al. (2017) who observed that the activity of *T. asperellum* is favored by higher temperatures due to the increased production of conidia in a shorter time.

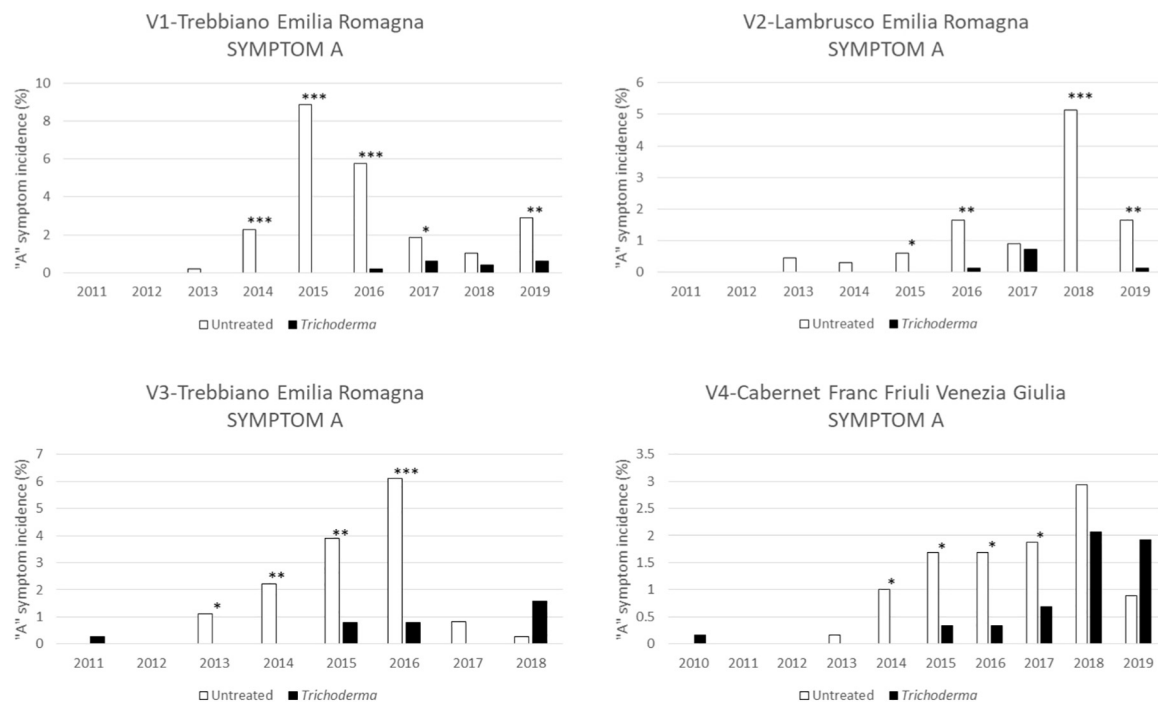
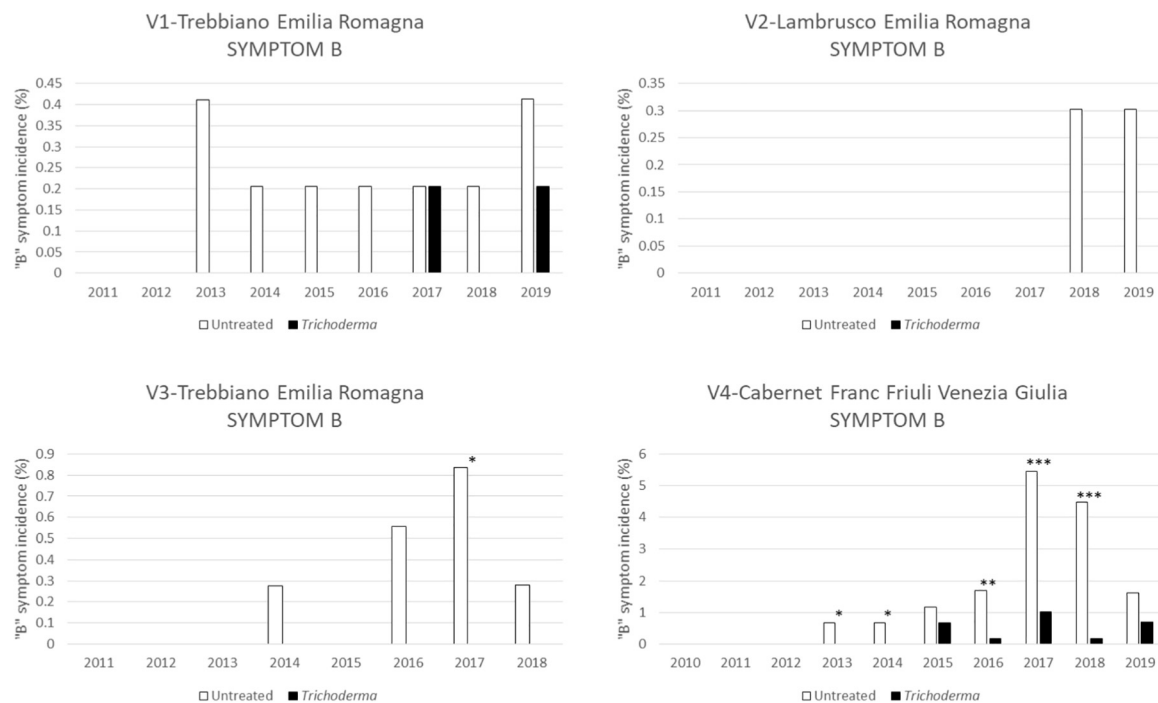
Although *T. gamsii* ICC 080 did not show any activity in competitive growth, it provided indirect activity, presumably due to volatile and non-volatile antibiotic compounds as described by Anees et al. (2010) and Chen et al. (2016). This isolate also showed efficacy at low temperatures. This strain of *T. gamsii* was originally classified as *Trichoderma viride*, which was found to include several cold-tolerant strains (Kredics et al., 2003). Furthermore, *T. gamsii* was indicated as being well suited for low-temperature environments (Rinu et al., 2014). The adaptability

to act at low temperatures can be a relevant feature in pruning operations carried out in the winter season.

The registered product applied in the field trials includes both strains of the two species. The coexistence of different species of *Trichoderma* is conditioned by a variety of extracellular lytic enzymes and secondary metabolites produced by each strain (Cardoza et al., 2005). Carro-Huerga et al. (2021) isolated several species of *Trichoderma* spp. from the bark of grapevine and tested their biocontrol capacity. The authors obtained promising results on the use of combinations of some of the tested species, highlighting the importance of assessing their intra- and inter-specific compatibility for determining their possible combinations.

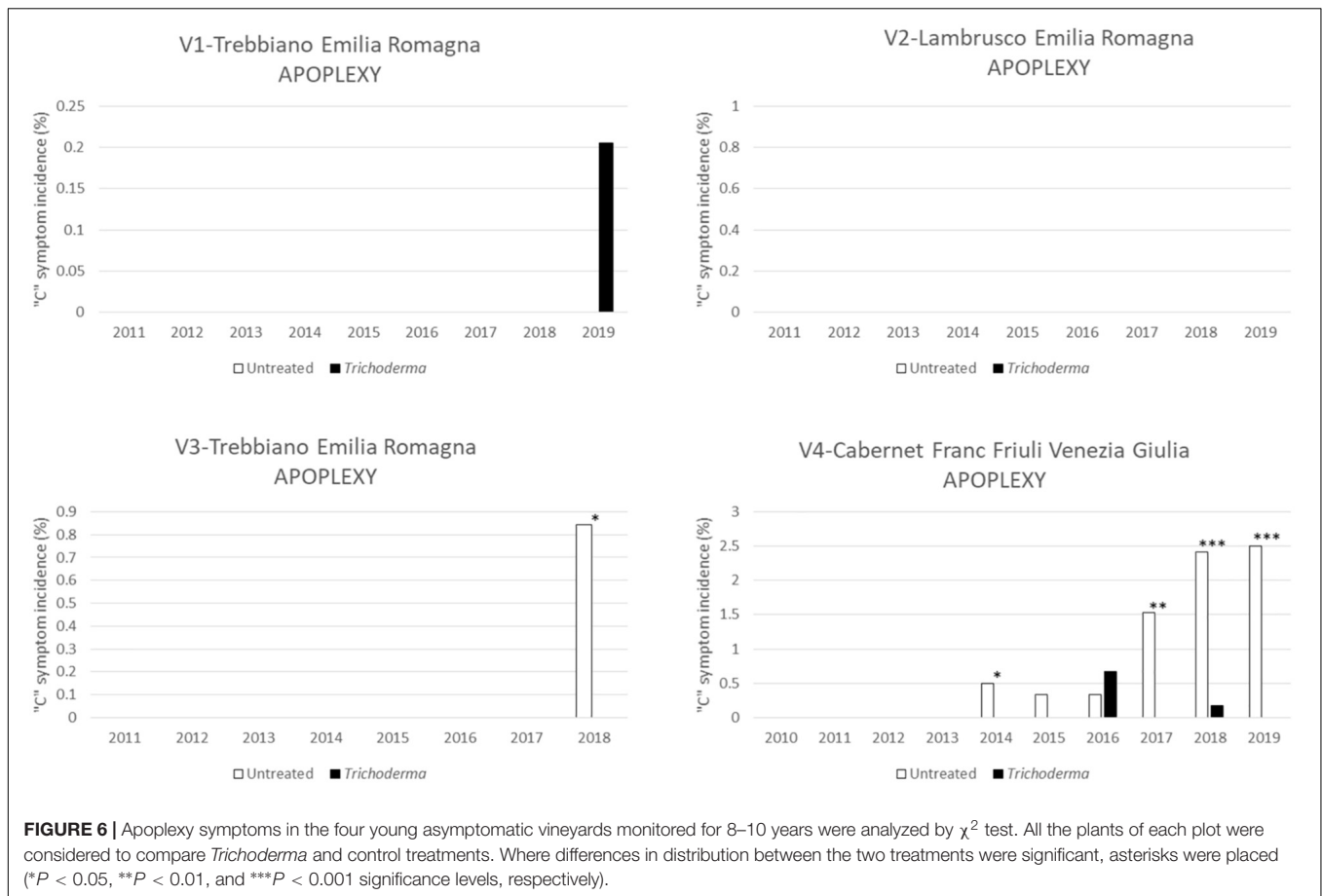
The re-isolation of the two species from inoculated canes during this study confirmed the ability of the strains to persistently colonize the wood, thus providing a long-lasting protection. Nevertheless, their efficiency was strongly influenced by the environment as the protection achieved from *Pch* infections on the most superficial section varied considerably in the 2 years, but in both years, it prevented the deeper colonization of the canes by the pathogen.

The field study offered a new view on the preventive action of these biocontrol agents when applied to fresh wounds by treating new vineyards in the first 1 or 2 years after planting before symptom development. The significant reduction in symptom development (foliar symptoms and apoplexy) recorded in the following years is a clear demonstration of the preventive activity of applications to the pruning wounds in commercial vineyards. It is also clearly demonstrated that preventive actions, as stated

**A****B**

**FIGURE 5 |** Severity of foliar symptoms in the four young asymptomatic vineyards monitored for 8–10 years: Symptom “A”—low severity (**A**) and symptom “B”—high severity (**B**) were analyzed by  $\chi^2$  test. All the plants of each plot were considered to compare *Trichoderma* and control treatments. Where differences in distribution between the two treatments were significant, asterisks were placed (\* $P < 0.05$ , \*\* $P < 0.01$ , and \*\*\* $P < 0.001$  significance levels, respectively).





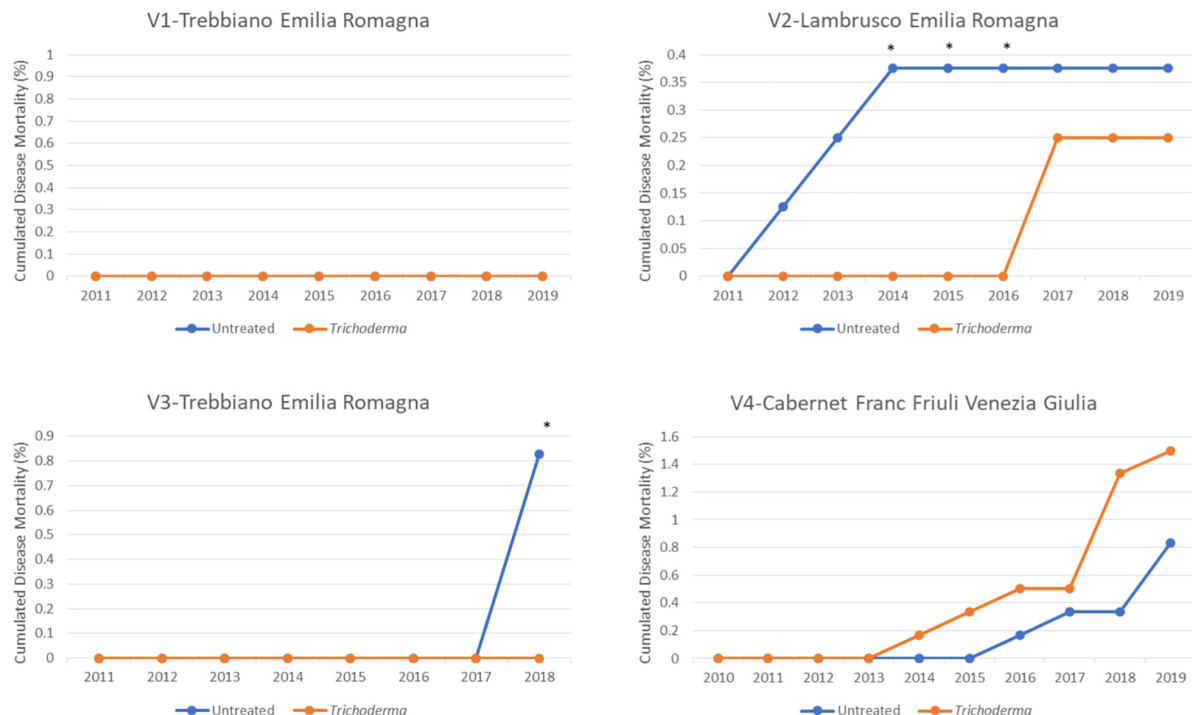
in Hills et al. (2016), are the only really rewarding approach to control GTDs.

In contrast to other trials, the efficacy of symptom reduction was clear since the first year in all four vineyards. The early efficacy in symptom reduction after treatment application may suggest a possible role of the infection in a new wound, close to the bud that will sprout in that year, in foliar disease expression, as also postulated by Larignon (2017). This hypothesis might be indirectly supported by the increasing reduction of symptom incidence over the years in *Trichoderma*-treated plots observed in the present study, assuming that the other factors associated with symptom expression remained unchanged in the treated and untreated plots. Therefore, although more research is required, it might not be excluded that new wound infections can reach the shoots developing from the buds close to that wound, having a higher probability to contribute to the formation of leaf symptoms. Anyway, pruning wound infections, well known as the most important point of entry of wood pathogens in the vineyard (Mugnai et al., 1999; Bertsch et al., 2013), remain of utmost importance for disease spread in vineyards.

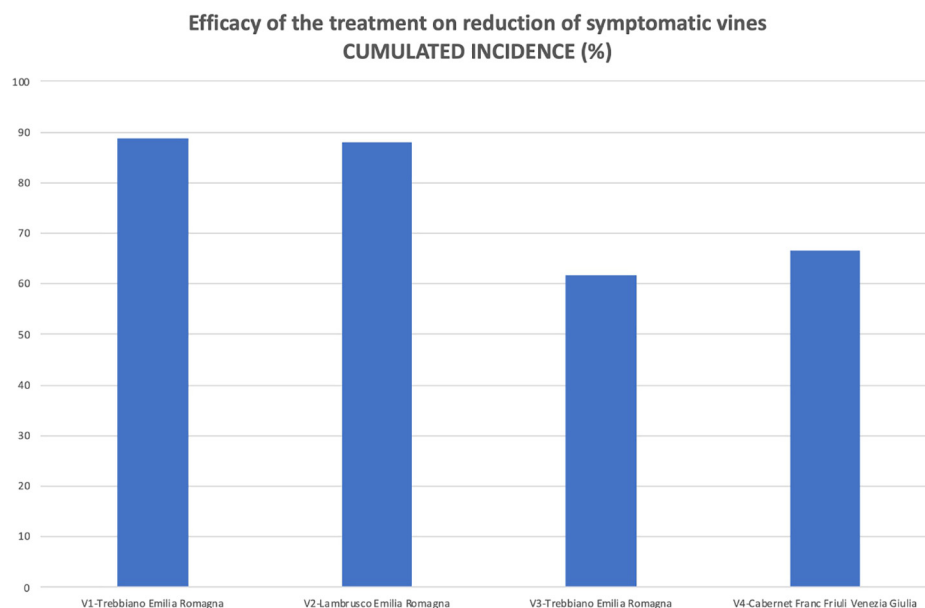
The application of *Trichoderma* was carried out in March when the average daily mean temperatures were not lower than 10°C to favor wood colonization by the biocontrol agents. Temperatures can play an important role in the activity of *Trichoderma* species (Pertot et al., 2016;

Martinez-Diz et al., 2021). Formulations based on *T. atroviride* I-1237 strain (biologically active at temperatures above 5°C) and *T. atroviride* SC1 (biologically active at temperatures equal to or higher than 10°C) showed good colonization when applied after pruning (Prodrutti et al., 2012; Mounier et al., 2016; Reis et al., 2017; Berbegal et al., 2020). As demonstrated by the *in vitro* assay, the presence of *T. gamsii* ICC 080 in the formulation can probably ensure some activity even at low temperatures, as it was shown to be biologically active at 10°C. Overall, temperatures above 10°C, even if not essential, favor the establishment and activity of different species of *Trichoderma* (Kredics et al., 2003). Furthermore, although it is necessary to consider the vineyard climate, environment, and cultural practices, it is also relevant to apply the product as soon as possible, i.e., on a fresh wound. Applications of *Trichoderma* carried out soon after pruning can increase the efficacy of wound protection (Mutawila et al., 2016).

The *Trichoderma* species used in this study showed the ability to effectively colonize wounds, very likely reducing the growth and viability of pathogens that reached the wound surface and providing long-term protection. In trials carried out with the same *Trichoderma* formulation for the protection of pruning wounds in symptomatic vineyards, the activation of host defense mechanisms [as had been described by Zehra et al. (2017)] promoted by the *Trichoderma* application was also hypothesized



**FIGURE 7 |** Cumulated mortality in the four young asymptomatic vineyards after 8–10 years of survey was analyzed by  $\chi^2$  test. All the plants of each plot were considered to compare *Trichoderma* and control treatments. Where differences in distribution between the two treatments were significant, an asterisk was placed ( $P < 0.05$ ).



**FIGURE 8 |** The efficacy of wound protection by the *Trichoderma* commercial product in reducing the number of symptomatic vines was calculated on the final number of vines that showed symptoms at least once during the whole survey time (cumulated incidence at the end of the trial).

(Bigot et al., 2020). The activation of polyphenol biosynthesis (Patel and Saraf, 2017) with effects on *Pch* and other wood pathogens has previously been reported (Mutawila et al., 2011b).

The vineyards treated with *Trichoderma* since the first or second year of planting, when fully asymptomatic, clearly showed a large delay in the onset of leaf symptoms, which moreover

occurred on a much smaller number of plants and with reduced severity.

Other trials carried out in older vineyards and started when the disease was already present report a reduction of 22% of “Esca symptoms” (Bigot et al., 2020) or 50% of GTD symptoms (Mounier et al., 2016). In the present trial, the cumulated incidence was reduced by 61.7–88.7% over the total number of vines showing the disease in the two plots in each vineyard. Young vineyards, usually not yet affected by the disease, are therefore the ideal target for the preventive protection of pruning wounds by *Trichoderma* toward infections that may occur every year through the pruning wounds. Furthermore, early application proved to be effective from the first year of symptom development, while Bigot et al. (2020) revealed that application of the same *Trichoderma* product on older vineyards resulted in significant effects on already symptomatic vineyards only from the third year of application. Nevertheless, even if applications before the first appearance of symptoms are so efficient, applications of *Trichoderma* may be recommended also in older symptomatic vineyards because the reduction in the number of symptomatic plants resulting from the treatment is linked to a reduction in yield losses, not only in terms of the number of productive vines but also in terms of quality losses as demonstrated by the correlation between leaf symptom and loss in quality of must and wine (Calzarano et al., 2004b; Lorrain et al., 2012).

A positive and increasing efficacy of *Trichoderma* applications in reducing apoplexy over the years could also be noticed, leading to the hypothesis that the reduction of annual infection might be correlated with a better plant defense reaction as suggested by Bigot et al. (2020). Biological control agents and *Trichoderma*, in particular, are known to show multiple effects that may have a role in the interaction between the host plant and the pathogen (Yacoub et al., 2016).

Finally, chemical fungicide formulations applied before (i.e., 24 h or a few days) the inoculation of pruning wounds with GTD pathogens proved to be effective in reducing infections (Brown et al., 2021; Martinez-Diz et al., 2021). The level of activity of these chemicals was superior to that of *Trichoderma* or *Bacillus amyloliquefaciens* formulations, and the authors commented on the need of a few days for growth and wound colonization and/or repeated applications of *B. amyloliquefaciens*. However, the ability of *Trichoderma* to get established and persist on pruning wounds for a long time on wounds that remain susceptible for months and against pathogens that produce new inoculum at every rain event is surely a competitive advantage.

In conclusion, the adaptability and versatility of *Trichoderma* species to several climatic and environmental conditions allow the fungus to display its activity under a wide range of climatic conditions (Hermosa et al., 2004), including those in which the grapevine is cultivated. Therefore, the protection of pruning wounds by *Trichoderma* can be likely recommended in all grapevine-growing areas. Moreover, the multiple interactions with the host plant proved to be effective for plant adaptation to climate change (Kashyap et al., 2017).

## CONCLUSION

Since the current management of the disease has limited control options (Mondello et al., 2018a), *Trichoderma* can be an effective tool for the reduction of both pruning wound infections and consequent wood colonization and degradation by fungal pathogens, of the expression of foliar symptoms in the vineyard, and of consequent losses in the quality and quantity of production. The efficiency of early and yearly protection soon after planting suggests the usefulness of applying efficient pruning wound protectants in mother vine fields, both for rootstock and scion vineyards, given the impact of GTD pathogens on nursery material.

Applications proved to be much more effective the earlier that they are carried out, that is, in young asymptomatic vineyards before the occurrence and spread of the disease. The treatment gives the highest efficacy after *Trichoderma* has established and grown on pruning wounds for a few days. Of course, the treatments need to be carried out every year on new wounds to protect the plants from new infections but, in this way, may also contribute to a reduction of the inoculum in the vineyard, which could be a useful integration with the recommended sanitary measures (Gramaje et al., 2018).

The disease reduction obtained by the early protection of pruning wounds by *Trichoderma* does not exclude further positive effects on the disease obtainable by other *Trichoderma* formulations as potential innovative formulations for curative trunk injection treatment (Peil et al., 2020).

Finally, it is important to remember that the *Trichoderma* species assessed in this study proved to be resistant to different pesticides used in viticulture, thus increasing the possibility to integrate chemical and biocontrol methods for the development of an effective and environmentally friendly control strategy for one of the most damaging grapevine trunk diseases worldwide.

This study demonstrated the relevance of pruning wound infections in causing leaf stripe symptoms (GLSD, with or without wood rot) and apoplexy within the Esca complex of diseases. It also confirms that multiple mechanisms and plant interactions are involved in the protective activity of *Trichoderma*, as stated by other authors (Druzhinina et al., 2011). Above all, it highlights the importance of early wound protection in maximizing the preventive activity and persistence of *Trichoderma* on annual infections and symptom expression of diseases in the Esca complex, such as leaf stripe and apoplexy.

## DATA AVAILABILITY STATEMENT

The original contributions presented in the study are included in the article/supplementary material, further inquiries can be directed to the corresponding author/s.

## AUTHOR CONTRIBUTIONS

SD and LM substantially conceptualized the study, designed the trials, acquired the data, and wrote the manuscript. EGM carried out the *in vitro* tests. SM and AP performed the data analysis.

MN, GC, and FO did the *in vivo* inoculations and field surveys. FO and EB substantially contributed in discussion of the results and revision of the manuscript. All authors contributed to the article and approved the submitted version.

## FUNDING

This study was partially funded by the Isagro Srl.

## REFERENCES

- Abbott, W. S. (1925). A method of computing the effectiveness of an insecticide. *J. Econ. Entomol.* 18, 265–267. doi: 10.1093/jee/18.2.265a
- Alfonzo, A., Lo Piccolo, S., Conigliaro, G., Ventorino, V., Burruano, S., and Moschetti, G. (2012). Antifungal peptides produced by *Bacillus amyloliquefaciens* AG1 active against grapevine fungal pathogens. *Ann. Microbiol.* 62, 1593–1599. doi: 10.1007/s13213-011-0415-2
- Aloi, C., Bigot, G., Bortolotti, P., Cotromino, M., Di Marco, S., Faccini, F., et al. (2017). Six years of trials on the activity of Remedier® against Esca disease complex in young and mature Italian vineyards. *Phytopathol. Mediterr.* 56, 566.
- Anees, M., Tronsmo, A., Edel-Hermann, V., Hjeljord, L. G., Heraud, C., and Steinberg, C. (2010). Characterization of field isolates of *Trichoderma* antagonistic against *Rhizoctonia solani*. *Fungal Biol.* 114, 691–701. doi: 10.1016/j.funbio.2010.05.007
- Berbegal, M., Ramón-Albalat, A., León, M., and Armengol, J. (2020). Evaluation of long-term protection from nursery to vineyard provided by *Trichoderma atroviride* SC1 against fungal grapevine trunk pathogens. *Pest Manag. Sci.* 76, 967–977. doi: 10.1002/ps.5605
- Bertsch, C., Ramírez-Suero, M., Magnin-Robert, M., Larignon, P., Chong, J., Abou-Mansour, E., et al. (2013). Grapevine trunk diseases: complex and still poorly understood. *Plant Pathol.* 62, 243–265. doi: 10.1111/j.1365-3059.2012.02674.x
- Bigot, G., Sivilotti, P., Stecchina, M., Lujan, C., Freccero, A., and Mosetti, D. (2020). Long-term effects of *Trichoderma asperellum* and *Trichoderma gamsii* on the prevention of Esca in different vineyards of Northeastern Italy. *Crop Prot.* 137:105264. doi: 10.1016/j.cropro.2020.105264
- Bortolami, G., Farolfi, E., Badel, E., Burlett, R., Cochard, H., Ferrer, N., et al. (2021). Seasonal and long-term consequences of Esca grapevine disease on stem xylem integrity. *J. Exp. Bot.* 72, 3914–3928. doi: 10.1093/jxb/erab117
- Brown, A., Travadon, R., Lawrence, D. P., Torres, G., Zhuang, G., and Baumgartner, K. (2021). Pruning-wound protectants for trunk-disease management in California table grapes. *Crop Prot.* 141:105490. doi: 10.1016/j.cropro.2020.105490
- Bruez, E., Vallance, J., Gautier, A., Laval, V., Compant, S., Maurer, W., et al. (2020). Major changes in grapevine wood microbiota are associated with the onset of Esca, a devastating trunk disease. *Environ. Microbiol.* 22, 5189–5206. doi: 10.1111/1462-2920.15180
- Calzarano, F., D'Agostino, V., Seghetti, L., and Amalfitano, C. (2007). Foliar treatment of Esca-proper affected vines with nutrients and bioactivators. *Phytopathol. Mediterr.* 46, 207–217. doi: 10.14601/Phytopathol\_Mediterr-2152
- Calzarano, F., and Di Marco, S. (2018). Further evidence that calcium, magnesium and seaweed mixtures reduce grapevine leaf stripe symptoms and increase grape yield. *Phytopathol. Mediterr.* 57, 459–471. doi: 10.14601/phyto-23636
- Calzarano, F., Di Marco, S., D'Agostino, V., Schiff, S., and Mugnai, L. (2014). Grapevine leaf stripe disease symptoms (Esca complex) are reduced by a nutrients and seaweed mixture. *Phytopathol. Mediterr.* 53, 543–558. doi: 10.14601/phyto-15253
- Calzarano, F., Osti, F., Baránek, M., and Di Marco, S. (2018). Rainfall and temperature influence expression of foliar symptoms of grapevine leaf stripe disease (Esca complex) in vineyards. *Phytopathol. Mediterr.* 57, 488–505. doi: 10.14601/phyto-23787
- Calzarano, F., Osti, F., D'Agostino, V., Pepe, A., Della Pelle, F., De Rosso, M., et al. (2017a). Levels of phytoalexins in vine leaves with different degrees of grapevine leaf stripe disease symptoms (Esca complex of diseases). *Phytopathol. Mediterr.* 56, 494–501. doi: 10.14601/phyto-22055
- Calzarano, F., Osti, F., D'Agostino, V., Pepe, A., and Di Marco, S. (2017b). Mixture of calcium, magnesium, and seaweed affects leaf phytoalexin contents and grape ripening on vines with grapevine leaf stripe disease. *Phytopathol. Mediterr.* 56, 445–457. doi: 10.14601/Phytopathol\_Mediterr-22023
- Calzarano, F., Pagnani, G., Pisante, M., Bellocci, M., Cillo, G., Metruccio, E. G., et al. (2021). Factors involved on tiger-stripe foliar symptom expression of Esca of grapevine. *Plants* 10:1041. doi: 10.3390/plants10061041
- Calzarano, F., Seghetti, L., Del Carlo, M., and Cichelli, A. (2004b). Effect of Esca on the quality of berries, musts and wines. *Phytopathol. Mediterr.* 43, 125–135. doi: 10.14601/Phytopathol\_Mediterr-1729
- Calzarano, F., Di Marco, S., and Cesari, A. (2004a). Benefit of fungicide treatment after trunk renewal of vines with different types of Esca necrosis. *Phytopathol. Mediterr.* 43, 116–124. doi: 10.14601/Phytopathol\_Mediterr-1725
- Cardoza, R., Hermosa, R., Vizcaino, J., Sanz, L., Monte, E., and Gutiérrez, S. (2005). “Secondary metabolites produced by *Trichoderma* and their importance in the biocontrol process,” in *Microorganisms for Industrial Enzymes and Biocontrol*, eds E. Mellado and J. L. Barredo (Trivandrum: Research Signpost).
- Carro-Huerga, G., Mayo-Prieto, S., Rodríguez-González, Á., González-López, Ó., Gutiérrez, S., and Casquero, P. A. (2021). Influence of fungicide application and vine age on *Trichoderma* diversity as source of biological control agents. *Agronomy* 11:446. doi: 10.3390/agronomy11030446
- Chen, J. L., Sun, S. Z., Miao, C. P., Wu, K., Chen, Y. W., Xu, L. H., et al. (2016). Endophytic *Trichoderma gamsii* YIM PH30019: a promising biocontrol agent with hyperosmolar, mycoparasitism, and antagonistic activities of induced volatile organic compounds on root-rot pathogenic fungi of *Panax notoginseng*. *J. Ginseng Res.* 40, 315–324. doi: 10.1016/j.jgr.2015.09.006
- Claverie, M., Notaro, M., Fontaine, F., and Wery, J. (2020). Current knowledge on grapevine trunk diseases with complex etiology: a systemic approach. *Phytopathol. Mediterr.* 59, 29–53. doi: 10.14601/phyto11150
- Del Frari, G., Oliveira, H., and Boavida Ferreira, R. (2021). White rot fungi (Hymenochaetales) and Esca of grapevine: insights from recent microbiome studies. *J. Fungi* 7:770. doi: 10.3390/jof7090770
- Di Marco, S., and Osti, F. (2007). Applications of *Trichoderma* to prevent *Phaeoemiella chlamydospora* infections in organic nurseries. *Phytopathol. Mediterr.* 46, 73–83. doi: 10.14601/Phytopathol\_Mediterr-1851
- Di Marco, S., and Osti, F. (2008). Foliar symptom expression of wood decay in *Actinidia deliciosa* in relation to environmental factors. *Plant Dis.* 92, 1150–1157. doi: 10.1094/pdis-92-1150
- Di Marco, S., Osti, F., Calzarano, F., Roberti, R., Veronesi, A., and Amalfitano, C. (2011a). Effects of grapevine applications of fosetyl-aluminium formulations for downy mildew control on “Esca” and associated fungi. *Phytopathol. Mediterr.* 50, S285–S299. doi: 10.14601/Phytopathol\_Mediterr-9802
- Di Marco, S., Osti, F., and Mugnai, L. (2011b). First studies on the potential of a copper formulation for the control of leaf stripe disease within Esca complex in grapevine. *Phytopathol. Mediterr.* 50, S300–S309. doi: 10.14601/phyto-10233
- Di Marco, S., Osti, F., and Cesari, A. (2004). Experiments on the control of Esca by *Trichoderma*. *Phytopathol. Mediterr.* 43, 108–115. doi: 10.14601/Phytopathol\_Mediterr-1730
- Di Marco, S., Osti, F., Roberti, R., Calzarano, F., and Cesari, A. (2002). Attività di specie di *Trichoderma* nei confronti di *Phaeoemiella chlamydospora*, patogeno associato al mal dell'Esca della vite. *Atti Giornate Fitopatol.* 2, 419–424.

## ACKNOWLEDGMENTS

The authors would like to thank Franca Reggiori and Filippo Faccini from Isagro Srl, Roberta Nannini and Paolo Bortolotti from Regional Plant-Health Service (Regione Emilia-Romagna), and Giovanni Bigot (Perleuve Srl) for the technical and logistical support in performing field surveys. The authors would also like to thank Alan Phillips for providing a careful review of this manuscript.



- Diaz, G. A., Auger, J., Ximena, B., Bordeu, E., and Latorre, B. A. (2013). Prevalence and pathogenicity of fungi associated with grapevine trunk diseases in Chilean vineyards. *Crop. Prot.* 40, 327–339. doi: 10.1016/j.cropro.2013.06.008
- Druzhinina, I. S., Seidl-Seiboth, V., Herrera-Estrella, A., Horwitz, B. A., Kenerley, C. M., Monte, E., et al. (2011). *Trichoderma*: the genomics of opportunistic success. *Nat. Rev. Microbiol.* 9, 749–759. doi: 10.1038/nrmicro2637
- Egger, E., Marinelli, E., and Storch, P. (1998). “Tecnica del rinnovo tempestivo delle branche in viti colpite dal mal dell’Esca nel comprensorio di Montalcino,” in *Atti del Convegno “Il mal dell’Esca Nella Viticoltura Toscana”*. Montalcino, Siena, 14 Novembre 1997, Arsia, 33–39.
- Elena, G., and Luque, J. (2016). Seasonal susceptibility of grapevine pruning wounds and cane colonization in Catalonia, Spain following artificial infection with *Diplodia seriata* and *Phaeoconiella chlamydospora*. *Plant Dis.* 100, 1651–1659. doi: 10.1094/PDIS-10-15-1186-RE
- Eskalen, A., Feliciano, A., and Gubler, W. (2007). Susceptibility of grapevine pruning wounds and symptom development in response to infection by *Phaeoacremonium aleophilum* and *Phaeoconiella chlamydospora*. *Plant Dis.* 91, 1100–1104. doi: 10.1094/Pdis-91-9-1100
- Eskalen, A., and Gubler, W. D. (2001). Association of spores of *Phaeoconiella chlamydospora*, *Phaeoacremonium inflatipes*, and *P. aleophilum* with grapevine cordons in California. *Phytopathol. Mediterr.* 40, S429–S432. doi: 10.14601/phyto-1613
- Feliciano, A., Eskalen, A., and Gubler, W. (2004). Differential susceptibility of three grapevine cultivars to *Phaeoconiella chlamydospora* in California. *Phytopathol. Mediterr.* 43, 66–69. doi: 10.14601/Phytopathol\_Mediterr-1727
- Fontaine, F., Pinto, C., Vallet, J., Clément, C., Gomes, A. C., and Spagnolo, A. (2016). The effects of Grapevine Trunk Diseases (GTDs) on vine physiology. *Eur. J. Plant Pathol.* 144, 707–721. doi: 10.1007/s10658-015-0770-0
- Fourie, P. H., and Halleen, F. (2004). Proactive control of petri disease of grapevine through treatment of propagation material. *Plant Dis.* 88, 1241–1245. doi: 10.1094/PDIS.2004.88.11.1241
- Fourie, P. H., and Halleen, F. (2006). Chemical and biological protection of grapevine propagation material from trunk disease pathogens. *Eur. J. Plant Pathol.* 116, 255–265. doi: 10.1007/s10658-006-9057-9
- Gramaje, D., and Di Marco, S. (2015). Identifying practices likely to have impacts on grapevine trunk disease infections: a European nursery survey. *Phytopathol. Mediterr.* 54, 313–324. doi: 10.14601/Phytopathol\_Mediterr-16317
- Gramaje, D., Úrbez-Torres, J. R., and Sosnowski, M. R. (2018). Managing grapevine trunk diseases with respect to etiology and epidemiology: current strategies and future prospects. *Plant Dis.* 102, 12–39. doi: 10.1094/PDIS-04-17-0512-FE
- Guerin-Dubrana, L., Fontaine, F., and Mugnai, L. (2019). Grapevine trunk disease in European and Mediterranean vineyards: occurrence, distribution and associated disease-affecting cultural factors. *Phytopathol. Mediterr.* 58, 49–71. doi: 10.14601/phyto-25153
- Halleen, F., van der Vyver, J., Fourie, P. H., and Schreuder, W. (2001). Effect of *Trichoderma* treatments on the occurrence of decline pathogens in the roots and rootstocks of nursery grapevines. *Phytopathol. Mediterr.* 40, 473–478. doi: 10.14601/Phytopathol\_Mediterr-1619
- Harman, G., Howell, C., Viterbo, A., Chet, I., and Lorito, M. (2004). *Trichoderma* species — opportunistic, avirulent plant symbionts. *Nat. Rev. Microbiol.* 2, 43–56. doi: 10.1038/nrmicro797
- Hermosa, M. R., Keck, E., Chamorro, I., Rubio, B., Sanz, L., Vizcaino, J. A., et al. (2004). Genetic diversity shown in *Trichoderma* biocontrol isolates. *Mycol. Res.* 108, 897–906. doi: 10.1017/S0953756204000358
- Hills, V., Lubell, M., Kaplan, J., Doll, D., and Baumgartner, K. (2016). The role of pest control advisers in preventative management of grapevine trunk diseases. *Phytopathology* 106, 339–347. doi: 10.1094/PHYTO-10-15-0250-R
- Hunt, J. S., Gale, D. S. J., and Harvey, I. C. (2001). Evaluation of *Trichoderma* as bio-control for protection against wood-invading fungi implicated in grapevine trunk diseases. *Phytopathol. Mediterr.* 40, 485–486. doi: 10.14601/Phytopathol\_Mediterr-1605
- Kashyap, P. L., Rai, P., Srivastava, A. K., and Kumar, S. (2017). *Trichoderma* for climate resilient agriculture. *World J. Microbiol. Biotechnol.* 33:155. doi: 10.1007/s11274-017-2319-1
- Kott, M., Gigolashvili, T., Großkinsky, K., and Piechulla, B. (2015). *Trichoderma* volatiles affecting *Arabidopsis*: from inhibition to protection against phytopathogenic fungi. *Front. Microbiol.* 6:995. doi: 10.3389/fmicb.2015.00995
- Kotze, C., Van Niekerk, J., Halleen, F., Mostert, L., and Fourie, P. (2011). Evaluation of biocontrol agents for grapevine pruning wound protection against trunk pathogen infection. *Phytopathol. Mediterr.* 50, 247–263.
- Kredics, L., Antal, Z., Manczinger, L., Szekeres, A., Kevei, F., and Nagy, E. (2003). Influence of environmental parameters on *Trichoderma* strains with biocontrol potential. *Food Technol. Biotechnol.* 41, 37–42.
- Larignon, P. (2017). Effect of sodium arsenite on the life cycles of the pathogenic agents involved in wood grapevine diseases. *Phytopathol. Mediterr.* 56:537. doi: 10.14601/phyto-21865
- Larignon, P., and Dubos, B. (1997). Fungi associated with esca disease in grapevine. *Eur. J. Plant Pathol.* 103, 147–157. doi: 10.1023/A:1008638409410
- Lecomte, P., Diarra, B., Carbonneau, A., Rey, P., and Chevrier, C. (2018). Esca of grapevine and training practices in France: results of a 10-year survey. *Phytopathol. Mediterr.* 57, 472–487. doi: 10.14601/phyto-22025
- Lengyel, S., Gold, R. E., Fischer, J., Yemelin, A., Thines, E., and Kühn, A. (2019). Early detection project – detection and quantification of *Phaeoconiella chlamydospora* and *Botryosphaeria* spp. in *Vitis vinifera* wood samples. *Phytopathol. Mediterr.* 58, 406–407. doi: 10.14601/phyto-10627
- Lorrain, B., Ky, I., Pasquier, G., Jourdes, M., Guérin-Dubrana, L., Gény, L., et al. (2012). Effect of Esca disease on the phenolic and sensory attributes of Cabernet Sauvignon grapes musts and wines. *Aust. J. Grape Wine Res.* 18, 64–72. doi: 10.1111/j.1755-0238.2011.00172.x
- Marchi, G., Peduto, F., Mugnai, L., Di Marco, S., Calzarano, F., and Surico, G. (2006). Some observations on the relationship on manifest and hidden Esca to rainfall. *Phytopathol. Mediterr.* 45, 117–126. doi: 10.1400/phyto-52267
- Markakis, E. A., Koubouris, G. C., Sergeantani, C. K., and Ligoigakis, E. K. (2017). Evaluation of Greek grapevine cultivars for resistance to *Phaeoconiella chlamydospora*. *Eur. J. Plant Pathol.* 149, 277–283. doi: 10.1007/s10658-017-1186-9
- Martinez-Diz, M. P., Díaz-Losada, E., Díaz-Fernández, A., Bouzas-Cid, Y., and Gramaje, D. (2021). Protection of grapevine pruning wounds against *Phaeoconiella chlamydospora* and *Diplodia seriata* by commercial biological and chemical methods. *Crop Prot.* 143:105465. doi: 10.1016/j.cropro.2020.105465
- Mary, S., Laveau, C., Lecomte, P., Birebent, M., and Roby, J. P. (2017). Impact of grafting type on Esca foliar symptoms. *Oeno One* 51, 221–230. doi: 10.20870/oeno-one.2016.50.4.1408
- Mondello, V., Larignon, P., Armengol, J., Kortekamp, A., Vaczy, K., Prezman, F., et al. (2018a). Management of grapevine trunk diseases: knowledge transfer, current strategies and innovative strategies adopted in Europe. *Phytopathol. Mediterr.* 57, 369–383. doi: 10.14601/phyto-23942
- Mondello, V., Songy, A., Battiston, E., Pinto, C., Coppin, C., Trotel-Aziz, P., et al. (2018b). Grapevine trunk diseases: a review of fifteen years of trials for their control with chemicals and biocontrol agents. *Plant Dis.* 102, 1189–1217. doi: 10.1094/PDIS-08-17-1181-FE
- Moretti, S., Pacetti, A., Pierron, R., Kassemeyer, H. H., Fischer, M., Pèros, J. P., et al. (2021). *Fomitiporia mediterranea* M. Fisch., the historical Esca agent: a comprehensive review on the main grapevine wood rot agent in Europe. *Phytopathol. Mediterr.* 60, 351–379. doi: 10.36253/phyto-13021
- Mounier, E., Boulisset, F., Elbaz, N., Dubournet, P., and Pajot, E. (2016). “Esquive® WP limits development of grapevine wood diseases and reductions in the productive potential of land,” in *Proceedings of the 5th Conférence Internationale sur les Méthodes Alternatives de Protection des Plantes, 11–13 May 2015, Nouveau Siècle, Lille*, 251–261.
- Mugnai, L., Graniti, A., and Surico, G. (1999). Esca (black measles) and brown wood streaking: two old and elusive diseases of grapevines. *Plant Dis.* 83, 404–418. doi: 10.1094/pdis.1999.83.5.404
- Mutawila, C., Fourie, P. H., Halleen, F., and Mostert, L. (2011a). Grapevine cultivar variation to pruning wound protection by *Trichoderma* species against trunk pathogens. *Phytopathol. Mediterr.* 50, S264–S276. doi: 10.14601/phyto-8981
- Mutawila, C., Fourie, P. H., Halleen, F., and Mostert, L. (2011b). Histo-pathology study of the growth of *Trichoderma harzianum*, *Phaeoconiella chlamydospora* and *Eutypa lata* on grapevine pruning wounds. *Phytopathol. Mediterr.* 50, 46–60. doi: 10.14601/Phytopathol\_Mediterr-8643
- Mutawila, C., Vinale, F., Halleen, F., Lorito, M., and Mostert, L. (2016). Isolation, production and *in vitro* effects of the major secondary metabolites produced

- by *Trichoderma* species used for the control of grapevine trunk diseases. *Plant Pathol.* 65, 104–113. doi: 10.1111/ppa.12385
- Ouadi, L., Bruez, E., Bastien, S., Yacoub, A., Coppin, C., Guérin-Dubrana, L., et al. (2021). Sap flow disruption in grapevine is the early signal predicting the structural, functional, and genetic responses to Esca disease. *Front. Plant Sci.* 12:695846. doi: 10.3389/fpls.2021.695846
- Pacetti, A., Moretti, S., Pinto, C., Compant, S., Farine, S., Bertsch, C., et al. (2021). Trunk surgery as a tool to reduce foliar symptoms in diseases of the Esca complex and its influence on vine wood microbiota. *J. Fungi* 7:521. doi: 10.3390/jof7070521
- Patel, S., and Saraf, M. (2017). Biocontrol efficacy of *Trichoderma asperellum* MSST against tomato wilting by *Fusarium oxysporum* f. sp. *lycopersici*. *Arch. Phytopathol. Pflanzenschutz* 50, 228–238. doi: 10.1080/03235408.2017.1287236
- Peil, S., Beckers, S. J., Fischer, J., and Wurm, F. R. (2020). Biodegradable, lignin-based encapsulation enables delivery of *Trichoderma reesei* with programmed enzymatic release against grapevine trunk diseases. *Mater. Today Biol.* 7:100061. doi: 10.1016/j.mtbio.2020.100061
- Pertot, I., Prodorutti, D., Colombini, A., and Pasini, L. (2016). *Trichoderma atroviride* SC1 prevents *Phaeoconiella chlamydospora* and *Phaeoacremonium aleophilum* infection of grapevine plants during the grafting process in nurseries. *Biocontrol* 61, 257–267. doi: 10.1007/s10526-016-9723-6
- Pouzoulet, J., Pivovarov, A. L., Santiago, L. S., and Rolshausen, P. E. (2014). Can vessel dimension explain tolerance toward fungal vascular wilt diseases in woody plants? Lessons from Dutch elm disease and Esca disease in grapevine. *Front. Plant Sci.* 5:253. doi: 10.3389/fpls.2014.00253
- Prodorutti, D., Pellegrini, A., Colombini, A., Charlot, B., and Pertot, I. (2012). *Trichoderma atroviride* SC1 is a good wound colonizer and can protect grapevine from infections of *Phaeoacremonium aleophilum* and *Phaeoconiella chlamydospora* in nurseries and vineyards. *Phytopathol. Mediterr.* 51, 447–448. doi: 10.14601/phyto-11353
- Qui, Z., Wu, X., Zhang, J., and Huang, C. (2017). High temperature enhances the ability of *Trichoderma asperellum* to infect *Pleurotus ostreatus* mycelia. *PLoS One* 12:e0187055. doi: 10.1371/journal.pone.0187055
- Reis, P., Letousey, P., and Rego, C. (2017). *Trichoderma atroviride* strain I-1237 protects pruning wounds against grapevine wood pathogens. *Phytopathol. Mediterr.* 56:580.
- Reis, P., Magnin-Robert, M., Nascimento, T., Spagnolo, A., Abou-Mansour, E., Fioretti, C., et al. (2016). Reproducing *Botryosphaeria* dieback foliar symptoms in a simple model system. *Plant Dis.* 100, 1071–1079. doi: 10.1094/PDIS-10-15-1194-RE
- Rinu, K., Sati, P., and Pandey, A. (2014). *Trichoderma gamsii* (NFCCI 2177): a newly isolated endophytic, psychrotolerant, plant growth promoting, and antagonistic fungal strain. *J. Basic Microbiol.* 54, 408–417. doi: 10.1002/jobm.201200579
- Rolshausen, P. E., Urbez-Torres, J. R., Rooney-Latham, S., Eskalen, A., Smith, R. J., and Gubler, W. D. (2010). Evaluation of pruning wound susceptibility and protection against fungi associated with grapevine trunk diseases. *Am. Soc. Enol. Vitic.* 61, 113–119.
- Serra, S., Mannoni, M. A., and Ligios, V. (2008). Studies on the susceptibility of pruning wounds to infection by fungi involved in grapevine wood diseases in Italy. *Phytopathol. Mediterr.* 47, 234–246. doi: 10.14601/Phytopathol\_Mediterr-2727
- Sparapano, L., Graniti, A., and Bruno, G. (2001). Three-year observation of grapevines cross-inoculated with Esca-associated fungi. *Phytopathol. Mediterr.* 40, 376–386. doi: 10.14601/Phytopathol\_Mediterr-1643
- Surico, G. (2009). Towards a redefinition of the diseases within the Esca complex of grapevine. *Phytopathol. Mediterr.* 48, 5–10. doi: 10.14601/Phytopathol\_Mediterr-2870
- Surico, G., Bandinelli, R., Braccini, P., Di Marco, S., Marchi, G., Mugnai, L., et al. (2004). On the factors that may have influenced the Esca epidemic in the eighties in Tuscany. *Phytopathol. Mediterr.* 43, 136–143. doi: 10.14601/Phytopathol\_Mediterr-1734
- Van Niekerk, J., Bester, W., Halleen, F., Crous, P., and Fourie, P. (2011). The distribution and symptomatology of grapevine trunk disease pathogens are influenced by climate. *Phytopathol. Mediterr.* 50, 98–111. doi: 10.14601/Phytopathol\_Mediterr-8645
- Verma, M., Satinder, K., Brar, R. D., Tyagi, J. R., Surampalli, R. Y., and Valero, J. R. (2007). Antagonistic fungi, *Trichoderma* spp.: panoply of biological control. *Biochem. Eng. J.* 37, 1–20. doi: 10.1016/j.bej.2007.05.012
- Wu, Q., Sun, R., Ni, M., Yu, J., Li, Y., Yu, C., et al. (2017). Identification of a novel fungus, *Trichoderma asperellum* GDFS1009, and comprehensive evaluation of its biocontrol efficacy. *PLoS One* 12:e0179957. doi: 10.1371/journal.pone.0179957
- Yacoub, A., Gerbore, J., Magnin, N., Chambon, P., Dufour, M. C., Corio-Costet, M. F., et al. (2016). Ability of *Pythium oligandrum* strains to protect *Vitis vinifera* L., by inducing plant resistance against *Phaeoconiella chlamydospora*, a pathogen involved in Esca, a grapevine trunk disease. *Biol. Control* 92, 7–16. doi: 10.1016/j.biocontrol.2015.08.005
- Zehra, A., Meena, M., Dubey, M. K., Aamir, M., and Upadhyay, R. S. (2017). Synergistic effects of plant defense elicitors and *Trichoderma harzianum* on enhanced induction of antioxidant defense system in tomato against *Fusarium wilt* disease. *Bot. Stud.* 58:44. doi: 10.1186/s40529-017-0198-2

**Conflict of Interest:** The authors declare that the research was conducted in the absence of any commercial or financial relationships that could be construed as a potential conflict of interest.

**Publisher's Note:** All claims expressed in this article are solely those of the authors and do not necessarily represent those of their affiliated organizations, or those of the publisher, the editors and the reviewers. Any product that may be evaluated in this article, or claim that may be made by its manufacturer, is not guaranteed or endorsed by the publisher.

Copyright © 2022 Di Marco, Metruccio, Moretti, Nocentini, Carella, Pacetti, Battiston, Osti and Mugnai. This is an open-access article distributed under the terms of the Creative Commons Attribution License (CC BY). The use, distribution or reproduction in other forums is permitted, provided the original author(s) and the copyright owner(s) are credited and that the original publication in this journal is cited, in accordance with accepted academic practice. No use, distribution or reproduction is permitted which does not comply with these terms.



# *Myxococcus xanthus* R31 Suppresses Tomato Bacterial Wilt by Inhibiting the Pathogen *Ralstonia solanacearum* With Secreted Proteins

Honghong Dong<sup>1</sup>, Xin Xu<sup>1,2</sup>, Ruixiang Gao<sup>1,2</sup>, Yueqiu Li<sup>1</sup>, Anzhang Li<sup>1</sup>, Qing Yao<sup>1,3</sup> and Honghui Zhu<sup>1\*</sup>

<sup>1</sup> Key Laboratory of Agricultural Microbiomics and Precision Application – Ministry of Agriculture and Rural Affairs, Guangdong Provincial Key Laboratory of Microbial Culture Collection and Application, State Key Laboratory of Applied Microbiology Southern China, Guangdong Microbial Culture Collection Center (GDMCC), Institute of Microbiology, Guangdong Academy of Sciences, Guangzhou, China, <sup>2</sup> Guangdong Province Key Laboratory of Microbial Signals and Disease Control, College of Plant Protection, South China Agricultural University, Guangzhou, China, <sup>3</sup> Guangdong Province Key Laboratory of Microbial Signals and Disease Control, College of Horticulture, South China Agricultural University, Guangzhou, China

## OPEN ACCESS

### Edited by:

Jochen Fischer,  
Institut für Biotechnologie und  
Wirkstoff-Forschung (IBWF), Germany

### Reviewed by:

Juanni Chen,  
Southwest University, China  
Yong-Qiang He,  
Guangxi University, China

### \*Correspondence:

Honghui Zhu  
zhuhh@gdim.cn

### Specialty section:

This article was submitted to  
Microbe and Virus Interactions with  
Plants,  
a section of the journal  
Frontiers in Microbiology

Received: 24 October 2021

Accepted: 02 December 2021

Published: 07 February 2022

### Citation:

Dong H, Xu X, Gao R, Li Y, Li A,  
Yao Q and Zhu H (2022) *Myxococcus*  
*xanthus* R31 Suppresses Tomato  
Bacterial Wilt by Inhibiting the  
Pathogen *Ralstonia solanacearum*  
With Secreted Proteins.  
Front. Microbiol. 12:801091.  
doi: 10.3389/fmicb.2021.801091

The pathogenic bacterium *Ralstonia solanacearum* caused tomato bacterial wilt (TBW), a destructive soil-borne disease worldwide. There is an urgent need to develop effective control methods. Myxobacteria are microbial predators and are widely distributed in the soil. Compared with other biocontrol bacteria that produce antibacterial substances, the myxobacteria have great potential for biocontrol. This study reports a strain of *Myxococcus xanthus* R31 that exhibits high antagonistic activity to *R. solanacearum*. Plate test indicated that the strain R31 efficiently predated *R. solanacearum*. Pot experiments showed that the biocontrol efficacy of strain R31 against TBW was 81.9%. Further study found that the secreted protein precipitated by ammonium sulfate had significant lytic activity against *R. solanacearum* cells, whereas the ethyl acetate extract of strain R31 had no inhibitory activity against *R. solanacearum*. Substrate spectroscopy assay and liquid chromatography-tandem mass spectrometry (LC-MS/MS) analysis of secreted proteins showed that some peptidases, lipases, and glycoside hydrolases might play important roles and could be potential biocontrol factors involved in predation. The present study reveals for the first time that the use of strain *M. xanthus* R31 as a potential biocontrol agent could efficiently control TBW by predation and secreting extracellular lyase proteins.

**Keywords:** *Myxococcus xanthus* R31, *Ralstonia solanacearum*, predation, biocontrol, extracellular proteins, tomato bacteria wilt

## INTRODUCTION

Tomato bacterial wilt (TBW) caused by *Ralstonia solanacearum* is a devastating soil-borne disease (Salanoubat et al., 2002). A survey indicated that *R. solanacearum* ranks second among the top 10 most concerned pathogenic bacteria based on the scientific and economic importance (Mansfield et al., 2012). The pathogen *R. solanacearum* is a complex species with obvious physiological differentiation and genetic diversity and a very wide host range. *R. solanacearum* can infect more

than 200 species in 54 families of plants (Prior et al., 2016), including tomato, tobacco, potato, banana, pepper, etc., thereby posing a serious threat to food security (Zhang et al., 2020). TBW is a vascular disease that often breaks out under the conditions of high temperatures and high humidity (Choi et al., 2020). Pathogen infection can lead to substantial crop production losses, especially in tropical, subtropical, and other regions with warm temperature (Wang et al., 2018). Now, how to achieve green and efficient control of TBW is a major concern that needs to be solved urgently in agricultural production worldwide.

The traditional methods of controlling soil-borne diseases mainly include physical control and chemical control (Posas et al., 2007). These methods can effectively reduce the number of rhizosphere pathogens and the occurrence of diseases in a short period of time. However, the non-specific bactericidal chemicals not only target the pathogenic bacteria, but also destroy the plant rhizosphere microbial community structure and microecological balance. Consequently, these traditional methods are not conducive for the sustainable development of plant rhizosphere and disease control (Liar et al., 2015). The rhizosphere microbiome is known as the “second genome” of crops and plays a pivotal role in maintaining crop health. Beneficial rhizosphere bacteria-based biocontrol can effectively protect the plants from infection of soil-born pathogenic bacteria, and at the same time can effectively maintain the homeostasis of the rhizosphere microbial community without causing pollution to the environment. Therefore, the use of beneficial rhizosphere microorganisms to control plant diseases has increasingly become a research hotspot and an important direction of applied research (Wei et al., 2018; Elsayed et al., 2020; Im et al., 2020; Ling et al., 2020).

Myxobacteria, as important bacterial predators, are indigenous and dominant bacteria that are widely distributed in the soil (Muñoz-Dorado et al., 2016). It is well documented that myxobacterial isolates can produce rich and diverse secondary metabolites and hydrolytic enzymes, and have broad application prospects in plant disease biocontrol, drug development, waste resources utilization, etc. (Thiery and Kaimer, 2020). In addition, myxobacteria are at the top of the soil microbial food web, and their predation of soil-borne pathogens directly affects the soil microecological environment and plays a pivotal role in maintaining the soil microecological balance and plant health (Marshall and Whitworth, 2019). Moreover, myxobacteria have high abundance in the soil, strong resistance to stresses, high potential for producing active substances, and a wide range of predation. These characteristics endow the myxobacteria with unique biocontrol advantages.

In recent years, numerous researches have suggested myxobacteria to be a type of promising biocontrol agent with higher potentials to inhibit the agricultural pathogen. Some greenhouse experiments and field trials determine that the application of myxobacteria remarkably alleviates damping-off disease of tree seedlings (Hocking and Cook, 1972; Dahm et al., 2015), cucumber *Fusarium* wilt (Löbmann et al., 2016; Ye et al., 2020), hot peppers anthracnose (Kim and Yun, 2011; Raza et al., 2017), and rice blast (Li et al., 2017). Intriguingly, most studies report the biocontrol potentials of myxobacteria against a variety of plant fungal diseases rather than bacterial

diseases (Homma, 1984; Iizuka et al., 1998; Taylor and Draughon, 2001; Bull et al., 2002). For example, myxobacteria *Coralloccoccus* sp. EGB secretes a new type of  $\beta$ -1,6-glucanase GluM, which specifically targets  $\beta$ -1,6-glucan in the cell wall of phytopathogenic fungi by destroying the integrity of the cell wall, and thus inhibits fungal infection (Li et al., 2019b). Strain EGB also secretes a chitin hydrolase, CcCti1, which exerts an antibacterial effect by inhibiting the germination of *Magnaporthe oryzae* and the formation of appressorium (Li et al., 2019a). In contrast, only a few experiments report the application of myxobacteria in the biocontrol of bacterial diseases, where *Myxococcus* sp. strain BS effectively reduced the incidence of calla lily soft rot caused by *Pectobacterium carotovorum* (Li et al., 2018). Recently, we found that myxobacteria could efficiently predate *R. solanacearum*, the primary bacterial pathogen of TBW, in laboratory assays. In this scenario, we propose that myxobacteria may be developed as a robust biocontrol agent to suppress TBW, and the predation mechanisms of myxobacteria on the phytopathogenic bacterium *R. solanacearum* deserve further elucidation.

The present study aimed to isolate and screen myxobacterial isolates that can effectively control TBW and to explore the underlying biocontrol mechanisms. Here, by using *E. coli* and *R. solanacearum* as the prey bacteria, we isolated fifty myxobacteria from the healthy tomato rhizosphere soil of the TBW field. With the combination of plate predation assay and pot experiments, we found that *M. xanthus* R31 not only effectively predated *R. solanacearum* on plates, but also exhibited an excellent biocontrol potential against TBW in pot experiments. Further studies indicated that the extracellular enzyme proteins, especially peptidase, lipases, and glycoside hydrolases secreted by strain R31 played a significant role in the predation process. The present study provides a new insight into the biocontrol against TBW and the recognition of myxobacteria predation against phytopathogen bacteria.

## MATERIALS AND METHODS

### Strains and Culture Conditions

The phytopathogen bacterial strains *R. solanacearum* RsH, GIM 1.70, RS04, GMI 1000, GIM 1.335, and CFP-tagged RsH were maintained in our laboratory under  $-80^{\circ}\text{C}$  with 25% glycerol as the cryoprotectant. Strains were grown on triphenyl tetrazolium chloride (TTC) solid medium (Popoola et al., 2015) at  $30^{\circ}\text{C}$ . When necessary, gentamycin (Gm) at a final concentration of  $30\text{ }\mu\text{g mL}^{-1}$  was added to the culture medium. For pathogen infection assay, a single colony of RsH was inoculated into TTC liquid broth and cultured in a horizontal shaker at  $30^{\circ}\text{C}$  with 200 rpm for 2 days. Myxobacteria strains and the new isolates were cultured on Casitone-Tris (CTT) (Nair et al., 2019) or VY/4 medium (Li et al., 2017) at  $28^{\circ}\text{C}$ . *Escherichia coli* 1.173 was grown at  $37^{\circ}\text{C}$  in LB broth.

### Isolation of Myxobacteria in the Soil of the Diseased Area

Soil samples were collected from the experiment field (N23°9'44", E113°22'22") of South China Agricultural



University, Guangzhou, China. Approximately 200 g of soil was collected from the upper 5–15 cm layer. The samples were air-dried as quickly as possible after collection and stored at room temperature after passing through a 2-mm pore-sized mesh. The isolation procedure of myxobacteria with the induction of fruiting body formation was performed as described before with minor revision (Iizuka et al., 1998). Briefly, a sterile needle was used to pick the fruiting bodies that were induced by *R. solanacearum* RsH or *E. coli* 1.173, and then the fruiting bodies were transferred to VY/4 purifying medium and cultured at 28°C for 3–7 days, and this step was repeated for several times until no other bacterial taxa grew.

## Identification of the Myxobacterium Isolates

The purified myxobacterial isolates were inoculated on VY/4 medium for morphological observation. For the phylogenetic analysis, the 16S rRNA gene was amplified using the primers 27F (5'-AGAGTTTGATCCTGGCTCAG-3') and 1492R (5'-GGTTACCTTGTACGACTT-3') (Weisburg et al., 1991). The PCR amplification was conducted in a T100™ PCR system (Bio-Rad, Hercules, CA, United States) using *EasyTaq* DNA polymerase (Transgene, China) with following conditions: 94°C for 5 min, followed by 35 cycles at 94°C for 15 s, 58°C for 30 s, and 72°C for 2 min, and a final extension at 72°C for 5 min. PCR amplification products were detected using 1% agarose gel electrophoresis analysis and sequenced by Shanghai Sangon Biotechnology Co., Ltd. (Shanghai, China). The similarity search of the 16S rRNA gene was performed using EzBioCloud database.<sup>1</sup>

## Predation Activity Assay

Predation activity was assayed using the colony-induced predation method as described (Berleman et al., 2006). Firstly, the predation ability of the isolated myxobacteria strains against *R. solanacearum* on the TPM plate was estimated to screen the strains with strong predation ability for further research. A total of 100  $\mu$ L RsH cell suspension was pipetted onto the TPM plates and allowed to dry, and then 4  $\mu$ L myxobacterial suspension was spotted at a 2 mm distance from the prey colony. Plates were cultured at 28°C for 7 days. The lawn growths were examined under a stereoscope and photographed. Here, strain of *M. xanthus* R31 displayed a high predation activity against *R. solanacearum*. Therefore, predation activity of strain R31 was further evaluated on WA (No nutrition) and CFL (Oligotrophic) plates with the same methods as above. Predator area rate which was evaluated based on its swarming area against the pathogenic lawn area, and the numbers of fruiting bodies were used to quantify the predation efficacy of strain R31. Additionally, strain R31 and RsH were co-cultured on CFL plate as described above, and the bacterial lawn comprising both of strain R31 and RsH was taken for scanning electron microscope (SEM, Hitachi S-3000N) examination.

<sup>1</sup><https://www.ezbiocloud.net/>

## Pot Experiments With Tomato Bacterial Wilt

The field soil grown with tomato all year round was used as the substrate in the pot experiments. The soil was air-dried soon after collection, screened through a 2-mm pore-sized mesh, and stored at room temperature. A susceptible tomato cultivar Zhongshu No. 4 was used as the test plant. Tomato plants were grown in a greenhouse under 80% relative humidity at 28°C and in a 16 h/8 h light/dark cycle.

Three treatments were designed: (1) only pot soil used as control; (2) pot soil inoculated with RsH at  $1 \times 10^7$  colony-forming units (CFU)  $\text{g}^{-1}$  soil; and (3) pot soil simultaneous inoculated with strains R31 ( $5 \times 10^5$  cells/mL) and RsH ( $1 \times 10^7$  CFU  $\text{g}^{-1}$  soil). One tomato plant was grown in each pot, and each treatment included six pots representing six biological replicates. The experiments were repeated three times.

The typical wilt symptoms of TBW were evaluated in terms of five disease severity scores from 0 to 4, where 0 represents no symptoms, and 1, 2, 3, 4 represent <25, 26–50, >50, and 100% of leaves being wilted, respectively. The disease index (DI) and biocontrol efficacy were subsequently calculated as following:  $\text{DI} = \left[ \frac{\sum (\text{number of diseased plants} \times \text{disease degree})}{(\text{total number of plants} \times \text{highest disease degree})} \right] \times 100$ .  $\text{Biocontrol efficacy} = \frac{(\text{control disease index} - \text{treatment disease index})}{\text{control disease index}} \times 100\%$  (Wang et al., 2019).

## Real-Time Quantitative PCR Analysis

The abundances of *R. solanacearum* RsH in the rhizosphere soil, tomato root, and stem tissues were determined by RT-qPCR quantification of the *filC* gene. RT-qPCR was performed with an Applied Biosystems Quant Studio 6 and 7 Flex Real-Time PCR system (Applied Biosystems, Foster City, CA, United States) using a TransStart Tip Green qPCR Super Mix (Transgene, China). The primers *filC*-F (5'-GAACGCCAACGGTGCGAACT-3') and *filC*-R (5'-GGCGGCCTTCAGGGAGGTC-3') were used for the detection of the abundance of RsH (Schönfeld et al., 2003).

## Confocal Laser Scanning Microscopy Observation

Colonization of *R. solanacearum* RsH in roots and stems of tomato inoculated with CFP-tagged RsH or strain R31 + CFP-tagged RsH were examined using confocal observation. Microscope observation of the sliced plant tissues was performed under a confocal Laser-scanning microscope (LSM 700, Zeiss) equipped with filter blocks with spectral properties matching the fluorescence of CFP (excitation wavelength at 405 nm and emission wavelength at 485 nm) and the autofluorescence of tomato tissues (excitation wavelength at 543 nm and emission wavelength at 590 nm).

## Evaluation of Secondary Metabolites and Extracellular Proteins of Strain R31 in the Predation Against RsH

Strain R31 was cultured in CTT liquid for 7 days at 30°C and shaking at 160 rpm. The culture suspension was collected

by centrifugation at 8,000g, and secondary metabolites were extracted from the supernatant with an equal volume of ethyl acetate, whereas the intracellular metabolites were extracted after the cells were ultrasonically broken up. The extracts were dissolved in an appropriate volume of methanol to a final concentration of 50 mg mL<sup>-1</sup>. For bacteriostatic assay, 30 µL methanol extract was added to a circular filter paper (6 mm diameter), and after methanol was completely removed by evaporation, the filter paper was overlaid on TTC medium spread with strain RsH. Methanol and Gm were used as the negative control and positive control, respectively. The inhibitory activity of ethyl acetate extract against RsH was determined according to the inhibitory zone size.

To investigate the lysis activity of extracellular proteins of strain R31 against RsH, strain R31 was cultured in CTT liquid medium at 30°C for 3 days with shaking at 180 rpm, and the spent culture was collected by centrifugation at 12,000g. Protein in the spent culture was precipitated with ammonium sulfate at various saturations (Li et al., 2019b), dissolved in PBS buffer (0.01 M, pH 7.2), and then dialyzed in a 3.5 kDa molecular weight dialysis bag to remove the residual ammonium sulfate. The dialyzate was then concentrated with an Amicon ultrafiltration tube of 3 kDa (Millipore, United States) and added with the newly cultured RsH cells. After incubation at 37°C for 2 h, the cell integrity of strain RsH cells was examined under a transmission electron microscope (TEM, Hitachi H-7650). The heat-inactivated protein solution was used as a blank control. For cell viability of RsH detection, extracellular proteins of strain R31 and newly cultured RsH cells were incubated at 37°C for 0, 3, 5, 8, and 12 h, respectively. Then, the plate gradient dilution method was used to calculate the numbers of live RsH cells.

## Substrate Spectrum Analysis of Extracellular Enzyme Crude

Laminarin and carboxymethyl cellulose were used as the substrates to assay the polysaccharide lyase activity in the extracellular protein. The enzyme activity was determined with 3,5-dinitrosalicylic acid (DNS) method using DNS assay kits (Beijing Solarbio Science Technology Co., Ltd., China) according to the manufacturer's protocol. Each experiment was repeated three times. The 4-nitrophenyl octanoate and *p*-nitrophenyl palmitate were used as substrates for lipase activity assay by spectrophotometry, as described by Zheng et al. (2011), and a series diluted *p*-nitrophenol was used to produce the standard curve. Inactivated crude enzyme solution was used as a negative control, and each test was repeated three times.

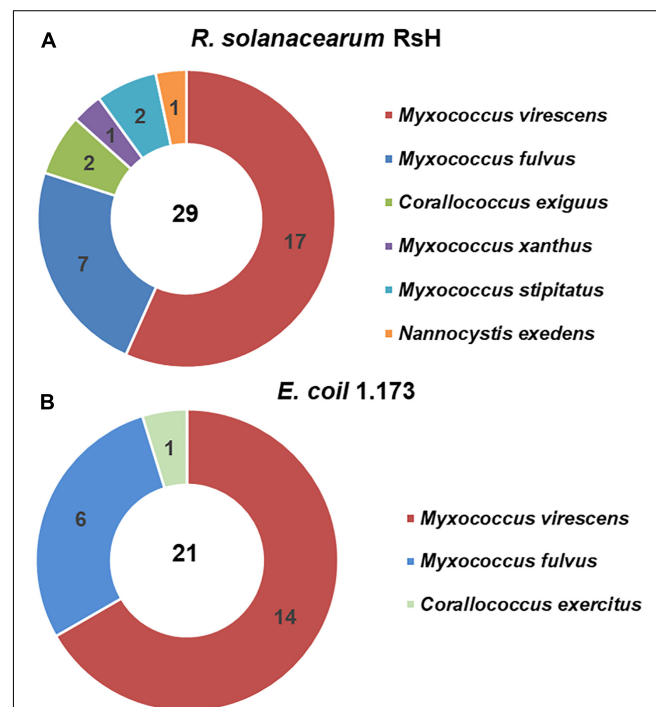
## Liquid Chromatography-Tandem Mass Spectrometry Analysis of Extracellular Proteins With Lysis Activity

Proteins in 40% saturated ammonium sulfate precipitation were reduced with 0.05 M Tris (2-carboxyethyl)phosphine (TCEP) for 1 h at 60°C. The protein was alkylated with 55 mM methyl

methanethiosulfonate (MTS) for 45 min at room temperature in darkness, then added into 10 K Millipore, centrifuged at 12,000g at 4°C for 20 min, and the filtrate was discarded. One hundred microliters of UA buffer (8 M urea, 0.1 M Tris-HCl, pH 8.5) was added into Millipore and centrifuged at 12,000g at 4°C for 20 min two times, and the filtrate was discarded. Then 100 µL 0.25 M triethylammonium bicarbonate (TEAB) was added into the Millipore and centrifuged at 12,000g at 4°C for 20 min three times, and the filtrate was discarded. Trypsin was added at 1:50 trypsin-to-protein mass ratio for the first digestion overnight and 1:100 trypsin-to-protein mass ratio for a second 4 h-digestion. The mixture was centrifuged at 12,000g at 4°C for 20 min. The filtrate was collected, added with 50 µL of 0.5 M TEAB, then centrifuged at 12,000g for 10 min, the filtrate was collected and vacuum dried at low-temperature until LC-MS/MS analysis.

In this study, LC-MS/MS analysis was entrusted to Guangzhou FitGene Biotechnology Co., Ltd. (Guangzhou, China) to be completed, and the specific experimental procedures are shown in **Supplementary File 1**. Finally, protein identification was performed with Mascot search engine (v2.3.0) by searching strain R31 protein databases.<sup>2</sup>

<sup>2</sup>[https://www.ncbi.nlm.nih.gov/nuccore/NZ\\_CP068048](https://www.ncbi.nlm.nih.gov/nuccore/NZ_CP068048)



**FIGURE 1 |** Isolated mycobacteria species from the healthy tomato rhizosphere soil of the tomato bacteria wilt (TBW) field. Using *Ralstonia solanacearum* RsH (A) and *Escherichia coli* 1.173 (B) as the prey bacteria, the mycobacteria strains were isolated from the TBW soil sample. The 50 isolates were identified based on the 16S rRNA gene identity analysis. The pie charts showed the species and numbers of the mycobacteria isolates using the two prey bacteria.

## RESULTS

### Myxobacteria Isolates From the Healthy Tomato Rhizosphere Soil of the Tomato Bacterial Wilt Field Display Predatory Activity on RsH

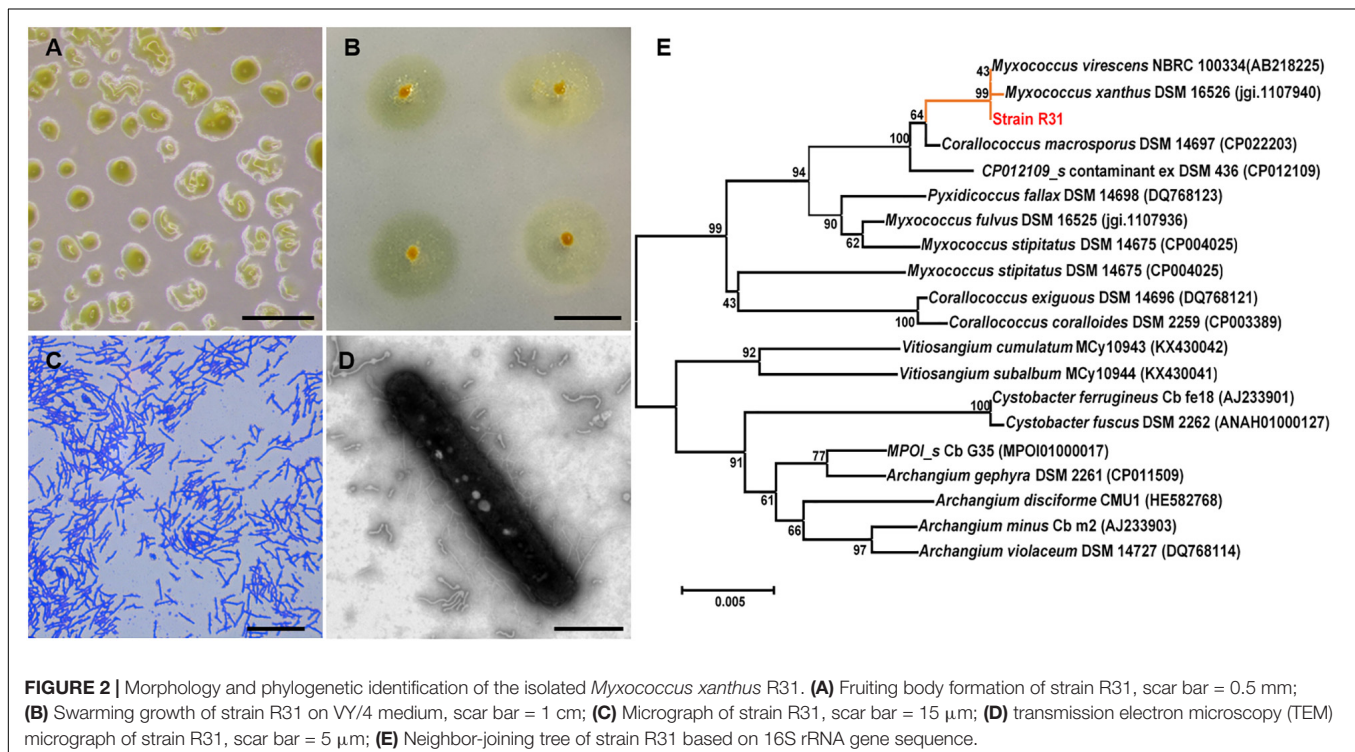
To obtain the potential biocontrol agent of myxobacteria to suppress TBW, we used *E. coli* 1.173 and *R. solanacearum* RsH as the prey bacteria and isolated 50 myxobacteria strains (Supplementary Table 1). Based on the 16S rRNA gene sequence homology analysis, the 50 myxobacterial strains were identified as three genera and seven species were affiliated to Myxococcaceae and Nannocystaceae families. Six myxobacterial species were isolated using *R. solanacearum* RsH as prey, in contrast to only three using *E. coli* 1.173 as prey, although similar numbers of the myxobacteria isolates with the same representative species (*M. virescens* and *M. fulvus*) were obtained using two different prey species (Figure 1). This probably implies that the phytopathogen *R. solanacearum* could be a preferential prey of myxobacteria.

Next, we evaluated the predatory activity of the myxobacteria isolates against *R. solanacearum* using plate experiment. Excitingly, *M. xanthus* R31 displayed a high predation activity against all five tested *R. solanacearum* strains (Figure 2 and Supplementary Figure 1). Within 7 days of co-culture, strain R31 swarmed into a large part of lawns of the prey *R. solanacearum* (Supplementary Figure 2). This indicates that strain R31 could be potential to suppress *R. solanacearum*.

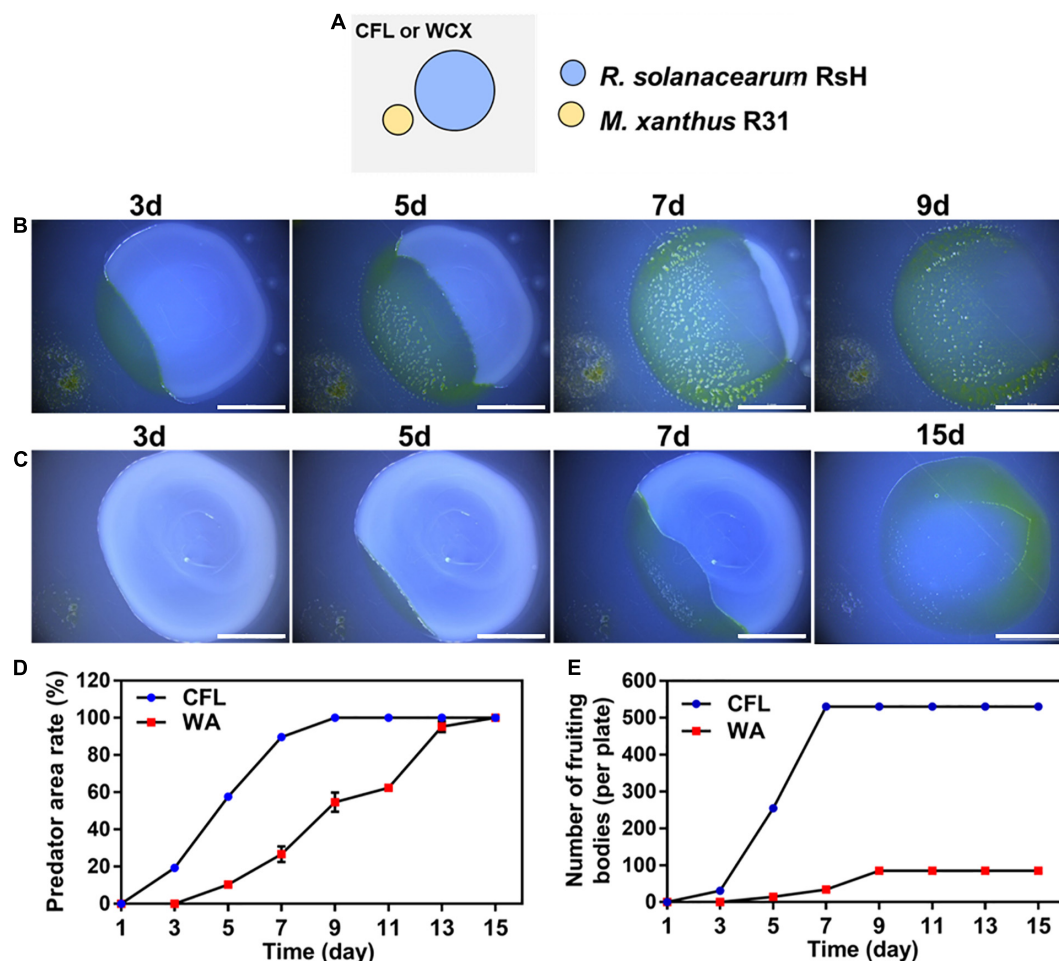
### Strain R31 Predates and Breaks Up the Prey RsH Cells

To further estimate the predatory ability of strain R31 in various environments, two media, CFL (Oligotrophic), and WA (No nutrition) were used. In co-culture of strain R31 and the RsH, swarming growth of strain R31 occurred in the two media (Figure 3). However, the active swarming growth of strain R31 toward RsH was faster on CFL medium than that on WA medium. Specifically, strain R31 almost completely extended into the prey lawn within 7 days co-culture, whereas it took 15 days for strain R31 on WA medium (Figures 3B,C). Calculation indicates that strain R31 exhibited a higher predatory activity on CFL medium than on WA medium (Figures 3D,E). In addition, more fruiting bodies were observed for strain R31 on CFL medium compared with WA medium (Figure 3E).

Scanning electron microscopy was further used *in situ* to observe the predation of RsH cells by strain R31 (Figure 4A). The strain R31 that have finished predation formed a clear fruit body structure (Figure 4B), but swarmed in the direction of the RsH cells during the predation (Figure 4C). RsH cells were densely clustered with complete morphological structure before being predated by strain R31 (Figure 4D). Once the strain R31 came into contact with and predated the RsH cells, the morphological structure of the RsH cells was destroyed and the cells were broken into small pieces (Figures 4F–I). Interestingly, the destroyed RsH cells were surrounded by many filamentous substances (Figure 4F), which might be some extracellular material secreted by strain R31 to lyse the RsH cells.







**FIGURE 3 |** Predation activity of strain R31 against RsH on CFL and WA media. Schematic of the predation assay (A), 100  $\mu$ L RsH cell suspension was pipetted onto the CFL (B) and WA plates (C) and allowed to dry, and then 4  $\mu$ L of strain R31 suspension was spotted at 2 mm distance from the prey colony, scar bar = 5 mm; Predator area ratio on two different media (D) and the numbers of strain R31 fruiting bodies formed on two media (E) was calculated. Triplicate experiments were performed, and the averages and standard deviations are shown.

### Strain R31 Increases Tomatoes Resistance Against Tomato Bacterial Wilt by Decreasing the Abundance of RsH

We conducted greenhouse pot experiments to verify the biocontrol potential of strain R31. The result showed that the tomato plants simultaneously inoculated with strain R31 and RsH almost grew as healthy as the control plants, whereas the plants inoculated with only RsH were seriously ill or even died (Figure 5A). Calculation indicates that the biocontrol efficacy of strain R31 against TBW was 81.9%, and the DI decreased from 100 in the R31 + RsH treatment to 18 in the RsH treatment (Figure 5B).

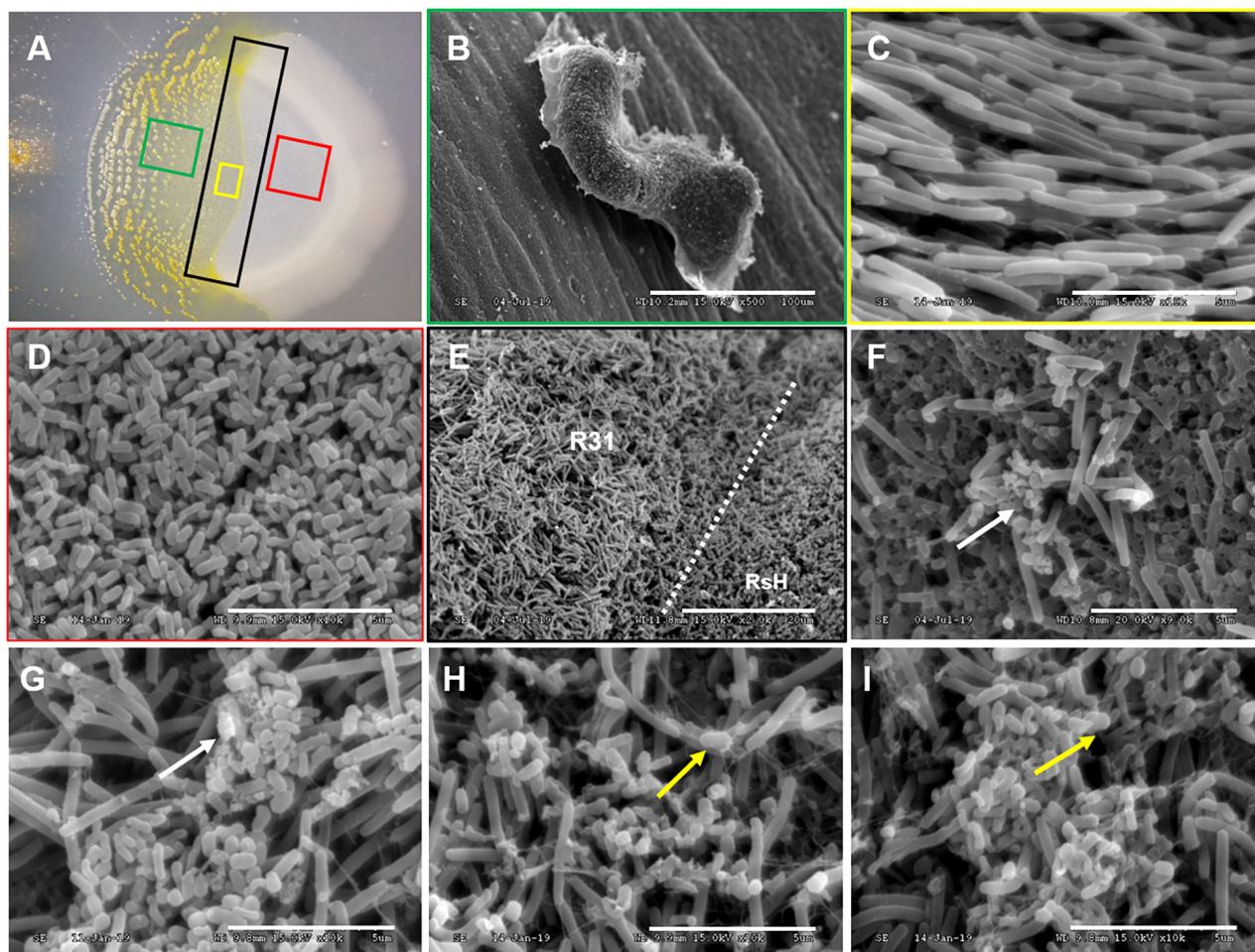
Furthermore, we analyzed the abundance of RsH in rhizosphere soil, tomato root and stem tissues, respectively, and found that strain R31 significantly decreased the abundance of RsH in soil and plant tissues (Figures 5C,D). Histological observation assay showed a similar result (Supplementary Figure 3). Collectively, these results indicate that strain R31

increased tomato resistance against TBW by decreasing the abundance of RsH.

### Extracts of Strain R31 Fermentation Broth Have No Antibacterial Activity Against RsH

Since secondary metabolites play a pivotal role during the predation event of myxobacteria, we extracted the secondary metabolites in fermentation supernatant and bacterial cells of strain R31 using the ethyl acetate. The LC-MS analysis of strain R31 fermentation supernatant and the extracts in the bacterial cells revealed that the kind of substances extracted from the fermentation supernatant was more than that extracted from the bacterial cells (Supplementary Figure 4). Antibacterial activity test shows that compared with the positive control, the ethyl acetate extract from strain R31 cells and supernatant had no inhibitory activity against RsH (Supplementary Figure 5). Therefore, we speculated that the





**FIGURE 4 |** SEM demonstrating the predation of RsH by strain R31. Taking a sample of the strain R31 predation on RsH in CFL plate (A) for scanning electron microscope (SEM) observation, (B) strain R31 that have completed predation in panel (A) green box formed a clear fruit body structure, scar bar = 100  $\mu$ m, (C) strain R31 preparing to predation in panel (A) yellow box showed tropism, scar bar = 5  $\mu$ m, (D) normal RsH cell was densely distributed with complete morphological structure, scar bar = 5  $\mu$ m, (E) the boundary line where strain R31 predation on RsH, strain R31, and RsH exist at the same time, and strain R31 swarmed in the direction of the RsH cells during predation, scar bar = 20  $\mu$ m, (F–I) strain R31 came into contact with RsH cells, the morphological structure of RsH cell is destroyed, and the cells were broken into small pieces. The white arrows indicated the *R. solanacearum* cells whose cell structure has been destroyed. The yellow arrows indicated that strain R31 secretes a large amount of filamentous extracellular substance entangled RsH cells, scar bar = 5  $\mu$ m.

strain R31 predation on RsH might not be attributed to the secondary metabolites.

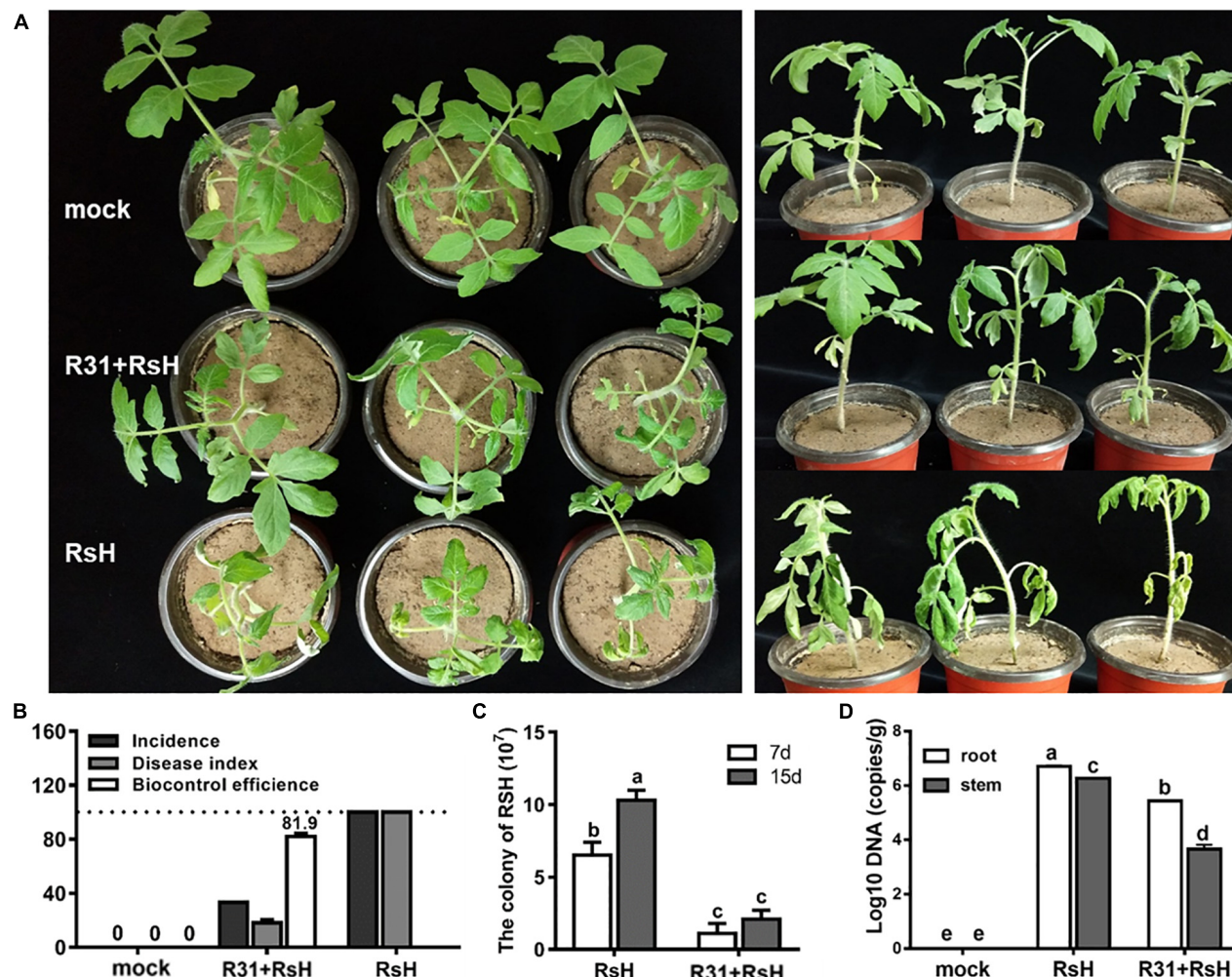
## Extracellular Proteins of Strain R31 Efficiently Lyse RsH Cells

We extracted the extracellular proteins of the strain R31 to determine their lytic bacteria ability against RsH cells. Excitingly, compared with the control (Figures 6A–C), we found that the protein components were precipitated with 40% saturation ammonium sulfate, showing a significant lysis effect on RsH cells (Figures 6D–F). The structure of RsH cells became loose and irregular, cell contents overflowed, and the integrity was destroyed (Figures 6D–F), whereas the protein components precipitated by saturated ammonium sulfate of other concentrations (40–60, 70–80, and 80–100%) showed no

activity (Supplementary Figure 6). These results indicate that the effective proteins might exist in the fraction precipitated by 40% saturation ammonium sulfate. The cell viability of RsH before and after treatment with the extracellular protein was further tested using the method of plate gradient dilution, and the result showed that the treatment with the extracellular proteins of strain R31 significantly reduced the cell viability of RsH along with the time (Figure 6G).

We tested the lytic activity of strain R31 on different substrates. The results showed that strain R31 degraded skimmed milk, sodium carboxymethyl cellulose, and tributyrin (Figures 6H–J), but did not degrade chitin and starch (Figures 6K,L).

Next, we further analyzed the substrate spectrum of the extracellular proteins fraction with lysis effect. Laminarin with  $\beta$ -1,6 glycosidic bonds and carboxymethyl cellulose with  $\beta$ -1,4 glycosidic bonds were hydrolyzed by the extracellular



**FIGURE 5 |** Pot experiments assayed strain R31 suppressing TBW. **(A)** Greenhouse pot experiments of strain R31 for biocontrol of TBW, mock was a sterile water control, R31 + RsH was for simultaneous inoculated of strain R31 and RsH, and RsH was only inoculated with RsH. After continued cultivation for another 7 days, the treatments were photographed. The left and right panels show the top and the side views, respectively. **(B)** Biocontrol effect statistics of strain R31 against TBW, plant disease status was evaluated based on equation that is described in the “Materials and Methods” section. **(C)** The abundance of RsH was tested by counting the colony formation units. Each 10 g of soil was sampled from the tomato rhizospheres that were added only with RsH (RsH) and with strain R31 and RsH (R31 + RsH), respectively. After a 10-fold series dilution, the soil suspension was spread on TTC plate. Colony was counted after 2 days incubation. **(D)** Quantitative results of RsH in tomato root and stem tissues were obtained through RT-qPCR, uninoculated tomato root and stem tissues as a mock. Triplicate experiments were carried out, and the averages and standard deviations are shown. The lowercase letters at each bar top show the statistically significant differences by Duncan’s test ( $p < 0.05$ ).

proteins, and the lipase substrates 4-nitrophenyl octanoate and *p*-nitrophenyl palmitate were also effectively hydrolyzed (Table 1). In contrast, the extracellular proteins showed no active reaction to D-glucan with  $\beta$ -1,3-glycosidic bonds and xylan. Therefore, it is possible that the extracellular proteins of strain R31 might have the lipase activity, the cellulase activity, and the glycoside hydrolase activity of hydrolyzing  $\beta$ -1,6-glycosidic bonds.

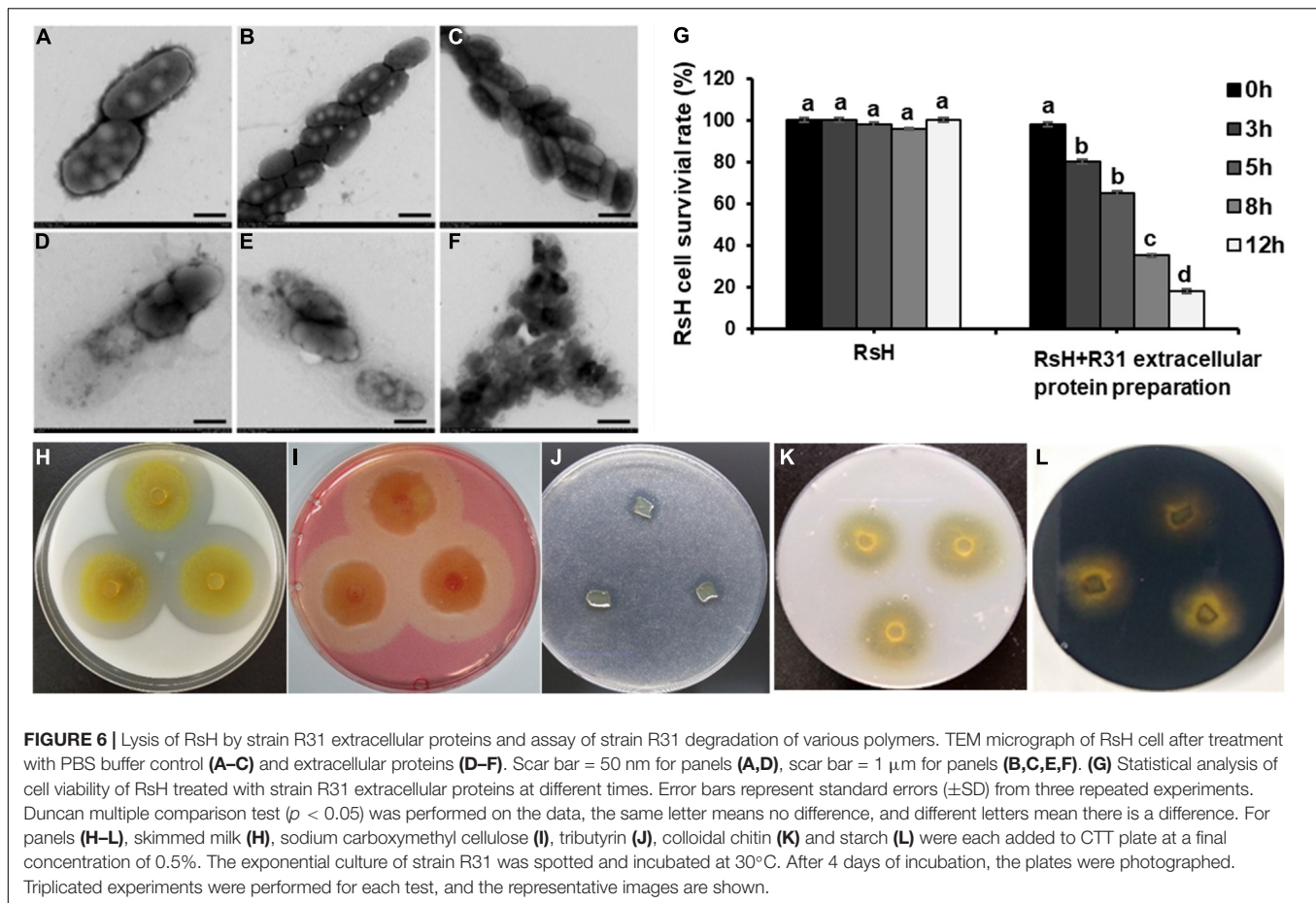
The LC-MS/MS analysis revealed a total of 178 proteins in the extracellular proteins precipitated with 40% saturation ammonium sulfate (Supplementary Table 2). Among them, we identified 9 enzymes with lytic activity, including one M4 family metalloprotease, three peptidase, one endopeptidase, two

glycoside hydrolases, one esterase, and one lipase. To sum up, these results suggest that these extracellular enzyme proteins may play a significant role in the predation of strain R31.

## DISCUSSION

In recent years, biocontrol agents based on beneficial soil microorganisms have attracted the attention of scientists to control TBW and have also achieved certain results. In this study, we successfully isolated and screened a strain R31 for potential use as an effective biocontrol agent against TBW and showed that it effectively suppressed this disease in pot experiment.





While many species have been used for biological control of TBW, including *Streptomyces* (Ling et al., 2020), *Bacillus methylotrophicus* (Im et al., 2020), *Bacillus amyloliquefaciens* (Wei et al., 2011; Ho et al., 2020), *Bacillus velezensis* (Chen et al., 2020), *Streptomyces microflavus* (Shen et al., 2021), information on the use of myxobacteria as biocontrol agents in controlling TBW is blank. In fact, myxobacteria have great potential in biocontrol of plant diseases. Antifungal myxobacteria, such as *Corallococcus* (Li et al., 2017; Ye et al., 2020), *Myxococcus* (Kim and Yun, 2011), *Sorangium cellulosum* (Hocking and Cook, 1972), *Nannocystis exedens* (Taylor and Draughon, 2001), and also other predatory myxobacteria (Homma, 1984; Meliah et al., 2020), have shown good biocontrol effects on a variety of plant fungal diseases. Actually, myxobacteria have stronger ability to prey on bacteria, and their potential for biocontrol of plant bacterial diseases is more promising. *Myxococcus* sp. strain BS as an efficient biocontrol agent for soft rot of calla lily (Li et al., 2018) is a good example. To the best of our knowledge, our study is the first report demonstrating the biocontrol of TBW by myxobacteria in pot experiments.

*Ralstonia solanacearum* is a soil-borne pathogen, which is extremely difficult to prevent and control due to the high degree of adaptability and variability (Genin and Denny, 2012). While the predation range of myxobacteria is very wide, and its

preference for prey bacteria is generally reflected in the level of large taxonomic units such as phylum and class, the physiological differentiation of the same bacteria is normally ignored (Morgan et al., 2010). In the present study, we found that strain R31 showed efficient predation on five strains of *R. solanacearum*. Therefore, we speculate that myxobacteria have an important biocontrol significance for TBW.

As a model species, *M. xanthus* is often used to study the multicellular behavior of myxobacteria (Muñoz-Dorado et al., 2016). Previous research has shown that in the process of predation, myxobacteria can secrete a large number of hydrolytic enzymes to kill and decompose prey cells and release the hydrolyzate into the extracellular environment, which is consumed by it for growth (Evans et al., 2012). Myxobacteria can produce a variety of enzymes, including proteases, amylases, cellulases, lipases, chitinases, xylanase enzymes, etc., which are the material basis for their predatory ability (Muñoz-Dorado et al., 2016). Myxobacteria can predate a variety of prey microorganisms through their unique wolf-pack behavior. The hypothesis is that when the cell density is high, the myxobacteria secrete a variety of hydrolytic enzymes. Myxobacterial cells gather together in the external environment to increase the concentration of enzymes and jointly play a lysis effect, creating a shared pool of hydrolyzates, which is convenient for individual

**TABLE 1** | Substrate specificity of extracellular crude enzymes of strain R31.

Substrate	Bond types	Enzyme activity
Xylan	$\beta$ -1,4-(Xylopyranosyl)	0
D-Glucan	$\beta$ -1,3 (Glucose)	0
Chitin	$\beta$ -1, 4-N-Acetylaminoglycoside bond	0
Laminarin	$\beta$ -1,3- $\beta$ -1,6-(Glucose)	$4.296 \pm 0.021 \text{ U mL}^{-1}$
Carboxymethyl cellulose	$\beta$ -1,4 (Glucose)	$0.252 \pm 0.009 \text{ U mL}^{-1}$
p-Nitrophenyl palmitate	Ester linkage	$0.163 \pm 0.008 \text{ U mL}^{-1}$

cells to absorb the lysates to achieve growth and reproduction (Berleman and Kirby, 2009). Recently, Li et al. (2017) suggested that the extracellular supernatant of strain EGB effectively reduced the infection ability of the *M. oryzae* on rice seedlings. The authors isolated a  $\beta$ -1,6-glucanase (GluM) and confirmed that it played a role in lysing fungal cell walls in the process of myxobacteria preying on fungi (Li et al., 2019b). Myxobacteria can use lipolytic enzymes to remove the cell membrane barrier of the prey and empty the cytoplasmic content of the prey (Moraleda-Munñoz and Shimkets, 2007). In line with these results, we also identified some enzyme proteins in strain R31 extracellular proteins, which have a lysis activity against RsH. Therefore, we speculate that the extracellular enzyme proteins, especially some peptidase, lipase, glycoside hydrolases etc., have a significant role in the predation of strain R31 against *R. solanacearum* and thus in the biocontrol of TBW. Certainly, further study to verify these speculations is necessary.

Secondary metabolites produced by myxobacteria are considered as small-molecule weapons that can penetrate prey cells, stop metabolism, or kill them (Pérez et al., 2020). In *M. xanthus* DK1622, the antibiotic TA has been proven to inhibit the growth of *E. coli* MG1655, but has no inhibitory effect on the growth of the gram-positive bacterium *Micrococcus luteus*, indicating that TA shows selective activity against bacterial species (Goldman et al., 2006; Xiao et al., 2011). Moreover, the killing ability of TA depends on the metabolic activity of the prey cells. The production of TA is very important for killing the metabolically vigorous and growing *E. coli*. In this study, however, we found that small molecules extracted with ethyl acetate had no antibacterial activity on RsH. Therefore, we inferred that the secondary metabolites produced by strain R31 may not play a role in the biocontrol of TBW. Similarly, Li et al. (2017) found that the secondary metabolites secreted by the *Corallococcus* sp. EGB had no antibacterial activity against phytopathogenic fungi. Interestingly, we found that *Citricoccus inhibens* gen. nov. sp. nov. M34 suppressed or predated a variety of phytopathogen mainly by secreting secondary metabolisms (Zhou et al., 2021). Generally speaking, we speculate that this may be related to the differences between different species in the coevolution process of myxobacteria, plants, and microorganisms.

Predation is an important survival strategy for most myxobacteria. The predation of myxobacteria on gram-negative and gram-positive bacteria is mediated by different bactericidal

mechanisms (Arend et al., 2021). During the predation of fungi by *Corallococcus* sp. EGB, the strain EGB destroyed the fungi cell wall by secreting GluM and CcCti1 (Li et al., 2019a,b). In the preset study, we found that peptidase, lipases, and glycoside hydrolases played a key role during the predation of strain R31 against *R. solanacearum*. These results might suggest that the kind of enzymes secreted by myxobacteria to lyse prey cells during predation is probably related to the composition of the cell wall of prey cells. Certainly, the types of lytic enzymes secreted by myxobacteria during predation and their mode of action on prey cells need further research. More detailed transcriptome and proteomes sequencing data, and also the analysis of the interaction between myxobacteria, prey, and plants will be expected to help identify specific extracellular lyase species involved in predation and to clarify the predation mechanism of myxobacteria in the future.

Rhizosphere exudates cannot only provide nutrients for indigenous microorganisms, but can also be used by plants to attract or repel related microorganisms (Dayakar et al., 2009). Ye et al. (2020) reported that the myxobacteria strain EGB responds chemotaxis to cucumber root exudates. In this study, strain R31 showed a good biocontrol effect on TBW. Therefore, it is necessary to further study how tomato root exudates affect the interaction between strain R31 and *R. solanacearum*. It helps to better apply myxobacteria to the biocontrol of TBW.

## CONCLUSION

In this study, we successfully isolated fifty myxobacteria strains from the healthy tomato rhizosphere soil of the TBW field. We showed that myxobacteria strain R31 can be used as a potential biocontrol agent of TBW. The strain R31 exhibited efficient predation against *R. solanacearum* in the plate assay and effectively reduced the abundance of *R. solanacearum* in the pot experiment, which was significant to ensure an effective biocontrol of TBW. In addition, our results also indicate that the extracellular enzyme proteins secreted by strain R31, especially some peptidase, lipases, and glycoside hydrolases played a significant role in the predation process. The present study provides a new insight into the biocontrol of TBW and the recognition of myxobacteria predation against bacterial phytopathogen.

## DATA AVAILABILITY STATEMENT

The original contributions presented in the study are included in the article/**Supplementary Material**, further inquiries can be directed to the corresponding author.

## AUTHOR CONTRIBUTIONS

HD and AL designed the experiments. HD, XX, and RG performed the experiments. HD and YL analyzed the data. HD,



QY, and HZ revised the manuscript. HD wrote the manuscript and responsible for the funding support. All authors read and approved the final manuscript.

## FUNDING

This research was funded by the GDAS' Project of Science and Technology Development (2021GDASYL-2021010309), the Natural Science Foundation of Guangdong Province (2020A1515110655), and the National Natural Science Foundation of China (32102276).

## REFERENCES

- Arend, K. I., Schmidt, J. J., Bentler, T., Luchtelfeld, C., Eggerichs, D., Hexamer, H., et al. (2021). *Myxococcus xanthus* predation of gram-positive or gram-negative bacteria is mediated by different bacteriolytic mechanisms. *Appl. Environ. Microb.* 87, e02382–20. doi: 10.1128/AEM.02382-20
- Berleman, J. E., Chumley, T., Cheung, P., and Kirby, J. R. (2006). Rippling is a predatory behavior in *Myxococcus xanthus*. *J. Bacteriol.* 188, 5888–5895. doi: 10.1128/jb.00559-06
- Berleman, J. E., and Kirby, J. R. (2009). Deciphering the hunting strategy of a bacterial wolfpack. *FEMS Microbiol. Rev.* 33, 942–957. doi: 10.1111/j.1574-6976.2009.00185.x
- Bull, C. T., Shetty, K. G., and Subbarao, K. V. (2002). Interactions between Myxobacteria, plant pathogenic fungi, and biocontrol agents. *Plant Dis.* 86, 889–896. doi: 10.1094/pdis.2002.86.8.889
- Chen, M., Wang, J., Liu, B., Zhu, Y., Xiao, R., Yang, W., et al. (2020). Biocontrol of tomato bacterial wilt by the new strain *Bacillus velezensis* FJAT-46737 and its lipopeptides. *BMC Microbiol.* 20:160. doi: 10.1186/s12866-020-01851-2
- Choi, K., Choi, J., Lee, P. A., Roy, N., Khan, R., Lee, H. J., et al. (2020). Alteration of bacterial wilt resistance in tomato plant by microbiota transplant. *Front. Plant Sci.* 11:1186. doi: 10.3389/fpls.2020.01186
- Dahm, H., Brzezińska, J., Wrótniak-Drzewiecka, W., Golińska, P., and Rai, M. (2015). Myxobacteria as a potential biocontrol agent effective against pathogenic fungi of economically important forest trees. *Dendrobiology* 74, 13–24. doi: 10.12657/denbio.074.002
- Dayakar, V. B., Tiffany, L. W., Daniel, L., and Jorge, M. V. (2009). Rhizosphere chemical dialogues: plant-microbe interactions. *Curr. Opin. Biotech.* 20, 642–650. doi: 10.1016/j.copbio.2009.09.014
- Elsayed, T., Jacquiod, S., Nour, E., Sørensen, S., and Smalla, K. (2020). Biocontrol of bacterial wilt disease through complex interaction between tomato plant, antagonists, the indigenous rhizosphere microbiota, and *Ralstonia solanacearum*. *Front. Microbiol.* 10:28355. doi: 10.3389/fmicb.2019.02835
- Evans, A., Davey, H., Cookson, A., Currinn, H., Cookefox, G., Stanczyk, P. J., et al. (2012). Predatory activity of *Myxococcus xanthus* outer-membrane vesicles and properties of their hydrolase cargo. *Microbiology* 158, 2742–2752. doi: 10.1099/mic.0.060343-0
- Genin, S., and Denny, T. P. (2012). Pathogenomics of the *Ralstonia solanacearum* species complex. *Annu. Rev. Phytopathol.* 50, 67–89. doi: 10.1146/annurev-phyto-081211-173000
- Goldman, B. S., Niernan, W. C., Kaiser, D., Slater, S. C., Durkin, A. S., Eisen, J. A., et al. (2006). Evolution of sensory complexity recorded in a myxobacterial genome. *Proc. Natl. Acad. Sci. U.S.A.* 103, 15200–15205. doi: 10.1073/pnas.0607335103
- Ho, T., Chuang, C., Zheng, J., Chen, H., Liang, Y., Huang, T., et al. (2020). *Bacillus amyloliquefaciens* strain PMB05 intensifies plant immune responses to confer resistance against bacterial wilt of tomato. *Phytopathology* 110, 1877–1885. doi: 10.1094/PHYTO-01-20-0026-R
- Hocking, D., and Cook, F. D. (1972). Myxobacteria exert partial control of damping-off and root disease in container-grown tree seedlings. *Can. J. Microbiol.* 18:1557. doi: 10.1139/m72-237

## ACKNOWLEDGMENTS

The authors are very grateful to Guoping Wang in College of Horticulture, South China Agricultural University for providing field soil.

## SUPPLEMENTARY MATERIAL

The Supplementary Material for this article can be found online at: <https://www.frontiersin.org/articles/10.3389/fmicb.2021.801091/full#supplementary-material>

- Homma, Y. (1984). Perforation and lysis of hyphae of *Rhizoctonia solani* and conidia of *Cochliobolus miyabeanus* by soil myxobacteria. *Phytopathology* 74, 1234–1239. doi: 10.1094/phyto-74-1234
- Iizuka, T., Jojima, Y., Fudou, R., and Yamanaka, S. (1998). Isolation of myxobacteria from the marine environment. *FEMS Microbiol. Lett.* 169, 317–322. doi: 10.1111/j.1574-6968.1998.tb13335.x
- Im, S., Yu, N., Joen, H., Kim, S., Park, H., Park, A., et al. (2020). Biological control of tomato bacterial wilt by oxydiflicidin and diflicidin-producing *Bacillus methylotrophicus* DR-08. *Pestic. Biochem. Phys.* 163, 130–137. doi: 10.1016/j.pestbp.2019.11.007
- Kim, S., and Yun, S. (2011). Biocontrol with *Myxococcus* sp. KYC 1126 against anthracnose in hot pepper. *Plant Pathol. J.* 27, 156–163. doi: 10.5423/PPJ.2011.27.2.156
- Li, Z., Wang, T., Luo, X., Li, X., Xia, C., Zhao, Y., et al. (2018). Biocontrol potential of *Myxococcus* sp. strain BS against bacterial soft rot of calla lily caused by *Pectobacterium carotovorum*. *Biol. Control* 126, 36–44. doi: 10.1016/j.biocontrol.2018.07.004
- Li, Z., Ye, X., Chen, P., Ji, K., Zhou, J., Wang, F., et al. (2017). Antifungal potential of *Corallococcus* sp. strain EGB against plant pathogenic fungi. *Biol. Control* 110, 10–17. doi: 10.1016/j.biocontrol.2017.04.001
- Li, Z., Ye, X., Liu, M., Xia, C., Zhang, L., Luo, X., et al. (2019b). A novel outer membrane  $\beta$ -1,6-glucanase is deployed in the predation of fungi by myxobacteria. *ISME J.* 13, 2223–2235. doi: 10.1038/s41396-019-0424-x
- Li, Z., Xia, C., Wang, Y., Li, X., Qiao, Y., Li, C., et al. (2019a). Identification of an endo-chitinase from *Corallococcus* sp. EGB and evaluation of its antifungal properties. *Int. J. Biol. Macromol.* 132, 1235–1243. doi: 10.1016/j.ijbiomac.2019.04.056
- Liar, Y., Nion, Y., and Toyota, K. (2015). Recent trends in control methods for bacterial wilt diseases caused by *Ralstonia solanacearum*. *Microbes Environ.* 30, 1–11. doi: 10.1264/jisme2.ME14144
- Ling, L., Han, X., Li, X., Zhang, X., Wang, H., Zhang, L., et al. (2020). A *Streptomyces* sp. NEAU-HV9: Isolation, identification, and potential as a biocontrol agent against *Ralstonia solanacearum* of tomato plants. *Microorganisms* 8:351. doi: 10.3390/microorganisms8030351
- Löbmann, M., Vetukuri, R. R., Zinger, L. Z., Alsanian, B. W., Grenville-Briggs, L. J., and Walter, A. J. (2016). The occurrence of pathogen suppressive soils in Sweden in relation to soil biota, soil properties, and farming practices. *Appl. Soil Ecol.* 107:57. doi: 10.1016/j.apsoil.2016.05.011
- Mansfield, J., Genin, S., Magori, S., Citovsky, V., Sriariyanum, M., Ronald, P., et al. (2012). Top 10 plant pathogenic bacteria in molecular plant pathology. *Mol. Plant Pathol.* 13, 614–629. doi: 10.1111/j.1364-3703.2012.00804.x
- Marshall, R. C., and Whitworth, D. E. (2019). Is “wolf-pack” predation by antimicrobial bacteria cooperative? Cell behaviour and predatory mechanisms indicate profound selfishness, even when working alongside kin. *Bioessays* 41:1800247. doi: 10.1002/bies.201800247
- Meliah, S., Kusumawati, D. I., and Ilyas, M. (2020). Preliminary study of myxobacteria as biocontrol agents for panama disease pathogen, tropical race 4 *Fusarium odoratissimum*. *IOP Conf. Ser. Earth Environ. Sci.* 457:12060. doi: 10.1088/1755-1315/457/1/012060
- Moraleda-Munñoz, A., and Shimkets, L. J. (2007). Lipolytic enzymes in *Myxococcus xanthus*. *J. Bacteriol.* 189:3072. doi: 10.1128/JB.01772-06

- Morgan, A. D., MacLean, R. C., Hillesland, K. L., and Velicer, G. J. (2010). Comparative analysis of myxococcus predation on soil bacteria. *Appl. Environ. Microb.* 76, 6920–6927. doi: 10.1128/AEM.00414-10
- Muñoz-Dorado, J., Marcos-Torres, F. J., García-Bravo, E., Moraleda-Muñoz, A., and Pérez, J. (2016). Myxobacteria: moving, killing, feeding, and surviving together. *Front. Microbiol.* 7:781. doi: 10.3389/fmicb.2016.00781
- Nair, R. R., Vasse, M., Wielgoss, S., Sun, L., Yu, Y. N., and Velicer, G. J. (2019). Bacterial predator-prey coevolution accelerates genome evolution and selects on virulence-associated prey defences. *Nat. Commun.* 10:4301. doi: 10.1038/s41467-019-12140-6
- Pérez, J., Contreras-Moreno, F. J., Marcos-Torres, F. J., Moraleda-Muñoz, A., and Muñoz-Dorado, J. (2020). The antibiotic crisis: how bacterial predators can help. *Comput. Struct. Biotechnol. J.* 18, 2547–2555. doi: 10.1016/j.csbj.2020.09.010
- Popoola, A. R., Ganiyu, S. A., Enikuomehin, O. A., Bodunde, J. G., Adedibu, O. B., Durosomo, H. A., et al. (2015). Isolation and characterization of *Ralstonia solanacearum* causing bacterial wilt of tomato in Nigeria. *Nig. J. Biotechnol.* 29, 1–10. doi: 10.4314/njb.v29i1.1
- Posas, M. B., Toyota, K., and Islam, T. M. (2007). Inhibition of bacterial wilt of tomato caused by *Ralstonia solanacearum* by sugars and amino acids. *Microbes Environ.* 22, 290–296. doi: 10.1264/jsme2.22.290
- Prior, P., Ailloud, F., Dalsing, B. L., Remenant, B., Sanchez, B., and Allen, C. (2016). Genomic and proteomic evidence supporting the division of the plant pathogen *Ralstonia solanacearum* into three species. *BMC Genomics* 17:90. doi: 10.1186/s12864-016-2413-z
- Raza, W., Ling, N., Zhang, R., Huang, Q., Xu, Y., and Shen, Q. (2017). Success evaluation of the biological control of *Fusarium* wilts of cucumber, banana, and tomato since 2000 and future research strategies. *Crit. Rev. Biotechnol.* 37:202212. doi: 10.3109/07388551.2015.1130683
- Salanoubat, M., Genin, S., Artiguenave, F., Gouzy, J., Mangenot, S., Arlat, M., et al. (2002). Genome sequence of the plant pathogen *Ralstonia solanacearum*. *Nature* 415, 497–502. doi: 10.1038/415497a
- Schönfeld, J., Heuer, H., Van Elsland, J. D., and Smalla, K. (2003). Specific and sensitive detection of *Ralstonia solanacearum* in soil on the basis of PCR amplification of *fliC* fragments. *Appl. Environ. Microbiol.* 69, 7248–7256. doi: 10.1128/AEM.69.12.7248-7256.2003
- Shen, T., Lei, Y., Pu, X., Zhang, S., and Du, Y. (2021). Identification and application of *Streptomyces microflavus* G33 in compost to suppress tomato bacterial wilt disease. *Appl. Soil. Ecol.* 157:103724. doi: 10.1016/j.apsoil.2020.103724
- Taylor, W., and Draughon, F. (2001). *Nannocystis exedens*: a potential biocompetitive agent against *Aspergillus avus* and *Aspergillus parasiticus*. *J. Food Protect.* 64:1030. doi: 10.1111/j.1745-4549.2001.tb00456.x
- Thiery, S., and Kaimer, C. (2020). The predation strategy of *Myxococcus xanthus*. *Front. Microbiol.* 11:2. doi: 10.3389/fmicb.2020.00002
- Wang, G., Jie, K., Cui, D., Zhao, H., Zhao, P., Feng, S., et al. (2018). Comparative proteomic analysis of two *Ralstonia solanacearum* isolates differing in aggressiveness. *Int. J. Mol. Sci.* 19:2444. doi: 10.3390/ijms19082444
- Wang, G., Kong, J., Cui, D., Zhao, H., Niu, Y., Xu, M., et al. (2019). Resistance against *Ralstonia solanacearum* in tomato depends on the methionine cycle and the  $\gamma$ -aminobutyric acid metabolic pathway. *Plant J.* 97, 1032–1047. doi: 10.1111/tpp.14175
- Wei, Z., Hu, J., Gu, Y., Yin, S., Xu, Y., Jousset, A., et al. (2018). *Ralstonia solanacearum* pathogen disrupts bacterial rhizosphere microbiome during an invasion. *Soil Biol. Biochem.* 118, 8–17. doi: 10.1016/j.soilbio.2017.11.012
- Wei, Z., Yang, X., Yin, S., Shen, Q., Ran, W., and Xu, Y. (2011). Efficacy of *Bacillus*-fortified organic fertiliser in controlling bacterial wilt of tomato in the field. *Appl. Soil Ecol.* 48, 152–159. doi: 10.1016/j.apsoil.2011.03.013
- Weisburg, W. G., Barns, S. M., Pelletier, D. A., and Lane, D. J. (1991). 16S ribosomal DNA amplification for phylogenetic study. *J. Bacteriol.* 173, 697–703. doi: 10.1128/jb.173.2.697-703.1991
- Xiao, Y., Wei, X., Ebright, R., and Wall, D. (2011). Antibiotic production by Myxobacteria plays a role in predation. *J. Bacteriol.* 193, 4626–4633. doi: 10.1128/JB.05052-11
- Ye, X., Li, Z., Luo, X., Wang, W., Li, Y., Li, R., et al. (2020). A predatory Myxobacterium controls cucumber *Fusarium* wilt by regulating the soil microbial community. *Microbiome* 8:49. doi: 10.1186/s40168-020-00824-x
- Zhang, Y., Hu, A., Zhou, J., Zhang, W., and Li, P. (2020). Comparison of bacterial communities in soil samples with and without tomato bacterial wilt caused by *Ralstonia solanacearum* species complex. *BMC Microbiol.* 20:89. doi: 10.1186/s12866-020-01774-y
- Zheng, X., Chu, X., Zhang, W., Wu, N., and Fan, Y. (2011). A novel cold-adapted lipase from *Acinetobacter* sp. XMZ-26: gene cloning and characterisation. *Appl. Microbiol. Biotechnol.* 90, 971–980. doi: 10.1007/s00253-011-3154-1
- Zhou, Y., Yi, S., Zang, Y., Yao, Q., and Zhu, H. (2021). The predatory myxobacterium *Citricoccus inhibens* gen. nov. sp. nov. showed antifungal activity and bacteriolytic property against phytopathogens. *Microorganisms* 9:2137. doi: 10.3390/microorganisms9102137

**Conflict of Interest:** The authors declare that the research was conducted in the absence of any commercial or financial relationships that could be construed as a potential conflict of interest.

**Publisher's Note:** All claims expressed in this article are solely those of the authors and do not necessarily represent those of their affiliated organizations, or those of the publisher, the editors and the reviewers. Any product that may be evaluated in this article, or claim that may be made by its manufacturer, is not guaranteed or endorsed by the publisher.

Copyright © 2022 Dong, Xu, Gao, Li, Li, Yao and Zhu. This is an open-access article distributed under the terms of the Creative Commons Attribution License (CC BY). The use, distribution or reproduction in other forums is permitted, provided the original author(s) and the copyright owner(s) are credited and that the original publication in this journal is cited, in accordance with accepted academic practice. No use, distribution or reproduction is permitted which does not comply with these terms.



# Interactive Effects of Filamentous Fungi and Cucurbitacin Phytonematicide on Growth of Cowpea and Suppression of *Meloidogyne enterolobii*

Kgabo Martha Pofu\* and Phatu William Mashela

Plant Production, Soil Science and Agricultural Engineering, Green Biotechnologies Research Centre of Excellence, University of Limpopo, Sovenga, South Africa

## OPEN ACCESS

### Edited by:

Florence Fontaine,  
Université de Reims  
Champagne-Ardenne, France

### Reviewed by:

Tariq Mukhtar,  
Pir Mehr Ali Shah Arid Agriculture  
University, Pakistan  
Saroj Yadav,  
Chaudhary Charan Singh Haryana  
Agricultural University, India

### \*Correspondence:

Kgabo Martha Pofu  
kgabo.pofu@ul.ac.za

### Specialty section:

This article was submitted to  
Microbe and Virus Interactions with  
Plants,  
a section of the journal  
Frontiers in Microbiology

**Received:** 26 August 2021

**Accepted:** 17 January 2022

**Published:** 08 February 2022

### Citation:

Pofu KM and Mashela PW (2022)  
Interactive Effects of Filamentous  
Fungi and Cucurbitacin  
Phytonematicide on Growth  
of Cowpea and Suppression  
of *Meloidogyne enterolobii*.  
Front. Microbiol. 13:765051.  
doi: 10.3389/fmicb.2022.765051

Cowpea [*Vigna unguiculata* (L.) Walp]] is highly susceptible to the emerging guava root-knot nematode, *Meloidogyne enterolobii*, with available management options being limited due to the withdrawal of effective fumigant nematicides from the agrochemical markets. Filamentous fungi, available as Biocult (a.i. *Glomus* species + *Trichoderma asperellum* Lieckf and Nirenberg) and Nemafric-BL phytonematicide (a.i. cucurbitacin B) each improves plant growth and suppresses nematode population densities. However, when filamentous fungi like Biocult are combined with other biocontrol agents, the combined effects either have synergistic or antagonistic effects on the test variables. The combined effects of Biocult and cucurbitacin phytonematicides on plant growth and nematode suppression remain undocumented. The objective of this study was therefore to determine the combined effects of Biocult and Nemafric-BL phytonematicide on growth of cowpea var. Eureka and suppression of *M. enterolobii* population densities. Eureka was subjected to the effects of the two products in a 2 × 2 factorial experiment on a field infested with *M. enterolobii*. At harvest, the interaction of Biocult and Nemafric-BL phytonematicide was highly significant ( $P \leq 0.01$ ) on plant and nematode variables, with a two-way table used to assess the findings. Relative to untreated control, Biocult alone increased plant growth variables from 15 to 74%. Similarly, NemafricBL phytonematicide increased plant variables from 14 to 61%, whereas the combined effects significantly increased dry shoot mass (19%) and dry harvestable leaf mass (21%), but did not have significant effects on plant height and stem diameter. Relative to untreated control, Biocult alone reduced nematode eggs in root (80%), J2 in root (84%) and J2 in soil (53%), whereas the combined relative effects of the two products did not have significant effects on nematode population densities. In conclusion, Biocult and Nemafric-BL phytonematicide had antagonistic effects on growth of cowpea and suppression of *M. enterolobii* population densities and therefore, should be used separately in cowpea production.

**Keywords:** arbuscular mycorrhizae, Biocult, cucurbitacin phytonematicides, *Glomus* species, *Meloidogyne enterolobii*, *Trichoderma* species

## INTRODUCTION

In semi-arid regions, cowpea [*Vigna unguiculata* (L.) Walp] is one of the mandated crops for ameliorating food insecurity, where it is primarily cultivated for use as a leafy vegetable and secondarily as grains for consumption, feed and seed. Even though the crop is drought-tolerant, when cultivated as a low input crop, the productivity of the crop is substantially low due to an assortment of challenges, which include the availability of nutrient elements such as phosphorus and the incidence of high population densities of root-knot (*Meloidogyne* species) nematodes. Generally, *Meloidogyne* species are a serious threat in crop production systems, with crops without nematode resistance to the genus suffering losses from as high as 50% to total crop failure (Thies et al., 2016). Fortunately, certain cowpea cultivars/landraces with resistance to *Meloidogyne* species had been identified (Ononuju and Nzenwa, 2011; Ruanpanun and Somta, 2015). Nevertheless, the crop is also susceptible to cowpea aphid (*Aphis craccivora* Koch). Findings suggested that when infestations of phloem-sucking insects such as aphids and greenhouse whiteflies (*Trialeurodes vaporariorum* Westwood) when unchecked on sweet stem sorghum and wild *Cucumis* species, resistance to *Meloidogyne* species was invariably lost (Pofu et al., 2012; Mashela et al., 2017a; Maleka et al., 2021). Incidentally, another emerging *Meloidogyne* species, the guava root-knot nematode [*Meloidogyne enterolobii* (Jang and Eisenback)], with a wide range of host plants and, the shortest ontogeny of 15 days among thermophilic *Meloidogyne* species (Collet, 2020), was not affected by Mi resistance genes that affect most *Meloidogyne* species in *Solanum* species (Philbrick et al., 2020). Globally, *M. enterolobii* is being viewed as the most aggressive among *Meloidogyne* species (Castagnone-Sereno, 2012; Dareus et al., 2021). Due to the high damage impact induced by the genus, it is imperative that management strategies be in place for suppressing the population densities of this nematode to below the economic threshold level for crops without nematode resistance (Proveda et al., 2020).

Traditionally, nematode population densities were effectively managed using fumigant nematicides. However, their withdrawal from the agrochemical markets due to environmental issues that included climate change, shifted nematode management strategies to alternatives perceived as being sustainable and environment-friendly (Mashela et al., 2017b).

Filamentous fungi such as *Glomus* species (AMF) and *Trichoderma* species have capabilities for improving plant growth and suppressing various soil-borne pathogens, including plant nematodes (Baltruschat and Schonbeck, 1975; Richardson et al., 2011). Colonization of roots by *Glomus* species improve nutrient absorption, particularly phosphorus and certain micronutrient elements, along with conferring drought tolerance and disease resistance to plants (Ozbay and Newman, 2004; Chandanie et al., 2009). In contrast, colonization of roots by *Trichoderma* species confer resistance to pathogens, including plant nematodes (Vasundhara et al., 2016; Proveda et al., 2020). In root-free soil, *Trichoderma* species had antagonistic effects on AMF (Green et al., 1999). On tomato plants, *T. feltiae* and cucurbitacin phytonematicides had synergistic effects on plant

growth variables and suppression of *M. incognita* population densities under greenhouse conditions (Madaure et al., 2019). As noted in other reports, the efficacy of *Trichoderma* species is both fungus-specific and plant-specific, with numerous contradicting effects (Stewart and Hill, 2014; Proveda et al., 2020).

The cucurbitacin phytonematicides, Nemarioc-AL and Nemafric-BL phytonematicides, with active ingredients cucurbitacin A ( $C_{32}H_{46}O_9$ ) and cucurbitacin B ( $C_{32}H_{46}O_8$ ), respectively, are being developed from fruits of indigenous wild *Cucumis* species to South Africa as alternatives to fumigant nematicides (Mashela et al., 2017a). The two phytonematicides each consistently improved plant growth and suppressed nematode population densities of various *Meloidogyne* species under a wide range of conditions (Mashela et al., 2017a). Efficacies of the two phytonematicides were comparable to those of the carbamate and organophosphate nematostatic products (Mashela et al., 2008). Filamentous fungi and cucurbitacin phytonematicides are ideal for use as cost-effective products in low-input crops such as cowpeas. Biocult WS (Biocult Pty, Sommerset West, South Africa) is a South African product, with each gram containing 400 propagules of *Glomus* species +  $1 \times 10^9$  CFU *Trichoderma asperellum*. Lieckf and Nirenberg. Although both Biocult and cucurbitacin phytonematicides are separately being researched and developed for improving plant growth and suppressing nematode population densities. Generally, the combined effects of filamentous fungi with other agricultural biocontrol agents have had antagonistic effects (Proveda et al., 2020). The combined effects of the two test variables on leguminous crops and suppression of nematodes had not been documented. The objective of this study was therefore to investigate the interactive effects of Biocult and Nemafric-BL phytonematicide on growth of cowpea and suppression of *M. enterolobii* population densities under field conditions.

## MATERIALS AND METHODS

### Study Location

The trial was conducted in autumn (March-May) 2019 and repeated in 2020 under field conditions at the Green Biotechnologies Research Centre of Excellence, University of Limpopo (23°53'10"S, 29°44'15"E), South Africa. The location is semi-arid with summer rainfall averaging less than 450 mm per annum and summer temperature averaging 28°C. Hutton soil at the experimental site comprised 65% sand, 30% clay, 5% silt, which was thus classified as loam, with pH (H<sub>2</sub>O) 6.5 and EC 1.87 dS/m.

### Treatments and Experimental Design

Nemafric-BL phytonematicide was prepared through fermentation using oven-dried fruit from cultivated wild watermelon (*Cucumis africanus* L.) and effective microorganisms (EM) as described previously (Mashela et al., 2017a). Biocult and Nemafric-BL phytonematicide, as the first and the second main factors, respectively, were laid out in a 2 × 2 factorial experiment. The four treatments (B<sub>0</sub>P<sub>0</sub>, B<sub>1</sub>P<sub>0</sub>, B<sub>0</sub>P<sub>1</sub>, B<sub>1</sub>P<sub>1</sub>) were arranged



in randomized complete block design with 10 replications ( $n = 40$ ), with blocking being for shading by windbreaks in the morning and in the afternoon. Due to the factorial nature of the experiment, there was no need to repeat the experiment (Little and Hills, 1978).

## Cultural Practices

A drip irrigation line was laid out resulting in planting stations at 1.0 m  $\times$  0.45 m spacing, with each drip hole discharging 2 L chlorine-free water/h. A day before sowing, each station was irrigated with 3 L half-strength Hoagland solution without N (Hoagland and Arnon, 1950). Primed cowpea var. Eureka seeds were inoculated with *Rhizobium leguminosarium biovar phaseoli* spores while still moist and placed on laboratory bench for 3 days prior to sowing. Four seeds were sown per drip hole and at 5 days after complete emergence, seedlings were thinned to one per drip hole.

## Initiation of Treatments

Soil samples were collected adjacent to each seedling using a Soil Sampler Probe 52 cm (Mylawncare, Johannesburg, South Africa), composited and mixed. Second-stage juveniles (J2) were extracted from 250 ml soil subsample using the modified sugar-centrifugation floatation method (Marais et al., 2017), with J2 counted under a 60  $\times$  magnification stereomicroscope, with mounted specimen identified as *M. enterolobii* using morphometric characters. The initial nematode population density (Pi) averaged 35 J2/250 ml soil subsample, which necessitated augmentation of each seedling with 250 eggs + J2 *M. enterolobii* collected from roots of tomato plant cv. “Floradade.” Eggs + J2 were dispensed using a 20 ml plastic pipette around each seedling with holes covered using soil. Five days after thinning, Biocult was applied by placing 2 g in a shallow furrow around each seedling and covering with soil. Five days thereafter, Nemafric-BL phytonematicide was applied at 2%, with biweekly reapplication until harvest. Aphid populations were monitored daily, with plants sprayed once at 35 days after seedling emergence using malasol at 5 ml/5 L chlorine-free water to contain the aphid infestations.

## Data Collection and Analysis

At 60 days after the phytonematicide treatment, whole plants were removed. Plant length was measured from the severed end to the tip of the flag leaf of the longest vine using a measuring tape. Stem diameter was measured at 5 cm above the severed distal end using a digital Vernier caliper. Tender leaves usually harvested for use as leafy vegetable were harvested and dried with shoots in air-forced ovens at 60°C for 72 h for dry leaf and shoot mass. Root systems were removed from each station, immersed in water to remove soil particles, blotted dry, with eggs and J2 extracted from 10 g roots using the modified sugar floatation method (Marais et al., 2017). From each planting site, 300 ml soil sample was collected, mixed and J2 extracted from a 250 ml soil subsample (Marais et al., 2017), with root and soil nematodes separately counted under a stereomicroscope. Nematode data were transformed using  $\log_{10}(x + 1)$  to normalize the variances. All datasets were separately subjected to the Shapiro-Wilk

test using Statistix 10 software to assess the normality of the distribution of data (Shapiro and Wilk, 1965; Ghasemi and Zahedias, 2012). The data exhibited normal distribution and were therefore subjected to factorial analysis of variance.

## RESULTS

The seasonal interactions for variables were not significant and data were pooled ( $n = 80$ ) and reanalyzed. The interactions on plant and nematode variables were highly significant ( $P \leq 0.01$ ), and therefore the data were expressed using a two-way table (Little, 1981), with treatment means compared at the probability level of 5% using Tukey HSD All-Pairwise Comparison test. Due to the factorial nature of the study, there was no need to validate the results Little and Hills, 1978). Unless otherwise stated, only treatment effects which were significant at 5% level of probability were discussed.

### Plant Growth Variables

At harvest, the interaction of Biocult and Nemafric-BL phytonematicide was highly significant ( $P \leq 0.01$ ) on plant growth variables. Relative to untreated control, Biocult alone increased plant variables from 15 to 74% (Table 1). Similarly, NemafricBL phytonematicide increased plant variables from 14 to 61%. However, the combined effects significantly increased dry shoot mass by 19% and dry harvestable leaf mass by 21%, but did not have significant effects on plant height and stem diameter.

### Nematode Suppression

The interaction of the two products was also highly significant on nematode variables. Relative to untreated control, Biocult alone reduced nematode eggs in root, J2 in root and J2 in soil by 80, 84, and 53%, respectively (Table 2). However, the combined effects of the two products did not have significant effects on any of the test nematode variables in roots, but significantly reduced J2 in soil by 30%.

## DISCUSSION

### Plant Growth

In the current study Biocult and Nemafric-BL phytonematicide each significantly increased growth variables of cowpea plants. *Glomus* species and *Trichoderma* species in Biocult have the potential of increasing soil biological activities that improve soil health by inducing the root system to exudate various secondary metabolites, including enzymes, into the rhizosphere (Stirling, 2014; Yan et al., 2021). Additionally, *Glomus* species, the arbuscular mycorrhizal fungi, provide benefits that include improved absorption of phosphorus and certain micronutrient elements (Richardson et al., 2011) and nematode suppression (Gough et al., 2020). The species can also accord the host plant the ability to access water beyond the normal wilting point, thereby according the plants the drought tolerance status, particularly under suboptimal conditions (Proveda et al., 2020).

**TABLE 1 |** Relative impact (RI) of Biocult (B) and Nemafric-BL phytonematicide (P) on dry harvestable leaf mass (DHLM), dry shoot mass (DSM), plant height (PHT), and stem diameter (STD) of cowpea var. Eureka at 56 days after the treatments under field conditions ( $n = 80$ ).

BL	Biocult															
	DSM (kg) <sup>y</sup>				DHLM (kg)				PHT (cm)				STD (mm)			
	B <sub>0</sub>	RI (%) <sup>z</sup>	B <sub>1</sub>	RI (%)	B <sub>0</sub>	RI (%)	B <sub>1</sub>	RI (%)	B <sub>0</sub>	RI (%)	B <sub>1</sub>	RI (%)	B <sub>0</sub>	RI (%)	B <sub>1</sub>	RI (%)
P <sub>0</sub>	3.71 <sup>c</sup>	–	6.45 <sup>a</sup>	74	0.97 <sup>b</sup>	–	1.40 <sup>a</sup>	44	25.05 <sup>b</sup>	–	28.81 <sup>a</sup>	15	7.51	–	8.14	11
P <sub>1</sub>	5.98 <sup>a</sup>	61	4.43 <sup>b</sup>	19	1.32 <sup>a</sup>	37	1.17 <sup>a</sup>	21	28.61 <sup>a</sup>	14 <sup>a</sup>	25.81 <sup>a</sup>	3	8.30	14	7.53	–0.4
	Standard error = 1.07				Standard error = 0.96				Standard error = 1.12				Standard error = 1.89			

<sup>y</sup>Means with the same letter within the variable were not different ( $P \leq 0.05$ ) according to Tukey test.

<sup>z</sup>RI (%) =  $[(\text{Treatment}/\text{Control}) - 1] \times 100$ .

**TABLE 2 |** Relative impact (RI) of Biocult (B) and Nemafric-BL phytonematicide (P) on eggs in roots, second-stage juveniles (J2) in root, J2 in soil on cowpea var. Eureka at 60 days after the treatments under field conditions ( $n = 80$ ).

Nemafric-BL	Biocult											
	Eggs/10 g root <sup>y</sup>				J2/10 g root				J2/250 ml soil			
	B <sub>0</sub>	RI (%) <sup>z</sup>	B <sub>1</sub>	RI (%)	B <sub>0</sub>	RI (%)	B <sub>1</sub>	RI (%)	B <sub>0</sub>	RI (%)	B <sub>1</sub>	RI (%)
P <sub>0</sub>	954 <sup>a</sup>	–	188 <sup>c</sup>	–80	3,490 <sup>a</sup>	–	560 <sup>b</sup>	–84	2,094 <sup>a</sup>	–	977 <sup>b</sup>	–53
P <sub>1</sub>	103 <sup>b</sup>	–89	594 <sup>a</sup>	–38	210 <sup>c</sup>	–94	27 95 <sup>a</sup>	–20	90	–96	1,459 <sup>c</sup>	–30
	Standard error = 2.11				Standard error = 1.86				Standard error = 3.12			

<sup>y</sup>Means with the same letter within the variable were not different ( $P < 0.05$ ) according to Tukey test.

<sup>z</sup>RI (%) =  $[(\text{Treatment}/\text{Control}) - 1] \times 100$ .

Another endophytic fungi, *Trichoderma* species, in addition to promoting plant growth through various mechanisms (Ozby and Newman, 2004), which include mineral solubilization and boost nutrient uptake, also provide certain degree of protection against soil pathogens, including nematodes (Stewart and Hill, 2014). Colonization of roots by *Trichoderma* species had been associated with improved chlorophyll content, alleviation of abiotic stress, increased exudation of secondary metabolites and the production of various plant growth regulators hormones (Yan et al., 2021). However, the effects of *Glomus* species and *Trichoderma* species on plant growth are plant- and species-specific (Stewart and Hill, 2014; Gough et al., 2020). Combined, *Glomus* species and *T. asperellum* in Biocult were previously observed to have synergistic effects on increasing dry shoot mass in cucumber (*Cucumis sativa* L.) plants when compared with individual treatment effects (Chandanie et al., 2009).

In our study, Nemafric-BL phytonematicide had consistent effects on improving growth variables of cowpea plants. In other studies, where the product was used to manage nematode population densities of *M. incognita* and *M. javanica*, the product consistently improved crop growth variables (Mashela et al., 2017a). Cucurbitacins in phytonematicides can either have stimulation, neutral or inhibition effects on plant growth. However, since the dosage accumulates in the rhizosphere with repeated phytonematicide application, response in different plant organs can also be concentration-specific as shown in different studies (Mashela et al., 2017a). Cucurbitacin B in Nemafric-BL phytonematicide is able to penetrate the apoplastic pathways in roots, but cannot penetrate the symplastic pathway which is accorded by the pericycle and the endodermis in root systems (Van Wyk and Wink, 2014). In our study, as shown by the plant

growth responses, concentration of cucurbitacin B in apoplastic spaces remained within the stimulation range for all the test plant variables since growth was significantly increased.

Notably, the combined effects of Biocult and Nemafric-BL phytonematicide, had antagonistic effects on plant growth when compared with that of either of product. In colonized root systems, mycelia of the filamentous fungi penetrate the root system to establish mutual relationships (Stewart and Hill, 2014; Proveda et al., 2020). Such relationships change the morphology and metabolism of the root system, along with the bioactive chemical compounds of affected plant roots (Vasundhara et al., 2016; Yan et al., 2021). Apparently, when the two products are combined, there are both physical and chemical limitations in roots. Firstly, the proliferation of mycelia in the apoplast spaces, alter the available physical spaces in which free water that carries cucurbitacin molecules percolate. Consequently, the reduced free-passage of free water, invariably results in reduced concentration of cucurbitacin B in apoplastic spaces. Secondly, although reduced cucurbitacin B could have stimulation effects on plant growth variables, for lower organisms such as *Glomus* and *Trichoderma* species, the concentration could have been at the inhibition range, technically, the cytotoxic range. Under *in vitro* conditions, which mimic apoplastic conditions, *T. harzianum* suppressed mycelia of *G. intraradices* (Green et al., 1999).

## Nematode Suppression

Cowpea var. Eureka is a host to *Meloidogyne* species (Mashela and Pofu, 2012). In our study, Biocult and Nemafric-BL phytonematicide each consistently suppressed nematode population densities of *M. enterolobii* in root and in soil, which

confirmed observations in other studies (Mashela et al., 2017a; Proveda et al., 2020; Yan et al., 2021). *Trichoderma* species are primarily biocontrol agents that have inherent capabilities of triggering plants to release chemicals with nematocidal properties (Proveda et al., 2020; Yan et al., 2021). Such chemicals include flavonoids, phenols and chitinase,  $\beta$ -1,3 glucanase, protease, amylase, which are known as plant genes that confer nematode resistance in plants (Mashela et al., 2017b). The induced plant resistance as observed in var. Eureka in our study, had been referred to as systemic acquired resistance (Stirling, 2014; Proveda et al., 2020). The effects of Nemafric-BL phytonematicide on population densities of *M. enterolobii* in the current study, confirmed those of this product on a wide range of other *Meloidogyne* species and races (Mashela et al., 2017b), which we do not wish to discuss further in the current study.

Both *Glomus* species and *Trichoderma* species are endophytes, with different roles and capabilities of inducing nematode resistance in plants (Proveda et al., 2020). However, the two species, when combined, were at times shown to have significant antagonistic effects on population densities of *Meloidogyne* species (Yan et al., 2021), with the effects not being limited to the induced chemicals. After J2 hatch, J2 move out of roots into soil solution, from where search for penetration sites occurs. After penetration, J2 move to the tip of root and enter the vascular bundle and then move upward through the xylem to the zone of differentiation, where feeding sites are established (Mashela et al., 2017b). In addition to inducing chemicals with nematocidal properties (Yan et al., 2021), mycelia and spores of the endophytes can physically impede J2 mobility (Stewart and Hill, 2014; Gough et al., 2020; Proveda et al., 2020).

Generally, the effects of cucurbitacins on entities are both concentration- and size-specific. Concentrations that have stimulation effects on plant growth were previously shown to have significant inhibition effects on various bioactivities on minute entities like plant nematodes (Dube, 2016). In Nemarioc-AL phytonematicide, with active ingredient cucurbitacin A, which is partly polar and therefore slightly soluble in water. Nodules induced by *Bradyrhizobium japonicum* on cowpea vs. increasing concentration of Nemarioc-AL phytonematicide exhibited quadratic positive relationships, with nodules being highly sensitive to the product (Kola et al., 2018). Although in the current study we observed consistent antagonistic effects of Biocult and Nemafric-BL phytonematicide, *T. harzianum* in short-term studies was tolerant to Nemarioc-AL and Nemafric-BL phytonematicides at concentrations used in nematode management (Madaure et al., 2019). In our study, Nemafric-BL phytonematicide was applied biweekly, with the likelihood that the stable cucurbitacin B accumulated within the apoplastic spaces, thereby inhibiting both mycelia and spore development. In other studies (Vasundhara et al., 2016; Proveda et al., 2020) the combined effects of *Trichoderma* species with either

*Paecilomyces lilacinus* biocontrol agent, neem (*Azadirachta indica* A. Juss) phytonematicide or castor (*Ricinus communis* L.) oil had synergistic effects in suppressing population densities of *Meloidogyne* species, which contradicted observations in our study. However, our findings confirm the assertion that the efficacy of filamentous fungi on inducing beneficial effects is dependent upon the fungal species, plant species and pathogen type and species (Gough et al., 2020). Additionally, in interaction with agricultural remedies of botanical nature, the degree of sensitivity of filamentous fungi to the active ingredients of the test product could also play an indispensable role in the expression of the interactive effects.

## CONCLUSION

Biocult and Nemafric-BL phytonematicide each consistently promoted growth of cowpea var. Eureka and suppressed population densities of *M. enterolobii* in both root and soil. In contrast, the combined effects of the two products had antagonistic effects on growth of the test plant and suppression of nematode population densities. In conclusion, the two products should be applied separately in cowpea production until the issues of antagonism are resolved.

## DATA AVAILABILITY STATEMENT

The original contributions presented in the study are included in the article/supplementary material, further inquiries can be directed to the corresponding author/s.

## AUTHOR CONTRIBUTIONS

KP conducted the field experiments over two seasons and analyzed the data. Both authors contributed equally to the discussion of the results, formulated the objectives, and designed the study.

## FUNDING

This work was based on the research supported in part by the National Research Foundation of South Africa (Grant No. 135451).

## ACKNOWLEDGMENTS

The Agricultural Research Council of South Africa provided cowpea var. Eureka seeds from its seedbank.

## REFERENCES

- Baltruschat, H., and Schonbeck, F. (1975). The influence of endotrophic mycorrhiza on the infestation of tobacco *Thielaviopsis basicola*. *Phytopathol. Z.* 84, 172–188.
- Castagnone-Sereno, P. (2012). *Meloidogyne enterolobii* (= *M. mayaguensis*): profile of an emerging, highly pathogenic, root-knot nematode species. *Nematology* 14, 133–138. doi: 10.1163/156854111X601650
- Chandanie, W. A., Kubota, M., and Hyakumachi, M. (2009). Interaction between the arbuscularmycorrhizal fungus *Glomus mosseae* and plant growth promoting

- fungi and their significance for enhancing plant growth and suppressing damping off of cucumber (*Cucumis sativus* L.). *Appl. Soil Ecol.* 41, 336–341. doi: 10.1016/j.apsoil.2008.12.006
- Collet, R. L. (2020). *A comparative study of the development and reproduction of Meloidogyne enterolobii and other thermophilic South African Meloidogyne species*. Ph.D. thesis. Potchefstroom, South Africa: North-West University, doi: 10.13140/RG.2.2.27857.56169
- Dareus, R., Porto, A. C., Bogale, M., DiGennaro, P., Chase, C. A., and Rios, E. F. (2021). Resistance to *Meloidogyne enterolobii* and *Meloidogyne incognita* in cultivated cowpea. *HortScience* 56, 460–468.
- Dube, Z. P. (2016). *Nemarioc-AL and Nemafric-BL phytonematicides: bioactivities in Meloidogyne incognita, tomato crop, soil type and organic matter*. Ph.D. thesis. Sovenga South Africa: University of Limpopo.
- Ghasemi, A., and Zahedias, S. (2012). Normality tests for statistical analysis: a guide for non-statisticians. *Int. J. Endocrinol. Metab.* 10, 486–489. doi: 10.5812/ijem.3505
- Gough, E. C., Owen, K. J., Zwart, R. S., and Thompson, J. P. (2020). A systemic review of the effects of arbuscular mycorrhizal fungi on root-lesion nematodes, *Pratylenchus* spp. *Front. Plant Sci.* 11:923. doi: 10.3389/fpls.2020.00923
- Green, H., Larsen, J., Olsson, P. A., Jensen, D. F., and Jakobsen, I. (1999). Suppression of the biocontrol agent *Trichoderma harzianum* by mycelium of the arbuscular mycorrhizal fungus *Glomus intraradices* in root-free soil. *J. Appl. Environ. Microbiol.* 65, 1428–1434. doi: 10.1128/AEM.65.4.1428-1434.1999
- Hoagland, D. R., and Arnon, D. I. (1950). *The Water-Culture method for growing plants without soil*. Berkeley, Calif: University of California, College of Agriculture, Agricultural Experiment
- Kola, M. E., Mashela, P. W., and Lukhele-Olorunju, P. (2018). Response of *Bradyrhizobium japonicum* nodule variables to cucurbitacin-containing phytonematicides in cowpea (*Vigna unguiculata*) on N-deficient soil. *Res. Crops* 19, 480–485. doi: 10.31830/2348-7542.2018.0001.19
- Little, T. M. (1981). Interpretation and presentation of results. *HortScience* 16, 19–22.
- Little, T. M., and Hills, F. J. (1978). *Agricultural experimentation: design and analysis*. New York: Wiley, 350.
- Madaure, J. T., Mashela, P. W., and De Waele, D. (2019). Interactive effects of Nemarioc-AL phytonematicide, *Steinernema feltiae* and *Trichoderma harzianum* on the reproduction of *Meloidogyne incognita* race 2 under greenhouse conditions. *Acta Agric. Scand. B Soil Plant Sci.* 69, 235–240. doi: 10.1080/09064710.2018.1539190
- Maleka, K. G., Pofu, K. M., and Mashela, P. W. (2021). Interference of sugarcane aphid (*Melanaphis scirpae*) with sugar content in sweet stem sorghum (*Sorghum bicolor*) and its resistance to *Meloidogyne* species under field conditions. *Res. Crops* 22, 360–368.
- Marais, M., Swart, A., Fourie, H., Berry, S. D., Knoetze, R., and Malan, A. P. (2017). “Techniques and Procedures,” in *Nematology in South Africa: a View From the 21<sup>st</sup> Century*, eds H. Fourie, V. W. Spaull, R. K. Jones, M. S. Daneel, and D. De Waele (Cham: Springer International), 73–118. doi: 10.1007/978-3-319-44210-5\_4
- Mashela, P. W., De Waele, D., Dube, Z., Khosa, M. C., Pofu, K. M., Tefu, G., et al. (2017a). “Alternative Nematode management Strategies,” in *Nematology in South Africa: a View From the 21<sup>st</sup> Century*, eds H. Fourie, V. W. Spaull, R. K. Jones, M. S. Daneel, and D. De Waele (Cham: Springer International), 151–182. doi: 10.1007/978-3-319-44210-5\_7
- Mashela, P. W., Ndhlala, A. R., Pofu, K. M., and Dube, Z. P. (2017b). “Phytochemicals of nematode-resistant transgenic plants,” in *Transgenesis and Secondary Metabolism. Reference Series in Phytochemistry*, ed. S. Jha (Cham: Springer), 553–568. doi: 10.1007/978-3-319-28669-3\_26
- Mashela, P. W., and Pofu, K. M. (2012). Interactive effects of *Meloidogyne incognita* race 2, *Bradyrhizobium japonicum* and crude extracts of *Cucumis myriocarpus* fruit on *Vigna unguiculata*. *Crop Prot.* 42, 124–127. doi: 10.1016/j.cropro.2012.06.013
- Mashela, P. W., Shimelis, H. A., and Mudau, F. N. (2008). Comparison of the efficacy of ground wild cucumber fruits, aldicarb and fenamiphos on suppression of the root-knot nematode on tomato. *J. Phytopathol.* 156, 264–267. doi: 10.1111/j.1439-0434.2007.01353.x
- Ononuju, C. C., and Nzenwa, O. P. (2011). Assessment of six-cowpea (*Vigna unguiculata* (L.) Walp) varieties for resistance to root-knot nematodes. *Int. J. Appl. Agric. Res.* 6, 77–82.
- Ozbay, Y. N., and Newman, S. E. (2004). Effect of *Trichoderma harzianum* strains to colonize tomato roots and improve growth. *Pak. J. Biol. Sci.* 7, 253–257.
- Philbrick, A. N., Adhikari, T. B., Lous, F. J., and Gorny, A. M. (2020). *Meloidogyne enterolobii*, a major threat to tomato production: current status and future prospects for its management. *Front. Plant Sci.* 11:606395. doi: 10.3389/fpls.2020.606395
- Pofu, K., Mashela, P., and Shimelis, H. (2012). Host-status and host-sensitivity of wild *Cucumis* species to *Meloidogyne incognita* race 4. *Acta Agric. Scand. B Soil Plant Sci.* 62, 329–334. doi: 10.1080/09064710.2011.614633
- Proveda, J., Abril-Urias, P., and Escobar, C. (2020). Biological control of plant-parasitic nematodes by filamentous fungi inducers of resistance: *trichoderma*, mycorrhizal and endophytic fungi. *Front. Microbiol.* 11:992. doi: 10.3389/fmicb.2020.00992
- Richardson, A. E., Lynch, J. P., Ryan, P. R., Delhaize, E., Smith, F. A., Smith, S. E., et al. (2011). Plant and microbial strategies to improve the phosphorus efficiency of agriculture. *Plant Soil* 349, 121–156. doi: 10.1007/s11104-011-0950-4
- Ruanpanun, P., and Somta, P. (2015). Identification and resistant characterization of legume sources against *Meloidogyne incognita*. *J. Integ. Agric.* 20, 168–177. doi: 10.1016/S2095-3119(20)63414-1
- Shapiro, S. S., and Wilk, M. B. (1965). An analysis of variance test for normality (Complete samples). *Biometrika* 52, 591–611. doi: 10.2307/2333709
- Stewart, A., and Hill, R. (2014). “Application of *Trichoderma* in Plant Growth Promotion,” in *Biotechnology and Biology of Trichoderma*, eds V. K. Gupta, M. Schmoll, M. A. Herrera-Estrella, R. S. Upadhyay, I. Druzhining, and M. G. Taohy (Amsterdam: Elsevier), 415–428.
- Stirling, G. R. (2014). *Biological control of plant-parasitic nematodes: soil ecosystem management in sustainable agriculture*. Boston: CABI, 510.
- Thies, J. A., Ariss, J., Kousik, C., Hassell, R., and Levi, A. (2016). Resistance to southern root-knot nematode (*Meloidogyne incognita*) in wild watermelon (*Citrullus lanatus* var. *citroides*). *J. Nematol.* 48, 14–19. doi: 10.21307/jofnem-2017-004
- Van Wyk, B., and Wink, M. (2014). *Phytomedicines, herbal drugs and poisons*. Chicago: The University of Chicago Press, 304.
- Vasundhara, M., Kumar, A., and Reddy, M. S. (2016). Molecular approaches to screen bioactive compounds from endophytic fungi. *Front. Microbiol.* 7:1774. doi: 10.3389/fmicb.2016.01774
- Yan, Y., Wang, Y., Zhao, J., Fu, Y., Yang, Z., Peng, X., et al. (2021). *Trichoderma harzianum* induces resistance to root-knot nematodes by increasing secondary metabolite synthesis and defense-related enzyme activity in *Solanum lycopersicum* L. *Biol. Control* 158:104609.

**Conflict of Interest:** The authors declare that the research was conducted in the absence of any commercial or financial relationships that could be construed as a potential conflict of interest.

**Publisher's Note:** All claims expressed in this article are solely those of the authors and do not necessarily represent those of their affiliated organizations, or those of the publisher, the editors and the reviewers. Any product that may be evaluated in this article, or claim that may be made by its manufacturer, is not guaranteed or endorsed by the publisher.

Copyright © 2022 Pofu and Mashela. This is an open-access article distributed under the terms of the Creative Commons Attribution License (CC BY). The use, distribution or reproduction in other forums is permitted, provided the original author(s) and the copyright owner(s) are credited and that the original publication in this journal is cited, in accordance with accepted academic practice. No use, distribution or reproduction is permitted which does not comply with these terms.





# Modification of Early Response of *Vitis vinifera* to Pathogens Relating to Esca Disease and Biocontrol Agent Vintec® Revealed By Untargeted Metabolomics on Woody Tissues

Justine Chervin<sup>1,2,3</sup>, Ana Romeo-Oliván<sup>4</sup>, Sylvie Fournier<sup>1,2,3</sup>, Virginie Puech-Pages<sup>1,2,3</sup>, Bernard Dumas<sup>1</sup>, Alban Jacques<sup>4</sup> and Guillaume Marti<sup>1,2,3\*</sup>

<sup>1</sup> Laboratoire de Recherche en Sciences Végétales, Université de Toulouse, CNRS, UPS, Toulouse INP, Toulouse, France,

<sup>2</sup> Metatoul-AgromiX Platform, LRSV, Université de Toulouse, CNRS, UPS, Toulouse INP, Toulouse, France,

<sup>3</sup> MetaboHUB-MetaToul, National Infrastructure of Metabolomics and Fluxomics, Toulouse, France, <sup>4</sup> Unité de Recherche Physiologie, Pathologie, et Génétique Végétales (PPGV), INP PURPAN, Université de Toulouse, Toulouse, France

## OPEN ACCESS

### Edited by:

Florence Fontaine,  
Université de Reims  
Champagne-Ardenne, France

### Reviewed by:

Marta R. M. Lima,  
Virginia Tech, United States  
Julie Chong,  
University of Upper Alsace, France

### \*Correspondence:

Guillaume Marti  
guillaume.marti@univ-tlse3.fr

### Specialty section:

This article was submitted to  
Microbe and Virus Interactions with  
Plants,  
a section of the journal  
Frontiers in Microbiology

Received: 14 December 2021

Accepted: 19 January 2022

Published: 02 March 2022

### Citation:

Chervin J, Romeo-Oliván A,  
Fournier S, Puech-Pages V, Dumas B,  
Jacques A and Marti G (2022)  
Modification of Early Response of *Vitis*  
*vinifera* to Pathogens Relating to Esca  
Disease and Biocontrol Agent Vintec®  
Revealed By Untargeted  
Metabolomics on Woody Tissues.  
Front. Microbiol. 13:835463.  
doi: 10.3389/fmicb.2022.835463

Esca disease is one of the most destructive grapevine trunk diseases. *Phaeoacremonium minimum* and *Phaeomoniella chlamydospora* are two of the known fungal pathogens associated with this disease. Today, biocontrol agents against Esca are mainly based on the use of the strain of the mycoparasite fungal genus *Trichoderma* such as the Vintec® product. The aim of this study was to investigate early response of woody tissues to Esca pathogens and identify metabolites that could be correlated with a biocontrol activity within a complex woody matrix. An untargeted liquid chromatography–high-resolution mass spectrometry metabolomic approach coupled to a spectral similarity network was used to highlight clusters of compounds associated with the plant response to pathogens and biocontrol. Dereplication highlighted the possible role of glycerophospholipids and polyphenol compounds, the latest mainly belonging to stilbenoids. Antifungal activity of some relevant biomarkers, evaluated *in vitro* on *Phaeomoniella chlamydospora* and *Botrytis cinerea*, suggests that some of these compounds can play a role to limit the development of Esca pathogens in planta.

**Keywords:** *Vitis vinifera*, Esca disease, metabolomics, biomarkers, biocontrol

## INTRODUCTION

Grapevine trunk diseases (GTDs) are of growing concern among worldwide viticulture. These diseases concern different organs of the plant, some causing the progressive death of vines in vineyards. These losses influence the productivity of the vineyard and, therefore, represent a considerable economic impact in the viticultural sector (Hofstetter et al., 2012; Fontaine et al., 2016). Grapevine trunk diseases are associated with the presence of different pathogenic fungal species, which can affect vines at different stages of their life cycle (Bertsch et al., 2013; Bruez et al., 2014).

Esca is one of the most complex and destructive trunk diseases. The Esca disease comprises different syndromes, depending on the symptoms, the age of the plant, and the fungal species associated (Graniti et al., 2000; Surico, 2009; Bertsch et al., 2013). One of the syndromes, named Esca, is associated with white rot in the trunk, and it is caused by fungal species of the genus *Formitiporia* (Bruno and Sparapano, 2007). The three vascular syndromes—brown wood streaking (Mugnai et al., 1999), Petri disease, and grapevine leaf stripe disease (GLSD) (Bertsch et al., 2013)—are associated with *Phaeoconiella chlamydospora* (*P. chlamydospora*), *Phaeoacremonium minimum* (*P. minimum*), and other *Phaeoacremonium* spp. (Luque et al., 2009; Úrbez-Torres et al., 2014). The presence of these pathogens in the wood affects not only the trunk but also leaves and berries. Symptoms on leaves start with chlorotic areas becoming necrotic and conferring a “tiger striped” appearance. On berries, dark purple spots on the epidermis can be observed (Mugnai et al., 1999). The last syndrome, Esca proper, corresponds to the co-occurrence of Esca and GLSD in the same plant (Surico, 2009).

In the absence of curative methods, since the banishment of sodium arsenite, there are numerous strategies to limit the occurrence of GTDs both in nurseries and in the field (Mondello et al., 2018a,b). One of these strategies includes the use of biocontrol agents (BCAs). Biocontrol agents represent promising alternatives to conventional phytosanitary products (Ram et al., 2018). *Trichoderma* spp. have been largely studied and are of great interest as biocontrol agents (Moya et al., 2020; Poveda, 2021). In viticulture, there exist two *Trichoderma*-based commercial solutions to control GTDs: Vintec® (Belchim Crop Protection) and Esquive® (Agrauxine by Lesaffre). Some microorganisms have also achieved good results in grapevine protection against GTDs, such as the oomycete *Pythium oligandrum* (Yacoub et al., 2016) or a number of bacteria (Trotel-Aziz et al., 2019; Haidar et al., 2020). *Pythium oligandrum* is known to have an antifungal effect against different plant fungal pathogens (Gerborne et al., 2014). Concerning GTDs, the presence of this oomycete reduces *P. chlamydospora* infection (Yacoub et al., 2016). The known modes of action of *P. oligandrum* are diverse and, as well as *Trichoderma* spp., it can enhance plant defense responses (Yacoub et al., 2020). In the case of bacteria, Trotel-Aziz et al. (2019) found that *Bacillus subtilis* protects grapevine against *Neofusicoccum parvum*, the causal agent of Botryosphaeria dieback, by the activation of detoxification process in the plant. In addition, Haidar et al. (2021) found that bacteria from the genus *Paenibacillus* produced antifungal metabolites and volatile organic compounds that reduced the infection of *N. parvum* in the grapevine's trunk.

*Trichoderma* species have been widely studied for this purpose. Their ability to protect plants resides in the combination of several factors: (i) the enhancement of nutrient uptake and mobilization, (ii) mycoparasitism and competition with the pathogens, and (iii) induction of plant systemic resistance (Vinale et al., 2008; Braun et al., 2018). Vintec®, a formulation of *Trichoderma atroviridae* SC1 (TASC1), is one of the main approved BCAs today to fight trunk diseases (Esca, black dead arm, eutypiose). Its efficiency has been successfully tested in both nursery and vineyard (Berbegal et al., 2020).

In order to better understand this disease, different studies were focused on the physiological modifications on Esca-affected vines (Fontaine et al., 2016). Early studies reported the accumulation of stress metabolites in the wood of Esca-diseased vines (Amalfitano et al., 2000, 2011). Modifications in phenolic compounds in roots showing an early decline were also observed (Del Rio et al., 2001). However, most available works are based on targeted approaches linked with polyphenol compound changes as described in Amalfitano et al. (2011); Lima et al. (2012), or Rusjan et al. (2017), for example.

Untargeted approaches as transcriptomics and metabolomics are of prime interest to study the overall modifications induced in plants during disease outcomes. Recently, several omic studies were assessed in the context of Botryosphaeria dieback issue. A metabolomic study based on wood response with the pathosystem *Neofusicoccum parvum* revealed significant modifications of primary and secondary metabolites after inoculation, in particular a decrease in sugars and an increase in stilbenes and flavonoids (Labois et al., 2020). Another study also reported the importance of lipids in understanding this disease and showed that in diseased vines, phytochemicals, in particular stilbenes and flavonoids, mainly characterized the brown stripe area, whereas lipids, in particular phospholipids, mainly characterized the adjacent white area (Lemaitre-Guillier et al., 2020).

Regarding the Esca issue, a first report on the pathosystem *Vitis vinifera*/Esca upon untargeted metabolomics through nuclear magnetic resonance spectroscopy-based metabolomic showed that a double stress induced by fungi and drought led to the change of several amino acids (Lima et al., 2017b). Nowadays, the majority of studies focus on leaf metabolomes such as the investigation of phenolic modification in leaves of *Vitis vinifera* cv. Alvarinho revealing an apparent accumulation of phenolic compounds in diseased leaves (Lima et al., 2017a). Another work focusing on alterations in leaf metabolome reported that changes, especially concerning phenylpropanoids but also carbohydrates and amino acids, could already be observed prior to symptom appearance (Magnin-Robert et al., 2017). Lipidomic analysis of leaves of Esca-affected grapevine was also conducted (Goufo and Cortez, 2020) and notably showed a general increase in most lipids that correlated with symptom progression.

The present study investigates the response of grapevine woody tissue to fungal infection with the biocontrol agent (BCA) Vintec® (IV), a mixture of both fungi *P. chlamydospora* and *P. minimum* (IPP), as it is usually observed in a natural context, and their combination (IVPP), at an early stage of infection by an ultra-high-performance liquid chromatography–high-resolution mass spectrometry (UHPLC–HRMS)-based metabolomic approach.

The aim of this UHPLC–HRMS approach is to highlight metabolite changes that could be further considered as early biomarkers of infection. This is crucial since fungi associated with Esca disease are known to colonize grapevines during several years without any detectable symptoms in aerial organs like leaves (Bruez et al., 2016).

For this study, a pathosystem was set up to mimic the natural events by co-inoculation of pathogens with and without a

biocontrol agent in the trunk of canes. The aim is to be as close as possible to the vineyard to propose biomarkers to monitor both Esca pre-emergence and biocontrol effects.

## MATERIALS AND METHODS

### Standards

Individual solutions of natural products (NPs) compounds from Metasci (Metasci, Toronto, Canada) and Chemfaces (Wuhan, Hubei) were prepared at 100 µg/ml according to suppliers' recommendations. Belchim Crop Protection (Lissieu, France) supplied the BCA Vintec®.

### Fungal Material

*Phaeoacremonium minimum* (CBS 100398), *Phaeomoniella chlamydospora* (CBS 239.74), and *Botrytis cinerea* (CBS 131.28) strains came from the fungal biodiversity center (Centraalbureau voor Schimmelcultures, CBS, Utrecht, the Netherlands). Fungal isolates were grown in individual Petri plates containing the malt extract-agar (MEA) medium for five weeks at 26°C in obscurity before use.

### Plant Culture

One-year-old canes of *Vitis vinifera* L. cv Cabernet-Sauvignon clone 15 purchased from a French nursery (Pépinières Daydé, Montans, Midi-Pyrénées, France) of the 2019 and 2021 seasons were divided in cuttings containing two dormant nodes. Cuttings were then kept at 5°C for one night. Before planting, their surface was disinfected. At first, cuttings were soaked for 30 s in a 10-L water bath with 5-ml bleach (2.6% active chlorine) and then rinsed twice with 10 L of tap water. Then, cuttings were stored overnight at 4°C in a 10-L water bath containing 5-ml 8-hydroxyquinoline sulfate (0.05% Cryptonol®, Chauvin, France), rinsed three times with 10 L of demineralized water. They were planted in moist autoclaved (121°C, 15 min) rock wool to allow disbudding and rooting. At this point, plants were watered twice a week. Four weeks later, cuttings were transferred from the rock wool into individual pots containing 100 g of autoclaved soil (PAM2, PROVEEN Substrates). Plants were finally grown in a plant growth chamber at 25°C, with 45% of humidity, a photoperiod of 12 h/12 h, and watered three times weekly.

### Plant Inoculation

The following conditions were studied, and for each, 16 plants were used: Injured/Not inoculated (INi); Injured/Vintec® (IV); Injured/*P. minimum* + *P. chlamydospora* (IPP); Injured/Vintec® + *P. minimum* + *P. chlamydospora* (IVPP).

The injured plants were drilled at the internode, as described in Reis et al. (2019). Plants injured but not inoculated with Vintec® received 20 µl in the hole of sterile distilled water; plants injured and inoculated with the biocontrol received 20 µl in the hole of a suspension of the product Vintec® at 2 g L<sup>-1</sup> of formulated product 5 days before infection with Esca fungi (T-5d). The injury was covered with a strip of Parafilm (American National Can, Chicago, IL).

Inoculation with fungi *P. minimum* and *P. chlamydospora* at T0 was performed by drilling again all the plants at the same

spot, and a plug of agar-agar colonized by fungi was directly introduced. All the plants were grown in a plant growth chamber at 25°C, with 45% of humidity and a photoperiod of 12 h/12 h for 3 or 6 weeks.

### Wood Sample Extraction for Metabolomic Analysis and Fungal Colonization Quantification

For metabolomic analysis, samples were harvested at 3 weeks (T3) and 6 weeks (T6) after treatment. We performed an analysis on samples collected above and behind the inoculation site, and these preliminary data did not show a systemic response. This observation agreed with Pierron et al. (2015), showing that wood responses to *P. minimum* (*P. aleophilum*) were mainly restricted to the inoculation point six weeks post-infection. Thus, around 1 cm of wood in the inoculation part (I) was collected and immediately dipped in liquid nitrogen. Likewise, wood samples of the same treatment were pooled in 6 tubes containing 3 pieces of wood from 3 different plants. Each sample was then grounded with a Mixer Mill MM 300 (Retsh, Eragny sur Oise, France) by applying 28 oscillations per second for 1 min. Around 100 mg of powder was then placed in a FastPrep tube (MP Biomedicals Lysing Matrix D, Illkirch, France) and kept at -80°C.

For sample extraction, 1 ml of 70% EtOH was added per 100 mg followed by three cycles of 20 s at 6 m/s in the FastPrep while keeping samples in ice between each cycle. After a centrifugation at 4°C and 12,000 rpm for 10 min, the supernatant was collected and a second extraction was achieved on the residue. The two supernatants were pooled, transferred to vials, and kept at -20°C before injection. An extraction blank (without plant material) and quality control (QC) samples were also prepared for extraction and analytical validation.

A set of three plants of each treatment was reserved for evaluating fungal colonization six weeks post-inoculation via qPCR quantifications. DNA extraction was performed using a CTAB/CIA-based protocol combined with a Qiagen DNA extraction kit (DNeasy plant mini Kit, Qiagen, United States), as described in Romeo-Oliván et al. (2021). qPCR reactions were conducted with the GoTaq® qPCR System (Promega) and ABI 7500 Real-Time PCR Cycler (Applied Biosystems, Foster City, United States) following this cycling program: 15 min at 95°C (denaturation), 40 cycles of 15 s at 95°C and 45 s at 62°C (annealing and extension), and 40 min from 60 to 95°C (melting analysis). Specific primers targeting the β-tubulin gene of *P. chlamydospora* and *P. minimum* were previously described (Pouzoulet et al., 2013) as well as those amplifying the endochitinase 42 gene of *T. atroviridae* SC1 for Vintec® (Savazzini et al., 2008). They were used at 0.5 µM in a final reaction volume of 10 µl. The number of gene copies of *P. chlamydospora* and *P. minimum* was estimated using a standard curve (Pouzoulet et al., 2013). Two-way ANOVA and Dunnett's *post hoc* test ( $p \leq 0.05$ ) were used to compare the gene copy number of the various modalities using GraphPad Prism 8 version 8.3.0 (San Diego, California).

For Vintec®, we only considered the presence/absence of amplification.



## Ultra-High-Performance Liquid Chromatography–High-Resolution Mass Spectrometry Profiling

Ultra-high-performance liquid chromatography-high-resolution MS (UHPLC-HRMS) analyses were performed on a Q Exactive Plus quadrupole (Orbitrap) mass spectrometer, equipped with a heated electrospray probe (HESI II) coupled to a U-HPLC Ultimate 3000 RSLC system (Thermo Fisher Scientific, Hemel Hempstead, United Kingdom). Separation was done on a Luna Omega Polar C18 column (150 mm × 2.1 mm i.d., 1.6 μm, Phenomenex, Sartrouville, France) equipped with a guard column. The mobile phase A (MPA) was water with 0.05% formic acid (FA), and the mobile phase B (MPB) was acetonitrile with 0.05% FA. The solvent gradient was 0 min, 100% MPA; 1 min, 100% MPA; 22 min, 100% MPB; 25 min, 100% MPB; 25.5 min, 100% MPA; and 28 min, 100% MPA. The flow rate was 0.3 ml/min, the column temperature was set to 40°C, the autosampler temperature was set to 5°C, and the injection volume was fixed to 5 μl. Mass detection was performed in positive ionization (PI) mode at resolution 35,000 power [full width at half-maximum (fwhm) at 400 m/z] for MS1 and 17,500 for MS2 with an automatic gain control (AGC) target of  $1 \times 10^6$  for full scan MS1 and  $1 \times 10^5$  for MS2. Ionization spray voltages were set to 3.5 kV, and the capillary temperature was kept at 256°C. The mass scanning range was m/z 100–1500. Each full MS scan was followed by data-dependent acquisition of MS/MS spectra for the six most intense ions using stepped normalized collision energy of 20, 40, and 60 eV.

## Data Processing

Ultra-high-performance liquid chromatography-high-resolution mass spectrometry (UHPLC-HRMS) raw data were processed with MS-DIAL version 4.70 (Tsugawa et al., 2015) for mass signal extraction between 100 and 1,500 Da from 0.5 to 18.5 min. Respectively, MS1 and MS2 tolerance were set to 0.01 and 0.05 Da in the centroid mode. The optimized detection threshold was set to  $1.5 \times 10^6$  concerning MS1 and 10 for MS2. Peaks were aligned on a QC reference file with a retention time tolerance of 0.1 min and a mass tolerance of 0.015 Da. Peak annotation was performed with an in-house database built on an MS-FINDER model (Tsugawa et al., 2016).

MS-DIAL data were then cleaned with the MS-CleanR workflow (Fraisier-Vannier et al., 2020) by selecting all filters with a minimum blank ratio set to 0.8, a maximum relative standard deviation (RSD) set to 40, and a relative mass defect (RMD) ranging from 50 to 3,000. The maximum mass difference for feature relationships detection was set to 0.005 Da and the maximum RT difference to 0.025 min. The Pearson correlation links were considered with correlation  $\geq 0.8$  and statistically significant with  $\alpha = 0.05$ . Two peaks were kept in each cluster with the most intense and the most connected. The kept features (m/z × RT pairs) were annotated with MS-FINDER version 3.52. The MS1 and MS2 tolerances were, respectively, set to 5 and 15 ppm. Formula finders were only processed with C, H, O, N, P, and S atoms. Databases (DBs) based on *Vitis* (genus), Vitaceae (family), *Trichoderma* (genus of the BCA strain), and Togniniaceae (the family of the two pathogenic fungi) were

constituted with the dictionary of natural product (DNP, CRC press, DNP on DVD v. 28.2). The internal generic DBs from MS-FINDER used were KNApSACk, PlantCyc, HMDB, LipidMaps, NNPDB, and UNPD. Annotation prioritization was done by ranking *Vitis* DB, followed by Vitaceae DB, *Trichoderma* and Togniniaceae DBs, and finally generic DBs using the final MS-CleanR step.

## Statistical Analysis

Statistical analyses were made with Orange 3.30.1 (Demsar et al., 2013). All data were scaled by unit variance scaling (UV) before multivariate analysis. ANOVA models were proposed to rank features and highlight biomarkers of plant response to the various studied treatments. Models confronting only two treatments at once were built taking as reference the sample Injured/Not inoculated (INi). A random forest model was used to validate the comparisons based on the cross-validation algorithm. Two-way ANOVA and Dunnett's *post hoc* test ( $p \leq 0.05$ ) were used to check biomarker significance for both kinetics in comparison to references INi with GraphPad Prism 8 version 8.3.0 (San Diego, California).

The heatmap of revealed biomarkers based on average peak area was built with the web-interface MetaboAnalyst version 4.0 (Chong et al., 2019).

## Mass Spectral Similarity Network

The.msp PI and metadata files generated at the end of the MS-CleanR workflow were imported into MetGem version 1.2.2. A mass spectral similarity network was built with a cosine score cutoff fixed at 0.6, a maximum of ten connections between nodes, and at least four matched peaks. The resulting network was imported into Cytoscape12 version 3.7.2 to tune visualization. Node color was based on chemical classes, and the size of revealed biomarkers was increased. The edge width was deepened according to the cosine score.

## In vitro Bioassays

Antifungal activity of pure available standard metabolites was investigated *in vitro* in 96-well plate cultures by measuring fungal growth. Standard solutions were previously dissolved in 8% DMSO in water with concentration ranging from 0.1 to 1.6 mg/ml. Three final concentrations in each well were investigated for each standard, based on antifungal activity results found in the literature: 100, 10, and 1 μg/ml for α-viniferin (Langcake and Pryce, 1977); 50, 5, and 0.5 μg/ml for viniferin (Langcake, 1981), and finally 25, 2.5, and 0.25 μg/ml for pterostilbene (Jeandet et al., 2002). As no information was found on oxyresveratrol, a higher range of concentration was studied: 400, 40, and 4 μg/ml.

To obtain *Botrytis cinerea* and *P. chlamydospora* spores, two plugs of agar colonized by the mycelium of each were cut, placed in 1-ml sterile water, and vortexed. The spore concentration was adjusted under a microscope using a Malassez counting chamber to  $10^3$  spores/ml with water.

Triplicates using *Botrytis cinerea* spores as the positive control as well as *P. chlamydospora* spores as the target pathogen were prepared for each standard concentration. To the well, 130 μl of malt extract medium (0.01 g/ml) was added, followed by 20 μl



of the spore suspension and 50  $\mu$ l of standard solutions. For the negative control, 20  $\mu$ l of the spore suspension was replaced by 20  $\mu$ l of sterile distilled water. Plates were then incubated at 26°C for three days. The absorbance was measured at 600 nm in a microplate reader (Infinite 200 Pro Nano, Tecan, Austria). IC<sub>50</sub> (concentrations causing an inhibition of 50% of fungal growth) were then calculated using GraphPad Prism 8 version 8.3.0 (San Diego, California). Control replicates were prepared to subtract the compound absorbance.

## RESULTS

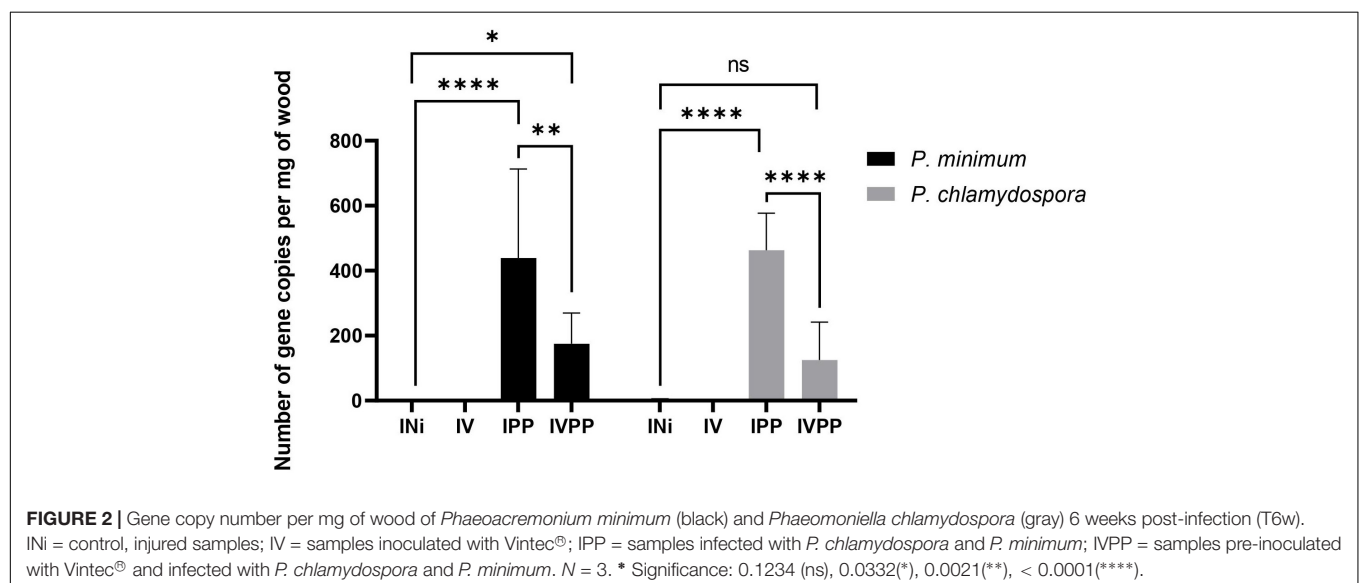
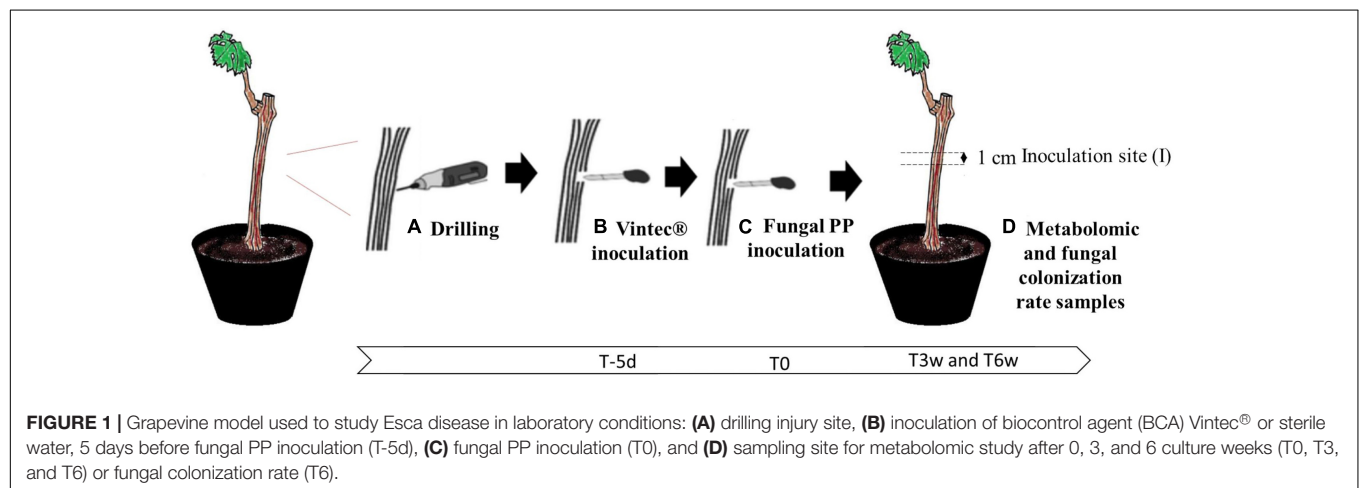
### Fungal Inoculation on *Vitis vinifera*

The dataset was built on a reductionist model to study the local effect of the BCA Vintec® in the metabolic regulation of a plant challenged or not with the two fungal pathogens and highlight early biomarkers of pathogens and biocontrol presence (Figure 1).

*Phaeomoniella chlamydospora* and *P. minimum* colonization was estimated via quantifications by qPCR of their  $\beta$ -tubulin gene (Figure 2). The results indicated that the wood was still colonized six weeks post-infection by the two fungal pathogens in IPP and IVPP samples. Moreover, a significant reduction of colonization by *P. chlamydospora* and *P. minimum* due to the BCA Vintec® was observed. As expected, control samples (INi) and samples inoculated with Vintec® (IV) were free of pathogenic DNA. The presence of *T. atroviridae* SC1 for Vintec® pretreatment was also assessed via qPCR, confirming the colonization by *T. atroviridae* in the biocontrol-treated IV and IVPP samples (Supplementary Table 1). Altogether, these results corroborated that the data obtained further are related to the presence of either the pathogens, the BCA, or the combination of the three.

### Metabolomic Analysis of Wood Samples

Ultra-high-performance liquid chromatography–high-resolution mass spectrometry (UHPLC–HRMS) profiles of all the extracts afforded 239 features ( $m/z$ -RT pairs) in the PI mode after



application of the MS-CleanR workflow. Among these features, 85% of them were annotated using different DBs: 3% (*Trichoderma*), 1% (Togniniaceae), 4% (Vitaceae), 42% (*Vitis*), and 35% (generic internal MS-FINDER DBs). Fungal metabolites were found in samples inoculated, and their intensity was between  $5 \times 10^5$  and  $3 \times 10^6$ . As the background threshold was estimated to  $1.5 \times 10^6$ , they appeared in the minority not only in terms of number but also in terms of intensity. Thus, separation of samples in principal component analysis (PCA) was mainly due to plant metabolites, and we only focused on them in the rest of the paper.

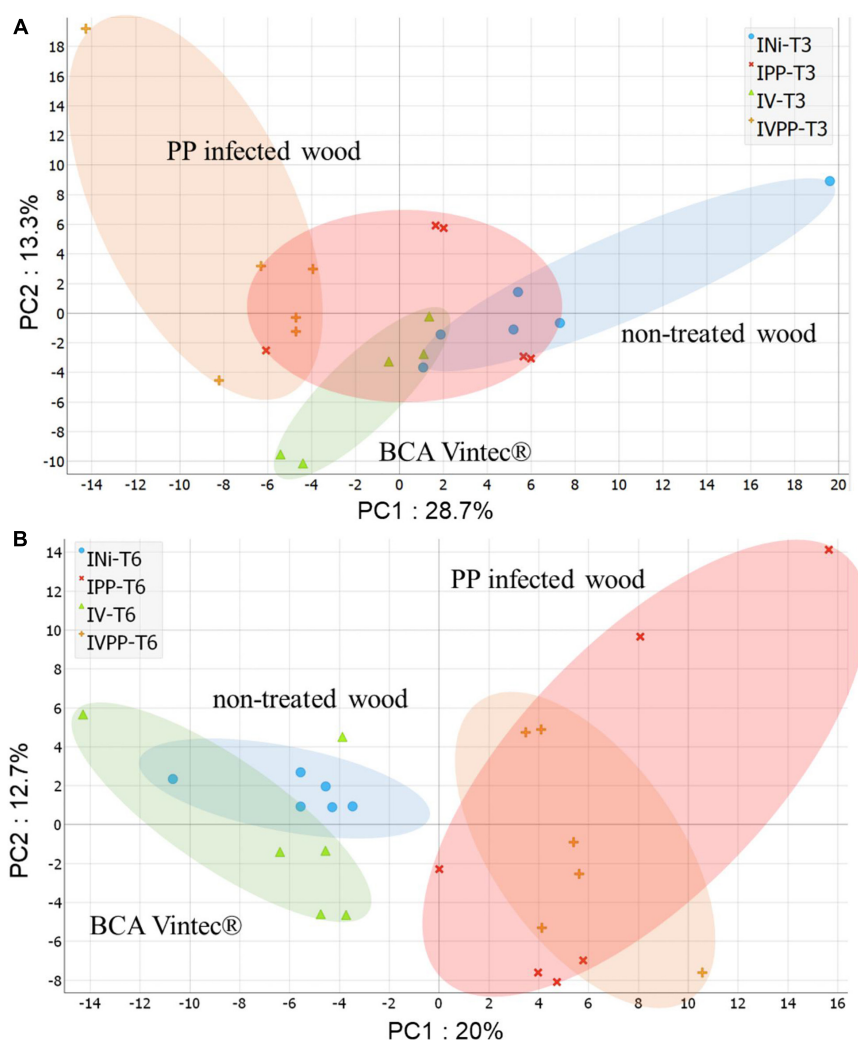
PCA score plots of respective kinetics T3 (**Figure 3A**) and T6 (**Figure 3B**), providing an unsupervised overview of UHPLC-HRMS fingerprints, marked sample-to-sample variability particularly for PP-infected wood at T3 and T6. It, respectively, displayed 42% and 32.7% of total explained variance using the first two principal components. Quality control samples

of the whole dataset (**Supplementary Figure 1**) were centered on the PCA plot, demonstrating the high reproducibility of the analysis.

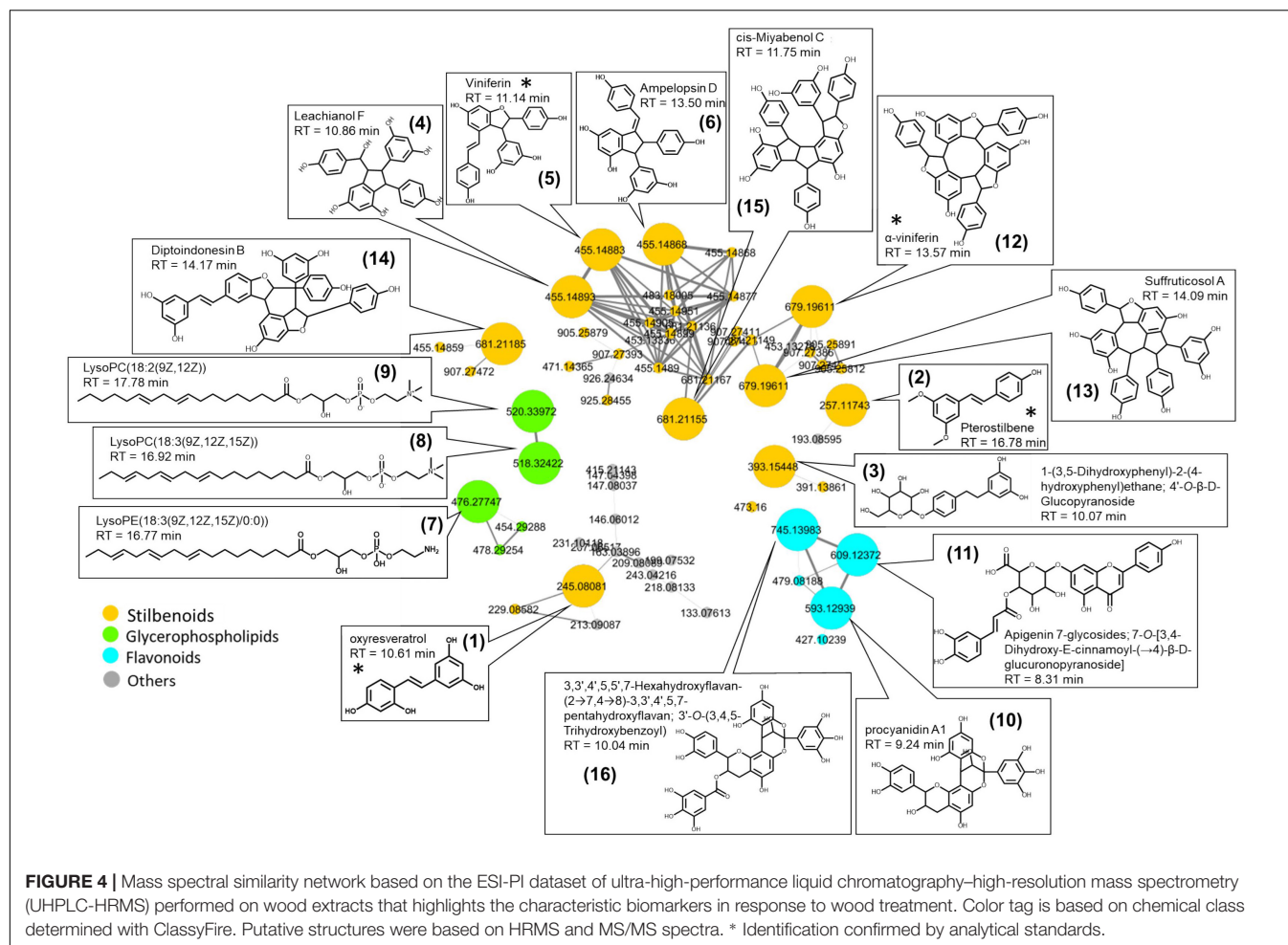
More generally, a separation of samples can be seen according to treatment type. Non-treated wood composed of INi class and wood infected with fungi composed of IPP and IVPP classes are separated by PC1 in both kinetics. Interestingly, wood samples only treated with Vintec® are separated by PC1 for kinetics T3 and by PC2 for kinetics T6.

Using the MS-CleanR workflow (Fraisier-Vannier et al., 2020), a cleaner mass spectral similarity network was built to highlight common chemical classes related to plant response to pathogens and Vintec® (**Figure 4**). Potential biomarkers were revealed by ANOVA models to obtain a classification of the features ( $m/z$ -RT pairs) for each treatment in comparison with the reference.

All the two-to-two comparisons models were validated by random forest models based on the ROC curve coupled with



**FIGURE 3 |** PCA score plot of ESI-PI data from wood extract of *Vitis* cuttings of kinetics T3 (**A**) and kinetics T6 (**B**) (in color). Colored circles arbitrarily enclose treatment types: Injured/Not inoculated (INi) samples; Injured/Vintec® (IV); Injured/*P. chlamydospora* + *P. minimum* (IPP) and Injured/*P. chlamydospora* + *P. minimum* + Vintec® (IVPP).



the area under the curve (AUC). We observed a high AUC score around 0.9 (**Supplementary Table 2**) indicating a good prediction ability.

Sixteen significant biomarkers correlated to the highest ANOVA coefficient scores were tentatively annotated by interrogating simultaneously *Vitis*, Vitaceae, *Trichoderma*, Togniniaceae, and local databases of natural products in MS-FINDER (**Table 1**). Three main biomarker clusters were observed, and annotation results gathered from the aligned peak list of LCMS features allowed the highlight of three main chemical classes: stilbenoid, flavonoid, and glycerophospholipids. The molecular formulae of these compounds matched structures already identified in the *Vitis* genus, except the three glycerophospholipids found in generic databases. No biomarkers were annotated with fungal databases.

The majority of the biomarkers belong to the stilbenoid class. They are resveratrol monomers (compounds 1, 2, and 3), dimers (compounds 4, 5, and 6), and trimers (compounds 12, 13, 14, and 15). Four of them displayed the identification level 1 according to the Metabolomics Standards Initiative (MSI) (Sumner et al., 2007) as their retention time, and MS/MS fragments perfectly match with the standards injected in the same conditions as samples (RT similarity score > 850; similarity

spectrum score > 800): oxyresveratrol, pterostilbene,  $\alpha$ -viniferin, and viniferin. For all other compounds, the identification level 2 was proposed according to the MSI.

The three glycerophospholipids were annotated as lysophosphatidylcholines lysoPC (18:2) (9) and lysoPC (18:3) (8), and as lysophosphatidylethanolamine LysoPE (18:3) (7).

Two flavonoids were annotated as procyanidin derivatives (10 and 16), while the last one was annotated as an apigenin derivative (11).

After tentative annotation, we compared their distribution among treated conditions. On the heatmap representing the average peak intensity by class of each biomarker (**Figure 5**), it can be seen that these significant features are overproduced in the presence of pathogenic fungi alone (IPP) and in combination with BCA Vintec® (IVPP), validating our approach. In addition, the hierarchical clustering analysis, based on the sample class, separates well the non-infected wood samples, including those with Vintec® alone, from the pathogen-inoculated infected wood samples.

Among the different metabolites, flavonoids are mainly present at kinetics T3 and T6 with IPP and IVPP (metabolites 10, 11, and 16) and glycerophospholipids at kinetics T3 with IPP and IVPP (metabolites 7, 8, and 9). Suffruticosol A (13)

**TABLE 1** | Summary of annotated compounds most differentially present in the tested conditions.

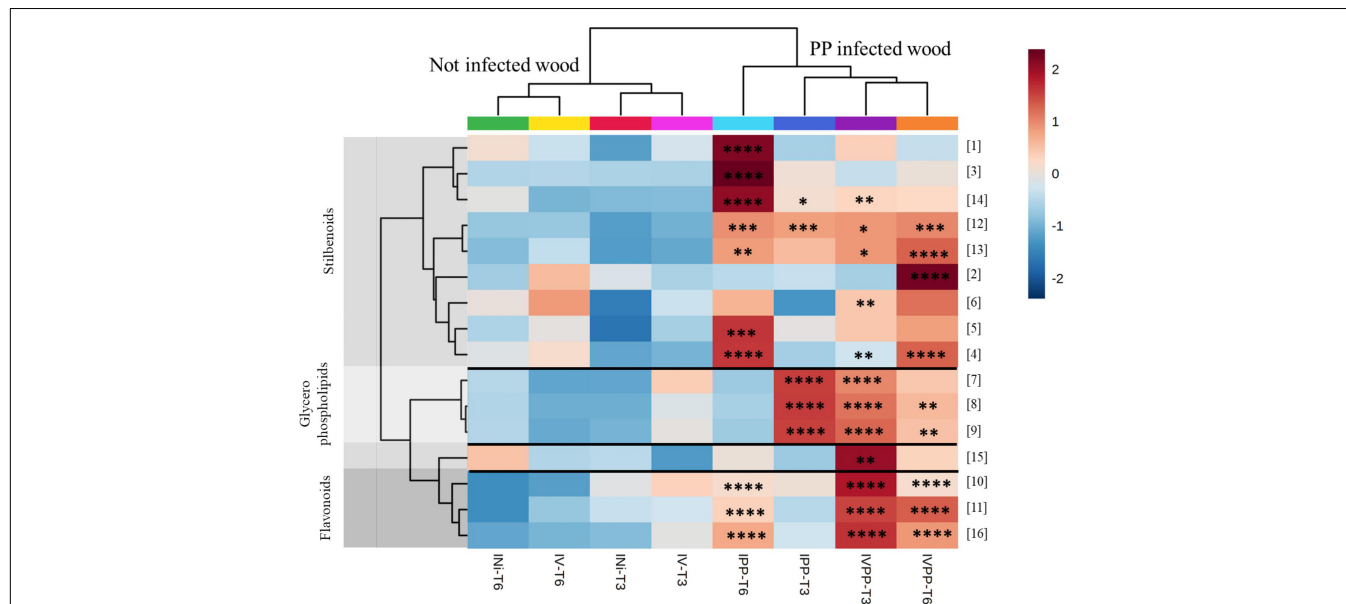
N°	m/z	RT (min)	Molecular Formula	Error (ppm)	Chemical class <sup>a</sup>	Putative annotation
1	245.08081	10.608	C <sub>14</sub> H <sub>12</sub> O <sub>4</sub>	4.5781	Stilbenoid	Oxyresveratrol <sup>b</sup>
2	257.11743	16.784	C <sub>16</sub> H <sub>16</sub> O <sub>3</sub>	3.4537	Stilbenoid	Pterostilbene <sup>b</sup>
3	393.15448	10.065	C <sub>20</sub> H <sub>24</sub> O <sub>8</sub>	2.5715	Stilbenoid	1-(3,5-Dihydroxyphenyl)-2-(4-hydroxyphenyl)ethane; 4'-O-β-D-glucopyranoside <sup>c</sup>
4	455.14893	10.863	C <sub>28</sub> H <sub>20</sub> O <sub>5</sub>	2.3772	Stilbenoid	Leachianol F <sup>c</sup>
5	455.14883	11.139	C <sub>28</sub> H <sub>22</sub> O <sub>6</sub>	2.5969	Stilbenoid	Viniferin <sup>b</sup>
6	455.14868	13.502	C <sub>28</sub> H <sub>22</sub> O <sub>6</sub>	2.9265	Stilbenoid	Ampelopsin D <sup>c</sup>
7	476.27747	16.766	C <sub>30</sub> H <sub>37</sub> NO <sub>4</sub>	4.2820	Glycerophospholipids	LysoPE[18:3(9Z,12Z,15Z)/0:0] <sup>d</sup>
8	518.32422	16.922	C <sub>26</sub> H <sub>48</sub> NO <sub>7</sub> P	1.9158	Glycerophospholipids	LysoPC [18:3(9Z,12Z,15Z)] <sup>d</sup>
9	520.33972	17.781	C <sub>26</sub> H <sub>50</sub> NO <sub>7</sub> P	2.1966	Glycerophospholipids	LysoPC [18:2(9Z,12Z)] <sup>d</sup>
10	593.12939	9.237	C <sub>30</sub> H <sub>24</sub> O <sub>13</sub>	1.1363	Flavonoid	Procyanidin A1 <sup>c</sup>
11	609.12372	8.31	C <sub>30</sub> H <sub>24</sub> O <sub>14</sub>	2.0669	Flavonoid	Apigenin 7-glycosides; 7-O-[3,4-Dihydroxy-E-cinnamoyl-(→4)-β-D-glucuronopyranoside] <sup>c</sup>
12	679.19611	13.571	C <sub>42</sub> H <sub>30</sub> O <sub>9</sub>	1.8345	Stilbenoid	α-viniferin <sup>b</sup>
13	679.19611	14.085	C <sub>42</sub> H <sub>30</sub> O <sub>9</sub>	1.8345	Stilbenoid	Suffruticosol A <sup>c</sup>
14	681.21185	14.168	C <sub>42</sub> H <sub>32</sub> O <sub>9</sub>	0.0866	Stilbenoid	Diptoindonesin B <sup>c</sup>
15	681.21155	11.753	C <sub>42</sub> H <sub>32</sub> O <sub>9</sub>	0.5270	Stilbenoid	cis-Miyabenol C <sup>c</sup>
16	745.13983	10.039	C <sub>37</sub> H <sub>28</sub> O <sub>17</sub>	1.6010	Flavonoid	3,3',4',5,5',7-Hexahydroxyflavan-(2→7,4→8)- 3,3',4',5,7-pentahydroxyflavan; 3'-O-(3,4,5-Trihydroxybenzoyl) <sup>c</sup>

<sup>a</sup>Determined with ClassyFire (Djombou Feunang et al., 2016).

<sup>b</sup>Compounds confirmed by injection of standard in the same analytical conditions.

<sup>c</sup>Putative annotation based on experimental HRMS, MS/MS, and in silico fragmentation matches restricting interrogation to *Vitis* genus and Vitaceae family databases.

<sup>d</sup>Putative annotation based on experimental HRMS, MS/MS, and in silico fragmentation matches by interrogation of natural product databases within the MS-FINDER software.

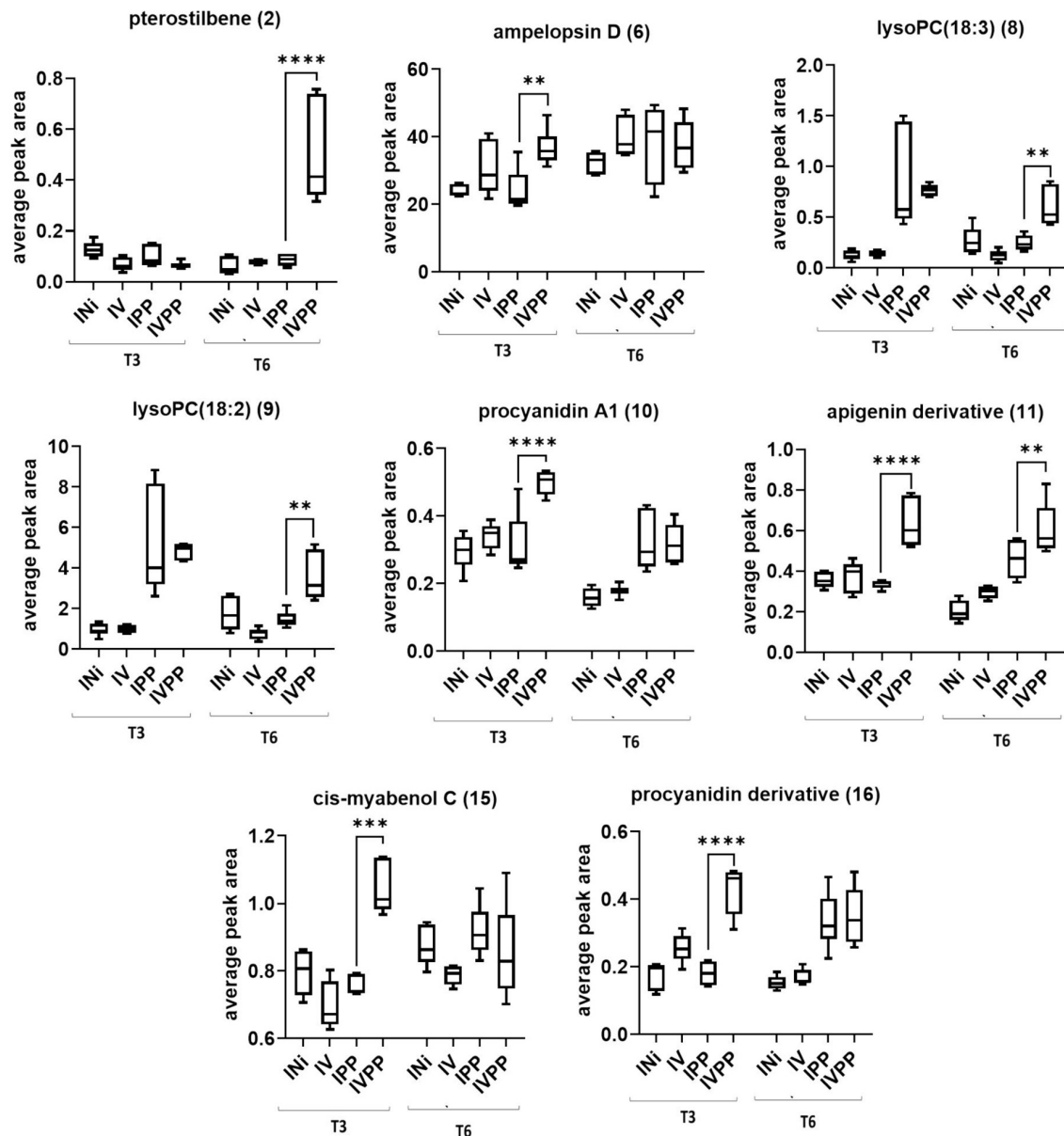


**FIGURE 5** | Heatmap of the annotated biomarkers at kinetics 3 weeks (T3) and 6 weeks (T6). The color key is based on the average peak intensity of each feature by class: red color for higher peak intensity and blue color for lower peak intensity. Injured/Not inoculated (INi) samples; Injured/Vintec® (IV); Injured/*P. chlamydospora* + *P. minimum* (IPP) and Injured/*P. chlamydospora* + *P. minimum* + Vintec® (IVPP). Report to **Table 1** for metabolite annotation. \* Significance in comparison to INi for each kinetics independently [0.0332(\*), 0.0021(\*\*), 0.0002(\*\*\*), < 0.0001(\*\*\*\*)].

and α-viniferin (12), two resveratrol trimers, are overall equally expressed with IPP and IVPP at both kinetics. *Cis*-miyabenol C (15) and ampelopsin D (6) are mainly overproduced with IVPP at kinetics T3, while pterostilbene (2) is mainly overproduced with

IVPP at kinetics T6. Oxyresveratrol (1), the bibenzyl derivative (3), and diptoindonesin B (14) are mainly overproduced with IPP at kinetics T6. Finally, all other annotated resveratrol dimers (metabolites 4 and 5) are overproduced with IPP and





**FIGURE 6 |** Two-way ANOVA and Dunnett's *post hoc* test ( $p \leq 0.05$ ) of metabolites overproduced with the combination Vintec®-pathogens. 0.0021(\*\*), 0.0002(\*\*\*), < 0.0001(\*\*\*\*).

IVPP at kinetics T6. ANOVA comparisons can be found in **Supplementary Figure 2**.

Interestingly, all biomarkers overproduced with IVPP were not significantly overproduced in the presence of BCA Vintec® alone, as well as for kinetics T3 and for kinetics T6. Thus, it resulted that Vintec® treatment alone induces a weak grapevine defense response, which seemed rather correlated with plant reaction to pathogenic fungal infection. Nevertheless, some metabolites, in particular oxyresveratrol (1), the bibenzyl derivative (3), and diptioindonesin B (14), were less produced with pathogens in combination with Vintec® than with pathogens alone.

Thus, Vintec® seems to reduce some metabolic response to pathogen attack.

From another side, Vintec® increases plant response to pathogen treatment (**Figure 6**), in particular regarding the expression of stilbenoids pterostilbene (2) at T6 and *cis*-miyabenol C (15) at T3, as well as flavonoids 10, 11, and 16 at T3. To a lesser extent, it also stimulates the production of lysoPCs 8 and 9 at T6 and ampelopsin D at T3.

The reproducibility of the experiment and the raw materials were confirmed for kinetics T3 with canes of *Vitis vinifera* L. cv Cabernet-Sauvignon clone 15 during the 2021 season (data not shown). UHPLC-HRMS analysis revealed a metabolic response

quite constant as 11 of the 16 highlighted biomarkers were also overproduced in IPP and IVPP samples comparatively to control or BCA Vintec® treatment of the 2021 season (Supplementary Figure 3).

## Validation of Stilbenoids Antifungal Activity

Antifungal activity of four stilbenoids standards was investigated on *Botrytis cinerea* and *P. chlamydospora* fungal growth. IC<sub>50</sub> was determined (Table 2), and the results pointed out that all stilbenes showed an antifungal activity on both fungi, *P. chlamydospora* being the more susceptible. Pterostilbene and viniferin had the highest antifungal activities for both fungi, whereas oxyresveratrol presented the lowest activity.

## DISCUSSION

The objective of this study was to characterize the grapevine wood metabolome changes, during a 6-week kinetics, after the inoculation of the Esca pathogens *Phaeoconiella chlamydospora* and *Phaeoacremonium minimum*, and of the commercialized BCA Vintec® formulated with *Trichoderma atroviridae* SC1, within the framework of Esca disease. This work was expected to identify some biomarkers of Esca attack that could be used to further evaluate BCA efficiency in vineyard conditions. Even if BCA can exhibit many different modes of action on targeted disease, the objective was to demonstrate the prime interest of metabolomics on the semi-ligneous and quite challenging Esca pathosystem.

From an analytical point of view, the PI mode was preferred as MS/MS spectra were of better quality than in the NI mode, thus improving feature annotation using MS-FINDER and network feature clusterization. In order to highlight significant features based on pathogens and BCA presence, a classification model between treatment and UHPLC-HRMS fingerprints was realized by random forest. In addition, a mass spectral similarity network was built and allowed the distinction of three main significant clusters from three chemical classes: flavonoids, glycerophospholipids, and mainly stilbenoids as resveratrol monomers, dimers, and trimers. The majority of highlighted biomarkers were annotated from a *Vitis* database. Interestingly, none of them were fungal metabolites even if nearly 5% of all features were annotated with fungal databases. Indeed, the peak intensity of these metabolites was lower than the one of plant metabolites, and they were often close to the background noise demonstrating the prevalence of wood metabolites using this untargeted metabolomic approach. However, their presence is a

very good indicator of the presence of pathogens as well as BCA. These results can stimulate further investigation to follow the presence/absence of these different partners in the time course of Esca disease, which show a slow decaying evolution. This could be particularly helpful to understand the first steps of this disease especially when there are no symptoms.

Stilbenoids belong to the phenylpropanoid pathway and include stilbenes, bibenzyls, and phenanthrenes derivatives. They are found as constitutive compounds in several plant families especially Vitaceae (Rivière et al., 2012). As mentioned above, they are synthesized through the phenylpropanoid pathway as well as the flavonoids. However, there is an early divergence between these classes at the p-coumaroylCoA level that can enter either the stilbenoid way through the key stilbene synthase or the flavonoids way thanks to chalcone synthase isomerase (Ali et al., 2011). They are widely considered as phytoalexins as they play a protective role in plant defense to fungal pathogen infection, such as the detected pterostilbene in the presence of *Plasmopara viticola* (Langcake et al., 1979; Pezet et al., 2004). These compounds are also of great interest since they exhibit many biological properties, in particular cardioprotection, neuroprotection, antidiabetic properties, depigmentation, anti-inflammation, cancer prevention, and treatment (Akinwumi et al., 2018). Several other particular stilbenoids were previously reported in literature and isolated from diseased grapevine wood: the resveratrol dimers leachianol F as well as the resveratrol trimers  $\alpha$ -viniferin and cis-miyabenol C (Amalfitano et al., 2011). It was also previously shown that infection of *Vitis vinifera* with *Phaeoconiella chlamydospora* induced changes in phenolic compounds with a significant increase in their production after this fungal inoculation. The production of viniferin-type stilbenes was, in particular, observed, absent from the control condition (Lima et al., 2012).

The role of stilbenes as plant defense compounds was strengthened by antifungal bioassays on four available standards. Our results on positive control *Botrytis cinerea* support the data from literature. It was previously shown that ED<sub>50</sub> (effective dose to obtain 50% mortality) of pterostilbene on *B. cinerea* was around 18 to 20  $\mu$ g/ml (Jeandet et al., 2002). Regarding  $\alpha$ -viniferin, an IC<sub>50</sub> around 97  $\mu$ g/ml was observed on *B. cinerea* (Langcake and Pryce, 1977). *P. chlamydospora* appeared to be more sensitive than *B. cinerea*. Pterostilbene and viniferin presented the highest antifungal activities for both fungi, whereas oxyresveratrol showed the lowest activity. A detailed analysis of stilbenoids antifungal activity on various fungi involved in wood disease showed a weak sensibility of *P. chlamydospora* and *P. aleophilum*. *Phaeoconiella chlamydospora* growth was inhibited by pterostilbene and two resveratrol tetramers, vitisins A and B, whereas no stilbenoids had an impact on *P. aleophilum* growth (Lambert et al., 2012). Nevertheless, they found that pterostilbene was the most active stilbenoids agreeing with our results. Still, the apparent divergence regarding sensitivity could be explained by the use of different fungal isolates and by the experimental conditions as our analysis was realized on fungal spores and not mycelium. These results support the key role of stilbenoids in the framework of wood disease.

**TABLE 2 |** IC<sub>50</sub> of the standard solutions on *Botrytis cinerea* and *Phaeoconiella chlamydospora* spores 3 days after onset of treatment.

	IC <sub>50</sub> <i>Botrytis</i> ( $\mu$ g/ml)	IC <sub>50</sub> <i>Pch</i> ( $\mu$ g/ml)
Oxyresveratrol (1)	162	40.0
Pterostilbene (2)	20.3	7.3
Viniferin (5)	37.5	8.6
$\alpha$ -viniferin (12)	92.8	13.5

Flavonoids are also a class of compounds known to play a role in plant defense against pathogens and other environmental stresses (Treutter, 2005). They are often constitutive compounds of the plant with a production enhanced by the stress. In *Vitis vinifera*, they are mainly distributed in leaves, stems, and canes (Goufo et al., 2020). In addition, accumulation of flavonoids, namely procyanidin derivatives, was also highlighted in wood parts of Esca-infected grapevines (Rusjan et al., 2017).

The third class of compounds identified was phospholipids. It was also previously reported that phospholipids lysophosphatidylcholines (lysoPCs), in particular lysoPCs C18:2 and C18:3 identified in this study, increase after pathogen inoculation (Cho et al., 2012). Regarding the leaves of Esca-affected grapevine, a lipidomic study also reported a progressive increase in lipids, including lysophospholipids as lysoPCs C18:2 and C18:3, with symptom progression (Goufo and Cortez, 2020). These compounds are enzymatically produced through phospholipase A activity linked to the signaling pathways of jasmonic acid leading to defense induction (Chandra et al., 1996). However, the precise role of lysoPCs in the interaction between wood tissues and wood pathogens needs further investigation. Nevertheless, lipids appeared to be good biomarkers of grapevine disease as a higher accumulation of them was also observed in asymptomatic diseased grapevine (Lemaitre-Guillier et al., 2020).

*Trichoderma* spp. strains are known to reduce infections caused by trunk disease pathogens, such as *Phaeoemoniella chlamydospora* (Pertot et al., 2016) and *Phaeoacremonium minimum* (Carro-Huerga et al., 2020) in a preventive way, as we confirmed here at 6 weeks post-inoculation. Different modes of action have been described for *Trichoderma* spp. to explain their capacity to protect plants against different biotic and abiotic stresses. These explain (i) the competition for resources and space, (ii) the production of toxic compounds, and (iii) the stimulation of plant natural defenses. The ability of *Trichoderma* spp. to enhance plant defenses against different organisms has been already described several times in different pathosystems (Perazzolli et al., 2011; Mastouri et al., 2012; Mathys et al., 2012; Hermosa and Rubio, 2013; Banani et al., 2014; Singh et al., 2019). For instance, a recent study of the application on *T. harzianum* on tomato reported a protective effect against root-knot nematode by the overproduction of reactive oxygen species (ROS), secondary metabolites, and defense-related hormones (Yan et al., 2021). It has also been observed that the application of different *Trichoderma* spp. in eggplant resulted in a higher total phenolic content during the infection with *S. sclerotium* (Pratap Singh et al., 2021).

Metabolomic results revealed that Vintec® composed of a *Trichoderma atroviride* (TASC1) strain induces a weak metabolomic response alone, sufficient enough to differentiate the treated and not treated plants by metabolomics comparison, but therefore does not have plant defense stimulating effect.

Nevertheless, BCA Vintec® seems to have not only an effect on pathogens but also a priming effect after infection with fungi. Indeed, some metabolites were more produced in IPP samples compared to IVPP samples, especially at T6. This observation could indicate a weaker virulence of pathogens in the presence of Vintec® corroborating BCA capacity to compete and

interact with these pathogens. This effect appears within a certain period probably due to the time necessary for the sufficient strain development. On the other hand, Vintec® increases plant response to challenge inoculation with a clear stimulation of the phenylpropanoid pathway with increasing amounts of stilbenoid pterostilbene as well as an increase in flavonoids. Thus, these compounds appear to be good BCA indicators as they are still observable after 3 weeks and even 6 weeks after infection.

## CONCLUSION

A UHPLC-HRMS based metabolomic study was performed and allowed the dereplication of plant defense metabolites in the framework of Esca disease. Comparison with injured reference (INi) was conducted and significant metabolic changes were observed. Sixteen biomarkers were highlighted and annotated based on MS/MS fragmentation patterns. Four of them were clearly identified thanks to the injection of corresponding standards. These compounds belong mainly to the stilbenoid chemical class, as well as flavonoids and glycerophospholipids known to be involved in plant defense. They were mainly accumulated after two wood treatments: inoculation of the pathogenic fungi, *Phaeoacremonium minimum* and *Phaeoemoniella chlamydospora*, and in combination with BCA Vintec®. One stilbenoid and three flavonoids were highly associated with the synergy between the BCA and the pathogens. Indeed, they were mainly overproduced when Vintec® was in the presence of fungi. Thus, these four compounds appear to be good indicators of BCA effects in field condition.

## DATA AVAILABILITY STATEMENT

The datasets presented in this study can be found in online repositories. The names of the repository/repositories and accession number(s) can be found below: 10.5281/zenodo.5779519.

## AUTHOR CONTRIBUTIONS

GM, VP-P, SF, BD, and AJ supervised the project and revised the article. JC was in charge of the plant extraction, the analytical workflow, and the data processing and interpretation. AR-O was in charge of the plant culture and treatment and realized the bioassays. JC and AR-O wrote the article. All authors have read and agreed the published version of the manuscript.

## FUNDING

Financial support was received from the French National Infrastructure for Metabolomics and Fluxomics, Grant MetaboHUB-ANR-11-INBS-0010, and the PSCP SOLSTICE Project (SOLutionS pour des Traitements Intégrés dans une Conduite Environnementale) managed by Belchim Crop

Protection and partly funded by the French state within the framework of the Programme d'Investissements d'Avenir.

## ACKNOWLEDGMENTS

We thank Wilfried Remus-Borel and Gabriel D' Enjoy from Belchim Crop Protection for fruitful discussions and for supplying the Vintec® product. MetaToul (Toulouse metabolomics & fluxomics facilities, [www.metatoul.fr](http://www.metatoul.fr)) is part

of the French National Infrastructure for Metabolomics and Fluxomics MetaboHUB-ANR-11-INBS-0010.

## SUPPLEMENTARY MATERIAL

The Supplementary Material for this article can be found online at: <https://www.frontiersin.org/articles/10.3389/fmicb.2022.835463/full#supplementary-material>

## REFERENCES

- Akinwumi, B., Bordun, K.-A., and Anderson, H. (2018). Biological activities of stilbenoids. *Int. J. Mol. Sci.* 19:792. doi: 10.3390/ijms19030792
- Ali, M. B., Howard, S., Chen, S., Wang, Y., Yu, O., Kovacs, L. G., et al. (2011). Berry skin development in norton grape: distinct patterns of transcriptional regulation and flavonoid biosynthesis. *BMC Plant Biol.* 11:7. doi: 10.1186/1471-2229-11-7
- Amalfitano, C., Agrelli, D., Arrigo, A., Mugnai, L., Surico, G., and Evidente, A. (2011). Stilbene Polyphenols in the brown red wood of *Vitis vinifera* Cv. sangiovese affected by "Esca Proper". *Phytopathol. Mediter.* 50, S224–S235.
- Amalfitano, C., Evidente, A., Surico, G., Tegli, S., Bertelli, E., and Mugnai, L. (2000). Phenols and stilbene polyphenols in the wood of esca-diseased grapevines. *Phytopathol. Mediter.* 39:6.
- Banani, H., Roatti, B., Ezzahi, B., Giovannini, O., Gessler, G., Pertot, I., et al. (2014). Characterization of resistance mechanisms activated by *Trichoderma harzianum* T39 and benzothiadiazole to downy mildew in different grapevine cultivars. *Plant Pathol.* 63, 334–343. doi: 10.1111/ppa.12089
- Berbegal, M., Ramón-Albalat, A., León, M., and Armengol, J. (2020). Evaluation of long-term protection from nursery to vineyard provided by trichoderma atroviride SC1 against fungal grapevine trunk pathogens. *Pest Manag. Sci.* 76, 967–977. doi: 10.1002/ps.5605
- Bertsch, C., Ramírez-Suero, M., Magnin-Robert, M., Larignon, P., Chong, J., Abou-Mansour, E., et al. (2013). Grapevine trunk diseases: complex and still poorly understood: grapevine trunk diseases. *Plant Pathol.* 62, 243–265. doi: 10.1111/j.1365-3059.2012.02674.x
- Braun, H., Woitsch, L., Hetzer, B., Geisen, R., Zange, B., and Schmidt-Heydt, M. (2018). *Trichoderma harzianum*: inhibition of mycotoxin producing fungi and toxin biosynthesis. *Int. J. Food Microbiol.* 280, 10–16. doi: 10.1016/j.jifoodmicro.2018.04.021
- Bruet, E., Baumgartner, K., Bastien, S., Travadon, R., Guérin-Dubrana, L., and Rey, P. (2016). Various fungal communities colonise the functional wood tissues of old grapevines externally free from grapevine trunk disease symptoms: fungal microflora of gtd-free old vines. *Austral. J. Grape Wine Res.* 22, 288–295. doi: 10.1111/ajgw.12209
- Bruet, E., Vallance, J., Gerbore, J., Lecomte, P., Da Costa, J. P., Guérin-Dubrana, L., et al. (2014). Analyses of the temporal dynamics of fungal communities colonizing the healthy wood tissues of esca leaf-symptomatic and asymptomatic vines. *PLoS One* 9:e95928. doi: 10.1371/journal.pone.0095928
- Bruno, G., and Sparapano, L. (2007). Effects of three esca-associated fungi on *Vitis vinifera* L.: V. changes in the chemical and biological profile of xylem sap from diseased Cv. sangiovese vines. *Physiol. Mol. Plant Pathol.* 71, 210–229. doi: 10.1016/j.pmp.2008.02.005
- Carro-Huerga, G., Compant, S., Gorfer, M., Cardoza, R. E., Schmoll, M., Gutierrez, S., et al. (2020). Colonization of *Vitis vinifera* L. by the *Endophyte trichoderma* Sp. Strain T154: biocontrol activity against phaeoacremonium minimum. *Front. Plant Sci.* 11:15. doi: 10.3389/fpls.2020.01170
- Chandra, S., Heinsteins, P. F., and Low, P. S. (1996). Activation of phospholipase a by plant defense elicitors. *Plant Physiol.* 110, 979–986. doi: 10.1104/pp.110.3.979
- Cho, K., Kim, Y., Wi, S. J., Seo, J. B., Kwon, J., Chung, J. H., et al. (2012). Nontargeted metabolite profiling in compatible pathogen-inoculated tobacco (*Nicotiana tabacum* L. Cv. Wisconsin 38) Using UPLC-Q-TOF/MS. *J. Agric. Food Chem.* 60, 11015–11028. doi: 10.1021/jf303702j
- Chong, J., Wishart, D. S., and Xia, J. (2019). Using metaboanalyst 4.0 for comprehensive and integrative metabolomics data analysis. *Curr. Protoc. Bioinformatics* 68:e86. doi: 10.1002/cpbi.86
- Del Rio, J. A., Gonzalez, A., Fuster, M. D., Botia, J. M., Gomez, P., Frias, V., et al. (2001). Tylose formation and changes in phenolic compounds of grape roots infected with *Phaeoacremonium chlamydospora* and *Phaeoacremonium* Species. *Phytopathol. Mediter.* 40, S394–S399.
- Demsar, J., Curk, T., Erjavec, A., Demsar, J., Curk, T., Erjavec, A., et al. (2013). Orange: data mining toolbox in python. *J. Mach. Learn. Res.* 14, 2349–2353.
- Djombou Feunang, Y., Eisner, R., Knox, C., Chepelev, L., Hastings, J., Owen, G., et al. (2016). ClassyFire: automated chemical classification with a comprehensive, computable taxonomy. *J. Cheminform.* 8:61. doi: 10.1186/s13321-016-0174-y
- Fontaine, F., Pinto, C., Vallet, J., Clément, C., Gomes, A. C., and Spagnolo, A. (2016). The effects of grapevine trunk diseases (GTDs) on vine physiology. *Eur. J. Plant Pathol.* 144, 707–721. doi: 10.1007/s10658-015-0770-0
- Fraisier-Vannier, O., Chervin, J., Cabanac, G., Puech, V., Fournier, S., Durand, V., et al. (2020). MS-CleanR: a feature-filtering workflow for untargeted LC–MS based metabolomics. *Anal. Chem.* 92, 9971–9981. doi: 10.1021/acs.analchem.0c01594
- Gerbore, J., Benhamou, N., Vallance, J., Le Floch, G., Grizard, D., Regnault-Roger, C., et al. (2014). Biological control of plant pathogens: advantages and limitations seen through the case study of *Pythium oligandrum*. *Environ. Sci. Pollut. Res.* 21, 4847–4860. doi: 10.1007/s11356-013-1807-6
- Goufo, P., and Cortez, I. (2020). A lipidomic analysis of leaves of esca-affected grapevine suggests a role for galactolipids in the defense response and appearance of foliar symptoms. *Biology* 9:268. doi: 10.3390/biology9090268
- Goufo, P., Singh, R. K., and Cortez, I. (2020). A reference list of phenolic compounds (including stilbenes) in grapevine (*Vitis vinifera* L.) roots, woods, canes, stems, and leaves. *Antioxidants* 9:398. doi: 10.3390/antiox9050398
- Graniti, A., Surico, G., and Mugnai, L. (2000). Esca of grapevine: a disease complex or a complex of diseases? *Phytopathol. Mediter.* 39:5.
- Haidar, R., Amira, Y., Roudet, J., Marc, F., and Patrice, R. (2021). Application Methods and Modes of Action of *Pantoea agglomerans* and *Paenibacillus* Sp. to control the grapevine trunk disease-pathogen, *Neofusicoccum parvum*. *OENO One* 55, 1–16. doi: 10.20870/oenone.2021.55.3.4530
- Haidar, R., Yacoub, A., Pinard, A., Roudet, J., Fermaud, M., and Rey, P. (2020). Synergistic effects of water deficit and wood-inhabiting bacteria on pathogenicity of the grapevine trunk pathogen *Neofusicoccum parvum*. *Phytopathol. Mediter.* 59, 473–484. doi: 10.14601/Phyto-11990
- Hermosa, R., and Rubio, M. B. (2013). The contribution of trichoderma to balancing the costs of plant growth and defense. *Int. Microbiol.* 16, 69–80. doi: 10.2436/20.1501.01.181
- Hofstetter, V., Buyck, B., Croll, D., Viret, O., Couloux, A., and Gindro, K. (2012). What if esca disease of grapevine were not a fungal disease? *Fungal Divers.* 54, 51–67. doi: 10.1007/s13225-012-0171-z
- Jeandet, P., Douillet-Breuil, A.-C., Bessis, R., Debord, S., Sbaghi, M., and Adrian, M. (2002). Phytoalexins from the Vitaceae: biosynthesis, phytoalexin gene expression in transgenic plants, antifungal activity, and metabolism. *J. Agric. Food Chem.* 50, 2731–2741. doi: 10.1021/jf011429s



- Labois, C., Wilhelm, K., Laloue, H., Tarnus, C., Bertsch, C., Goddard, M.-L., et al. (2020). Wood metabolomic responses of wild and cultivated grapevine to infection with *Neofusicoccum parvum*, a trunk disease pathogen. *Metabolites* 10:232. doi: 10.3390/metabo10060232
- Lambert, C., Bisson, J., Waffo-Tégou, P., Papastamoulis, Y., Richard, T., Corio-Costet, M.-F., et al. (2012). Phenolics and their antifungal role in grapevine wood decay: focus on the Botryosphaeriaceae family. *J. Agric. Food Chem.* 60, 11859–11868. doi: 10.1021/jf303290g
- Langcake, P. (1981). Disease resistance of *Vitis* Spp. and the production of the stress metabolites resveratrol,  $\epsilon$ -Viniferin,  $\alpha$ -Viniferin and pterostilbene. *Physiol. Plant Pathol.* 18, 213–226. doi: 10.1016/S0048-4059(81)80043-4
- Langcake, P., Cornford, C. A., and Pryce, R. J. (1979). Identification of pterostilbene as a Phytoalexin from *Vitis vinifera* leaves. *Phytochemistry* 18, 1025–1027. doi: 10.1016/S0031-9422(00)91470-5
- Langcake, P., and Pryce, R. J. (1977). A new class of phytoalexins from grapevines. *Experientia* 33, 151–152. doi: 10.1007/BF02124034
- Lemaître-Guillier, C., Fontaine, F., Roullier-Gall, C., Harir, M., Magnin-Robert, M., Clément, C., et al. (2020). Cultivar- and Wood area-dependent metabolomic fingerprints of grapevine infected by Botryosphaeria Dieback. *Phytopathology* 110, 1821–1837. doi: 10.1094/PHYTO-02-20-0055-R
- Lima, M. R. M., Felgueiras, M. L., Cunha, A., Chicau, G., Ferreres, F., and Dias, A. C. P. (2017a). Differential phenolic production in leaves of *Vitis vinifera* Cv. alvarinho affected with esca disease. *Plant Physiol. Biochem.* 112, 45–52. doi: 10.1016/j.plaphy.2016.12.020
- Lima, M. R. M., Machado, A. F., and Gubler, W. D. (2017b). Metabolomic study of chardonnay grapevines double stressed with esca-associated fungi and drought. *Phytopathology* 107, 669–680. doi: 10.1094/PHYTO-11-16-0410-R
- Lima, M. R. M., Ferreres, F., and Dias, A. C. P. (2012). Response of *Vitis vinifera* Cell Cultures to *Phaeoacremonium chlamydospora*: changes in phenolic production, oxidative state and expression of defence-related genes. *Eur. J. Plant Pathol.* 132, 133–146. doi: 10.1007/s10658-011-9857-4
- Luque, J., Martos, S., Aroca, A., Raposo, R., and Garcia-Figueres, F. (2009). Symptoms and fungi associated with declining mature grapevine plants in Northeast Spain. *J. Plant Pathol.* 91, 381–390.
- Magnin-Robert, M., Adrian, M., Trouvelot, S., Spagnolo, A., Jacquens, L., Letousey, P., et al. (2017). Alterations in grapevine leaf metabolism occur prior to esca apoplexy appearance. *Mol. Plant Microbe Interact.* 30, 946–959. doi: 10.1094/MPMI-02-17-0036-R
- Mastouri, F., Björkman, T., and Harman, G. E. (2012). *Trichoderma harzianum* enhances antioxidant defense of tomato seedlings and resistance to water deficit. *Mol. Plant Microbe Interact.* 25, 1264–1271. doi: 10.1094/MPMI-09-11-0240
- Mathys, J., De Cremer, K., Timmermans, P., Van Kerckhove, S., Lievens, B., Vanhaecke, M., et al. (2012). Genome-wide characterization of ISR induced in *Arabidopsis thaliana* by *Trichoderma hamatum* T382 against botrytis cinerea infection. *Front. Plant Sci.* 3:108. doi: 10.3389/fpls.2012.00108
- Mondello, V., Larignon, P., Armengol, J., Kortekamp, A., Vaczy, K., Prezma, F., et al. (2018a). Management of grapevine trunk diseases: knowledge transfer, current strategies and innovative strategies adopted in Europe. *Phytopathol. Medit.* 57, 369–383. doi: 10.14601/Phytopathol\_Mediterr-23942
- Mondello, V., Songy, A., Battiston, E., Pinto, C., Coppin, C., Trotel-Aziz, P., et al. (2018b). Grapevine trunk diseases: a review of fifteen years of trials control with chemicals and biocontrol agents. *Plant Dis.* 102, 1189–1217. doi: 10.1094/PDIS-08-17-1181-FE
- Moya, P., Barrera, V., Cipollone, J., Bedoya, C., Kohan, L., Toledo, A., et al. (2020). New isolates of *Trichoderma* Spp. as biocontrol and plant growth-promoting agents in the pathosystem pyrenophora teres-barley in Argentina. *Biol. Control* 141:104152. doi: 10.1016/j.biocontrol.2019.104152
- Mugnani, L., Graniti, A., and Surico, G. (1999). Esca (Black Measles) and brown wood-streaking: two old and elusive diseases of grapevines. *Plant Dis.* 83, 404–418. doi: 10.1094/PDIS.1999.83.5.404
- Perazzolli, M., Roatti, B., Bozza, E., and Pertot, I. (2011). *Trichoderma harzianum* T39 induces resistance against downy mildew by priming for defense without costs for grapevine. *Biol. Control* 58, 74–82. doi: 10.1016/j.biocontrol.2011.04.006
- Pertot, I., Prodanutti, D., Colombini, A., and Pasini, L. (2016). *Trichoderma atroviride* SC1 prevents *Phaeoacremonium chlamydospora* and *Phaeoacremonium aleophilum* infection of grapevine plants during the grafting process in nurseries. *BioControl* 61, 257–267.
- Pezet, R., Gindro, K., Viret, O., and Richter, H. (2004). Effects of resveratrol, viniferins and pterostilbene on *Plasmopara viticola* zoospore mobility and disease development. *Vitis, J. Grapevine Res.* 43, 145–148.
- Pierron, R., Gorfer, M., Berger, H., Jacques, A., Sessitsch, A., Strauss, J., et al. (2015). Deciphering the niches of colonisation of *Vitis vinifera* L. by the esca-associated fungus *Phaeoacremonium aleophilum* using a Gfp marked strain and cutting systems. *PLoS One* 10:e0126851. doi: 10.1371/journal.pone.0126851
- Pouzoulet, J., Mailhac, N., Couderc, C., Besson, X., Daydé, J., Lummerzheim, M., et al. (2013). A method to detect and quantify phaeoacremonia chlamydospora and *Phaeoacremonium aleophilum* DNA in grapevine-wood samples. *Appl. Microbiol. Biotechnol.* 97, 10163–10175. doi: 10.1007/s00253-013-5299-6
- Poveda, J. (2021). Trichoderma as biocontrol agent against pests: new uses for a mycoparasite. *Biol. Control* 159:104634. doi: 10.1016/j.biocontrol.2021.104634
- Pratap Singh, S., Keswani, C., Pratap Singh, S., Sansinenea, E., and Xuan Hoat, T. (2021). Trichoderma Spp. Mediated induction of systemic defense response in brinjal against *Sclerotinia sclerotiorum*. *Curr. Res. Microb. Sci.* 2:100051. doi: 10.1016/j.crmicr.2021.100051
- Ram, R. M., Keswani, C., Bisen, K., Tripathi, R., Singh, S. P., and Singh, H. B. (2018). “Biocontrol technology: eco-friendly approaches for sustainable agriculture,” in *Omics Technologies and Bio-Engineering*, Vol. 2, eds D. Barh and V. Azevedo (San Diego, CA: Academic Press), 177–190. doi: 10.1016/B978-0-12-815870-8.00010-3
- Reis, P., Pierron, R., Larignon, P., Lecomte, P., Abou-Mansour, E., Farine, S., et al. (2019). Vitis methods to understand and develop strategies for diagnosis and sustainable control of grapevine trunk diseases. *Phytopathology* 109, 916–931. doi: 10.1094/PHYTO-09-18-0349-RVW
- Rivière, C., Pawlus, A. D., and Mérillon, J.-M. (2012). Natural stilbenoids: distribution in the plant kingdom and chemotaxonomic interest in vitaceae. *Nat. Prod. Rep.* 29:1317. doi: 10.1039/c2np20049j
- Romeo-Oliván, A., Pagès, M., Breton, C., Lagarde, F., Cros, H., Yobréat, O., et al. (2021). Ozone dissolved in water: an innovative tool for the production of young plants in grapevine nurseries? *Ozone Sci. Eng.* 1–15. doi: 10.1080/01919512.2021.1984203
- Rusjan, D., Persic, M., Likar, M., Biniari, K., and Mikulic-Petkovsek, M. (2017). Phenolic responses to esca-associated fungi in differently decayed grapevine woods from different trunk parts of “Cabernet Sauvignon”. *J. Agric. Food Chem.* 65, 6615–6624. doi: 10.1021/acs.jafc.7b02188
- Savazzini, F., Longa, C. M. O., Pertot, I., and Gessler, C. (2008). Real-time PCR for detection and quantification of the biocontrol agent *Trichoderma atroviride* strain SC1 in soil. *J. Microbiol. Methods* 73, 185–194. doi: 10.1016/j.mimet.2008.02.004
- Singh, B. N., Padmanabh, D., Sarma, B. K., and Singh, H. B. (2019). *Trichoderma Asperellum* T42 induces local defense against *Xanthomonas oryzae* Pv. *Oryzae* under nitrate and ammonium nutrients in tobacco. *RSC Adv.* 9, 39793–39810. doi: 10.1039/C9RA06802C
- Sumner, L. W., Amberg, A., Barrett, D., Beale, M. H., Beger, R., Daykin, C. A., et al. (2007). Proposed minimum reporting standards for chemical analysis: chemical analysis working group (CAWG) metabolomics standards initiative (MSI). *Metabolomics* 3, 211–221. doi: 10.1007/s11306-007-0082-2
- Surico, G. (2009). Towards a redefinition of the diseases within the esca complex of grapevine. *Phytopathol. Medit.* 48, 5–10.
- Treutter, D. (2005). Significance of flavonoids in plant resistance and enhancement of their biosynthesis. *Plant Biol.* 7, 581–591. doi: 10.1055/s-2005-873009
- Trotel-Aziz, P., Abou-Mansour, E., Courteaux, B., Rabenoelina, F., Clément, C., Fontaine, F., et al. (2019). Bacillus subtilis PTA-271 counteracts botryosphaeria dieback in grapevine, triggering immune responses and detoxification of fungal phytotoxins. *Front. Plant Sci.* 10:25. doi: 10.3389/fpls.2019.00025
- Tsugawa, H., Cajka, T., Kind, T., Ma, Y., Higgins, B., Ikeda, K., et al. (2015). MS-DIAL: data-independent MS/MS deconvolution for comprehensive metabolome analysis. *Nat. Methods* 12, 523–526. doi: 10.1038/nmeth.3393
- Tsugawa, H., Kind, T., Nakabayashi, R., Yukihira, D., Tanaka, W., Cajka, T., et al. (2016). Hydrogen rearrangement rules: computational MS/MS fragmentation

- and structure elucidation using MS-FINDER software. *Anal. Chem.* 88, 7946–7958. doi: 10.1021/acs.analchem.6b00770
- Úrbez-Torres, J. R., Haag, P., Bowen, P., and O’Gorman, D. T. (2014). Grapevine trunk diseases in British Columbia: incidence and characterization of the fungal pathogens associated with Esca and Petri diseases of grapevine. *Plant Dis.* 98, 469–482. doi: 10.1094/PDIS-05-13-0523-RE
- Vinale, F., Sivasithamparam, K., Ghisalberti, E. L., Marra, R., Woo, S. L., and Lorito, M. (2008). Trichoderma–plant–pathogen interactions. *Soil Biol. Biochem.* 40, 1–10. doi: 10.1016/j.soilbio.2007.07.002
- Yacoub, A., Gerbore, J., Magnin, N., Chambon, P., Dufour, M.-C., Corio-Costet, M.-F., et al. (2016). Ability of *Pythium oligandrum* strains to protect *Vitis vinifera* L., by inducing plant resistance against *Phaeomoniella chlamydospora*, a pathogen involved in Esca, a grapevine trunk disease. *Biol. Control* 92, 7–16. doi: 10.1016/j.biocontrol.2015.08.005
- Yacoub, A., Haidar, R., Gerbore, J., Masson, C., Dufour, M.-C., Guyoneaud, R., et al. (2020). *Pythium Oligandrum* induces grapevine defence mechanisms against the trunk pathogen *Neofusicoccum parvum*. *Phytopathol. Mediter.* 59, 565–580. doi: 10.14601/Phyto-11270
- Yan, Y., Mao, Q., Wang, Y., Zhao, J., Fu, Y., Yang, Z., et al. (2021). *Trichoderma harzianum* induces resistance to root-knot nematodes by increasing secondary metabolite synthesis and defense-related enzyme activity in *Solanum lycopersicum* L. *Biol. Control* 158:104609. doi: 10.1016/j.biocontrol.2021.104609
- Conflict of Interest:** The authors declare that the research was conducted in the absence of any commercial or financial relationships that could be construed as a potential conflict of interest.
- Publisher’s Note:** All claims expressed in this article are solely those of the authors and do not necessarily represent those of their affiliated organizations, or those of the publisher, the editors and the reviewers. Any product that may be evaluated in this article, or claim that may be made by its manufacturer, is not guaranteed or endorsed by the publisher.

Copyright © 2022 Chervin, Romeo-Oliván, Fournier, Puech-Pages, Dumas, Jacques and Marti. This is an open-access article distributed under the terms of the Creative Commons Attribution License (CC BY). The use, distribution or reproduction in other forums is permitted, provided the original author(s) and the copyright owner(s) are credited and that the original publication in this journal is cited, in accordance with accepted academic practice. No use, distribution or reproduction is permitted which does not comply with these terms.



# Gene *sdaB* Is Involved in the Nematocidal Activity of *Enterobacter ludwigii* AA4 Against the Pine Wood Nematode *Bursaphelenchus xylophilus*

Yu Zhao<sup>1,2†</sup>, Zhibo Yuan<sup>1,2†</sup>, Shuang Wang<sup>3</sup>, Haoyu Wang<sup>1,2</sup>, Yanjie Chao<sup>4</sup>, Ronald R. Sederoff<sup>5</sup>, Heike Sederoff<sup>6</sup>, He Yan<sup>7</sup>, Jialiang Pan<sup>7</sup>, Mu Peng<sup>8</sup>, Di Wu<sup>1,2</sup>, Rainer Borriss<sup>9,10\*</sup> and Ben Niu<sup>1,2\*</sup>

## OPEN ACCESS

### Edited by:

Jochen Fischer,  
Institut für Biotechnologie und  
Wirkstoff-Forschung (IBWF), Germany

### Reviewed by:

Kgabo Martha Pofu,  
University of Limpopo, South Africa  
Florence Fontaine,  
Université de Reims  
Champagne-Ardenne, France

### \*Correspondence:

Rainer Borriss  
rainer.borriss@rz.hu-berlin.de

Ben Niu  
ben\_niu@nefu.edu.cn

<sup>†</sup>These authors have contributed  
equally to this work

### Specialty section:

This article was submitted to  
Microbe and Virus Interactions with  
Plants,  
a section of the journal  
Frontiers in Microbiology

Received: 06 February 2022

Accepted: 25 March 2022

Published: 06 May 2022

### Citation:

Zhao Y, Yuan Z, Wang S, Wang H,  
Chao Y, Sederoff RR, Sederoff H,  
Yan H, Pan J, Peng M, Wu D,  
Borriss R and Niu B (2022) Gene  
*sdaB* Is Involved in the Nematocidal  
Activity of *Enterobacter ludwigii* AA4  
Against the Pine Wood Nematode  
*Bursaphelenchus xylophilus*.  
Front. Microbiol. 13:870519.  
doi: 10.3389/fmicb.2022.870519

<sup>1</sup> State Key Laboratory of Tree Genetics and Breeding, Northeast Forestry University, Harbin, China, <sup>2</sup> College of Life Science, Northeast Forestry University, Harbin, China, <sup>3</sup> Administrative Office of the Summer Palace, Beijing Municipal Administration Center of Parks, Beijing, China, <sup>4</sup> The Center for Microbes, Development and Health (CMDH), Institut Pasteur of Shanghai, Chinese Academy of Sciences, Shanghai, China, <sup>5</sup> Forest Biotechnology Group, Department of Forestry and Environmental Resources, North Carolina State University, Raleigh, NC, United States, <sup>6</sup> Department of Plant and Microbial Biology, North Carolina State University, Raleigh, NC, United States, <sup>7</sup> Center for Biological Disaster Prevention and Control, National Forestry and Grassland Administration, Shenyang, China, <sup>8</sup> College of Biological Science and Technology, Hubei Minzu University, Enshi, China, <sup>9</sup> Nord Reet UG, Greifswald, Germany, <sup>10</sup> Institute of Marine Biotechnology e.V. (IMaB), Greifswald, Germany

*Bursaphelenchus xylophilus*, a plant parasitic nematode, is the causal agent of pine wilt, a devastating forest tree disease. Essentially, no efficient methods for controlling *B. xylophilus* and pine wilt disease have yet been developed. *Enterobacter ludwigii* AA4, isolated from the root of maize, has powerful nematocidal activity against *B. xylophilus* in a new *in vitro* dye exclusion test. The corrected mortality of the *B. xylophilus* treated by *E. ludwigii* AA4 or its cell extract reached 98.3 and 98.6%, respectively. Morphological changes in *B. xylophilus* treated with a cell extract from strain AA4 suggested that the death of *B. xylophilus* might be caused by an increased number of vacuoles in non-apoptotic cell death and the damage to tissues of the nematodes. In a greenhouse test, the disease index of the seedlings of Scots pine (*Pinus sylvestris*) treated with the cells of strain AA4 plus *B. xylophilus* or those treated by AA4 cell extract plus *B. xylophilus* was 38.2 and 30.3, respectively, was significantly lower than 92.5 in the control plants treated with distilled water and *B. xylophilus*. We created a *sdaB* gene knockout in strain AA4 by deleting the gene that was putatively encoding the beta-subunit of L-serine dehydratase through Red homologous recombination. The nematocidal and disease-suppressing activities of the knockout strain were remarkably impaired. Finally, we revealed a robust colonization of *P. sylvestris* seedling needles by *E. ludwigii* AA4, which is supposed to contribute to the disease-controlling efficacy of strain AA4. Therefore, *E. ludwigii* AA4 has significant potential to serve as an agent for the biological control of pine wilt disease caused by *B. xylophilus*.

**Keywords:** *sdaB*, L-serine dehydratase, *Enterobacter ludwigii*, nematocidal activity, *Bursaphelenchus xylophilus*, pine wilt disease, methuosis

## INTRODUCTION

The pine wood nematode (PWN) *Bursaphelenchus xylophilus* causes serious damage to forest ecosystems and massive economic losses by inducing pine wilt disease (PWD) (Zhao et al., 2014; Lee et al., 2019; Guo et al., 2020). PWD may result in destruction of conifer forests and has long been a huge threat to Asian and European forestry for a long time (Kikuchi et al., 2011; Faria et al., 2015). As a pathogenic nematode native to North America (Li et al., 2015; Proenca et al., 2017), *B. xylophilus*, feeding on live trees and fungi colonizing dead or dying trees, is a migratory endoparasite transmitted by the insect vector *Monochamus alternatus* (Japanese pine sawyer beetle) (Kim et al., 2019, 2020). The annual economic cost of the PWN (Soliman et al., 2012) in the European Union (EU) alone is estimated at a billion euros for each of the past 22 years. The rapid death of pine trees infected by the PWN could be attributed to the dysfunction of the water-conducting system caused by the death of parenchyma cells. The secreted enzymes and surface coat proteins of *B. xylophilus* are involved in its pathogenicity (Futai, 2013; Nunes da Silva et al., 2015; Wen et al., 2021). The molecular mechanisms of PWN pathogenesis are still largely unknown, hindering the prospects for control of this pathogen and PWD. Chemical insecticides and nematicides used to control *B. xylophilus* by jet-sprays or trunk injections for decades (Qiu et al., 2019; Guo et al., 2020; Faria et al., 2021) have become a major social concern. More environmental-friendly strategies, such as beneficial microorganisms that suppress PWN, have recently gained more attention (Tian et al., 2007; Wu et al., 2013; Cai et al., 2022).

Biological control of plant parasitic nematodes (PPNs) using nematocidal bacteria or their metabolites, which are toxic to nematodes, is a potentially sustainable alternative to chemical nematicides (Haegeman et al., 2009; Kumar and Dara, 2021). Nematocidal prokaryotes mainly belonging to bacterial genera, such as *Bacillus* (Crickmore, 2005; Ponpandian et al., 2019; Park et al., 2020), *Streptomyces* (Kang et al., 2021), *Serratia* (Paiva et al., 2013; Nascimento et al., 2016; Abd El-Aal et al., 2021), *Stenotrophomonas* (Huang et al., 2009; Ponpandian et al., 2019), *Pseudoduganella* (Fang et al., 2019; Abd El-Aal et al., 2021), *Novosphingobium* (Topalović et al., 2020), *Pasteuria* (Tian et al., 2007), *Pseudomonas* (Chan et al., 2020), *Enterobacter* (Munif et al., 2000; Oh et al., 2018), and *Curtobacterium* (Kumar and Dara, 2021), are capable of suppressing PPNs by diverse modes of action, including parasitism (Wu et al., 2013; Proenca et al., 2017; Ponpandian et al., 2019), production of toxins (Abd El-Aal et al., 2021; Kahn et al., 2021), antibiotics plus enzymes (Yang et al., 2007; Huang et al., 2009), competition for nutrients (Proenca et al., 2019), and induction of systemic resistance of plants (Liang et al., 2019; Han et al., 2021). Within these nematocidal groups, some bacterial strains have exhibited efficient killing activity against the PWNs. *Bacillus thuringiensis* zjfc85 caused 90% mortality of *B. xylophilus* by producing a Cry protein named Cry5Ba3 (Kahn et al., 2021). Two *Streptomyces* strains did kill the hatched PWNs and affected egg hatching via biosynthesis of the toxic compounds, teleocidin B4, and spectinabilin, which effectively suppressed the development of PWD under field

conditions (Kang et al., 2021). A 70 kD serine protease produced by *Serratia* sp. A88copa13 was majorly responsible for the toxicity of this PWN-killing strain (Paiva et al., 2013). Thus, the application of nematocidal bacteria is a promising strategy in suppressing PWD.

*Enterobacter* is an exceptionally diverse genus of bacteria found in various habitats in association with soil (El-Sayed et al., 2014; Habibi et al., 2019; Danish et al., 2020), plants (Park et al., 2015; Andres-Barrao et al., 2017; Sarkar et al., 2018), and animals, including humans (Mokracka et al., 2004; Peng et al., 2009). Many *Enterobacter* strains are characterized as plant beneficial bacteria. Such procaryotic microbes promote the growth of their plant hosts under favored or adverse abiotic conditions by producing indole-acetic acid (IAA) (Park et al., 2015; Srisuk et al., 2018; Habibi et al., 2019; Li et al., 2022), siderophores (Mokracka et al., 2004; Nurjadi et al., 2021; Li et al., 2022), hydrocyanic acid (Mpongwana et al., 2016; Mahdi et al., 2020; Javaheri Safa et al., 2021), salicylic acid (Kang et al., 2015) plus exopolysaccharides (Sayyed et al., 2015; Niu et al., 2018; Dhanya et al., 2021), solubilizing phosphate (Adhikari et al., 2020; Roslan et al., 2020; Aeron et al., 2021), by fixing nitrogen (Kämpfer et al., 2005; Peng et al., 2009; El-Sayed et al., 2014), reducing Na<sup>+</sup> uptake (Um et al., 2017; Sarkar et al., 2018), and inducing the activity of enzymes with action as antioxidants (Andres-Barrao et al., 2017; Danish et al., 2020). At present, it has been demonstrated that some *Enterobacter* species exhibit inhibitory effects against the oomycete pathogen *Pythium ultimum* (Lohrke et al., 2002; Kageyama and Nelson, 2003; Windstam and Nelson, 2008), the fungal pathogens *Fusarium moniliforme* (Hinton and Bacon, 1995; Demirci et al., 2000; Rodrigues et al., 2018), *F. oxysporum* (El-Sayed et al., 2014; Del Barrio-Duque et al., 2019; Abdelshafy Mohamad et al., 2020), *Aspergillus niger* (Yadav et al., 2016; Kaushik et al., 2017; Batyrova et al., 2020), and *Aspergillus flavus* (Etcheverry et al., 2009; Mahmood et al., 2020), and the bacterial pathogen *Ralstonia solanacearum* (Sarkar and Chaudhuri, 2015; Yin et al., 2020; Zaki et al., 2021), indicating their protective efficacy on plants. A few *Enterobacter* strains exhibited significant nematocidal activity against the root-knot nematodes (Munif et al., 2000; El-Sayed et al., 2014; Oh et al., 2018). *Enterobacter asburiae* HK169 was able to reduce root gall formation rate by 66% and killed all juveniles of *Meloidogyne incognita* within 48 h (Oh et al., 2018). Similarly, an endophytic *E. intermedius* strain isolated from tomato roots remarkably decreased the number of root galls (Munif et al., 2000). Our knowledge of the molecular mechanisms underlying the inhibitory effects of *Enterobacter* strains against PPNs is still very limited.

In the present study, we identified a powerful PWN-killing bacterial strain, *Enterobacter ludwigii* AA4, which was previously isolated from maize roots (Niu et al., 2017) by screening the nematocidal activities of 374 bacterial strains against *B. xylophilus* using a new fluorescent staining-based PWN-killing activity test. *E. ludwigii* AA4 had a remarkable inhibitory effect against PWD under greenhouse conditions. After deleting the *sdaB* gene, presumed to encode the beta subunit of L-serine dehydratase, the nematocidal and disease-suppressing effects of the mutant strain were significantly reduced. The robust colonization of *P. sylvestris* seedling needles by *E. ludwigii* AA4, presumed to contribute to



the disease-controlling efficacy of strain AA4, was quantified and compared to the strain carrying a *sdaB* gene deletion.

## MATERIALS AND METHODS

### Microbial Strains and Growth Conditions

Bacterial strains kept frozen with 15% (v/v) glycerol at  $-80^{\circ}\text{C}$  were streaked on Luria-Bertani (LB) agar plates and incubated at  $30^{\circ}\text{C}$  for 16 h. Then, a single colony of each strain was inoculated into 5 ml LB liquid medium and shaken at  $30^{\circ}\text{C}$ , 200 rpm for another 16 h. Antibiotics were supplemented where necessary at the following concentrations: kanamycin 50  $\mu\text{g/ml}$ , tetracycline 50  $\mu\text{g/ml}$ , gentamicin 25  $\mu\text{g/ml}$ , streptomycin 50  $\mu\text{g/ml}$ , and gentamicin 25  $\mu\text{g/ml}$  (Table 1).

The spores of *Botrytis cinerea* were deposited at  $-80^{\circ}\text{C}$  in 15% (v/v) glycerol. Ten microliters of fungal spores were dropped on a potato dextrose agar (PDA) plate and incubated at  $25^{\circ}\text{C}$  in the dark. When *B. cinerea* mycelia covered PDA plates, the fungal culture was used for inoculating *B. xylophilus*.

### The Source and Culture of Pine Wood Nematodes

Cultures of the PWN, *Bursaphelenchus xylophilus*, were obtained from Dr. Hongtao Li at the Hebei Academy of Agriculture and Forestry Sciences and Dr. Kai Guo at Zhejiang A&F University. The fungus *B. cinerea* was purchased from the Shanghai Bioresource Collection Center (SHBCC).

*Bursaphelenchus xylophilus* was inoculated on a PDA culture of *B. cinerea* and incubated at  $25^{\circ}\text{C}$  in the dark until the fungal mycelia were completely consumed by *B. xylophilus*. Nematodes were collected using the modified Baermann funnel technique (Kitazume et al., 2018; Cesarz et al., 2019; Maehara et al., 2020) and washed with a mixture of 0.1% streptomycin sulfate and 0.002% actinone three times to remove surface microbial contaminants (Liu et al., 2016). Then, these nematodes were used for PWN-killing activity test and *in planta* biocontrol assays.

For microscopic image analysis of PWN morphology, about 10,000 nematodes were decanted into a burette containing 25 ml of 0.3% carboxymethyl cellulose (CMC) solution. After 12 h, the second-stage juveniles were collected from the top of the burette (Qiu et al., 2016, 2019). These worms were fed with *B. cinerea*. After 48 h, the L4 juveniles were collected in sterile water and washed with a mixture of 0.1% streptomycin sulfate and 0.002% actinone three times. These L4 juveniles were used for the image analysis.

### Preparation of Cell Extracts of *E. ludwigii* AA4

Wild-type AA4, AA4 $\Delta$ *sdaB* (derivative of wild-type AA4 that lacks *sdaB*), and C $\Delta$ *sdaB* (AA4 $\Delta$ *sdaB* complemented with wild-type *sdaB* gene) kept frozen with 15% (v/v) glycerol at  $-80^{\circ}\text{C}$  were streaked on LB agar plates with corresponding antibiotics (Table 1) and incubated at  $30^{\circ}\text{C}$  for 16 h. Then, a single colony of each strain was inoculated into 5 ml LB liquid medium and shaken at  $30^{\circ}\text{C}$ , 200 rpm for another 16 h. One milliliter

of the culture of each strain was transferred into 50 ml LB liquid medium and shaken at  $30^{\circ}\text{C}$ , 200 rpm for 2–3 h until Optical Density at 600 nm ( $\text{OD}_{600}$ ) value reached 0.6–0.8 (early stationary phase). Cells were harvested by centrifuging at 9,100 rpm ( $8,000 \times g$ ) at  $4^{\circ}\text{C}$  for 20 min (Thermo, Multifuge X1R, Germany) and washed by phosphate-buffered saline (PBS). The cell precipitations were resuspended in 5 ml PBS before sonication. An ultrasound processor (Sonics, VCX130PB, United States) was used to sonicate the resuspended cell suspensions. The probe was immersed into the suspensions and sonicated the cells on ice for 60 min at a power of 130 W (pulse duration: 2 s on, 1 s off). The resulting cell lysates were centrifuged at 15,300 rpm ( $14,000 \times g$ ) for 30 min. The supernatant was collected and used as cell extracts. The concentration of total protein in cell extract was measured by using a biuret protein assay reagents kit (Solarbio, PC0010, China).

### Fluorescent Staining-Based Pine Wood Nematode-Killing Activity Test

The nematocidal activity of the 43 efficient PWN-killing bacterial strains of AA4 $\Delta$ *sdaB* and C $\Delta$ *sdaB* was evaluated by the fluorescent staining-based PWN-killing activity test, while *Bacillus pumilus* YLT40 and *Paenibacillus polymyxa* M-1 were utilized for confirming the reliability of the assay. The cell density of bacterial culture suspension was adjusted to  $\text{OD}_{600} = 1.0$  for each strain used in the test. Each well of the 96-well microplates was added with 40  $\mu\text{l}$  of bacterial culture suspension and 20  $\mu\text{l}$  of worm suspension containing 40–50 nematodes, while 40  $\mu\text{l}$  of LB liquid medium or PBS and 20  $\mu\text{l}$  of worm suspension was employed as negative control. Five wells were used for each treatment designated with the code of the strain listed in Supplementary Tables 1, 2. The inoculated microplates were incubated at  $25^{\circ}\text{C}$  in the dark for 24 h. Then, a plate washer (Biobase, BK-9622, China) was employed to change the liquid cultures with sterile water. 4'-diamidino-2-phenylindole (DAPI, Solarbio, C0065, China) was used to stain the PWNs, and the final concentration of DAPI in each well was 5  $\mu\text{g/ml}$ . After being stained for 1 h, the nematodes were observed by a confocal laser scanning microscope (Zeiss, LSM 800, Germany) using an excitation laser of 353 nm and collecting emission of 465 nm, where the dead worms displayed bright fluorescence while the live ones were dim.

To test the nematocidal activity of the cell extract of wild-type AA4, AA4 $\Delta$ *sdaB*, and C $\Delta$ *sdaB*, the extract containing total proteins of 5 mg/ml was mixed with 20  $\mu\text{l}$  of worm suspension containing 40–50 nematodes in one well of a 96-well microplate. The remaining steps are the same as those for the assays with bacterial cell suspensions.

The mortality and corrected mortality of *B. xylophilus* were calculated as follows (Faria et al., 2013; Guo et al., 2016; Liu et al., 2019):

$$\text{The mortality (\%)} = \frac{\text{number of dead nematodes}}{\text{number of all nematodes}} \times 100$$

**TABLE 1 |** Strains and plasmids used for genetic manipulation of *Enterobacter ludwigii* AA4.

Strain or plasmid	Description
<b>Strains</b>	
T1	Tn10 transposon inserting into genome of wild-type AA4; <i>Kan<sup>R</sup></i> .
AA4Δ <i>sdaB</i>	Derivative of wild-type AA4 that lacks <i>sdaB</i> ; <i>Kan<sup>R</sup></i> .
CΔ <i>sdaB</i>	AA4Δ <i>sdaB</i> complemented with wild-type <i>sdaB</i> gene; <i>Kan<sup>R</sup></i> , <i>Tet<sup>R</sup></i> .
AA4-GFP	Green fluorescent protein (GFP)-labeled wild-type AA4; <i>Tet<sup>R</sup></i> , <i>Gen<sup>R</sup></i> .
AA4Δ <i>sdaB</i> -GFP	GFP-labeled AA4Δ <i>sdaB</i> ; <i>Kan<sup>R</sup></i> , <i>Tet<sup>R</sup></i> , <i>Gen<sup>R</sup></i> .
CΔ <i>sdaB</i> -GFP	GFP-labeled CΔ <i>sdaB</i> ; <i>Kan<sup>R</sup></i> , <i>Tet<sup>R</sup></i> , <i>Gen<sup>R</sup></i> .
DH5a	Competent cells for cloning.
<b>Plasmids</b>	
pKD4	Kanamycin cassette; <i>Kan<sup>R</sup></i> .
pKD46	Template plasmid containing Red recombinase system under arabinose-inducible promoter; <i>Kan<sup>R</sup></i> .
pUC19	Vector for construction of recombinant plasmid; <i>Kan<sup>R</sup></i> .
pBBR1	Vector for construction of complement plasmid; <i>Tet<sup>R</sup></i> .
pGPF78	Vector with green fluorescent protein (GFP); <i>Tet<sup>R</sup></i> , <i>Gen<sup>R</sup></i> .

*Kan<sup>R</sup>*, kanamycin resistance; *Tet<sup>R</sup>*, tetracycline resistance; *Gen<sup>R</sup>*, gentamicin resistance.

**TABLE 2 |** Primers used in this study.

Primer	5'–3' sequence
<b>For 16S rRNA gene sequencing analysis</b>	
27F	AGAGTTTGATCATGGCTCAG
1492R	TACGGTTACCTTGTTACGACTT
<b>For gene deletions</b>	
<i>sdaB</i> -H1up	TCTGATTCCGCTGATCATCATGGCTATCATTGCCTTC
<i>sdaB</i> -H1down	GTAATGCTGCAATCTGATGCGTCCATTGCTTTTCAGTCAGAGGGGGAGGAG
<i>sdaB</i> -H2up	GAAGAAGCCTCGCATAACGAGGCTTCCTGAAAGGCATATCCTCCTTAGTTCCTATTCC
<i>sdaB</i> -H2down	GTGCGATATGGTTGAGAAGCCAGCAAAGTGGCC
Kup	GGCTTCCTGAAAGGCATATCCTCCTTAGTTCCTATTCC
Kdown	AGCAATGGACGCATCAGATTGCAGCATTACACGCTTT
pUC19up	CATGATGATCAGCGGAATCAGATCGCGGTTTCGGTGATGACGGTGAAAACCTCTGAC
pUC19down	CACCTTCTTCGCGGTCGTGATACGACGAAAGGGCCTCGTGATACGCCTATTTTATAGG
<b>For complementing the mutation</b>	
<i>sdaB</i> -DF	ATGGAACCACTCAAACCAGCACCGTTGCTTCGATTG
<i>sdaB</i> -UR	CGAGCTGCGTGTGAAAGTCGCGGATACCAACGAAAGC
<i>sdaB</i> -PBBR1-DF	AAGACAGAATCAGAATCAATTGCCCCATAGTGAGTCGTATTA
<i>sdaB</i> -PBBR1-UR	TTGTGACCTGCGATTAAACAGCTTTTGTTCCCTTTAG

Corrected mortality (%) =

$$\frac{\text{mortality in treatment (\%)} - \text{mortality in control (\%)}}{100 - \text{mortality in control (\%)}} \times 100$$

Two-tailed *t*-test (GrapPad Prism 8) was used for the statistical analysis. All these experiments above were repeated five times.

Z'factor, a combination of signal interval and variation, is a parameter used to evaluate the reliability of results obtained from an experiment for guiding a larger-scale experimentation. It is calculated as:

$$z'\text{factor} = 1 - \frac{3(\sigma_p + \sigma_n)}{|\mu_p - \mu_n|}$$

where  $\sigma_p$  and  $\sigma_n$  represent the standard deviations of positive control and negative control, respectively, and  $\mu_p$  and  $\mu_n$  represent the means of positive control and negative control, respectively. Z'factor was calculated by using the software Excel (Microsoft). The theoretical value of Z'factor is 1, and a Z'factor value between 0.5 and 1 indicates the outcomes of a given experiment is highly reliable, while a test of low reliability usually possesses a Z'factor value of less than 0.5 (Zhang X. D. et al., 2020).

## Identification of the Efficient Bacterial Pine Wood Nematode-Killing Strains

Identification of the efficient bacterial PWN-killing strains were carried out by using 16S rRNA gene sequencing analysis. Genomic DNA was extracted from an overnight LB culture of

each strain by utilizing a bacterial genomic DNA extraction kit (Tiangen, DP302-02, China) following the manufacturer's protocol. The 16S rRNA gene was amplified in 25- $\mu$ l PCR reactions using the universal primers 27F and 1492R (Table 2) (Monciardini et al., 2002; Niu et al., 2013; López and Alippi, 2019). The reaction mixture contained 1  $\mu$ l of template DNA, 12.5  $\mu$ l of master mix (Takara, RR350Q, Japan), 1  $\mu$ l of each of the forward and reverse primers, and 9.5  $\mu$ l of sterile deionized water. Amplifications were performed using a T100 Thermal Cycler (Bio-Rad, 621BR47532, United States) with the following cycle conditions: initial denaturation at 95°C for 5 min; 30 cycles at 94°C for 30 s, 58°C for 30 s, and 72°C for 1.5 min; and a final extension at 72°C for 10 min. Amplicons were purified using a PCR purification kit (Omega, D6492-02, China) and sequenced using 27F primer at Tsingke Biotechnology Co., Ltd. DNA sequences were inspected for base-caller errors and were trimmed by removing any ambiguous trailing or leading bases using the software GAP4 in the STADEN Package<sup>1</sup>. The sequences were compared with those of the reference organisms by Basic Local Alignment Search Tool (BLAST) at the National Center for Biotechnology Information (NCBI) website<sup>2</sup> and by Sequence Match at the Ribosomal Database Project (RDP) website<sup>3</sup>. The 16S rRNA gene sequences of efficient nematocidal strains were deposited in the GenBank database. The accession numbers were listed in **Supplementary Table 1**.

## In planta Assays for Biocontrol Effect Against Pine Wilt Disease

The biological control effects of wild-type AA4, AA4 $\Delta$ *sdaB*, and C $\Delta$ *sdaB* were examined by using both 3-year-old and 1-month-old Scots pine (*Pinus sylvestris*) tree seedlings grown under greenhouse conditions. The 3-year-old seedlings were purchased from Longsheng nursery at Harbin. Ten milliliters of bacterial suspension (OD<sub>600</sub> = 1.0) were inoculated on the 3-year-old seedlings by spraying. Then, a 2–4 cm silt was made on the surface of bark located at approximately 10–15 cm above the soil. One hundred microliters of PWN suspension containing about 5,000 worms were injected into the trunk. A small piece of sterilized cotton was fixed on the trunk to cover the silt (Xue et al., 2019). The plants were placed in a greenhouse under the following conditions: 16 h of light (day) and 8 h of dark (night), 25°C, and a relative humidity of 70%. Plants were watered periodically and maintained in the greenhouse. Thirty days after inoculation, the symptoms present on the seedlings were recorded with a camera (Canon, 80D, Japan). The severities of PWD were evaluated based on the disease ranks described in earlier studies (Qiu et al., 2016, 2019) as follows: In rank 0, all needles are green. In rank 1, less than a quarter of needles turn yellow. In rank 2, 25–75% of needles turn yellow. In rank 3, more than 75% of needles turn yellow and less than 50% of needles get wilted. In rank 4, more than 50% of the needles get wilted. Five plants were used for each of the two treatments designated as PWN (inoculation of

seedlings with PWN alone) and PWN + AA4 (inoculation of seedlings with PWN jointly with wild-type AA4), respectively.

For the experimentations with 1-month-old *Pinus sylvestris* seedlings, the seeds were surface-sterilized by immersing in 5% KMnO<sub>4</sub> for 60 min and placing in a growth chamber at 30°C in the light for 48 h. After germination, the seeds with roots were sown in the plant growth substrates prepared by mixing soil and vermiculite in a ratio of 3:1. Thirty days after emergence, 5 ml of bacterial suspensions (OD<sub>600</sub> = 1.0) or cell extracts (containing total proteins of 5 mg/ml) of wild-type AA4, AA4 $\Delta$ *sdaB*, and C $\Delta$ *sdaB* were sprayed on the needles of Scots pine seedlings, respectively. In the meantime, 100  $\mu$ l of PWN suspension containing approximately 3,000 worms were injected into the needles by using a syringe. A small piece of sterile cotton was fixed on the needles to cover the pinhole. The plants were incubated in greenhouse under the same condition on which the 3-year-old seedlings grew. The number of dead seedlings and symptoms were recorded on the ninth day after inoculation. Ten plants were used for each of the 11 treatments designated as PWN (inoculation of seedlings with PWN alone), PWN +  $\Delta$ *sdaB* (inoculation of seedlings with PWN jointly with AA4 $\Delta$ *sdaB* cell suspension), PWN + C $\Delta$ *sdaB* (inoculation of seedlings with PWN jointly with AA4C $\Delta$ *sdaB* cell suspension), PWN + WT (inoculation of seedlings with PWN jointly with wild-type AA4 cell suspension), PWN +  $\Delta$ *sdaB*CE (inoculation of seedlings with PWN jointly with AA4 $\Delta$ *sdaB* cell extract), PWN + C $\Delta$ *sdaB*CE (inoculation of seedlings with PWN jointly with AA4C $\Delta$ *sdaB* cell extract), PWN + WTCE (inoculation of seedlings with PWN jointly with wild-type AA4 cell extract), PWN +  $\Delta$ *sdaB*S (inoculation of seedlings with PWN jointly with AA4 $\Delta$ *sdaB* culture supernatant), PWN + C $\Delta$ *sdaB*S (inoculation of seedlings with PWN jointly with AA4C $\Delta$ *sdaB* culture supernatant), PWN + WTS (inoculation of seedlings with PWN jointly with wild-type AA4 culture supernatant), and DW (treatment with distilled water), respectively.

The severities of PWD were evaluated based on the disease ranks shown in **Supplementary Figure 3**. The disease severity indices were calculated as follows:

$$\text{Disease Index (DI)} = \frac{\sum (X_i \times A_i)}{(X \times A_{\max})}$$

where  $X_i$  is the number of pine trees in each disease rank,  $A_i$  is the disease rank,  $X$  is the total number of pine trees, and  $A_{\max}$  is the maximum rank (Qiu et al., 2019; Xue et al., 2019). Two-tailed *t*-test (GrapPad Prism 8) was used for the statistical analysis. These experiments were repeated three times.

## Image Analysis of Pine Wood Nematode Morphology

The cell extract of *E. ludwigii* AA4 was prepared as above. Forty microliters of cell extract containing total proteins of 5 mg/ml and 20  $\mu$ l of worm suspension containing 40–50 L4 juveniles of PWNs were added in a single well of the 96-well microplates. At the meantime, the combination of 40  $\mu$ l of PBS and 20  $\mu$ l of worm

<sup>1</sup> <http://staden.sourceforge.net/>

<sup>2</sup> <https://blast.ncbi.nlm.nih.gov/>

<sup>3</sup> <http://rdp.cme.msu.edu>

suspension was employed as negative control. The microplates were stored at 25°C in the dark for 24 h. Then, the worms were picked and put into 10 µl of PBS by injector pinhead. After being washed three times, the worms were transferred to a slide. Ten microliters of PBS were then dropped on the samples. The morphological changes of *B. xylophilus* were observed and recorded by a light microscope (Olympus, BX43, Japan).

## Construction of Mutants of *E. ludwigii* AA4

The *sdaB* gene knock-out mutant of *E. ludwigii* AA4 was created by using the Red recombinase system (Datsenko and Wanner, 2000; Dahyot et al., 2020; Guérin et al., 2020). Primers were designed according to the information obtained from the whole genome sequence of strain AA4 (Niu et al., 2017). The upstream border sequence of the AA4 *sdaB* gene was amplified from AA4 chromosomal DNA using primers *sdaB*-H1up and *sdaB*-H1down (Table 2), while the downstream border sequence of *sdaB* was amplified with primers *sdaB*-H2up and *sdaB*-H2down (Table 2). A kanamycin resistance cassette, flanked by 23-bp-long sequences homologous with *sdaB* gene, was amplified from plasmid pKD4 DNA with primers Kup and Kdown (Table 2). Another fragment flanked by 22-bp-long sequences homologous with *sdaB* gene was amplified from plasmid pUC19 by using primers pUC19up and pUC19down (Table 2). The purified PCR products were assembled by Gibson DNA assembly technology, using a SoSoo Cloning Kit (Tsingke, T-TSV-S1, China) following the manufacturer's instructions and then cloned into *Escherichia coli* DH5α. Clones containing the resulting recombinant pU19Δ*sdaB* vector were selected on LB agar supplemented with kanamycin. The recombinant plasmid pUC19Δ*sdaB* was isolated with a plasmid extraction kit (Omega, D6943-02, China) following the manufacturer's instructions and used as template DNA for PCR amplification with the primers *sdaB*-H1up and *sdaB*-H2down (Table 2). After purification, the PCR products were introduced into the competent cells of AA4 carrying a Red helper plasmid pKD46 by electroporation (Bio-Rad, 411BR11661, United States) at 2.5 KV. The resulting transformants were selected on LB agar supplemented with kanamycin after incubation for 24 h at 30°C. Homologous recombination was confirmed by PCR and sequencing. Then, the elimination of pKD46 was performed by culturing the correct transformant by shaking at 37–42°C, 200 rpm overnight. The knock-out mutant can only grow at 30°C on the LB agar supplemented with kanamycin but not streptomycin.

To construct a complement strain of AA4Δ*sdaB*, the complete open reading frame of *sdaB* gene was amplified by PCR with primers *sdaB*-DF and *sdaB*-UR (Table 2) from the genomic DNA of strain AA4 and linked with the fragment flanked by 22-bp-long sequences homologous with *sdaB* gene and amplified from plasmid pBBR1 using primers *sdaB*-PBBR1-DF and *sdaB*-PBBR1-UR (Table 2) by the Gibson DNA assembly technology. The complement plasmid pBBR1-*sdaB* was introduced into the competent cells of AA4Δ*sdaB* by electroporation at 2.5 KV, and the resulting transformants were selected on LB agar supplemented with kanamycin and tetracycline after incubation

at 30°C for 24 h. The complementation was then confirmed by PCR and sequencing.

To create a random transposon library, *E. ludwigii* AA4 was transformed with pDL1093 via conjugation at 30°C and outgrown at 42°C in the presence of kanamycin to induce transposition of miniTn10 (Duncan et al., 2018).

For the sake of constructing fluorescence protein-labeled AA4, plasmid pGFP78, obtained from Dr. Qi Wang at China Agricultural University, harboring the gene encoding for green fluorescent protein (GFP), was introduced into the competent cells of wild-type AA4, AA4Δ*sdaB*, or CΔ*sdaB* by electroporation at 2.5 KV. The resulting transformants were selected on LB agar supplemented with tetracycline, or kanamycin and tetracycline, or a combination of kanamycin, tetracycline, and gentamicin where necessary after incubation at 30°C for 24 h. The correctness of the transformants were then confirmed by PCR, sequencing, and fluorescence microscopy.

## Assay for L-Serine Dehydratase Activity

The cell extract of *E. ludwigii* AA4 was prepared as above, except washing and resuspending in the extraction buffer (50 mM K<sub>2</sub>HPO<sub>4</sub>, 2.5 mM serine protease inhibitors) (Velayudhan et al., 2004). Three aliquots of 1 ml of cell extract containing total proteins of 10 mg/ml was incubated with 500 µl of 300 mM L-serine at 37°C for 6 min. Then, the concentration of pyruvate was determined by using a pyruvate assay kit (Solarbio, BC2205, China). The L-serine hydrolase activity was calculated as:

$$\text{L-serine hydrolase activity nmol/min-mg of protein} =$$

$$\frac{\frac{c \times v}{M}}{T \times m} \times 10^3 \quad (1)$$

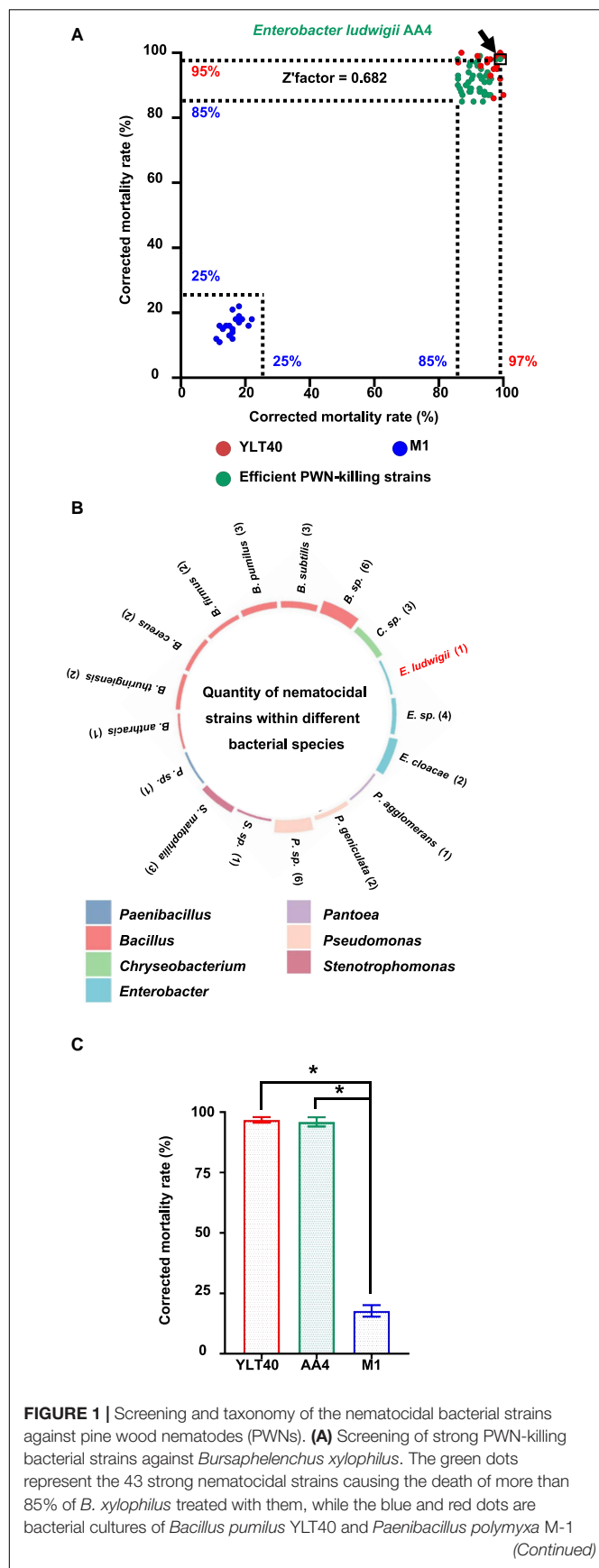
where c is the concentration of pyruvate in µg/ml, v is the total reaction volume in ml, M is the relative molecular mass of pyruvate, T is the reaction time in minutes, and m is the weight of cell extract in mg.

Two-tailed *t*-test (GrapPad Prism 8) was used for the statistical analysis. This experiment was repeated five times.

## Assays for Colonization of Scots Pine Needles

In order to investigate the ability of *E. ludwigii* AA4 to colonize Scots pine needles, 50 ml of LB cultures (OD<sub>600</sub> = 1.0) of GFP-labeled wild-type AA4, AA4Δ*sdaB*, and CΔ*sdaB* were sprayed on 21 1-month-old seedlings, respectively. The plants were placed in a greenhouse under the following conditions: 16 h of light (day) and 8 h of dark (night), 25°C, and a relative humidity of 70%. Three aliquots of 50 mg of needles were sampled at the 4th, 48th, 72th, 96th, 120th, and 144th, and 168th hour post inoculation, respectively, for bacterial quantification. The needles were crushed with 1 ml of PBS by using a sterile mortar. The resulting suspensions were diluted and spread on LB agar plates supplemented with tetracycline and incubated at 30°C for 16 h. The colony-forming unit (CFU) numbers were recorded. Two-tailed *t*-test (GraphPad Prism 8) was used for the statistical analysis. This experiment was repeated five times.





**FIGURE 1 |** used as controls to confirm the reliability of the screening. The position of each dot was determined by the two values (showing on the x- and y-axis, respectively) of corrected mortality rate of PWNs calculated in two independent tests. The dot standing for *Enterobacter ludwigii* AA4 is framed and pointed out by an arrow. **(B)** The number of nematocidal strains within each bacterial species. The colors of the columns on the circle indicate the genus names of the 43 nematocidal strains, while histogram heights are consistent with the numbers (showing in the brackets) of the strains belonging to each bacterial species. **(C)** Nematocidal effect of *E. ludwigii* AA4 against PWNs. Asterisks indicate that differences among the means represented by the columns are statistically significant ( $p < 0.0001$ ). Two-tailed t-test (GrapPad Prism 8) was used for the analysis.

For image analysis, 48 h after inoculation, the needle slices were washed with PBS and transferred to a slide. Ten microliters of PBS were dropped on the samples. The colonization of needles by bacteria was visualized by a Confocal Laser Scanning Microscopy (CLSM; Zeiss, LSM 800, Germany) using an excitation laser of 480 nm.

## RESULTS

### Screening of Bacterial Strains for Nematocidal Activity Against *Bursaphelenchus xylophilus*

To find microorganisms possessing strong nematocidal activity against *B. xylophilus* for potential biological control of the PWD, we performed a PWN-killing test with 374 bacterial strains from our lab collection. First, we used an efficient PWN-killer *Bacillus pumilus* YLT40 and a moderate PWN-killing strain *Paenibacillus polymyxa* M-1 (Niu et al., 2013), identified previously (data not shown), as controls (**Figure 1A**) to verify if the PWN-Bacterium interaction system employed in this study was reliable for a large-scale screening. The corrected mortality rates of the nematode *B. xylophilus* treated by *B. pumilus* YLT40 and *P. polymyxa* M-1 were more than 85% and less than 25% (**Figure 1A**), respectively. We calculated a Z'factor score of 0.682 (**Figure 1A**) which indicated that the screening procedure utilized is sufficiently reliable for selecting powerful PWN-killing strains.

We detected 43 efficient nematocidal bacterial strains exhibiting *B. xylophilus* mortality rates above 85% (**Figure 1A**, **Supplementary Figure 1**, and **Supplementary Table 1**). Based on 16S rRNA gene sequencing, we found that these bacterial strains belong to 21 species from seven genera, including *Bacillus*, *Pseudomonas*, *Enterobacter*, *Chryseobacterium*, *Stenotrophomonas*, *Pantoea*, and *Paenibacillus* (**Figure 1B**), all genera with known nematocidal activity. Among the seven genera, *Bacillus* harbored 19 nematocidal strains, while *Pantoea* and *Paenibacillus* possessed only one PWN-killing strain (**Figure 1B**). Interestingly, seven *Enterobacter* strains, including the plant beneficial bacterium *E. ludwigii* AA4 isolated from maize roots (Niu et al., 2017), exhibited high nematocidal activity against the PWN (**Figure 1B**). In addition, AA4 did kill almost all of the *B. xylophilus* clones (96%) in our assay (**Figure 1C**). In our collection, we found 43 strong PWN-killing strains involving

*E. ludwigii* AA4. Next, we validated the PWN-killing function of strain AA4 in both *in vitro* and *in planta* experiments.

## Biocontrol Effect of *E. ludwigii* AA4 Against *B. xylophilus*

To confirm the nematocidal effect of *E. ludwigii* AA4 against *B. xylophilus*, we developed a fluorescent dye-exclusion viability test to visualize PWN-killing activity. We used DAPI which differentially stains live and dead PWNs. Dead worms take up DAPI rapidly and show bright fluorescence, while the live ones are relatively non-fluorescent and look dim (Figure 2A).

In our assay, the majority (68%) of PWNs co-cultured with wild-type *E. ludwigii* AA4 cells in very low density ( $OD_{600} = 0.063$ ) for 24 h were killed (Figure 2B). The corrected mortality rate of the nematodes treated with wild-type AA4 cells tends to increase with enhanced cell density. The percentage of dead worms dramatically increased from less than 70% to more than 92% when the  $OD_{600}$  value of the bacterial culture was raised from 0.063 to 0.5. The corrected mortality rate rose slowly to a maximum of 98.3% when the  $OD_{600}$  value of the cell suspension reached 2 (Figure 2B). Our visual test documented that nearly all the nematodes incubated with wild-type AA4 emitted intense fluorescent signals, while almost no fluorescence was detected without bacteria (Figure 2A). These results well corroborated the high mortality rate of *B. xylophilus* when exposed to wild-type AA4. *E. ludwigii* AA4 exhibited a remarkable *in vitro* PWN-killing effect.

We then investigated the disease-suppressing efficacy of *E. ludwigii* AA4 against PWD on 3-year-old *Pinus sylvestris* greenhouse-grown seedlings. Thirty days after inoculation, we found that the needles of the seedlings treated with PWNs together with wild-type AA4 were much greener and less wilted than those inoculated with *B. xylophilus* only (Figure 3A). The disease index of PWD on the *P. sylvestris* plants treated with PWNs together with wild-type AA4 (19.5) was significantly lower than that treated with *B. xylophilus* alone (86.9) (Figure 3B), indicating that the PWD severity was substantially reduced by treatment with wild-type AA4. *E. ludwigii* AA4 was capable of efficiently suppressing PWNs not only under *in vitro* conditions but also in *in planta* and was a strong bacterial biocontrol strain against PWD caused by *B. xylophilus*.

## *E. ludwigii* AA4 Causes Morphological Defects in *B. xylophilus*

To further understand the PWN-killing effect of *E. ludwigii* AA4, culture supernatants and cell extracts were prepared for the DAPI-staining based nematocidal activity test. Treatment of *B. xylophilus* with the culture supernatant of wild-type AA4 did not affect the mortality rate of the nematode (Figure 2A). Wild-type AA4 cells did dramatically enhance fluorescence of the *B. xylophilus* nematodes (Figure 2A). This result was corroborated by the mortality rate of the PWNs, suggesting that the death rate of worms exposed to wild-type AA4 culture supernatant (less than 20%) was significantly less than that of *B. xylophilus* incubated with cells of wild-type AA4 (more than 60%) (Figure 2B). By contrast, we

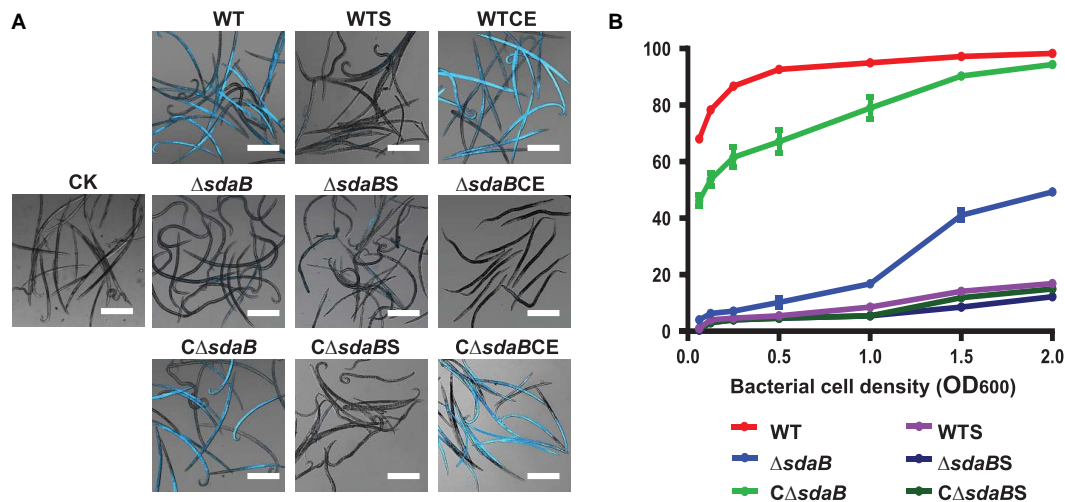
detected intense fluorescent signals from the worms treated with wild-type AA4 cell extract (Figure 4A) and found that more than 80% of PWNs were dead after being exposed to the extract (Figure 4A), indicating its strong nematocidal effect. Thus, our data indicates that the cell extract of wild-type AA4 rather than the culture supernatant contains the nematocidal activity.

To elucidate the mode of action of the nematocidal effect of *E. ludwigii* AA4 against PWN, we choose its cell extract for investigating morphological variations of AA4-treated *B. xylophilus*. The L4 stage nematodes were incubated with wild-type AA4 cell extract. Afterward, the morphological changes of the worms were observed and recorded using an optical light microscope. Exposure of PWN to cell extract-induced formation of vast amounts of vacuoles filled the internal tissues of nematodes completely (Figures 4Bi,iii). Newly formed small vacuoles accumulate and progressively fuse into giant ones, leading to membrane rupture and death (Maltese and Overmeyer, 2014; Armenta and Dixon, 2020). This process is defined as methuosis (Cai et al., 2013; Chen et al., 2014; Nirmala and Lopus, 2020), a type of non-apoptotic cell death widely described in animals (Jang et al., 2016; Rajasekharan et al., 2017; Song et al., 2021). The death of *B. xylophilus* caused by AA4 might be attributed to methuosis induced by the damage to cell membranes.

In these vacuolated worms, some vital organs, e.g., intestine, pharynx, and genital glands, disappeared in the mass of bubbles. We also failed to capture a clear structure of stylet at the head of PWN treated with wild-type AA4 cell extract (Figures 4Bi,iii). The reproductive organ of male worms, the copulatory spicule, dispersed after being incubated with cell extract (Figure 4Bv). In contrast, we observed fewer vacuoles in the control nematodes exposed only to PBS. All the critical internal organs were intact and clearly visible in the control worm bodies (Figures 4Bii,iv,vi). Therefore, *E. ludwigii* AA4 appeared to destroy crucial internal organs of *B. xylophilus* through causing a series of morphological defects.

## The *sdaB* Gene Is Involved in the Nematocidal Effect of *E. ludwigii* AA4 Against *B. xylophilus*

To resolve the molecular mechanisms underlying the strong nematocidal effect of *E. ludwigii* AA4, we characterized genes involved in its PWN-killing efficacy using transposon and PCR-targeted mutagenesis. First, by screening a miniTn10 transposon mutant library of strain AA4, we identified a mutant with greatly reduced nematocidal activity against *B. xylophilus*. We further analyzed the genomic site where the transposon was located and found a miniTn10 element that was inserted into an open reading frame (ORF) located between kilobase positions 3,956,912 and 3,955,545 (Supplementary Figure 4). This ORF was identified as the *sdaB* gene encoding the L-serine dehydratase beta subunit, indicating that the *sdaB* gene might be involved in the PWN-killing effect of AA4.



**FIGURE 2 |** Nematocidal effect of *E. ludwigii* AA4 and its *sdaB* gene knock-out mutant against *B. xylophilus*. **(A)** Imaging analysis of the PWN-killing efficacy of wild-type *E. ludwigii* AA4 and AA4 $\Delta sdaB$  against *B. xylophilus*. The dead nematodes showed cyan fluorescence when excited by 353 nm wavelength after being stained by 4'6-diamidino-2-phenylindole (DAPI), while the live worms stained by DAPI were dim under excitation with the same wavelength. These images were taken using a confocal laser scanning microscope (scale bars: 2 mm). **(B)** Mortality of the PWNs treated with bacterial cells or culture supernatants. *B. xylophilus* was co-cultured with cells of wild-type AA4 and AA4 $\Delta sdaB$  or incubated with culture supernatants of wild-type AA4 and AA4 $\Delta sdaB$  for 24 h, respectively. CK, sterile LB liquid medium; WT, cell culture of wild-type AA4; WTS, supernatant of wild-type AA4 culture; WTCE, cell extract of wild-type AA4;  $\Delta sdaB$ , cell culture of AA4 $\Delta sdaB$ ;  $\Delta sdaBS$ , supernatant of AA4 $\Delta sdaB$  culture;  $\Delta sdaBCE$ , cell extract of AA4 $\Delta sdaB$ ;  $C\Delta sdaB$ , cell culture of AA4 $\Delta sdaB$  complemented with the wild-type *sdaB* gene;  $C\Delta sdaBS$ , supernatant of culture of AA4 $\Delta sdaB$  complemented with the wild-type *sdaB* gene;  $C\Delta sdaBCE$ , cell extract of AA4 $\Delta sdaB$  complemented with the wild-type *sdaB* gene.



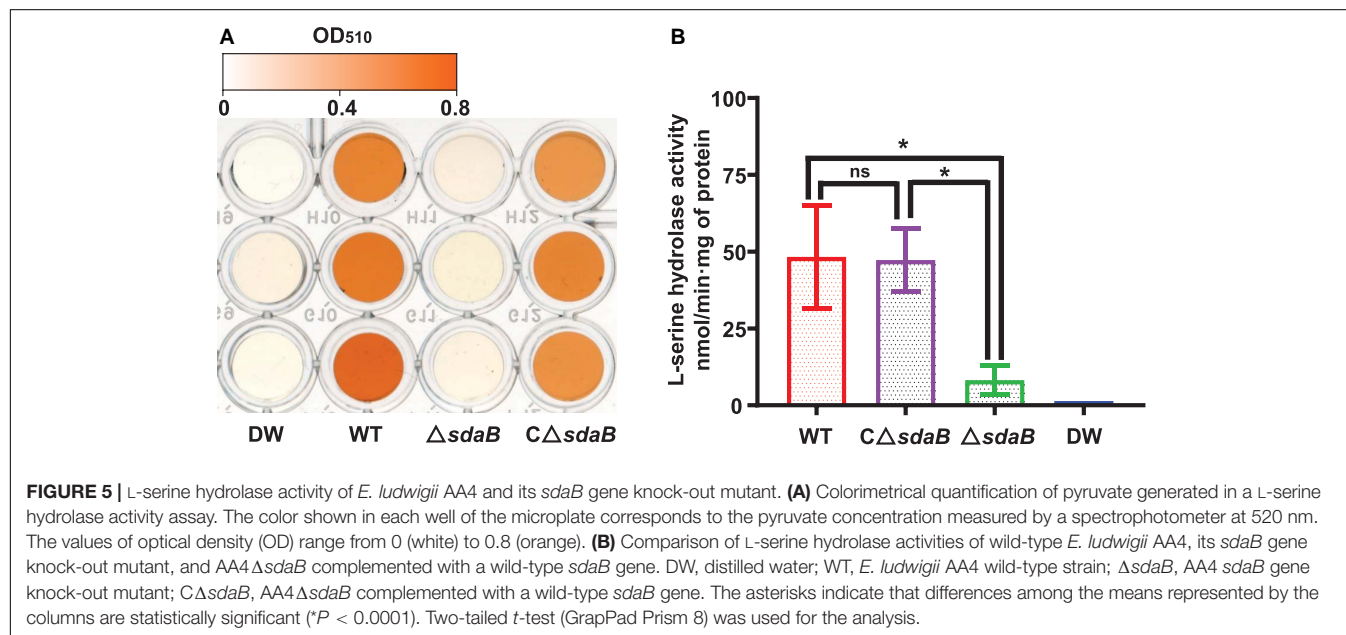
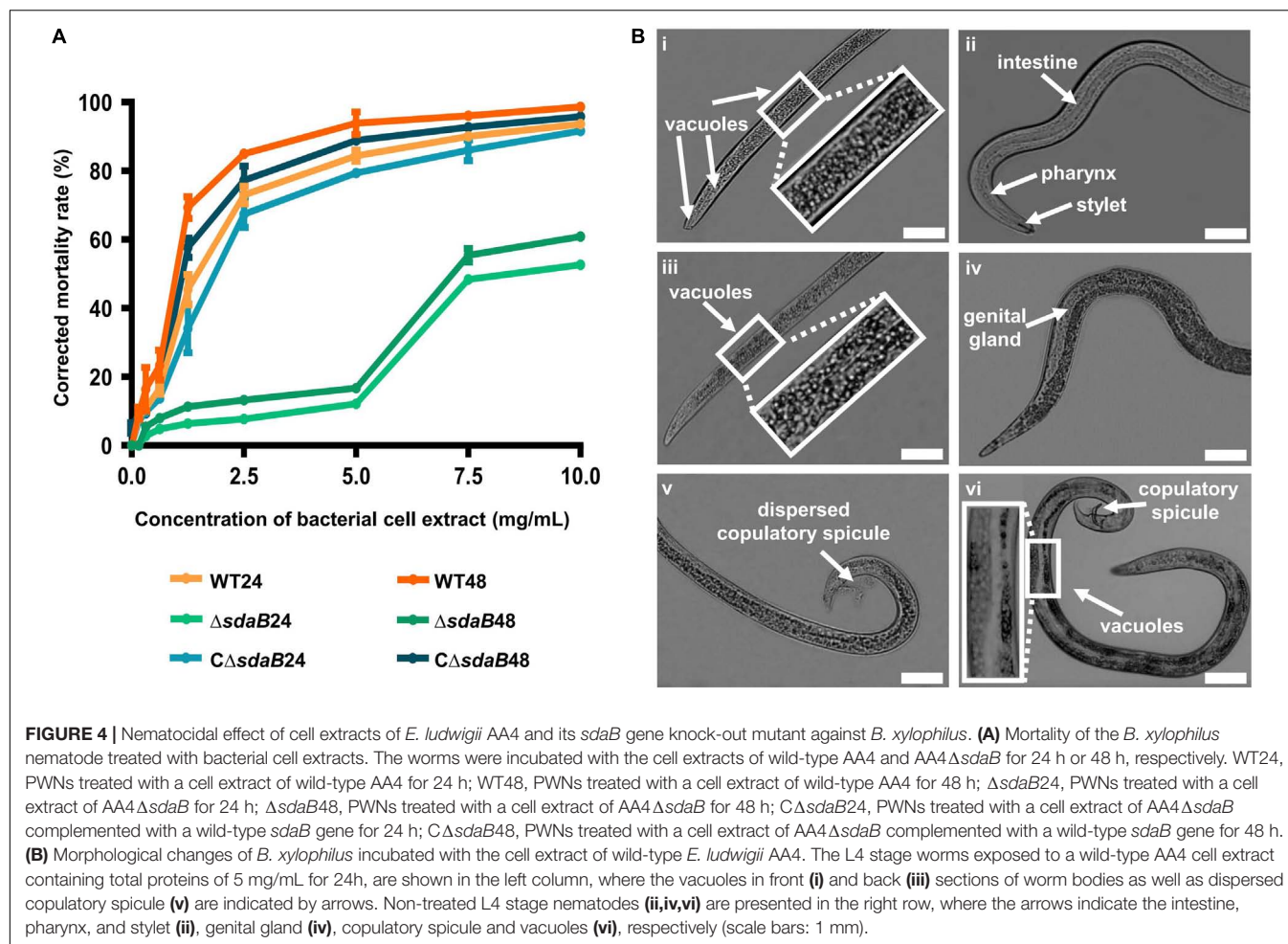
**FIGURE 3 |** Biocontrol effect of *E. ludwigii* AA4 against PWD caused by *B. xylophilus*. **(A)** Symptoms on the 3-year-old *Pinus sylvestris* seedlings inoculated with PWN alone or PWN jointly with *E. ludwigii* AA4 (PWN + AA4). Photographs were taken 30 days after inoculation (Scale bars: 15 cm). **(B)** Severity of PWD on the 3-year-old *P. sylvestris* seedlings inoculated with PWN alone and PWN jointly with *E. ludwigii* AA4 (PWN + AA4). The asterisk indicates that differences among the means represented by the columns are statistically significant (\* $p < 0.0001$ ). Two-tailed *t*-test (GrapPad Prism 8) was used for the analysis.

We next created a knock-out mutant of the *sdaB* gene by employing the Red ( $\lambda$ ,  $\beta$ ,  $\text{exo}$ )-mediated DNA homologous recombination system. The L-serine hydrolase activity of the *sdaB* gene knock-out deletion mutant AA4 $\Delta sdaB$  was significantly lower than that of the wild-type AA4 or the AA4 $\Delta sdaB$  mutant strain complemented with the *sdaB* wild-type gene (Figure 5B), which indicated that the interruption of the *sdaB* gene affected the biosynthesis of L-serine dehydratase. Then, we compared the PWN-killing activities of the wild-type AA4 and AA4 $\Delta sdaB$  by using the fluorescent staining-based nematocidal activity assay (Figure 2A). Nearly no fluorescence could be detected in the worms treated with AA4 $\Delta sdaB$  cells or their extracts, which confirmed the loss of nematocidal activity of the miniTn10 insertional mutant. Complementation of the mutant with a recombinant plasmid harboring *sdaB* partially

restored the PWN-killing activity (Figure 2A). These results were corroborated by the nematode mortality curves, which documented that the corrected death rate of the PWNs treated by AA4 $\Delta sdaB$  was significantly lower than those incubated with wild-type AA4, while the mortality of nematodes exposed to the mutant strain complemented with the *sdaB* wild-type gene increased remarkably (Figure 2B). Therefore, *sdaB* gene product has a major impact on the nematocidal activity of *E. ludwigii* AA4.

Then, we investigated the role of the *sdaB* gene product on the protective effect of *E. ludwigii* AA4 on *P. sylvestris* against PWD. Using a Pine-Nematode-Bacterium tripartite interaction system with 1-month-old *P. sylvestris* seedlings, a lower disease index was estimated when wild-type AA4 cells or their extracts were added to the system. Under these conditions, much less wilted and fewer chlorotic pine seedlings were observed compared







to the control containing *B. xylophilus* alone (Figure 6B). We found more wilted and chlorotic seedlings when AA4 $\Delta$ *sdaB* cells or their extracts were added instead of wild-type AA4 cells or their extracts. The number of diseased plants was reduced when the seedlings were treated with PWNs together with cells or cell extracts of the AA4 $\Delta$ *sdaB* mutant strain complemented with the *sdaB* wild-type gene (Figure 6A). These findings were supported by disease severity analysis, where the disease index of plants treated with PWNs and AA4 $\Delta$ *sdaB* mutant cells or cell extracts was significantly higher than that with PWNs treated with the cells or cell extracts of wild-type AA4 or the *sdaB* mutant complemented with the *sdaB* wild-type gene (Figure 6B). The indices of the PWN infected seedlings treated with cells or cell extracts of the AA4 $\Delta$ *sdaB* mutant complemented with the wild-type *sdaB* gene and seedlings treated with PWNs plus the wild-type AA4 strain cells or cell extracts showed no significant differences. The culture supernatants of the wild-type AA4, the AA4 $\Delta$ *sdaB* mutant strain, or AA4 $\Delta$ *sdaB* mutant complemented with the *sdaB* wild-type gene not only exhibited nearly no nematocidal activity against *B. xylophilus* *in vitro*, but also failed to display biocontrol efficacy against PWD (Figure 6). The *sdaB* gene encoding the beta subunit of L-serine dehydratase, is highly related to the PWN-killing activity of *E. ludwigii* AA4 and may be a key molecular element controlling the interplay between strain AA4 and PWNs.

## Colonization of *E. ludwigii* AA4 on Needles of *P. sylvestris*

Efficient colonization of plant surfaces and tissues is fundamental for successful inhibition of pathogens by biological control agents. To investigate the ability of *E. ludwigii* AA4 to colonize *P. sylvestris*, we sprayed the needles with a GFP-labeled transgenic strain of AA4. We observed by CLSM that strain AA4 was capable of adhering to the surface of *P. sylvestris* needles by forming robust biofilms (Figure 7A). Although there was a dramatical reduction of the abundance of AA4 cells sticking to the needles, from around  $1.9 \times 10^7$  CFU (colony-forming unit)/g (of pine needle fresh weight) 4 h after inoculation to  $3.8 \times 10^4$  CFU/g 144 h after inoculation, the colonization rates of AA4 at days 6 and 7 ( $2.8 \times 10^4$  CFU/g) showed no significant difference (Figure 7B). This indicates that *E. ludwigii* AA4 can colonize the needles of *P. sylvestris*, presumably a precondition for its disease-controlling efficacy against PWD. AA4 $\Delta$ *sdaB* cells were equally able to colonize pine needles compared to the wild-type AA4 (Figure 7A), demonstrating that the *sdaB* gene function is not needed for colonization. The biomass accumulation rate of both strains was at the same level along our 7-day-long experiment (Figure 7B). Therefore, *E. ludwigii* AA4 may be an efficient colonizer of pine needles, and that the eradication of *sdaB* gene did not affect its adherence to needles.

## DISCUSSION

Compared to the control of phytopathogens in agroecosystems, forest disease suppression puts more emphases on the sustainable management of pests due to the vital functionality of forests

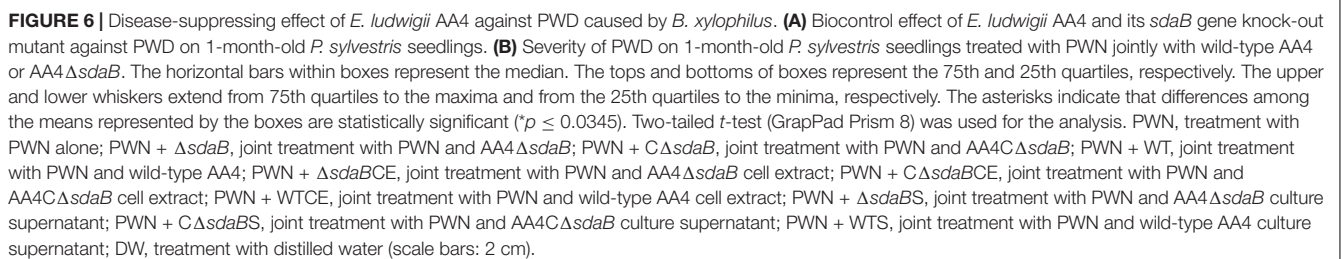
in maintaining the balance and health of their ecosystems (Nascimento et al., 2015; Proenca et al., 2017; Khan et al., 2020; Ozair et al., 2020). To this end, biological control of forest pathogens, including the PWNs, by beneficial microbes have been receiving increasing attention (Nunes da Silva et al., 2015; Ponpandian et al., 2019; Proenca et al., 2019). A considerable number of nematocidal microbial strains suppressing *B. xylophilus* have been identified and characterized. These strains are, mainly, species of *Bacillus* (Crickmore, 2005; Niu et al., 2011; Park et al., 2020), *Streptomyces* (Kang et al., 2021), *Serratia* (Paiva et al., 2013; Nascimento et al., 2016; Abd El-Aal et al., 2021), and *Stenotrophomonas* (Huang et al., 2009; Ponpandian et al., 2019).

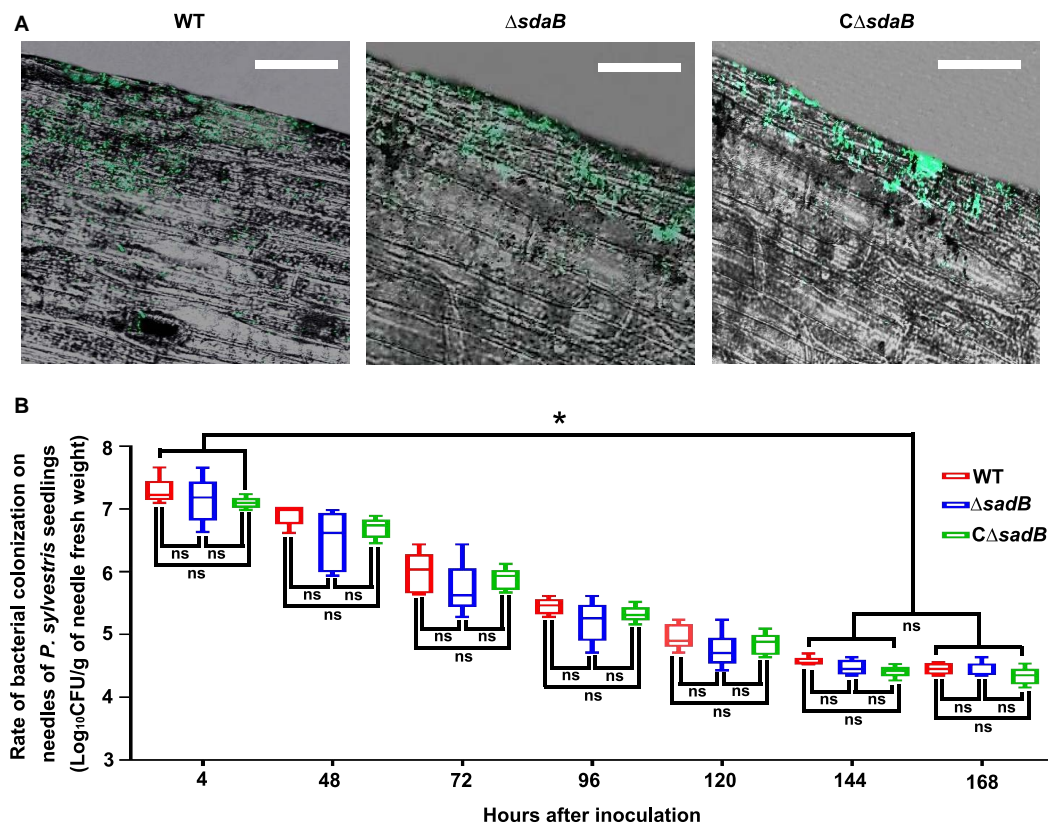
We selected a PWN-killing *Enterobacter ludwigii* strain, designated as AA4 from a large-scale screening of nematocidal activity and inhibition of PWD (Figures 1C, 3). Representatives of the genus *Enterobacter* are able to inhibit a wide range of phytopathogens (Demirci et al., 2000; Kageyama and Nelson, 2003; Windstam and Nelson, 2008; Del Barrio-Duque et al., 2019; Batyrova et al., 2020), including plant pathogenic nematodes, such as root-knot nematodes (Munif et al., 2000; El-Sayed et al., 2014; Oh et al., 2018). To our knowledge, *E. ludwigii* AA4 is the first *Enterobacter* strain described as a nematocidal agent suppressing *B. xylophilus*. Our findings expand the knowledge of the biocontrol potential of the genus *Enterobacter*, one of the most expanding bacterial taxa in recent decades (Taghavi et al., 2010; Ibort et al., 2018; François et al., 2021).

Accurate and rapid determination of the mortality of nematodes is the key to efficient screening and selection of microbial strains with nematocidal activity. In earlier studies on PPN-bacterium interactions, the killing rate of nematodes was estimated mainly by the morphology of the worms, where rigid nematodes were considered dead, while the curved ones were considered alive (Liu et al., 2016, 2019; Ponpandian et al., 2019; Qiu et al., 2019). Such criteria do not always work well. We found that a significant number of apparently rigid nematodes could still move after being touched with a needle, suggesting that they were still alive. In addition, counting dead nematodes under a microscope is time consuming and tedious.

We developed a visual PWN-killing activity DAPI dye exclusion which is faster and more reliable (Figure 2). DAPI passes slowly through intact cell membranes of living nematodes, and thus preferentially stains the dead nematodes. Once entering the cells and binding to the minor groove of A-T-rich regions of DNA, DAPI fluorescence is greatly enhanced (Atale et al., 2014). As a result, dead worms display intense fluorescent signals. A similar method was employed in a previous study, where the dead *Caenorhabditis elegans* nematodes were stained with the fluorophore Sytox Orange (Natalia et al., 2013; Rajamuthiah et al., 2015; Xie et al., 2020). Applying fluorescence staining in the identification of PWN-killing bacterial strains may be amenable to high throughput or automated screening for biocontrol agents against other plant pathogenic nematodes.

In present study, we observed that the PWNs treated with cell extracts of wild-type *E. ludwigii* AA4 displayed dramatic morphological defects associated with the accumulation of numerous vacuoles, recognized as a sign of reversible cell





**FIGURE 7 |** Colonization of *E. ludwigii* AA4 on needles of *P. sylvestris* seedlings. **(A)** Image analysis of needle colonization of green fluorescent protein (GFP)-labeled wild-type AA4, AA4 *sdaB* gene knock-out mutant, and AA4Δ*sdaB* complemented with a wild-type *sdaB* gene. These images were taken using a confocal laser scanning microscope at 48 h post inoculation (Scale bars: 20 μm). **(B)** The abundance of wild-type AA4, AA4 *sdaB* gene knock-out mutant, and AA4Δ*sdaB* complemented with a wild-type *sdaB* gene colonizing on the needles of *P. sylvestris* seedlings. WT, AA4 wild-type strain; Δ*sdaB*, AA4 *sdaB* gene knock-out mutant; CΔ*sdaB*, AA4Δ*sdaB* complemented with a wild-type *sdaB* gene. The asterisks indicate that differences among the means represented by the columns are statistically significant (\* $p \leq 0.0041$ ). Two-tailed *t*-test (GrapPad Prism 8) was used for the analysis.

injury (RCI) and methuosis, resulting in the destruction of internal organs of *B. xylophilus* needed for absorbing nutrients, pathogenicity, and reproduction (Figure 4). Similar changes in morphology were also reported in *B. xylophilus* incubated with indoles and abamectin (Rajasekharan et al., 2017). Another plant pathogenic nematode, *Meloidogyne incognita*, the causal agent of root knot in several crops, showed bubbling in its body when meeting toxic compounds as well (Jang et al., 2016). A large number of vacuoles were present in the transgenic *C. elegans* with an ectopically expressed and activated *mek-1* gene (Koga et al., 2000). Intracytoplasmic vacuolation may commonly occur when nematodes live under stressful conditions, which can be triggered by fluid accumulation within the cytoplasm due to  $\text{Ca}^{2+}$  and water influx caused by RCI (Jurkowitz-Alexander et al., 1992; Basavappa et al., 1998; Rajasekharan et al., 2017). The death of *B. xylophilus* caused by AA4 might be attributed to methuosis induced by damage to the cell membrane caused by this nematocidal bacterial strain. The mechanisms underlying the PWN-killing function of *E. ludwigii* AA4 remains to be determined.

Some mechanisms of nematocidal activity against *B. xylophilus* have been recently documented, such as parasitization (Proenca et al., 2017; Ponpandian et al., 2019), production of toxins (Abd El-Aal et al., 2021; Kahn et al., 2021), antibiotics and destructive enzymes (Yang et al., 2007; Huang et al., 2009) or competing for nutrients (Proenca et al., 2019), and inducing systemic resistance of plants (Liang et al., 2019; Han et al., 2021). The molecular mechanisms underlying these PWN-killing effects are still largely unknown. In this work, we demonstrate that the *sdaB* gene encoding the beta subunit of L-serine dehydratase is involved in the nematocidal activity of *E. ludwigii* AA4 against PWNs. The deletion of this gene caused significant impairment in both L-serine hydrolase activity (Figure 5) and ability to inhibit PWN (Figures 2, 6), but not the growth of *E. ludwigii* AA4 *in vitro* or *in planta* (Supplementary Figure 2). L-serine dehydratase activity is widely found in diverse organisms. It specifically deaminates L-serine to produce pyruvate and ammonia (Xu et al., 2011; Grant, 2012; Thoden et al., 2014), and plays a critical role in maintaining amino acid homeostasis during shifts in nutrient availability (Velayudhan et al., 2004; Zhang et al., 2010;



Chen et al., 2012). Until now, little or no data about the contribution of L-serine dehydratase to microbial nematocidal activities has been reported. L-serine is an important biomolecule, and excessive amounts of intracellular serine inhibit the biosynthesis of other amino acids (Zhang et al., 2018, 2019; Révora et al., 2020; Wang et al., 2020) essential to the production of certain bacterial toxins *via* the non-ribosomal peptide synthetase (NRPS) pathway (Cao et al., 2008; Soeriyadi et al., 2021).

Here, we assume that the *sdaB* gene product might control *B. xylophilus* by regulation of potential anti-nematode compounds in *E. ludwigii* AA4. Considering the tight relationship between L-serine and methylation reactions (Kalhan and Hanson, 2012; Datta et al., 2016; Bignell et al., 2018; Kriner and Subramaniam, 2020), such modulation may be linked to bacterial epigenetics. We noticed that the supernatant of strain AA4 cell culture has almost no effect (Figures 2, 6), which may be due to the low concentration of nematocidal compounds in the broth or suggests that the PWN-killing efficacy of AA4 might be contact-dependent. In future work, we will more deeply analyze the function of the *sdaB* gene in the nematocidal activity of *E. ludwigii* AA4.

Colonization of plant hosts is a necessary precondition for efficient pathogen inhibition by microbial biocontrol agents (Vurukonda et al., 2018; Niu et al., 2020; Zhang J. et al., 2020; Vandana et al., 2021). *E. ludwigii* AA4 was capable of colonizing the needles of *P. sylvestris* by forming sturdy biofilms (Figure 7), indicating its high affinity to pine needles, despite its presumed origin from herbaceous host plants. This finding underlines the great adaptability of the genus *Enterobacter*, which appears to be highly adaptable to diverse environments (Shoebitz et al., 2009; Singh et al., 2017; Shastry et al., 2020; Ranawat et al., 2021). These features may facilitate the development of an AA4-based biopesticide against *B. xylophilus*. Identification of genes and proteins involved in resistance to pests and pathogens is of long-term interest because such molecules represent the next generation of targets for creation of nematode resistant plants through genetic engineering or targeted mutagenesis. Our findings also pave the way for introducing agriculture biocontrol agents in forest disease management.

## DATA AVAILABILITY STATEMENT

The data presented in the study are deposited in the Genbank repository, accession numbers CP018785, OM883853, OM899759-OM899796, OM899810, OM900025, and OM900026.

## AUTHOR CONTRIBUTIONS

BN and RB designed the project. YZ and BN wrote the manuscript. BN, RB, ZY, RS, and HS revised the manuscript. YZ and ZY performed the experiments. YZ, SW, DW, and BN analyzed the data. YC created the random transposon library. HW, HY, JP, and MP performed the *in planta* biocontrol assays.

All authors listed have made a substantial, direct, and intellectual contribution to the work, and approved it for publication.

## FUNDING

This work was supported by National Science Foundation of China Grant No. 32071741 (to BN), Heilongjiang Provincial Science Foundation of China Grant No. YQ2019C002 (to BN), Beijing Municipal Administration Center of Parks Science and Technology Project Grant No. zx2021002 (to SW), Fundamental Research Funds for the Central Universities Grant No. 2572018AA36 (to ZY), Northeast Forestry University International Forest Biotech Center Project Grant (to BN), and Heilongjiang Touyan Innovation Team Program (Tree Genetics and Breeding Innovation Team).

## ACKNOWLEDGMENTS

We thank Yaxin Shi for performing the screening of nematocidal bacterial strains, Hongtao Li, Kai Guo, and Ben Fan for offering the cultures of pinewood nematodes, Qi Wang for providing the pGFP78, Mingyue Wang for help with the construction of mutant strains, and members of the BN laboratory for the valuable advice.

## SUPPLEMENTARY MATERIAL

The Supplementary Material for this article can be found online at: <https://www.frontiersin.org/articles/10.3389/fmicb.2022.870519/full#supplementary-material>

**Supplementary Figure 1** | The corrected mortality of 43 efficient pine wood nematode (PWN)-killing bacterial strains. *Bacillus pumilus* YLT40 and *Paenibacillus polymyxa* M-1 were used as positive and negative controls, respectively. Asterisk indicates that differences among the means represented by the columns are statistically significant (\* $p < 0.0001$ ). Two-tailed *t*-test (GrapPad Prism 8) was used for the analysis.

**Supplementary Figure 2** | Growth curves of wild-type *E. ludwigii* AA4, its *sdaB* gene knock-out mutant, and AA4  $\Delta sdaB$  complemented with a wild-type *sdaB* gene. WT, *E. ludwigii* AA4 wild-type strain;  $\Delta sdaB$ , AA4 *sdaB* gene knock-out mutant; C $\Delta sdaB$ , AA4  $\Delta sdaB$  complemented with a wild-type *sdaB* gene; LB, sterile Luria-Bertani liquid medium.

**Supplementary Figure 3** | Disease ranks of the pine wilt disease (PWD) caused by *B. xylophilus* under greenhouse conditions on day 9 after inoculation (scale bars: 20  $\mu$ m). In rank 0, stems and needles are green and plump. In rank 1, yellowish speckles are presented on stems, and stems and needles appear slightly shriveled. In rank 2, stems turn yellow and shriveled, and less than 25% needles are partially wilted. In rank 3, stems turn yellow and shriveled, among which 25–50% of needles are partially wilted. In rank 4, stems turn brownish and completely shriveled, and more than 50% of needles are completely wilted and turn yellowish. W, the whole views of *P. sylvestris* seedlings; T, the top views of *P. sylvestris* seedlings; S, the stems of *P. sylvestris* seedlings; N, the needles of *P. sylvestris* seedlings.

**Supplementary Figure 4** | The location of miniTn10 transposon on the genome sequence of *E. ludwigii* AA4. The site of miniTn10 transposon insertion is indicated by a black triangle.

**Supplementary Table 1** | Corrected mortality rates for the 43 efficient pine wood nematode (PWN)-killing strains.



## REFERENCES

- Abd El-Aal, E. M., Shahan, M., Sayed, S., Kesba, H., Ansari, M. J., El-Ashry, R. M., et al. (2021). In vivo and in vitro management of *Meloidogyne incognita* (Tylenchida: Heteroderidae) using rhizosphere bacteria, *Pseudomonas* spp. and *Serratia* spp. compared with oxamyl. *Saudi J. Biol. Sci.* 28, 4876–4883. doi: 10.1016/j.sjbs.2021.06.078
- Abdelshafy Mohamad, O. A., Ma, J. B., Liu, Y. H., Zhang, D., Hua, S., Bhute, S., et al. (2020). Beneficial endophytic bacterial populations associated with medicinal plant *Thymus vulgaris* alleviate salt stress and confer resistance to *Fusarium oxysporum*. *Front. Plant Sci.* 11:47. doi: 10.3389/fpls.2020.00047
- Adhikari, A., Lee, K. E., Khan, M. A., Kang, S. M., Adhikari, B., Imran, M., et al. (2020). Effect of silicate and phosphate solubilizing rhizobacterium *Enterobacter ludwigii* GAK2 on *Oryza sativa* L. under cadmium stress. *J. Microbiol. Biotechnol.* 30, 118–126. doi: 10.4014/jmb.1906.06010
- Aeron, A., Dubey, R. C., and Maheshwari, D. K. (2021). Next-generation biofertilizers and novel biostimulants: documentation and validation of mechanism of endophytic plant growth-promoting rhizobacteria in tomato. *Arch. Microbiol.* 203, 3715–3726. doi: 10.1007/s00203-021-02344-0
- Andres-Barrao, C., Lafi, F. F., Alam, I., Zelicourt, A., Eida, A. A., Bokhari, A., et al. (2017). Complete genome sequence analysis of *Enterobacter* sp. SA187, a plant multi-stress tolerance promoting endophytic bacterium. *Front. Microbiol.* 8:2023. doi: 10.3389/fmicb.2017.02023
- Armenta, D. A., and Dixon, S. J. (2020). Investigating nonapoptotic cell death using chemical biology approaches. *Cell Chem. Biol.* 27, 376–386. doi: 10.1016/j.chembiol.2020.03.005
- Atale, N., Gupta, S., Yadav, U. C., and Rani, V. (2014). Cell-death assessment by fluorescent and nonfluorescent cytosolic and nuclear staining techniques. *J. Microsc.* 255, 7–19. doi: 10.1111/jmi.12133
- Basavappa, S., Mobasheri, A., Errington, R., Huang, C. C., Al-Adawi, S., and Ellory, J. C. (1998). Inhibition of Na<sup>+</sup>, K<sup>+</sup>-ATPase activates swelling-induced taurine efflux in a human neuroblastoma cell line. *J. Cell. Physiol.* 174, 145–153. doi: 10.1002/(SICI)1097-4652(199802)174:2<145::AID-JCP1>3.0.CO;2-O
- Batyrova, K. A., Khusnutdinova, A. N., Wang, P. H., Di Leo, R., Flick, R., Edwards, E. A., et al. (2020). Biocatalytic in Vitro and in Vivo FMN prenylation and (De)carboxylase activation. *ACS Chem. Biol.* 15, 1874–1882. doi: 10.1021/acscchembio.0c00136
- Bignell, D., Cheng, Z., and Bown, L. (2018). The coronafacoyl phytotoxins: structure, biosynthesis, regulation and biological activities. *Antonie van Leeuwenhoek* 111, 649–666. doi: 10.1007/s10482-017-1009-1
- Cai, H., Liu, J., Fan, Q., and Li, X. (2013). Methuosis: a novel type of cell death. *J. Southern Med. Univ.* 33, 1844–1847.
- Cai, S., Jia, J., He, C., Zeng, L., Fang, Y., Qiu, G., et al. (2022). Multi-omics of pine wood nematode pathogenicity associated with culturable associated microbiota through an artificial assembly approach. *Front. Plant Sci.* 12:798539. doi: 10.3389/fpls.2021.798539
- Cao, L., Bandelac, G., Volgina, A., Korostoff, J., and DiRienzo, J. M. (2008). Role of aromatic amino acids in receptor binding activity and subunit assembly of the cytolethal distending toxin of *Aggregatibacter actinomycetemcomitans*. *Infect. Immunity* 76, 2812–2821. doi: 10.1128/IAI.00126-08
- Cesarz, S., Eva Schulz, A., Beugnon, R., and Eisenhauer, N. (2019). Testing soil nematode extraction efficiency using different variations of the Baermann-funnel method. *Soil Org.* 91, 61–72. doi: 10.25674/so91201
- Chan, S. Y., Liu, S. Y., Seng, Z., and Chua, S. L. (2020). Biofilm matrix disrupts nematode motility and predatory behavior. *Int. Soc. Microb. Ecol. J.* 15, 260–269. doi: 10.1038/s41396-020-00779-9
- Chen, D., Song, M., Mohamad, O., and Yu, S. P. (2014). Inhibition of Na<sup>+</sup>/K<sup>+</sup>-ATPase induces hybrid cell death and enhanced sensitivity to chemotherapy in human glioblastoma cells. *BMC Cancer* 14:716. doi: 10.1186/1471-2407-14-716
- Chen, S., Xu, X. L., and Grant, G. A. (2012). Allosteric activation and contrasting properties of L-serine dehydratase types 1 and 2. *Biochemistry* 51, 5320–5328. doi: 10.1021/bi300523p
- Crickmore, N. (2005). Using worms to better understand how *Bacillus thuringiensis* kills insects. *Trends Microbiol.* 13, 347–350. doi: 10.1016/j.tim.2005.06.002
- Dahyot, S., Oxaran, V., Nieperon, M., Dupart, E., Legris, S., Destruel, L., et al. (2020). Role of the *LytSR* two-component regulatory system in *Staphylococcus lugdunensis* biofilm formation and pathogenesis. *Front. Microbiol.* 11:39. doi: 10.3389/fmicb.2020.00039
- Danish, S., Zafar-Ul-Hye, M., Mohsin, F., and Hussain, M. (2020). ACC-deaminase producing plant growth promoting rhizobacteria and biochar mitigate adverse effects of drought stress on maize growth. *PLoS One* 15:e0230615. doi: 10.1371/journal.pone.0230615
- Datsenko, K. A., and Wanner, B. L. (2000). One-step inactivation of chromosomal genes in *Escherichia coli* K-12 using PCR products. *Proc. Natl. Acad. Sci. U.S.A.* 97, 6640–6645. doi: 10.1073/pnas.120163297
- Datta, A., Bhattacharyya, D., Singh, S., Ghosh, A., Schmidtchen, A., Malmsten, M., et al. (2016). Role of aromatic amino acids in lipopolysaccharide and membrane interactions of antimicrobial peptides for use in plant disease control. *J. Biol. Chem.* 291, 13301–13317. doi: 10.1074/jbc.M116.719575
- Del Barrio-Duque, A., Ley, J., Samad, A., Antonielli, L., Sessitsch, A., and Compant, S. (2019). Beneficial endophytic bacteria-*Serendipita indica* interaction for crop enhancement and resistance to phytopathogens. *Front. Microbiol.* 10:2888. doi: 10.3389/fmicb.2019.02888
- Demirci, F., Işcan, G., Güven, K., Kirimer, N., Demirci, B., and Başer, K. H. (2000). Antimicrobial activities of *Ferulago* essential oils. *Z. Naturforsch. C J. Biosci.* 55, 886–889. doi: 10.1515/znc-2000-11-1207
- Dhanya, B. E., Athmika, and Rekha, P. D. (2021). Characterization of an exopolysaccharide produced by *Enterobacter* sp. YU16-RN5 and its potential to alleviate cadmium induced cytotoxicity in vitro. *3 Biotech* 11:491. doi: 10.1007/s13205-021-03034-w
- Duncan, M. C., Forbes, J. C., Nguyen, Y., Shull, L. M., Gillette, R. K., Lazinski, D. W., et al. (2018). *Vibrio cholerae* motility exerts drag force to impede attack by the bacterial predator *Bdellovibrio bacteriovorus*. *Nat. Commun.* 9:4757. doi: 10.1038/s41467-018-07245-3
- El-Sayed, W. S., Akhkha, A., El-Naggar, M. Y., and Elbadry, M. (2014). In vitro antagonistic activity, plant growth promoting traits and phylogenetic affiliation of rhizobacteria associated with wild plants grown in arid soil. *Front. Microbiol.* 5:651. doi: 10.3389/fmicb.2014.00651
- Etcheverry, M. G., Scandolaria, A., Nesci, A., Vilas Boas Ribeiro, M. S., Pereira, P., and Battilani, P. (2009). Biological interactions to select biocontrol agents against toxigenic strains of *Aspergillus flavus* and *Fusarium verticillioides* from maize. *Mycopathologia* 167, 287–295. doi: 10.1007/s11046-008-9177-1
- Fang, W., Qunqun, G., Linsong, W., Yi, M., Tingting, Z., and Ronggui, L. (2019). Nematicidal activities of bacterial volatiles from *Pseudoduganella violaceinigra* G5-3 and *Novosphingobium pokkali* G8-2 against the pine wood nematode *Bursaphelenchus xylophilus*. *Chiang Mai J. Sci.* 46, 236–246.
- Faria, J. M., Barbosa, P., Bennett, R. N., Mota, M., and Figueiredo, A. C. (2013). Bioactivity against *Bursaphelenchus xylophilus*: nematotoxics from essential oils, essential oils fractions and decoction waters. *Phytochemistry* 94, 220–228. doi: 10.1016/j.phytochem.2013.06.005
- Faria, J. M., Sena, I., Vieira da Silva, I., Ribeiro, B., Barbosa, P., Ascensao, L., et al. (2015). In vitro co-cultures of *Pinus pinaster* with *Bursaphelenchus xylophilus*: a biotechnological approach to study pine wilt disease. *Planta* 241, 1325–1336. doi: 10.1007/s00425-015-2257-9
- Faria, J., Barbosa, P., Vieira, P., Vicente, C., Figueiredo, A. C., and Mota, M. (2021). Phytochemicals as biopesticides against the pinewood nematode *Bursaphelenchus xylophilus*: a review on essential oils and their volatiles. *Plants (Basel, Switzerland)* 10:2614. doi: 10.3390/plants10122614
- François, C. J., Batinovic, S., Petrovski, S., and Gendall, A. R. (2021). Draft genome sequence of *Enterobacter asburiae* NCR1, a plant growth-promoting rhizobacterium isolated from a cadmium-contaminated environment. *Microbiol. Resour. Announc.* 10:e0047821. doi: 10.1128/MRA.00478-21
- Futai, K. (2013). Pine wood nematode, *Bursaphelenchus xylophilus*. *Annu. Rev. Phytopathol.* 51, 61–83. doi: 10.1146/annurev-phyto-081211-172910
- Grant, G. A. (2012). Kinetic evidence of a noncatalytic substrate binding site that regulates activity in *Legionella pneumophila* L-serine dehydratase. *Biochemistry* 51, 6961–6967. doi: 10.1021/bi3008774
- Guérin, F., Lallement, C., Goudergues, B., Isnard, C., Sanguinetti, M., Cacaci, M., et al. (2020). Landscape of in vivo fitness-associated genes of *Enterobacter cloacae* complex. *Front. Microbiol.* 11:1609. doi: 10.3389/fmicb.2020.01609
- Guo, Q. Q., Du, G. C., Zhang, T. T., Wang, M. J., Wang, C., Qi, H. T., et al. (2020). Transcriptomic analysis of *Bursaphelenchus xylophilus* treated by a potential phytonematicide, punicalagin. *J. Nematol.* 52, 1–14. doi: 10.21307/jofnem-2020-001

- Guo, Q., Du, G., He, H., Xu, H., Guo, D., and Li, R. (2016). Two nematocidal furocoumarins from *Ficus carica* L. leaves and their physiological effects on pine wood nematode (*Bursaphelenchus xylophilus*). *Nat. Prod. Res.* 30, 1969–1973. doi: 10.1080/14786419.2015.1094804
- Habibi, S., Djedidi, S., Ohkama-Ohtsu, N., Sarhadi, W. A., Kojima, K., Rallos, R. V., et al. (2019). Isolation and screening of indigenous plant growth-promoting rhizobacteria from different rice cultivars in Afghanistan soils. *Microbes Environ.* 34, 347–355. doi: 10.1264/jsm2.ME18168
- Haegeman, A., Vanholme, B., Jacob, J., Vandekerckhove, T., Claeys, M., Borgonie, G., et al. (2009). An endosymbiotic bacterium in a plant-parasitic nematode: member of a new *Wolbachia* supergroup. *Int. J. Parasitol.* 39, 1045–1054. doi: 10.1016/j.ijpara.2009.01.006
- Han, G., Mannaa, M., Kim, N., Jeon, H. W., Jung, H., Lee, H. H., et al. (2021). Response of pine rhizosphere microbiota to foliar treatment with resistance-inducing bacteria against pine wilt disease. *Microorganisms* 9:688. doi: 10.3390/microorganisms9040688
- Hinton, D. M., and Bacon, C. W. (1995). *Enterobacter cloacae* is an endophytic symbiont of corn. *Mycopathologia* 129, 117–125. doi: 10.1007/BF01103471
- Huang, X., Liu, J., Ding, J., He, Q., Xiong, R., and Zhang, K. (2009). The investigation of nematocidal activity in *Stenotrophomonas maltophilia* G2 and characterization of a novel virulence serine protease. *Can. J. Microbiol.* 55, 934–942. doi: 10.1139/w09-045
- Ibort, P., Molina, S., Ruiz-Lozano, J. M., and Aroca, R. (2018). Molecular insights into the involvement of a never ripe receptor in the interaction between two beneficial soil bacteria and tomato plants under well-watered and drought conditions. *Mol. Plant Microbe Interact.* 31, 633–650. doi: 10.1094/MPMI-12-17-0292-R
- Jang, J. Y., Choi, Y. H., Shin, T. S., Kim, T. H., Shin, K. S., Park, H. W., et al. (2016). Biological control of *Meloidogyne incognita* by *Aspergillus niger* F22 producing oxalic acid. *PLoS One* 11:e0156230. doi: 10.1371/journal.pone.0156230
- Javaheri Safa, Z., Olya, A., Zamani, M., Motalebi, M., Khalili, R., Haghbeen, K., et al. (2021). Biodegradation of cyanide to ammonia and carbon dioxide by an industrially valuable enzyme from the newly isolated *Enterobacter* zs. *J. Environ. Sci. Health A Tox. Hazard. Subst. Environ. Eng.* 56, 1131–1137. doi: 10.1080/10934529.2021.1967653
- Jurkowitz-Alexander, M. S., Altschuld, R. A., Hohl, C. M., Johnson, J. D., McDonald, J. S., Simmons, T. D., et al. (1992). Cell swelling, blebbing, and death are dependent on ATP depletion and independent of calcium during chemical hypoxia in a glial cell line (ROC-1). *J. Neurochem.* 59, 344–352. doi: 10.1111/j.1471-4159.1992.tb08910.x
- Kageyama, K., and Nelson, E. B. (2003). Differential inactivation of seed exudate stimulation of *Pythium ultimum* sporangium germination by *Enterobacter cloacae* influences biological control efficacy on different plant species. *Appl. Environ. Microbiol.* 69, 1114–1120. doi: 10.1128/AEM.69.2.1114-1120.2003
- Kahn, T. W., Duck, N. B., McCarville, M. T., Schouten, L. C., Schwei, K., Zaitseva, J., et al. (2021). A *Bacillus thuringiensis* Cry protein controls soybean cyst nematode in transgenic soybean plants. *Nat. Commun.* 12:3380. doi: 10.1038/s41467-021-23743-3
- Kalhan, S. C., and Hanson, R. W. (2012). Resurgence of serine: an often neglected but indispensable amino acid. *J. Biol. Chem.* 287, 19786–19791. doi: 10.1074/jbc.R112.357194
- Kämpfer, P., Ruppel, S., and Remus, R. (2005). *Enterobacter radicincitans* sp. nov., a plant growth promoting species of the family *Enterobacteriaceae*. *Syst. Appl. Microbiol.* 28, 213–221. doi: 10.1016/j.syapm.2004.12.007
- Kang, M. K., Kim, M. H., Liu, M. J., Jin, C. Z., Park, S. H., Lee, J., et al. (2021). Nematocidal activity of teleocidin B4 isolated from *Streptomyces* sp. against pine wood nematode, *Bursaphelenchus xylophilus*. *Pest Manag. Sci.* 77, 1607–1615. doi: 10.1002/ps.6095
- Kang, S. M., Radhakrishnan, R., You, Y. H., Khan, A. L., Lee, K. E., Lee, J. D., et al. (2015). *Enterobacter asburiae* KE17 association regulates physiological changes and mitigates the toxic effects of heavy metals in soybean. *Plant Biol. (Stuttgart, Germany)*. 17, 1013–1022. doi: 10.1111/plb.12341
- Kaushik, C. P., Luxmi, R., Singh, D., and Kumar, A. (2017). Synthesis and antimicrobial evaluation of ester-linked 1,4-disubstituted 1,2,3-triazoles with a furyl/thienyl moiety. *Mol. Divers.* 21, 137–145. doi: 10.1007/s11030-016-9710-y
- Khan, M. A., Ahmed, L., Mandal, P. K., Smith, R., and Haque, M. (2020). Modelling the dynamics of pine wilt disease with asymptomatic carriers and optimal control. *Sci. Rep.* 10:11412. doi: 10.1038/s41598-020-67090-7
- Kikuchi, T., Cotton, J. A., Dalzell, J. J., Hasegawa, K., Kanzaki, N., McVeigh, P., et al. (2011). Genomic insights into the origin of parasitism in the emerging plant pathogen *Bursaphelenchus xylophilus*. *PLoS Pathog.* 7:e1002219. doi: 10.1371/journal.ppat.1002219
- Kim, H. M., Jeong, S. G., Choi, I. S., Yang, J. E., Lee, K. H., Kim, J., et al. (2020). Mechanisms of insecticidal action of *Mmetarhizium anisopliae* on adult Japanese pine sawyer beetles (*Monochamus alternatus*). *ACS Omega* 5, 25312–25318. doi: 10.1021/acsomega.0c03585
- Kim, J. C., Baek, S., Park, S. E., Kim, S., Lee, M. R., Jo, M., et al. (2019). Colonization of *Metarhizium anisopliae* on the surface of pine tree logs: a promising biocontrol strategy for the Japanese pine sawyer, *Monochamus alternatus*. *Fungal Biol.* 124, 125–134. doi: 10.1016/j.funbio.2019.12.006
- Kitazume, H., Dayi, M., Tanaka, R., and Kikuchi, T. (2018). Assessment of the behaviour and survival of nematodes under low oxygen concentrations. *PLoS One* 13:e0197122. doi: 10.1371/journal.pone.0197122
- Koga, M., Zwaal, R., Guan, K. L., Avery, L., and Ohshima, Y. (2000). A *Caenorhabditis elegans* MAP kinase kinase, MEK-1, is involved in stress responses. *EMBO J.* 19, 5148–5156. doi: 10.1093/emboj/19.19.5148
- Kriner, M. A., and Subramaniam, A. R. (2020). The serine transporter SdaC prevents cell lysis upon glucose depletion in *Escherichia coli*. *Microbiol. Open* 9:e960. doi: 10.1002/mbo3.960
- Kumar, K. K., and Dara, S. K. (2021). Fungal and bacterial endophytes as microbial control agents for plant-parasitic nematodes. *Int. J. Environ. Res. Public Health* 18:4269. doi: 10.3390/ijerph18084269
- Lee, I. H., Han, H., Koh, Y. H., Kim, I. S., Lee, S. W., and Shim, D. (2019). Comparative transcriptome analysis of *Pinus densiflora* following inoculation with pathogenic (*Bursaphelenchus xylophilus*) or non-pathogenic nematodes (*B. thailandae*). *Sci. Rep.* 9:12180. doi: 10.1038/s41598-019-48660-w
- Li, J., Zou, C., Xu, J., Ji, X., Niu, X., Yang, J., et al. (2015). Molecular mechanisms of nematode-nematophagous microbe interactions: basis for biological control of plant-parasitic nematodes. *Annu. Rev. Phytopathol.* 53, 67–95. doi: 10.1146/annurev-phyto-080614-120336
- Li, Y., Mo, L., Zhou, X., Yao, Y., Ma, J., Liu, K., et al. (2022). Characterization of plant growth-promoting traits of *Enterobacter* sp. and its ability to promote cadmium/lead accumulation in *Centella asiatica* L. *Environ. Sci. Pollut. Res. Int.* 29, 4101–4115. doi: 10.1007/s11356-021-15948-2
- Liang, L. M., Zou, C. G., Xu, J., and Zhang, K. Q. (2019). Signal pathways involved in microbe-nematode interactions provide new insights into the biocontrol of plant-parasitic nematodes. *Philos. Trans. R. Soc. B Biol. Sci.* 374:1767. doi: 10.1098/rstb.2018.0317
- Liu, G., Lai, D., Liu, Q., Zhou, Z. L., and Liu, Z. L. (2016). Identification of nematocidal constituents of *Notopterygium incisum* rhizomes against *Bursaphelenchus xylophilus* and *Meloidogyne incognita*. *Molecules* 21:1276. doi: 10.3390/molecules21101276
- Liu, M. J., Hwang, B. S., Jin, C. Z., Li, W. J., Park, D. J., Seo, S. T., et al. (2019). Screening, isolation and evaluation of a nematocidal compound from actinomycetes against the pine wood nematode, *Bursaphelenchus xylophilus*. *Pest Manag. Sci.* 75, 1585–1593. doi: 10.1002/ps.5272
- Lohrke, S. M., Dery, P. D., Li, W., Reedy, R., Kobayashi, D. Y., and Roberts, D. R. (2002). Mutation of *rpiA* in *Enterobacter cloacae* decreases seed and root colonization and biocontrol of damping-off caused by *Pythium ultimum* on cucumber. *Mol. Plant Microbe Interact.* 15, 817–825. doi: 10.1094/MPMI.2002.15.8.817
- López, A. C., and Alippi, A. M. (2019). Feasibility of using RFLP of PCR-amplified 16S rRNA gene(s) for rapid differentiation of isolates of aerobic spore-forming bacteria from honey. *J. Microbiol. Methods* 165:105690. doi: 10.1016/j.mimet.2019.105690
- Maehara, N., Kanzaki, N., Aikawa, T., and Nakamura, K. (2020). Potential vector switching in the evolution of *Bursaphelenchus xylophilus* group nematodes (Nematoda: Aphelenchoididae). *Ecol. Evol.* 10, 14320–14329. doi: 10.1002/ece3.7033
- Mahdi, I., Fahsi, N., Hafidi, M., Allaoui, A., and Biskri, L. (2020). Plant growth enhancement using rhizospheric halotolerant phosphate solubilizing bacterium *Bacillus licheniformis* QA1 and *Enterobacter asburiae* QF11 isolated from *Chenopodium quinoa* wildl. *Microorganisms* 8:948. doi: 10.3390/microorganisms8060948
- Mahmood, K., Akhter, Z., Asghar, M. A., Mirza, B., Ismail, H., Liaquat, F., et al. (2020). Synthesis, characterization and biological evaluation of novel

- benzimidazole derivatives. *J. Biomol. Struct. Dyn.* 38, 1670–1682. doi: 10.1080/07391102.2019.1617783
- Maltese, W. A., and Overmeyer, J. H. (2014). Methuosis: nonapoptotic cell death associated with vacuolization of macropinosome and endosome compartments. *Am. J. Pathol.* 184, 1630–1642. doi: 10.1016/j.ajpath.2014.02.028
- Mokracka, J., Koczura, R., and Kaznowski, A. (2004). Yersiniabactin and other siderophores produced by clinical isolates of *Enterobacter* spp. and *Citrobacter* spp. *FEMS Immunol. Med. Microbiol.* 40, 51–55. doi: 10.1016/S0928-8244(03)00276
- Monciardini, P., Sosio, M., Cavaletti, L., Chiocchini, C., and Donadio, S. (2002). New PCR primers for the selective amplification of 16S rDNA from different groups of actinomycetes. *FEMS Microbiol. Ecol.* 42, 419–429. doi: 10.1111/j.1574-6941.2002.tb01031.x
- Mpongwana, N., Ntwampe, S. K., Mekuto, L., Akinpelu, E. A., Dyantyi, S., and Mpentshu, Y. (2016). Isolation of high-salinity-tolerant bacterial strains, *Enterobacter* sp., *Serratia* sp., *Yersinia* sp., for nitrification and aerobic denitrification under cyanogenic conditions. *Water Sci. Technol.* 73, 2168–2175. doi: 10.2166/wst.2016.070
- Munif, A., Hallmann, J., and Sikora, R. A. (2000). “Evaluation of the biocontrol activity of endophytic bacteria from tomato against *Meloidogyne incognita*,” in *Proceedings of the Mededelingen Faculteit Landbouwkundige En Toegepaste Biologische Wetenschappen*, Vol. 65, (Belgium: Universiteit Gent), 471–480.
- Nascimento, F. X., Espada, M., Barbosa, P., Rossi, M. J., Vicente, C. S., and Mota, M. (2016). Non-specific transient mutualism between the plant parasitic nematode, *Bursaphelenchus xylophilus*, and the opportunistic bacterium *Serratia quinivorans* BXF1, a plant-growth promoting pine endophyte with antagonistic effects. *Environ. Microbiol.* 18, 5265–5276. doi: 10.1111/1462-2920.13568
- Nascimento, F. X., Hasegawa, K., Mota, M., and Vicente, C. S. (2015). Bacterial role in pine wilt disease development – review and future perspectives. *Environ. Microbiol. Rep.* 7, 51–63. doi: 10.1111/1758-2229.12202
- Natalia, V. K., Daniel, R. K., Jonah, L., Carolina, W., Gary, R., and Frederick, M. A. (2013). *Pseudomonas aeruginosa* disrupts *Caenorhabditis elegans* iron homeostasis, causing a hypoxic response and death. *Cell Host Microbe* 13, 406–416. doi: 10.1016/j.chom.2013.03.003
- Nirmala, J. G., and Lopus, M. (2020). Cell death mechanisms in eukaryotes. *Cell Biol. Toxicol.* 36, 145–164. doi: 10.1007/s10565-019-09496-2
- Niu, B., Paulson, J. N., Zheng, X., and Kolter, R. (2017). Simplified and representative bacterial community of maize roots. *Proc. Natl. Acad. Sci. U.S.A.* 114, E2450–E2459. doi: 10.1073/pnas.1616148114
- Niu, B., Vater, J., Rueckert, C., Blom, J., Lehmann, M., Ru, J. J., et al. (2013). Polymyxin P is the active principle in suppressing phytopathogenic *Erwinia* spp. by the biocontrol rhizobacterium *Paenibacillus polymyxa* M-1. *BMC Microbiol.* 13:137. doi: 10.1186/1471-2180-13-137
- Niu, B., Wang, W., Yuan, Z., Sederoff, R. R., Sederoff, H., Chiang, V. L., et al. (2020). Microbial interactions within multiple-strain biological control agents impact soil-borne plant disease. *Front. Microbiol.* 11:585404. doi: 10.3389/fmicb.2020.585404
- Niu, Q., Tian, Y., Zhang, L., Xu, X., Niu, X., Xia, Z., et al. (2011). Overexpression of the key virulence proteases Bace16 and Bae16 in *Bacillus* nematocidal B16 to improve its nematocidal activity. *J. Mol. Microbiol. Biotechnol.* 21, 130–137. doi: 10.1159/000332805
- Niu, X., Song, L., Xiao, Y., and Ge, W. (2018). Drought-tolerant plant growth-promoting rhizobacteria associated with foxtail millet in a semi-arid agroecosystem and their potential in alleviating drought stress. *Front. Microbiol.* 8:2580. doi: 10.3389/fmicb.2017.02580
- Nunes da Silva, M., Solla, A., Sampedro, L., Zas, R., and Vasconcelos, M. W. (2015). Susceptibility to the pinewood nematode (PWN) of four pine species involved in potential range expansion across Europe. *Tree Physiol.* 35, 987–999. doi: 10.1093/treephys/tpv046
- Nurjadi, D., Kocer, K., Chanthalangsy, Q., Klein, S., Heeg, K., and Boutin, S. (2021). New delhi metallo-beta-lactamase facilitates the emergence of cefiderocol resistance in *Enterobacter cloacae*. *Antimicrob. Agents Chemother.* 66:e0201121. doi: 10.1128/AAC.02011-21
- Oh, M., Han, J. W., Lee, C., Choi, G. J., and Kim, H. (2018). Nematicidal and plant growth-promoting activity of *Enterobacter asburiae* HK169: genome analysis provides insight into its biological activities. *J. Microbiol. Biotechnol.* 28, 968–975. doi: 10.4014/jmb.1801.01021
- Ozair, M., Hussain, T., Awan, A. U., Aslam, A., Khan, R. A., Ali, F., et al. (2020). Bio-inspired analytical heuristics to study pine wilt disease model. *Sci. Rep.* 10:3534. doi: 10.1038/s41598-020-60088-1
- Paiva, G. N., Proenca, D., Francisco, R., Verissimo, P., Santos, S. S., Fonseca, L., et al. (2013). Nematicidal bacteria associated to pinewood nematode produce extracellular proteases. *PLoS One* 8:e79705. doi: 10.1371/journal.pone.0079705
- Park, A. R., Jeong, S. I., Jeon, H. W., Kim, J., Kim, N., Ha, M. T., et al. (2020). A diketopiperazine, Cyclo-(L-Pro-L-Ile), derived from *Bacillus thuringiensis* JCK-1233 controls pine wilt disease by elicitation of moderate hypersensitive reaction. *Front. Plant Sci.* 11:1023. doi: 10.3389/fpls.2020.01023
- Park, J. M., Radhakrishnan, R., Kang, S. M., and Lee, I. J. (2015). IAA producing *Enterobacter* sp. I-3 as a potent bio-herbicide candidate for weed control: a special reference with lettuce growth inhibition. *Indian J. Microbiol.* 55, 207–212. doi: 10.1007/s12088-015-0515-y
- Peng, G., Zhang, W., Luo, H., Xie, H., Lai, W., and Tan, Z. (2009). *Enterobacter oryzae* sp. nov., a nitrogen-fixing bacterium isolated from the wild rice species *Oryza latifolia*. *Int. J. Syst. Evol. Microbiol.* 59, 1650–1655. doi: 10.1099/ijs.0.005967-0
- Ponpandian, L. N., Rim, S. O., Shanmugam, G., Jeon, J., Park, Y. H., Lee, S. K., et al. (2019). Phylogenetic characterization of bacterial endophytes from four *Pinus* species and their nematocidal activity against the pine wood nematode. *Sci. Rep.* 9:12457. doi: 10.1038/s41598-019-48745-6
- Proenca, D. N., Grass, G., and Morais, P. V. (2017). Understanding pine wilt disease: roles of the pine endophytic bacteria and of the bacteria carried by the disease-causing pinewood nematode. *Microbiol. Open* 6:e00415. doi: 10.1002/mbo3.415
- Proenca, D. N., Heine, T., Senges, C. H. R., Bandow, J. E., Morais, P. V., and Tischler, D. (2019). Bacterial metabolites produced under iron limitation kill pinewood nematode and attract *Caenorhabditis elegans*. *Front. Microbiol.* 10:2166. doi: 10.3389/fmicb.2019.02166
- Qiu, X. W., Wu, X. Q., Huang, L., and Ye, J. R. (2016). Influence of Bxp1 gene silencing by dsRNA interference on the development and pathogenicity of the pine wood nematode, *Bursaphelenchus xylophilus*. *Int. J. Mol. Sci.* 17:125. doi: 10.3390/ijms17010125
- Qiu, X., Yang, L., Ye, J., Wang, W., Zhao, T., Hu, H., et al. (2019). Silencing of cyp-33C9 gene affects the reproduction and pathogenicity of the pine wood nematode, *Bursaphelenchus xylophilus*. *Int. J. Mol. Sci.* 20:4520. doi: 10.3390/ijms20184520
- Rajamuthiah, R., Jayamani, E., Majed, H., Conery, A. L., Kim, W., Kwon, B., et al. (2015). Antibacterial properties of 3-(phenylsulfonyl)-2-pyrazinecarbonitrile. *Bioorg. Med. Chem. Lett.* 25, 5203–5207. doi: 10.1016/j.bmcl.2015.09.066
- Rajasekharan, S. K., Lee, J. H., Ravichandran, V., and Lee, J. (2017). Assessments of iodoindoles and abamectin as inducers of methuosis in pinewood nematode, *Bursaphelenchus xylophilus*. *Sci. Rep.* 7:6803. doi: 10.1038/s41598-017-07074-2
- Ranawat, B., Mishra, S., and Singh, A. (2021). *Enterobacter hormaechei* (MF957335) enhanced yield, disease and salinity tolerance in tomato. *Arch. Microbiol.* 203, 2659–2667. doi: 10.1007/s00203-021-02226-5
- Révora, V., Marchesini, M. I., and Comerici, D. J. (2020). *Brucella abortus* depends on l-Serine biosynthesis for intracellular proliferation. *Infect. Immunity* 88:e00840–19. doi: 10.1128/IAI.00840-19
- Rodrigues, A. A., Araújo, M., Soares, R. S., Oliveira, B., Ribeiro, I., Sibov, S. T., et al. (2018). Isolation and prospection of diazotrophic rhizobacteria associated with sugarcane under organic management. *Anais Acad. Bras. Cienc.* 90, 3813–3829. doi: 10.1590/0001-3765201820180319
- Roslan, M., Zulkifli, N. N., Sobri, Z. M., Zuan, A., Cheak, S. C., and Abdul Rahman, N. A. (2020). Seed biopriming with P- and K-solubilizing *Enterobacter hormaechei* sp. improves the early vegetative growth and the P and K uptake of okra (*Abelmoschus esculentus*) seedling. *PLoS One* 15:e0232860. doi: 10.1371/journal.pone.0232860
- Sarkar, A., Ghosh, P. K., Pramanik, K., Mitra, S., Soren, T., Pandey, S., et al. (2018). A halotolerant *Enterobacter* sp. displaying ACC deaminase activity promotes rice seedling growth under salt stress. *Res. Microbiol.* 169, 20–32. doi: 10.1016/j.resmic.2017.08.005
- Sarkar, S., and Chaudhuri, S. (2015). New report of additional *enterobacterial* species causing wilt in West Bengal, India. *Can. J. Microbiol.* 61, 477–486. doi: 10.1139/cjm-2015-0017
- Sayed, R. Z., Patel, P. R., and Shaikh, S. S. (2015). Plant growth promotion and root colonization by EPS producing *Enterobacter* sp.



- RZS5 under heavy metal contaminated soil. *Indian J. Exp. Biol.* 53, 116–123.
- Shastri, R. P., Welch, M., Rai, V. R., Ghate, S. D., Sandeep, K., and Rekha, P. D. (2020). The whole-genome sequence analysis of *Enterobacter cloacae* strain Ghats1: insights into endophytic lifestyle-associated genomic adaptations. *Arch. Microbiol.* 202, 1571–1579. doi: 10.1007/s00203-020-01848-5
- Shoebitz, M., Ribaud, C. M., Pardo, M. A., Cantore, M. L., Ciampi, L., and Curá, J. A. (2009). Plant growth promoting properties of a strain of *Enterobacter ludwigii* isolated from *Lolium perenne* rhizosphere. *Soil Biol. Biochem.* 41, 1768–1774. doi: 10.1016/j.soilbio.2007.12.031
- Singh, R. P., Runthala, A., Khan, S., and Jha, P. N. (2017). Quantitative proteomics analysis reveals the tolerance of wheat to salt stress in response to *Enterobacter cloacae* SBP-8. *PLoS One* 12:e0183513. doi: 10.1371/journal.pone.0183513
- Soeriyadi, A. H., Ongley, S. E., Kehr, J. C., Pickford, R., Dittmann, E., and Neilan, B. A. (2021). Tailoring enzyme stringency masks the multispecificity of a *Lyngbyatoxin* (Indolactam Alkaloid) nonribosomal peptide synthetase. *Chembiochem* 23:e202100574. doi: 10.1002/cbic.202100574
- Soliman, T., Mourits, M. C., Werf, W., Hengeveld, G. M., Robinet, C., and Lansink, A. G. (2012). Framework for modelling economic impacts of invasive species, applied to pine wood nematode in Europe. *PLoS One* 7:e45505. doi: 10.1371/journal.pone.0045505
- Song, S., Zhang, Y., Ding, T., Ji, N., and Zhao, H. (2021). The dual role of macropinocytosis in cancers: promoting growth and inducing methuosis to participate in anticancer therapies as targets. *Front. Oncol.* 10:570108. doi: 10.3389/fonc.2020.570108
- Srisuk, N., Sakpuntoon, V., and Nutarat, P. (2018). Production of indole-3-acetic acid by *Enterobacter* sp. DMKU-RP206 using sweet whey as a low-cost feed stock. *J. Microbiol. Biotechnol.* 28, 1511–1516. doi: 10.4014/jmb.1804.04043
- Taghavi, S., van der Lelie, D., Hoffman, A., Zhang, Y. B., Walla, M. D., Vangronsveld, J., et al. (2010). Genome sequence of the plant growth promoting endophytic bacterium *Enterobacter* sp. 638. *PLoS Genet.* 6:e1000943. doi: 10.1002/9781118297674.ch84
- Thoden, J. B., Holden, H. M., and Grant, G. A. (2014). Structure of L-serine dehydratase from *Legionella pneumophila*: novel use of the C-terminal cysteine as an intrinsic competitive inhibitor. *Biochemistry* 53, 7615–7624. doi: 10.1021/bi501253w
- Tian, B., Yang, J., and Qin, K. (2007). Bacteria used in the biological control of plant-parasitic nematodes: populations, mechanisms of action, and future prospects. *FEMS Microbiol. Ecol.* 61, 197–213. doi: 10.1111/j.1574-6941.2007.00349.x
- Topalović, O., Hussain, M., and Heuer, H. (2020). Plants and associated soil microbiota cooperatively suppress plant-parasitic nematodes. *Front. Microbiol.* 11:313. doi: 10.3389/fmicb.2020.00313
- Um, J., Kim, D. G., Jung, M. Y., Saratale, G. D., and Oh, M. K. (2017). Metabolic engineering of *Enterobacter aerogenes* for 2,3-butanediol production from sugarcane bagasse hydrolysate. *Bioresour. Technol.* 245, 1567–1574. doi: 10.1016/j.biortech.2017.05.166
- Vandana, U. K., Rajkumari, J., Singha, L. P., Satish, L., Alavilli, H., Sudheer, P., et al. (2021). The endophytic microbiome as a hotspot of synergistic interactions, with prospects of plant growth promotion. *Biology* 10:101. doi: 10.3390/biology10020101
- Velayudhan, J., Jones, M. A., Barrow, P. A., and Kelly, D. J. (2004). L-serine catabolism via an oxygen-labile L-serine dehydratase is essential for colonization of the avian gut by *Campylobacter jejuni*. *Infect. Immunity* 72, 260–268. doi: 10.1128/IAI.72.1.260-268.2004
- Vurukonda, S., Giovanardi, D., and Stefani, E. (2018). Plant growth promoting and biocontrol activity of *Streptomyces* spp. as endophytes. *Int. J. Mol. Sci.* 19:952. doi: 10.3390/ijms19040952
- Wang, C., Wu, J., Shi, B., Shi, J., and Zhao, Z. (2020). Improving L-serine formation by *Escherichia coli* by reduced uptake of produced L-serine. *Microb. Cell Fact.* 19:66. doi: 10.1186/s12934-020-01323-2
- Wen, T. Y., Wu, X. Q., Hu, L. J., Qiu, Y. J., Rui, L. Y., Zhang, X., et al. (2021). A novel pine wood nematode effector, BxSCD1, suppresses plant immunity and interacts with an ethylene-forming enzyme in pine. *Mol. Plant Pathol.* 22, 1399–1412. doi: 10.1111/mp.13121
- Windstam, S., and Nelson, E. B. (2008). Differential interference with *Pythium ultimum* sporangial activation and germination by *Enterobacter cloacae* in the corn and cucumber spermospheres. *Appl. Environ. Microbiol.* 74, 4285–4291. doi: 10.1128/AEM.00263-08
- Wu, X. Q., Yuan, W. M., Tian, X. J., Fan, B., Fang, X., Ye, J. R., et al. (2013). Specific and functional diversity of endophytic bacteria from pine wood nematode *Bursaphelenchus xylophilus* with different virulence. *Int. J. Biol. Sci.* 9, 34–44. doi: 10.7150/ijbs.5071
- Xie, F., Dai, S., Zhao, Y., Huang, P., Yu, S., Ren, B., et al. (2020). Generation of fluorinated amycolin siderophores against *Pseudomonas aeruginosa* infections by a combination of genome mining and mutasynthesis. *Cell Chem. Biol.* 27, 1532–1543.e6. doi: 10.1016/j.chembiol.2020.10.009
- Xu, X. L., Chen, S., and Grant, G. A. (2011). Kinetic, mutagenic, and structural homology analysis of L-serine dehydratase from *Legionella pneumophila*. *Arch. Biochem. Biophys.* 515, 28–36. doi: 10.1016/j.abb.2011.08.005
- Xue, Q., Xiang, Y., Wu, X. Q., and Li, M. J. (2019). Bacterial communities and virulence associated with pine wood nematode *Bursaphelenchus xylophilus* from different *Pinus* spp. *Int. J. Mol. Sci.* 20:3342. doi: 10.3390/ijms20133342
- Yadav, M., Shukla, A. K., Srivastava, N., Upadhyay, S. N., and Dubey, S. K. (2016). Utilization of microbial community potential for removal of chlorpyrifos: a review. *Crit. Rev. Biotechnol.* 36, 727–742. doi: 10.3109/07388551.2015.1015958
- Yang, J., Tian, B., Liang, L., and Zhang, K. (2007). Extracellular enzymes and the pathogenesis of nematophagous fungi. *Appl. Microbiol. Biotechnol.* 75, 21–31. doi: 10.1007/s00253-007-0881-4
- Yin, L., Liu, B., Wang, H., Zhang, Y., Wang, S., Jiang, F., et al. (2020). The rhizosphere microbiome of *Mikania micrantha* provides insight into adaptation and invasion. *Front. Microbiol.* 11:1462. doi: 10.3389/fmicb.2020.01462
- Zaki, S., Kamal, A., Ashmawy, N. A., and Shoeib, A. A. (2021). Nano-metals forming bacteria in Egypt. I. Synthesis, characterization and effect on some phytopathogenic bacteria in vitro. *Sci. Rep.* 11:12876. doi: 10.1038/s41598-021-92171-6
- Zhang, J., Fu, B., Lin, Q., Riley, I. T., Ding, S., Chen, L., et al. (2020). Colonization of *Beauveria bassiana* 08F04 in root-zone soil and its biocontrol of cereal cyst nematode (*Heterodera filipjevi*). *PLoS One* 15:e0232770. doi: 10.1371/journal.pone.0232770
- Zhang, X. D., Wang, D., Sun, S., and Zhang, H. (2020). Issues of Z-factor and an approach to avoid them for quality control in high-throughput screening studies. *Bioinformatics* 36, 22–23. doi: 10.1093/bioinformatics/btaa1049
- Zhang, X., El-Hajj, Z. W., and Newman, E. (2010). Deficiency in L-serine deaminase interferes with one-carbon metabolism and cell wall synthesis in *Escherichia coli* K-12. *J. Bacteriol.* 192, 5515–5525. doi: 10.1128/JB.00748-10
- Zhang, X., Xu, G., Shi, J., Koffas, M., and Xu, Z. (2018). Microbial production of L-Serine from renewable feedstocks. *Trends Biotechnol.* 36, 700–712. doi: 10.1016/j.tibtech.2018.02.001
- Zhang, X., Zhang, D., Zhu, J., Liu, W., Xu, G., Zhang, X., et al. (2019). High-yield production of L-serine from glycerol by engineered *Escherichia coli*. *J. Ind. Microbiol. Biotechnol.* 46, 221–230. doi: 10.1007/s10295-018-2113-6
- Zhao, L., Mota, M., Vieira, P., Butcher, R. A., and Sun, J. (2014). Interspecific communication between pinewood nematode, its insect vector, and associated microbes. *Cell Press* 30, 299–308. doi: 10.1016/j.pt.2014.04.007

**Conflict of Interest:** The authors declare that the research was conducted in the absence of any commercial or financial relationships that could be construed as a potential conflict of interest.

**Publisher's Note:** All claims expressed in this article are solely those of the authors and do not necessarily represent those of their affiliated organizations, or those of the publisher, the editors and the reviewers. Any product that may be evaluated in this article, or claim that may be made by its manufacturer, is not guaranteed or endorsed by the publisher.

Copyright © 2022 Zhao, Yuan, Wang, Wang, Chao, Sederoff, Sederoff, Yan, Pan, Peng, Wu, Borriss and Niu. This is an open-access article distributed under the terms of the Creative Commons Attribution License (CC BY). The use, distribution or reproduction in other forums is permitted, provided the original author(s) and the copyright owner(s) are credited and that the original publication in this journal is cited, in accordance with accepted academic practice. No use, distribution or reproduction is permitted which does not comply with these terms.



# Advantages of publishing in Frontiers



## OPEN ACCESS

Articles are free to read  
for greatest visibility  
and readership



## FAST PUBLICATION

Around 90 days  
from submission  
to decision



## HIGH QUALITY PEER-REVIEW

Rigorous, collaborative,  
and constructive  
peer-review



## TRANSPARENT PEER-REVIEW

Editors and reviewers  
acknowledged by name  
on published articles

## Frontiers

Avenue du Tribunal-Fédéral 34  
1005 Lausanne | Switzerland

Visit us: [www.frontiersin.org](http://www.frontiersin.org)

Contact us: [frontiersin.org/about/contact](http://frontiersin.org/about/contact)



## REPRODUCIBILITY OF RESEARCH

Support open data  
and methods to enhance  
research reproducibility



## DIGITAL PUBLISHING

Articles designed  
for optimal readership  
across devices



## FOLLOW US

@frontiersin



## IMPACT METRICS

Advanced article metrics  
track visibility across  
digital media



## EXTENSIVE PROMOTION

Marketing  
and promotion  
of impactful research



## LOOP RESEARCH NETWORK

Our network  
increases your  
article's readership